Experimental and Theoretical Study of Hydrogen and Benzene Destruction Chemistries

by

RICHARD ALLEN SHANDROSS

B. S. Environmental Engineering
Northwestern University
(1979)

Submitted to the Department of Chemical Engineering
in partial fulfillment of the requirements for the degree of

DOCTOR OF PHILOSOPHY
at the
MASSACHUSETTS INSTITUTE OF TECHNOLOGY

February 1996

Signature of author _____
Department of Chemical Engineering
September 18, 1995

Certified by _____
Jack B. Howard
Professor of Chemical Engineering
Thesis Supervisor

_____
John P. Longwell
Professor of Chemical Engineering Emeritus and Senior Lecturer
Thesis Supervisor

Accepted by _____
Robert E. Cohen
Bayer Professor of Chemical Engineering
Chair, Committee for Graduate Students

Experimental and Theoretical Study of Hydrogen and Benzene Destruction Chemistries

by

RICHARD ALLEN SHANDROSS

Submitted to the Department of Chemical Engineering on September 18, 1995, in partial fulfillment of the requirements for the degree of Doctor of Philosophy in Chemical Engineering.

Abstract

Benzene is postulated by some to be a crucial intermediate in the formation of soot and polycyclic aromatic hydrocarbons from both aliphatic and aromatic fuels, but critical testing of this hypothesis has been hindered by inadequate knowledge of benzene chemistry. In this research, mole fraction profiles of 44 species were measured using molecular beam mass spectrometry, in a low-pressure premixed fuel-rich H_2-O_2 flame with a small amount of benzene additive (P=22 torr, 31.3% Ar, $(C_6H_6)_0/(H_2)_0$=0.010, v_0=101 cm/sec). Sixteen species were identifed with reasonable certainty. A temperature profile was measured with a Pt/Pt13%Rh thermcouple, coated to prevent catalytic heating by a method developed in this work.

The data were used to test three literature benzene combustion mechanisms, two of which had previously been shown to predict stable species, plus H and OH, successfully in a rich C_6H_6 flame. In the present hydrogen-dominant flame, however, most of the same species are poorly predicted. In the H/O system, the overall rate of O_2 burnout is computed to be faster than observed, and radical mole fractions are overpredicted. This was found to be due to a defect in the high-temperature chemistry, primarily a lack of O consumption pathways and an imbalance of two fast shuttle reactions.

The computed scale for hydrocarbons burnout is correct, though there are systematic deficiencies in the profiles of intermediates, and a number of more-saturated species measured are not present in the models. Because of the H_2-O_2 chemistry problems, comparison of computed and measured net rates was found to be more suitable than analysis of mole fractions. With appropriate corrections for pressure effects, current benzene destruction chemistry agrees well with data. However, the net rates for the critical intermediates phenyl, phenol and cyclopentadiene are not well predicted by literature mechanisms.

With falloff adjustments and pathway corrections, the phenol net rate prediction is dramatically improved. Improvements were made to the chemistry of phenyl and phenoxy radicals, but their rates of destruction require further work and are shown to be the principal sources of error remaining in the aromatics chemistry of the models.

Overall, significant improvements in benzene destruction chemistry were achieved, and the remaining difficulties were clarified. High-temperature hydrogen chemistry problems were identified and partially solved, with directions for future attention recommended.

Thesis Supervisors and Titles:

Dr. Jack B. Howard, Professor of Chemical Engineering
Dr. John P. Longwell, Professor Emeritus of Chemical Engineering

Acknowledgements

Well, the end of the journey has finally arrived, hasn't it? (Yes, it has!) Steel yourself, because I've been here so long that I have a *lot* of people to thank.

First and foremost, I'd like to thank my wife, Randi Donnis. Her patience, endurance and support have meant more to me than words can say. I love you, sweetie, and here's to our life without an n-year unfinished project hanging over our heads!

So long as I've started off with the personal side, I might as well continue. Thanks to my family: Mom, for your support and love; Dad, for being the inspiration for my undertaking the project, both before and after your passing; Marianne and Joel, for being an outpost of sanity and insanity for me; Sue and Bob and Carrie and Kelly, for always showing your excitement about my (then future) achievements, and for brothorly love. Pearl, Marilyn, Ralph, Jacob, Jennie, Barry, Judy and Vher: thanks for making me your family, too.

To the Chicago crew for standing by me in the distance: Frank Sternberg, Dave and Debbie Harris, Ron Villejo and Karen Landrum, Michael and Irene Tobis (well...Madison is close enough), and Jane Cooperman. Here on the right coast, I'd like to thank Eric Hoffman and Angela Suescún-Hoffman, Doug and Nancy Thompson, Brian and Judy Galford, and Catherine Womack for standing by me in the nearness.

And down south, I'd like to send thanks to Larry Monroe, who taught me a lot about humor, talk radio, computer mania, and learning. We had some great political discussions, which moved me closer to the center of the road. Hopefully, I pulled him partly off the right shoulder. Thanks for your warm and personable next door friendship, Larry.

Thanks to Hallie Harris, Lois Glass, and especially Steve Krugman, for those special points of view. Bill Ryan and Al Dougall deserve a lot of credit for helping me go from limping back to walking, and on to running.

There are many to thank for their professional help. On that side of the aisle, I'd like to extend my gratitude to my advisors, Professors Jack Howard and John Longwell. Thanks for your confidence, your guidance, your prodding, and your friendship. (Thanks also to Carolyn Howard and Marion Longwell, for many enjoyable times at your respective houses.) All of my

thesis committee deserve thanks for their feedback and guidance: Professors Adel Sarofim and Phil Westmoreland, and Dr. Tony Dean.

The work was financially supported throughout by the Division of Chemical Sciences, Office of Basic Energy Sciences, Office of Energy Research of the U.S. Department of Energy, under Grant No. DE-DG02-84ER13282 — for which I am grateful, and on behalf of which I call on Congress to recognize the importance of grants such as this to the future of our environment and the efficient use of energy.

Phil Westmoreland and Carl Wikstrom deserve a paragraph to themselves. Phil, thanks for your close attention in those early years. You were like a big brother showing me the ropes. Especially, thanks for the technical, tactical ("Ready...fire!..aim, fire!...") support, the great expressions ("sad, but grim") and the confidence. Carl, well...what can I say? You singlehandedly taught me my crescent wrench from my toggle valve. As the next to last of the now-dead breed in Building 31, you were indeed a good buddy, and my only beef with you is that you left so soon.

I received the help of several UROPs: Bill Helfinstine mastered difficult thermocouple construction techniques and tutored me on cloning computers. Rob Snihur did an excellent job of coding and documenting several revisions of the RRKM program.

A number of people in other shops and labs here at MIT have given me invaluable assistance. I owe Tony Modestino thanks for his mock-begrudging help in countless ways, large and small. He helped me set up and attempt to set up Rayleigh scattering and sodium-D experiments on the McKinnon burner, lent me assorted pieces of equipment, helped out with the MicroVax, and on and on. You all should keep him employed here at MIT forever and ever. In fact, give him a raise. (How was that, Tony are we even yet?) Speaking of "McKinnon," Tom McKinnon was also a big help in various ways, including lending of equipment, providing technical expertise, his friendship, and (along with his student Hai-Yue Zhang) providing me with a computer copy of his model and QRRK calculations. Jack Brouwer deserves praise for his technical skill and generosity. He was invaluable in my sodium-D experiments, which alas never made it into this thesis. He was also someone I could have been close friends with had we not been so darn busy on our projects. Thanks to Art Lafleur for advice on getting my benzene feedstock analyzed for possible contaminants.

Acknowledgements

Back in the early days, there was a combustion chemistry research seminar called "10.731." I learned an awful lot in those classes, thanks to Bob Barat, Jack Brouwer, Fred Lam, Joe Marr, Chris Pope (whom I also thank for lots of interesting and diverting conversations in the combustion suite of Building 31), Craig Vaughn, Vikki Vlastnik, Phil Westmoreland and Carl Wikstrom.

Outside of MIT, many equipment folk lent their support over the sad but grim years. Brian Regel of Extrel Corporation was a life and project saver. Many an hour he spent (by phone) with me and my vintage Extranuclear mass spectrometer, talking me through the paces and out of the woods. Without Joe Lebiedzik of Advanced Research Instruments Corporation, I wonder if I might ever have solved my RF interference problem: thanks, Joe. Thanks to Don and Tom James of Eastern Scientific Sales and Service for innumerable pump repairs and advice. Also, to the master glassblower Gerhard Finkenbeiner, of G. Finkenbeiner, Inc., for spending a month of evenings in your shop learning how to make sampling probes. I hope I've sent you enough customers in return.

At other universities and research centers: Prof. John Kiefer and Dr. Wing Tsang helped me to better understand the chemistry of unimolecular and chemical activation reactions. Profs. Ken Brezinsky and Peter Lindstedt sent me copies of their models, and Prof. Lindstedt worked with me to get his running. Thanks also to Fran Rupley of Sandia National Laboratories, for the help with CHEMKIN, PREMIX and trying to get the Lindstedt and Skevis model to converge. Dr. Dan Seery provided technical assistance with H_2-O_2 flames, and encouraging feedback about what seemed like discouraging results.

We have had many, many esteemed visitors to MIT over the years and (I'm sure I'll leave someone out, but...) I'd like to extend thanks for the lectures and helpful private talks to: Prof. H.Gg. Wagner, Prof. Ken Brezinsky, Prof. John Kiefer, Dr. Bob Kee, Dr. Charles Westbrook, Prof. Klaus-Heinrich Homann, Prof. Joe Bozzelli (whom I also thank for help with the THERM and CHEMACT programs), Dr. Tony Dean, Dr. Steve Harris, Prof. Fred Dryer, Prof. Mitchell Smooke, and Prof. Houston Miller.

Finally, thanks to Kathy Brownell, Arline Benford, Carol Phillips, Gabrielle Joseph, Elaine Aufiero-Peters, Janet Fischer, for their administrative and support prowess, especially how they always had a smile, a word of support, or a dig (that means *you*, Ah-leen) for me.

Actually, finally, I'd like to thank Howard Covert for being last.

Oh...and anyone I've missed.

Table of Contents

List of Figures

List of Figures

List of Figures

List of Tables

Chapter 1: Introduction.

Soot and polycyclic aromatic hydrocarbons ("PAH") are frequently-found components of hydrocarbon combustion systems, sometimes welcome (e.g., in the formation of carbon black) and sometimes not (such as when they are emitted as pollutants). Their chemistry has generated a great deal of interest in the recent years, beginning with the energy shortage of 1979[1] (McKinnon, 1989).

Being composed of multiple fused aromatic rings, these compounds — if soot can be called a "compound" — have at least some of the chemical character of benzene. For example, according to Fenimore and Jones (1967), Neoh (1980), Puri et al. (1994), and others, OH is found to be one of the primary oxidizing species, as it is with benzene. Some have postulated (e.g., Lam et al., 1990; Frenklach and Wang, 1990; Kazarov, 1995) that single-ring aromatics such as benzene and phenyl play an important role as fundamental building blocks in soot and PAH formation in flames. To the extent that this is true, the fate of these high molecular weight species is tied to that of the first-ring aromatics. Benzene, the simplest aromatic in its class, is thus worthy of study for its potential impact on the ability to control the formation of soot and PAH.

The chemistry of benzene in flames may be divided into formation, destruction and molecular weight growth. The current state of knowledge in any of these categories is far from complete. The focus of this work is destruction. In particular, the initial focus was on oxidation, including reactions of benzene and phenyl with O, OH, and O_2. Benzene chemistry is reviewed in Chapters 2 and 7.

In his laminar, premixed flat flame study of C_6H_6-O_2-Ar flames, Bittner (1981) determined that the benzene consumption rate only began to accelerate when the flame temperature reached 1500-1650 K. As most previous investigations of benzene oxidation reactions have been conducted at temperatures below 1500 K, the high-temperature environment of flames such as Bittner's provides an opportunity to extend the prior level of understanding to a temperature range that is more practical for certain combustion systems. Further motivation was provided by

[1] As early as 1974, however, "Soot Formation and Behavior" was added as a major research topic in The Combustion Institute's international symposia.

the lack of agreement on the most important benzene oxidation pathways under combustionc conditions; see Lovell et al. (1989) and Lin and Lin (1984), for example.

One of the problems with studying stoichiometric and rich benzene flames such as Bittner's is that reactions of benzene with non-oxidant species obscure the oxidation chemistry. This is especially so because mechanisms and rate constants for those reactions are also in the main poorly known. Since the oxidants of interest all belong to the H/O system of flame species, the method of adding small amounts of benzene to an H_2-O_2 flame was used in this work (in the Bittner apparatus) to ensure that the overwhelming majority of bimolecular reactions involving C_6H_6 were of the type under investigation[2]. Rich H_2-O_2 conditions were chosen for the base flame, so that reactions with OH would stand out: much work had been done on hydrogen reactions with C_6H_6 and phenyl, and O atom reactions would be deemphasized under those conditions.

Doping or seeding of flames has been used in the past by a number of workers, to study (1) the effect on the primary flame (Halstead and Jenkins, 1969; Zachariah and Smith, 1987), (2) the nature of the primary flame itself (Fenimore and Jones, 1965), or (3) as in this study, reactions of the additive with primary flame species (Peeters et al., 1971; Seery and Zabielski, 1981). While not a new technique *per se*, the power of the additive method was enhanced in this work with modeling and net rate analysis.

In the planning and early stages of this work, no benzene flame models had been published. There was no concern that this might hamper efforts to analyze the results quantitatively, as H_2-O_2 flame chemistry was considered to be well understood. In the words of Baldwin et al. (1986), for example, when describing their study of trace amounts of C_6H_6 added to H_2 and O_2 at 773 K:

> "A comprehensive mechanism is available for the H_2 + O_2 system, so that the reaction provides a reproducible and controllable source of H, OH, O and HO_2 in an environment suitable for the study of oxidation reactions..."

With the mole fractions of H/O species predictable by computation, much information on benzene oxidation could then be derived from observations of the perturbations caused by the additive. The molecular-beam mass spectrometry ("MBMS") capability of the experiment allows for

[2] This technique was suggested by an anonymous grant proposal reviewer.

study of both radical and stable species, providing even more tools for investigation. The experimental apparatus and procedures are described in Chapter 3.

In spite of the well-laid plans described above, several events required a shift in the emphases and methods needed to accomplish the stated goals:

1. With recent progress in the modeling of C_3-C_5 chemistry, comprehensive benzene flame models have become possible. Proposed models have arisen from groups at NASA (Bittker, 1987; Bittker, 1991), Princeton (Emdee et al., 1992), Stuttgart (Chevalier and Warnatz, 1991), Imperial College (Lindstedt and Skevis, 1994) and Colorado School of Mines (Zhang and McKinnon, 1995). Since benzene destruction chemistry is now in a phase of being established for flame systems, it is no longer relevant to consider the elements of a preliminary model. Rather, it is more important to critically examine the existing models, and identify their strengths and weaknesses.
2. The intermediate and product hydrocarbon species measured in this work have revealed reduction as a strong competitor to oxidation, under rich H_2-O_2 conditions. Some types of reduction pathways were expected, for example $H+C_6H_6 \rightleftharpoons H_2+C_6H_5$, but others become apparent as well. Furthermore, model-proposed reduction pathways such as $H+C_6H_6 \rightleftharpoons C_6H_7$ lead to unrealistic results in the form originally put forth. Therefore, a study of reduction chemistry was added to the initial objectives, the goal being enlarged to an investigation of benzene *destruction* chemistry.
3. Measurements in the present flame reveal that, at the high temperatures of this work, H_2-O_2 models *do not* do an adequate job of predicting H/O species mole fractions. The inability to rely on a prediction of the base flame mole fractions affects both a perturbation analysis and a full modeling study. It was necessary to turn to the alternative technique of net rate analysis, where predicted mole fractions are not necessary to examine the validity of the various pathways and rate constants of the model.

The experimental data collected in this study are presented in Chapter 4. In Chapter 5, the predictions of three recently proposed benzene models are presented and compared to data.

The outcome of this work was an improved understanding of the high-temperature reactions of both the H/O system and benzene destruction chemistry. A discussion of H_2-O_2 chemistry is found in Chapter 6, from the standpoints of consistency tests of the measured mole fraction

and temperature profiles, identification of possible sources of error in literature models, and potential solutions to those problems. Benzene destruction chemistry is treated in Chapter 7, in which the chemistry of each of the species C_6H_6, C_6H_5OH, C_6H_5, C_6H_5O, C_6H_7 and C_6H_8 is examined in turn. Much of the current models was found to be valid, or at least to do a good job of predicting net rates. However, a more thorough accounting for pressure-induced kinetic effects in unimolecular and chemically activated reactions was found to be necessary, and was made. Also, a more careful review of chemical pathways revealed a number of improper reactions in the proposed models. A revised model was put forth, which includes all of the recommended changes, appropriate for ca. 22 torr flames. After the best efforts at improving the models, two areas of deficiency were found to remain: the destruction chemistries of phenyl and phenoxy radicals. Therefore, the identification of these areas for future work is considered a result of the present research.

A secondary result of this investigation was a clarification of the need for and utility of research techniques such as net rate analysis. Previous screening methods that utilized net rates (Cole, 1982; Cole et al., 1984a and b; Westmoreland, 1986; Westmoreland et al., 1989) were extended here to include predictions of entire model networks involving a particular species.

Chapter 2: Literature Review.

2.1 Hydrogen Destruction Chemistry

The following is a brief and admittedly very sketchy outline of H_2-O_2 combustion modelling, intended only as an introduction to history of the topic. The citations are only given as samples of important works published in a particular time period.

1950's: Solution of branched chain reaction kinetics in flame. Studies of recombination region of flames. Partial equilibrium calculations.

- Giddings and Hirschfelder (1957)
- Kaskan (1958)
- Padly and Sugden (1959)

1960's: Models to explain explosion limits and slow reaction rates in closed vessels. More complete and accurate flame solutions attempted (low-T flames, but including energy and diffusion equations).

- Baldwin and Mayor (1960)
- Dixon-Lewis (1967)

1970's: Compilation and evaluation of reaction rates. Continued development of explosion models. Further progress in kinetics and numerical methods, including sensitivity analysis.

- Baulch et al. (1972).
- Baldwin et al. (1974)
- Day et al. (1972)
- Dixon-Lewis (1979)
- Dougherty et al. (1979)

1980's: Comprehensive mechanisms pieced together from single-reaction studies, models for "slow" reaction systems, databases, etc. (Every combination of species considered: H+OH, H+H_2, H+O_2,..., H+x; O+OH, O+H_2, O+O_2,..., O+x; ...) Powerful reactor codes developed.

- Dougherty & Rabitz (1980)

- Westbrook (1982)
- Miller et al. (1983)
- Westbrook and Dryer (1984)
- Dixon-Lewis (1984)
- Warnatz (1983)
- Kee et al. (1985)

1990's: Continued refinement of kinetics.

- Yetter et al. (1991)

2.2 Benzene Destruction Chemistry

Products from destruction of benzene and other aromatics.

Knowledge of the products obtained in studies of the destruction of benzene and related aromatics is potentially helpful in the interpretation of results, or the identification of unknown species. The summary given below is organized by species being destroyed and type of experiment.

C_6H_6 pyrolysis. At low temperatures ($T \lesssim 1100$ K), products are almost exclusively biphenyl and H_2, though small amounts of CH_4 and larger aromatics have been seen (Brooks et al., 1979). Above this temperature, acetylene and polyacetylenes are the major products; minor products include species such as C_8H_6 (very high temperature), C_4H_4, C_4H_3 and C_3H_3 — but not phenyl radical (Singh and Kern, 1983; Kern et al., 1985; Colket, 1986). Phenyl was seen in a Knudsen cell (very low pressure pyrolysis, or VLPP), where bimolecular reactions are rare, by Smith and Johnson (1983).

C_6H_6 pyrolysis in the presence of H. All of the experiments discussed here were performed at low temperatures, that is, at or below about 500 K. In experiments with an abundance of H atom relative to benzene, such as those of Schiff and Steacie (1951) and Kim et al. (1973), CH_4 is the single most prevalent product. Schiff and Steacie reported that 85% of the reacted C_6H_6 was converted to methane. Kim et al. report the same figure, but it is not clear whether they are referring to 85% of total carbon or moles of benzene reacted. Ethane is also present in high quantities, and small amounts of cyclohexane has been observed (Kim et al. only). When

there is much more C_6H_6 than H atom, more-hydrogenated cyclo-C_6's appear (Sauer and Ward, 1967) as well as CH_4 (Hoyermann et al., 1975).

C_6H_6 and C_6H_5 pyrolysis in the presence of H_2. Experiments with benzene in H_2 at 773-1273 K, by Louw et al. (1984), yielded biaryls at low temperatures. At the higher end of the range, solid carbon, CH_4, and small amounts of C_2H_4 and C_2H_6 were found. In their study of chlorobenzene (hence phenyl, by fast loss of Cl) reduction by H_2, Ritter et al. (1990) measured benzene, soot, toluene, C_5H_6, C_2H_4, and CH_4. Biphenyl and naphthalene were also found.

C_6H_6 oxidation. In shock tube experiments at 1300-1700 K with small amounts of O_2, the products seen by Fujii and Asaba (1973) were CO, acetylene, biphenyl, CH_4 and C_2H_4. Baldwin et al. (1986) added a small amount of benzene to a rich H_2-O_2 mixture at 773 K. Principal products were CO and CH_4, and smaller amounts of H_2CO, C_2H_2, C_2H_4, C_4H_4, CO_2 and phenol were found. When benzene is present in a large excess of O_2, as in the 950-1150 K flow reactor study of Rotzoll (1985), a multitude of oxygenated species are found. The products mentioned above for small amounts of O_2, plus C_3-C_5 and C_8-C_{10} hydrocarbons, were measured too. However, species with more carbons decreased in concentration with increasing temperature: nothing above C_1 survived temperatures over 1075 K.

Phenol pyrolysis. The products of phenol pyrolysis depend on the residence time of the gases. At short times (170 ms), CO, benzene and c-C_5H_6 were found at 1 atm and 1064-1162 K by Lovell et al. (1989), with small amounts of acetylene, naphthalene and indene as well. The phenol introduced was diluted in N_2 at concentrations from 500-2016 ppm. At much longer times (2.5 sec), Cyprès and Bettens (1974) found that undiluted phenol at 1 atm and 938-1138 K produced a variety of products. The most abundant at 938 K were water, solids, dibenzofuran, CO, H_2 and benzene. At 1138 K, however, the major products were solids, CO, H_2, water, C_6H_6, CH_4, naphthalene, anthracene + phenanthrene, toluene, and cyclopentadiene. Spielmann and Cramers (1972) note, however, that under vacuum conditions only c-C_5H_6 and CO are produced. From this, the thermal instability of cyclopentadiene, and the fates of ^{14}C and ^{3}H from labeled phenols, Cyprès and Bettens concluded that c-C_5H_6 and CO are the earliest products produced. This is consistent with the finding of Spielmann and Cramer that the products from cracking of c-C_5H_6 are similar to those of phenol pyrolysis.

Phenol pyrolysis in H_2. Manion and Louw (1989) pyrolyzed phenol in excess H_2 in a flow reactor, from 922-1175 K. They found CH_4, C_2H_2, C_2H_4, C_2H_6, c-C_5H_6, CO, C_6H_6,

napthalene, indene, styrene and other species. Except for CO, these products are similar to those found for benzene and phenyl in H_2.

Benzene destruction mechanisms. For the purpose of this work, reaction mechanisms for benzene destruction may (arbitrarily) be put into two categories: (1) those postulated to explain specific experimental results, and (2) those intended for use in a laminar (or other type of) flame code. Mechanisms of the former type are generally limited in the sorts of conditions to which they are applied: for example, to pyrolysis conditions or to oxidation at low temperatures. Table 2.1 lists some of those proposed benzene destruction mechanisms. It should be noted that a number of papers regarding specific reactions (e.g., $OH+C_6H_6 \rightleftharpoons$ products) propose small networks in the course of solving for the reaction of interest. Those are not included in Table 2.1. Flame code models for benzene have only recently begun to be proposed. The first to appear was that of Jackson and Laurendeau (1987). This model consisted of a set of benzene and phenyl reactions, plus a formation reaction for cyclohexadienyl, added to the acetylene model of

Table 2.1 Selected literature benzene destruction mechanisms developed to explain experimental results.

Source	Applicable Conditions and Comments
Norrish and Taylor (1956)	O_2 oxidation, around 950 K, 1 atm, flow system.
Bauer and Aten (1963)	Pyrolysis, 690-1900 K, shock tube.
Asaba and Fujii (1971)	Pyrolysis, 1400-1900 K, 2-8 atm, shock tube.
Fujii and Asaba (1973)	Pyrolysis with additive O_2, 1300-1700 K, shock tube.
Louw and Lucas (1973)	Pyrolysis with additives, around 800 K , 1 atm, flow system.
Brooks et al. (1979)	Pyrolysis, 873-1036 K, 1 atm, static system.
Santoro and Glassman (1979)	Oxidation, review paper.
McLain et al. (1979)	Oxidation, 1700-2800 K, 1.1-1.7 atm, shock tube.
Bittner (1981), Bittner and Howard (1981)	$\phi = 1.8$ C_6H_6-O_2-Ar flame study, to 1900 K, 20 torr.
Venkat (1981), Venkat et al. (1982)	Oxidation, about 1200 K, 1 atm, flow system.
Smith and Johnson (1983)	Pyrolysis, 300-2173 K, < 5 torr, Knudsen cell.
Louw et al. (1984)	Pyrolysis in H_2, around 1000 K, 1 atm, flow system.
Rotzoll (1985)	Oxidation, 950-1150 K, 0.4 atm, flow system.
Brezinsky (1986)	Oxidation, 875-1500 K, 1 atm, review paper.
Colket (1986a, b)	Pyrolysis, 7-8 atm, 1200-2400 K, shock tube.
Braun-Unkhoff et al. (1989)	Phenyl pyrolysis, 1300-1800 K, 1.5-7.8 atm, shock tube.

Miller et al. (1982) as a base. It was used to predict major stable species in a lean H_2-O_2-N_2 flame with benzene as an additive. The maximum temperaure in the flame was 1400 K. Phenyl destruction was modeled by the "semiglobal" reaction of McLain et al. (1979) (originally Fujii and Asaba, 1973):

$$C_6H_5+O_2 \rightleftharpoons 2CO+C_2H_2+C_2H_3 \qquad \text{(Ph6)}$$

Bittker (1991) proposed a more detailed benzene model[3], based in part on the scheme proposed by Brezinsky (1986). Some C_5 reactions were included as well. The model was tested against 1 atm, 1100 K flow reactor mole fraction profiles of major species, and was used to predict ignition delay times for shock tube experiments up to 1600 K.

Chevalier and Warnatz (1991) put forth a mechanism containing 57 species and 475 reactions, detailing only the benzene oxidation submechanism. The base model contained reactions for species up to C_4's. They tested the model by predictions of flame velocities and ignition delay times for shock tube experiments from about 1300-1600 K.

The third model proposed was that of Emdee et al. (1992) ("EBG"), nominally for toluene oxidation near 1200 K[4], but containing a full benzene submechanism. Also based on the Brezinsky (1986) outline of benzene oxidation, the model has 44 species and 130 reactions. There is no C_3 chemistry, and very little of C_4's. The authors tested the model against their 1 atm laminar flow reactor data (stable species), in the temperature region of 1100 K, finding it to do a reasonable job of predicting phenol, c-C_5H_6, C_4 species, and CO.

Most recently, Lindstedt and Skevis (1994) ("LS") and Zhang and McKinnon (1995) ("ZM") have published benzene models which they used to predict the $\phi = 1.8$, C_6H_6-O_2-Ar flame results of Bittner (1981). The LS model has 87 species and 454 reactions. The C_3-C_5 subnetworks are rather large, and a number of linear C_6H_5 and C_6H_6 isomers not found in other models are included. Formation and subsequent decyclization of cyclohexadienyl radical is also present. The ZM model has 75 species and 498 reactions. They used the EBG model as a starting point, but made a number of modifications, including falloff corrections for most reactions which

[3] Bittker did not publish the model as being intended for laminar flame predictions *per se*, but it was tested as such by Zhang and McKinnon (1994), and was the most detailed mechanism proposed at its time (120 reactions).

[4] The model was not published expressly for laminar flame either, but was also tested for that purpose by Zhang and McKinnon.

require it. There is a fair amount of chemistry for molecular weight growth species, up to $C_{10}H_8$. C_3-C_5 reactions are also significantly represented in the model.

Interestingly, both the LS and ZM models predict H, OH and major stable species quite well in the rich benzene flame, but do a much poorer job with the critically important intermediates C_6H_5, C_6H_5O, and C_6H_5OH. The consequences of and reasons for this are discussed in Chapter 7.

Selected specific reactions.

The following review of individual reactions is intended to provide background information relevant to the analysis of literature reaction networks for aromatics destruction presented in Chapter 7 and the falloff calculations found in Appendix C.

$C_6H_6+O \rightleftharpoons C_6H_5OH$, C_6H_5O+H - The chemistry of oxygen addition to olefins is an ongoing and active area of research. See, for example, Cvetanović and Singleton (1984) (review) and Koda et al. (1991) (experiments with several linear olefins). Intermediates are very short-lived, and in many cases a variety of products can be formed from the adduct. Because the adduct is a triplet biradical which undergoes rapid secondary reaction (Boocock and Cvetanović (1961), Mani and Sauer (1968), Grovenstein and Mosher (1970), Bonanno et al. (1972), and later studies), it has been difficult to study this reaction.

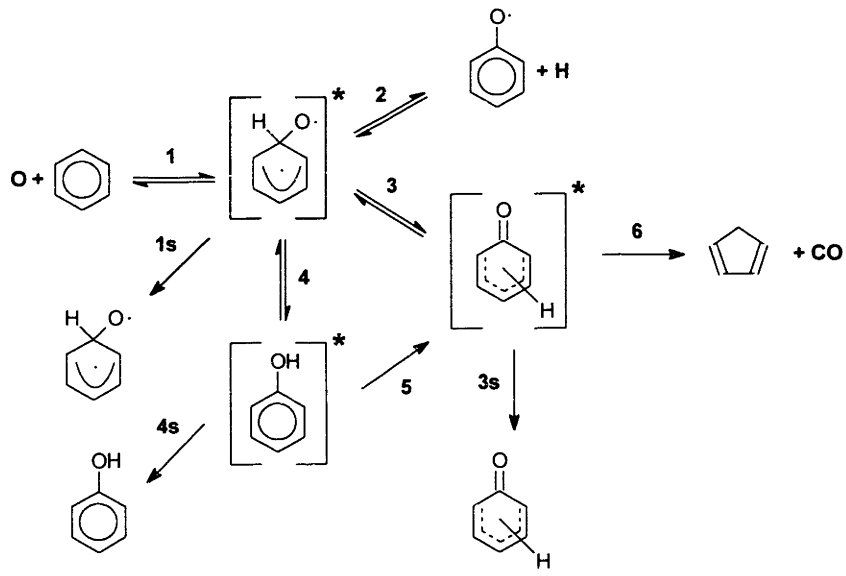

Figure 2.1 Possible reaction network for $O+C_6H_6$.

Figure 2.1 show a possible reaction network for this reaction, excluding reactions in which O is incorporated into the ring. The triplet biradical mentioned above is the product of reaction 1 in the figure. The migration of H from the site of O attack to another on the ring would follow a pattern frequently seen in O+olefin reactions, usually followed by decomposition of the isomerized adduct (Cvetanović and Singleton, 1984). This particular pathway for $O+C_6H_6$ is not found in the literature, though some have searched for the final product CO (see below).

The branching ratio for formation of phenol (or other C_6H_6O species) vs. phenoxy+H, as a function of both temperature and pressure, is not well-determined. Various studies (Boocock and Cvetanović (1961), Mani and Sauer (1968), Grovenstein and Mosher (1970), Bonanno et al. (1972), Sloane (1977), Sibener et al. (1980), and Sol et al. (1988)) have found formation of up to 30% phenol (or an undetermined C_6H_6O, in the cases of Sloane and Sibener et al.). Many of those studies were performed under multicollision conditions, in which phenol may have been formed by secondary reactions. The crossed molecular beams experiment of Sibener et al. seems to establish that the formation of a long-lived adduct (probably phenol) via intersystem crossing increases with energy, though the authors acknowledged that the higher energy work may have been contaminated by reaction of $O(^1D_2)+C_6H_6$. The study did not measure an activation energy for the crossing. (Sloane estimated it at 10 kcal/mol, in an SCF theoretical calculation.) Recent low-temperature (405 K) and low-pressure work of Bajaj and Fontijn (1994) confirm in part the findings of Sibener et al., in that little phenol was formed — and much less than that when a scavenger limited the amount of secondary reaction in the system ($I_{94}/I_{93} \sim 0.0025$, independent of pressure from 3-7 torr).

Studies of O + linear olefins do not show rearrangements to hydroxides. Bley et al. (1989) point out that in the case of O + ethylene, the alcohol would rapidly isomerize to acetaldehyde, which has only been observed in a matrix.

Leidreiter and Wagner (1989) studied $O+C_6H_6$ in a shock tube at 1200-1450 K. They fit a rate constant for the addition/stabilization channel by modeling the O atom concentration-time profile. The entire contribution from O plus benzene was assigned to this pathway, as the addition/elimination channel was not even considered. The basis for this assignment was the high pressure of the experiment and the large energy well for the overall reaction $C_6H_6+O \rightleftharpoons C_6H_5OH$. (From the temperature and approximate density they give, however, the pressure can be calculated to be only about 650 torr.) Their logic is based on the supposition that thermal

decomposition of phenol would be in the high-pressure limit, by analogy to toluene, apparently leading to the conclusion that isomerization from the triplet biradical to phenol would also have little falloff compared with elimination.

The amount and route of formation of CO as a further byproduct is another question without a definitive quantitative answer, though qualitatively it appears to be clearer than the issue of intersystem crossing. The bulk of evidence in the literature suggests that the CO formation channel is not significant. It is not clear either whether any CO formation which might result this reaction would be due to decomposition of C_6H_5OH or another isomer of C_6H_6O such as the cyclic ketone of Figure 2.1. Since a route from phenol has been proposed by some workers, CO formation from both phenol pyrolysis and $O+C_6H_6$ is discussed in the next section.

Most recently, a study of $O+C_6H_6 \rightarrow$ products over the large temperature range 600-1310 K was performed by Ko et al. (1991). The data were found to agree well with other literature measurements over the range 300-1450 K, including those of Leidreiter and Wagner, without curvature in the Arrhenius plot. The data cover a wide range of pressures as well, down to several torr. This behavior is suggestive of the "concerted displacement" pathway of Cvetanović and Singleton (1984), in which the elimination of hydrogen to form a >C=O bond — in this case forming phenoxy and H atom — was found to be pressure-independent.

Other isomerization pathways for the C_6H_6O adduct, besides the one leading to phenol, have been proposed by Boocock and Cvetanović (1961) (1,2- and 1,4-epoxides, cyclic ketones, and two c-C_5H_5CHO species) and Mani and Sauer (1968) (1,2-epoxide and the heterocyclic compound, oxepin). No studies have been performed which might prove or disprove these intersystem crossing channels.

In their aromatics destruction model, EBG chose the rate constant of Nicovich et al. (1982), which is fully consistent with that of Ko et al. ZM assigned the result of Avramenko et al. (1965), and performed a chemical activation calculation with outlet channels to C_6H_5OH, C_6H_5O+H, and C_5H_6+CO. As the only channel they found to be important was C_6H_5O+H, no other pathways were included in their model. LS assign the only product of $O+C_6H_6$ to be C_6H_5OH, following Leidreiter and Wagner.

In summary, the branching ratio of the $O+C_6H_6$ reaction has not been determined, and different conclusions have been reached by different investigators. The question is investigated in some detail in Chapter 7 and Appendix C.

$C_6H_5OH \rightleftharpoons C_5H_6+CO$ - This pathway was apparently first proposed for thermal systems by Spielmann and Cramers (1972), in their work on cyclopentadiene pyrolysis, though they may have derived it from carbon labelling work of Bettens and Cyprès (1971). Cyprès and Bettens (1974) later document the ^{14}C labelling study and therein embrace the mechanism. Both studies were conducted at 1 atm and temperatures in the general range of 823-1138 K. In addition, both propose the pathway on the basis of the distribution of products from thermal degradation of phenol; in the earlier work by comparison of products with those from c-C_5H_6 pyrolysis, in the later study by the product distribution and the appearance of most of the ^{14}C originally attached to the OH group in ^{14}CO.

In the reaction of O atom with benzene, CO has been observed by some to be a major product. For example, Boocock and Cvetanović (1961) found CO in significant quantities and noted its production at 298 K to decrease with pressure over their measurements, 49-592 torr. They proposed that CO might have derived from sources other than phenol (such as hot cyclopentadienyl formaldehyde from isomerization of the C_6H_6O adduct). Since (a) O and benzene were present in the system in similar amounts, and (b) no attempt was made to eliminate the considerable amount of surface reactions, no conclusion about the elementary reaction steps could truly be made. Avramenko et al. (1965) also found much CO (from 343-523 K) but surface reactions and/or secondary gas-phase reactions were not explicitly eliminated or accounted for.

Sloane (1977) studied O+C_6H_6 in a crossed molecular beams experiment, finding that formation of CO and a (probably linear) C_5H_6 species was a major pathway. However, Sibener et al. (1980), in a similar experiment in which angular distributions were also measured, concluded that the mass 66 seen by Sloane was created in his ionizer as a fragment and was not a reaction product.

Nicovich et al. (1982) also reacted O+C_6H_6, in a 298-950 K, 1 atm flash photolysis flow system, measuring CO with resonance fluorescence. The amount of O atom relative to benzene and N_2 diluent was very small, and other precautions were taken as well to reduce the effect of secondary reactions. They were unable to find any CO, at a maximum level of 5% of the quantity of $O(^3P)$ generated. The range of possible $(x_{CO})_{max}/(x_{C6H6})_0$ ranged from $1x10^{-7}$ to $1x10^{-2}$, depending on the combination of oxygen and initial benzene concentrations used. The authors published the amount of benzene used in each run, but only the *range* of O atom for the whole

experiment, therefore one must assume as much as 1% CO might have been present. Even so, that is much less than earlier studies, in support of the conclusions of Sibener et al.

The most recent $O+C_6H_6$ study to look at CO formation was that of Bajaj and Fontijn (1994). Their 3-12 torr discharge flow system was sampled by molecular beam mass spectrometry, with which they measured masses 93, 94 and 28. Phenoxy dominated their system, but the signal ratio of CO to C_6H_5O was as high as $7x10^{-3}$. Without a calibration factor, however, the exact ratio of mole fractions cannot be ascertained. Furthermore, the source of the CO — phenol or phenoxy — cannot be determined positively from an experiment such as this.

In a mechanistic study of phenol decomposition in H_2 and/or N_2 at 922-1175 K, Manion and Louw (1989) concluded that the direct CO-formation pathway was insignificant. Their study was performed using C_6H_5OD, and they found that ortho deuterium transfer did occur (but not the meta or para forms). In spite of the formation of the cyclohexadieneone, the low amount of deuterated cyclopentadiene — corrected for possible scrambling and other reaction effects — showed that the Spielmann and Cramers pathway was not important. They confirmed this by performing additional experiments with a reactor whose surface was treated to enhance surface reactions.

In spite of the above evidence that this reaction is probably absent or not important, the ZM model includes it, with a rate taken from Bruinsma et al. (1988). In the Bruinsma et al. study, phenol was pyrolyzed in a carbon-coated flow reactor at 1040-1140 K, where the products were cyclopentadiene and CO, and benzene. It is clear, however, that there was no way to know if the decomposition of phenol was via the Spielmann and Cramers mechanism or some other. The Bruinsma et al. rate constant for phenol decomposition would be $2.7x10^{-2}s^{-1}$ at 1040 K, which is almost exactly the first order rate constant for CO formation in the untreated reactor in the Manion and Louw study and about an order of magnitude or more higher than the rate in the treated reactor. Since the Bruinsma et al. rate is at or above that in the Manion and Louw study, and the latter conclude that unimolecular phenol decomposition is not significant in formation of CO, the formation of products in the Bruinsma et al. study was probably from a pathway involving phenoxy decomposition and H atom recombination with C_5H_5.

$C_6H_6+OH \rightleftharpoons C_6H_5OH+H$ (EBG, ZM, LS) - The rate constant for $OH+C_6H_6$ was first measured at room temperature by Davis et al. (1975), and by Doyle et al. (1975). Davis et al.

discovered the reaction to be in the falloff region over the pressure range of their experiment, 3-100 torr. Neither study elucidated the products of the reaction.

Perry et al. (1977) studied the reaction at 100 torr over the temperature range 296-473 K, and found a peculiar non-exponential behavior in the temperature region 325-380 K. They attributed the behavior to a duel-pathway mechanism consisting of H atom abstraction (high temperature) and addition/stabilization (low temperature), with decomposition of the adduct back to reactants above 325 K. In a crossed effusive molecular beam experiment at 300 K using OD instead of OH, Sloane (1978) confirmed a mass 96 adduct and the absence of abstraction, but also observed a mass 95 product of H elimination. The hydroxy-cyclohexadienyl adduct was also directly observed by cw-UV-laser absorption, by Fritz et al. (1985).

Tully et al. (1981) extended the range of measurements to $213 \leq T \leq 1150$ K and $20 \leq P \leq 200$ torr, and to reaction of OH with deuterated benzene as well. Their results were similar to Perry et al.; additionally, they determined that at 298 K the high-pressure limit was reached at 25 torr. The non-exponential region was also somewhat wider, ranging from about 320-500 K. Domination of the mechanism by abstraction was determined to take place above 500 K. Lorenz and Zellner (1983) prepared a 298 K falloff curve with all of the data collected thus far, and concluded that the high-pressure limit was 30 torr. They also showed that the shape of the transition region between addition and abstraction found by various workers was dependent on the time resolution of the experiment.

Lin and Lin (1984) postulated a different mechanism from that previously considered, that the high-temperature behavior observed in previous systems was a result of H elimination from the energized adduct, overcoming decomposition back to reactants. Using an RRKM analysis which included addition/stabilization, addition/elimination and redissociation back to reactants, their computations showed an excellent fit to previous data over the entire temperature range. According to their calculations, abstraction never played a significant part. The details of their falloff calculation were not specified, except for the energy barrier to H elimination, which they gave as 1 kcal/mol. The source of their abstraction rate constant was not given either.

Madronich and Felder (1985) concluded differently from Lin and Lin in their analysis of non-exponential OH decays at 1300 K, 87-138 torr, and high H_2O concentration. They fit the OH decay to models with various assumptions, finding that the only model to portray the data accurately was that with reversible abstraction only. Having an addition/elimination channel

overpredicted the transient OH profile. For a particular channel in question (abstraction or addition/elimination) the assumption was made that the rate constant was equal to the experimentally measured value for $OH+C_6H_6 \rightarrow$ products, at low H_2O concentration where the reverse of the abstraction reaction is negligible. The main cause of the change of OH prediction was the *product* of the reaction, H in the addition/elimination case or H_2O in the abstraction case.

Witte et al. (1986) are the only workers to determine the decomposition rate of the adduct from the experiment. As in the case of Madronich and Felder, this was accomplished by solving for [OH] vs. time with a proposed reaction network, under pseudo-first-order conditions with respect to C_6H_6. The network included k_{rev}, and measurements were made up to 150 torr — clearly at the high-pressure limit. They estimate one order of magnitude as the limit of error of the reverse rate constant. Based on the observation of "quasi-equilibrium" of OH at long times, they believe the addition/elimination channel to be negligible at the temperatures studied (239-354 K).

The temperature dependence of the addition rate constant is quite weak, leading to a fairly large variation in the activation energies assigned by various workers, from 0 kcal/mol (Wallington et al., 1987) to 4.6 kcal/mol (Madronich and Felder, 1985).

The first high-temperature experimental investigation of addition/elimination reaction proposed by Lin and Lin was that of He et al. (1988). They studied the reaction $H+C_6H_5OH \rightleftharpoons C_6H_6+OH$ in a single-pulse shock tube at 1000-1150 K and 2.5-5 atm, by measuring isobutene (produced in equal amounts as initial H atom) and benzene. The rate constants for this reaction and abstraction were determined directly, and were subsequently used with a model calculation to derive the rate of H recombination with phenoxy. Decomposition of C_6H_5O to $CO+C_5H_5$ was not a part of that model. The rate constant for $C_6H_6+OH \rightleftharpoons C_6H_5OH+H$ was inferred from microscopic reversibility, and the authors concluded that abstraction is the preferred reaction at their temperatures. No pressure effect was found.

The rate constant for H+phenol measured subsequently by Manion and Louw (1989) at 1 atm was in substantial agreement with that of He et al. over the experimental temperature range, though the specific Arrhenius parameters differed somewhat. The two rate constants are at most variance at high and low temperatures. Rate constants for abstraction from phenol by H, and for H recombination with phenoxy, were estimated as well.

In summary, the relative importance of abstraction and addition has been somewhat controversial, but the experimental data supports abstraction as the dominant channel at higher temperatures, at least at pressures above 87 torr. The nature of this reaction at 22 torr, the pressure of the present work, is explored in a QRRK analysis.

$C_6H_5O+H \rightleftharpoons C_6H_5OH$ (EBG, ZM, LS) - The first appearance of this reaction in the literature was in the article by He et al. (1988) mentioned above. Shortly thereafter, Lovell et al. (1989) published an estimate for the reverse direction, by analogy to other (unmentioned), similar reactions. Their concern with using the experimental rate constant stemmed from the large sensitivity of this rate to uncertainties in the phenol/phenoxy thermochemistry. The thermochemistry in question is that of Burcat et al., (1985), which was derived from experimental measurements and appropriate modifications of the same but suffered from a lack of literature data for specific comparison. The Lovell et al. estimated value is within a factor of 3-5 of He et al. (using the equilibrium constant) over the temperature range of their experiment, but varies from $1x10^{-2}$ to 12 times the latter's rate constant over the temperature range of the present flame. The rate constant estimated by Manion and Louw (1989) is about 50% that of He at al. over the same temperature range.

Despite the objections raise by Lovell et al., the EBG model proposed by the same group uses the He et al. rate constant for this reaction. The ZM model, which otherwise includes rate constants from the He et al. paper, uses a value for this reaction supposedly set forth by Avramenko et al. (1965). That work involved $O+C_6H_6$ rather than C_6H_5OH or C_6H_5O, and no specific elementary mechanism was proposed or discussed. Therefore, use of the Avramenko et al. rate constant for the $H+C_6H_5O$ reaction is erroneous. Lindstedt and Skevis (1995) report that their value for the reaction is from Leidreiter and Wagner (1989), but in the versions sent by Lindstedt (1994, 1995) for this work, they use the He et al. rate constant. Leidreiter and Wagner latter base their rate on H elimination from toluene.

$C_6H_5+O_2 \rightleftharpoons C_6H_5O+O$ (EBG, ZM, LS); $2CO+C_2H_2+C_2H_3$ (ZM); $C_6H_5O_2$, $C_6H_4O_2+H$ - The reaction of $C_6H_5+O_2$ has been long known to be slow, relative to the reaction of many other hydrocarbon radicals with oxygen (Russell and Bridger, 1963). The first suggestion that this reaction might be important in combustion came from Fujii and Asaba (1973) in their 1300-1700 K shock tube study of the effect of oxygen additive to the pyrolysis of benzene. They proposed a semi-global reaction, written as $C_6H_5+O_2 \rightarrow 2CO+C_2H_2+C_2H_3$, with the product of initial

formation speculated to be $[C_6H_5O_2]^*$. Bittner (1981) found, though, that under rich C_6H_6-O_2 flame conditions the reaction of phenyl with oxygen to form any products would have to take place at nearly the collision frequency to account for the destruction of C_6H_5.

In a turbulent flow study, Venkat et al. (1982) postulated that under their lower temperature (1118-1280 K) and smaller radical pool conditions the reaction to form C_6H_5O+O was the primary consumer of phenyl. Hsu et al. (1984) suggested the possibility of the alternate pathway,

$$C_6H_5 + O_2 \longrightarrow C_6H_5OO \longrightarrow \text{ 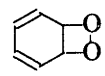 } + H \longrightarrow 2CO + C_4H_4 + H$$

though Venkat et al. and later Lin and Lin (1987) discounted mechanisms which do not involve C_6H_5O because of the lack of a route to the observed product phenol.

An experimental investigation which studied this reaction specifically at high temperatures was performed by Lin and Lin (1987), in a shock tube from 1030-1670 K and 0.32-0.54 atm. They assumed the primary mechanism to be formation of phenoxy and secondarily $C_6H_5O_2$ under the conditions studied. They derived the rate constant by modeling the observed CO and performed an RRKM analysis to confirm the dominance of the branching ratio by addition/decomposition.

The most recent and far-reaching work on C_6H_5+O_2 to date has been performed by Frank et al. (in press) and Yu and Lin (1994). The former studied the reaction behind reflected shocks at 900-1800 K and 975-1875 torr, using resonance absorption to monitor H, O and CO. The latter investigators used a cavity-ring-down method to examine the reaction at 297-473 K and 20-80torr. Laser absorption was used to measure the adduct, $C_6H_5O_2$. The picture put together by Yu and Lin from the results of these studies is that at low temperatures addition/stabilization is most important, but at high temperatures addition/elimination to C_6H_5O+O dominates. For example, at the pressures of the Frank et al. experiment, the low temperature regime is below about 1000 K, and the high temperature region is above about 1300 K. Between those temperatures, the two pathways compete. The H elimination channel shown above is never as important as the other two.

An RRKM analysis performed by Yu and Lin is discussed in detail in Appendix C. The results of their analysis are in agreement with every previous measurement of the reaction, except for a "preliminary value" put forth by Baldwin et al. (1986), a measurement by Preidel and

Zellner (1989), and Lin and Lin (1987). The Preidel and Zellner study was shown by Yu and Lin to be in error because of a strong coabsorption by the adduct at the wavelength in which C_6H_5 was monitored.

The falloff calculation of Yu and Lin is extended to the present temperatures and pressure in this work.

All three of the models reviewed in this study use the Lin and Lin (1987) rate constant for $C_6H_5+O_2 \rightleftharpoons C_6H_5O+O$. That rate constant should be updated to be consistent with the Yu and Lin measurements.

$C_6H_5 \rightleftharpoons l\text{-}C_6H_5$ (unspecified isomer) (ZM); HC≡CCH=CHCH=CH (LS); $C_2H_2+HC=CHC\equiv CH$ (ZM) - The nature of this decomposition reaction — decyclization, concerted decomposition, or both — has been the object of scrutiny for some time. Bauer and Aten (1963) first proposed two concerted pathways to products,

$$C_6H_5 \rightarrow C_4H_4+C_2H \qquad (a)$$

$$C_6H_5 \rightarrow C_4H_3+C_2H_2 \qquad (Ph13)$$

Asaba and Fujii (1971) pointed out that reaction Ph13 was really decyclization followed by β-scission, though they declined to write the steps separately in their model because "A-factors of these reactions are difficult to estimate."

Bittner (1981) was apparently the first to attempt such an estimate. His interest was in computing an overall rate constant for reaction Ph13, and he concluded from his estimate that the rate of recyclization was much faster than decomposition, below 1900 K. Therefore, the rate overall was rather low. All rates used were high-pressure limits.

Colket (1986a) also proposed an estimated value for the elementary steps, attributing the sequence to the reverse of that proposed by Frenklach et al. (1985) rather than Asaba and Fujii. In this case, decomposition of the linear species would be equal to recyclization at 1700 K, and exceeded it above that temperature. Use of the separate reactions in modeling the shock tube pyrolysis of benzene at 7 atm and 1200-2400K resulted in a good fit to data. The linear species was proposed to be HC≡CCH=CHCH=CH. As the thermochemistry implied by the forward and reverse reactions given by Colket was inconsistent with accepted values, he later revised the rate constants, in his modeling study of the shock tube pyrolysis of acetylene and vinylacetylene

(Colket, 1986b). With the revision, decomposition to acetylene and C_4H_3 never would be as fast as cyclization below 1940 K, though it would get within 30%. The ratio $\frac{k_{cycl}}{k_{decomp}}$ is 2 at 1850 K.

In the time period between Asaba and Fujii and Colket, several other groups, including Smith and Johnson (1983), Singh and Kern (1983), Kern et al. (1984) and Kiefer et al. (1985), had embraced the concerted pathway. The departure taken by Colket was motivated by the conclusions of his excellent analysis of the kinetics, thermochemistry and product distributions of the various theories of benzene pyrolysis (Colket, 1986a). He concluded that the A-factor required for a multibond pathway was unrealistically high, given the minumum E_a needed for the reaction.

Westmoreland (1986) pointed out that after the complex decyclizes it still possesses excess energy, which could go into the decomposition channels H+l-C_6H_4 and 1-C_4H_3+C_2H_2. According to his analysis, at a pressure of 1 atm the H elimination reaction becomes as important as simple decyclization above 2000 K, and skeletal fragmentation competes with simple decyclization above about 1750 K.

Shortly thereafter, Dewar et al. (1987) performed a semi-empirical quantum chemical (MINDO/3) calculation of the transition state structure for cyclization/decyclization, combined with an RRKM calculation of falloff over the ranges 0.5-4 atm and 1500-2500 K. The computed heats of formation of benzene and phenyl were each off by about 9 kcal/mol, in opposite (accumulative rather than compensatory) directions. Frenklach and Wang (1991) extended the RRKM calculation to 20 torr.

Rao and Skinner (1988) pyrolyzed benzene-d_6 and halobenzenes in a shock tube at 0.4 atm and 1450-1900 K, also deriving a rate constant for the decyclization reaction from fitting with a kinetic model. They then perform an RRKM falloff calculation to estimate the high-pressure limit, which is 0.1-0.5 times the Colket (1986b) rate over the temperature range of their study. The rate of Colket (1986a) was used for l-C_6H_5 decomposition. Relative to Colket's revised decomposition rate (Colket, 1986b), the Rao and Skinner high-pressure recyclization rate is much slower than estimated previously by others. The two rate constants are equal at about 1225 K, and $\frac{k_{cycl}}{k_{decomp}}$ gets as low as 0.043 with the temperature profile for the flame of this work.

Recently, Braun-Unkhoff et al. (1989) pyrolyzed phenyl behind reflected shock waves from 1125-5850 torr and 1300-1800 K. They argue for linearization as a first step using a

thermochemical kinetics argument similar to Colket (1986a), and derive a rate constant by modeling their data. Their rate constant, which is apparently not the high-pressure limit, is 0.07-0.16 that of Colket (1986b) over the temperature range of the study. With their rate constants and thermochemistry, decomposition would be equal to recyclization, above 1500 K.

In their paper on benzene formation, Westmoreland et al. (1989) perform a QRRK calculation for the reverse reaction,

$$1\text{-}C_4H_3 + C_2H_2 \rightleftharpoons (n\text{-}C_6H_5)^* \rightleftharpoons \text{phenyl}$$

at 20 torr, in a similar fashion as Westmoreland (1986). The high-pressure limits for both steps were estimated.

Athough no particular isomer was given by ZM for the single product reaction, the source cited was Braun-Unkhoff et al. who in turn cite Colket (1986a) as the source of their structure. For their rate constant for the concerted channel, ZM cite Bittker (1991), who mistakenly assigned the Braun-Unkhoff et al. rate for decylization to a multibond pathway. The use of both pathways, concerted and step-wise, is in any case redundant.

Baulch et al. (1992) recommend the rate constant of Braun-Unkhoff et al.

In summary, the experimental evidence points to decyclization as the first step in unimolecular phenyl destruction, rather than the concerted pathway. The linear species then decomposes further.

$C_6H_5+O \rightleftharpoons C_5H_5+CO$ - This rate constant was measured recently by Frank et al. (1995), representing a chemically activated pathway through the adduct $(C_6H_5O)^*$.

$H+C_6H_6 \rightleftharpoons C_6H\text{-}(LS);\ l\text{-}C_6H\text{-};\ fulvene+H;\ c\text{-}C_5H_4CH_3$ - This reaction has received a great deal of attention. An early investigation of the reaction of H atom with benzene was performed by Schiff and Steacie (1951), who produced H and D by the "discharge method" and reacted them with C_6H_6. As they formed no c-C_6H_8 or c-C_6H_{10}, they concluded that secondary hydrogenation was minimal. The major product was CH_4 (85%), with the rest being straight chain hydrocarbons of six or fewer carbons. The residence time in their 20 cm reaction tube was 0.6 sec. At the end of the tube, they exposed the gases to platinum gauze to "recombine H atoms." Condensable products (such as any hydrogenated cyclics) were trapped by liquid nitrogen, distilled and measure by a mass spectrometer. It is not clear what the sensitivity of the analytical

technique might have been, and clearly, in this study experimental results were strongly affected by secondary reactions.

Sauer and Ward (1967) produced H atoms by pulsed radiolysis — bombardment with 12-15 MeV electrons for 1 μsec — and also reacted them in various proportions with benzene at room temperature and 357 K. They observed a transient spectrum which they identified as cyclohexadienyl radical. Both c-C_6H_8 isomers were observed in their GC product analysis, along with bicyclo-hexadienyl. They latter they concluded was formed by disproportionation of two C_6H_7 molecules. They found essentially no pressure effect on the rate constant, over a range of about 1-61 atm.

Benson and Shaw (1967b) deduced an addition mechanism followed by H elimination back to reactants in their low-pressure study of 1,3-c-C_6H_8 pyrolysis at 603 K and 663 K, because of the formation of HD when C_6D_6 was added. Sauer and Mani (1970) observed a Hammett correlation of rate constants[5] for H plus substituted benzenes, in which the rate constant decreased with increasing σ, and concluded that electrophilic addition was the operating reaction mechanism. A similar conclusion was drawn for reaction in aqueous solution by Pryor et al. (1973) and others.

Other workers who confirmed the addition reaction with formation of more hydrogenated species include Kim et al. (1973) (273-511 K and 0.14-1.38 torr) and Hoyermann et al. (1975) (296-493 K and 2.4-9.1 torr). Neither group measured any falloff. Hoyermann et al. (1975) postulated the addition of H atoms to both the *energized complex* and the stabilized adduct, forming more hydrogenated species and unspecified decomposition products. Furukawa et al. (1974) produced C_6H_7 from c-C_6H_8 species and invoked H addition back to the cyclohexadienyl radical to explain their results.

Nicovich and Ravishankara (1984) extended measurements up to 1000 K, in a flow system at 10-200 torr, and computed the reverse reaction rate from non-exponential H atom decay curves. They were careful to reduce and account for secondary reactions, which they showed to be responsible for inconsistencies in some previous measurements of this relatively slow reaction. No pressure effect was observed at or below 470 K, the highest temperature for which they varied pressure. The authors argue that the reverse rate constant they derive is applicable to the

[5] The Hammett equation correlates reactions of substituted to unsubstituted compounds. The formula is $k = k_0 * 10^{\rho\sigma}$, where k_0 is the rate constant for the unsubtituted species, ρ is a reaction constant, and σ is a substituent constant (Morrison and Boyd, 1973).

reaction of thermalized C_6H_7, and not the energized complex. The first appearance of the reverse reaction was at 500 K, and by 600 K there was no discernible net reaction taking place.[6]

Despite Nicovich and Ravishankara's excellent results, some differences still existed between their value for the reverse decomposition reaction and earlier work, in particular that of James and Suart (1968). Furthermore, the A-factor was uncharacteristically high for a radical decomposition. These facts motivated Tsang (1986) to re-evaluate the thermochemistry of C_6H_7 from a "third-law" perspective rather than the "second-law" method used by Nicovich and Ravishankara. With the revised thermochemistry and using the measured forward rate constant, the H elimination rate constant was re-derived. The result of that analysis resolved the noted inconsistencies, including the high pre-exponential factor.

Fontijn and Mahmud (1989) repeated the measurements of Nicovich and Ravishankara in a HTP (high-temperature photochemistry) pseudo-static system, monitoring the disappearance of H atom. Below 600 K their results agreed well, but above that temperature Fontijn and Mahmud measured a higher rate constant and a negative pressure dependence.

Other routes for the energized complex have been proposed by Louw et al. (1984). In their flow system at 1 atm and 773-1273 K they observed large amounts of CH_4 formation which

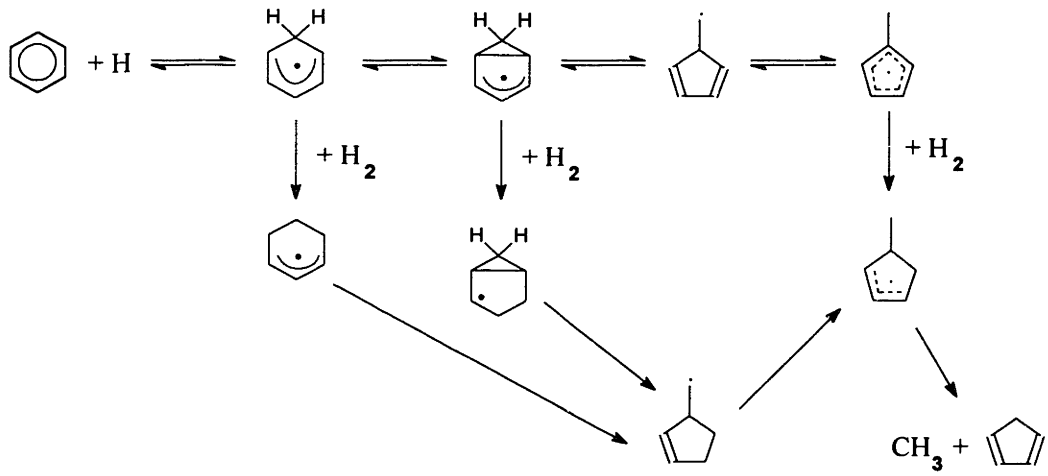

Figure 2.2 Louw et al. (1984) cyclohexadienyl mechanism.

[6] The loss of C_6H_7 by diffusion and reaction was found to be about 60% that of H atom. Since the larger species diffuses much less than H, more of the loss should be due to reaction with other cyclohexadienyl molecules, benzene or H atom. No reactions were found in the literature for $C_6H_6+C_6H_7$, the likely products of such a reaction which would be either the same species or $C_6H_5+C_6H_8$. The heat of reaction for the latter case is 35 kcal/mol, making that reaction (cont'd) unlikely. Therefore, some of the loss was probably due to further reaction of H atoms.

could not be explained by decomposition of C_2 species. Thermochemical arguments ruled out a molecular concerted elimination reaction. Seeing CH_3 formation as more likely to come from C_6H_7 than phenyl or benzene, they proposed the mechanism of Figure 2.2.

Ritter et al. (1990) estimated rate parameters for a similar mechanism, one with no H_2 addition pathways. Instead, the methyl cyclopentadienyl radical undergoes further unimolecular reaction to fulvene+H. A decyclization pathway was also proposed, with an estimate rate constant.

In short, the $H+C_6H_6$ reaction proceeds by an addition pathway with a rate constant (Tsang, 1986) that is consistent with experiments conducted by various groups. Additional isomerization and decomposition pathways have been proposed. The possible impact of those other channels on benzene destruction and product distributions is discussed further in the analysis of benzene chemistry.

$H_2+C_6H_6 \rightleftharpoons C_6H_8$ (1,3- and 1,4- isomers) - Benson and Shaw (1967a) show that H_2 elimination from 1,4-C_6H_8 is in the high-pressure limit at 22 torr, 635-694K. Ellis and Frey (1966) give a rate constant for 1,4-$C_6H_8 \rightleftharpoons C_6H_6+H_2$ over 3-30 torr and 573-616K, mentioning no pressure dependence. However, at flame temperatures, the reaction might be in the falloff range.

Regarding the 1,3 reaction, Benson and Shaw (1967b) show that hydrogenation is generally a chain mechanism, but they do give an estimate for the molecular reaction. That is, for elimination they estimate that $A_{1,4} \sim A_{1,3}$ and $E_{1,4} > 53$ kcal/mol. Later, Alfassi et al. (1973) studied the 1,3 reaction in a VLPP reactor where the rate of bimolecular gas collisions was so low that only the unimolecular reaction was taking place. They performed an RRKM fitting to get high-pressure limit parameters for the reaction. They conclude that the rate parameters are consistent with *either* a conversion to 1,4-C_6H_8 via a biradical intermediate or with a concerted, orbital symmetry forbidden pathway. In either case, a simple RRKM analysis can be applied, because in the biradical mechanism the elimination of H_2 from 1,4-C_6H_8 is rapid compared to the interconversion.

Contemporaneously with the Alfassi et al. work, a photochemical study by Orchard and Thrush (1974) was performed, showing very similar results. They concluded that the biradical mechanism is operative.

Rate constants appropriate to the pressures of the present flame were calculated in this work using RRKM. Their importance to benzene chemistry and the formation of hydrogenated C_6's is analyzed in Chapter 7.

Chapter 3: Experimental Program.

As discussed in Chapter 1, the goal of this work was to study the destruction chemistry of benzene, by determining the structure and chemical composition of a rich H_2-O_2-Ar flame[7] with small amounts of added C_6H_6. The experimental apparatus used was the premixed, laminar flat flame system built by Wersborg (1972). Sampling and analysis for mole fraction data was performed with the molecular-beam mass spectrometer ("MBMS") system added by Bittner (1981) and modified by Cole (1982) and Westmoreland (1986). Temperature was measured with a Pt/Pt13%Rh thermocouple.

The design, construction and operation of the entire system has been described previously by the above-mentioned investigators. Therefore, only a brief explanation will be presented here. No changes were made to the overall design of the system in this work, however changes in hardware were found to be necessary, and are documented below in Sections 3.1-3.3. Improvements were also made to data collection, reduction and analysis methods. These are described in Sections 3.2-3.4.

3.1 Low-Pressure Flat-Flame Burner System

Cylindrical flat flames such as the one studied here are by nature one-dimensional (the axial direction) in concentration and temperature. Equations describing the flame structure are given in Section 3.4. The flame was stabilized on a 39.7 cm^2 circular, water-cooled, copper burner. A 15 cm diameter, water-jacketed, stainless steel burner chamber surrounded the burner. The burner height was measured with a cathetometer, as the difference between the height of the probe tip and that of the closest edge of the burner surface. For the most accurate readings, the burner surface was made as parallel to the floor as possible, by shims under the apparatus' support legs and rotation of the wedge-shaped burner mounting flange insert.

All gases were metered directly from cylinder regulators, using critical orifices (0.038 cm for Ar, 0.032 cm for O_2, and 0.016 cm for H_2) for flow control. The pressures upstream of the O_2 and Ar orifices were monitored with 1600 mm mercury manometers, while the pressure before

[7] Flame conditions: P = 22 torr, ϕ = 1.79 (51.6% H_2, 16.6% O_2, 0.52% C_6H_6. 31.3% Ar), v_0 = 101 cm/sec.

the H_2 orifice was monitored with a pressure transducer. Purity information about gases and benzene used in this work is contained in Appendix F.

The small benzene flow was fed from the constant-temperature bath vaporizer and metering system used by Bittner for calibration flows[8]. Three critical orifices were installed in the system: 0.018 cm, 0.0064 cm, and 0.012 cm. The 0.012 cm orifice was used for standard flame experiments in this work; for certain ionization efficiency measurements in a flame with more hydrocarbons (described in Chapter 4 as an 'analogue' flame), the 0.018 cm orifice was used. For flame data experiments the bath temperature was maintained at 61.35°C and the critical orifice at 98.9°C. Monitoring thermocouples were of type T (Cu-CuNi) from Omega, with Special Limits of Error. In other respects, the system was operated as described by Bittner (1981).

The typical flame startup procedure used was as follows:

1. The benzene bath startup procedure was initiated.
2. Feed gas lines were evacuated (with the burner chamber pump), to the cylinder regulators.
3. The toggle valves from the regulators to the control board was shut, and the regulators opened to pressurize the lines upstream of the valves.
4. The O_2 manometer was zeroed.
5. The C_2H_2 system was flushed and pressurized. (Since experiments were not being performed with acetylene, the purification system to remove acetone was not operated.)
6. Because of its dirty glass around zero reading, the Ar manometer was zeroed by comparison with O_2, at atmospheric pressure.
7. The H_2 pressure transducer was calibrated against the O_2 manometer, directly at the pressure at which it would be used.
8. Once the benzene bath and orifice temperatures were close to operating temperatures, a final evacuation of He from the C_6H_6 flask was performed.
9. A lean C_2H_2-O_2-Ar flame was then lit.
10. The flame was switched rapidly to lean H_2-O_2-Ar, which was then adjusted to rich conditions.
11. The benzene feed valve was slowly and carefully opened to avoid blowing off the flame.

[8] Interestingly, he anticipated the system's use for experiments such as this.

12. Once the C_6H_6 flow was established, all flows were adjusted to data conditions. The burner chamber was warmed up for at least 45 minutes, and the flows checked and re-adjusted as needed before beginning experiments.

To be certain that the flame was not blown out when no hydrocarbon fuel was being fed, a thermocouple was kept in the burner chamber, below the level of the burner surface. This thermocouple monitored exhaust gases, and would have a characteristic temperature ranges when the H_2-O_2 flame was lit or extinguished.

Under the conditions studied, the flame exhibited a slight green tint in the otherwise blue emission. This behavior has been observed by others. Schiff and Steacie (1951) reported a "green fluorescence" in their room temperature experiment of H atom reactions with C_6H_6, and cite a previous similar observation by Bonhoeffer and Harteck (1928). In any event, the flame was rather attractive, helping to ameliorate the punishing effects of 12-25 hour experiments.

3.2 Molecular-Beam Sampling, Mass Spectrometer, and Calibration

Sampling and beam formation.

Flame gas sampling and analysis were performed online in the present system. That is, no handling or manual preparation of samples was required. This was accomplished via a fixed quartz sampling probe, and subsequent formation of a portion of the sampled gas into a molecular beam. The beam was aligned to enter the ionizer of a quadrupole mass spectrometer. A schematic of the burner, sampling and MBMS portions of the system is shown in Figure 3.1.

The sampling probe used in the present experiment was of the 40°-90° hybrid type invented by Biordi et al. (1974). It was fabricated by Gerhard Finkenbeiner, a master quartz glassblower and owner of G. Finkenbeiner, Inc. in Waltham, MA. After grinding and polishing, the orifice diameter was 0.59-0.60 mm. The height of the 90° section from the probe base was 47 mm, and the 40° section was approximately 14 mm.

A new brass skimmer tip was also fabricated for the experiment by the Machine Shop of MIT's Center for Materials Science and Engineering. The skimmer orifice diameter was 0.91 mm. After installation and alignment, the tip of the skimmer was measured to be 19.3 mm upstream of the probe tip.

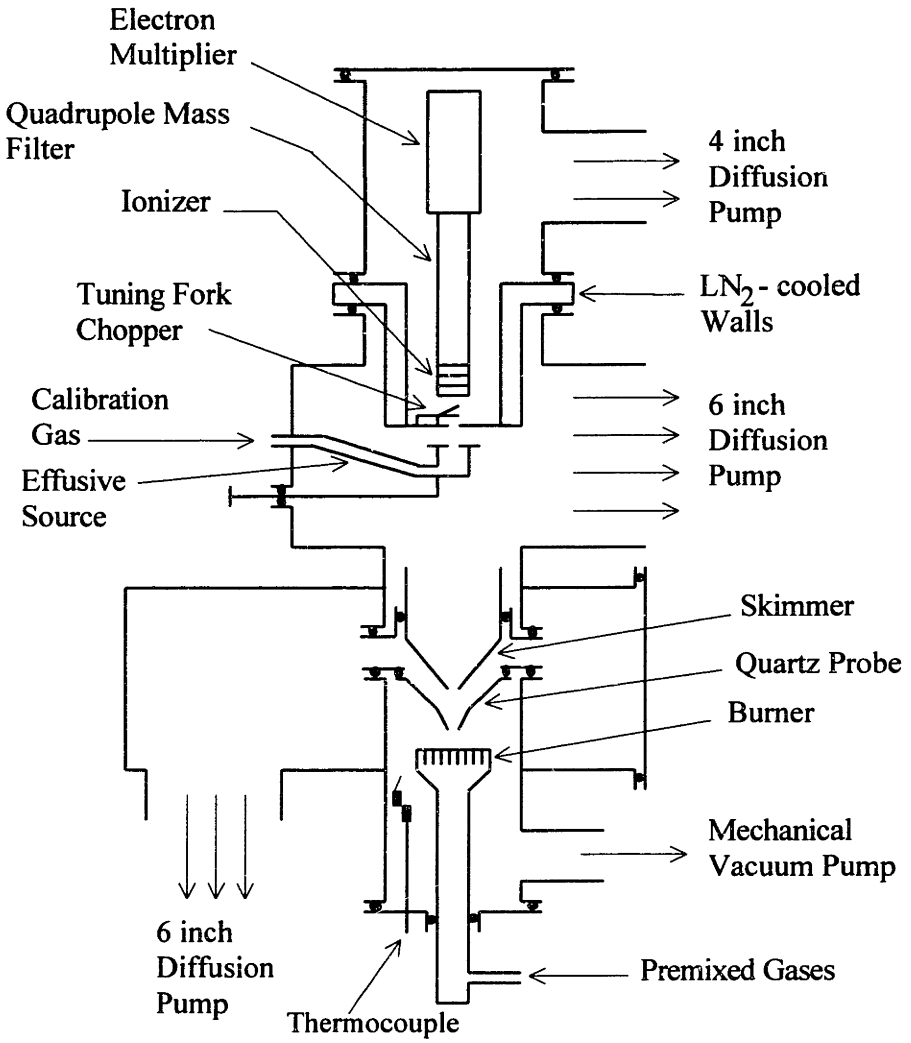

Figure 3.1 Cross-section of burner, sampling and calibration systems, and mass spectrometer chamber of MBMS apparatus.

Mass spectrometer signal collection and processing.

Several pieces of equipment relevant to the operation of the mass spectrometer and the vacuum system required replacement in the course of this research:

- The thermocouple gauge and controller used to monitor first stage pressure in the diffusion pump startup phase was replaced by a Pirani gauge system, HPS model 917.

- The ionization gauge system used to monitor the pressure of all stages was replaced with a HPS SensiVac Model 919. The system uses Bayard-Alpert type 563 ionization gauges.
- A new tuning fork chopper was installed, a Philamon SC3-TFLC-7338. The 220 Hz frequency was retained, but the quiesent aperature (the distance between tuning fork tines with no power applied) was half the area of the collimator hole[9] instead of straddling it. This eliminated the signal advantage in pulse counting without use of the chopper, a technique utilized by Westmoreland (1986).
- The Princeton Applied Research HR-8 lock-in amplifier was replaced with an EG&G PARC Model 5209. A helpful aspect of that instrument were digital tuning and output readouts.
- The EG&G PARC Model 1112 photon counter (for pulse counting experiments) was replaced with Stanford Research's Model SR400 and the computer control software (SR465).

The design of the new lock-in amplifier allowed for easy application of a modified procedure to account for the phase shift of the beam in travelling from chopper to ionizer. The method, that of Jones et al. (1972), is especially useful for cases of weak or erratic signals. Two signal readings are made, the first with the input signal in phase with the reference signal (s_0) and the second at a phase 90° from it (s_{90}). The phase angle Φ is then calculated as

$$\Phi = \tan^{-1}\left(\frac{s_{90}}{s_0}\right).$$

Significant problems were encountered in setting up and using the SR400 pulse counter. The first obstacle to be overcome was the instrument's limitation of ±300 mV discrimination, too low to be able to handle DC-offset TTL pulses from the pulse counting preamplifier. To remove the DC component, the preamplifier output signal was sent to the electrometer, and then taken from the "AC" connection to the pulse counter. This electrometer output is merely the preamp output, run through a 1 mfd capacitor. A modification of the preamplifier was needed to allow the standard preamp-electrometer cable to be used. A 1:7 voltage divider was also needed to make the TTL level pulses compatible with input requirements.

[9] The collimator is the orifice at the entrance of the mass spectrometer compartment.

A more serious problem was RF interference. The bandwidth of the SR400 is $3x10^8$ pulses/sec, three times that of the previous counter. Therefore, the instrument was much more sensitive to RF. With the advice of an expert in RF shielding (Lebiedzik, 1992), the mass spectrometer wires inside the vacuum system were reworked to provide complete coverage of signal and RF connections with shielding and to eliminate contact of shielding with the metal walls. The grounding system was also rewired. The modifications ultimately proved successful.

3.3 Temperature Measurement

The temperature measurement technique used was that described by Westmoreland (1986), with several modifications. As in that work, both unheated and electrically-heated measurements were made with a Pt/Pt13%Rh thermocouple, coated with a BeO-Y_2O_3 ceramic to reduce catalytic heating. However, the coating method of Shandross et al. (1991), developed in the course of this research, was used instead of the earlier technique put forth by Kent (1970). A copy of the Shandross et al. article is included here as Appendix G. Additionally, the thermcouple configuration was modified slightly so that a portion of the (uncoated) support wires would lie along a flame isotherm, thus reducing potential heat conduction error. The revised shape is shown in Figure 3.2. The two flame data profiles taken with the bent-support type of thermocouple — one with a 20 mm junction wire — gave identical readings in the preheat and early

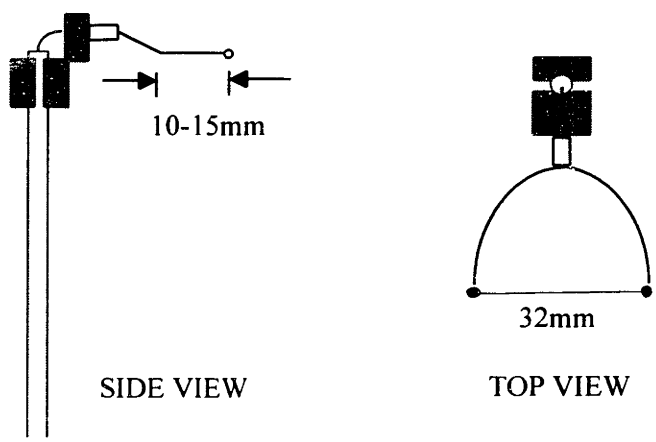

Figure 3.2 Modified thermocouple shape for reduced potential heat conduction error. Figure is not drawn to scale.

reaction zones, but were about 100 K lower in that region than the single profile taken with a straight-support thermocouple. Above 1200 K, all of the thermocouples gave the same flame temperature. A replication of the test is warranted to verify the apparent improvement.

With the coated thermocouple there was no evidence of the temperature drift or electrical heating hysteresis characteristic of catalytic recombination effects. At each position, the thermocouple was heated electrically for radiation compensation, starting at zero current, then brought back to zero current at the end. Had there been catalytic heating, when the current was dropped back to zero the temperatures would have been higher than at the starting point. This was not found to be the case.

The equation describing heat transfer to and from the thermocouple is:

$$h(T_{flame} - T_{TC}) - \sigma\varepsilon(T_{TC}^4 - T_{surroundings}^4) + 4\frac{\rho_e I^2}{\pi^2 d^3} = 0 \qquad (3\text{-}1)$$

where

h = heat transfer coefficient between the wire and the flame,

T_{TC} = thermocouple reading,

σ = Stephan-Boltzmann constant,

ε = thermocouple emissivity,

ρ_e = electrical resistivity of wire,

I = heating current, and

d = thermocouple wire diameter.

In electrical-compensation measurements, when the thermocouple and flame temperatures are equal, the equation reduces to same formula of a thermocouple heated electrically in a vacuum. A calibration curve for the latter case is taken in a vacuum calibration apparatus. The thermocouple temperature at the intersection of the calibration and flame curves is therefore the flame temperature.

In the case of measurements taken without electrical heating, the third term drops out the the equation. The emissivity of the thermocouple is measured with an optical pyrometer, and the diameter of the wire with a light microscope. The flame temperature may therefore be calculated if the heat transfer coefficient can be determined. This was accomplished by solving the expression of Kramers (1946) for transverse laminar flow across a cylinder:

$$h = \frac{k}{d}\left[0.42\left(\frac{\mu C_p}{k}\right)^{0.2} + 0.57\left(\frac{\mu C_p}{k}\right)^{0.333}\left(\frac{\rho v d}{\mu}\right)^{0.5}\right] \tag{3-2}$$

with

k = thermal conductivity of flame gas at T_{film},

μ = viscosity of flame gas at T_{film},

C_p = specific heat of flame gas at T_{film},

ρ = density of flame gas at T_{film},

v = flame gas velocity, and

$T_{film} = (T_{TC}+T_{flame})/2$.

The flame gas properties were calculated from mole fraction measurements, in an iterative process with respect to T_{flame}, using Lotus 1-2-3® Release 4 for Windows™. A wrinkle in the process that is peculiar to the present flame is the strong temperature dependence of the mass discrimination factors used in computing mole fractions (Subsection 3.4.2). To account for this, the mass discrimination factors — and therefrom, mole fractions — were initially calculated with an estimated temperature profile in which the flame temperature was approximated as

$$T_{flame} \approx T_{TC,unheated} + \left(\frac{\sigma\varepsilon}{d}\right)_{est}\left(T^4_{TC,unheated} - 298^4\right), \tag{3-3}$$

where

$$\left(\frac{\sigma\varepsilon}{d}\right)_{est} = \left[\frac{T_{flame} - T_{TC,unheated}}{T^4_{TC,unheated} - 298^4}\right]_{\substack{\text{average of two highest electrical} \\ \text{compensation measurements}}}. \tag{3-4}$$

The gas properties computed with the first estimated temperature profile were used to get a second estimated profile. The second profile was then used to recalculate mole fractions. Since the resulting mole fraction changes were found to be less than 2% (most points less than 0.5%), no further iterations were made.

3.4 Data Collection, Reduction and Analysis

3.4.1 Data Collection

Ionization efficiency problems with C_6H_6.

An important part of the process of determining the identity of a species is the measurement of an *ionization efficiency curve*. This term refers to graph of mass spectrometer signal vs. electron energy, for a particular mass number. There is typically a linear section in the curve, the intercept of which is taken as the experimental ionization potential for the species. The offset of the experimental intercept from the literature ionization potential is used as an energy correction to the electron energy scale, and is a function of tuning and instrumental factors. Unless an electron impact ionizer is designed to use monoenergetic electrons, the ionization efficiency curve will exhibit a low-energy tail due to electrons of higher-than-average energy in the thermal distribution. A good discussion of electron impact ionizers and ionization efficiency curves is found in Field and Franklin (1970). Bittner (1981) describes the practical use of these curves for species identification.

It was empirically observed by Bittner (1981)[10] that the experimentally determined intercept ("ICP") for benzene in ionization efficiency curves, when referenced to argon or other low molecular weight stable species, was about 1 eV higher than the literature intercept ("IP") of C_6H_6. This behavior was found to occur in the present work as well. A search of the literature on benzene ionization potential measurements showed that IP's as low as 9.14 eV (Dibeler et al., 1957) and as high as 9.9 eV (Majer and Patrick, 1962) have been recorded. The accepted literature value is 9.22-9.25 eV. The large variation is only found in electron impact determinations, the range of results from other types of experiments being 9.20-9.39 eV. There is no correlation between the time in which the electron impact studies were done and the IP's measured. It appears then that instrumental factors play a large part in the electron impact IP measured for C_6H_6.

One possible source of this peculiar behavior is the existence of fine structure in the ionization behavior of benzene (Fox and Hickam, 1954). That is, ionization experiments with monoenergetic electrons show multiple linear portions with different slope in the signal response curve, as electron energy ("EE") is increased. This is not particularly unique behavior. For example, it is seen in CH_4 (Frost and McDowell, 1957), C_2H_2 (Collins et al., 1968), and O_2 (Herron and Schiff, 1958). However, in few other cases is there a sharp break with as great a change of slope as there is for C_6H_6, and at an EE greater than 1-1.5 eV above the ionization potential — but not so great as to be unnoticeable in a typical ionization efficiency measurement.

After all the data were collected and the ionization efficiency curves were measured, the

[10] Page 369.

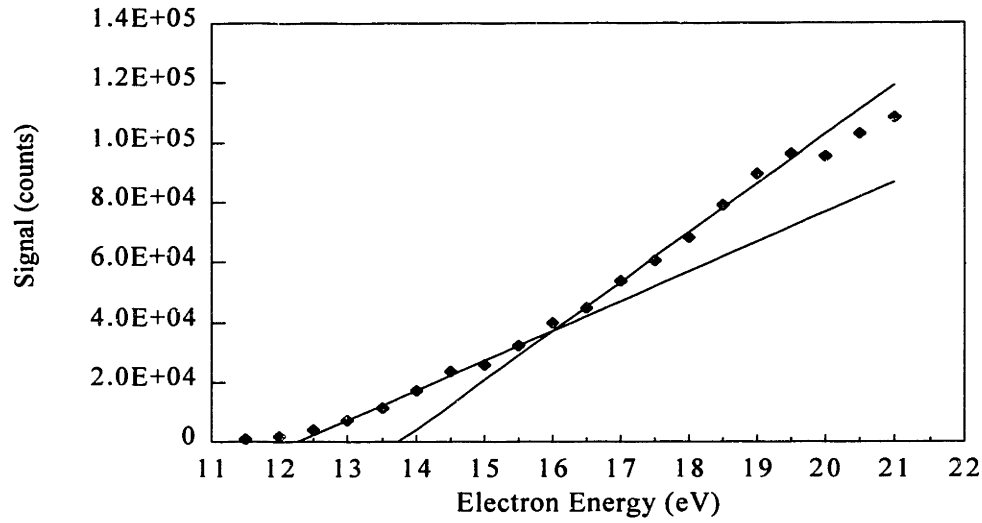

Figure 3.3 Sample ionization efficiency curve for benzene.

latter measurements for benzene were reviewed. From measurements with relatively good energy resolution, it was discovered that there are *two* linear sections in the graph, as can be seen with a sample ionization efficiency curve in Figure 3.3. It was found that, for those ionization efficiency curves in which signals were measured at small enough energies to permit a lower line to be drawn, the average difference between the lower ICP and the IP was very close to that of other species which were measured at the same time. That is, there was a method of measuring the IP of benzene which was consistent with species that did not display the peculiar energy offset.

Unfortunately, fine structure information is only available for a few species, and there is no proposed or accepted method for quantitatively accounting for this effect. In any case, instrumental factors for electron impact ionizers are too variable (Field and Franklin, 1970) to hold much hope that some such correlation can be made.

Literature electron impact IP data for phenol are also scattered, ranging from 8.5-9.16 eV; the photoelectron and photoionization values range from 8.37-8.69 eV. An ionization efficiency curve for phenol, with the pure substance introduced effusively, showed double linear section whose upper intercept had an energy correction within 0.3 eV of benzene's. The energy corrections for the lower intercepts differed by 0.25 eV. This is just the amount of scatter shown in literature IP's taken by the more accurate methods. The energy corrections of masses 94 and 78

interpreted from flame ionization efficiency curves are also close. No fine structure information on phenol could be found; however, a study of toluene was made by Melton and Hamill (1964) within 1eV of the IP. In that limited range, the fine structure of toluene was very similar in appearance to that of benzene. It is therefore possible that the structure possessed by C_6H_6 is common to many single-ringed aromatic species, and the energy offsets of these species would be about the same.

Scans for species present in flame.

To ensure that every detectable species would be measured, the flame was scanned for signals at every mass number at several locations. Complete scans were made at 3.0 and 6.0 mm, and high mass scans were performed at 4.4 mm (type B [11] high-Q head; maximum mass of about 118 amu), 3.0 and 6.1 mm (type E [15] high-Q head; maximum mass of 1000 amu).

All of the scanning experiments were performed with pulse counting for the greatest sensitivity. For every mass number, the ionization potential literature was searched to determine the range of IP for species which might be expected to appear in the flame. The EE setting used for each species was 3 eV above the anticipated ICP, so that a strong signal might be measured with little fragmentation. The average IP was used as a basis in the case of masses with species that had a wide range of possible IP's: for example, 9.4 eV for mass 64 with it's IP range of 8.7-10.1 eV. For species 1-2 amu higher than another mass with a significant signal, isotopic corrections were made. The correction factors used for isotopic adjustment are given in Appendix Q.

The scans were performed with several mass spectrometer tunings. The first complete scan at 3.0 mm was made with a tuning optimized for benzene. It was then repeated with an H_2O-based tuning, which afforded better sensitivity but a worse peak shape at higher masses. For the 6.0 mm complete scan, the spectrometer was tuned for maximum Ar signal with only a partial regard for the peak shape. The high mass scans were tuned for a high benzene signal without regard for perfection in shape and with only fair resolution.

Because of noise and the low concentration of hydrocarbon species overall, classification of a species as "detectable," "barely detectable," or "undetectable" was somewhat arbitrary. In spite of this, an attempt was made to be consistent in the methodology used. Typically, the following were considered in setting the criteria for those classifications during a particular experiment:

1. The signal measured for mass numbers known not to represent any possible species (e.g., mass 47) or probable species (e.g., masses 88-90 and 113).
2. The amount of fluctuation observed in the signal. Based on oscilloscope observations of electrometer output, signals which fluctuate around zero[11] generally were found to represent species that are present in the background, or almost detectable. Very small signals which fluctuated a great deal, but not around zero, were considered barely detectable.
3. In cases of some doubt, measurements were also taken with the beam block in place to obtain a true background.

3.4.2 Data Reduction

Calibration of mole fractions measured in the MBMS system is performed in several different ways. For certain stable species, direct calibration was possible. In situations where a pure gas cannot be introduced into the calibration system, the Relative Ionization Cross-Section ("RICS") method of Lazarra et al. (1973) and Peeters and Vinckier (1975) was used.

In the direct method, the mole fraction of a species relative to argon was computed from the relationship

$$\frac{x_i}{x_{Ar}} = \frac{1}{\alpha_{i,Ar} S_{i,Ar}} \left(\frac{I_i}{I_{Ar}} \right) \tag{3-5}$$

where

$\alpha_{i,Ar}$ = mass discrimination factor for species i, relative to argon,

$S_{i,Ar}$ = sensitivity of species i, relative to argon, and

I = mass spectrometer signal.

Sensitivities were measured using the method described by Bittner, except that the effusive source pressure was always set to be the same for both species, rather than introducing methane to account for beam density differences.

Raw mole fraction profiles were shifted by 2.5 probe diameters toward the burner, to account for probe sampling effects (Biordi et al., 1974). The temperature profile was shifted away from the burner by 4.5 wire diameters, in accord with the observation of Fristrom and

[11] In pulse counting, a negative signal can result when the signal collected in the background window is greater than that in the foreground window.

Westenberg (1965) that a thermocouple wire displaces isothermal surfaces four to five bead diameters downstream due to its wake.

Mass discrimination factors.

The mass discrimination factor is a measure of the effect of the molecular beam on the relative mole fractions of two species. Bittner (1981) contains an excellent discussion of its nature and measurement.

In the hydrocarbon flames previously measured with the present equipment, mass discrimination factors for all species except H_2 were found to be relatively constant (within ±3% for most species) with respect to changes in sampled gas density and gas composition. The variation for hydrogen was 16-19%. In the present flame, *all* species measured had high degrees of variability in mass discrimination factor over the range of densities and compositions tested. Table 3.1 shows the mass discrimination factors measured for two mixtures, designed to simulate

Table 3.1 Mass discrimination factors, measured relative to argon, for various flame temperatures and gas compositions. $\phi = 1.79$, H_2-O_2-C_6H_6-Ar flame.

	Early reaction zone set						*Post-flame zone set*					
	H_2	O_2	C_6H_6	CO	Ar	CH_4*	H_2	O_2	C_6H_6	CO	Ar	CH_4*
$x_{mixture}$:	0.26	0.17	0.0052	0.01	0.46	0.10	0.27	0.011	0.0011	0.035	0.36	0.33
$\alpha_{300\ K}$	0.151	0.803	2.02	0.649			0.138	0.732	1.94	0.627		
$\alpha_{900\ K}$	0.179	0.830	1.73	0.703			0.166	0.805	1.65	0.702		
$\alpha_{1500\ K}$	0.196	0.844	1.63	0.731			0.183	0.845	1.54	0.743		
$\alpha_{2100\ K}$	0.209	0.853	1.56	0.751			0.197	0.873	1.47	0.773		
Maximum deviation from ave†	18.4%	3.8%	18.3%	8.9%			20.0%	10.6%	19.6%	12.4%		

*Surrogate for H_2O.
†Average taken over 100 K intervals from 300-2100 K.

flame gases close to the burner and in the post-flame zone. As noted by Bittner, for a cold gas measurement the equivalent flame temperature is the temperature at which $\rho_{flame} = \rho_{cold\ gas}$.

To a very good approximation, it was found that plots of $\frac{1}{\alpha_{i,Ar}}$ vs. ln P_b were linear, where P_b is the burner chamber pressure of the measurement. Using $T_{flame} = 298\left(\frac{P_{flame}}{P_b}\right)$, one derives:

$$\alpha_{i,Ar} = a/\ln\left(\frac{c}{T_{flame}}\right) \tag{3-6}$$

where a is $\frac{1}{\text{slope}}$ of the linear fit, and $c = 298*P_{flame}*\exp\left(\frac{\text{intercept}}{\text{slope}}\right)$. This relationship held true for both gas mixtures.

At any particular temperature, a graph of mass discrimination factors vs. molecular weight were sufficiently close to linear that a good estimation for $\alpha_{i,Ar}$ was possible for species not measured. This technique was used to estimate mass discrimination factors for CH_4, C_2H_2 and CO_2.

The question then arises of how best to use this information in performing direct calibrations. A zeroth order approximation would be to apply the method used for hydrocarbon flames, i.e., constant $\alpha_{i,Ar}$. Obviously, this would result in a great deal of error. A large improvement can be obtained by using Equation 3-6 for an average composition, but flame gas composition changes would still be unmodeled.

The best situation of all would be to make measurements for a large number of potential flame compositions, and use them on the basis of estimated compositions, or in an interative scheme. However, this level of detail was not considered to be necessary because (a) the mole fractions of major species vary roughly linearly from preheat to post-flame zones, and (b) the composition effect is secondary to the impact of temperature. The second order approximation adopted was the linear estimate, $\alpha(T_{flame}) = m \times HAB + b$, where HAB is the height above the burner surface, $m = (\alpha_{post\text{-}flame}-\alpha_{feed\ gas})/10$, and $b = \alpha_{feed\ gas}$. This approximation was used for the first 10 mm, after which α was assigned the value $\alpha_{post\text{-}flame}$.

This method of calculating mass discrimination factors results in a situation where the calibration factors depend on the temperature profile, and the temperature profile depends on the calibration factors. In Section 3.3, the iterative procedure used to determine mole fractions and the temperature profile simultaneously was described. The interdependence turns out to be weak enough that mole fractions based on the initial temperature estimate did not need to be changed.

Communication with Seery (1994) of United Technologies Research Center revealed that the type of mass discrimination factor behavior observed here has been seen by other workers using MBMS for H_2-O_2 flames. A method is in use at United Technologies, similar to the one developed here, for accounting for the strong temperature variation of the calibration factor.

Relative Ionization Cross-Section calibration.

The current of positive ions of a species k, $i_{+,k}$, in an electron impact ionizer has been described by Fite (1971) as

$$i_{+,k} = n_k Q_k X i_e \tag{3-7}$$

where

n_k = number density of molecule k in the ionizer,

Q_k = electron impact ionization cross-section for k,

X = thickness of neutral molecular beam (in the ionizer), and

i_e = electron current in ionizer.

Q_k is a function of the energy of the electron. The ratio of ion currents of two species would then be

$$\frac{i_{+j}}{i_{+,k}} = \left(\frac{n_j}{n_k}\right)\left(\frac{Q_j}{Q_k}\right). \tag{3-8}$$

Since the mole fraction is proportional to the number density, this expression shows a potential way of computing the relative mole fractions of two species, at least as found in the ionizer. If the electron multiplier sensitivities of the two species are equal, the ratio of measured signals is the same as the ratio of ion currents. Then

$$\left(\frac{x_j}{x_k}\right)_{\text{ionizer}} \approx \left(\frac{I_j}{I_k}\right)\left(\frac{Q_k}{Q_j}\right), \tag{3-9}$$

where I refers to the signal measured from the electron multiplier.

A mole fraction ratio for flame gases is needed, however. If Bittner's assumption that the mass discrimination occurring in the molecular beam is offset by the opposite type of discrimination in the quadrupole mass filter is true, then no conversion is required, and

$$\left(\frac{x_j}{x_k}\right)_{\text{flame}} \approx \left(\frac{x_j}{x_k}\right)_{\text{ionizer}} \approx \left(\frac{I_j}{I_k}\right)\left(\frac{Q_k}{Q_j}\right). \tag{3-10}$$

This is the operating equation for the RICS method.

The typical method of application of this method is to measure signals for the two species at the same amount of energy above their respective ionization potentials. This presumes that the ratio of 70 eV ionization cross-sections is the same as the same ratio at the energies measured. Smith et al. (1982) have noted two sources of error in using typical 70 eV ionization cross-sections: (1) the ratio at 70 eV might be different than that at the energies measured, and (2)

reported values are usually total cross-sections, including fragmentation if it occurs and not just the ionization process of interest. It should be noted that total cross-sections also include multiple ionizations, isomerizations, and other events which are different than what is occurring in the ionizer during an experiment.

The ideal cross-sections to use are those for single ionization alone at the energy for which the measurement was made in the experiment. Unfortunately, this type of cross-section is rarely available, or is only available for one of the species. Nevertheless, it was possible to perform several RICS calibrations using more appropriate cross-sections. These are described in detail Appendix E.

Even 70 eV cross-sections are unavailable for many species, especially radicals. In previous MBMS work with the present equipment, Bittner (1981) and Cole (1982) used the cross-section approximation methods of Otvos and Stevenson (1956), Lampe et al. (1957), Harrison et al. (1966), and Beran and Kevan (1969). In recent years, several other estimation methods have been put forth. Fitch and Sauter (1983) proposed a revised approximation technique for 70 eV total ionization cross-sections, based on additivity of atomic cross-sections, which distinguishes between different hybridizations for carbon and oxygen. Derived from linear regression of 179 literature cross-sections, the average error of the method was 4.69%, though it was larger for gases as a class and for species with a cross-section below $5x10^{-16}$ cm^2. Deutsch and Schmidt (1985) extended the Fitch and Sauter method to 20 eV and 35 eV. Because they could only access a database of 31 compounds at the lower energies, errors are higher.

In the present work, a combination of methods for estimation of ionization cross-sections was used. In general the Fitch and Sauter (or occasionally, Deutcsh and Schmidt) additivity method was used. For species whose measurements were reasonably accurate in the first place, the average of the Beran and Kevan, Harrison, and Fitch and Sauter approximation was sometimes used. This was found to give the best results in a comparison with larger hydrocarbon species with high cross-sections. RICS calibration factors are documented in Appendix E.

A study of the suitability of the Fitch and Sauter method, as extended to lower energies, for radical species was conducted by Deutsch et al. (1989). They tested the additivity rule against the only radical cross-section data in the literature that they considered to be reliable, which were for CH_2, CH_3, SiF, SiF_2 and SiF_3. The hydrocarbon radicals were well predicted, but not the silicon species.

The cited factor of two error expected for RICS calibration is a result of the assumptions about mass discrimination, electron multiplier sensitivities and ionization cross-sections.

Calibration factor conversions for unknown species.

As discussed in Chapter 4, a number of species remained unidentified because the signals were too small or noisy for ionization efficiency curves to be collected, or the results were ambiguous. In such cases, an identity was assumed for purposes of calculation and presentation in this thesis. Although an attempt to choose an assumed identity was made before the data were collected, in not every case was the final computation based on the original choice. Therefore, a technique was devisd to correct the calibration factor for the different species hypothesis. A similar method was anticipated to be necessary for the purpose of conversion of a data profile given here from a basis of one assumed species to that of any of the other remaining species which could have that mass number.

Under the RICS method, two quantities need to be adjusted to make a species conversion. Those are the signal itself (which is based on the assumed IP) and the ionization cross-section, both for the species being "changed." For each of the species tentatively identified in this work, a set of calibration conversion factors was computed, which are reported in Appendix E. A description of the energy correction to the signal measurement is given here.

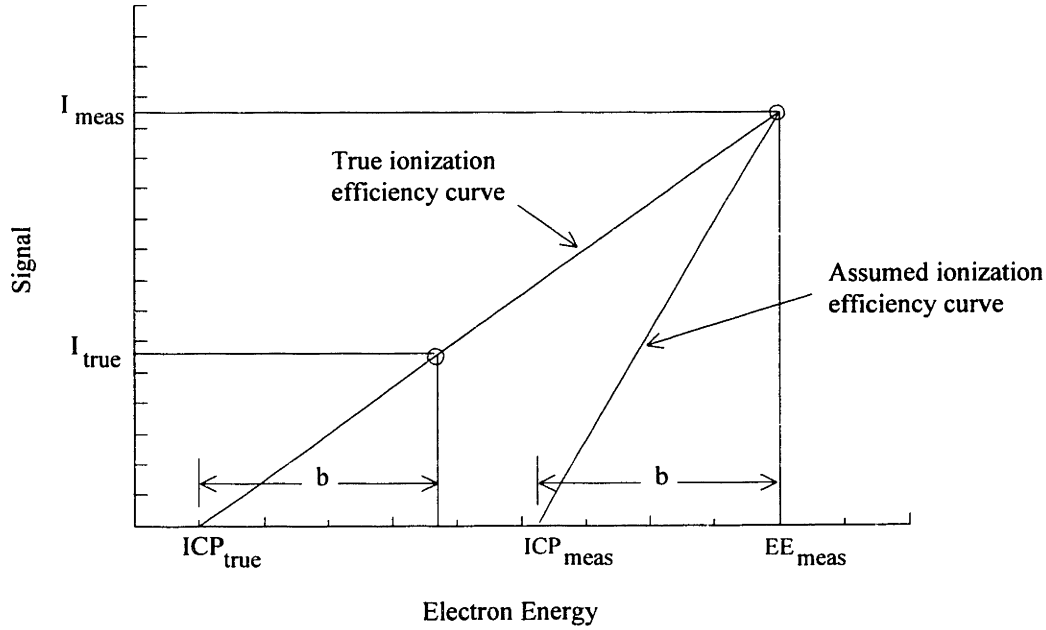

Figure 3.4 RICS energy correction schematic.

Figure 3.4 is a schematic of situation in which a measurement was taken at a particular electron energy, "EE_{meas}", for a species which would have an ionization efficiency intercept at ICP_{true}. It is assumed that the electron energy level of the reference species was *b* eV above $ICP_{reference}$. If the true species identity had been known, the correct energy for the measurement would have been (ICP_{true}+b). However, with the data having been taken higher than that, the effective intercept is $ICP_{meas} = (EE_{meas}\text{-}b)$. The problem is to convert I_{meas} to I_{true}. The solution lies in equating the following two ways of solving for the slope of the true ionization efficiency line which would encompass both points:

$$m_{true} = \frac{I_{true}}{b}, \text{ and} \tag{3-11}$$

$$m_{true} = \frac{I_{meas}}{(ICP_{meas} - ICP_{true}) + b} \tag{3-12}$$

Solving for I_{true},

$$I_{true} = I_{meas} \times \frac{b}{b + ICP_{meas} - ICP_{true}} \tag{3-13}$$

or, assuming that ICP-IP is a constant ($\equiv \Delta$),

$$I_{true} = I_{meas} \times \frac{b}{b + IP_{meas} - IP_{true}} \tag{3-14}$$

where $IP_{meas} = (ICP_{meas} - \Delta) = (EE_{meas} - b - \Delta)$. So another way of writing it is

$$I_{true} = I_{meas} \times \frac{b}{EE_{meas} - (IP_{true} + \Delta)}. \tag{3-15}$$

When correcting for a measurement of an unknown made at the wrong energy, 'true' refers to the assumed species.

For the situation where one wants to convert from one assumed species (A) to another (B), note that

$$I_A = I_{meas} \times \frac{b}{EE_{meas} - (IP_A + \Delta)} \tag{3-16}$$

and

$$I_B = I_{meas} \times \frac{b}{EE_{meas} - (IP_B + \Delta)}, \tag{3-17}$$

so the conversion is:

$$I_B = I_A \times \frac{EE_{meas} - (IP_A + \Delta)}{EE_{meas} - (IP_B + \Delta)}. \tag{3-18}$$

Fragmentation magnitude analysis.

A number of species were determined by ionization efficiency curves to have intercepts which were higher than any known species. The molecules being measured are therefore fragments of larger species. In some cases, possible parents of fragment molecules are themselves unidentified. If one supposes that all the parent candidates for a fragment, other than a particular unidentified species at mass X, could be ruled out because their magnitudes are too low to produce the measured quantity of fragment, then the species at mass X might thus be determinable.

To perform this type of analysis, the signals of the daughter and all possible parents would ideally all be taken at the same height above the burner, on the same day and over a range of electron energies from below the appearance potential to a few eV above it. Also, where the parent species can be introduced into the burner or effusive source, cold gas fragmentation calibration experiments would be performed. Since the analyses were attempted after experiments were completed, conditions were less than perfect for most of the cases attempted. Corrections and estimations required included:

- use of a third, reference species that was measured on both days, to get the parent and daughter species on the same basis,
- energy corrections, such as those described above, and
- interpolation or use of a data curve to approximate the signal at a different height than that measured.

Two other factors had to be considered: the type of fragmentation (skeletal or H atom elimination) and the energy level with respect to the appearance potential. Measurements of CH_3 appearance from CH_4 revealed that for some H eliminations a much higher amount of fragment would appear at a particular energy above the appearance potential than for skeletal fragmentations. In the other cases measured, C_6H_5 from C_6H_6, comparatively little fragment showed up in the first several eV above the appearance potential. Although there was no way of determining which type of behavior a postulated H elimination might exhibit, for those types of fragmentations it was necessary to allow for the possibility of a high fragment signal close to the appearance potential. In general, of course, within the first several eV of the appearance potential more daughter species would be expected at higher electron energies.

Computation of argon and water mole fractions.

Calibration of the water signal was performed by an oxygen balance in the post-flame zone, at 28.5 mm. At that height, the only species present which contain oxygen were OH, H_2O, CO and CO_2. The computation of a calibration factor was therefore particularly simple:

$$\frac{x_{H_2O}}{x_{Ar}} = C_{H_2O,Ar}\left(\frac{I_{H_2O}}{I_{Ar}}\right) = 2\left(\frac{x_{O_2}}{x_{Ar}}\right)_{unburnt} - 2\left(\frac{x_{CO_2}}{x_{Ar}}\right) - \frac{x_{CO}}{x_{Ar}} - \frac{x_{OH}}{x_{Ar}} \qquad (3\text{-}19)$$

or

$$C_{H_2O,Ar} = \left(\frac{I_{Ar}}{I_{H_2O}}\right) \times \left(2\left(\frac{x_{O_2}}{x_{Ar}}\right)_{unburnt} - 2\left(\frac{x_{CO_2}}{x_{Ar}}\right) - \frac{x_{CO}}{x_{Ar}}\right) / \left(1 + \frac{x_{OH}}{x_{Ar}}\right), \qquad (3\text{-}20)$$

since the OH mole fraction was measured relative to H_2O. The calibration factor might have been calculated on the basis of a hydrogen balance, but the mole fractions of H and H_2 which dominate that balance are more uncertain than those of the oxygen system.

The argon mole fraction was calculated at every height above the burner from the simple mole fraction balance,

$$\frac{1}{x_{Ar}} = 1 + \sum_{i \neq Ar} \frac{x_i}{x_{Ar}} \qquad (3\text{-}21)$$

The mole fractions of species measured relative to another species by the RICS method were converted to an argon basis by the formula:

$$\frac{x_i}{x_{Ar}} = \left(\frac{x_i}{x_j}\right)\left(\frac{x_j}{x_{Ar}}\right) \qquad (3\text{-}22)$$

Limits of error for experimental data.

Table 3.2 lists the estimated limits of error for species calibrated directly, i.e., with calibration gases. Species calibrated by the RICS method are expected to be accurate to within a factor of two. The basis for these estimates is discussed in Appendix A.

Table 3.2 Estimated limits of error for directly-calibrated species.

Species	Limits of error for x/x_{Ar} (%)
C_6H_6	19.1
O_2	18.2
H_2	33.5
CO	18.5
CO_2	18.4
C_2H_2	18.0
CH_4	18.6

3.4.3 Data Analysis

Computation of fluxes and net rates.

The equations for a pre-mixed, laminar, (quasi-) one-dimensional flame have been given by Fristrom and Westenberg. The continuity equation in such a flame is

$$(\rho v)_0 = \rho v A = \dot{M} \tag{3-23}$$

where ρ is the mass density, v the mass average velocity, A is the area expansion ratio (ratio of the area of a stream tube at a particular height to one at the burner surface), and $\dot{M}$ the total mass flux. The molar flux of species i, F_i, at a particular height is

$$F_i = N_i(v + V_i)A \tag{3-24}$$

with N_i being the number of moles of i per unit volume, and V_i the diffusion velocity. Finally, the net chemical reaction rate, $\dot{W}_i$, is the derivative of the molar flux with respect to the height above burner:

$$\dot{W}_i = \frac{1}{A}\left(\frac{dF_i}{dz}\right) \tag{3-25}$$

A computer program called FBR was written to perform flux and net rate calculations from these equations, using the temperature and experimental mole fraction profiles. Complete documentation of that program is given in Appendix D. The value for A for this burner and C_6H_6 flame conditions was experimentally determined by Bittner (1981). He modeled the flame gases using cold gases under two conditions: (1) with the cold gas mass flux identical to that of the flame, and (2) with the Reynolds ($\rho VL/\mu$) number of the cold gases equal to that of "the hot flame gases."

The mass flux of the present flame is 2.34×10^{-3} g/cm^{2}s, almost identical to the 2.18×10^{-3} g/cm^{2}s for the rich C_6H_6-O_2-Ar flame. In addition, the Reynolds numbers throughout the two flames are very similar, as can be seen in Figure 3.5. Therefore, the area expansion ratios measured by Bittner are appropriate for the H_2-O_2-C_6H_6-Ar flame studied in this research. The ratio based on Reynolds number was chosen for this work, since it used by all previous investigators using this apparatus. That formula is $A(z) = (1\text{-}0.0116z)^{-1}$, where z is in millimeters. The difference between the area expansion ratios measured by the two methods is only 2% at 20 mm.

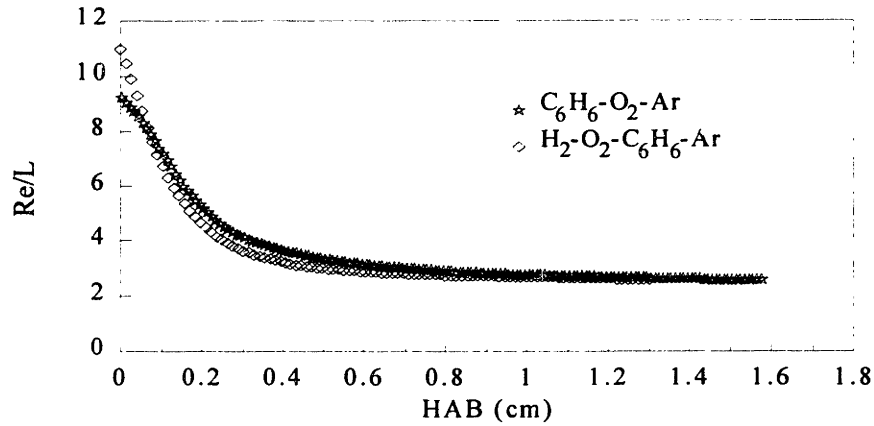

Figure 3.5 Reynolds number (divided by the identical length dimension in both cases) for rich C_6H_6-O_2-Ar and H_2-O_2-C_6H_6-Ar flames.

Chapter 4: Results - Temperature and Mole Fraction Data, and Identification of Species.

The molecular-beam mass spectrometry (MBMS) technique was used to measure species concentrations in the 22 torr, $\phi = 1.79$ (51.6% H_2, 16.6% O_2, 0.52% C_6H_6, 31.3% Ar) flame. Forty-four species were measured, some with full mole fraction profiles and others simply to obtain an order of magnitude estimate and general location in the flame. Sixteen species were identified with reasonable certainty, and several others have likely, but not certain, identities. A temperature profile was also measured, using the method described in Chapter 3.

Most of the data collection was performed in the preheat, reaction, and early post-flame zones; that is, from 0-13 mm. Height Above Burner ("HAB") data were also collected at 28.5 mm, deep in the post-flame zone, to investigate partial equilibrium relationships.

4.1 Overview of Experimental Data

Most of the flame (≥ 98%) is composed of — in order of abundance — Ar, H_2O, H_2, O_2

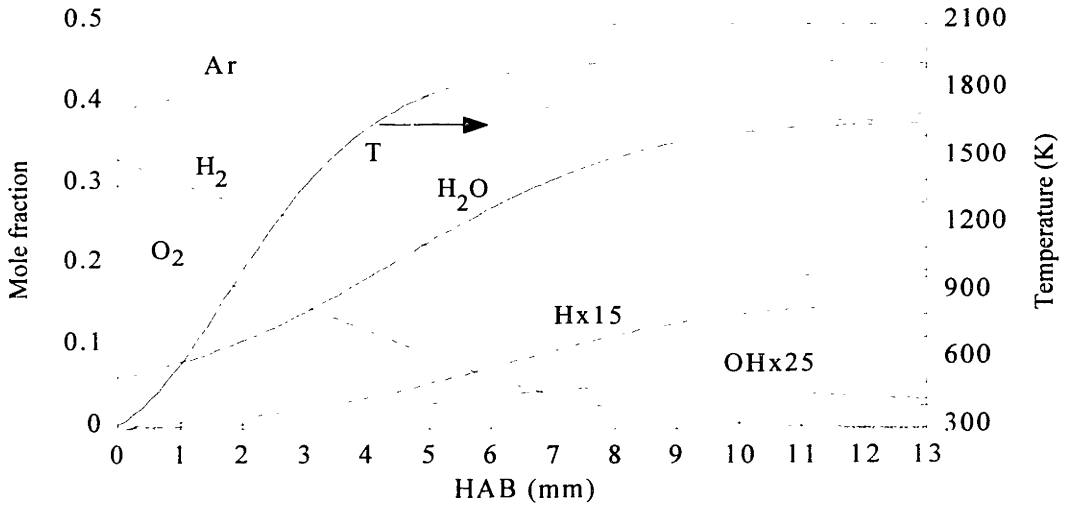

Figure 4.1 Profiles of temperature and mole fractions of major species of the H/O system, plus argon. Taken in a 22 torr laminar, premixed H_2-O_2-C_6H_6-Ar flame, $\phi = 1.79$, 31.3% Ar, $(x_{C6H6}/x_{H2})_0 = 0.010$, $v_0 =$ 101 cm/sec. Individual data points are not shown, only smoothed curves.

and CO. Next in quantity are H, CO_2, C_6H_6, CH_4, OH, C_2H_4, H_2CO and C_2H_2. The mole fractions of these species in the first 13 millimeters from the burner are shown in Figures 4.1 and 4.2. Argon and the species of the H/O system are plotted, along with the temperature profile, in the first figure. The argon mole fraction was computed by difference as described in Chapter 3. The major species of the C/H/O system are found in Figure 4.2..

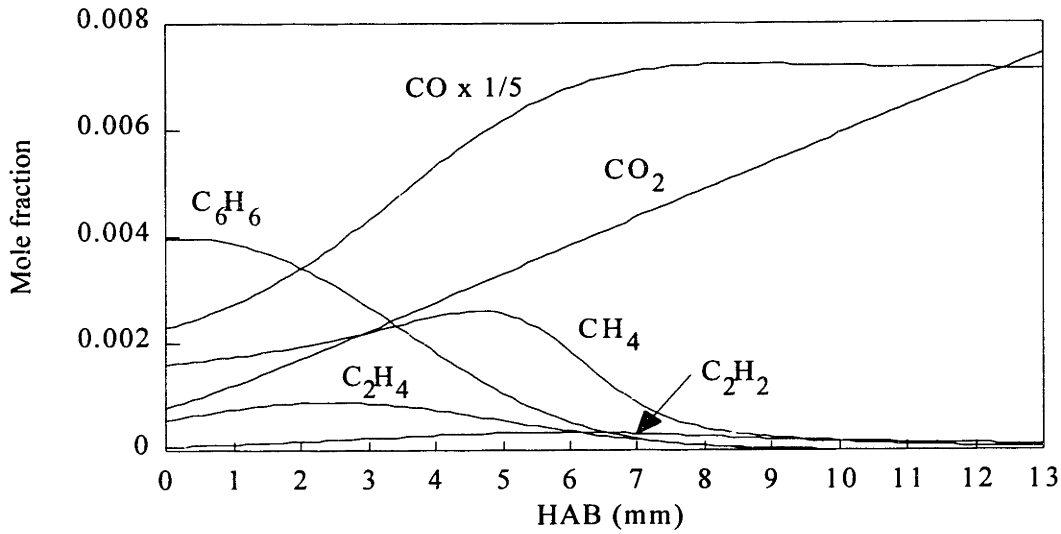

Figure 4.2 Profiles of mole fractions of major species of the C/H/O system. Taken in a 22 torr laminar, premixed H_2-O_2-C_6H_6-Ar flame, ϕ = 1.79, 31.3% Ar, $(x_{C6H6}/x_{H2})_0 = 0.010$, v_0 = 101 cm/sec. Individual data points are not shown, only smoothed curves.

Judging from the onset of rapid temperature rise and appearance of radical species, the reaction zone begins at about 1.5 mm. The fuels and O_2 are burnt out (or reach a stable level, in the case of H_2) by 10 mm, signalling the end of the reaction zone and start of the post-flame zone.

It is interesting to compare the relative magnitudes and locations of the various intermediates and products in this flame with those in the ϕ = 1.8, C_6H_6-O_2-Ar flame of Bittner (1981). The widths of the reaction zones are identical in the two flames, but CO is produced a few millimeters earlier in the present flame. This is probably due to the more intense radical environment of the H_2 flame close to the burner. In both cases, O_2 lasts about 2 mm longer than C_6H_6. The relative amounts and locations of H and OH are similar in both flames. The most abundant hydrocarbon product present in the benzene flame is acetylene, whereas methane has the strongest

signal in a hydrogen flame, and ethylene is the most abundant C_2 species. This is consistent with product distributions in pyrolysis of C_6H_6 alone (corresponding to benzene flame data) and in the presence of H atom (corresponding to H_2-O_2-C_6H_6 flame data).

As can be seen in the profiles given in the next section, this trend of having more of the more hydrogenated versions of a particular hydrocarbon is commonly followed in the H_2 flame. This is reflective of the greater amount of H and H_2, and the absence of significant amounts of other hydrocarbons with which a species may react.

The internal consistency of the data was tested by computation of elemental mass flux balances, as Bittner (1981) and Westmoreland (1986) did previously on their measurements from the same equipment. The results are shown in Figure 4.3 for carbon, hydrogen, oxygen and

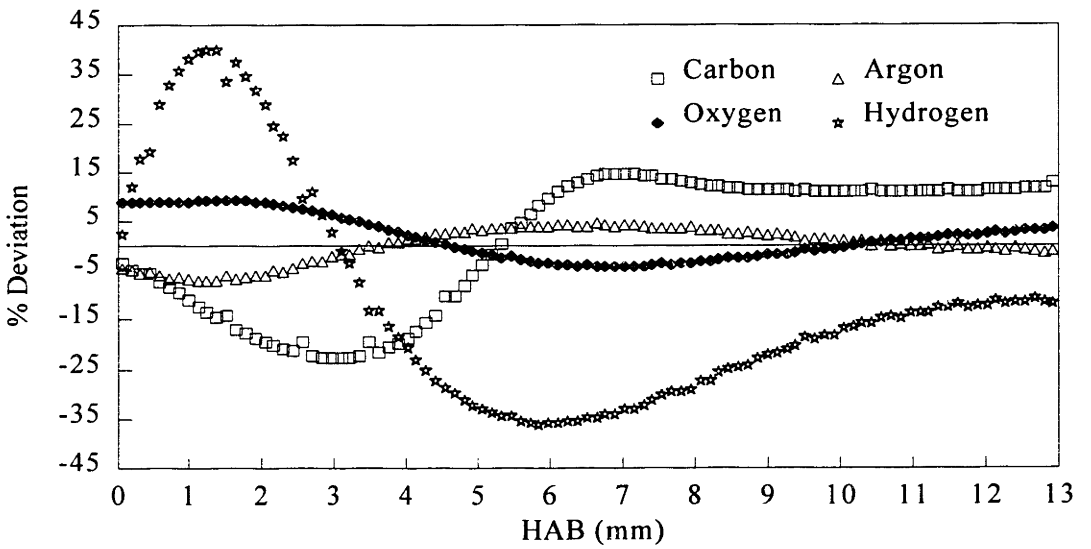

Figure 4.3 Element mass flux balances on carbon, hydrogen, oxygen and argon.

argon. The extent of closure of the mass balance for these reaction zone data is quite similar to that of Westmoreland, except for carbon. Several factors probably account for the higher deviation in the carbon balance. First, the species included in the carbon balance were C_6H_6, CH_4, CH_3, CO, CO_2, C_2H_2, C_2H_4, H_2CO and C_6H_5OH. Not including diffusion effects, the carbon in species not accounted for amounts to as much as 7.3% of the original C_6H_6 carbon, appearing primarily in the first 4.5 mm. In that region, the extra carbon serves to improve the balance. Another factor is that the inital elemental flux of carbon is only 1.9% of the total flux. That is,

carbon species are in low concentration relative to others and therefore suffer from a higher signal to noise ratio. Finally, the product with the strongest signal was CO, which was subject to interference from both N_2 and C_2H_4. As is discussed in the section below, attempts were made to remove or account for the effect of those interferences, but they were not entirely successful. Therefore much of the deviation in the carbon flux is likely to lie in the CO profile.

As was discussed in Chapter 3, mass discrimination factors revealed a very strong impact of high H_2 concentration on molecular beam diffusion. The effect is also present in the flame itself, as Figure 4.4 reveals using the element flux balance for hydrogen. In the base case situation — that used for the calculations in this thesis — thermal diffusion was incorporated, and the

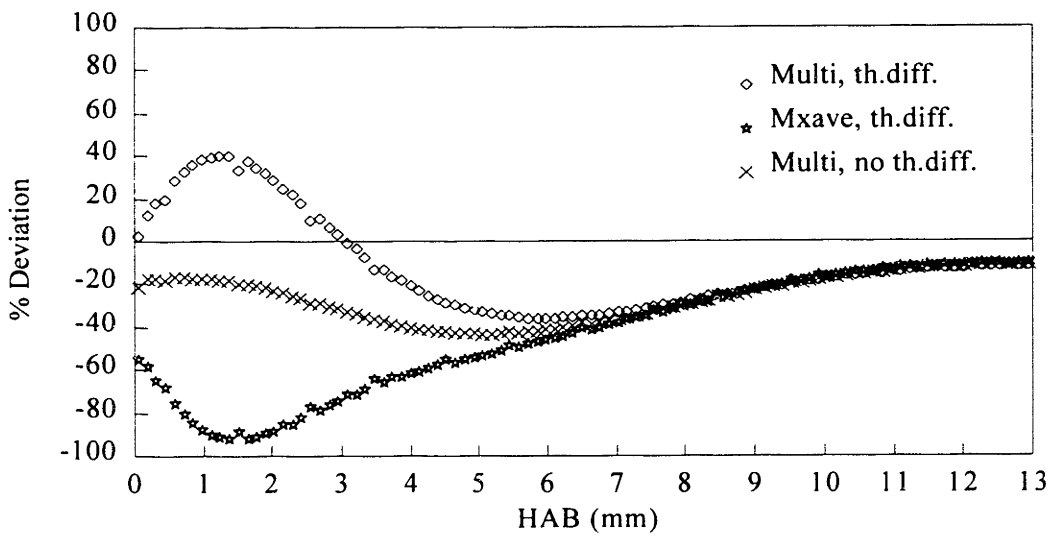

Figure 4.4 Element mass flux balances for hydrogen, calculated with different types of diffusion: (a) multicomponent and thermal diffusion, (b) mixture-averaged and thermal diffusion, and (c) multicomponent diffusion only (Kee et al., 1986).

multicomponent formulation of Dixon-Lewis (1968) was used for ordinary diffusion. (In contrast, for their hydrocarbon flames, Bittner and Westmoreland used the mixture-averaged formulation given by Fairbanks and Wilke (1950), and ignored thermal diffusion.) Two other cases are presented; in each, one of the two "extra" levels of computation was replaced by the simpler version. Use of multicomponent diffusivity is clearly needed to get good results in the flux balance for this H_2 flame, and thermal diffusivity is seen to have a strong impact on the balance as well. The carbon and oxygen balances are hardly affected by the type of diffusivity equations used.

For example, using mixture-averaged diffusion only changes the maximum carbon deviation from -21% to -15%.

Except for a few profiles noted in Section 4.2, all mole fraction data were collected by pulse counting.

4.2 Discussion of Temperature and Individual Species

The presence or absence of a signal at a particular mass number was determined by scans of the mass numbers from 14 to 118. The surveys were performed at heights of 3.0 mm, 4.4 mm (high masses only) and 6.0 mm, corrected, and 3 eV above the average ionization potential ("IP") or the IP of the most likely species at that mass number. Data were collected for species for which the scans revealed the signal to be above the detection limit. (The scanning process was discussed in greater detail in Chapter 3.)

Signals of many species were too low to be able to measure an ionization efficiency curve for identification of the isomer or isomers present. In some cases, ionization efficiency curves were measured but found to be too noisy to draw an accurate line through the points. Other times, the correct reference species (e.g., C_6H_6 or Ar) to use for electon energy ("EE") scale correction was unclear. When benzene was used as a reference species, it was not always clear whether the high or low intercept (see Chapter 3) was appropriate for the comparison. Even when a clean curve was obtained and the energy scale was unambiguous, there were several mass numbers — especially the larger ones with more isomers — for which a number of species had ionization potentials ("IP's") equally close to the measured intercept ("ICP").

For all of these reasons, most of the species for which data were collected could not be positively identified. Table 4.1 summarizes ionization efficiencies taken and identifications made for the species measured in the flame. A "high certainty" identification is one in which species is almost unambiguously identified; "medium certainty" means that there is good reason to believe that a species is the one identified, but the evidence is not conclusive; species of "low certainty" were not assigned a possible identity. In cases of low certainty, a likely isomer was chosen for the purposes of calculation and presentation, and calibration conversion factors for other possible isomers were computed (Appendix E).

Numeric tables of the information presented in this chapter are found in Appendixes H (data points) and I (smoothed curves). In addition, flux balances and profiles are given in

Table 4.1 Summary of ionization efficiency measurements for species in $\phi = 1.79$, H_2-O_2-C_6H_6-Ar flame.

Mass no.	Ionization efficiency?	Level of certainty	Species
1	yes	high	H
2	yes	high	H_2
15	yes	high	CH_3
16	yes	high	CH_4
17	yes	high	OH
18	yes	high	H_2O
26	yes	high	C_2H_2
28	yes	high	CO, C_2H_4 (,N_2)
30	yes	high	H_2CO
32	yes	high	O_2
34	yes	high	^{18}OO
39	yes	high	C_3H_3 formed in ionizer
40	yes	high	Ar
41	yes	high	C_3H_5 formed in ionizer
42	yes	(multiple species possible)	C_3H_6, c-C_3H_6, possibly HC≡COH; H_2C=CO not ruled out
44	yes	high; (multiple species possible)	CO_2; CH_3CHO and/or c-C_2H_4O
52	yes	high	C_4H_4 formed in ionizer
53	no	---	---
54	no	---	---
55	no	---	---
56	yes	(multiple species possible)	CH_2=CHCHO, HC≡CCH_2OH, CH_2=$CHCH_2CH_3$, c-C_4H_8, c-$C_3H_5(CH_3)$
57	no	---	---
58	no	---	---
59	no	---	---
60	no	---	---
65	yes	(multiple species possible)	c-C_5H_5 or HC=C=C=CO, possibly HC≡CCHCH=CH_2
66	yes	(multiple species possible)	(see species section below)
67	yes	medium	C_5H_7 fragment formed in ionizer; possibly trace amount of same in flame
68	yes	(multiple species possible)	(see species section below)
69	no	---	---
70	no	---	---
71	no	---	---
72	no	---	---

Mass no.	Ionization efficiency?	Level of certainty	Species
77	yes	(multiple species possible)	phenyl or HC≡CCH=CHCH=CH
78	yes	high	C_6H_6
79	yes	high	$^{13}CC_5H_6$ and C_6H_5D (isotopes of benzene)
80	yes	(multiple species possible)	(see species section below)
81	no	---	---
82	no	---	---
83	no	---	---
84	no	---	---
85	no	---	---
86	no	---	---
91	no	---	---
92	no	---	---
93	no	---	---
94	yes	medium-high	C_6H_5OH
95	yes	high	$^{13}CC_5H_5OH$, C_6H_5OD and C_6H_4DOH
96	no	---	---
110	no	---	---

Appendix J, and net rates in Appendix K. Similar to Westmoreland (but unlike Bittner), raw mole fraction data were shifted by 2.5 probe diameters toward the burner, to account for probe sampling effects (Biordi et al., 1974). Temperature data were shifted away from the burner by 4.5 wire diameters, as recommended by Fristrom and Westenberg (1965).

Unless specified otherwise, all ionization potentials referred to in this chapter are given on an *energy-corrected* basis. Certain species which were were determined to be formed as a fragment of a larger molecule were studied by comparing the signal intensity to the known or potential mole fraction of a possible parent, via fragmentation magnitude analysis (see Chapter 3). The details of these analyses are given in Appendix L.

Temperature profile.

No catalytic heating of any significance was observed in the collection of temperature data. In addition, measurements with the burner moving toward the thermocouple were in good agreement with those in the opposite direction. Good reproducibility was found with several thermocouples. In conjunction with the thermocouple heat transfer equation discussed in Chapter 3, smoothed mole fractions were used to calculate h/εd for measurements where electrical

heating radiation compensation was not used. The flame temperature was then calculated from $T_{unheated\ TC}$ by means of Equation 3-3.

Iteration of the temperature-$\alpha_{i,Ar}$ equations resulted in minimal correction to the original values on the first pass. The raw temperature profile was adjusted by being: (a) reduced 100 K to account for the heat sink effect of the probe (Biordi et al., 1974), and (b) shifted 4.5 bead diameters away from the burner to account for wake displacement (Fristrom and Westenberg, 1965). The flame temperature, shown in Figure 4.5, reaches a maximum of 1937 K at 9.6 mm, being 1500 K already at 3.4 mm. The particular smoothing curve used extrapolates to a burner temperature of 316 K, or 43°C.

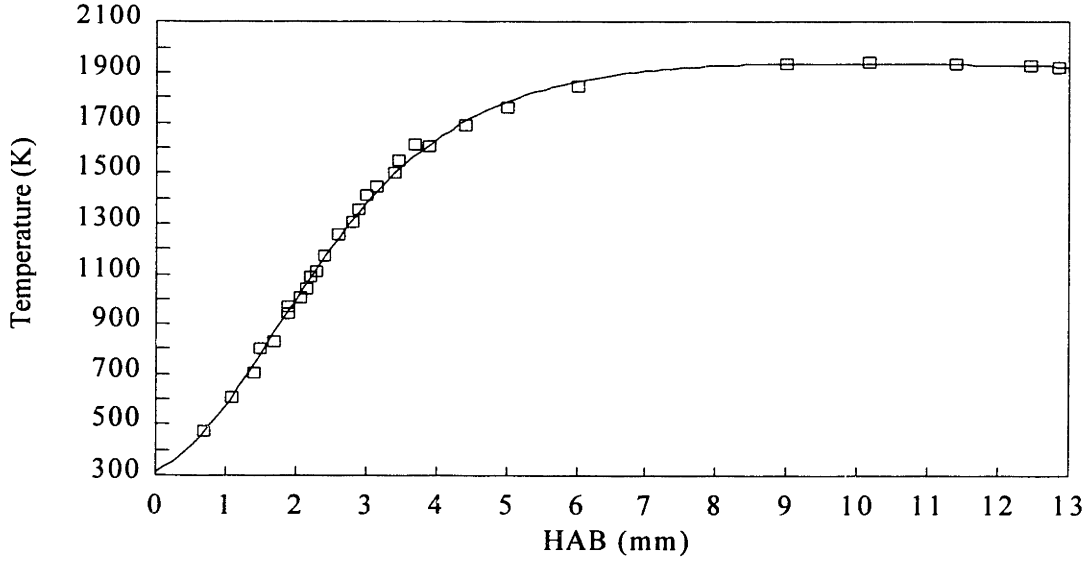

Figure 4.5 Temperature in the reaction zone of a 22 torr laminar, premixed H_2-O_2-C_6H_6-Ar flame. ϕ = 1.79, 31.3% Ar, $(x_{C6H6}/x_{H2})_0$ = 0.010, v_0 = 101 cm/sec. Data points and smoothed curve are shown.

H atom profile.

As expected, H atom was one of the most difficult mass spectrometer peaks to tune. In spite of a great deal of day-to-day variability in the H_2 signal, the ratio $\frac{I_H}{I_{H_2}}$ remained reasonably constant, on the average deviating 40% in three measurements over two months' time. Unlike in rich hydrocarbon flames measured with MBMS (Bittner, 1981; Cole, 1982; Westmoreland, 1986), no drifting or hysteresis of the H signal was observed. The data profile was taken with H_2 as the reference species, at an electron energy 2.55 eV above the ICP. The appearance of H from

H_2 was measured to occur at least 2.5 eV above this energy. In some ionization efficiency curves, no H_2 fragmentation occurs at all in the electron energy range measured, as evidenced by a lack of upturn in the H atom signal.

The mole fraction of H, relative to argon, is shown in Figure 4.6. Two calibration methods were used for H atom. Initially the Relative Ionization Cross Section ("RICS") method was used, but a second method based on partial equilibration of the H_2-O_2 system in the post-flame zone was ultimately preferred. The latter method is discussed in detail in Chapter 6. Conversion of the partial equilibrium data presented here to the RICS calibration simply involves multiplying the curve points by 1.66.

The data are themselves quite smooth. The mole fraction peak occurs somewhere beyond 10.5 mm.

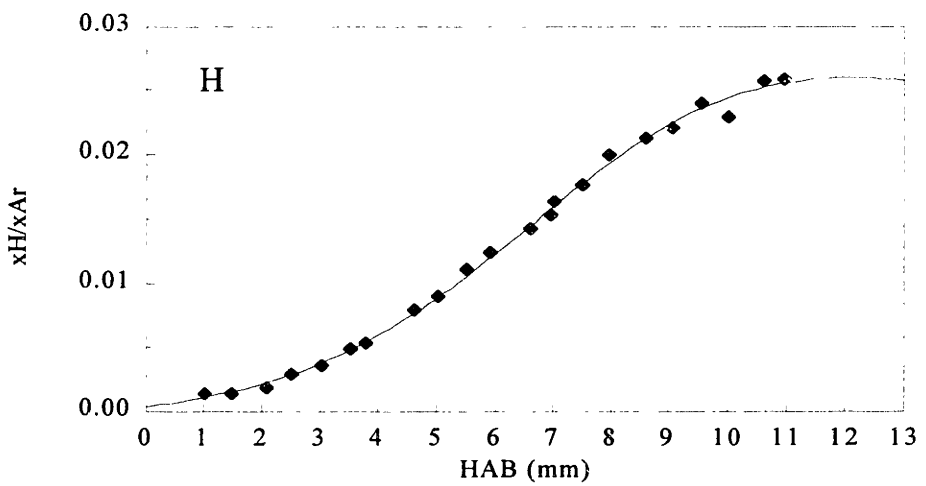

Figure 4.6 Mole fraction of H atom relative to Ar, in a 22 torr laminar, premixed H_2-O_2-C_6H_6-Ar flame. ϕ = 1.79, 31.3% Ar, $(x_{C6H6}/x_{H2})_0$ = 0.010, v_0 = 101 cm/sec. Data points and smoothed curve are shown.

H_2 profile.

The H_2 signal was found to be stable with respect to a particular day's measurements, but unstable from day to day. Hydrogen is well known to be difficult to measure with MBMS, a situation which was probably exacerbated in this instance by the age of the mass spectrometer. Whatever the source of the discrepancy, the ratio $\frac{I_{H_2}}{S_{H_2,Ar}I_{Ar}}$ at a particular location in the flame fluctuated between two nearly constant values. One of these, if used, would result in an element

flux balance for H with nearly three times the deviation as the other. The more realistic of the two sets of measurements was used, and is shown relative to argon in Figure 4.7.

The absolute calibration technique was used for hydrogen, which (along with Ar) was collected with analog signal processing. The IP 's of H_2 and Ar are nearly identical at 15.5 eV and 15.75 eV, respectively, so the mole fractions for both species were measured at 17.7 eV. As with H atom, there was little scatter, and no hysteresis with respect to burner position.

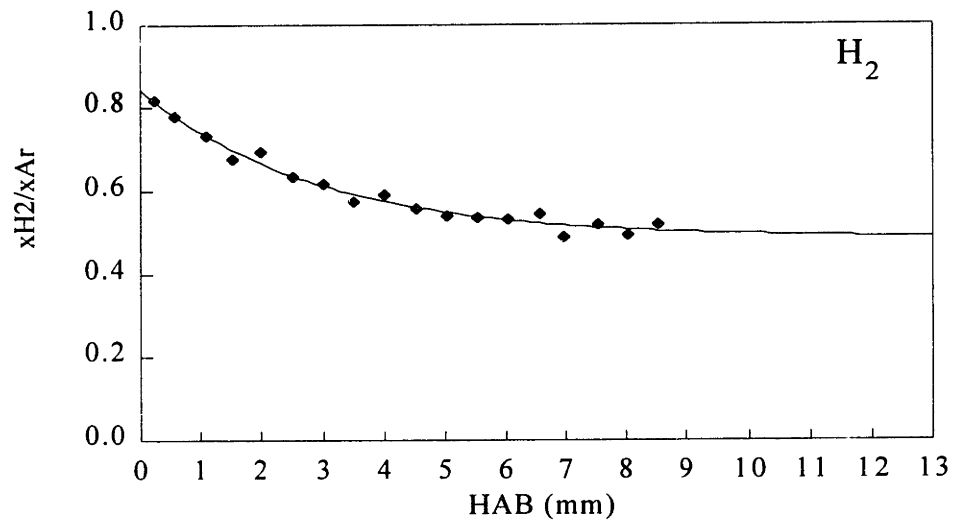

Figure 4.7 Mole fraction of H_2 relative to Ar, in a 22 torr laminar, premixed H_2-O_2-C_6H_6-Ar flame. ϕ = 1.79, 31.3% Ar, $(x_{C6H6}/x_{H2})_0$ = 0.010, v_0 = 101 cm/sec. Data points and smoothed curve are shown.

CH_3 profile.

Since no species other than CH_3 and fragments of CH_3 from larger molecules could have a signal at mass 15, species identification was not necessary. Methyl could, however, be formed by fragmentation of CH_4. To prevent this, CH_3 was measured at 11.0 eV, below the experimental appearance potential ("AP"). Methyl was calibrated by the RICS method, with mass 16 measured as the reference species at 14.9 eV. The mass 16 signal was first corrected for (a) fragmentation to CH_3+H, using a calibration curve measured with cold CH_4 (see below), and (b) the contribution of CH_2D and $^{13}CH_3$.

Some of the CH_3 data points were measured at 16.0 eV, when mass 15 was used to account for the presence of CH_3 isotopes in the mass 16 signal. (Mass 16 was being measured at that time, also at 16.0 eV, to quantify its isotopic contribution during collection of OH data; see

below.) The combined mole fraction data are shown in Figure 4.8. The raw data required quite a bit of correction to be usable as mole fractions. First, the isotopic signal had to be subtracted. Next, the contribution of CH_3 from fragmentation of CH_4 was accounted for with a cold-gas CH_4 calibration curve[12] of I_{CH3}/I_{CH4} vs. ($EE\text{-}ICP_{CH4}$). This curve was measured three times over the course of 2½ years, and was found to be quite reproducible. Fragmentation to CH_2 was ignored. Finally, because the reference species for CH_4 (H_2O) in the OH measurement was different from

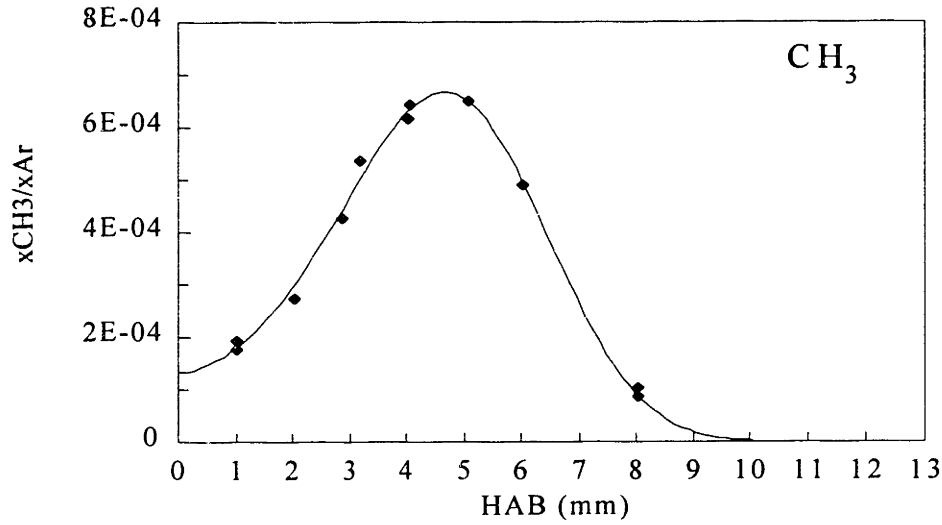

Figure 4.8 Mole fraction of CH_3 relative to Ar, in a 22 torr laminar, premixed H_2-O_2-C_6H_6-Ar flame. ϕ = 1.79, 31.3% Ar, $(x_{C6H6}/x_{H2})_0$ = 0.010, v_0 = 101 cm/sec. Data points and smoothed curve are shown.

the species used when CH_3-CH_4 data were being collected (Ar), the data were normalized so that the CH_4 peak mole fractions were equal.

The functioning of the calibration curve was as follows. For the cold gas calibration experiments, define $a[E] \equiv \left(\frac{I_{CH_3}}{I_{CH_4}}\right)[E]$, where $E \equiv EE\text{-}ICP_{CH4}$. That is, for a particular energy, $I_{CH_3,frag} = a \times I_{CH_4,meas}$. In a flame experiments at some energy above the appearance potential

[12] It could legitimately be argued — as Hausmann et al. (1992) do in their response to Symposium comments — that calibration fragmentation under flame conditions is not only not possible, but cannot be approximated by cold gas measurements because of the differences in vibrational excitation levels. It should be pointed out, though, that any molecule extracted from a flame would have *at a minimum* the same amount of vibrational energy as the cold gas. Therefore, a cold gas calibration curve represents the *minimum* fragmentation expected, and is an improvement over no fragmentation correction at all. Also, the closer to the ICP one is, the more accurate one could expect the cold gas calibration to be.

for CH_3 from CH_4,

$$I_{CH_3,total} = \frac{I_{CH_3,meas} - a \times I_{CH_4,meas}}{1 - P_{n+1}^{CH_3}},$$

where P_n is the probability of having an isotope of mass n for a particular species; that is, $\frac{I_{mass\,n}}{I_{all\ isotopes}}$. This is shown schematically in Figure 4.9 for the case of measurements made during the OH data experiment. A diagram for the case of CH_3 measurements made below the appearance potential is given in Figure 4.10.

From the coincidence of the results at the three heights where points were measured in both sets, it can be seen that the data are all consistent and reproducible. Methyl is primarily produced in the center of the flame's reaction zone, and is destroyed by about 9 mm.

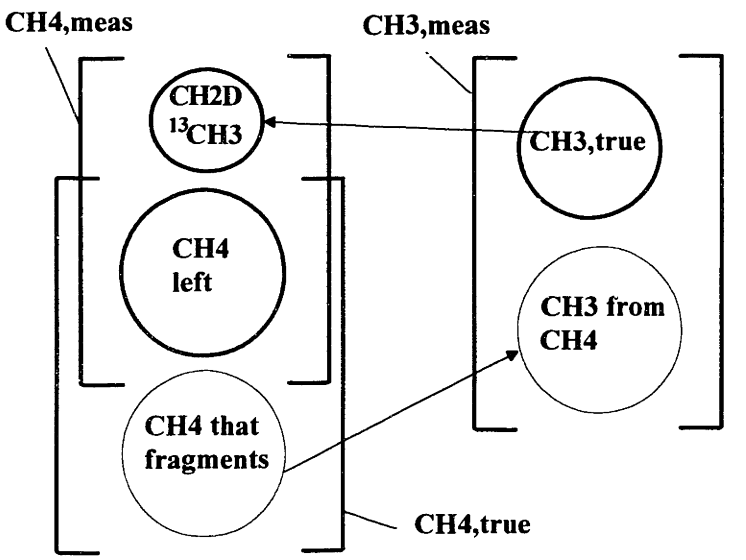

$$I_{CH_3,true} = \frac{I_{CH_3,meas} - a \times I_{CH_4,meas}}{1 - P_{n+1}^{CH_3}}$$

$$I_{CH_4,true} = (I_{CH_4,meas} - P_{n+1}^{CH_3} \times I_{CH_3,meas})\left(\frac{1+a}{1 - a \times P_{n+1}^{CH_3}}\right)$$

Figure 4.9 Calibration scheme for CH_3 and CH_4 in OH data set. Both mass 15 and mass 16 were measured above the $CH_4 \rightarrow CH_3$ appearance potential.

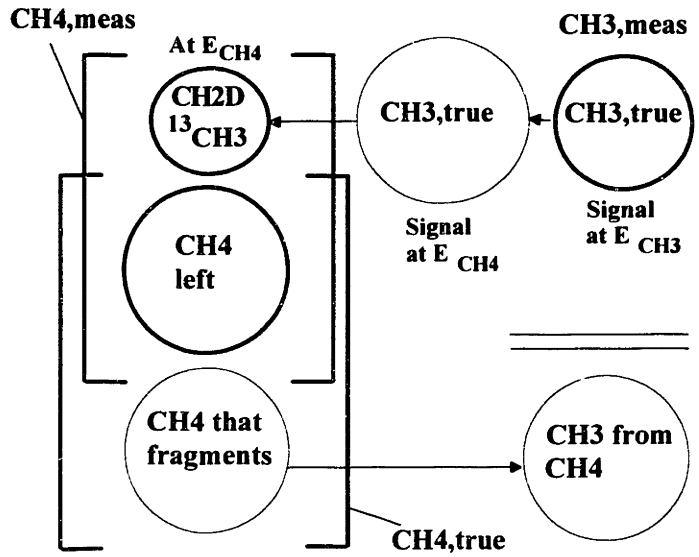

$$I_{CH_3,true} = I_{CH_3,meas}$$

$$I_{CH_4,true} = \left(I_{CH_4,meas} - I_{CH_3,meas} \times P_{n+1}^{CH_3} \times \left(\frac{E_{CH_4} - ICP_{CH_3}}{E_{CH_3} - ICP_{CH_3}} \right) \right)(1 + a)$$

Figure 4.10 Calibration scheme for CH_3 and CH_4 in mass 15-16 data set. Mass 15 was collected below the $CH_4 \rightarrow CH_3$ appearance potential, mass 16 above it.

CH_4 (mass 16) profile.

The first consideration with regard to mass 16 is the identity of the species: O, CH_4, or some combination of the two. In their fuel-rich hydrocarbon flames, Westmoreland (1986) and Bittner (1981) determined mass 16 to be CH_4. In the present flame, dominated as it is by H/O chemistry, one might expect a significant contribution from O atom. However, preliminary ionization efficiency investigations showed this not to be the case. Rather, mass 16 was found to be all (or at least overwhelmingly) CH_4. As this result was counterintuitive, the identity of the mass 16 signal was studied further in a number of different ways:

- Ionization efficiency curves were measured and compared to those taken in: (1) a CH_4 flame, where mass 16 should be overwhelmingly methane; (2) an H_2-O_2 flame without benzene, so that mass 16 was O atom; and (3) cold-gas experiments with CH_4. Measurements of H_2O and O_2 were used in some cases as reference species, to establish the energy scale. In other cases, the post-flame zone of various H_2-O_2-C_6H_6

flames were used as reference, on the basis that mass 16 would be O atom there. Except for several measurements in the late reaction zone and higher (≥ 8.0 mm) which could be consistent with O atom or a combination of O and CH_4, every ionization efficiency curve indicated that mass 16 was CH_4 rather than O atom.

- The "appearance" (CH_4 fragmentation to CH_3) portions of flame ionization efficiency curves for mass 15 were used in conjunction with the fragmentation calibration curve to predict an expected mass 16 signal, on the basis of 100% CH_4. The CH_4 signal thus computed was close to the mass 16 ionization efficiency curve, though slightly above it. (If the cold gas calibration curve were underpredicting flame gas fragmentation because of the lower vibrational energy content, the amount of CH_4 predicted in this calculation would indeed be higher than the true amount.) If mass 16 were primarily O atom, the computed CH_4 points should fall quite a bit *below* the ionization efficiency curve. In fairness, without further information it is impossible to rule out the possibility that any overprediction due to the use of cold gas calibration might be so great as to cause the results to *appear* to be in agreement with an identity of CH_4. This is probably not the case, though, as it was also true that as a function of EE-ICP_{CH4}, the fraction by which masses 16 plus excess mass 15 exceeded the mass 16 signal was very close to that in the cold gas calibration experiment[13]. Therefore, the back-calibration result is very consistent with domination by CH_4.
- Data taken with constant flows of H_2, O_2 and Ar, with and without benzene added, were compared with model predictions for these two cases. The model prediction (that mass 16 in the current flame should be nearly entirely O atom) was shown to be inconsistent with the measurements. The analysis is documented fully in Chapter 5.
- The O atom peak location in several other relevant flames was compared with the mass 16 peak location in the present flame. First, in the rich (ϕ = 1.91) H_2-O_2-Ar flame of Vandooren and Bian (1990), the peak was found to be at 6 mm, precisely where the OH peak occurred. In the stoichiometric C_6H_6-O_2-Ar flame of Bittner, both O atom and OH have very gradual slopes after the peak, making the precise location difficult. Both maxima appear to occur at 9.3±0.5 mm, the O profile rising to its peak faster, and therefore later, than OH. On the other hand, the CH_4 profile in Bittner's

[13] In the case of the cold gas experiment, *all* of the mass 15 signal was "excess."

rich (ϕ = 1.8) C_6H_6-O_2-Ar flame tops out at 7.5 mm, as opposed to 11.8 mm for OH. Therefore, when mass 16 is O atom, in either a hydrogen or a hydrocarbon flame, its location is close to that of OH; but when mass 16 is CH_4, the peak is several millimeters closer to the burner. Figures 4.11 and 4.12 show that in the present flame, the mass 16 profile maximizes at 4.6 mm, or 3.7 mm before OH does. This behavior supports the hypothesis that little or no O atom is present.

- Baldwin et al. (1986) found very high CH_4 production (25% on a mole per mole benzene basis) in a reactor in which small amounts of C_6H_6 were added to a rich H_2-O_2 mixture at 773K. Methane is a common major product in higher-temperature benzene pyrolysis studies: Louw et al. (1984) (C_6H_6 in an H_2 atmosphere), Brooks et al. (1979), Fujii and Asaba (1973) (C_6H_6 with O_2 additive), Hoyermann et al. (1975) (low-temperature C_6H_6 plus H atom), Schiff and Steacie (1951) (same as Hoyermann et al.) and Kim (1973) (same as Hoyermann et al.). Methane is even an important product for phenol (Manion and Louw, 1989) and phenyl (from C_6H_5Cl, Ritter et al., 1990) in an H_2 environment .

Ionization efficiency measurements taken in the *post-flame* zone of a rich H_2-O_2-C_6H_6-Ar flame were indicative of a mass 16 identity of O atom, rather than CH_4. This is supported by the lack of a mass 15 signal at 28.5 mm — in rich benzene and acetylene flames, CH_3 equals or exceeds CH_4 in the post-flame zone, to keep the partial equilibrium of $H+CH_4 \rightleftharpoons CH_3+H_2$ (Bittner 1981; Westmoreland, 1986). There is no reason to expect that reaction not to be partially equilibrated in the hydrogen flame as well; indeed, partial equilibrium of this reaction is predicted at 20 mm for these flame conditions, by the model of Zhang and McKinnon (1995). If the reaction is so equilibrated, the experimental mole fraction of CH_3 is calculated to be $0.8*x_{CH4}$, if H is calibrated by the partial equilibrium method. Therefore, identification of mass 16 as O atom at 28.5 mm is logical.

Given then that mass 16 is CH_4 in the preheat and reaction zones, calibration was effected using the same CH_3-CH_4 relationships as employed previously. As with CH_3, data were derived from two sources: (a) a CH_3-CH_4-Ar measurement for the purpose of mass 15-16 species (absolute calibration for CH_4), and (b) a CH_3-CH_4-OH-H_2O measurement made in the collection of OH data. The first case is diagrammed in Figure 4.10, the second in Figure 4.9. After correction for

CH_2D, $^{13}CH_3$ and fragmentation, the mass 16 signals measured during collection of the OH data set were normalized to the previous set so that the peak CH_4 mole fractions were equal. The heights with double measurements are in good agreement, as before.

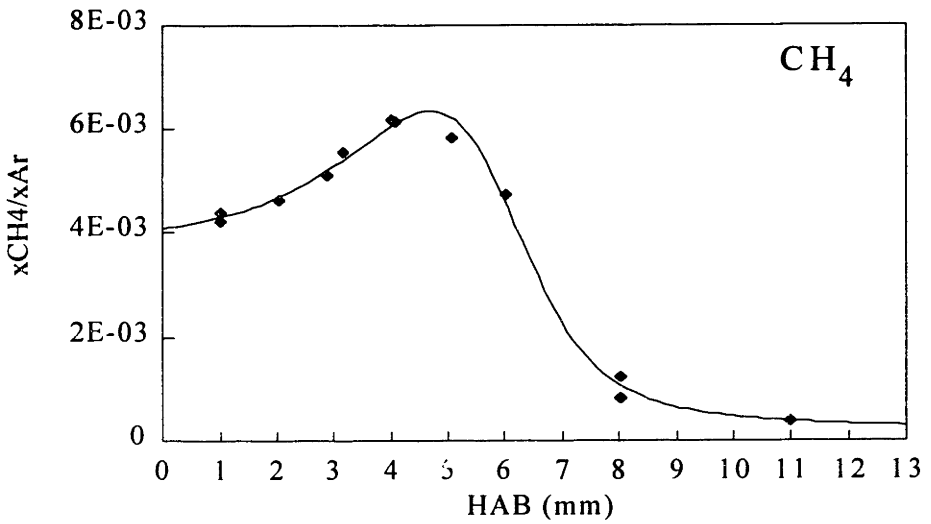

Figure 4.11 Mole fraction of CH_4 relative to Ar, in a 22 torr laminar, premixed H_2-O_2-Ar flame. $\phi = 1.79$, 31.3% Ar, $(x_{C6H6}/x_{H2})_0 = 0.010$, $v_0 = 101$ cm/sec. Data points and smoothed curve are shown.

As Figure 4.11 shows, CH_4 is an order of magnitude higher in concentration than CH_3. In Bittner's rich benzene flame, the two species were roughly the same magnitude. Also, unlike CH_3 in the present flame or CH_4 in a rich benzene flame, methane remains in relatively high concentration near the burner.

OH profile.

Ionization efficiency curves showed mass 17 to be OH, with a contribution from H_2O fragmentation at higher energies. As mentioned above, the contribution of CH_3D and $^{13}CH_4$ to the mass 17 signal was subtracted out, with the isotope calculated from $I_{CH4,true}$. Water was used as the reference species for a RICS calibration. OH was measured at 16.0 eV, and H_2O at 15.6 eV. No drift or hysteresis with respect to burner position was found. Measurements taken over a one-year period were generally within 30% of the final profile, showing good reproducibility for a radical species.

As with H atom, fir[illegible]alibration based on partial equilibrium was found to be more

appropriate. Conversion to the RICS calibration involves multiplication of the points in Figure 4.12 by 0.543. This factor, while fairly small, remains within the factor of two expected for RICS results.

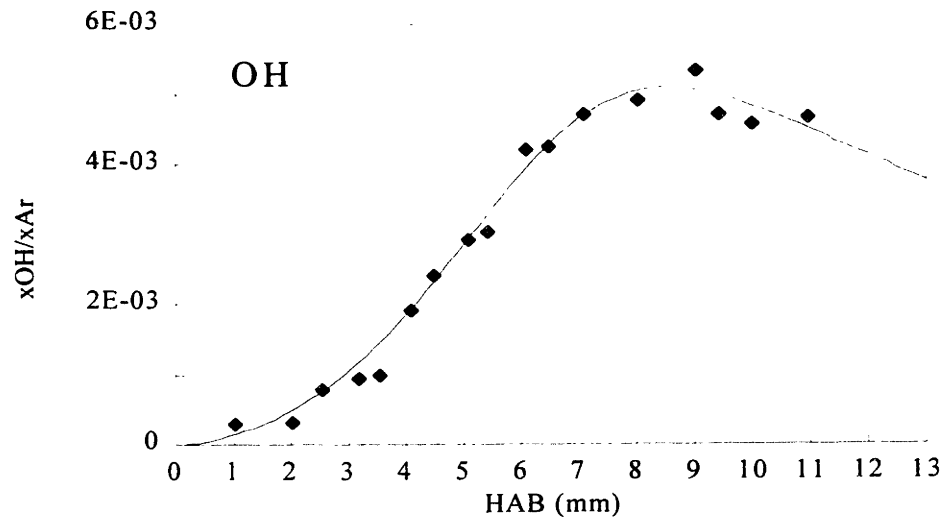

Figure 4.12 Mole fraction of OH relative to Ar, in a 22 torr laminar, premixed H_2-O_2-C_6H_6-Ar flame. ϕ = 1.79, 31.3% Ar, $(x_{C6H6}/x_{H2})_0$ = 0.010, v_0 = 101 cm/sec. Data points and smoothed curve are shown.

The smoothed curve chosen to fit the data points had two features which involved somewhat arbitrary assumptions. First, the mole fraction at the burner was chosen to be zero, though if H and CH_3 are an indication of the behavior of radicals, extrapolation to a positive value would not have been unreasonable. Second, as no data were taken between 11 mm and 13 mm (corrected), it is unknown whether the true slope above about 9.5 mm is as great as shown in Figure 4.12, or somewhat more gentle. The post-flame zone datum at 28.5 mm was used as an indicator of the possible shape in the region. In any event, the peak would still be in the range of 8 mm to 9.5 mm.

H_2O profile.

Ionization efficiency curves for H_2O were unremarkable. Water was measured with respect to argon, at 17.3 eV for both species. The signal showed excellent temporal and spatial stability, plus low scatter. The late maximum in the mole fraction profile is perfectly consistent with the O_2 and H_2 burnout scales.

As discussed in Chapter 3, a calibration factor was derived from the O element balance at

the 28.5 mm post-flame zone data point. Species included in the balance were OH, H_2O, CO and CO_2.

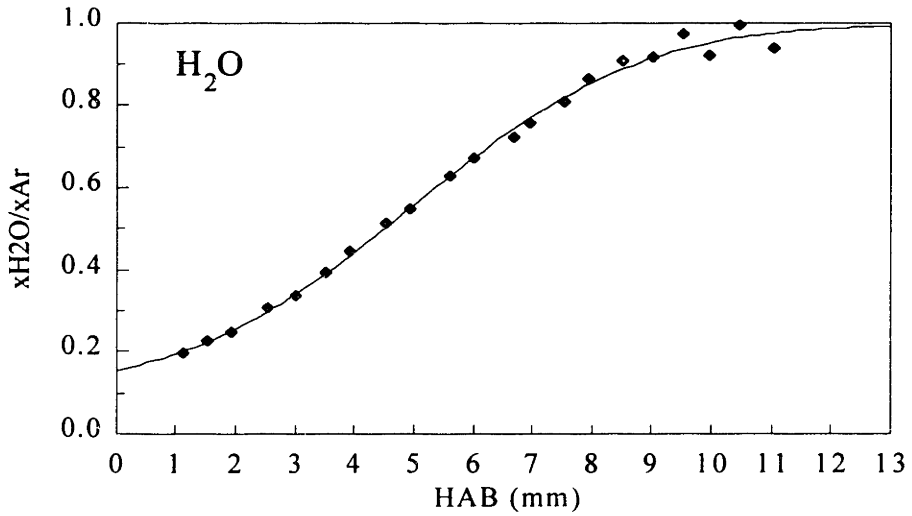

Figure 4.13 Mole fraction of H_2O relative to Ar, in a 22 torr laminar, premixed H_2-O_2-C_6H_6-Ar flame. ϕ = 1.79, 31.3% Ar, $(x_{C6H6}/x_{H2})_0$ = 0.010, v_0 = 101 cm/sec. Data points and smoothed curve are shown.

C_2H_2 profile and C_2H_3.

Only one species, acetylene, can exist at mass 26. A contribution from fragmentation of C_2H_4 appeared above 13.6-14.7 eV in the early and middle sections of the flame. The literature appearance potential ranges from 13.0 eV to 13.6 eV. Acetylene was measured with respect to argon, at 12.9 eV and 19.2 eV respectively, and was calibrated directly. The mole fraction profile with respect to argon is shown in Figure 4.14. The signal showed the good stability and low scatter typical of a major stable species.

The C_2H_2 profile is quite a bit lower, and about 3.3 mm later in the flame, than C_2H_4. (In contrast, in the rich C_6H_6 flame of Bittner, acetylene is only 2 mm later than ethylene and is more than 100 times higher in concentration.) The high ethylene concentration implies that C_2H_3 should also be relatively prevalent. Because of the low quantity of hydrocarbons in general, in the scans of flame species C_2H_3 had to be measured above the IP of acetylene. This required an accounting for the isotopic contribution of C_2HD and $^{13}CCH_2$ to mass 27. It was found that C_2H_3 was not detected above the expected isotopic acetylene signal, which fixes its maximum mole

fraction at roughly 1-5 ppm. The small amount of C_2H_3 of should perhaps not be unexpected, since x_{C2H3} in Bittner's benzene flame is only about 2% of $x_{C2HD}+x_{13CCH2}$. Even in the rich acetylene flame of Westmoreland, vinyl is at most only 6% of mass 27 acetylene.

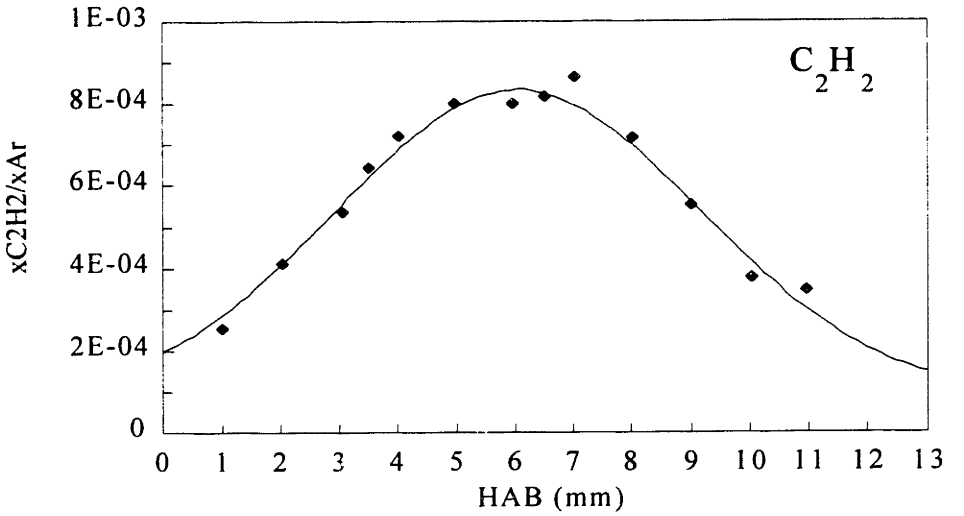

Figure 4.14 Mole fraction of C_2H_2 relative to Ar, in a 22 torr laminar, premixed H_2-O_2-C_6H_6-Ar flame. ϕ = 1.79, 31.3% Ar, $(x_{C6H6}/x_{H2})_0$ = 0.010, v_0 = 101 cm/sec. Data points and smoothed curve are shown.

Mass 28 (C_2H_4 and CO).

This mass number is not only composed of the flame species C_2H_4 and CO, but also N_2 from background gas, beam entrainment and small leaks. Background levels are not an important contributor to the signal if correctly subtracted out using the beam block, though there still could be some contribution to the noise level. In spite of efforts to eliminate leaks, and the fact that the ionization potentials of the three species are sufficiently distinct (10.5, 14.1 and 15.6 eV) that species differentiation should be possible, in practice it was found that the CO and C_2H_4 profiles were relatively noisy and less reproducible than desired. This could in part be due to a lower CO concentration relative to N_2 in a hydrogen flame, than in a hydrocarbon flame. While CO could be a fragmentation product of other species, such as C_6H_5OH, no evidence of such a contribution was seen in the ionization efficiency curves.

Ethylene was readily distinguishable from the CO signal in ionization efficiency curves. Direct calibration was used, with measurements made relative to argon. Even with the scatter

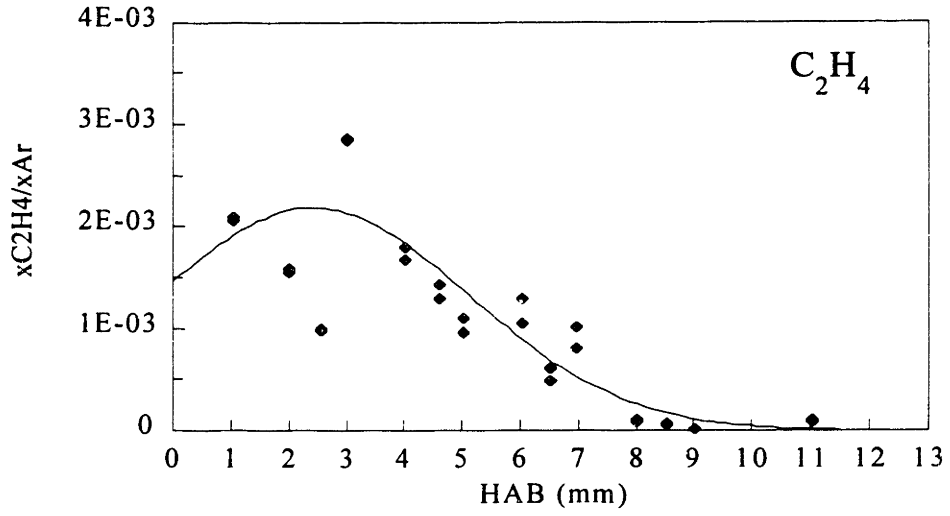

Figure 4.15 Mole fraction of C_2H_4 relative to Ar, in a 22 torr laminar, premixed H_2-O_2-C_6H_6-Ar flame. ϕ = 1.79, 31.3% Ar, $(x_{C6H6}/x_{H2})_0$ = 0.010, v_0 = 101 cm/sec. Data points and smoothed curve are shown.

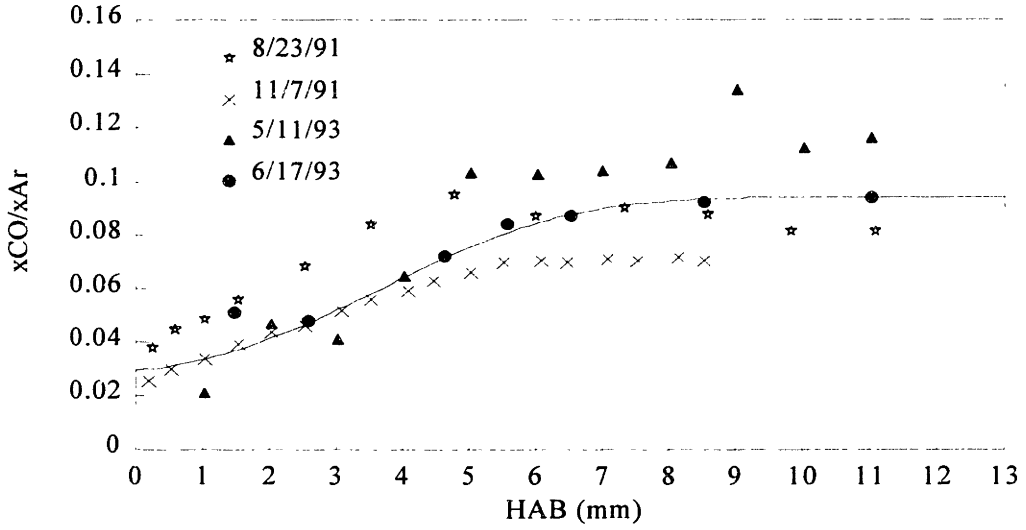

Figure 4.16 Mole fraction of CO relative to Ar, in a 22 torr laminar, premixed H_2-O_2-C_6H_6-Ar flame. ϕ = 1.79, 31.3% Ar, $(x_{C6H6}/x_{H2})_0$ = 0.010, v_0 = 101 cm/sec. Data points and smoothed curve are shown.

evident in Figure 4.15, overall the C_2H_4 profile was reproducible.

The CO intensity was adjusted for the contribution of C_2H_4, linearly compensated for the difference in energies between the two measurements. CO was also calibrated directly. An electron energy was chosen such that with the beam blocked, the mass 28 signal in the post-flame

zone was small relative to the unblocked intensity. Because the measurement had to be taken in the linear portion of the ionization efficiency curve, only a small electron energy window was usually available. Four CO profiles, taken over a two-year period, are shown in Figure 4.16. The first two profiles were measured with analog signal processing. As some of the points from different sets are close to each other, the smoothed curve was drawn so that it would approximately pass through the places where the most points were clustered. The choice of smoothed curve has little impact on the overall argon profile or O atom balance, and the net rate of CO was not used in any analyses in this thesis. Therefore, the scatter has little effect on any conclusions drawn here[14].

Mass 30 profile (H_2CO).

Only one ionization efficiency curve was taken, at 4 mm. Mass 30 isotope signals of CO and C_2H_4 were subtracted out. The resulting ICP, when the energy scale was corrected, was very close to the IP of formaldehyde, and about 0.7 eV above that of C_2H_6. As there can be as much as 0.5 eV error in the measurement of IP's (Bittner, 1981), it is possible that some of mass 30 is ethane. This would not be unreasonable, given the general trend of larger mole fractions for

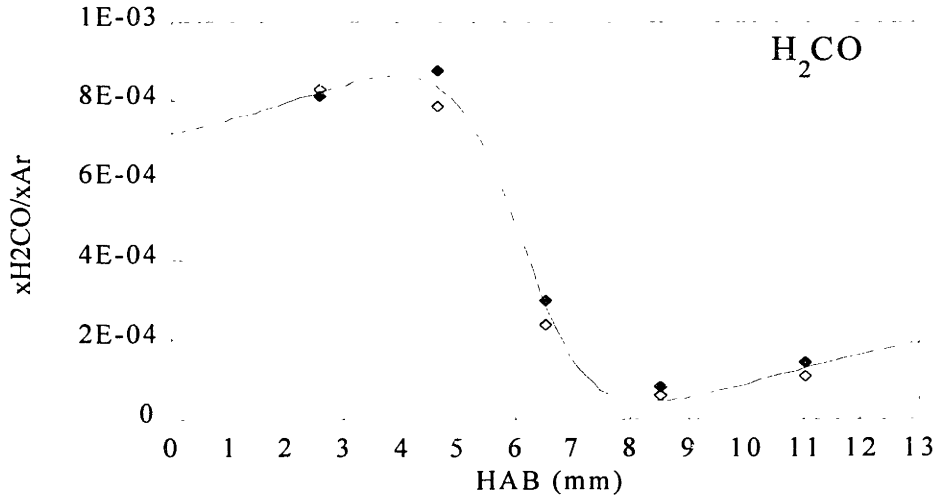

Figure 4.17 Mole fraction of H_2CO relative to Ar, in a 22 torr laminar, premixed H_2-O_2-C_6H_6-Ar flame. ϕ = 1.79, 31.3% Ar, $(x_{C6H6}/x_{H2})_0$ = 0.010, v_0 = 101 cm/sec. Data points and smoothed curve are shown.

[14] The data points taken in 1991 were *not* corrected for C_2H_4 contribution. The net effect of the adjustment would be a slight increase in mole fraction in the main reaction zone.

more hydrogenated species, and the large C_2H_4 concentration. On the other hand, the abundance of CO and hydrogen, relative to the amount of C_2H_4, implies that H_2CO is not an unreasonable conclusion. Baldwin et al. (1986) found H_2CO as a product, along with C_2H_4 and C_2H_2, in their study of additive C_6H_6 in an H_2-O_2 mixture at 773K. C_2H_6 was apparently below the detection limit in that work. The mass 30 signal was therefore assigned entirely to formaldehyde on the basis of the Baldwin et al. study and the ionization efficiency curve. RICS calibration was used, with the reference species being CO. Taken at the same time as the 6/16/93 CO profile, mass 30 was measured at 12.3 eV, carbon monoxide at 15.5 eV. Since mass 28 was found to be quite scattered, two of the four CO profiles shown above were used for the conversion of $\frac{x_{H_2CO}}{x_{CO}}$ to $\frac{x_{H_2CO}}{x_{Ar}}$. As one can see in Figure 4.17, the two resulting points at each height are close enough to consider the differences insignificant. Since the double points represent different reference species curves and not separate measurements, the upturn seen after 8.3 mm may be within the scatter and/or error of the data.

O_2 profile.

Identification of mass 32 as O_2 is nearly automatic, as the only other species which can exist are CH_3OH and isotopes of H_2CO that are clearly too low in abundance to make any difference. Methanol has an IP which is only 1.3 eV lower than that of oxygen. Therefore, any CH_3OH present in the flame would show up in the thermal energy tail. To check for this

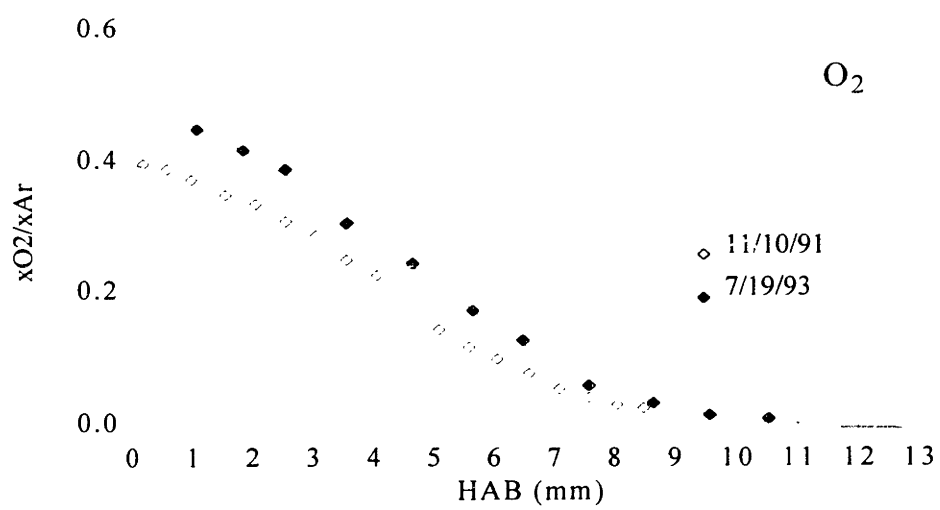

Figure 4.18 Mole fraction of O_2 relative to Ar, in a 22 torr laminar, premixed H_2-O_2-C_6H_6-Ar flame. ϕ = 1.79, 31.3% Ar, $(x_{C6H6}/x_{H2})_0$ = 0.010, v_0 = 101 cm/sec. Data points and smoothed curve are shown.

possibility, ionization efficiency curves were taken for cold O_2 in the effusive source and for mass 32 in the flame at 4 mm, on the same day. The tail sections of both curves were normalized to the signal at the beginning of the linear section, at 15.4 eV. If any CH_3OH were present in the tail, the normalized curves would look different because a signal which was not due to high energy electrons in the ionizer would be contributing. The two curves were superimposable, meaning that no methanol could be detected.

Like mass 28, mass 32 is also influenced by leaks and beam entrainment, as oxygen is the other major component of air. Two O_2 profiles were measured, almost two years apart (Figure 4.18). The early profile was measured with analog signal electronics; later tests showed no significant difference between analog and pulse counting results. The two differed from the mean by as much as 23%. Rather than using an average profile, the newer one was chosen because (1) it was taken in the same time frame as the bulk of the rest of the data, and (2) several measurements made in the preceeding month were closer to that data set than the first. Which curve is used makes little difference to the overall conclusions made in this thesis. Data were calibrated directly, with respect to argon. For the later profile, Ar and O_2 were both measured at 17.6 eV.

HO_2 and H_2O_2.

An attempt was made to measure these species in the flame. An ionization efficiency curve of mass 34 at 2.8 mm had an intercept indicative of ^{18}OO, rather than H_2O_2, with no lower linear section apparent. In addition, an experimental isotopic contribution ratio, $\left(\frac{I_{34}}{I_{O_2}}\right)_{\text{cold gas}}$, was measured with cold O_2 and then used with the oxygen ionization efficiency curve to subtract the ^{18}OO signal from mass 34. The resulting signal intensity was essentially noise. A number of sequential measurements of masses 32 and 33 were also made different multiplier high voltage settings, and masses 32-34 were also measured at different heights. The mass 34 signal was never greater than background. Therefore, H_2O_2 was not above the detection limit.

To check for HO_2, the ratio of mass 33 and mass 34 signals was examined at each HAB. In each case, the ratio was close to the experimental ratio, showing that HO_2 was not detectable either.

Because of the large amount of noise present in the O_2 signal and its isotopes no estimate could be made of maximum mole fractions for HO_2 and H_2O_2, and its detection limit should be higher than that of most other species. It is worth pointing out, though, that a mass 34 signal

one-fifth the size of ^{18}OO in the first few millimeters would have a mole fraction of about 120 ppm. A mass 33 signal one-fifth the size of ^{17}OO would have a mole fraction of about 23 ppm.

Mass 39.

A rather large mass 39 signal was detected in the scans for flame species. An ionization efficiency curve was measured at 4.6 mm, which had ambiguous features. There appeared to be two linear sections, though the lower energy portion could be short enough to be a tail. If an interpretation of two intercepts is accepted, the IP's would be 11.9 eV and 14.1 eV. If one considered there to be a single line, it would have an IP of 13.9 eV. No mass 39 species could be found in the literature having an ionization potential as high as 11.9 eV. Based solely on appearance potential, a number of species could be the parent of this species. Since knowing the parent of a particular fragment could help in species identification, the possible source of the signal was investigated by fragmentation magnitude analysis. Possible parents are masses 42 (two C_3H_6 species, AP 13.7-14.2 eV), 54 (AP 11-11.7 eV), 68 (AP 11.6-15.2 eV), and 78 (14.7-16.1 eV). With regard to the low linear section, the conclusion was that neither mass 54 nor mass 68 alone could explain it as an ionization event different from the energy tail. In all likelihood, the two together would not produce enough mass 39, either, so if that section of the ionization efficiency curve is from fragmentation, it probably is from a species not documented in the literature.

The average electron impact AP in the literature for C_3H_3 from benzene is 15.2 eV, and from C_3H_6 (cyclic and linear), 14.0 eV. Of the species which have AP's of 14±1 eV, these two are the only ones found in quantities near to or greater than the mass 39 signal in the flame. An experimental appearance potential of mass 39 from benzene was measured to be 14.3 eV, judged by the *onset* of C_3H_3 signal. (As opposed to a linear response; the intercept of the linear section was 16.1 eV.) This measurement was made with a different emission current than the mass 39 flame ionization efficiency curve, which could affect the result. However it seems that mass 39 was probably predominantly a product of benzene fragmentation, with a possible contribution from mass 42.

Mass 40.

An analysis of the normalized tail region of mass 40 ionization efficiency curves, similar to that done for mass 32, was performed to determine if C_3H_4 was present. As argon is the species with the highest concentration in the flame, detection of a trace species in its tail is the most

difficult. Furthermore, there was no case where mass 40 was measured to the end of the energy tail, in both a cold gas and the flame on the same day. Therefore, the comparison was made for ionization efficiency curves taken on different days. In fact, there were very few cases where the entire tail was measured. No evidence for C_3H_4 was seen in those curves. On the basis of the magnitude of the signal noise, the maximum mole fraction was estimated to be 25 ppm.

Mass 41.

Also identified by the mass scan, the experimental ionization/appearance potential was measured to be 12.3 eV. No ionization potentials this high could be found in the literature, the closest being 9.5 eV for HC=CO. Fragmentation magnitude analysis points to mass 42 (as C_3H_6, not C_2H_2O) as the likely parent, though mass 56 might contribute some.

Mass 42 profile.

Two separate measurements of the ionization efficiency at this mass number resulted in identical IP's of 10.1 eV. Possible species within a few tenths of an electron volt are linear and cyclic C_3H_6, and HC≡COH. The IP of H_2C=CO is a bit lower, at 9.6 eV. In addition, several larger species (masses 44, 56, 58, 70, 72 and 86) fragment into mass 42 at 10±1 eV. Fragmentation magnitude analysis rules out any major contributions from these parent molecules. The intercepts of mass 39 and mass 41 daughter species argue for mass 42 being nonoxygenated.

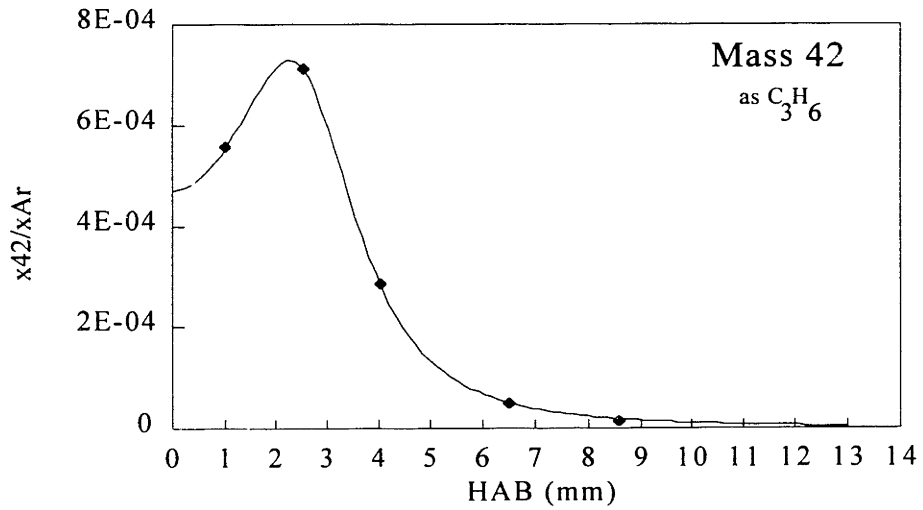

Figure 4.19 Mole fraction of mass 42 (calibrated as C_3H_6) relative to Ar, in a 22 torr laminar, premixed H_2-O_2-C_6H_6-Ar flame. ϕ = 1.79, 31.3% Ar, $(x_{C6H6}/x_{H2})_0$ = 0.010, v_0 = 101 cm/sec. Data points and smoothed curve are shown.

Mass 42 was calibrated as $CH_3CH{=}CH_2$ by the RICS method, referenced to CO_2. Data were taken at 12.2 eV for mass 42 and 15.8 eV for CO_2. Since only five data points were collected, the smoothed curve of Figure 4.19 merely approximates the correct profile. Regardless of that fact, it is clear that formation occurs early in the reaction zone, and the species does not survive long once the maximum flame temperature has been reached.

Mass 43.

During the first mass scan at 3.0 mm the signal at this peak was found to be at or below the detection limit. When the survey was repeated with a tuning optimized to H_2O, the signal was improved but the species was judged to be barely detectible. Later comparison with the mass 41 signals showed that the response of the two species was similar and mass 43 should have been investigated further.

A rough estimate of the quantity of mass 43 from the scan results can be made. Literature ionization potentials for C_3H_7 molecules are 7.36-8.6 eV (iso-C_3H_7) and 8.09-9.5 eV (n-C_3H_7). IP's for C_2H_3O range from 7.0-8.05 eV (CH_3CO). Because of the overlapping ranges for each species, a single energy of 8.0 eV was chosen to represent all three molecules. It was necessary to use C_2H_2 as the reference species for RICS calibration because CO_2 was not measured in the scans. The estimated mole fractions for both scans are 2 ppm for C_3H_7 and 3-4 ppm for CH_3CO. Error limits are high (-100%, + ≥100%) because of scatter, the calibration method, and the uncertainties involved in quantifying a scan that was optimized for qualitative purposes.

CO_2 and mass 44 low electron energy (CH_3CHO/c-C_2H_4O) profiles.

Only one of several ionization efficiency curves — that taken at 2.5 mm — clearly showed evidence of a second species present at mass 44. The experimental IP for the other species was 10.5-10.7 eV. Acetaldehyde and ethylene oxide have IP's that are close enough, but IP(C_3H_8) is reasonably close at 11.2 eV. If C_3H_8 is present, it is probably in much smaller amounts than the other two species. CH_3CHO was chosen as the species on which the calibration would be based, because of the probable presence of ketene (C_2H_2O) in rich benzene and acetylene flames. Hydrogenation of that species would result in acetaldehyde. There is something of an inconsistency here, however, because ketene was considered not to be a likely identity for mass 42. It is quite possible, though, that mass 42 is a combination of C_2H_2O and other species.

Two data sets were taken, $\frac{x_{EElow}}{x_{CO_2}}$ (RICS) and $\frac{x_{CO_2}}{x_{Ar}}$ (direct calibration). In the first

experiment, "CH_3CHO" and CO_2 were taken at 12.2 eV and 15.8eV. The low-EE signal, adjusted to 15.8eV, was subtracted out from the CO_2 intensity to get a resulting $\frac{I_{EElow}}{I_{CO_2}}$, rather than $\frac{I_{EElow}}{I_{44total}}$.

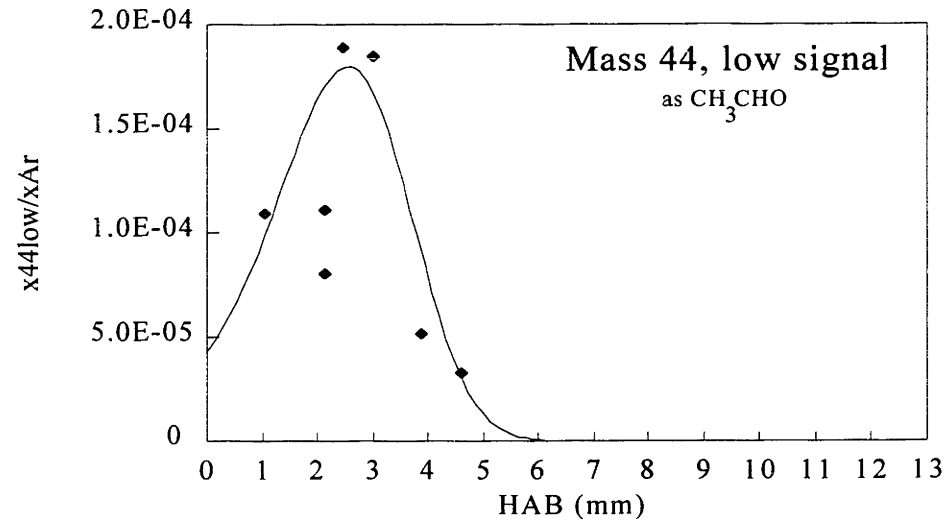

Figure 4.20 Mole fraction of mass 44 (low electron energy signal, calibrated as CH_3CHO) relative to Ar, in a 22 torr laminar, premixed H_2-O_2-C_6H_6-Ar flame. ϕ = 1.79, 31.3% Ar, $(x_{C6H6}/x_{H2})_0$ = 0.010, v_0 = 101 cm/sec. Data points and smoothed curve are shown.

One low-EE data point (2.5 mm) was derived from an ionization efficiency curve. The resulting profile, shown in Figure 4.20 with an admittedly tentative smoothing curve, is rather scattered with a peak in the early portion of the main reaction zone.

For the second data set, CO_2 and argon were measured at 17.4 eV and 19.4 eV, respectively. The smoothed low-EE profile was used to derive a net CO_2 signal. The CO_2 profile is plotted in Figure 4.21. It is not apparent from the three points at 11^+ mm that there is no maximum there, but a smoothing curve which continues to increase was chosen because of the data point at 28.5 mm, which is 2.9×10^{-2}. This is to be expected, as CO peaks somewhere above 10 mm and before 28.5 mm: at 28.5 mm the mole fraction is 15-20% less than at 10-11 mm.

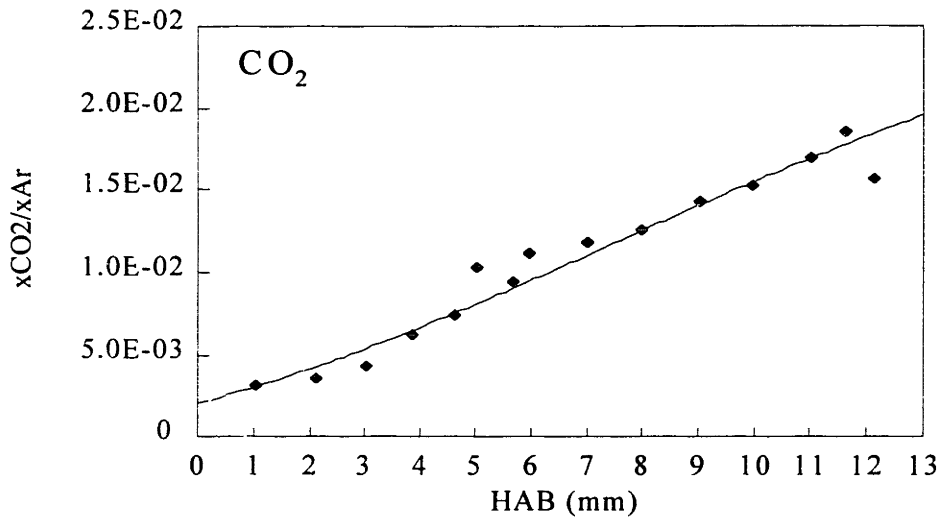

Figure 4.21 Mole fraction of CO_2 relative to Ar, in a 22 torr laminar, premixed H_2-O_2-C_6H_6-Ar flame. ϕ = 1.79, 31.3% Ar, $(x_{C6H6}/x_{H2})_0$ = 0.010, v_0 = 101 cm/sec. Data points and smoothed curve are shown.

Mass 52.

Ionization efficiency curves showed the experimental intercept to be 14.0-14.7 eV, far above the domain of any mass 52 species documented in the literature. Possible parents are masses 54, 78 (benzene), 80, and 82. Fragmentation magnitude analysis shows that only benzene is a viable candidate. An experimental appearance potential measurement showed the onset of mass 52 to be about 14 eV, consistent with that conclusion.

Mass 53-60 profiles.

Mass 56 was the only peak in this range for which an ionization efficiency curve was measured. The signal strengths of the other species did not permit such measurements. The experimental intercept for mass 56 was 10.0±0.3 eV. Unfortunately, five species (CH_2=CHCHO, HC≡CCH_2OH, CH_2=$CHCH_2CH_3$, c-C_4H_8, and c-$C_3H_5(CH_3)$) have IP's at or near that range, and it is impossible to determine which mass 56 might be. Masses 72, 84, 86 and 100 could theoretically be parents, but fragment magnitude analysis rules out any significant contribution from those molecules.

All of the species in this range were measured with respect to CO_2 and calibrated using RICS, with an assumed identity for each. The electron energies used for each species are shown

in Table 4.2. Mass 57 was taken above the AP for possible parents at masses 58, 72, and 86, but fragment magnitude analysis indicates that it is unlikely that any of those species are sufficiently high in concentration to explain the signal at 57. Several mass numbers were measured at two energies because different species of that molecular weight could have significantly different IP's. In the case of mass 58, there is little difference between data taken at either energy. The low-EE data of mass 60 was at or below the detection limit. Only in the case of mass 59 did it appear that two different species coexist, and then only at a height of 1 mm. The data collected

Table 4.2 Electron energies used to measure masses 53-60.

Mass	EE (eV)
44	16.3
53	11.9
54	12.2
55	10.3
56	11.7
57	12.3
58	12.0
58	13.4
59	9.0
59	12.4
60	9.0
60	12.4

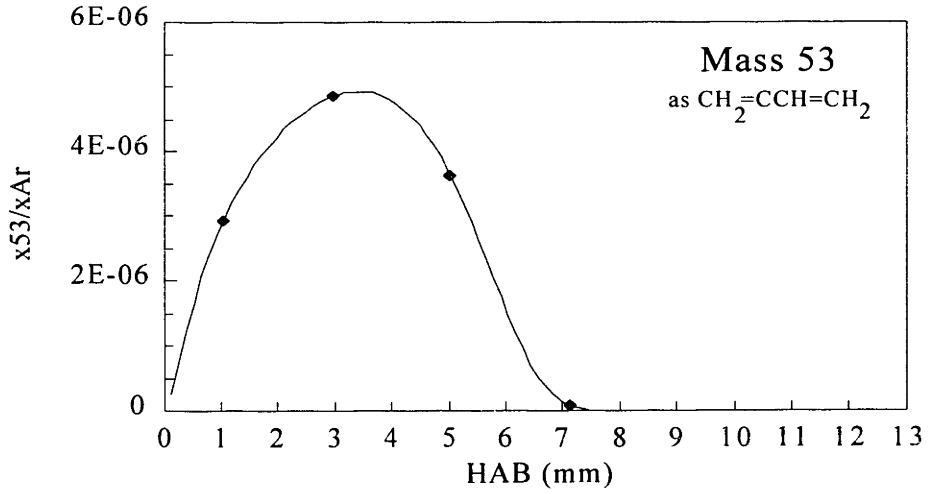

Figure 4.22 Mole fraction of mass 53 (calibrated as CH_2=CCH=CH_2) relative to Ar, in a 22 torr laminar, premixed H_2-O_2-C_6H_6-Ar flame. ϕ = 1.79, 31.3% Ar, $(x_{C6H6}/x_{H2})_0$ = 0.010, v_0 = 101 cm/sec. Data points and smoothed curve are shown.

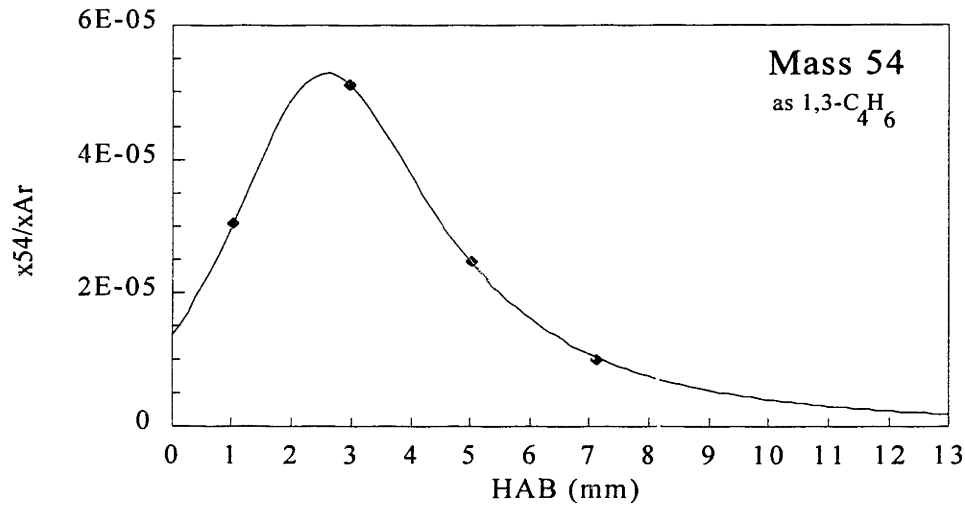

Figure 4.23 Mole fraction of mass 54 (calibrated as 1,3-C_4H_6) relative to Ar, in a 22 torr laminar, premixed H_2-O_2-C_6H_6-Ar flame. ϕ = 1.79, 31.3% Ar, $(x_{C6H6}/x_{H2})_0 = 0.010$, v_0 = 101 cm/sec. Data points and smoothed curve are shown.

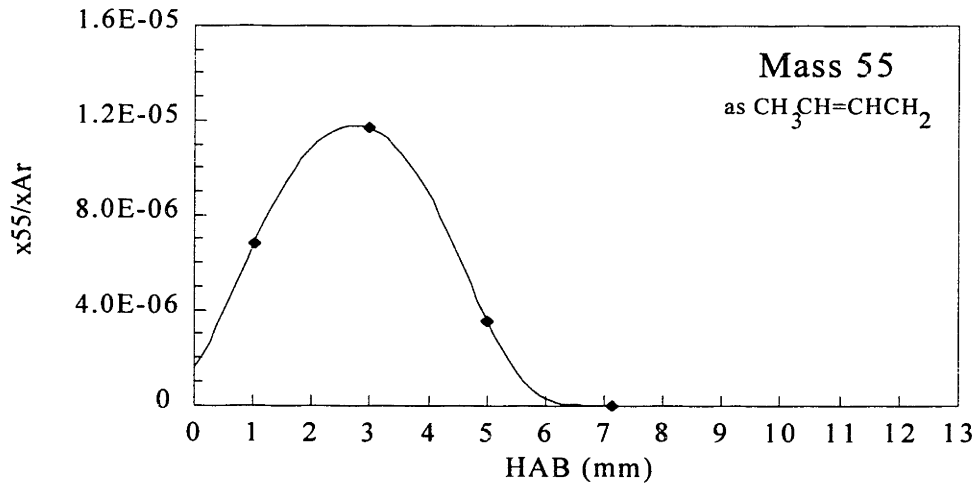

Figure 4.24 Mole fraction of mass 55 (calibrated as $CH_3CH{=}CHCH_2$) relative to Ar, in a 22 torr laminar, premixed H_2-O_2-C_6H_6-Ar flame. ϕ = 1.79, 31.3% Ar, $(x_{C6H6}/x_{H2})_0 = 0.010$, v_0 = 101 cm/sec. Data points and smoothed curve are shown.

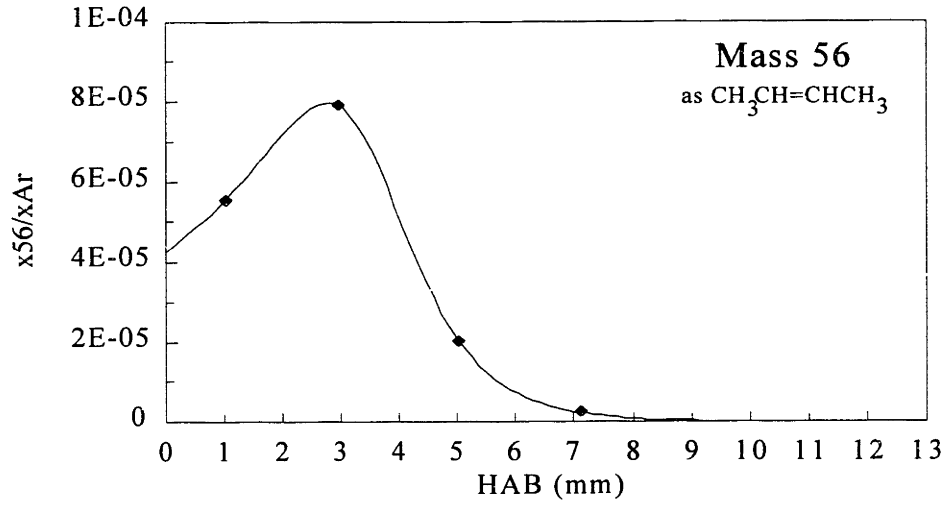

Figure 4.25 Mole fraction of mass 56 (calibrated as $CH_3CH=CHCH_3$) relative to Ar, in a 22 torr laminar, premixed H_2-O_2-C_6H_6-Ar flame. ϕ = 1.79, 31.3% Ar, $(x_{C6H6}/x_{H2})_0 = 0.010$, v_0 = 101 cm/sec. Data points and smoothed curve are shown.

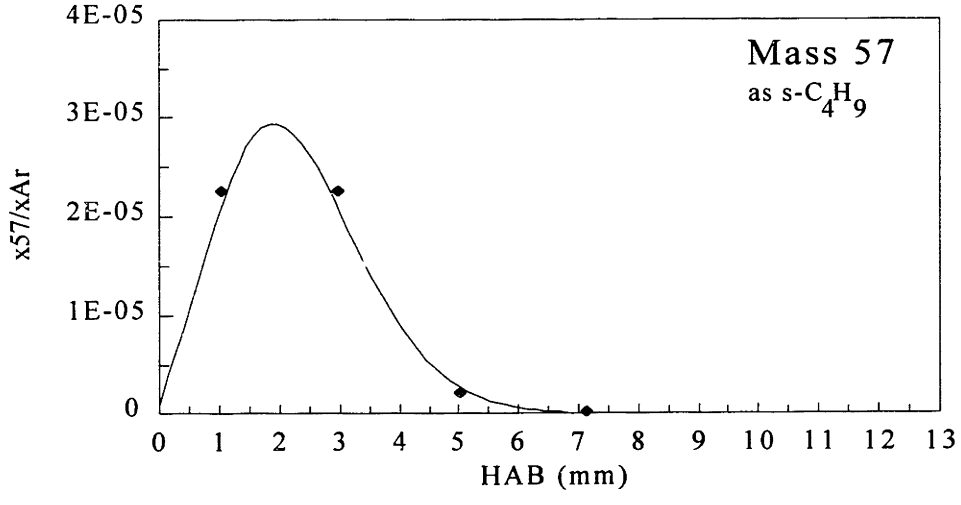

Figure 4.26 Mole fraction of mass 57 (calibrated as s-C_4H_9) relative to Ar, in a 22 torr laminar, premixed H_2-O_2-C_6H_6-Ar flame. ϕ = 1.79, 31.3% Ar, $(x_{C6H6}/x_{H2})_0 = 0.010$, v_0 = 101 cm/sec. Data points and smoothed curve are shown.

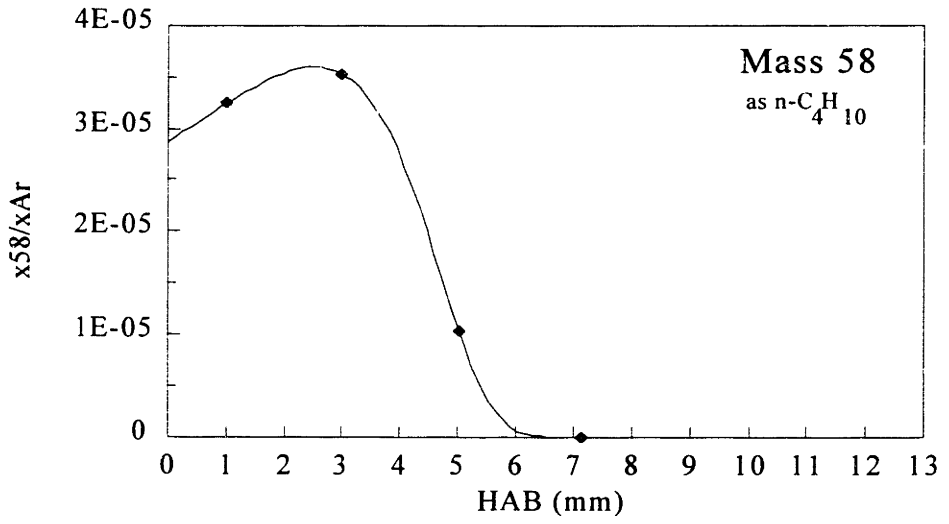

Figure 4.27 Mole fraction of mass 58 (calibrated as n-C_4H_{10}) relative to Ar, in a 22 torr laminar, premixed H_2-O_2-C_6H_6-Ar flame. ϕ = 1.79, 31.3% Ar, $(x_{C6H6}/x_{H2})_0$ = 0.010, v_0 = 101 cm/sec. Data points and smoothed curve are shown.

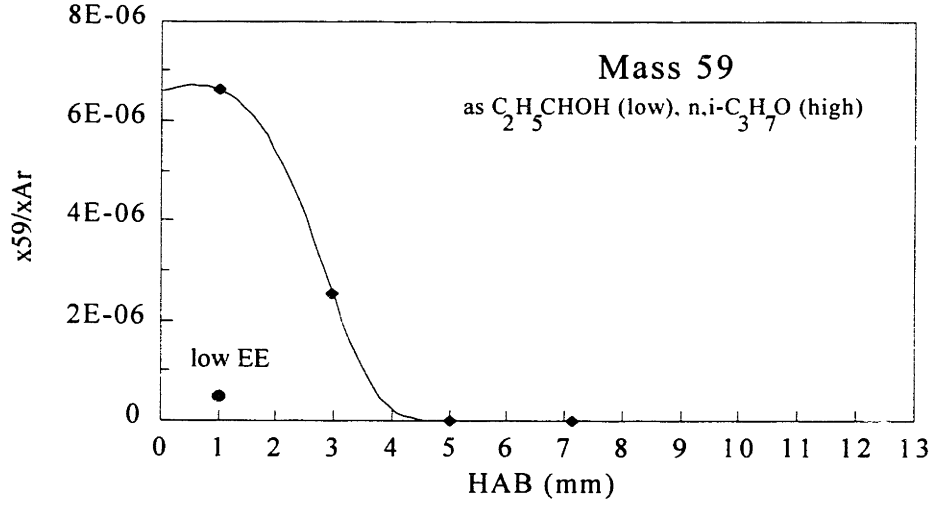

Figure 4.28 Mole fraction of mass 59 (calibrated as C_2H_5CHOH [low EE signal] and n- or i-C_3H_7O [high EE signal]) relative to Ar, in a 22 torr laminar, premixed H_2-O_2-C_6H_6-Ar flame. ϕ = 1.79, 31.3% Ar, $(x_{C6H6}/x_{H2})_0$ = 0.010, v_0 = 101 cm/sec. Data points and smoothed curve are shown.

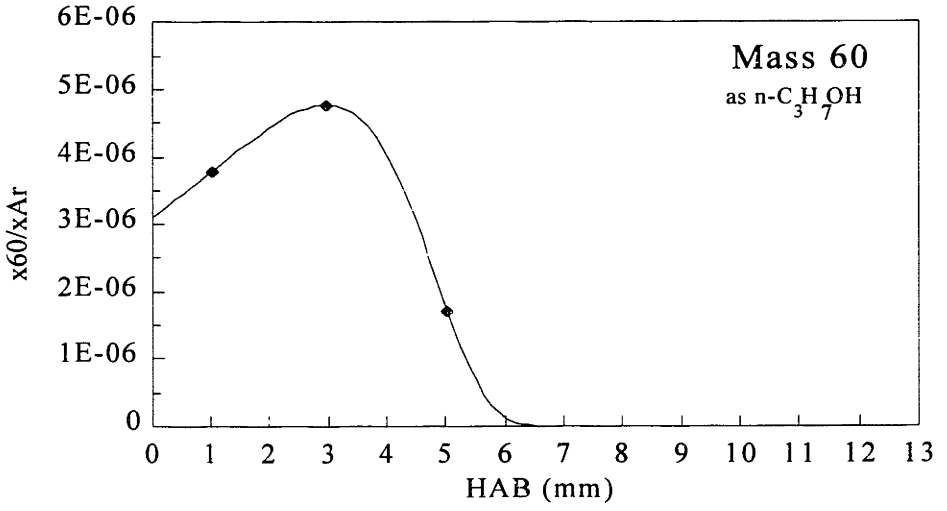

Figure 4.29 Mole fraction of mass 60 (calibrated as n-C_3H_7OH) relative to Ar, in a 22 torr laminar, premixed H_2-O_2-C_6H_6-Ar flame. $\phi = 1.79$, 31.3% Ar, $(x_{C6H6}/x_{H2})_0 = 0.010$, $v_0 = 101$ cm/sec. Data points and smoothed curve are shown.

in this mass range are graphed in Figures 4.22-4.29. Measurements were collected at four HAB's, only adequate for mapping a rough image of the true profiles. The actual locations of the mole fraction maxima could be within about ±1.5 mm of the guessed positions. Nevertheless, the peaks can be seen to reside in approximately the same location as C_2H_4, mass 42, and mass 44 (low-EE species), and are similarly destroyed by 6-7 mm.

If masses 53-58 are indeed nonoxygenated molecules, then the trend toward higher mole fractions of the more hydrogenated species in a radical/stable pair holds true. Of course, another perspective on this mass range is that the concentration of the stable species is usually higher than that of the radical, a phenomenon common to flames. However, it should still be noted that there seems to be a large spectrum of species, each separated by a hydrogen. Masses 59 and 60, much lower in concentration than most of the rest, can only be oxygenated molecules. The most prevalent species in the range are masses 54 and 56, C_4H_6 and C_4H_8 (or C_3H_2O and C_3H_4O).

Mass 65 profile.

This species was present in quantities so low that ionization efficiency curves had to be done in an 'analogue' flame; that is, a flame which is similar to the present one but has more hydrocarbon in it. The conditions chosen were $\phi = 1.3$, $(x_{C6H6}/x_{H2})_0 = 0.029$, 36% Ar, and $v_0 = 82$

cm/sec. Two clear linear sections were found in the curve, the intercept and curve break being at 9.6 eV and 14.4 eV when energy-corrected by the low intercept of benzene (cf. Chapter 3) and 8.4/13.1 eV using the high intercept. In either case, the higher section of the curve can only represent fragmentation from a larger species, most likely phenol and/or c-C_5H_6. The only species with IP's near experimental are c-C_5H_5 (8.41-8.69 eV) and HC=C=C=CO (9.5 eV estimated). Another species with a somewhat close IP is HC≡CCHCH=CH_2 (7.88 eV). As in the case of phenol (see below), it is possible that comparison with the low C_6H_6 intercept is appropriate for the highly resonant c-C_5H_5, in which case the IP and intercept match well. Comparison with the low intercept would be better for C_4HO, for which agreement is also found.

Based on intercepts alone, then, both species would be equally probable. For the purposes of calculation and presentation in this thesis, though, c-C_5H_5 was chosen because:

- Cyclopentadienyl is a well-known product of benzene decomposition (see Chapter 7).
- C_4HO is low in hydrogen, unlike most species found in the H_2-O_2-C_6H_6 flame.

Mass 65 was measured using C_6H_6 as a reference (11.8 eV and 12.8 eV, respectively), and was calibrated by the RICS method. The rather scattered curve is difficult to characterize, but the peak mole fraction appears to be in the 5-8 mm range.

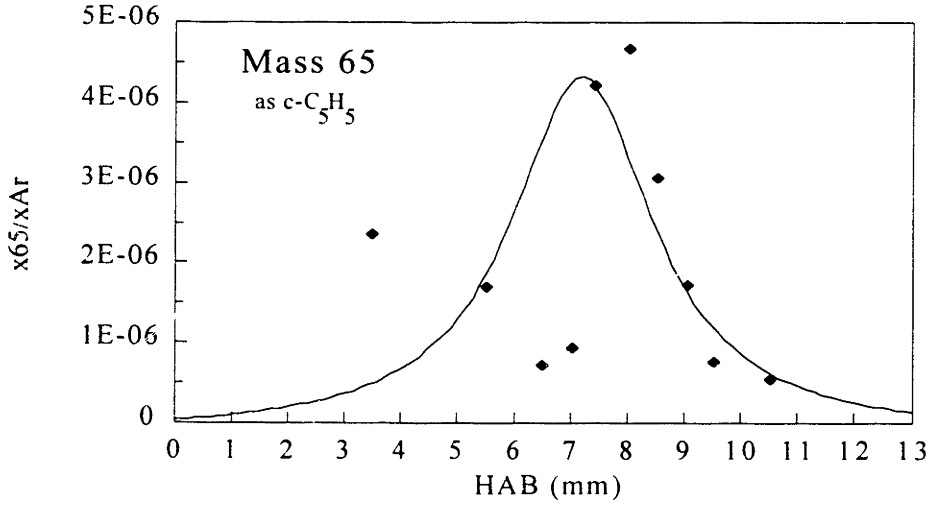

Figure 4.30 Mole fraction of mass 65 (calibrated as c-C_5H_5) relative to Ar, in a 22 torr laminar, premixed H_2-O_2-C_6H_6-Ar flame. ϕ = 1.79, 31.3% Ar, $(x_{C6H6}/x_{H2})_0$ = 0.010, v_0 = 101 cm/sec. Data points and smoothed curve are shown.

Mass 66 profile and mass 67.

The analogue flame (cf. mass 65) was used for the ionization efficiency curves collected for masses 66 and 67. The rather noisy mass 66 ionization efficiency curve had an intercept at 8.7 eV (high intercept of C_6H_6) or 9.5 eV (low intercept of C_6H_6). Table 4.3 documents ionization potentials of various candidate species which are close to the measured value. A molecule (c-C_5H_6) of this weight could also be produced from phenol in the mass spectrometer ionizer, though fragmentation magnitude analysis supports a conclusion that this is not so.

Table 4.3 Literature ionization potentials of candidate mass 66 species.

Species	IP (eV)
Around 8.6 eV:	
c-C_5H_6	8.56-9.00
$CH_3CH{=}CHC{\equiv}CH$	8.50, 9.14
$CH_2{=}C{=}CHCH{=}CH_2$	8.88
Bicyclo[2.1.0]pent-2-ene	8.00, 8.60
c-$C_3H_5C{\equiv}CH$	8.70, 9.58
$CH_2{=}CHC{\equiv}CCH_3$	8.10-9.40
Around 9.5 eV:	
$CH_2{=}C(CH_3)C{\equiv}CH$	9.23-10.10
$CH_2{=}CHC{\equiv}CCH_3$	8.10-9.40
c-$C_3H_5C{\equiv}CH$	8.70, 9.58
$HC{\equiv}CCH{=}C{=}O$	9.6 (estimated by analogy to ketene (Westmoreland, 1986), and revised here.)

The mechanism by which benzene and phenol possess two intercepts in the electron impact ionizer used in this experiment is not clearly understood (cf. Chapter 3), therefore it is not possible to determine if any of the species with IP around 8.6 eV would be expected to be comparable to the high intercept. Mass 66 is probably some form of C_5H_6, linear and/or cyclic, for the following reasons:

- Only one oxygenated species has the requisite IP, and that species (C_4H_2O) has a C/H ratio of 2, which is higher than most other species of similar concentration in the H_2-O_2-C_6H_6 flame.
- Faist (1979) and Vaughn (1988) identified mass 66 as C_5H_6 with GC analysis, in rich flames with benzene as fuel (Faist, GC-MS) or a major fuel component (Vaughn, GC-FTIR).

Mass 66 was calibrated using the RICS method, and was measured at 11.1 eV with respect to C_6H_6 at 11.8 eV. The signal ratio was stable with respect to time and burner position. The mole fraction profile, shown in Figure 4.31, is reasonably low in scatter. The peak occurs in the middle of the reaction zone, and the species persists until the start of the post-flame region.

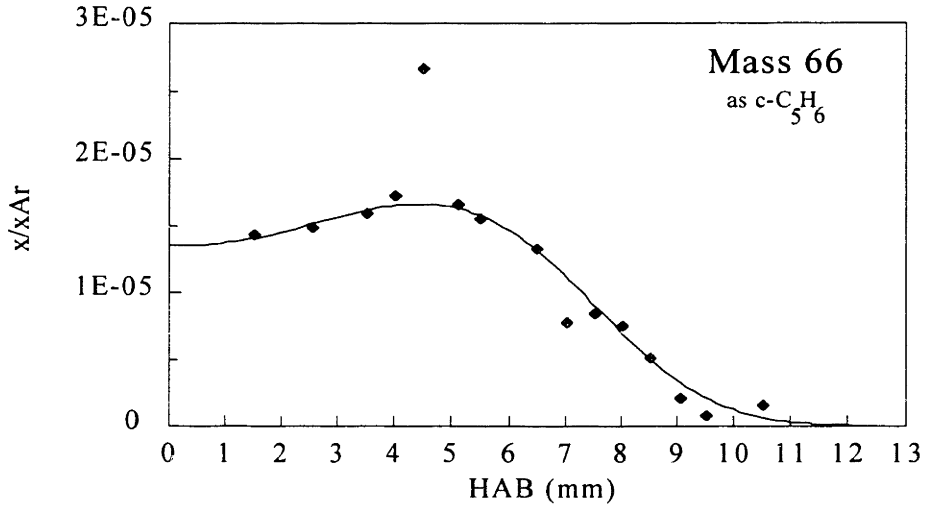

Figure 4.31 Mole fraction of masses 66 (calibrated as c-C_5H_6) relative to Ar, in a 22 torr laminar, premixed H_2-O_2-C_6H_6-Ar flame. ϕ = 1.79, 31.3% Ar, $(x_{C6H6}/x_{H2})_0$ = 0.010, v_0 = 101 cm/sec. Data points and smoothed curve are shown.

Several ionization efficiency curves were performed for mass 67, all of them in the analogue flame because of low signal intensity. The data suffer from a large amount of noise (scatter). The best interpretations yield an intercept of 9.8-10.2 eV, referenced to the low linear section of C_6H_6, 9.2 eV with respect to the upper section. There are no species with IP's of this order; only fragments of masses 68, 82, or 96 could produce the signal seen. There is insufficient information to legitimately perform a fragmentation magnitude analysis. One of the ionization efficiency curves could be read to have a break in the curve, i.e., evidence of a second ionization process. If that interpretation is valid[15], the second process would have an intercept of 7.9/7.0 eV (low/high intercept of C_6H_6 as reference). Five species were found in the IP literature: c-C_5H_7 (7.00 eV), CH_2=CHCHCH=CH_2 (7.25 eV), HC≡CC$(CH_3)_2$ (7.44 eV), HC≡CCHCH_2CH_3 (7.60 eV), and CH_2CHC(=CH_2)CH_2 (7.90 eV). Which of these species might be the mass 67

[15] Bittner (1981) reports no mass 67 species in his rich benzene flame, though he notes that Olson and Calcote (1981) document the presence of natural $C_5H_7^+$.

species (if one exists in the flame) cannot be determined from the existing information. No mass 67 profile was taken.

Mass 68-72 profiles.

A single ionization efficiency curve was made for mass 68, in the analogue flame. The experimental intercept of the rather noisy curve was 8.9 eV relative to the low intercept of benzene, and 8.0 eV with respect to the upper linear portion. As Table 4.4 shows, only one species was found with an IP around 8.0 eV. Most of the mass 68 isomers in the literature do in fact have IP's close to 8.9 eV.

Table 4.4 Literature ionization potentials of candidate mass 68 species.

Species	IP (eV)
Around 8.0 eV:	
CH_2=CHCH=C=O	8.29
Around 8.9 eV:	
c-C_4H_4O	8.8-9.04
CH_3CH=C=C=O	8.68
CH_2=C(OH)C≡CH	8.92
1-CH_3-c-C_3H_3-(=O)	9.15
c-C_3H_4(=C=O)	8.78
c-C_5H_8	9.0-9.27
CH_2=CHCH=$CHCH_3$	8.6-8.68
CH_3CH=C=$CHCH_3$	9.13
CH_2=CHC(CH_3)=CH_2	8.85-9.04
CH_2=C=C(CH_3)$_2$	8.9-9.02
CH_2=C=$CHCH_2CH_3$	9.22-9.25
c-C_4H_6=CH_2	9.16-9.35
Bicyclo[2.1.0]pentane	8.7
AP from c-C_5H_8=CH_2 (mass82)	9.2

Table 4.5 Electron energies used to measure masses 68-72.

Mass	EE (eV)
68	11.0
68	11.6
69	9.6
70	11.7
70	11.4
71	9.4
71	11.6
72	12.6
72	11.8
78	11.2

In keeping with the assumed assignment of masses 66 and 67 to C_5H_x species, and the general trend regarding the existence and relative importance of more hydrogenated species in a series, masses 68-72 were assumed to be nonoxygenated for calibration purposes. The electron energies used for the RICS measurements made with respect to benzene are documented in Table 4.5. Where two energies were used, the objective was to distinguish between any two (or more) species that had different IP's. In every case, measurements made at both energies were nearly the same. The average of the two was used as a final data point at each HAB. The higher benzene intercept was arbitrarily chosen to be the basis for the RICS energy offset; to convert to the other assumption, the data shown in Figures 4.32-4.35 should be multiplied by 1.8.

As with the data in the 50's mass range, there were fewer data points collected for masses 68-72 than are necessary to determine the shapes accurately, locations and magnitudes of the mole fraction profiles. With that caveat stated, the species in this range do seem to be very similar to masses 53-60 in regard to those profile characteristics. This also holds true with respect to the greater amount of the stable species in a radical/stable pairing and the wide spectrum of species (starting at mass 65) separated by one mass number.

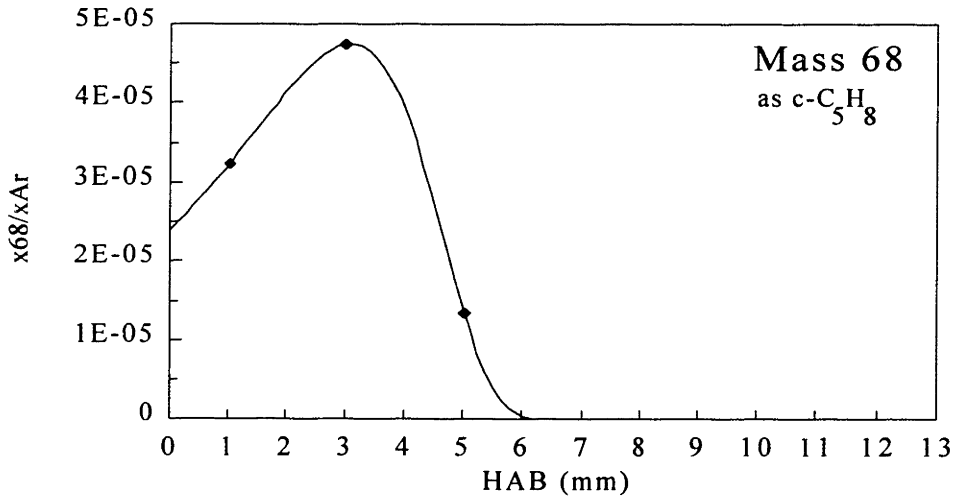

Figure 4.32 Mole fraction of mass 68 (calibrated as c-C_5H_8) relative to Ar, in a 22 torr laminar, premixed H_2-O_2-C_6H_6-Ar flame. ϕ = 1.79, 31.3% Ar, $(x_{C6H6}/x_{H2})_0$ = 0.010, v_0 = 101 cm/sec. Data points and smoothed curve are shown.

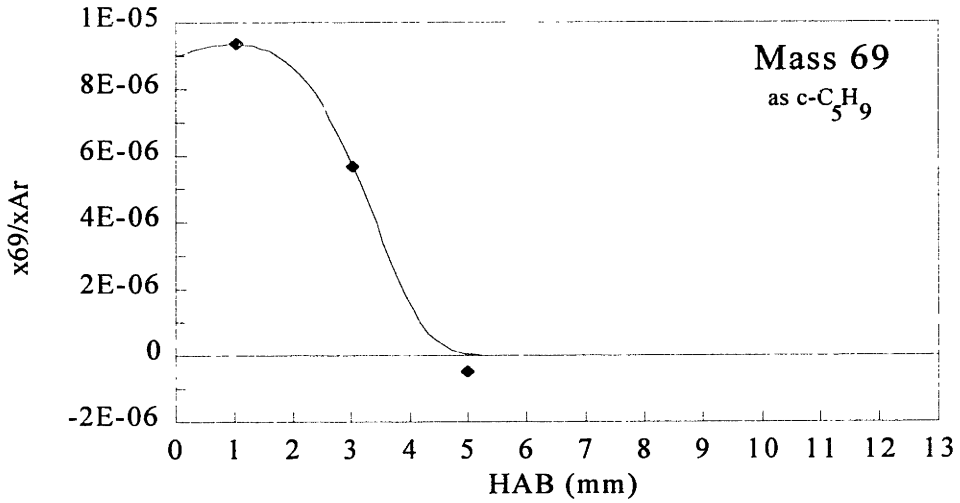

Figure 4.33 Mole fraction of mass 69 (calibrated as c-C_5H_9) relative to Ar, in a 22 torr laminar, premixed H_2-O_2-C_6H_6-Ar flame. ϕ = 1.79, 31.3% Ar, $(x_{C6H6}/x_{H2})_0$ = 0.010, v_0 = 101 cm/sec. Data points and smoothed curve are shown.

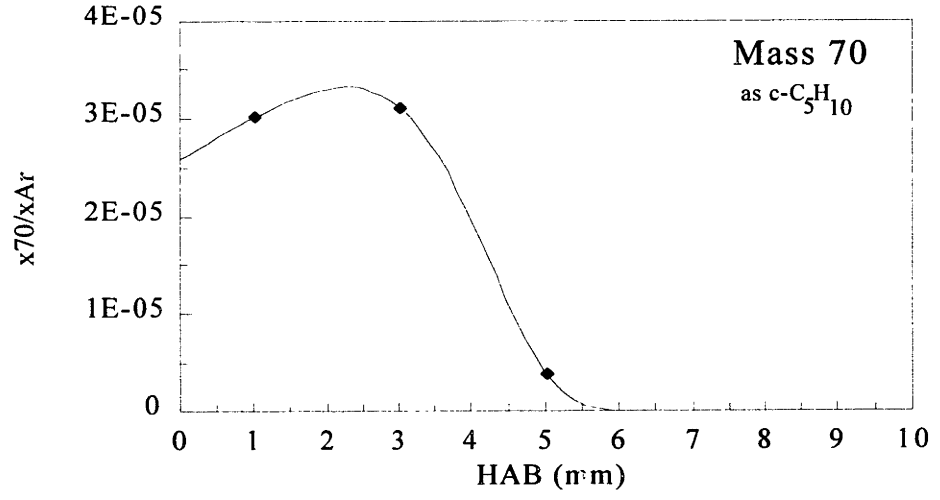

Figure 4.34 Mole fraction of mass 70 (calibrated as c-C_5H_8) relative to Ar, in a 22 torr laminar, premixed H_2-O_2-C_6H_6-Ar flame. ϕ = 1.79, 31.3% Ar, $(x_{C6H6}/x_{H2})_0$ = 0.010, v_0 = 101 cm/sec. Data points and smoothed curve are shown.

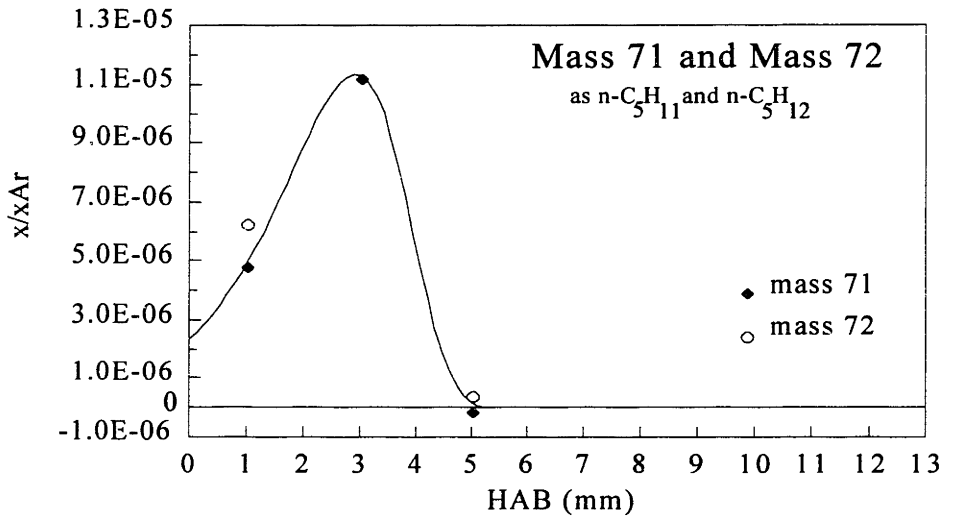

Figure 4.35 Mole fraction of masses 71 and 72 (calibrated as n-C_5H_{11} and n-C_5H_{12}) relative to Ar, in a 22 torr laminar, premixed H_2-O_2-C_6H_6-Ar flame. ϕ = 1.79, 31.3% Ar, $(x_{C6H6}/x_{H2})_0$ = 0.010, v_0 = 101 cm/sec. Data points and smoothed curve are shown.

C_6H_5 profile.

Ionization efficiency curves established the experimental AP of phenyl from C_6H_6 at 14.2 eV (first signal appearing at 12.7-13.0 eV), at least 3 eV above the IP of 8.25. The ionization potential of mass 77 could not be experimentally determined because the signal was too low.

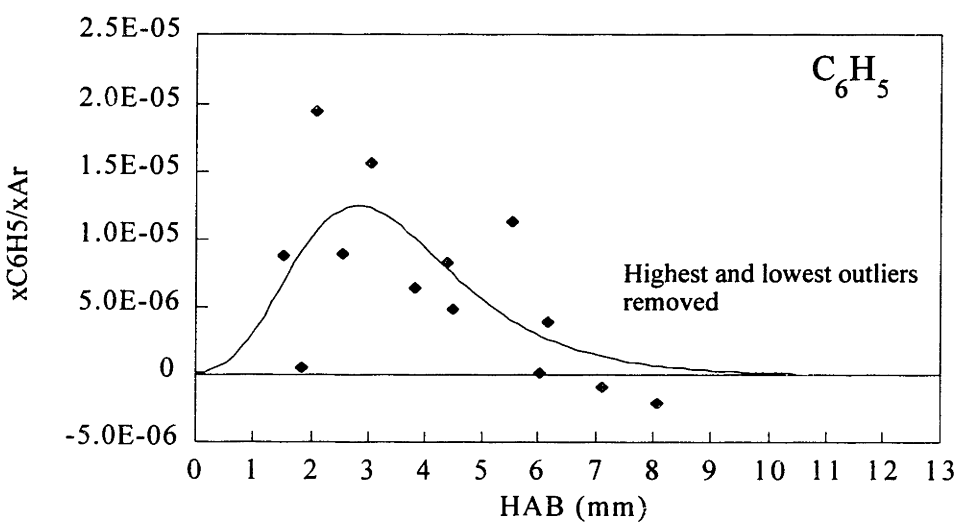

Figure 4.36 Mole fraction of C_6H_5 relative to Ar, in a 22 torr laminar, premixed H_2-O_2-C_6H_6-Ar flame. ϕ = 1.79, 31.3% Ar, $(x_{C6H6}/x_{H2})_0$ = 0.010, v_0 = 101 cm/sec. Data points and smoothed curve are shown.

C_6H_5 was measured at 12.1-2 eV, below any signal attributable to C_6H_6 fragmentation. Naturally, RICS calibration was used with benzene as a reference, collected at 1 eV higher. The resulting profile is exceptionally scattered (Figure 4.36), with the maximum occurring in the 1-4 mm range.

As will be shown in Chapter 7, modelling results are more consistent in a number of ways with a peak location in the 4-7 mm region. Furthermore, Bittner found phenyl to be centered at about 6.2 mm, after correction of the HAB scale for probe effects, in a rich benzene flame. In most other respects, the features of benzene destruction are the same in that flame and the H_2-O_2-C_6H_6-Ar flame measured here. Since the profile almost appears to follow that of benzene, the question could be raised as to whether the C_6H_5 measured here was not augmented by fragmentation after all. Bittner (1981) has suggested that some linear C_6H_6 or C_6H_8 species could contribute to the mass 77 signal at energies lower than the AP of phenyl from benzene. Indeed, some of those species have AP's in the range 10.2-12.7 eV, and therefore could theoretically be partially responsible for the early peak of mass 77. However, a steady-state prediction of l-C_6H_6 (see Section 7.2.2) shows that its mole fraction is far too small (~4×10^{-7} at most) to contribute to the mass 77 signal. Mass 80 does look similar in shape and location to C_6H_6, but is unlikely to be the source of much of the mass 77 signal since (1) its mole fraction is just a bit above that of mass 77, (2) the AP is the highest in the range cited (12.7 eV), and (3) cyclohexadiene isomers

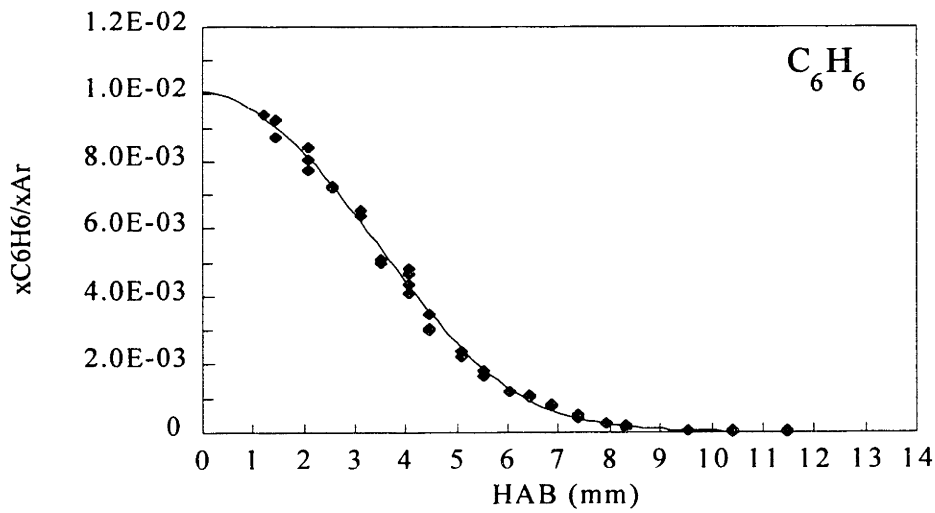

Figure 4.37 Mole fraction of C_6H_6 relative to Ar, in a 22 torr laminar, premixed H_2-O_2-C_6H_6-Ar flame. ϕ = 1.79, 31.3% Ar, $(x_{C6H6}/x_{H2})_0$ = 0.010, v_0 = 101 cm/sec. Data points and smoothed curve are shown.

have AP's of 13.9 eV.

C_6H_6 profile.

Benzene was calibrated directly with respect to argon, eliminating any possible ambiguity deriving from the multiple intercepts (cf. Chapter 3). The electron energies used were 17.2 eV (Ar) and 13.2 eV (C_6H_6). No signal drift or hysteresis was seen. The data are smooth, as Figure 4.37 reveals.

Mass 79.

Attempts were made to detect a cyclohexadienyl radical signal at mass 79. In every case, the signal was experimentally indistinguishable from the empirically-determined isotopic signal of C_6H_5D and $^{13}CC_5H_6$. If "detectable" is defined as one-fifth of the isotopic signal, then cyclohexadienyl — or to be more precise, mass 79 — is at most about 55 ppm, at the burner surface.

Mass 80-86 profiles.

Two ionization efficiency curves were taken of mass 80, one of them in the analogue flame. It was necessary to correct the signals for the contribution of $C_6H_4D_2$, $^{13}C_2C_4H_6$ and $^{13}CC_4H_5D$. The average experimental IP's were 9.2 eV relative to the lower intercept of benzene and 8.2 eV with respect to the upper. Table 4.6 lists the species with IP's close to 8.2 or 9.2 eV. There are clearly too many legitimate alternatives for a definitive identity to be established. Which intercept of benzene would be appropriate

Table 4.6 Literature ionization potentials of candidate mass 80 species.

Species	IP (eV)
Around 9.2 eV:	
2,4-cyclopentadiene-1-one (C_5H_4O)	9.49
1,4-c-C_6H_8	8.65-8.82
$CH_3C4CC(CH_3)=CH_2$	8.72
$C_2H_5C4CCH=CH_2$	8.91
1,3-c-$C_4H_4(CH_2)_2$	9.08
$C_4H_4(=CH_2)_2$ [generic]	8.77
AP from c-$C_5H_8=CH_2$ (mass 82)	8.70
Around 8.2 eV:	
2-c-$C_5H_5(CH_3)$	8.40
1-c-$C_5H_5(CH_3)$	8.40
1,2,trans-4-C_6H_8	8.32
2,3,5-C_6H_8	8.56
cis-$CH_2=CHCH=CHCH=CH_2$	8.31
trans-$CH_2=CHCH=CHCH=CH_2$	8.29

Species	IP (eV)
1,3-c-C_6H_8	8.30
1,3-c-$C_5H_5(CH_3)$	8.29-8.45
3-C_5H_6=CH_2	8.40
(E)-CH_2=C=CHCH=$CHCH_3$	8.32
CH_3CH=C=CHCH=CH_2	8.56

Table 4.7 Electron energies used to measure masses 80-86.

Mass number	EE (eV)
78	12.4
80	11.12
81	11.7
82	12.25
83	12.25
84	12.25
85	10.52
86	13.37

for comparison is also unknown. Because the mole fractions of masses 80-85 (Figures 4.38-4.43) follow that of benzene closely, and because of the extent of hydrogenation seen in the rich H_2-O_2 environment, species in this range were calibrated as C_6H_x and not C_6H_yO. Cyclic C_6's were chosen as the likely species on the basis of products found in low-temperature studies of benzene reacting with H (Sauer and Ward, 1967; Kim et al., 1973; Hoyermann et al., 1975). The

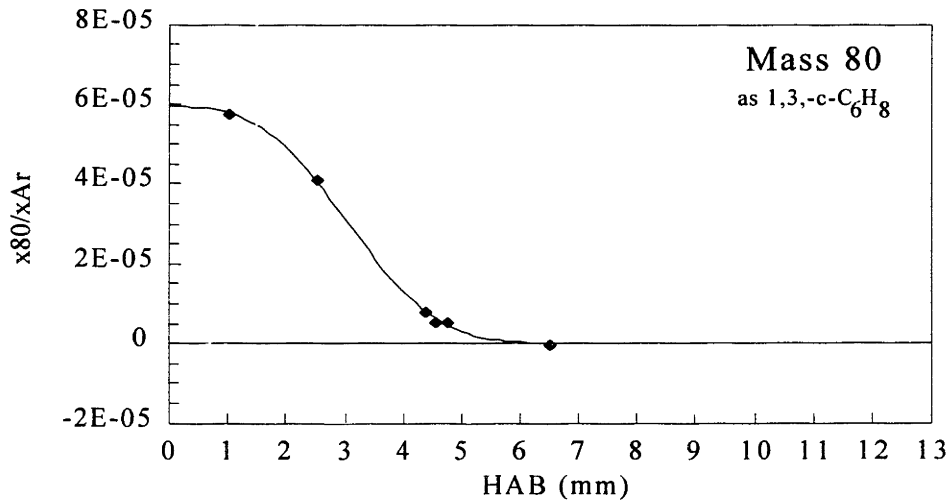

Figure 4.38 Mole fraction of mass 80 (calibrated as 1,3-c-C_6H_8) relative to Ar, in a 22 torr laminar, premixed H_2-O_2-C_6H_6-Ar flame. ϕ = 1.79, 31.3% Ar, $(x_{C6H6}/x_{H2})_0$ = 0.010, v_0 = 101 cm/sec. Data points and smoothed curve are shown.

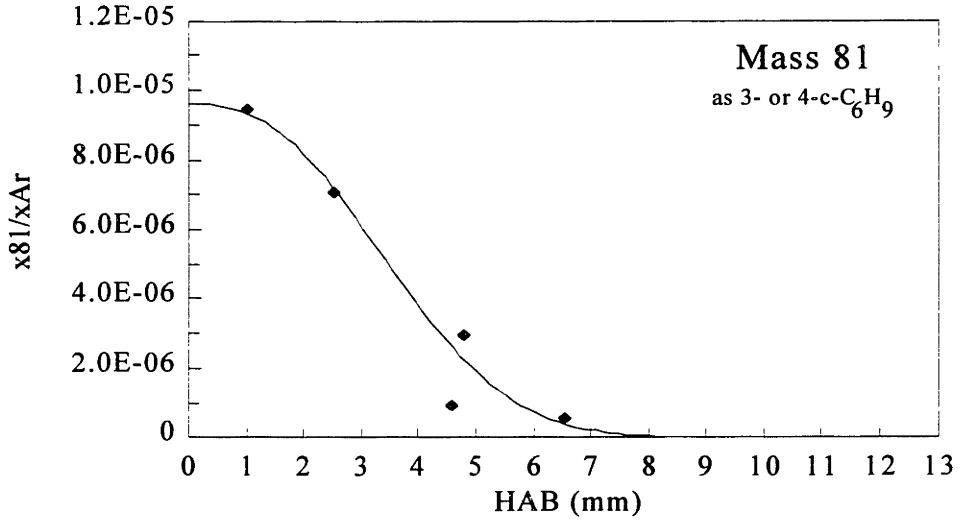

Figure 4.39 Mole fraction of mass 81 (calibrated as 3- or 4-c-C_6H_9) relative to Ar, in a 22 torr laminar, premixed H_2-O_2-C_6H_6-Ar flame. ϕ = 1.79, 31.3% Ar, $(x_{C6H6}/x_{H2})_0$ = 0.010, v_0 = 101 cm/sec. Data points and smoothed curve are shown.

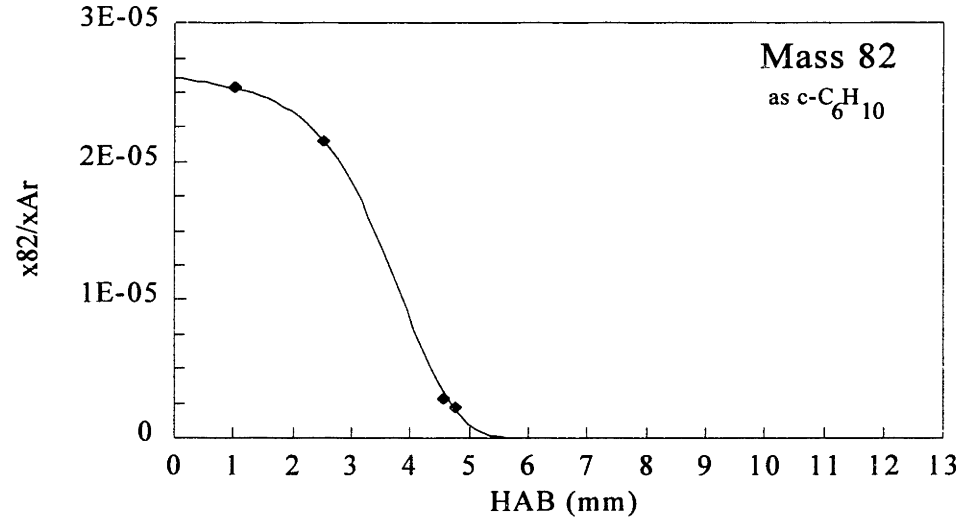

Figure 4.40 Mole fraction of mass 82 (calibrated as c-C_6H_{10}) relative to Ar, in a 22 torr laminar, premixed H_2-O_2-C_6H_6-Ar flame. ϕ = 1.79, 31.3% Ar, $(x_{C6H6}/x_{H2})_0$ = 0.010, v_0 = 101 cm/sec. Data points and smoothed curve are shown.

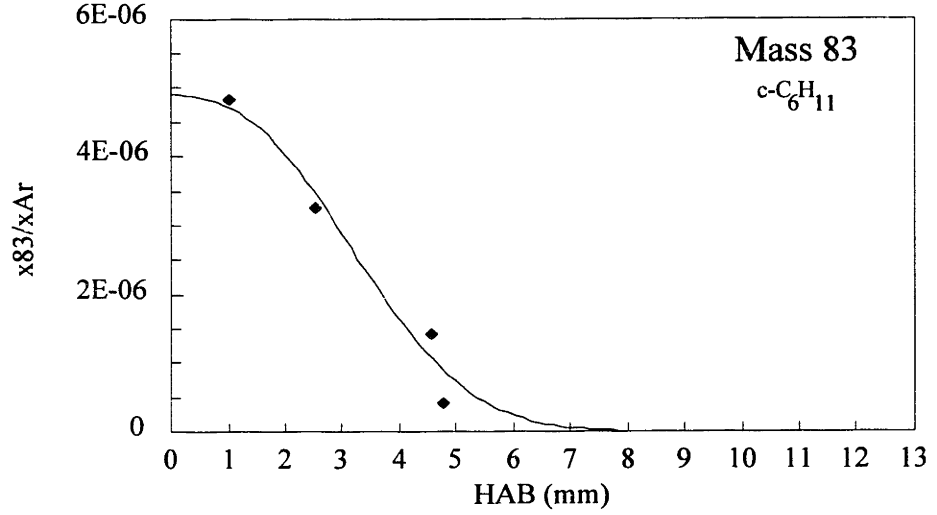

Figure 4.41 Mole fraction of mass 83 (calibrated as c-C_6H_{11}) relative to Ar, in a 22 torr laminar, premixed H_2-O_2-C_6H_6-Ar flame. ϕ = 1.79, 31.3% Ar, $(x_{C6H6}/x_{H2})_0$ = 0.010, v_0 = 101 cm/sec. Data points and smoothed curve are shown.

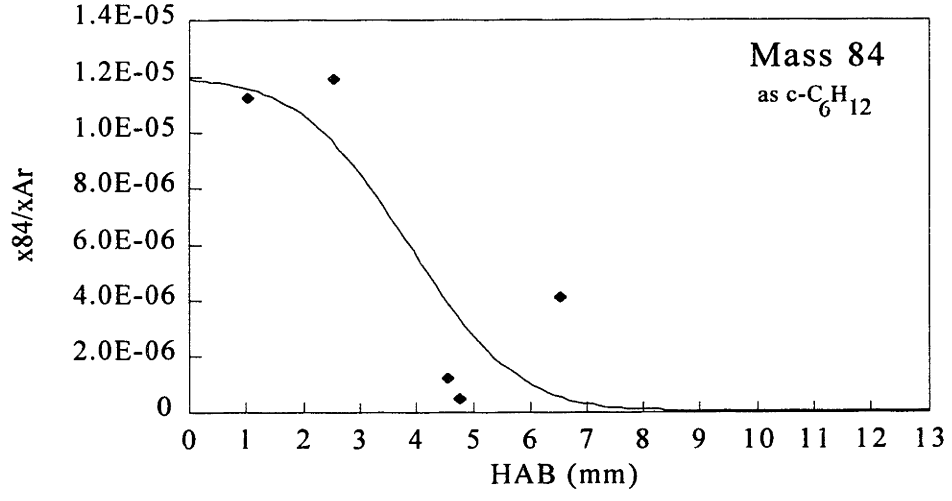

Figure 4.42 Mole fraction of mass 84 (calibrated as c-C_6H_{12}) relative to Ar, in a 22 torr laminar, premixed H_2-O_2-C_6H_6-Ar flame. ϕ = 1.79, 31.3% Ar, $(x_{C6H6}/x_{H2})_0$ = 0.010, v_0 = 101 cm/sec. Data points and smoothed curve are shown.

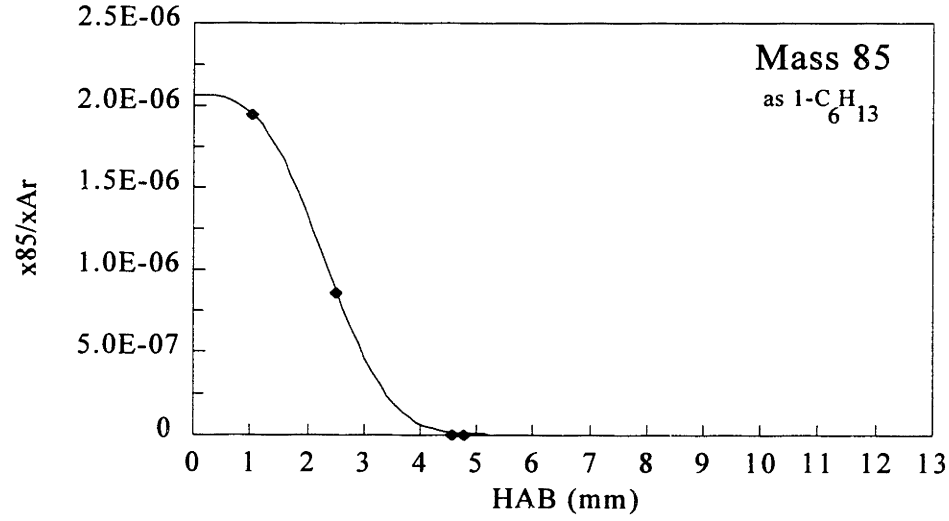

Figure 4.43 Mole fraction of mass 85 (calibrated as 1-C_6H_{13}) relative to Ar, in a 22 torr laminar, premixed H_2-O_2-C_6H_6-Ar flame. ϕ = 1.79, 31.3% Ar, $(x_{C6H6}/x_{H2})_0$ = 0.010, v_0 = 101 cm/sec. Data points and smoothed curve are shown.

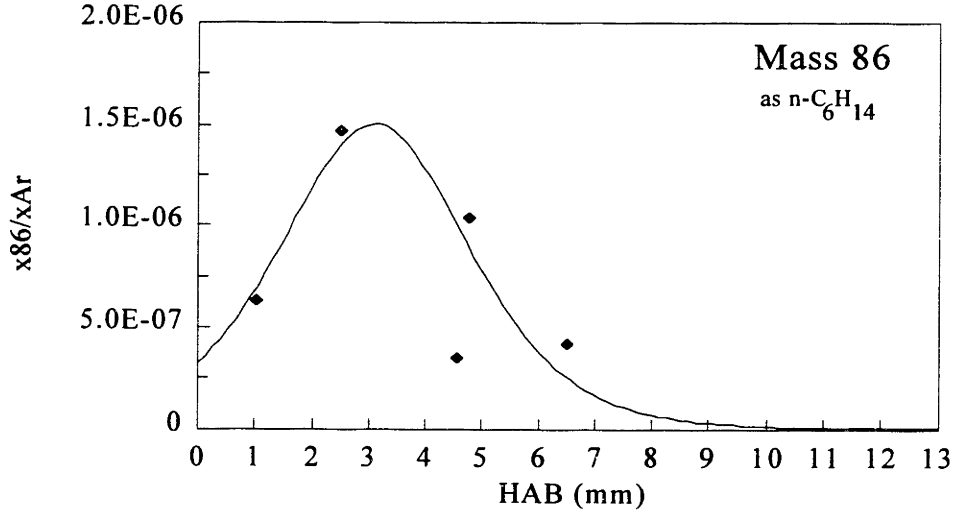

Figure 4.44 Mole fraction of mass 86 (calibrated as n-C_6H_{14}) relative to Ar, in a 22 torr laminar, premixed H_2-O_2-C_6H_6-Ar flame. ϕ = 1.79, 31.3% Ar, $(x_{C6H6}/x_{H2})_0$ = 0.010, v_0 = 101 cm/sec. Data points and smoothed curve are shown.

RICS method was used, with the reference species being benzene and the EE's listed in Table 4.7.

As with the other mass numbers for which few data points were collected, the smoothed profiles drawn in the figures are only schematic and not necessarily accurate. The purpose is served, though, of establishing the general trends for each species. Except for mass 86, all the profiles in this mass range appear to peak at or near the burner surface. Given the positioning of the lower molecular weight ranges (53-60 and 67-72), C_2H_4, and (possibly) C_3H_6, this suggests a potential scenario for benzene destruction of sequential hydrogenation followed by a series of decompositions into hydrocarbon fragments. For example,

$$c\text{-}C_6H_9 \rightarrow 1\text{-}C_6H_9 \rightarrow \underset{\beta\text{-scission}}{\rightarrow} \quad C_2H_2+C_2H_3+C_2H_4$$

The first step in the process, addition of hydrogen to benzene, is examined in some detail in Chapter 7.

Having peaks at or close to the burner suggests the possibility that these species might be contaminants in the benzene feedstock. To ensure that this was not the case, a sample of the benzene was sent to Herbert V. Shuster, Inc. for GC analysis of $c\text{-}C_6H_8$, $c\text{-}C_6H_{10}$ and $c\text{-}C_6H_{12}$. If mass 82 is not produced in the flame, it would have to be a contaminant at a level of $2.6x10^3$ ppm in order to explain the signal observed; the species was not detected. Mass 84 would have to be present at $1.2x10^3$ ppm, and was found at only 5.8 ppm. Cyclohexadiene would have had to be $5.9x10^3$ ppm, yet was not detected. Complete documentation of the laboratory methods and results is given in Appendix P.

In the several weeks prior to collection of data, cyclohexadiene and cyclohexene were used in the effusive source, for the purpose of tuning the mass spectrometer. Tests revealed that either one or both of the compounds was absorbed in the gas lines, along with C_6H_6, because signals for mass 78 and mass 80 were present when the effusive source gate valve was opened, and the amount of 80 was greater than the expected isotopic benzene. A contribution of effusive source contamination to the mass 80 data that was taken was ruled out because:

- the effusive source gate valve was closed during the data experiment,
- the mass 80-86 signals were a function of the burner position, reproducible for movements of the burner back and forth, and
- the mass 80-86 signals dropped to zero in the middle-to-late reaction zone.

Masses 91 and 92.

Although initially discounted because of their poor signal response during general species scans, masses 91 and 92 fared better in the high mass scans, which were tuned more specifically for molecules of their size. The signals were still quite low, so no profiles were measured. The results of the high mass scans were converted into crude data points which are plotted in Figures 4.45 and 4.46. For comparison, the same was done with the results of the early general scans. Benzene and C_6H_5OH (mass 94) were variously used as reference species. The quality of these data must be considered quite poor because of the low S/N ratio, and the use of mass spectrometer tunings which were not truly good enough for accurate data collection. (On the other hand, the high mass scan data taken for mass 95 proved to be in reasonable agreement with more carefully collected values, Figure 4.49.) Estimating the error would involve a factor for a tuning which was optimized more for signal level than accuracy, plus an increase in the factor for scatter (cf. Appendix A). Tuning error can very roughly be estimated to be about ±25%. For pulse counting data, the scatter is generally attributed to white noise, which is quantified by the statistical average of the square root of the signal (Fite et al., 1980). Signal levels for masses 91 and 92 in the high mass scans ranged from only 6-45 counts. For the worse-case scenario of 6 counts, the combined RICS error (factor of two) plus tuning and noise errors is a factor of two on the high side (the maximum) and three on the low side. It is clear to see from the points belonging

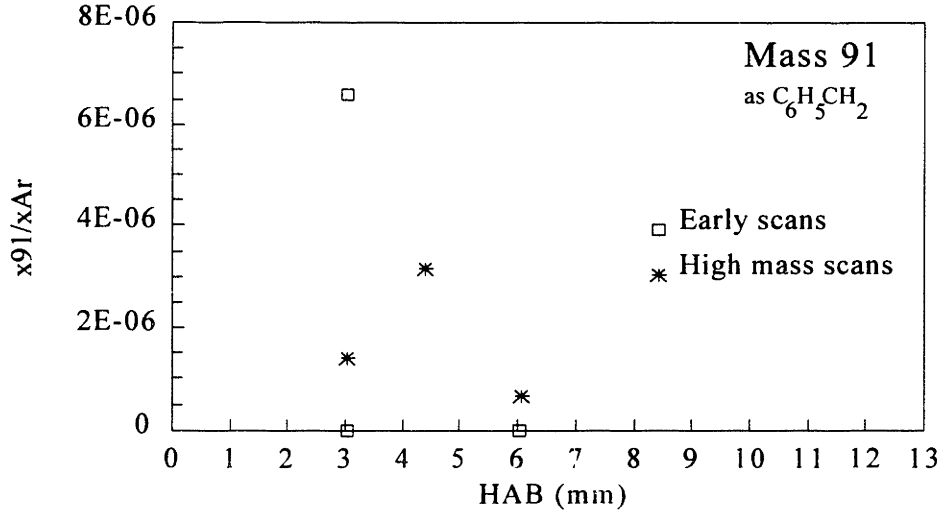

Figure 4.45 Mole fraction of mass 91 (calibrated as $C_6H_5CH_2$) relative to Ar, in a 22 torr laminar, premixed H_2-O_2-C_6H_6-Ar flame. $\phi = 1.79$, 31.3% Ar, $(x_{C6H6}/x_{H2})_0 = 0.010$, $v_0 = 101$ cm/sec.

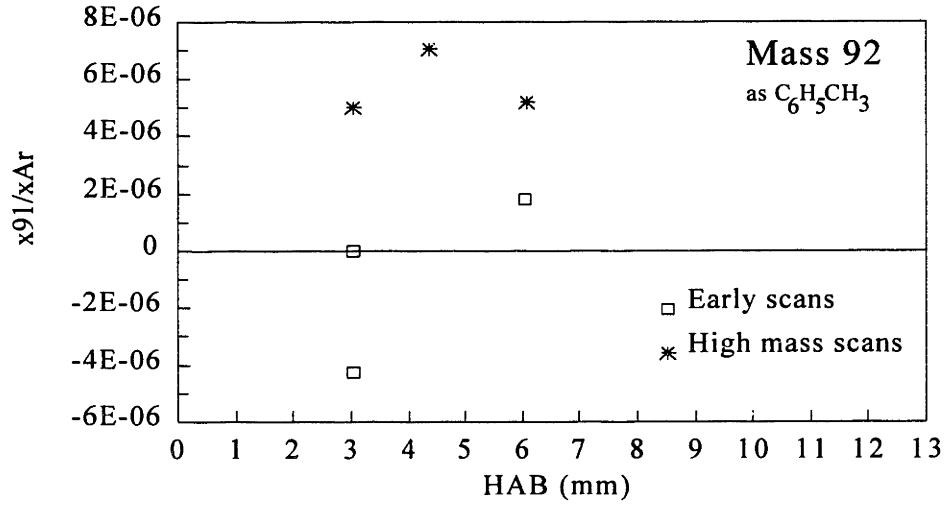

Figure 4.46 Mole fraction of mass 92 (calibrated as $C_6H_5CH_3$) relative to Ar, in a 22 torr laminar, premixed H_2-O_2-C_6H_6-Ar flame. $\phi = 1.79$, 31.3% Ar, $(x_{C6H6}/x_{H2})_0 = 0.010$, $v_0 = 101$ cm/sec.

to different sets that the actual reproducibility is much worse than that, showing how species that are too close to the detection limit exhibit fluctuation or scatter beyond that expected from white noise. Therefore, evaluations of the error for such species are not useful. The results can therefore best be summarized by saying that at most, these species are present at the ppm level.

Mass 93.

No ionization efficiency curve could be made for mass 93 because of its low signal intensity. Data were collected at 11.1 eV (high intercept of C_6H_6 as energy reference), under the assumption that the species is phenoxy. C_6H_6, the reference species for RICS calibration, was taken at 11.8 eV. The results are shown in Figure 4.47, along with estimates derived from the various scans. While it seems likely that mass 93 is present in some small amount, the high scatter shows that quantity to be just at the detection limit, which would probably be in the low ppm range. No smoothed curve was attempted.

Bittner (1981) was unable to detect mass 93 in a $\phi = 1.8$, C_6H_6-O_2-Ar flame, using analog signal measurement. The pulse counting technique used here is more sensitive, hence the ability to detect some signal, even with much lower initial benzene concentration. Using this technique, mass 93 was also detected in the $\phi = 1.8$ flame of Bittner. However, the type of experiment required to quantify the mole fraction was not performed.

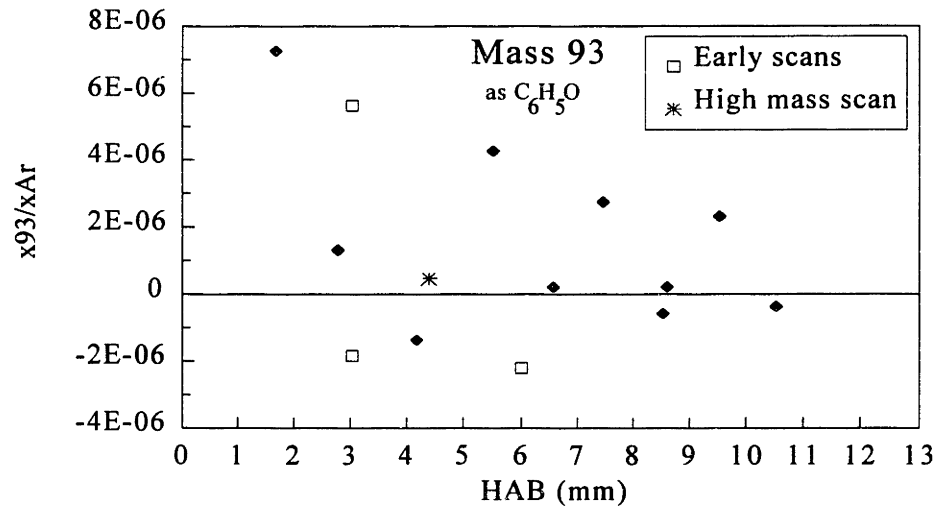

Figure 4.47 Mole fraction of mass 93 (calibrated as C_6H_5O) relative to Ar, in a 22 torr laminar, premixed H_2-O_2-C_6H_6-Ar flame. ϕ = 1.79, 31.3% Ar, $(x_{C6H6}/x_{H2})_0 = 0.010$, v_0 = 101 cm/sec.

Mass 94 profile (C_6H_5OH).

As discussed in Chapter 3, the ionization efficiency curve of pure phenol is very similar to that of benzene, in terms of the presence the two linear sections and an identical energy scale correction. Ionization efficiency curves were measured in the analogue flame, and were comparable to the pure gas measurements in both the existence of two linear sections, and the intercepts themselves (when photoionization or photoelectron IP's are used as reference). Several other species, listed in Table 4.8, have IP's close to phenol's 8.5 eV, or the 9.3 eV which the experimental mass 94 intercept would be if compared to the low intercept of benzene. Despite of the large number of species in this list, the species was identified as phenol because of (a) the excellent agreement of ionization efficiency curves with those of pure C_6H_5OH, and (b) Bittner's determination of mass 94 to be phenol[16] in his rich benzene flame.

Phenol was calibrated by the RICS method, with benzene as the reference species. C_6H_5OH was measured at 11.6 eV (energy corrected by higher intercept), benzene at 12.6 eV. The data are not smooth (see Figure 4.48), but are sufficiently numerous that a reasonable smoothed curve can be drawn through the points. Within the bounds of scatter, no burner position hysteresis was found. To examine the effect of a different but possible choice of smoothing

[16] Based on the experimental IP and products of C_6H_6+O_2 found in low-temperature studies. Another relevant study performed since then was Baldwin et al. (1986), in which small amounts of C_6H_6 were added to H_2-O_2 mixtures at 773K.

curve on the derived net rate, a second curve was drawn which went through the data points but had very different slopes at crucial points. As the flux and net rate are dependent on slope, the maximum possible slopes were chosen for peak region of the alternate curve.

Table 4.8 Ionization potential of candidate mass 94 species (except phenol).

Species	IP (eV)
$HC{\equiv}CC(C_2H_5){=}CHCH_3$	8.70
$C_2H_5C{\equiv}CC(CH_3){=}CH_2$	8.66
$CH_2{=}CHC(CH_3){=}CHCH{=}CH_2$-E	8.28
$CH_2{=}C{=}C(CH_3)C(CH_3){=}CH_2$	8.10
$CH_2{=}C(CH_3)CH{=}CHCH{=}CH_2$-E	8.31
trans-$CH_2{=}CHCH{=}CHCH{=}CHCH_3$	7.96-8.07
Bicyclo[2.2.1]hept-2-ene	8.8-8.96
Bicyclo[4.1.0]hept-2-ene	8.69
Bicyclo[3.2.0]hept-6-ene	9.38
1,3-c-C_7H_{10}	8.31-8.69
4-$C_6H_8{=}CH_2$	9.27
1,2-$C_5H_4(CH_3)_2$	8.58
5,5-$C_5H_4(CH_3)_2$	8.22
Norbornene	8.95
Other C_7H_{10}: (cyclopentanes, tricyclos, spiros, etc)	8.48-9.5

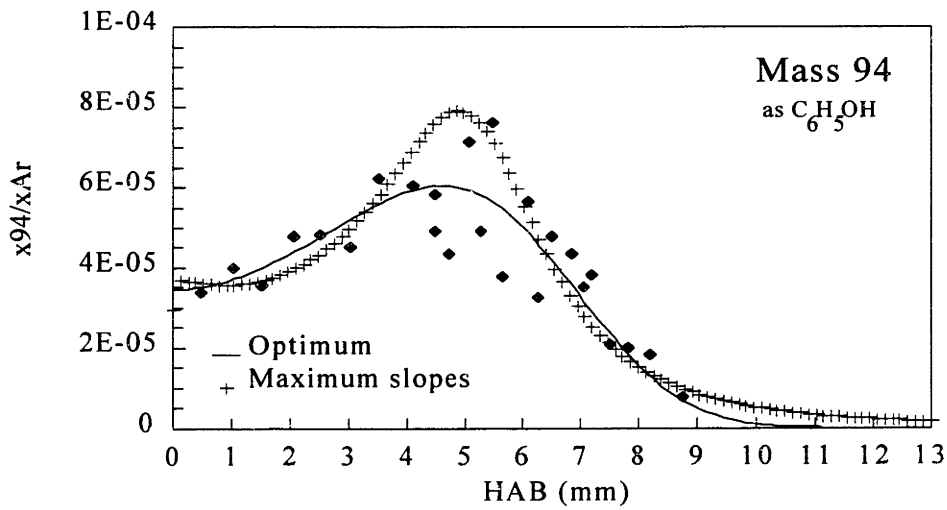

Figure 4.48 Mole fraction of mass 94 (calibrated as C_6H_5OH) relative to Ar, in a 22 torr laminar, premixed H_2-O_2-C_6H_6-Ar flame. $\phi = 1.79$, 31.3% Ar, $(x_{C6H6}/x_{H2})_0 = 0.010$, $v_0 = 101$ cm/sec. Data points and smoothed curves (optimum fit and maximum slopes) are shown.

As Bittner found in the rich benzene flame, phenol arises in the middle of reaction zone, indicative of its formation being a result of a high-temperature reaction. This is in contrast to the early destruction route through C_6H_8 hypothesized above for the current flame.

Masses 95 and 96.

An ionization efficiency curve taken for mass 95 was very scattered, with possible interpretations ranging from 8.5-9.1 eV relative to the high benzene intercept and 9.3-9.9 eV with respect to the low benzene intercept. The values calculated with respect to benzene's high intercept are similar to phenol. Mass 95 was initially assumed to be C_6H_6OH. Without any literature information on that species' IP, the IP of phenol was assumed for data collection. Calibration was by the RICS method, with benzene and phenol as the reference species. Data were collected at the same time as mass 93, and the mass 95 electron energy was 11.1 eV (same as for mass 93).

This EE is just 0.3 eV above what phenol would have been measured at, but 2.6 eV above what a later estimate showed should have been the proper energy[17]. However, the mass 95 signal

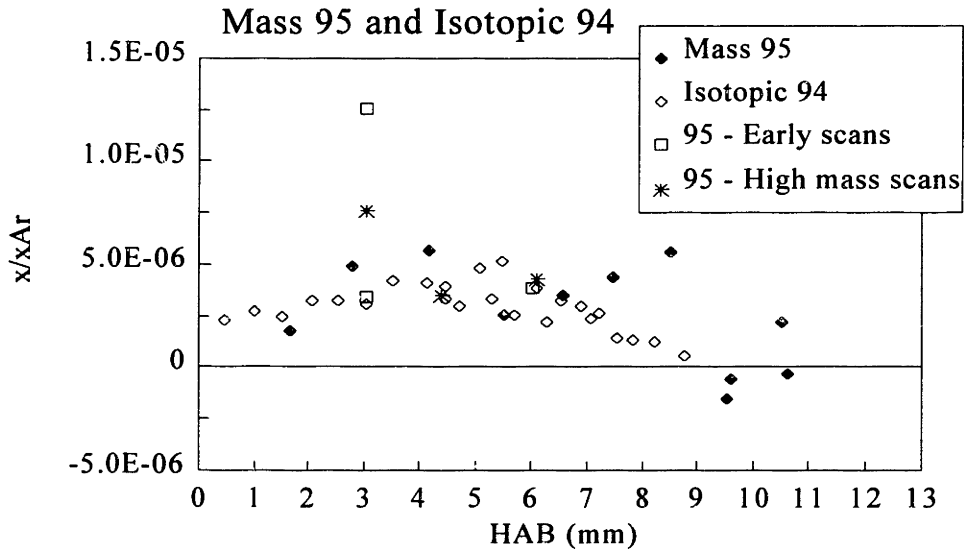

Figure 4.49 Mole fractions of mass 95 and the isotopic contribution of mass 94 to the mass 95 signal, both relative to Ar in a 22 torr laminar, premixed H_2-O_2-C_6H_6-Ar flame. ϕ = 1.79, 31.3% Ar, $(x_{C6H6}/x_{H2})_0$ = 0.010, v_0 = 101 cm/sec.

[17] Lias et al. (1988) report ΔH^0_f for $C_6H_6OH^+$ to be 146 kcal/mol. From thermochemical kinetics (using program THERM), the heat of formation of the neutral species is 8.3 kcal/mol, resulting in an estimated IP of 6.0 eV. Data were intended to have been taken at 2.5 eV above the IP.

so low at 11.1 eV that nothing would have been detected at the appropriate energy. In any event, the situation had a fortuitous aspect, as Figure 4.49 shows that the data taken at the mass 94 energy level is attributable to $^{13}CC_5H_5OH$, C_6H_4DOH and C_6H_5OD. That is, the mole fraction of C_6H_6OH is in reality below the detection limit. It can also be seen from the graph that the estimate made from high mass scans is reasonably close to the more careful data measurement, in the case of mass 95.

The mass 96 signal was so low as to merit classification as just at or below detection. The high mass scans confirm this and data estimated therefrom shows (Figure 4.50) that any signal species is roughly attributable to $C_6H_3D_2OH$, C_6H_4DOD, etc.

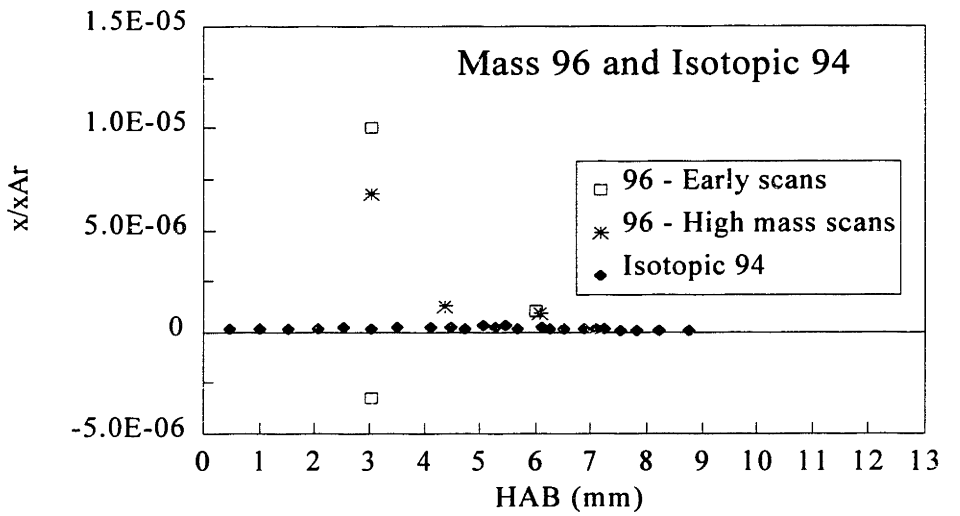

Figure 4.50 Mole fraction of mass 96 and the isotopic contribution of mass 94 to the mass 96 signal, both relative to Ar in a 22 torr laminar, premixed H_2-O_2-C_6H_6-Ar flame. ϕ = 1.79, 31.3% Ar, $(x_{C6H6}/x_{H2})_0$ = 0.010, v_0 = 101 cm/sec.

Mass 110.

Despite strong indications from early scans that this species was not present above the detection limit, the possible importance of an adduct of C_6H_6+O_2 motivates a second look. Figure 4.51 shows that data estimated from the high mass scans confirm that mass 110 is at most about 1 ppm.

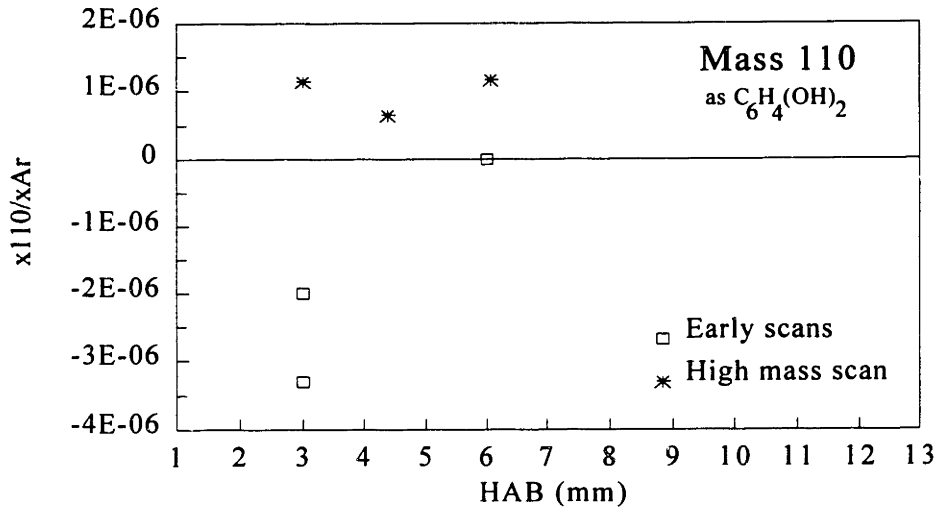

Figure 4.51 Mole fraction of mass 110 (calibrated as $C_6H_4(OH)_2$) relative to Ar, in a 22 torr laminar, premixed H_2-O_2-C_6H_6-Ar flame. ϕ = 1.79, 31.3% Ar, $(x_{C6H6}/x_{H2})_0$ = 0.010, v_0 = 101 cm/sec.

Chapter 5: Literature Model Predictions.

In this chapter, literature model predictions are presented, alongside measured mole fractions. The first step in the analysis of a literature flame mechanism is to see how well its solution compares with experimental data. A common perception is that one can learn much about the strengths and weaknesses of a model in this way. However, it will be shown in this and the following two chapters that mole fraction comparisons can give some insights but still be misleading in significant ways.

5.1 Literature Models Under Review

Three literature flame models with benzene destruction chemistry were chosen for comparison with experimental data. Those were the models of Emdee, Brezinsky and Glassman (1992) ("EBG"), Zhang and McKinnon (1995) ("ZM"), and Lindstedt and Skevis (1994) ("LS"). Two types of changes were made to the ZM model: (1) QRRK analyses were redone for 22 torr conditions and a bath gas which had weighted properties reflecting H_2-O_2-C_6H_6-Ar flame conditions, and (2) the H/O chemistry rate constants taken from Yetter et al. (1991) (via the EBG model) were corrected to apply to argon as a bath gas, instead of nitrogen. The EBG model was also somewhat modified: (1) rate constants for which Zhang and McKinnon had performed falloff calculations were replaced with the ZM values[18], and (2) the Yetter et al. H/O reactions were corrected for argon bath gas. The complete reaction sets of these models are documented in Appendix N; thermochemistry and transport parameters for flame code use are also given, in Appendix O.

The ZM model was the first to be chosen, because (a) it has a large and apparently thorough reaction set and list of species, (b) it was the first to incorporate important pressure effects, (c) the model performed well with respect to the rich benzene flame data of Bittner (1981), and (d) comparisons with the EBG and Bittker (1991) model were quite favorable. The EBG and Bittker models are considerably simpler than the ZM — 130 and 120 steps vs. 498. Since the

[18] The modifications to the EBG model were made prior to recalculation of ZM falloff reactions. Therefore, the revised EBG model contained the *original* Zhang and McKinnon QRRK rate constants. The recalculated rate constants were not in general much changed from the originals, but reaction path analyses in Chapter 7 do show differences in the predicted rates.

EBG model performed better than Bittker's in many respects, it was chosen as representative of the shorter models. Finally, the LS model was chosen as a second recent model which predicted rich C_6H_6 flame results well, but without accounting for pressure effects.

The H/O chemistry networks of the three models are taken from accepted literature sources and perform similarly. The EBG benzene destruction network was derived from various literature sources and estimates. ZM started with the EBG models, and drew from Bittker, the model of Chevalier and Warnatz (1991), and other sources. LS used much of the core EBG mechanism, with a somewhat different $O+C_6H_6$ set of reactions taken from Leidreiter and Wagner (1989), and several other minor differences. The reaction of H atom and benzene to form cyclohexadienyl is in LS alone, as are a number of reactions involving linear C_5 and C_6 species.

Text files of all three reaction sets, plus associated thermochemistry and transport parameters, were received in personal communications with the authors (Brezinsky, 1994; Zhang, 1994; Lindstedt, 1994). The QRRK input files used in the ZM model were also supplied by Zhang. All flame code computations were performed using the PREMIX code of Kee et al. (1985). The supporting programs CHEMKIN II (Kee et al., 1991) and TRANFIT (Kee et al., 1986) were used for associated thermochemical and transport calculations. All of these computations were performed on a Cray-2 computer at the Department of Energy's National Energy Research Supercomputer Center in Livermore, CA. The flame code output was post-processed with a program written for this purpose, FBR (Appendix D), and imported into a spreadsheet for additional analysis.

As discussed in Chapter 4, thermal diffusion effects are important in the present H_2-O_2 flame, hence the thermal diffusion option of the flame code was used. The use of the multicomponent diffusivity formalism, as opposed to the mixture-averaged approximation, was also shown to be important. The EBG and ZM models had no problem converging with these two options selected. However, the LS model as received was initially found to be intractable, even after many Cray-hours of computing time and assistance from one of the flame code authors (Rupley, 1994). Consultation with Lindstedt revealed that the published solution was reached with a different flame solver, and was computationally too stiff for PREMIX (Lindstedt, 1994 and 1995). A revised reaction set was then provided by Lindstedt, with which he had achieved convergence in the simulation of Bittner's rich benzene flame using PREMIX. To accomplish this, six minor reactions had to be removed and two others were rewritten in the reverse

direction. Several changes were also made to reactions involving species studied in this work, which are documented in Appendix N. Using the new reaction set, convergence was achieved for H_2-O_2-C_6H_6-Ar flame conditions, however only without multicomponent diffusivities.

5.2 Model Predictions of Argon and H/O System Species

All of the models using multicomponent diffusivities do a good job of predicting the argon mole fraction, as seen in Figure 5.1[19]. The same can be said for H_2, in Figure 5.2. Some

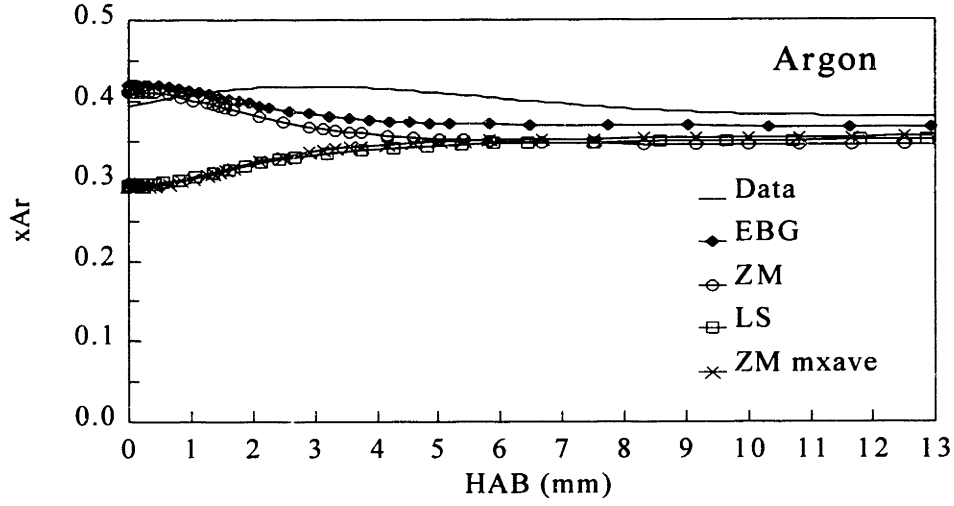

Figure 5.1 Mole fraction and model predictions of Ar, in a 22 torr laminar, premixed H_2-O_2-C_6H_6-Ar flame. ϕ = 1.79, 31.3% Ar, $(x_{C6H6}/x_{H2})_0$ = 0.010, v_0 = 101 cm/sec. "mxave" = mixture-averaged diffusivities.

deviation near the burner is evident for the mixture-averaged diffusion solutions, though. The LS and ZM models give identical solutions using that approximation.

Since the LS model could not be solved using the multicomponent formulation, it is important to understand the effect of diffusivity on its solution. The effect seen for both H_2 and Ar (and other species as well) is in fact mostly due to H_2 — the Ar dip is a result of the effect of the H_2 increase on the mole fraction balance. Since all of the mole fractions were collected with respect to argon as a reference (or converted to such a basis), the *ratio* of a particular mole fraction to argon is the best quantity to use in examining the effect of mixture-averaged diffusivity. Using this method no significant diffusivity effect was seen for the major stable species, and there

[19] In all of the figures, "Height Above Burner" is referred to as "HAB."

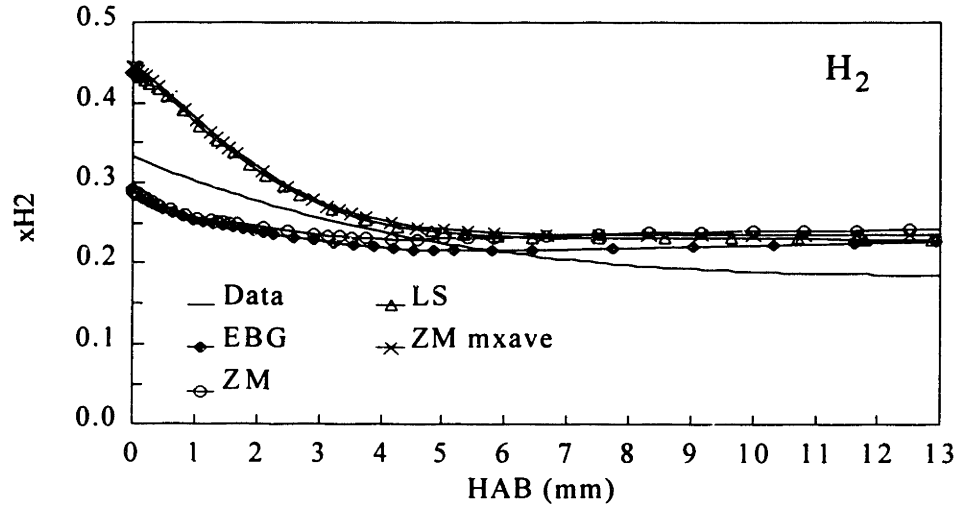

Figure 5.2 Mole fraction and model predictions of H_2, in a 22 torr laminar, premixed H_2-O_2-C_6H_6-Ar flame. ϕ = 1.79, 31.3% Ar, $(x_{C6H6}/x_{H2})_0$ = 0.010, v_0 = 101 cm/sec. "mxave" = mixture-averaged diffusivities.

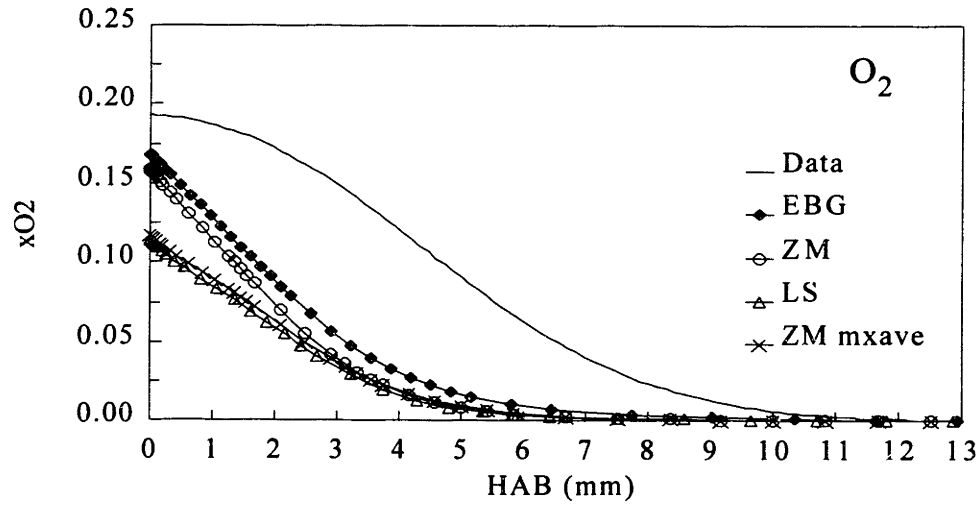

Figure 5.3 Mole fraction and model predictions of O_2, in a 22 torr laminar, premixed H_2-O_2-C_6H_6-Ar flame. ϕ = 1.79, 31.3% Ar, $(x_{C6H6}/x_{H2})_0$ = 0.010, v_0 = 101 cm/sec. "mxave" = mixture-averaged diffusivities.

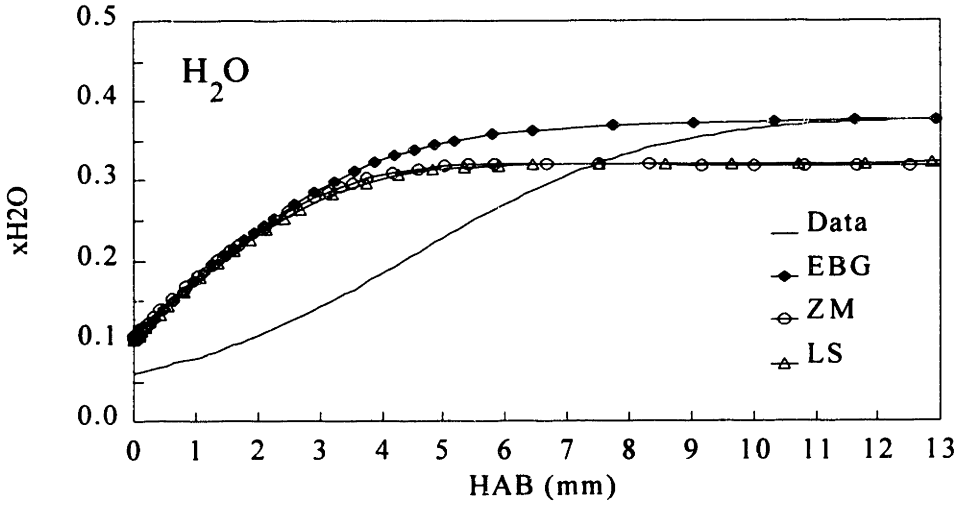

Figure 5.4 Mole fraction and model predictions of H_2O, in a 22 torr laminar, premixed H_2-O_2-C_6H_6-Ar flame. ϕ = 1.79, 31.3% Ar, $(x_{C6H6}/x_{H2})_0$ = 0.010, v_0 = 101 cm/sec.

is only a minor effect for other species. There are a few significant exceptions, which will be noted below.

Model predictions of O_2 and H_2O are not satisfactory, Figures 5.3 and 5.4, by comparison with the performance of these models for ϕ = 1.8, C_6H_6-O_2-Ar flame (Zhang and McKinnon; Lindstedt and Skevis). Again, the LS model prediction is no different from the ZM mixture-

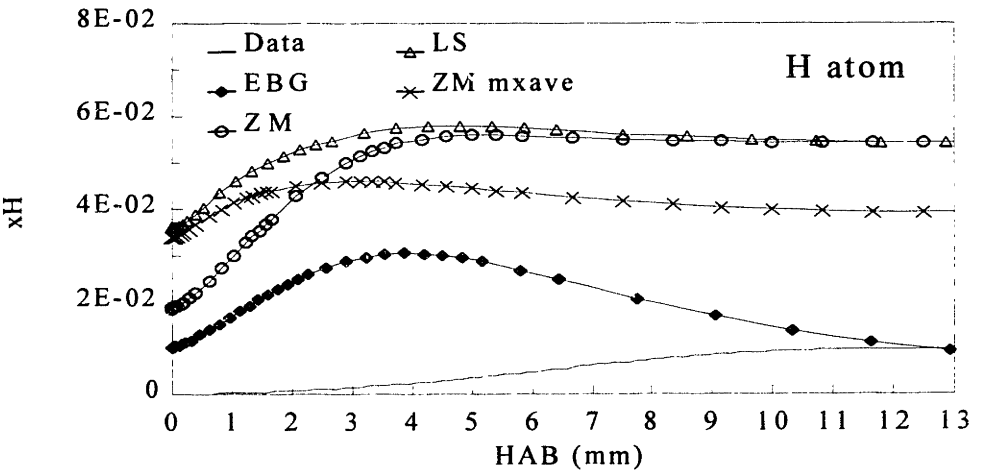

Figure 5.5 Mole fraction and model predictions of H atom, in a 22 torr laminar, premixed H_2-O_2-C_6H_6-Ar flame. ϕ = 1.79, 31.3% Ar, $(x_{C6H6}/x_{H2})_0$ = 0.010, v_0 = 101 cm/sec. "mxave" = mixture-averaged diffusivities.

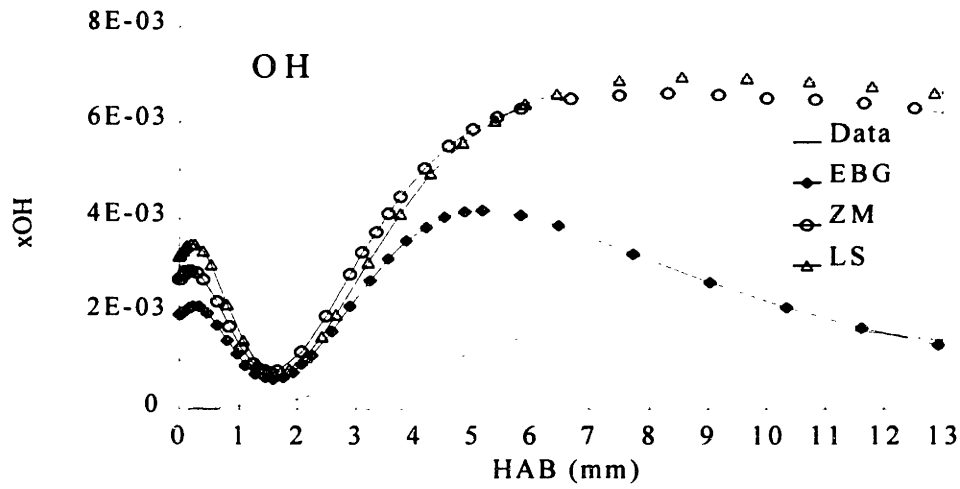

Figure 5.6 Mole fraction and model predictions of OH, in a 22 torr laminar, premixed H_2-O_2-C_6H_6-Ar flame. $\phi = 1.79$, 31.3% Ar, $(x_{C6H6}/x_{H2})_0 = 0.010$, $v_0 = 101$ cm/sec.

averaged solution. A feature common to predictions for both species — and on reflection, it is present for H_2 as well — is the length of the reaction or "burnout" zone. According to the models, the burnout zone is about 5 mm, but in reality it is 10 mm.

Predictions are even farther off for the radicals H and OH[20]. Figures 5.5 and 5.6 show that the model solutions have peak magnitudes from two to more than six times that of data. The reaction zone width is incorrectly predicted in the same way as for stable species, showing the problem to be consistent and systematic in the reaction set[21] — or the data.

The discrepancies observed in the H/O chemistry were unexpected because from examination of literature sources this reaction system appears to have been solved. For example, excellent results for various models have been presented by Laurendeau and Goldsmith (1989), Vandooren and Bian (1990), and Yetter et al. (1991). In Sections 6.2 and 6.4 it will be shown that the problem lies in the H_2-O_2 mechanisms, rather than the present results.

---

[20] Data for H and OH in this chapter were calibrated by the partial equilibrium method discussed in Chapter 6.

[21] The essential features of the problems noted here common to all of the H/O submechanisms tested. Those were: Miller et al. (1982), Warnatz (1984) (as modified by Westmoreland, 1986), and Yetter et al. (1991).

It was also found that the short reaction scale was not a function of hydrocarbon chemistry, as the same idiosyncrasy was observed when the models were run with only H_2-O_2 system reactions. Neither was the overprediction of radicals related to hydrocarbons, since without them the model predicts even higher mole fractions.

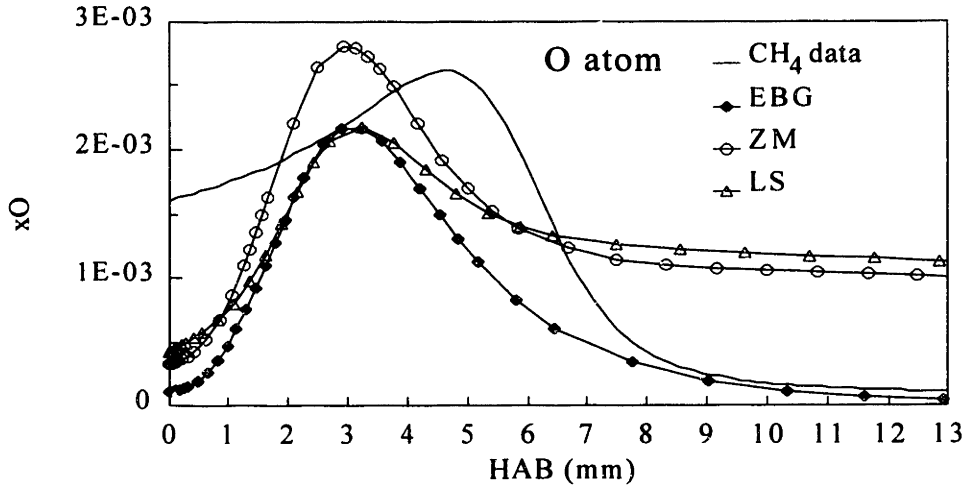

Figure 5.7 Mole fraction (mass 16 as CH_4) and model predictions of O atom, in a 22 torr laminar, premixed H_2-O_2-C_6H_6-Ar flame. $\phi = 1.79$, 31.3% Ar, $(x_{C6H6}/x_{H2})_0 = 0.010$, $v_0 = 101$ cm/sec.

The O atom prediction is shown in Figure 5.7, compared to the experimental mass 16 signal calibrated as CH_4. While there is strong evidence in favor of assigning the mass 16 signal to methane (see Section 4.2), the apparent agreement above provided motivation for further investigation into the matter.

One of the measurements taken during the species identification phase was a pair of ionization efficiency curves, the first at 4.4 mm in the $\phi = 1.79$, H_2-O_2-C_6H_6-Ar flame and the second at 6.6 mm with the same gas flows but no benzene. With these data points, a model could be tested by comparing measured values to the prediction of the additive effect of the presence of hydrocarbons. In particular, the ratio $\frac{(I_{CH_4} + I_O)_{\text{with C6H6}}}{(I_{O\ \text{atom}})_{\text{no C6H6}}}$ was computed and compared to data.

In addition to the simulation for the present flame reported here, it was necessary to run the model (ZM was chosen) for H_2-O_2-Ar conditions. Two assumed temperature profiles were used: (1) the profile shown in Figure 4.5, and (2) that profile modified by multiplication by 1.08, compression of the interval between points to 92% their original size, and shifting the profile toward the burner by 0.25 mm. The particular changes were designed to estimate the higher temperature profile that the leaner flame should have.

Conversion of mole fractions to estimated signals was performed with the Relative Ionization Cross Section ("RICS") equation (see Chapter 3), under the assumption that the density in the ionizer was approximately the same for both flames. In such a case, the constant of

proportionality between the mole fraction of a species and its signal is the same for each flame, and

$$\frac{(I_{CH_4}+I_O)_{\text{with C6H6}}}{(I_O)_{\text{no C6H6}}} = \frac{(I_{CH_4})_{\text{with C6H6}}}{(I_O)_{\text{no C6H6}}} + \frac{(I_O)_{\text{with C6H6}}}{(I_O)_{\text{no C6H6}}} = f \times \frac{(x_{CH_4})_{\text{with C6H6}}}{(x_O)_{\text{no C6H6}}} + \frac{(x_O)_{\text{with C6H6}}}{(x_O)_{\text{no C6H6}}},$$

where

$f \equiv$ (energy correction factor) x $\frac{Q_{CH_4}}{Q_O}$, and

Q_i = electron impact ionization cross-section.

The measured ratio was found to be 3.0, and with the above equation the predicted ratio was 0.27 (unchanged temperature profile) and 0.14 (modified profile). The discrepancy is at best a factor of eleven. Clearly then, the failure to predict the additive effect of hydrocarbon chemistry indicates that there is some problem with the model predictions for mass 16. The model would have much less mass 16 signal in the flame with benzene, while in reality there is three times as much.

Another way of studying the situation is to compute the O atom signal expected in the flame with benzene, given the measured signal in H_2-O_2-Ar and the predicted ratio $\frac{(I_O)_{\text{with C6H6}}}{(I_O)_{\text{no C6H6}}}$. The predicted O signal is then 0.026-0.047 mV, depending on the temperature assumptions. Since the total mass 16 signal measured in the flame with C_6H_6 was 0.57 mV, the amount attibutable to CH_4 would then be 0.52-0.54 mV. This strongly disagrees with the original prediction first observed in Figure 5.7. In addition, the CH_4 signal computed from the model-derived $\frac{(I_{CH_4})_{\text{with C6H6}}}{(I_O)_{\text{no C6H6}}}$ is 0.036 mV, also a factor of fifteen lower than estimated with O network. Therefore, assuming that the model's O chemistry is correct leads to the conclusion that its hydrocarbon (particularly CH_4) network is seriously in error, and vice versa.

Because of these findings about the literature mechanisms, the apparent agreement between mass 16 and O atom predictions was not considered to be inconsistent with the previous conclusion that mass 16 is CH_4.

In summary, comparisons between model computations and data for H/O system species reveals the following:

- Accepted literature H_2-O_2 models do not predict well either the reaction zone thickness for H/O system species, or the radical concentrations, under these conditions.

- One portion of the current H/O reaction networks which is particularly suspect is the O atom chemistry.

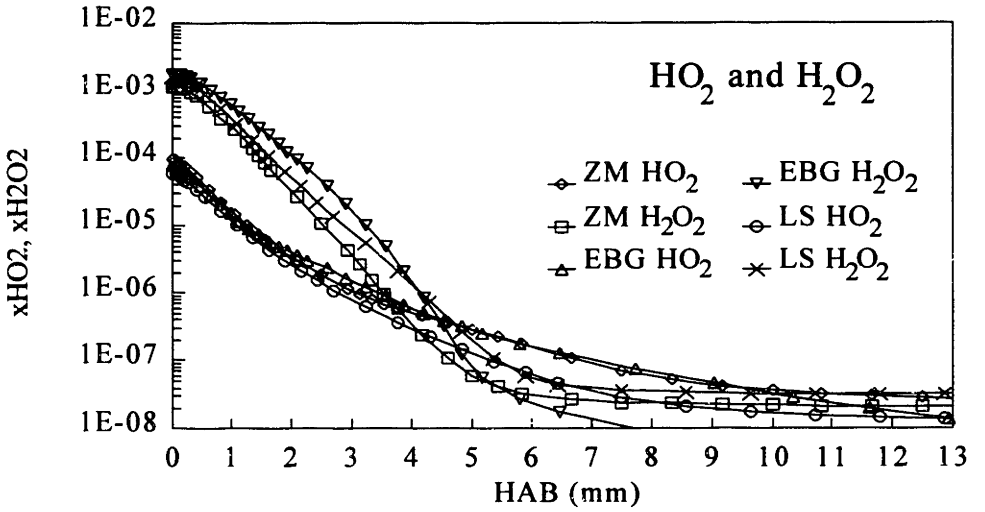

Figure 5.8 Model predictions of HO_2 and H_2O_2, in a 22 torr laminar, premixed H_2-O_2-C_6H_6-Ar flame. ϕ = 1.79, 31.3% Ar, $(x_{C6H6}/x_{H2})_0$ = 0.010, v_0 = 101 cm/sec.

5.3 Model Predictions of C/H/O System Species

The unreliability of H/O predictions creates serious problems for the interpretation of hydrocarbon results, because hydrocarbon-hydrocarbon chemistry is minor by comparison in the present flame. Most of the bimolecular reactions taking place for species such as benzene occur with the partners O_2, H_2, OH, H, and O. All of those reactions are significantly affected by the errant mole fractions. The power of model-data comparisons is thereby reduced to the point where only qualitative observations are meaningful. Therefore, this section contains few conclusions. Rather, the main products will be observations that will be helpful for the net rate analysis of Chapter 7, and those of general interest.

It is immediately obvious from Figures 5.9-5.32 that the hydrocarbon reaction scale predicted by the models is excellent, in contrast to the case for H/O chemistry. This explains why the scale problem does not show up for H_2-O_2 species in flames dominated by hydrocarbon chemistry.

Because of the additive nature of this flame, the amount of any hydrocarbon intermediate or product *formed* is dependent on the chemistry of the other hydrocarbon species, but the amount *destroyed* is more a function of the H/O environment. Because of this, and the uncertain nature of the consumption half of the equation, agreement or disagreement of mole fractions for most species is probably mostly fortuitous. A greater amount of information can be discerned from the relationship between related species, such as C_4H_6 and C_4H_7 or C_4H_8.

Benzene is not exempt from this circumstance, since reverse reactions (for example, recombination of C_6H_5+H) can cause it to be formed in the flame. However, right at the burner little formation or destruction is expected, and the predicted C_6H_6 should be close to the measured value. It can be seen in Figure 5.9 that this is not the case for the ZM and EBG models; rather, they overpredict the initial benzene mole fraction. The LS model, on the other hand, would have less benzene than experimentally determined, at the burner surface. Since the LS model was not run with multicomponent diffusion, some "translation" of its results is necessary[22]. Shown in the graph is the mixture-average computation of the ZM model, which has a burner mole fraction that is 67% of the multicomponent prediction. If the LS prediction is corrected on this basis, the

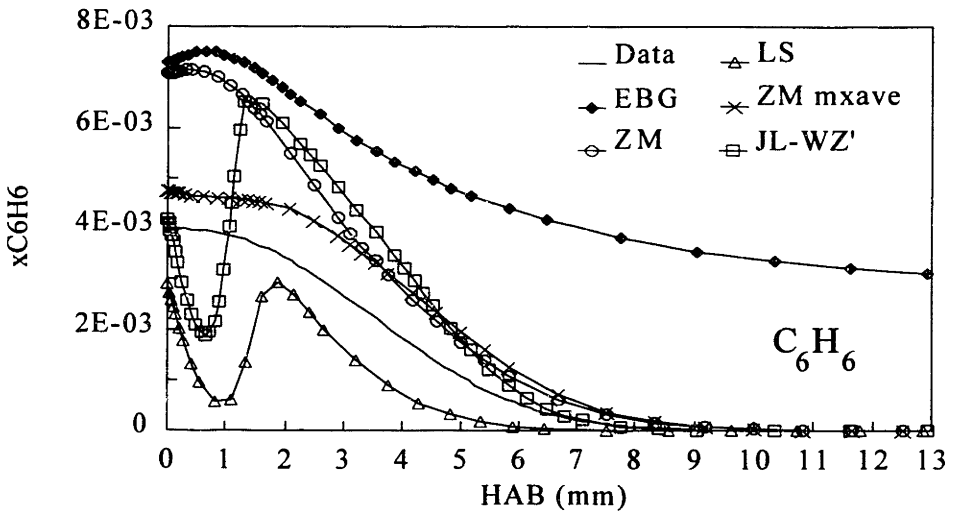

Figure 5.9 Mole fraction and model predictions of C_6H_6, in a 22 torr laminar, premixed H_2-O_2-C_6H_6-Ar flame. ϕ = 1.79, 31.3% Ar, $(x_{C6H6}/x_{H2})_0$ = 0.010, v_0 = 101 cm/sec. "mxave" = mixture-averaged diffusivities. "JL-WZ'" - see text.

[22] For species in the C/H/O system, the effect (on x_i/x_{Ar}) of using mixture-averaged diffusivities is similar to that of the H/O system. Exceptions are noted below.

initial benzene mole fraction would be within 10% of the data.

The reason for the difference in initial mole fraction, and the peculiar oscillation between the burner top and 2 mm, is the reaction $C_6H_6+H \rightleftharpoons C_6H_7$. According to the model, cyciohexadienyl radical is formed in large quantities in the first millimeter, then reverts back to H and benzene (primarily) in the next (Figure 5.26). The results produced by a much simplified benzene oxidation model that contains the C_6H_7 reaction, labelled "JL-WZ"[23], show that a multicomponent solution does in fact give an accurate mole fraction at the burner.

A pattern seen with a number of radical/stable species pairs is exemplified by CH_3-CH_4 and masses 65 and 66 (Figures 5.12, 5.13, 5.22 and 5.23). That is, either the radical is predicted well and the more hydrogenated stable species is strongly underpredicted (CH_3 and CH_4), or else the stable species is predicted well and the radical is strongly overpredicted (masses 65 and 66).

A number of similarities are seen between the results in the present flame and the predictions of the LS and ZM models for the rich C_6H_6-O_2-Ar flame of Bittner (1981):

1. Phenol is overpredicted.
2. Phenyl is overpredicted (ZM only).
3. Mass 66 is underpredicted (though not by much).
4. Mass 65 is overpredicted by the ZM model, and the LS model calculation is accurate in magnitude but slightly early in location.

These resemblances occur in spite of the difference in fit of H/O species. It would seem therefore that some relationships between these early intermediate species and their precursors and products are being maintained, even when the flame environment is incorrectly modeled. As will be shown in Chapter 7 unimolecular decomposition reactions of benzene, phenyl and phenoxy radical control much of the aromatics destruction rates. These reactions do not depend on H/O species, hence the "portability" of the model-data disagreements.

In several cases, the LS model approaches data much closer than the other two. Those are CH_4, C_2H_4, mass 42, mass 44, mass 54, mass 65, mass 70, C_6H_5, and C_6H_5O. Some of this

[23] Jackson and Laurendeau (1987), with Warnatz (1984) C_2H_2 submodel as modified by Westmoreland (1986). This model is simply an acetylene submechanism (containing, of course, H_2-O_2 and CO-CO_2 reactions as well) with 11 benzene destruction reactions, including cyclohexadienyl formation. The benzene reaction network contains key destruction elements (hence the good agreement at the burner), but intermediate chemistry is very unrealistic. For example, phenol is not even included in model. Hence, it was not reviewed here.

may be due to the closer fit of its benzene prediction to the data, and some to improved linear hydrocarbon treatment[24]. The lack of accounting for falloff may play some role. In the case of phenyl, though, the revised LS model used for flame code calculations has a phenyl decyclization rate constant which is about eight times that of the original LS model (from Braun-Unkhoff et al., 1989) and three times that of Rao and Skinner (1988). The revised LS rate constant therefore is probably incorrect, and the excessive destruction it predicts accounts for some of the improved fit. Regarding masses 44 (low electron energy) and 70, there are no species at these mass numbers in the other models. For masses 54 and 42, oxygenated species make up the difference.

In summary, mole fraction comparisons for C/H/O system species show the following:

- The models predict the hydrocarbon reaction zone size well.
- Direct interpretation of model calculations fits to mole fractions is not possible, except perhaps right at the burner surface.
- The H addition reaction near the burner surface is apparently necessary and sufficient to adjust the model prediction of C_6H_6 to agree with data.
- Current models need improvement with regard to their balance of more- to less-hydrogenated species.
- Relationships between early benzene destruction intermediates are not affected by the H/O chemistry problems.
- The LS model appears to have the best hydrocarbon submechanisms of the three. However, revisions for falloff and a corrected rate constant for $C_6H_5 \rightleftharpoons$ l-C_6H_5 should be incorportated before a final judgement is made on this issue.

[24] In the case of phenyl, the revised LS model used for the flame code calculations has a phenyl decyclization rate constant which is about eight times that of the original LS model (from Braun-Unkhoff et al., 1989) and three times that of Rao and Skinner (1988). Also, the rate constant was not corrected for falloff. The revised LS rate constant therefore seems to be in error, and the excessive destruction it predicts accounts for some of the improved fit.

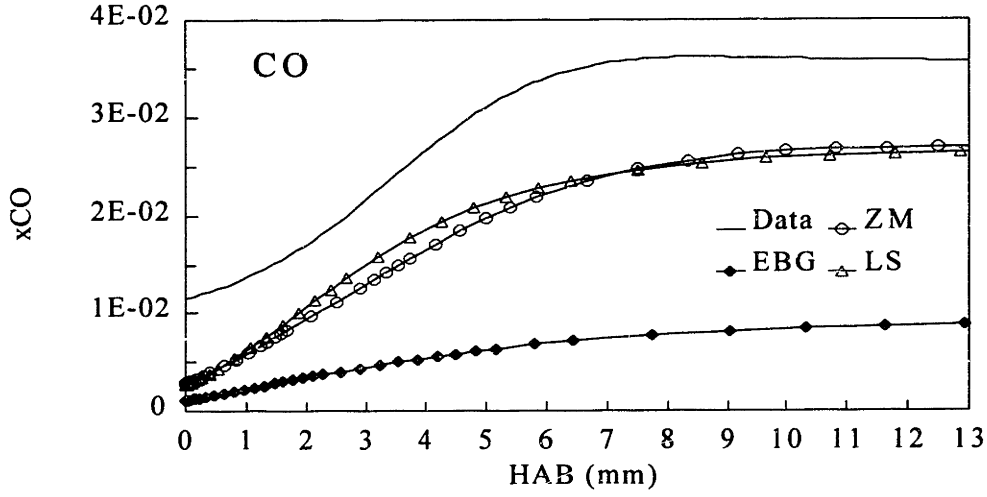

Figure 5.10 Mole fraction and model predictions of CO, in a 22 torr laminar, premixed H_2-O_2-C_6H_6-Ar flame. ϕ = 1.79, 31.3% Ar, $(x_{C6H6}/x_{H2})_0$ = 0.010, v_0 = 101 cm/sec.

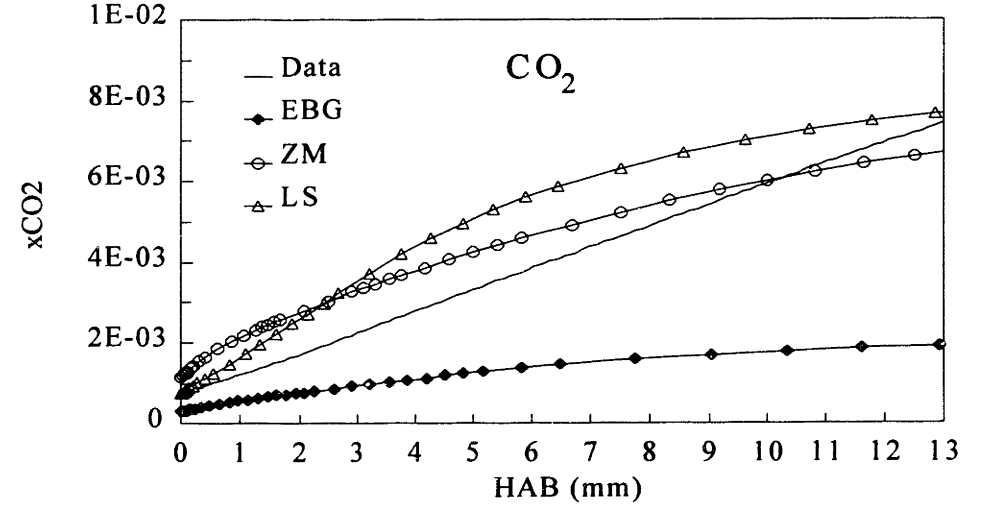

Figure 5.11 Mole fraction and model predictions of CO_2, in a 22 torr laminar, premixed H_2-O_2-C_6H_6-Ar flame. ϕ = 1.79, 31.3% Ar, $(x_{C6H6}/x_{H2})_0$ = 0.010, v_0 = 101 cm/sec.

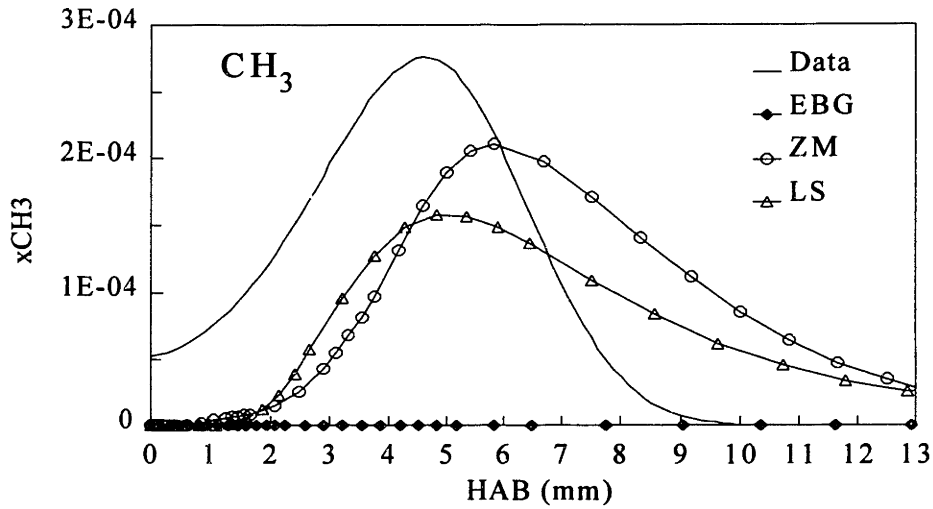

Figure 5.12 Mole fraction and model predictions of CH_3, in a 22 torr laminar, premixed H_2-O_2-C_6H_6-Ar flame. ϕ = 1.79, 31.3% Ar, $(x_{C6H6}/x_{H2})_0$ = 0.010, v_0 = 101 cm/sec.

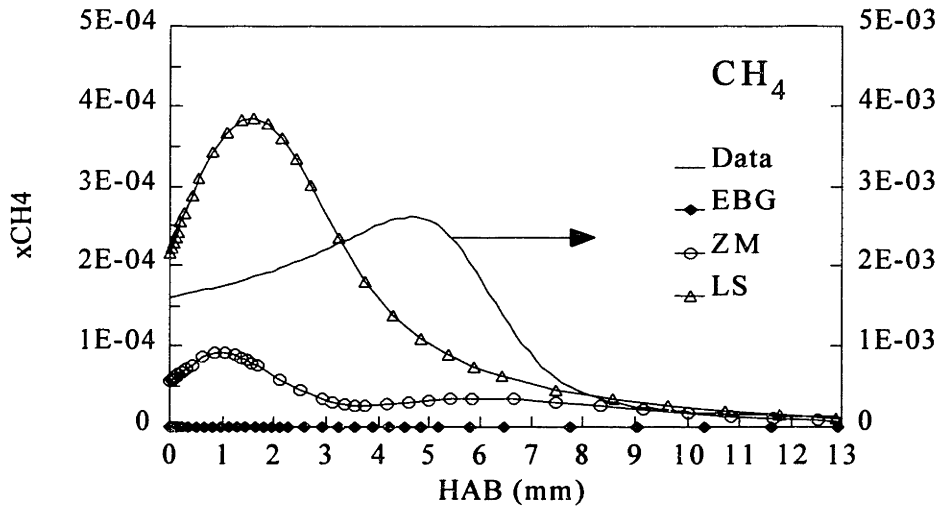

Figure 5.13 Mole fraction and model predictions of CH_4, in a 22 torr laminar, premixed H_2-O_2-C_6H_6-Ar flame. ϕ = 1.79, 31.3% Ar, $(x_{C6H6}/x_{H2})_0$ = 0.010, v_0 = 101 cm/sec.

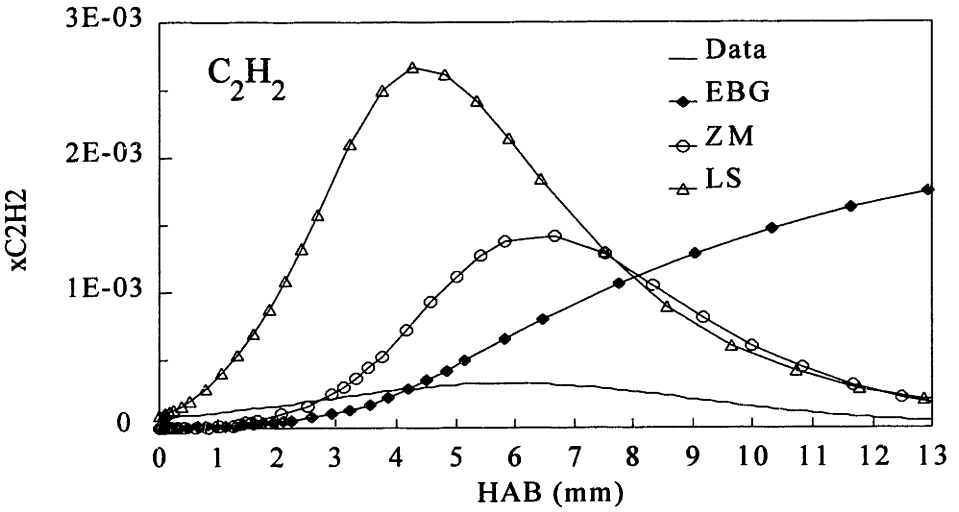

Figure 5.14 Mole fraction and model predictions of C_2H_2, in a 22 torr laminar, premixed H_2-O_2-C_6H_6-Ar flame. ϕ = 1.79, 31.3% Ar, $(x_{C6H6}/x_{H2})_0$ = 0.010, v_0 = 101 cm/sec.

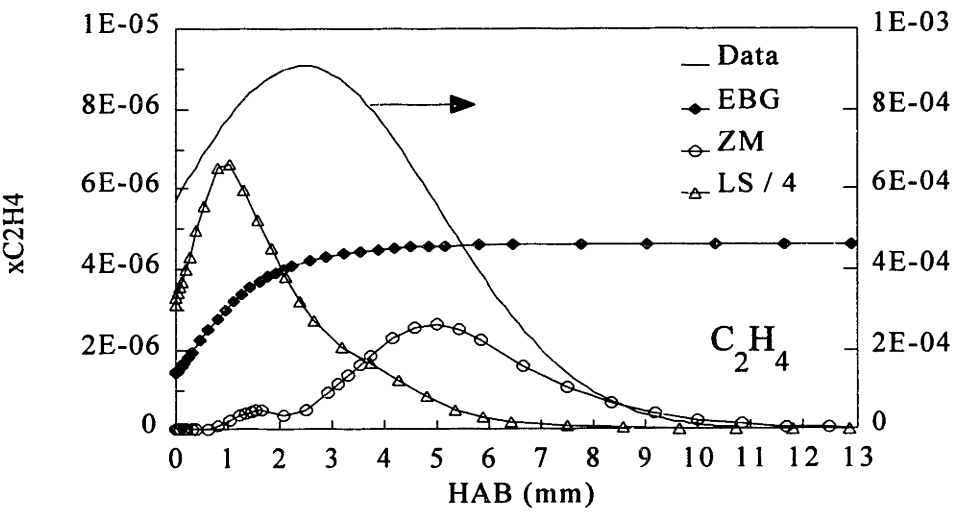

Figure 5.15 Mole fraction and model predictions of C_2H_4, in a 22 torr laminar, premixed H_2-O_2-C_6H_6-Ar flame. ϕ = 1.79, 31.3% Ar, $(x_{C6H6}/x_{H2})_0$ = 0.010, v_0 = 101 cm/sec.

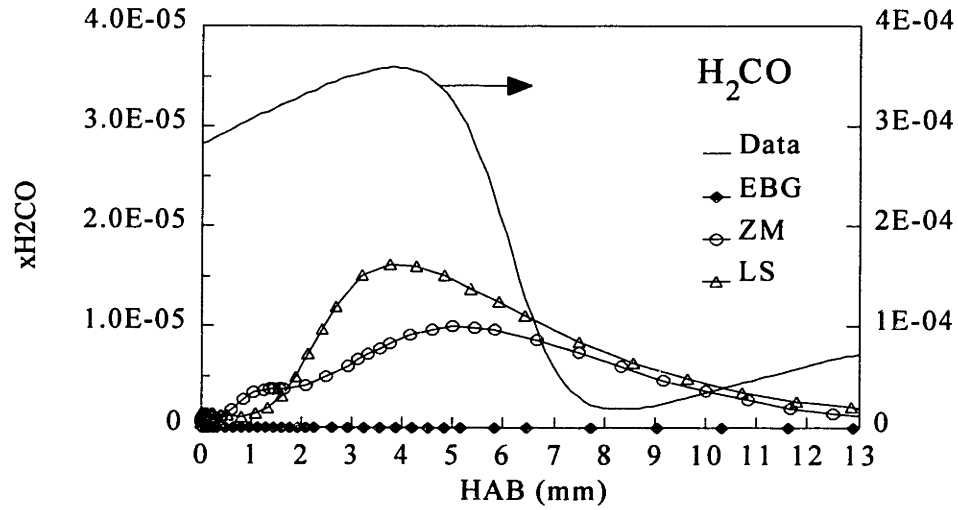

Figure 5.16 Mole fraction and model predictions of H_2CO, in a 22 torr laminar, premixed H_2-O_2-C_6H_6-Ar flame. ϕ = 1.79, 31.3% Ar, $(x_{C6H6}/x_{H2})_0$ = 0.010, v_0 = 101 cm/sec.

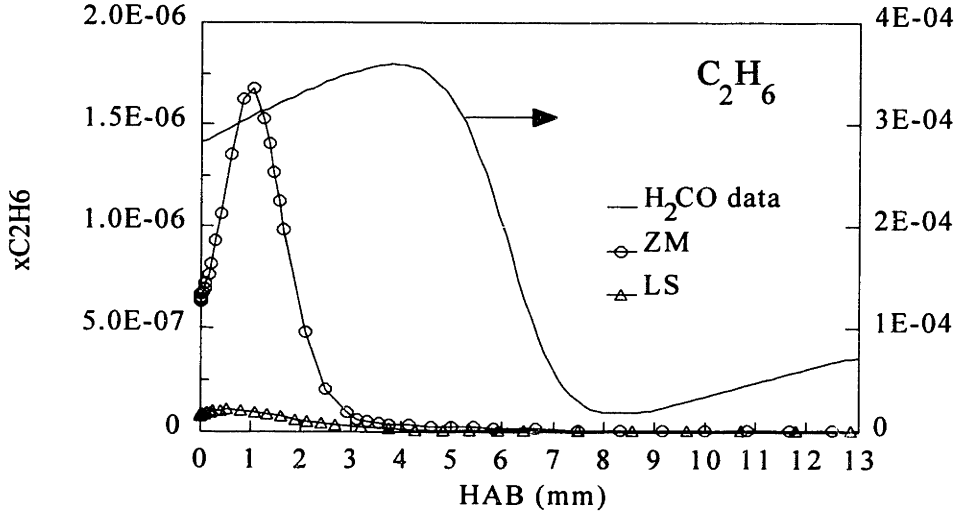

Figure 5.17 Mole fraction (mass 30 as H_2CO) and model predictions of C_2H_6, in a 22 torr laminar, premixed H_2-O_2-C_6H_6-Ar flame. ϕ = 1.79, 31.3% Ar, $(x_{C6H6}/x_{H2})_0$ = 0.010, v_0 = 101 cm/sec.

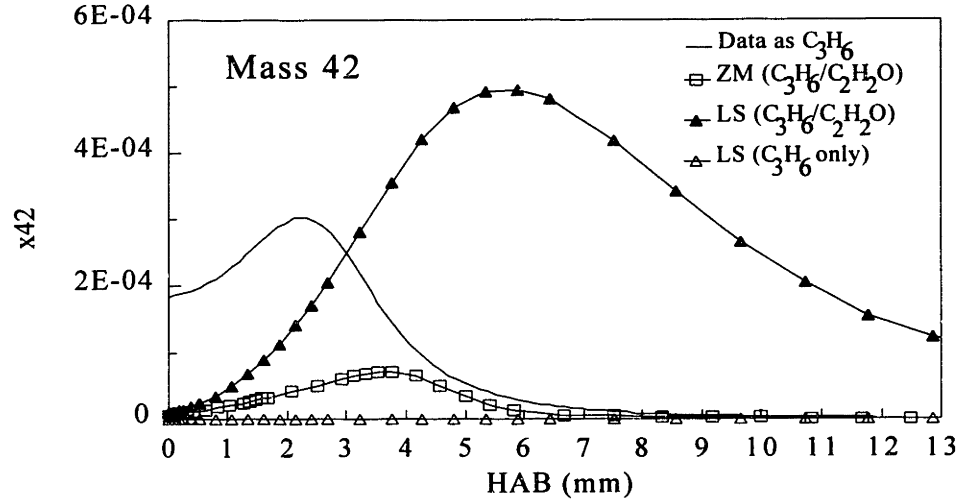

Figure 5.18 Mole fraction and model predictions of mass 42, in a 22 torr laminar, premixed H_2-O_2-C_6H_6-Ar flame. ϕ = 1.79, 31.3% Ar, $(x_{C6H6}/x_{H2})_0$ = 0.010, v_0 = 101 cm/sec.

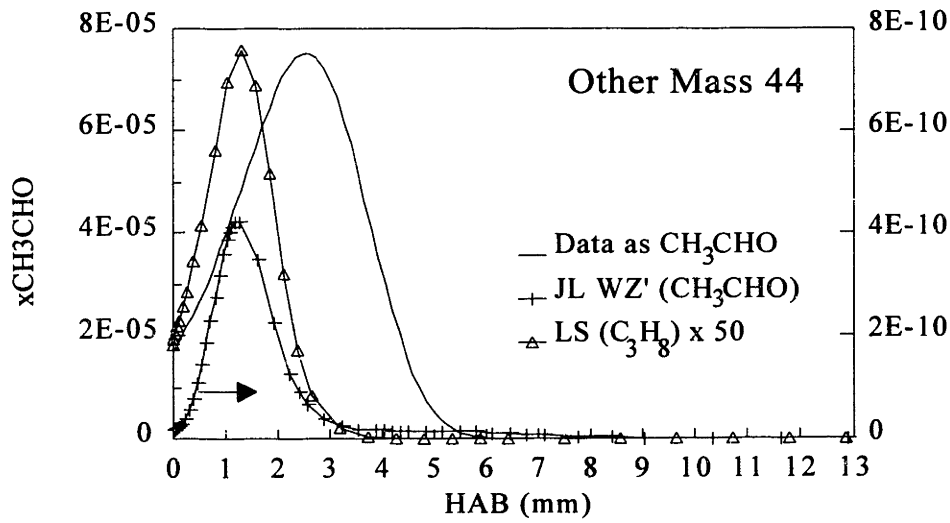

Figure 5.19 Mole fraction and model predictions of mass 44 species (other than CO_2), in a 22 torr laminar, premixed H_2-O_2-C_6H_6-Ar flame. ϕ = 1.79, 31.3% Ar, $(x_{C6H6}/x_{H2})_0$ = 0.010, v_0 = 101 cm/sec. "JL-WZ'" - see text.

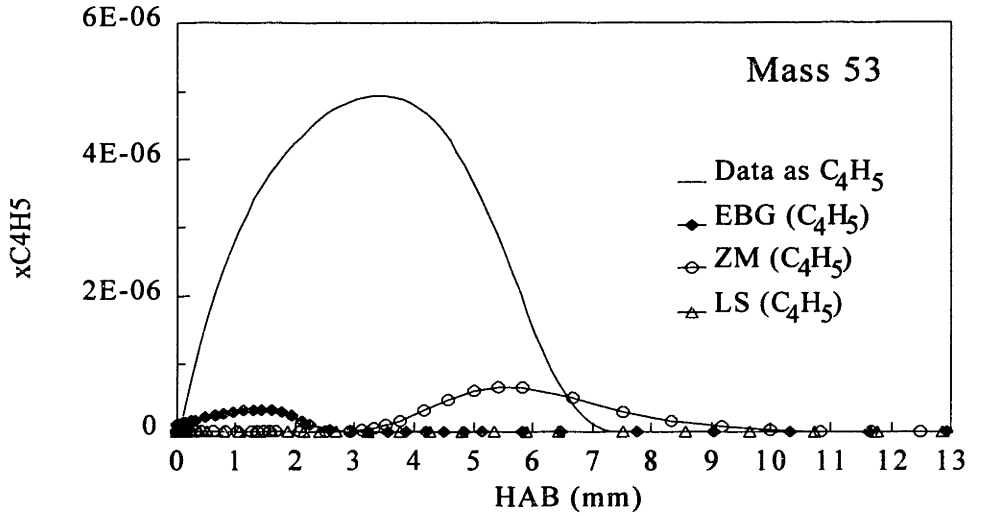

Figure 5.20 Mole fraction and model predictions of mass 53, in a 22 torr laminar, premixed H_2-O_2-C_6H_6-Ar flame. ϕ = 1.79, 31.3% Ar, $(x_{C6H6}/x_{H2})_0$ = 0.010, v_0 = 101 cm/sec.

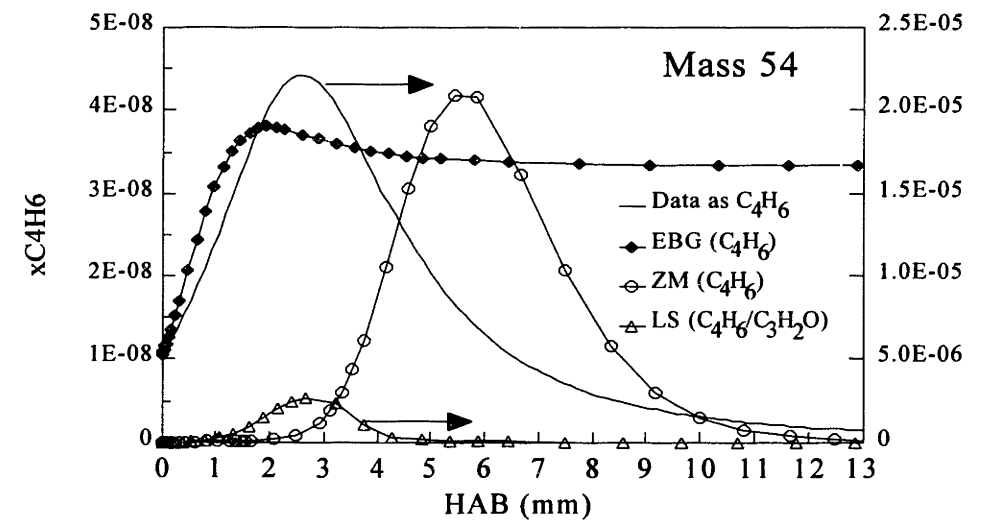

Figure 5.21 Mole fraction and model predictions of mass 54, in a 22 torr laminar, premixed H_2-O_2-C_6H_6-Ar flame. ϕ = 1.79, 31.3% Ar, $(x_{C6H6}/x_{H2})_0$ = 0.010, v_0 = 101 cm/sec.

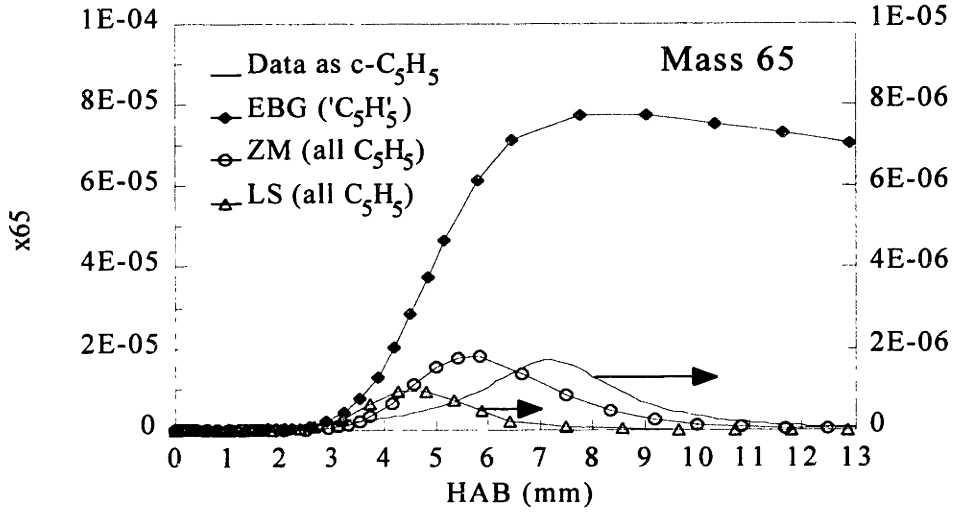

Figure 5.22 Mole fraction and model predictions of mass 65, in a 22 torr laminar, premixed H_2-O_2-C_6H_6-Ar flame. ϕ = 1.79, 31.3% Ar, $(x_{C6H6}/x_{H2})_0$ = 0.010, v_0 = 101 cm/sec. "'C_5H_5'" means unspecified isomer. "all C_5H_5" means linear and cyclic isomers combined.

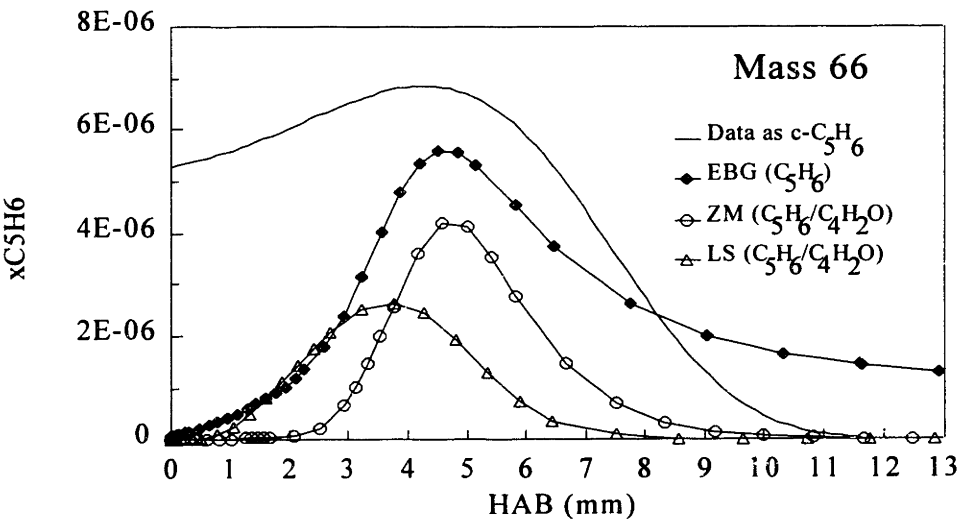

Figure 5.23 Mole fraction and model predictions of mass 66, in a 22 torr laminar, premixed H_2-O_2-C_6H_6-Ar flame. ϕ = 1.79, 31.3% Ar, $(x_{C6H6}/x_{H2})_0$ = 0.010, v_0 = 101 cm/sec.

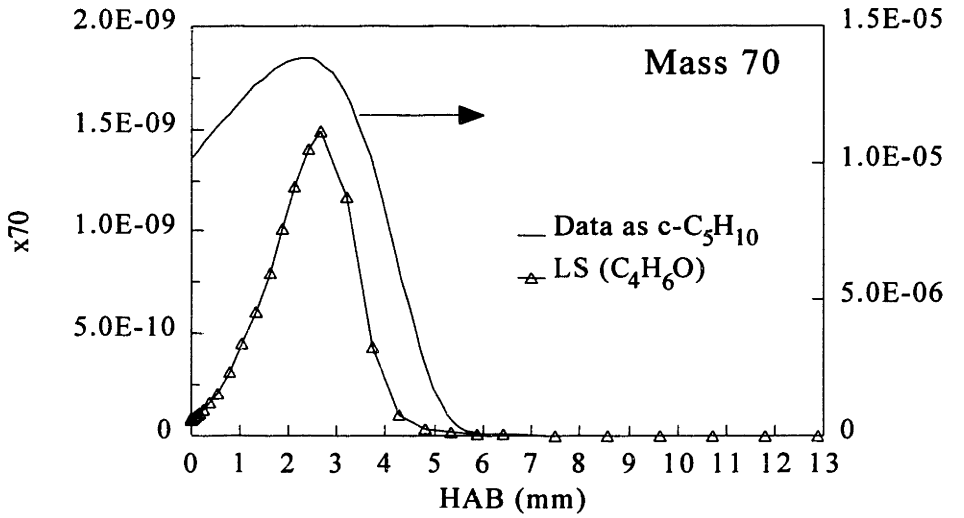

Figure 5.24 Mole fraction and model prediction of mass 70, in a 22 torr laminar, premixed H_2-O_2-C_6H_6-Ar flame. ϕ = 1.79, 31.3% Ar, $(x_{C6H6}/x_{H2})_0$ = 0.010, v_0 = 101 cm/sec.

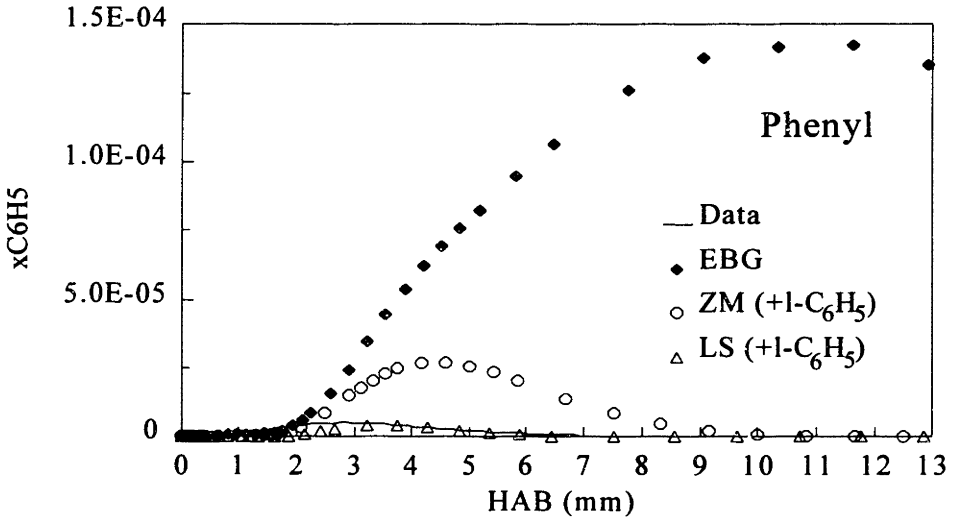

Figure 5.25 Mole fraction and model predictions of C_6H_5, in a 22 torr laminar, premixed H_2-O_2-C_6H_6-Ar flame. ϕ = 1.79, 31.3% Ar, $(x_{C6H6}/x_{H2})_0$ = 0.010, v_0 = 101 cm/sec. "+l-C_6H_5" means linear isomer included as well.

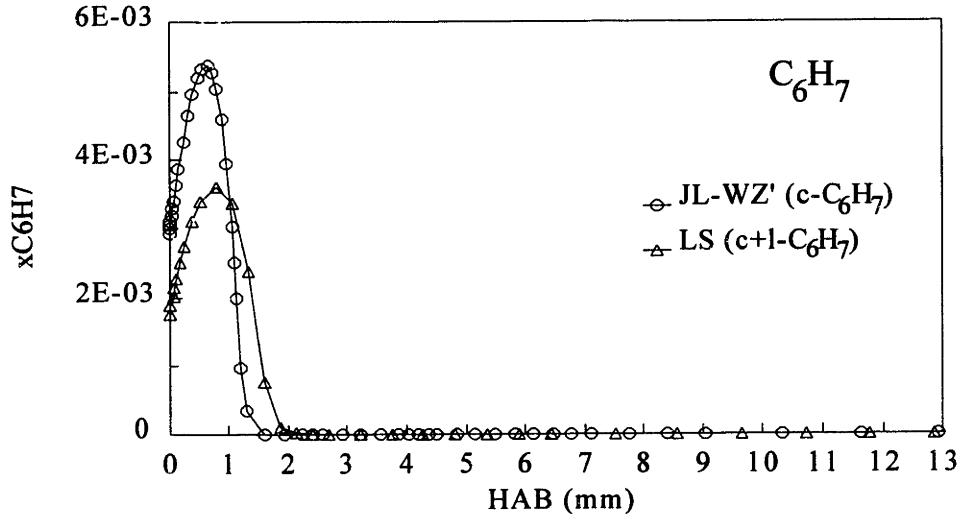

Figure 5.26 Model predictions of C_6H_7, in a 22 torr laminar, premixed H_2-O_2-C_6H_6-Ar flame. ϕ = 1.79, 31.3% Ar, $(x_{C6H6}/x_{H2})_0$ = 0.010, v_0 = 101 cm/sec. "c+l" = cyclic plus linear isomers. "JL-WZ'" - see text.

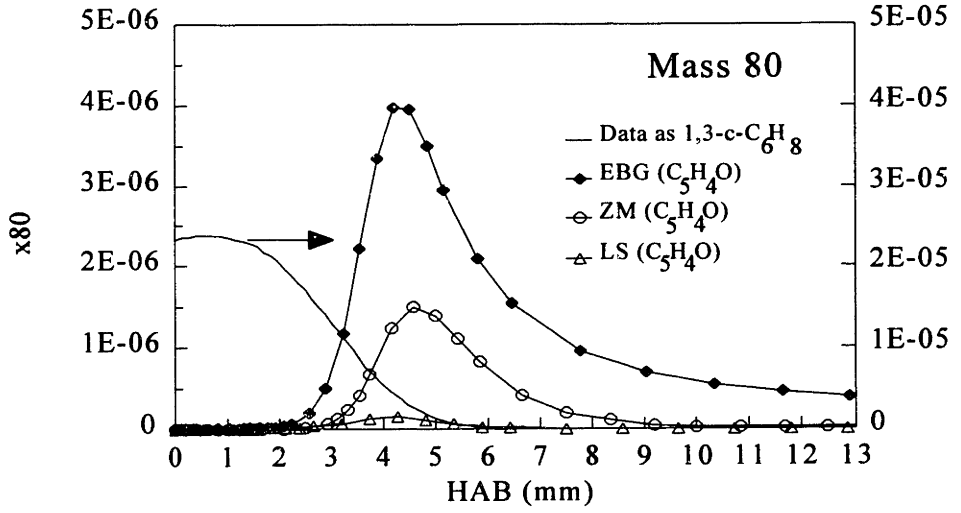

Figure 5.27 Mole fraction and model predictions of mass 80, in a 22 torr laminar, premixed H_2-O_2-C_6H_6-Ar flame. ϕ = 1.79, 31.3% Ar, $(x_{C6H6}/x_{H2})_0$ = 0.010, v_0 = 101 cm/sec.

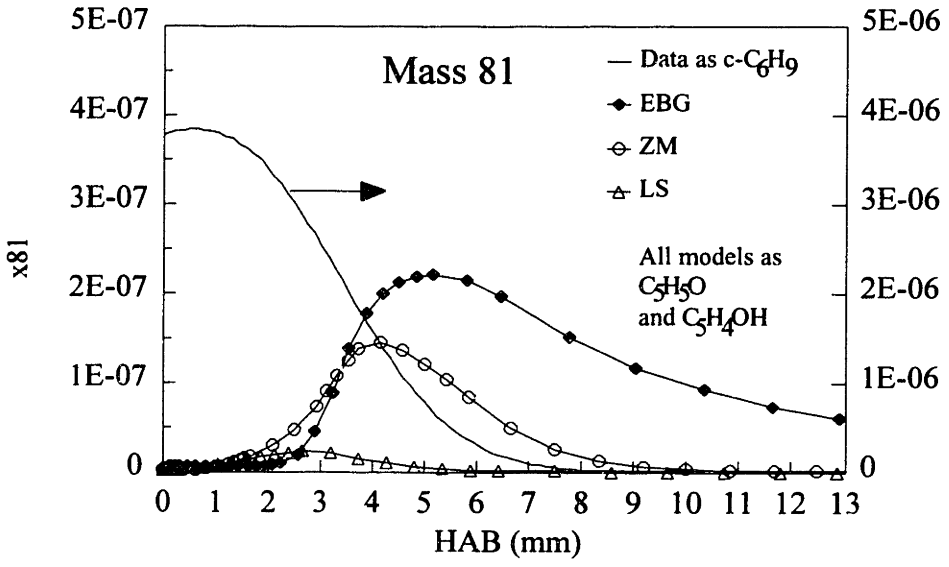

Figure 5.28 Mole fraction and model predictions of mass 81, in a 22 torr laminar, premixed H_2-O_2-C_6H_6-Ar flame. ϕ = 1.79, 31.3% Ar, $(x_{C6H6}/x_{H2})_0$ = 0.010, v_0 = 101 cm/sec.

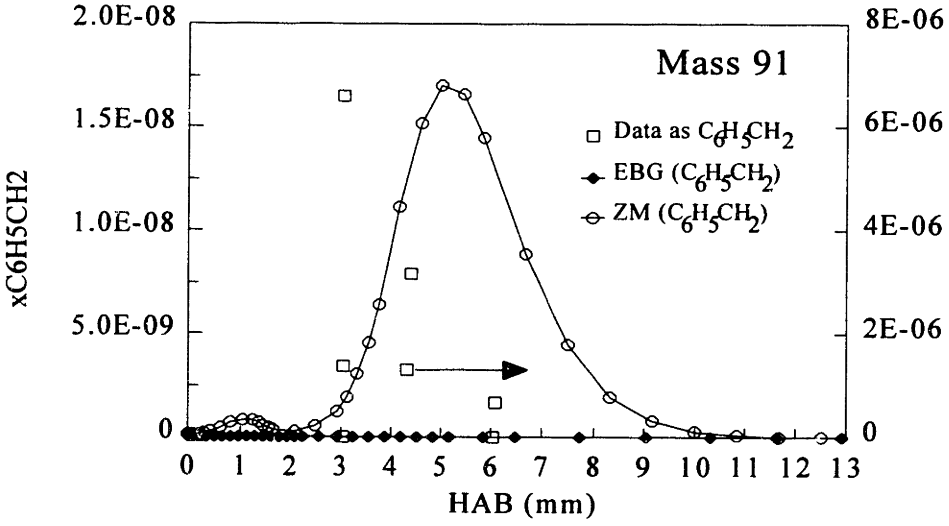

Figure 5.29 Mole fraction and model predictions of mass 91, in a 22 torr laminar, premixed H_2-O_2-C_6H_6-Ar flame. ϕ = 1.79, 31.3% Ar, $(x_{C6H6}/x_{H2})_0$ = 0.010, v_0 = 101 cm/sec.

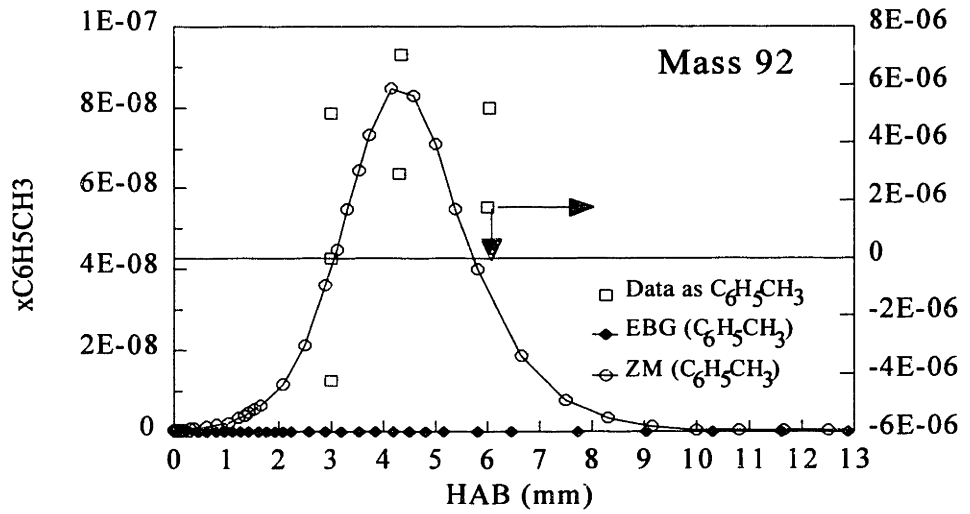

Figure 5.30 Mole fraction and model predictions of mass 92, in a 22 torr laminar, premixed H_2-O_2-C_6H_6-Ar flame. ϕ = 1.79, 31.3% Ar, $(x_{C6H6}/x_{H2})_0 = 0.010$, v_0 = 101 cm/sec.

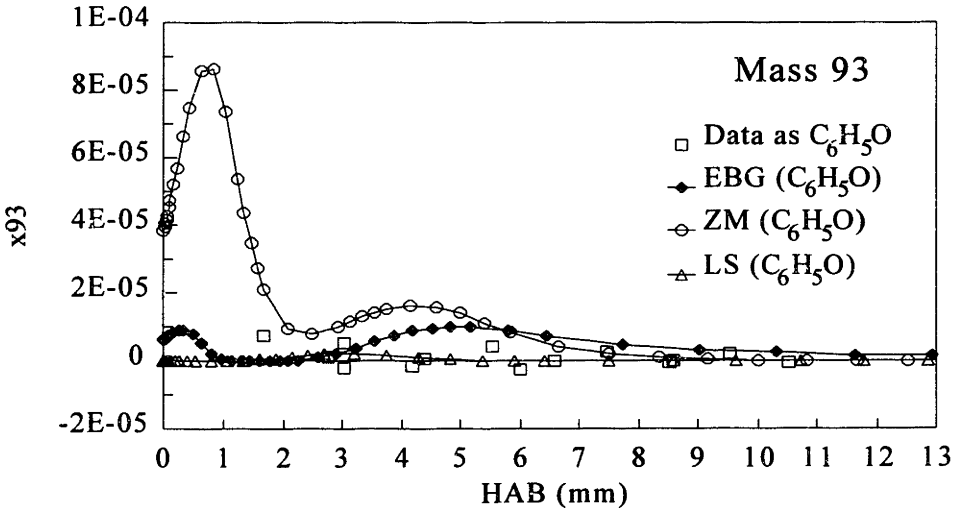

Figure 5.31 Mole fraction and model predictions of mass 93, in a 22 torr laminar, premixed H_2-O_2-C_6H_6-Ar flame. ϕ = 1.79, 31.3% Ar, $(x_{C6H6}/x_{H2})_0 = 0.010$, v_0 = 101 cm/sec.

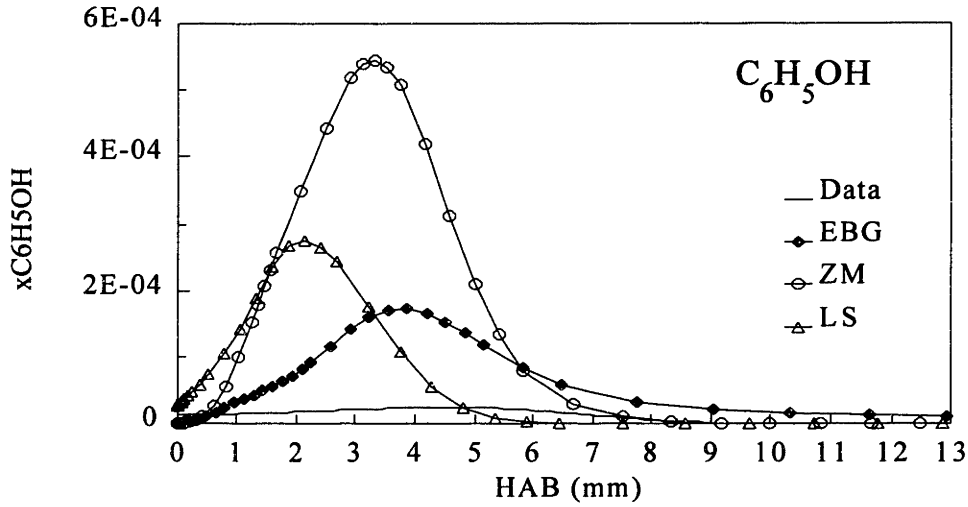

Figure 5.32 Mole fraction and model predictions of C_6H_5OH, in a 22 torr laminar, premixed H_2-O_2-C_6H_6-Ar flame. ϕ = 1.79, 31.3% Ar, $(x_{C6H6}/x_{H2})_0$ = 0.010, v_0 = 101 cm/sec.

Chapter 6: Analysis of H/O Destruction Chemistry.

It is clear from comparison of measured and computed mole fractions that nearly all of the species in the hydrogen-oxygen system are poorly predicted by the current reaction mechanisms in the literature. As mentioned previously in Chapter 5, this is not the case for comparison of the same models to benzene flame data previously collected with this experimental system. In addition, H_2-O_2 flame chemistry is generally considered to be well understood.

The unexpected disagreement between model and data in this flame is thus worthy of further analysis. The data were first evaluated in light of an important measure of data consistency — partial equilibrium — and found to be satisfactory. An examination of available experimental data in the literature was then undertaken, with an eye towards either validating the model predictions or finding disagreements similar to those seen in this study. The available information from previous sources is consistent with the data collected in this work.

Because the mole fraction of one species can affect the rate of formation or destruction of another, when there is serious disagreement between predicted and true mole fractions of important species one cannot even hope for a model to produce accurate reaction rates. Since accurate reaction rates are needed to arrive at an accurate solution, in such cases the mole fractions of other species will be strongly impacted, and the model cannot be meaningfully evaluated on the basis of its mole fraction predictions. An alternative method of assessing the strengths and weaknesses of the model which does not rely on model-produced mole fractions is needed. *Net rate analysis* is such a technique, and it is applied in this chapter to the chemistry of the H/O system of species. The hydrocarbon system — in particular aromatics, or "benzene destruction" chemistry — is analyzed in Chapter 7.

6.1 Evidence of Partial Equilibration of the H_2-O_2 System in the Post-flame Zone

Several reactions in the H/O chemical system are so fast that they are found to be equilibrated in the post-flame zone of H_2-O_2 flames, even when the entire chemistry cannot be said to be in equilibrium (for example, see Dixon-Lewis, 1979, and Zachariah and Smith, 1987). This condition is known as "partial equilibrium." In particularly rich flames, $\phi \geq 5$, this condition

weakens somewhat, but at the equivalence ratio of the present flame this is no problem (Dixon-Lewis, 1979). The fast reactions, known as "shuttle reactions," are:

$$H_2+OH \rightleftharpoons H+H_2O \quad (1)$$

$$O+H_2 \rightleftharpoons OH+H \quad (2)$$

$$H+O_2 \rightleftharpoons OH+O \quad (3)$$

Bittner (1981) found equilibration of reactions (1) and (3) in the post-flame zone of a stoichiometric C_6H_6-O_2-Ar flame, with the present experimental apparatus.

To test for partial equilibrium, one generally examines the ratio of experimental concentrations to the known equilibrium constant. So, taking reaction (1) for example,

$$K_{1,eq} \stackrel{?}{=} \frac{[H_2O][H]}{[H_2][OH]} \quad (6\text{-}1)$$

is the relevant relationship; or, one can see if the ratio of the right-hand side to the left is close to one. Calling the measured concentration ratio "K", a partial equilibrium ratio K/K_{eq} of 1.0 indicates perfect partial equilibrium.

For species calibrated by the Relative Ionization Cross-Section ("RICS") method, the ionization cross-section (Q) chosen will affect how close to equilibrium a reaction appears to be. As discussed in Chapter 3, some of the cross-sections used by Bittner can be improved upon, thanks to the use of more appropriate types. The partial equilibrium ratios for reactions (1)-(3) in the present H_2-O_2-C_6H_6-Ar flame and the stoichiometric C_6H_6-O_2-Ar flame are listed in Table 6.1. Since the accuracy of RICS calibrations is only a factor of two, and two or more species in each reaction are derived with that approximation, all of the RICS ratios indicate partial equilibrium[25]. In the case of the hydrogen flame, the ratio for reaction (1) is at the limit of partial equilibrium. With the updated cross-sections, no conclusions are changed but both reactions in the hydrogen flame are more comfortably within the acceptable range. In the benzene flame, the overall effect is improvement as well, judging by the total percentage deviation from 1.0 for the three reactions. Recalling that catalytic heating effects on thermocouples are stronger in stoichiometric than rich flames, Bittner checked for partial equilibrium with a temperature 80 K less

[25] If, for example, two species in the reaction are RICS-computed, then the range that the partial equilibrium ratio can take is $(0.50)^2 = 0.25$ to $(2.0)^2 = 4.0$. For three species — reactions (2) and (3) — the range is 0.125-8.0.

Table 6.1 Partial equilibrium ratios for H_2-O_2 system. "K" ≡ concentration ratio on right hand side of equation 6-1. Mass 16 data in the H_2-O_2-C_6H_6-Ar post-flame zone is taken as O atom.

Flame, Location	Radical Calibration Method	$\frac{K_1}{K_{1,eq}}$	$\frac{K_2}{K_{2,eq}}$	$\frac{K_3}{K_{3,eq}}$
H_2-O_2-C_6H_6-Ar 28.5 mm	RICS - Bittner Q's	4.34	0.16	*
H_2-O_2-C_6H_6-Ar 28.5 mm	RICS - updated Q's	3.23	0.58	*
H_2-O_2-C_6H_6-Ar 28.5 mm	partial equilibrium assumption	1.00	1.00	*
C_6H_6-O_2-Ar 36 mm	RICS - Bittner Q's (80 K catal. heating)	0.98 (0.76)	0.35 (0.36)	2.46 (3.25)
C_6H_6-O_2-Ar 36 mm	RICS - updated Q's (80 K catal. heating)	0.73 (0.57)	1.49 (1.53)	1.03 (1.35)

* Signal/noise ratio for the very low O_2 signal was too high to calculate concentration ratio.

than measured. Improvement is also seen with revised cross-sections, for the assumed lower temperature.

With partial equilibrium established in the post-flame zone of the hydrogen flame, the appropriate equilibrium relationships can be used to recalibrate the mole fractions of OH and H. Calibration on the assumption of partial equilibrium is an established technique (see, for example, Bittner, 1981, and Vandooren and Bian, 1990). In the present case, however, the mole fraction of O_2 is so small and the signal was so noisy that reaction (3) could not be used. As a third constraint, a requirement that the mole fractions of OH and H mole fractions remain within the factor of two expected from RICS calibration was substituted for reaction (3). The problem was solved using the "Solver" feature of Lotus 1-2-3® Release 4 for Windows™. All of the objectives could be achieved by multiplying the RICS-derived mole fractions by 1.84 for OH and 0.60 for H. The multiplicative factor for O is then 0.36, which is slightly more than a factor of two, but was considered acceptable because of the lower signal and higher noise for O than for the other two.

A second test for consistency of the data in the post-flame zone was to perform a steady-state analysis of the O atom mole fraction. The method was identical to that performed by Bittner (1981) (Chapter 8) for his rich benzene flame. Using RICS-calibrated mole fractions, the

estimated value of x_O was $1.2x10^{-5}$, as opposed to the experimental value of $3.0x10^{-5}$. With the revised calibration, $x_{O,est} = 1.5x10^{-5}$, and $x_{O,meas} = 1.1x10^{-5}$. Better agreement is seen when partial equilibrium calibrations are used.

In summary, experimental mole fractions of H/O species were found to meet standard measures of internally consistency in the post-flame zone. The partial equilibrium relationships were used to reevaluate calibrations of H, OH and O, and were found to result in better agreement of x_O to the steady-state estimation.

6.2 Tests of H_2-O_2 Models Against Literature Data

The discrepancies between model and data observed in Chapter 5 for the H/O system were motivation for an examination of published experiments involving H_2-O_2 flames and species. The purpose of this search was to see if the problem had been previously identified, or if modeling of others' data revealed similar problem trends.

As mentioned, it is commonly accepted in the combustion community that current models do a superb job of simulating H/O kinetics. However, published material on model development and testing have almost uniformly been made with respect to *lower-temperature* experiments, that is, at or below 1500 K. At higher temperatures, the results are not so clear.

For example, Warnatz (1979) and Cherian et al. (1981) were unable to model the 11.4% H_2 - 79.2% O_2 - 9.4% CO flame of Vandooren et al. (1975), with its temperature profile of $T_{max} \sim$ 1800 K. Using flame code programs which solved the energy equation as well as species concentrations, they found that the predicted temperature maximum for good mole fraction fits were as much as 500 K less than data. They concluded that the temperature data were in error, due to catalytic recombination on the thermocouple. This seems improbable, as (a) the amount of temperature rise which would have had to occur in the flame is at least 100 K higher than that typically found by Bittner in a stoichiometric benzene flame at half the pressure and a higher radical density, and (b) Vandooren et al. would probably have noticed the high drift.

Westmoreland (1986) measured stable and radical species in a lightly sooting C_2H_2-O_2-Ar flame (T_{max} = 1900K), and found that while the reaction scale of H/O species was reasonably well predicted, no model could do a good job with all the mole fractions. Nor could any model predict O atom, H_2 or H_2O well.

A third example is the lean (ϕ = 0.64) H_2-N_2O-Ar flame of Dayton et al. (1994), with its maximum temperature of 2161 K. This was not an H_2-O_2 system *per se*, but most H/O species[26] were present in significant amounts in the post-flame zone. Throughout the flame the nitrogen-containing species were well predicted, as was the reaction scale in general. In the reaction zone, though, the H atom prediction was a factor of seven high, and measured H_2 was about twice that calculated. O and OH were predicted to rise steadily from the preheat zone, while in reality the two showed an induction period, which lasted until the maximum flame temperature was reached and ended in a sharp rise. At 1750 K, for example, O and OH predictions were roughly five and fifteen times the measured values.

On the other hand, Zhang and McKinnon (1995) and Lindstedt and Skevis (1994) both found that H/O species were accurately modeled in ϕ = 1.8 C_6H_6-O_2-Ar.

Some perspective is needed to understand these results. The first question to be answered is the meaning of this information with respect to reaction scale. In the last three examples given, H/O chemistry was minor relative to C/H/O or N/H/O chemistry, implying that the latter two were the governing factors in setting the reaction scale. It has already been noted in Section 5.3 that the model-predicted reaction scale for C/H/O chemistry is accurate. In the case of the flame of Vandooren et al., undoubtably dominated by H/O chemistry, the modeling results showed that a lower temperature profile was needed to predict the species mole fractions well.

To understand the meaning of this result, model computations of the present flame were made with the temperature profile modified to be identical to that of the ϕ = 1.9 H_2-O_2-Ar flame of Vandooren and Bian (1990). The modified maximum temperature was then about 700 K lower than the measured peak for the present flame, analogous to the results computed by Warnatz and Cherian et al. for the Vandooren et al. flame. With this profile the Zhang and McKinnon ("ZM") model predicted H_2, O_2 and H_2O very well, with the reaction zone being several millimeters wider than measured, rather than half its width[27]. OH was nearly perfect, but H atom was still overpredicted by a factor of 5.6. In summary, good overall agreement could be achieved by a lowering of the temperature profile, showing that the error in modeling of the Vandooren et al. data might lie in the models themselves rather than the thermocouple measurements.

[26] HO_2 and H_2O_2 were either not present or not measured.

[27] Most significantly for the question of whether such a modified profile is realistic, C/H chemistry was nearly halted entirely.

The second feature to be explained is the comparison of mole fractions. In the H_2-N_2O flame most of the H/O species were as far mispredicted in the reaction zone as they are in the present flame. In the acetylene flame, each model tested predicted at least one species in the system correctly, but others poorly. Finally, in the benzene flame, everything was predicted accurately. The trend to be noted here is that as the chemistry and models *increase* in complexity, the fit of H/O computations approaches perfection. This is probably indicative of improvement by compensating errors.

What is needed then, to best document the incongruence between model and data in another experimental source, are high temperature H_2-O_2 data. The only examples found in the literature were the H_2-O_2 flames of Seery and Zabielski (1981). Two flames were modeled, using the H/O submechanism of Zhang and McKinnon (1995). They were:

1. $\phi = 1.22$ flame ($T_{max} = 1930$ K). No radical data were available for comparison. With regard to major species, the burnout zone was shortened to half its width, exactly as seen for the present flame.
2. $\phi = 0.88$ flame ($T_{max} = 1950$ K). The only radical reported was OH. The model predicted the magnitude correctly, but the peak was located at less than half the height of the experimental maximum. The major species' reaction zone was 3 mm, again half that of the measured width.

Analysis of the data available in the literature therefore leads to the conclusion that the present data are valid, and the problems with H_2-O_2 chemistry lie in the models instead. Further evidence of this is presented in the radical net rate analysis portion of Section 6.4.

6.3 Net Rate Analysis Methods

In previous work at MIT, Cole (1982) and Cole et al. (1984a,b) devised a method of screening proposed formation reactions, for regions of a flame where the net rate of the species of interest was expected to be little affected by consumption reactions. In that method, the rate of formation of the species was calculated by using the proposed rate constant and the measured temperature and mole fractions of reactants. That rate was then compared to the experimental net rate to explore the viability of that pathway to formation. This type of analysis is referred to here as "model-data," or "MD," analysis. In contrast, many reaction path analyses (cf., for

example: Zhang and McKinnon; Westmoreland, 1986; or Jackson and Laurendeau, 1987) involve a study of rates computed by combining the reaction rate constants with *model-predicted* mole fractions (concentrations). That method is referred to here as "model-model," or "MM," analysis. It has been little-acknowledged (or not at all) that when a mole fraction calculated by a model is significantly in error, one cannot take any rates which rely upon that species at face value. That is, in such cases one is dealing with the combined error of the rate constant and the mole fractions, which could easily compensate or aggravate the error in the rate constant (or pathway) alone. Chapter 7 contains several specific examples to illustrate this point in the present flame.

The model-data method was extended by Westmoreland et al. (1989) to comparison of the sum of several reactions to an experimental formation rate. Given the current state of development of reaction mechanisms, the MD method may be further extended in the following ways:

- The reverse reaction may be included, so as to give a net rate for the individual pathway.
- The entire submechanism of a proposed model, i.e. the sum of all net rates for each pathway in the model that involves the species of interest, may be compared to the measured net rate. Because current mechanisms are relatively comprehensive, one needn't search for specific regions dominated by formation or consumption. An accurate model should reproduce the measured net rate in all regions of the flame (except close to the burner, where flow nonidealities and probe effects affect the fluxes).

Analyses in the next section and Chapter 7 are of this type unless specified otherwise.

6.4 H/O Chemistry Net Rate Analysis

While differences do exist between the various literature H_2-O_2 models, the main features seen in the results obtained are identical in the present flame. Five H_2-O_2 reaction sets were tested, as submodels of the larger mechanisms: Miller et al. (1982), Warnatz (1984) (as modified by Westmoreland, 1986), Yetter et al. (1991), and a modified version of Yetter et al. found in the ZM model. Because of the similarity in solutions produced by the models, only one set of results is reported and analyzed here.

Major stable species.

Figures 6.1-6.3[28] show the data and model-predicted (MD) net rates for O_2, H_2O and H_2. Data net rates were calculated from the flame equations of Chapter 3, using the program FBR listed in Appendix D. Computations were performed on the Cray-2 computer at the Department of Energy's National Energy Research Supercomputer Center in Livermore, CA.

Two sets of net rates are presented, one derived from the full reaction set of the ZM model and the other from only the H_2-O_2 submechanism. The full-model net rates were

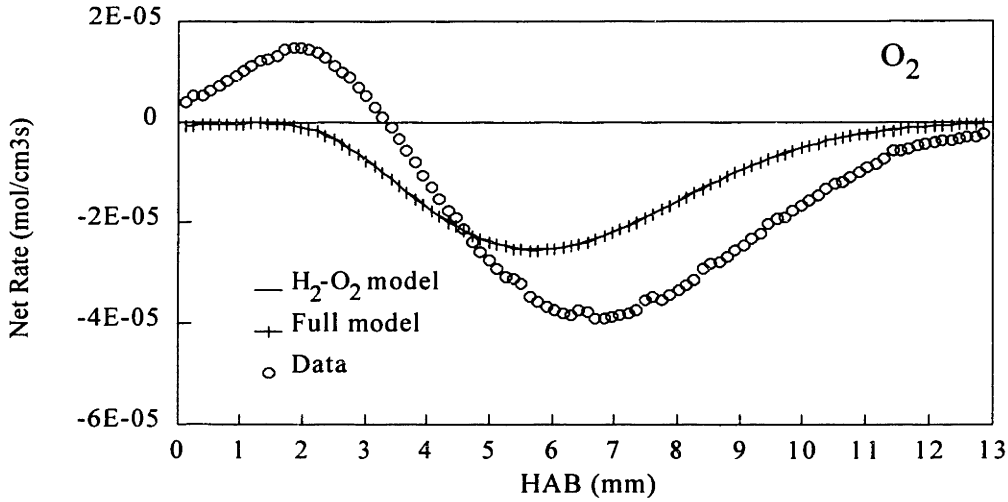

Figure 6.1 Data and MD model-predicted net rates for O_2.

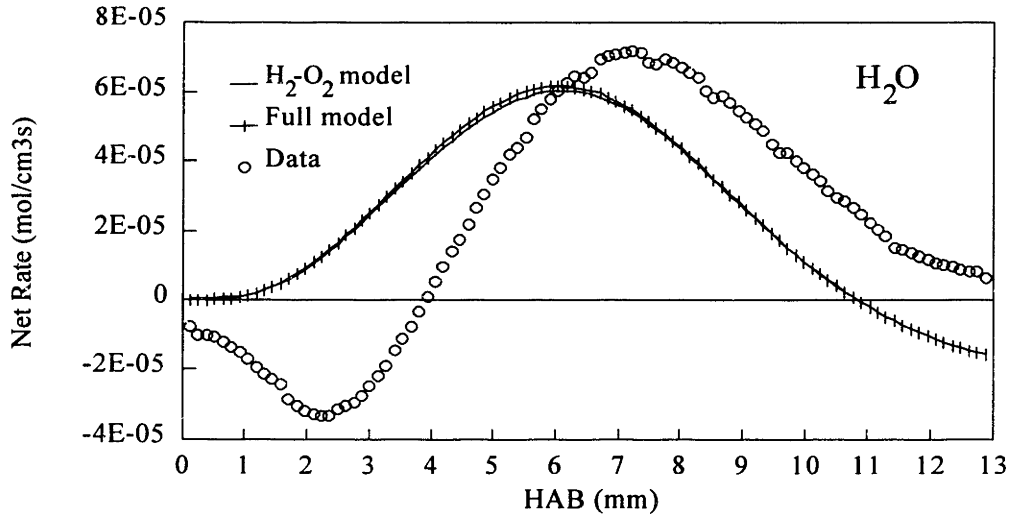

Figure 6.2 Data and MD model-predicted net rates for H_2O.

[28] In all figures, "Height Above Burner" is referred to as "HAB."

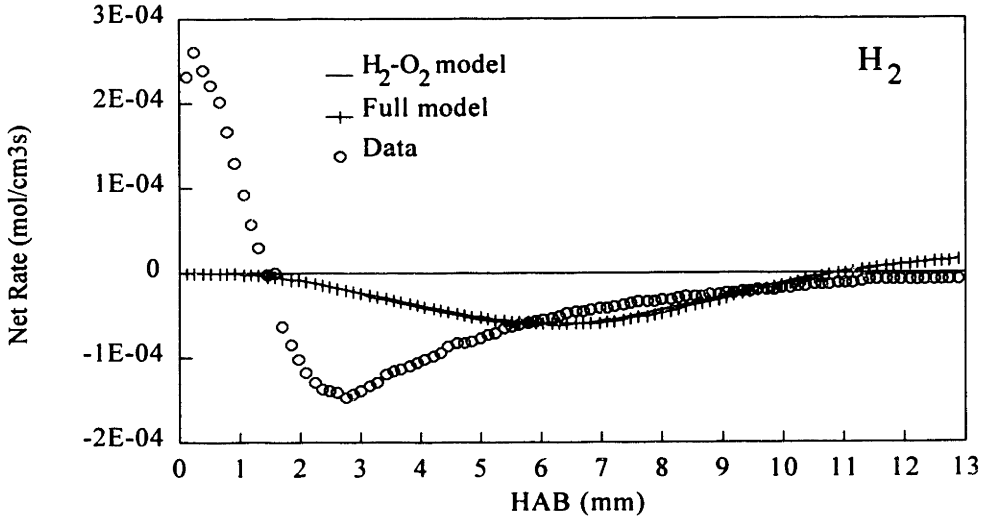

Figure 6.3 Data and MD model-predicted net rates for H_2.

calculated with FBR; the H_2-O_2 rates were computed in a spreadsheet on a personal computer. The near-perfect coincidence of the two predictions confirms that hydrocarbon chemistry has no effect on the stable H/O species.

The experimental net rates for the major H/O species compare favorably to those measured for the same species by Bittner in his rich benzene flame, in a qualitative sense. The positive rate for O_2 between the burner and 3.3 mm was also seen in rich C_6H_6, until 4 mm in that case[29]. As one would expect that right at the burner the rate should be zero or negative (indicating destruction), Bittner attributed the non-physical behavior to distortion by the large-orifice probe. The probe used in this study also had a relatively large orifice, with an area 70% of that used by Bittner. In particular, he cited O_2 as being sensitive to this effect because of its gradient and high diffusivity relative to benzene. In the present flame the diffusivity is even higher for all species, because of the large quantity of H and H_2 and small quantity of higher molecular weight species. Therefore, the early hump in the net rate is consistent with previous measurements. H_2 has an even larger hump, as expected because of its diffusivity. Interestingly, for H_2 the positive rate only occurs in the first 1.3 mm, though distortion may be present in the next few millimeters as well. In any event, measured net rates below several millimeters are subject to error and should

[29] All flame heights cited for the Bittner flames will be given on a basis of correction for probe perturbations. This is the same basis as the present flame data.

not be compared to predictions. The net rate of H_2O in the rich C_6H_6 flame was negative until 3.2 mm and positive above that height, similar to the H_2O rate in the present flame.

Despite its drawbacks when model predictions are in error, MM reaction path analysis can be useful for studying the nature of a model or submechanism of a model. One such case in which useful information can be gleaned is the major stable species predictions of the H_2-O_2 model. According the the ZM model MM analysis:

- above 2 mm the O_2 net rate is completely governed by reaction (3) alone,
- above 2 mm the H_2O net rate is completely due to one reaction as well — reaction (1),
- several reactions are responsible for the H_2 net rate, but reaction (1) accounts for 75% or more of the total above 1.5 mm.

In the MD analysis the same results are found, except that for H_2 reaction (1) is for all purposes 100% of the predicted consumption rate. The agreement of the model predictions with data above the first 3-4 mm — and therefore above 1500 K as well — is good, considering the error in experimental measurements and the larger uncertainty in most individual rate constants.

The net rate of O_2 consumption is not only predicted by a single reaction, but the contribution of reverse direction of the reaction is insignificant as well[30]; that is, $R_{O2,pred} \approx k_3[H][O_2]$. Since reaction (3) is one of the fast branching reactions in the H/O network, a lower activation energy would both cause the reaction zone to shrink and result in greater radical mole fractions. Therefore, k_3 could theoretically be the source of poor model performance. The net rate, the mole fractions of H and O_2, and the temperature profile are all experimental quantities, so good net rate agreement implies that the literature value of k_3 is not likely the source of the H/O chemistry problems. (Alternatively, one might take the point of view that since k_3 is a well-studied reaction up to 2500 K, agreement lends some support to the validity of x_H and x_{O2}. For more information about the history of this rate constant, see Baulch et al., 1992. The estimated error is a factor of 1.6 at 2500 K.)

Both directions of reaction (1) are important to the predictions of H_2 and H_2O, but all of the mole fractions are measured, leaving only the rate and equilibrium constants in question. As with k_3, k_1 could in principle be responsible for the undesirable features of the model predictions. The good agreement for both water (except for a position shift on the same order as oxygen's)

[30] This conclusion is highly insensitive to assumptions about the O atom profile.

and hydrogen above 4 mm argue favorably for the accuracy of k_1. The order of magnitude is well-determined up to 2500 K (though there is disagreement as to whether it follows Arrhenius bevahior at high temperatures), allowing again for an opinion that the prediction supports the data. In any event, nothing about the net rate analysis for major species leads one to question either the data or the rate constants.

Radical species: overall features.

Things are not so clear for H and OH. In those cases a number of reactions are important to the final net rate, in both the MM and the MD calculations. Furthermore, the predicted rates deviate from the data far more than for major species, in both peak position and magnitude (Figures 6.4 and 6.5). OH chemistry is much more in error than H chemistry, giving a net rate two orders of magnitude too high and with consumption alone throughout the reaction zone.
The experimental net rates are qualitatively very similar to those found in the rich benzene flame. In both flames, the net rate of H is negative until the middle-to-late reaction zone, and is positive thereafter. Similarly, in both environments peak OH formation occurs at the position where the H net rate is going from consumption to production, and OH is destroyed in the preheat and early reaction zone plus the post-flame zone[31].

With the exception of the H atom rate in the first millimeter, the model predicts that hydrocarbon chemistry has essentially no effect on the calculated net rate. (The large hydrogen

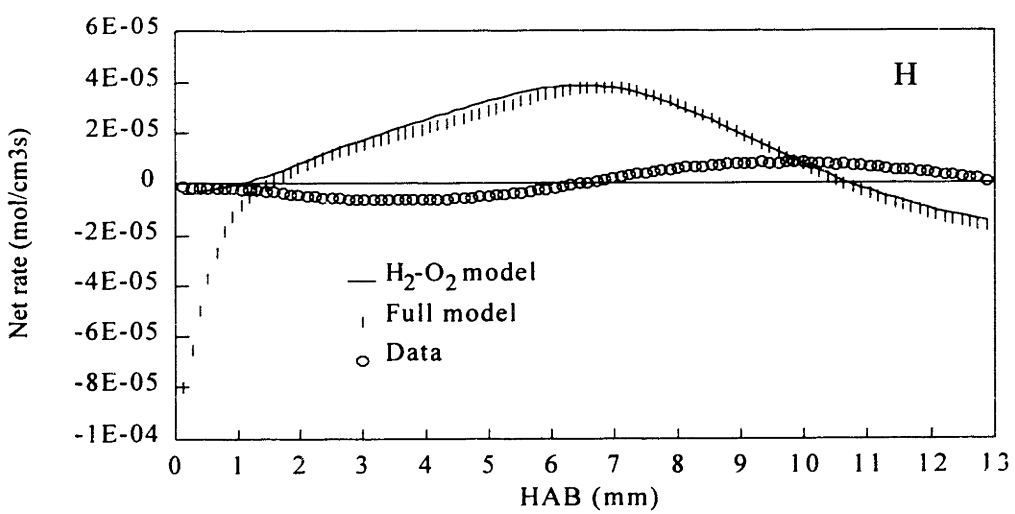

Figure 6.4 Data and MD model-predicted net rates for H atom.

[31] The exact positioning of the post-flame transition to destruction for OH in the present flame is an estimate, as no data points were collected above 11 mm.

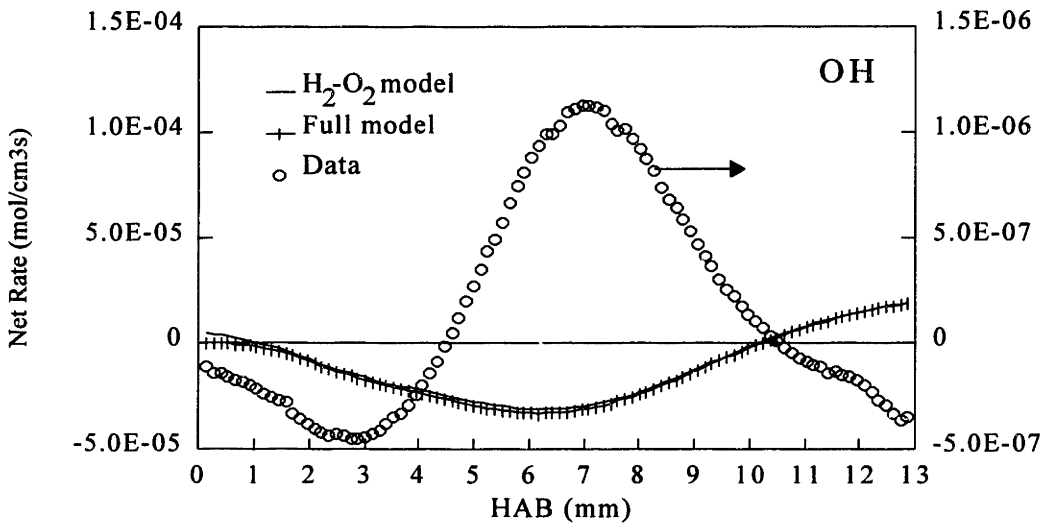

Figure 6.5 Data and MD model-predicted net rates for OH.

consumption predicted by the model near the burner is from the reaction $C_2H_4+H+M \rightleftharpoons C_2H_5+M$.) This is reasonably in accord with a measurement of the OH signal at 14.5 mm, made first in the H_2-O_2-C_6H_6-Ar flame, and then in a flame with identical flows but no benzene. The signal in the hydrocarbon-additive flame was 16% lower than the H_2-O_2 flame signal. That is, the presence of hydrocarbons has only minimal effect on the OH chemistry.

To test the model within the framework of its *own* mole fraction predictions, solutions were obtained for H_2-O_2-Ar flame conditions. Two runs were performed, the first with the same temperature profile as the benzene flame and the second with a modified profile intended to simulate a slightly hotter, faster, low ϕ flame. In both scenarios, the maximum x_{OH} predicted was at least three times more than the prediction for a flame with benzene, and the peak x_H was at least twice that of the benzene additive flame. A model-model reaction path analysis of the impact of hydrocarbons on the H/O system reveals that the primary effect is a drain on H atom by the pair of reactions:

$$C_6H_5+H \rightleftharpoons C_6H_6 \qquad \text{(B1)}$$

$$C_6H_6+H \rightleftharpoons C_6H_5+H_2 \qquad \text{(B4)}$$

The fast shuttle reactions (1) and (3) quickly propagate the effect to the other H/O species, with a slower reaction (3) shutting down part of the chain branching. Since the model phenyl and H atom mole fractions are much larger than the measured profile, $x_{C6H5,pred}$ and $x_{H,pred}$ both share

responsibility for the unrealistically large hydrocarbons impact predicted by the model. However, reaction (B4) and abstraction from benzene by OH, account for nearly all of the model's phenyl production. That is, H atom plays a hand both directly and in the excessive formation of C_6H_5.

To help sort out the contributions of hydrocarbons as opposed to H/O species, the net rate

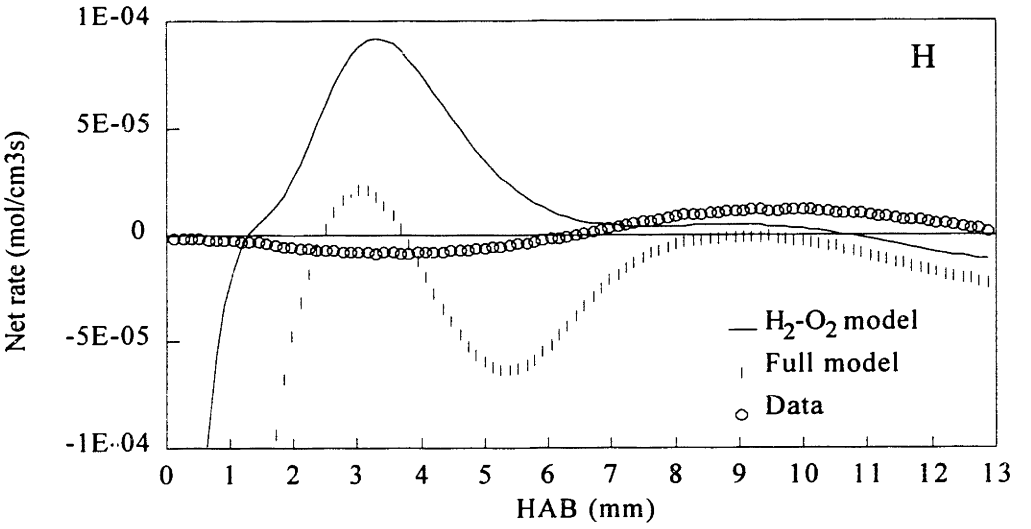

Figure 6.6 Data and MD model-predicted net rates for H. Mole fraction set was hybrid of measured hydrocarbons and model-predicted H/O species.

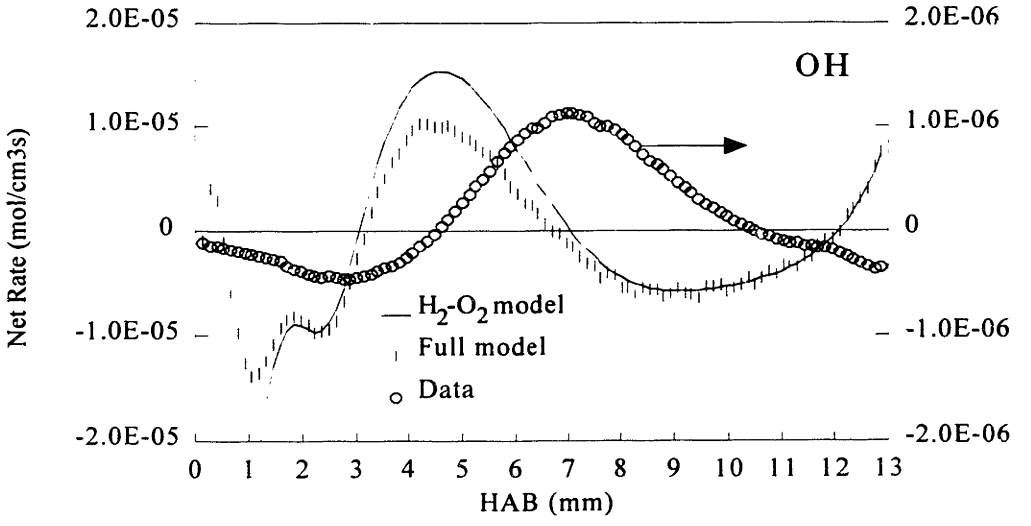

Figure 6.7 Data and MD model-predicted net rates for OH. Mole fraction set was hybrid of measured hydrocarbons and model-predicted H/O species.

analyses were redone with a hybrid set of mole fractions, in which the hydrocarbons were measured profiles and the H/O species were model predictions. With the model-predicted H_2-O_2 species imposed on the original data set, the effect of hydrocarbon chemistry is now predicted to be very large for H atom (Figure 6.6). The areas under the curves show there to be a great deal more H formation for the case of no hydrocarbons than for the full model — in fact, integration of the full model curve would result in more destruction than production, a non-physical situation. Figure 6.7 shows the areas under the OH curves are approximately equal. This should not be taken as meaning that the addition of hydrocarbons would not affect the mole fraction of OH. The change in the net rate curve of a species in going from "H_2-O_2" to "full model" corresponds to the *instantaneous* response of the chemistry of that species to the (hypothetical) imposition of the hydrocarbon mole fraction structure on the flame. In the case of the original analysis with a completely experimental set of profiles, none of the H/O species for which data were collected changed to any extent in response to that imagined stimulus. Therefore, the H_2-O_2 chemistry would be expected to remain stable. In the case of the hybrid model-data profile set, the tremendous leap in H production shows that the flame would *not* be expected to remain as is, hydrogen being capable of "jump-starting" the entire radical pool through branching action of reaction (3). OH would increase as a result. Another way of understanding the results is to recall from the discussion above that the reverse effect (quenching) occurs in the model calculation of a benzene additive to an H_2-O_2 flame, almost exclusively as a result of reactions which consume H. The resulting response of OH is even greater than that of H atom.

The conclusion to be drawn, then, is that the model H/O mole fraction solution is in great measure responsible for the incorrect prediction that addition of small amounts of benzene would cause a large change in the OH mole fraction. In contrast, experimental mole fractions are consistent with the OH observation.

The prediction of O atom's net rate is dependent on the assumptions made for the O profile, but for the assumptions used here and for each of several reasonable limiting cases (all described in Section 6.5), the predicted maximum net rate is on the order of ($\pm$) 10^{-5}-10^{-4} mol/cm^{3}s. Species with maximum net rates in the 10^{-5} range are O_2 and H atom; C_6H_6 has a maximum net rate less than $1/10^{th}$ that value, and CH_4 about $1/5^{th}$. As it was established in Chapters 4 and 5 that mass 16 is largely or entirely CH_4, the model prediction for O atom is far afield of the data.

Radical species: specific reaction paths.

Examination of the predicted MD net rates for H and OH reveals an interesting feature: unlike with the measured rates, the models predict the net rates to be equal and opposite for the two species. Reaction path analysis shows that two reactions, (1) and (3), are responsible for this condition. Reaction (2) contributes to both species as well, but not much relative to the other two reactions. The two reactions run in opposite directions with respect to H/OH production. That is, reaction (1) produces H and destroys OH, and reaction (3) does the opposite. This explains the mirror image nature of the two predicted net rates. O atom is predicted to be formed overwhelmingly by reaction (3), and is consumed at a low rate by (2).

Possible sources of H/O chemistry inadequacy at high temperature.

Further study of the H and OH net rates shows that the balance between production and formation for each species is skewed in that the maximum of rate of reaction (1) is a bit more than twice that of reaction (3). The error limits of the rate contants are such that the reactions could in fact be much more closely in balance than the predictions would indicate, which would lower the net rate and thus bring the predicted mole fractions closer to measurements. With lower H atom, the critical branching reaction (3) is slower and the consumption of O_2 is slowed as well. This would result in an increase in the predicted reaction zone width, as desired.

Having the proper balance of reactions (1) and (3) cannot fully explain the observations. OH would still be destroyed by these reactions when H is being produced, and vice versa, a behavior which is only seen between 4.6-6.5 mm and above 10.6 mm. Also, the mole fraction of OH is in reality much smaller than that of H, not approximately equal to it. Reaction (2), when added, is the pathway for production of asymmetrical net rate curves. While $O+H_2$ is unimportant when the other two reactions are not running at nearly equal rates, when balance is almost achieved the resulting small net reaction rate and the rate of reaction (2) can be the same order of magnitude. Since both H and OH are produced in this secondary branching reaction, the net result of the three reactions can be any combination of net formation or consumption of H and OH — even net consumption of both species, if the O mole fraction is so low that (2) runs in reverse. Indeed, with a crude adjustment[32] of $A'_1 = 0.65A_1$ and $A'_3 = 1.6A_3$, the predicted net rates of H and OH come far closer to data (as Figures 6.8 and 6.9 show), without negative effects on the fit

[32] The changes are needed more at high temperatures than low ones.

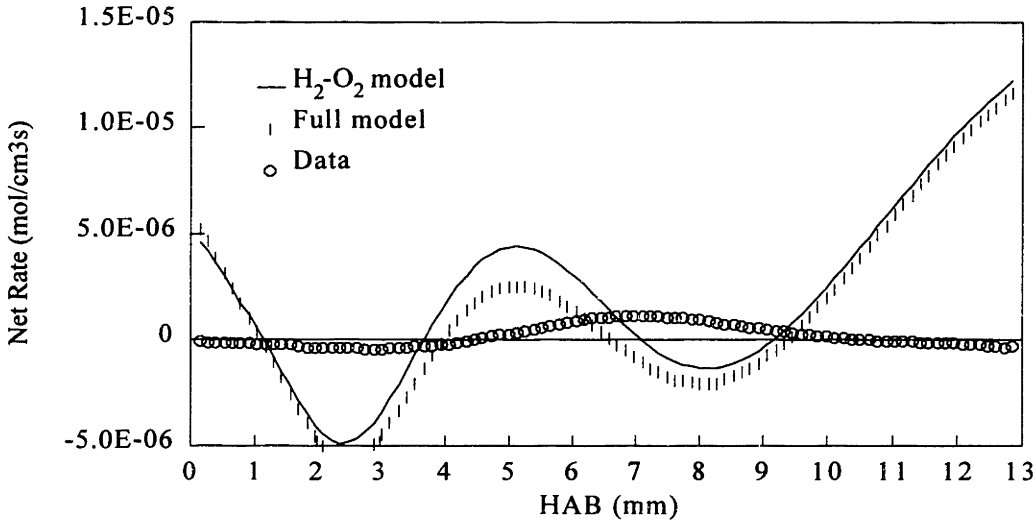

Figure 6.8 Data and MD model-predicted net rates for OH. Pre-exponential factors A_1 and A_3 were modified as noted in the text.

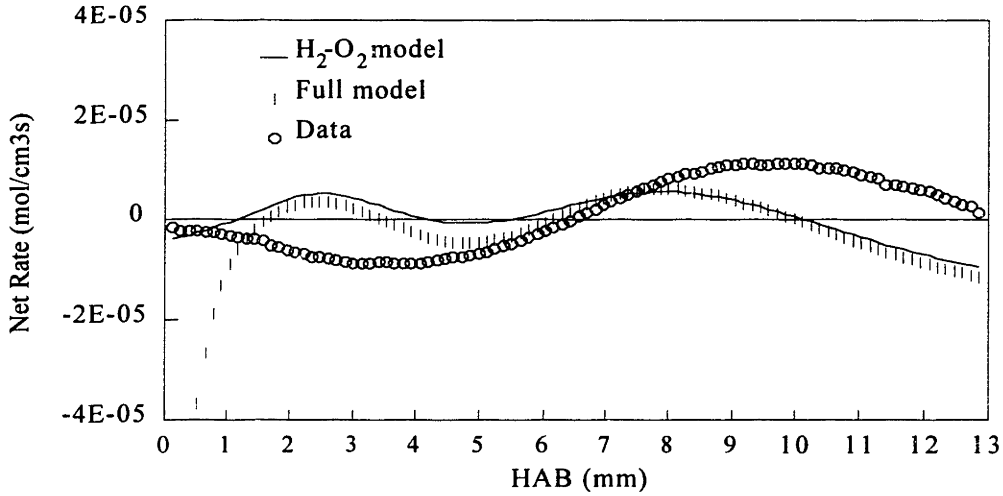

Figure 6.9 Data and MD model-predicted net rates for H. Pre-exponential factors A_1 and A_3 were modified as noted in the text.

for stable species[33]. Furthermore, the slightly larger difference between the full model prediction and that of the H_2-O_2 submodel alone is in better agreement with the 16% drop in OH signal observed with no hydrocarbons in the flame.

[33] The rapid increase in predicted OH rate above 10-11 mm is a result of reaction (1), and could be a function of assumptions made in the smoothing curves of the species involved above the region where measurements were made.

Unfortunately, as was already mentioned the large amount of O atom produced by (3) is not even close to being offset by consumption in reaction (2), and the aforementioned adjustments only make matters worse. Artificially increasing A_2 to a level in which the area under the net rate curve is roughly balanced between production and consumption throws the other radical predictions, particularly OH, back into disagreement. That is, increasing k_2 enough to offset O production would only upset the delicate balance achieved with H and OH.

It was noted in Section 6.2 that the model mole fraction solution can nearly be made to agree with the data if a temperature profile that has a lower maximum is used as input to the simulation. This is suggestive of a possible problem with spurious thermocouple heating by catalytic recombination. However, the hydrocarbon chemistry is then predicted to be almost entirely halted, clearly in conflict with the actual situation. Furthermore, the thermocouple temperature drift characteristic of catalytic heating was not observed either.

If one accepts the accuracy of high-temperature literature values of k_1-k_3, there appears to be only one possible explanation for the observed behavior: an alternative, very fast, pathway for O consumption that only opens up at higher temperatures.

6.5 Mole Fraction Assumptions and Sensitivity Analysis

Mole fraction assumptions and rationale.

O - same shape and location as OH, peak height $0.055*x_{OH,max}$. In their $\phi = 1.93$, H_2-O_2-Ar flame, Vandooren and Bian (1990) measured O atom and OH profiles using MBMS. The shapes and locations of the peaks were identical, though the O peak was about 2.5 times that of OH. Bittner (1981) measured these species with MBMS in a stoichiometric C_6H_6-O_2-Ar flame, and found the same situation with respect to the form of the profiles. However, with the main fuel being a hydrocarbon instead of H_2, the peak heights of the two species were the same. In his $\phi = 1.8$ benzene flame, Bittner assigned the mass 16 signal entirely to CH_4, on the basis of ionization potential measurements and the behavior of the signal in a region of the flame where polymeric material was deposited on the probe (8-18 mm). He also performed a steady-state analysis of reactions which form and destroy O atom, to estimate the mole fraction in the post-flame zone. The maximum O mole fraction estimated was 4.7×10^{-4} at 10 mm, not far from the OH peak location. This is about 30% of the highest CH_4 mole fraction, clearly an overestimate since the CH_4 mole fraction at 10 mm was also 4.7×10^{-4}. If one assumes that 10 mm is about the

peak height for O atom, and that $x_{O,10mm} \sim 0.1 * x_{CH4,10mm}$, then the ratio $\frac{x_{O,max}}{x_{CH_4,max}}$ would be about 0.03. For the present flame, a ratio of 0.04 was chosen, resulting in $x_{O,max} = 1x10^{-4}$.

HO_2, H_2O_2 - 5.0*(original ZM model prediction). As discussed in Chapter 4, the mass 33 and 34 signals were so noisy that these species could not be accurately measured. As the upper limit estimates were somewhat higher than the model predictions, the model profiles were multiplied by five. The ratio of HO_2 profile maximum to $x_{OH,max}$ for such an estimate was more than twice the same ratio found by Bittner (1981) in his rich benzene flame. Bittner apparently could not detect H_2O_2, but in the present flame with dominant H_2-O_2 chemistry more of that species would be expected.

Sensitivity to O atom assumptions. The result of O profile variations was studied. Three major cases are considered. In the first, the position and shape are identical to the OH profile (the default assumption); in the second, they are the same as the original ZM model prediction; in the third, they are the same as the methane profile. In the first case, the base-case magnitude was that noted at the beginning of this section; it was varied from 0 to 20 times the base magnitude. In the second case the base height is 8% of the ZM model's prediction, and in the last it was 8% of the CH_4 peak mole fraction; magnitude variations from 0.5 to 12.5 times the base case were made.

Original model - Stable species H_2, O_2, and H_2O are quite insensitive to the assumed O magnitude for the three test profiles. Water is the most sensitive, with the predicted net rate peak location moving almost a millimeter closer to the burner (except in the CH_4-based scenario) and dropping in height by about 15% when the O magnitude is highest.

H atom's net rate is increased with increasing O atom concentration, ultimately reaching three times the original prediction at the highest assumed x_O's. The peak location shifts 1.5 mm toward the burner with a CH_4-based profile, and becomes a 3 mm plateau starting 3 mm closer to the burner when the model-based profile is used.

The sensitivity of OH is also very strong. With enough O atom assumed, the destruction peak at 6.5 mm becomes a formation peak with a maximum as much as three times the original quantity of consumption. The peak location shifts with increasing $x_{O,max}$; towards the burner for the CH_4- and model-based O profiles, and away for the OH-derived profile. In no case does the

shape of the OH net rate begin to approximate a situation where the destruction and the formation levels both get closer to the measured quantities.

Model with revised k_1 and k_3 - The stable species respond in a similar way as for original model, though H_2O drops about 25% when the O magnitude is highest.

For H, the peak at about 8 mm is affected by the variations. Dropping the O mole fraction to 0.00 throughout decreases the H peak by a factor of three. At the highest $x_{O,max}$ tested, the predicted rate of H formation rises to 15 times the original height — but it is still only two-thirds the prediction with the original rate constants, for the same O assumptions. When there is a location shift, though, it is larger. The new peak location is the same; the location with an OH-based profile is simply 1.5 mm higher from the burner, which is closer to the measured maximum by the same amount. Therefore, except for a drop in assumed maximum O mole fraction, for all of the variations tested the net rate of H produced with revised rate constants is always better than the original model.

The OH net rate predicted by the revised model is even more sensitive to $x_{O,max}$ than for the original model. Above twice the base-case maximum mole fraction, the maximum formation rate increases proportionally to 25 times the value with an unvaried O profile. The greater sensitivity is expected by the very nature of the situation. The OH net rate in this case is in a more delicate balance between three reactions than H, and O atom is the most important species in the "tie-breaker" reaction, (2). When one looks at the *absolute* deviation of the prediction from the measured net rate, one finds:

- below (roughly) three times the base case $x_{O,max}$, the revised model performs better than the original, and
- above (roughly) three times the base case $x_{O,max}$, the relative performance of original and revised models is about the same as for H atom, i.e., the original model deviates about two-thirds as much as the revised.

In summary, for assumed O peak heights at or below about three times the base-case value, the revised model does much better than the original, particularly with respect to OH net rate. For variations with an O maximum above three times base-case, the two models would be judged to be equally inaccurate.

Sensitivity to HO_2 and H_2O_2 assumptions. The two mole fraction profiles were varied together from the base-case described above, from 0.1 to twice the original magnitude. There is very little sensitivity to these mole fractions, and that only in the first 1-1.5 mm. In that region, when the magnitudes of the mole fractions are doubled, the OH production and H destruction predicted there double as well.

It should be noted that the model profiles on which the assumed profiles are based are probably half the actual width, possibly accounting for some of the disagreements in predictions and measurements for H and OH in the early-to-middle reaction zone (less than about 4.5 mm, or twice the width of the model profile).

Sensitivity to H and OH calibration factors. As discussed in Section 6.1, the partial equilibrium calibration method was used instead of RICS for H and OH. To test the response of the predictions to calibration of these radicals, the mole fraction curves were varied from 50% to 150% of the original magnitude. As one would expect, the major species are not as sensitive to these changes as the radicals, though the fits do significantly improve or deteriorate. Generally, the predictions retain the same shape as the measured net rate profiles, but increase or decrease in magnitude, or appear slightly shifted in location. The radical species are highly sensitive to the changes, since they have to be in a fairly precarious balance to achieve reasonable agreement with the data. Improvements over the fits of original model net rates — sometimes large, in the case of H and OH — for most or all species are still possible by adjustments of A_1 and A_3 within a factor of 2-3.

Sensitivity to temperature profile. The temperature profile is subject to error in two primary ways: magnitude, and alignment with respect to mole fractions. Both of these features were varied within the expected maximum limits and the resulting effect on the model predictions was gauged. To test for magnitude error, the profile was multiplied by 0.948 and 1.052, which in both cases resulted in a maximum difference of 100 K from the original values. The modified temperature profiles were used as the basis for recalculating both the model predictions and the data net rates of H/O species.

The changes to data net rates and original model-predicted net rates were minor in all cases. With regard to net rates computed with revised k_1 and k_3, major species were only slightly changed. For minor species, small readjustments of the rate constants could be made to offset

changes due to temperature profiles, except for the increase in temperature magnitude. The revised prediction it still an improvement over the original model, but by a smaller amount.

6.6 Summary

Consistency of H/O species data.

1. Partial equilibrium of reactions (1) and (3) is achieved by the far post-flame zone. The electron impact ionization cross-sections of Chapter 3 appear to be more appropriate for RICS calibration than those used by other workers.
2. H atom and OH data were recalibrated on the basis of partial equilibrium at 28.5 mm. When used in a steady-state approximation of O atom at that point in the flame, the recalibrated mole fractions agree better with the data, supporting a conclusion that partial equilibrium calibration is preferable to RICS.

H/O chemistry: analysis.

1. The effect of additive levels of hydrocarbons on OH (in the early post-flame zone) is correctly predicted to be small.
2. H_2-O_2 models predict a very narrow burnout zone, and the radical mole fractions are much higher than data.
3. For each of the major species a single reaction, (1) or (3), is responsible or mostly responsible for the entire net rate. Using MD net rate analysis, the net rates are well-predicted, within the error limits of the data and rate constants, supporting literature values of high temperatures.
4. H and O atom is predicted to be formed in greater quantities than measured; O atom formation in particular is far overpredicted. The models predict OH be destroyed where it should be produced and at an extremely high rate relative to the measured values.
5. Reactions (1) and (3) result in a large amount of production and consumption of H and OH, such that the amount of consumption (production) of one species must be equal and opposite of the production (consumption) of the other. This behavior was not observed. O atom is produced by reaction (1) and destroyed by (2).

Evidence of H/O chemistry problems in others' data.

1. The few high temperature experiments in which H/O chemistry was predominant show behavior consistent with that seen in the present flame.
2. Overall reaction scale (burnout rate) seems to be governed by the amount of H/O chemistry occuring relative to other types. The amount of radical magnitude overprediction appears to be a function of the complexity of the chemistry, i.e., the size of the reaction set: the errors seem to be compensated in more complex models (or because the relative importance of H/O reactions diminishes greatly).
3. Because the discrepancies seen here are only important in high temperature H_2-O_2 flames or other flames of lower complexity, the problems have gone unnoticed by many.

H/O chemistry: possible solution and remaining problems.

1. In order for the H/O submechanisms to predict the observed net rates of H and OH, reactions (1) and (3) have to be proceeding at nearly equal rates, with the rate of reaction (2) being on about the same scale as the net of the other two. The crude revision of k_1 to 65% of the original value, and k_3 to 160% of its original, accomplishes the task reasonably well.
2. With reaction (2) proceeding at a level necessary to predict H and OH, the rate of O production is much higher than its consumption rate. The net result is a prediction of far more O atom than is observed, and which in any case if correct would throw off the possibility of an adequate balance between H and OH.
3. A large slowdown of reactions (1) and (3) could solve nearly all of the problems, but if the well-studied values of k_1 and k_3 are accepted as reasonable then the only way for this to occur is if the temperature profile is in error. This possibility is ruled out.
4. The only remaining explanation for the observed discrepancy in O atom appears to be the existence of an alternative, high-temperature, fast O consumption mechanism.

Sensitivity analysis.

1. Because of the postulated radical balance, H/O radical concentrations are sensitive to changes in the assumed O profile and calibration factors of H and OH.

2. When the assumed O profile or radical calibration factors are varied within reasonable limits, the revised model either performs better than the original version, or readjustments to A_1 and A_3 can be made so that a net improvement is maintained. Therefore, the conclusion that a better balance between reactions (1)-(3) is needed at high temperatures is not affected by expected limits of error in measurement or calibration.

Chapter 7: Analysis of C_6H_6 Destruction Chemistry.

As discussed in Chapters 5 and 6, the mole fraction profiles of H, O, OH and O_2 are poorly predicted by the current literature mechanisms. These species are the most important reactants for benzene and its products in the present H_2-O_2 flame, so the reaction rates calculated within flame code simulations are negatively impacted by the errors. Therefore, the resulting mole fractions of aromatic species do not adequately reflect the accuracy of the benzene portion of the kinetic model. It is necessary, then, to use *net reaction rate* analysis to study the state-of-the-art C_6H_6 destruction mechanisms.

In Section 6.4 measured mole fractions were applied to H_2-O_2 mechanism subnetworks, to compute net rates for comparison with the experimental values. The method used in this chapter for analysis of benzene destruction chemistry involves an initial comparison of model to data (Section 7.1), followed by consideration of individual rate constants within the C_6H_6, C_6H_5OH, C_6H_5 and C_6H_5O subnetworks and the subsequent effect of modifications on tne fit to data (Sections 7.2-7.5). The single cyclohexadienyl formation reaction found in the published models, plus the development of a preliminary C_6H_7-C_6H_8 submechanism, are discussed in Section 7.6.

In the model and reaction calculations made in this chapter, assumptions had to be made regarding the mole fractions of species which were not positively identifiable, below the detection limit or in some other way unmeasureable. The decisions made and there rationale are given in Section 7.7, along with an analysis of the sensitivity of the results to those assumptions.

Specific calculations mentioned in the chapter are found, for the most part, in the Appendices. The final model additions and modifications are found in Section 7.8, where the revised model is put to the test in a rich benzene flame. Finally, a summary of findings is presented in Section 7.9.

7.1 Net Rate Analysis of Published Models

Shown in Figure 7.1 are the net rates for benzene as predicted by the three models (Emdee, Brezinsky and Glassman (1992) ("EBG"), Zhang and McKinnon (1995) ("ZM"), and Lindstedt and Skevis (1994) ("LS"). In this chapter, the EBG and LS models were used as received by the authors. The version of the LS model used is that of Lindstedt and Skevis (1994),

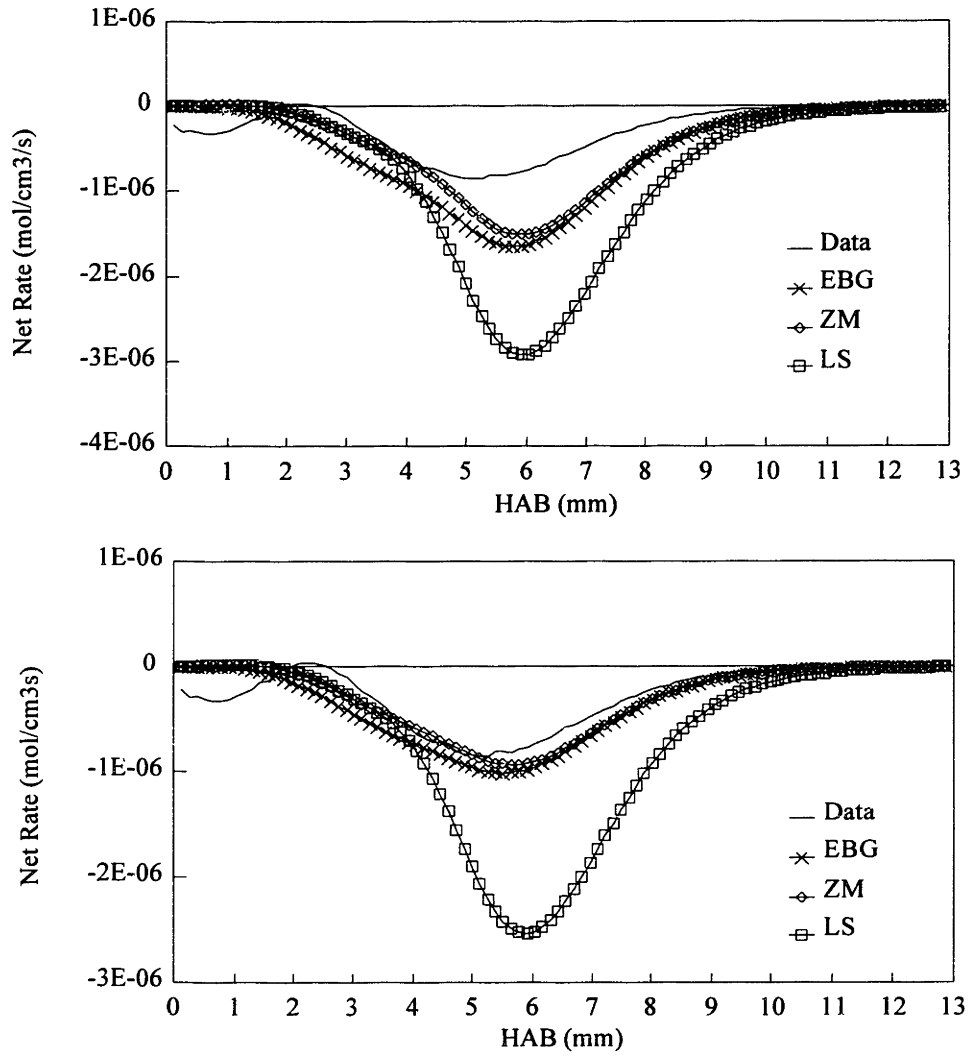

Figure 7.1 Data and model-predicted net rates for benzene. Top: Sandia thermochemistry. Bottom: modified Sandia thermochemistry. EBG = Emdee, Brezinsky and Glassman (1992); ZM = Zhang and McKinnon (1995); LS = Lindstedt and Skevis (1994).

rather than Lindstedt (1995), because of the incorrect phenyl decyclization rate constant in the latter. For the ZM model, the falloff calculations were redone for 22 torr and a bath gas with "average" H_2-O_2-C_6H_6-Ar properties.

In the top graph of Figure 7.1, the thermochemistry used to calculate equilibrium constants for reverse reactions was that used by ZM. This set, referred to herein as "Sandia thermochemistry," was a slightly modified version of the CHEMKIN Thermodynamic Database, Kee et

al. (1994). The changes made by ZM were to incorporate EBG values for several aromatic species, none of which are significant in this flame.

While much of the Sandia thermochemistry includes fits to experimental data, the values for C_6H_5, C_6H_5O, and C_6H_5OH are derived from BAC-MP4 *ab initio* quantum chemistry calculations (Kee et al., 1994). The heats of formation derived from those computations are 79.4, 10.35 and -25.0 kcal/mol respectively as compared with 78.4, 11.4, and -23.0 in Burcat et al. (1985). The Burcat et al. set of values, referred to here as "modified Sandia thermochemistry," was derived from experimental sources. One change was made for these calculations: ΔH_f^0(phenoxy) was set to 9.3 kcal/mol, the average of more recent recommendations, one by Back (1989) and two recommendations by Manion and Louw (1989). The 11.4 kcal/mol used by Burcat et al. was derived from Colussi et al. (1977). The remaining thermodynamic properties for phenoxy were calculated from the vibrational frequencies and moments of intertia given by the NASA group. The NASA entropies at 298 K are about 1-1.5 cal/mol lower than the *ab initio* values. The lower plot of Figure 7.1 shows the results for benzene when modified Sandia thermochemistry is used in the calculations. Unlike the Sandia set, in which the maximum consumption rate predicted by the ZM and EBG models is beyond the roughly ±20% limit of error of the measurement (see Appendix A), the NASA-based calculations show the models to do an excellent job of predicting the net rate. The accuracy of the LS mechanism is clearly in question, regardless of thermochemistry.

It should be mentioned that the LS net rate in Figure 7.1 does not include the reaction $C_6H_6+H \rightleftharpoons C_6H_7$, which is a part of that mechanism. Inclusion of that reaction causes the predicted rate to exhibit very peculiar behavior, the nature and remedy of which is discussed in Section 7.6. The significant additional benzene consumption seen in Figure 7.1 for the LS mechanism is due to the reaction $C_6H_6 \rightleftharpoons$ fulvene. Except for these two reactions, the C_6H_6 network of Lindstedt and Skevis is quite similar to that of the other two models. The reaction networks of the three models are discussed in detail in Section 7.2.1.

Net rate comparisons for C_6H_5OH are given in Figure 7.2. The results for both thermochemistry sets are very similar, except for a bit more formation with the Sandia set. Interestingly, while both heats of formation for C_6H_5O, if the BAC-MP4 value of 10.35 kcal/mol is substituted in the modified Sandia set (along with the BAC-MP4 heat capacity), there is a great deal more production of phenoxy and destruction of phenol. This topic is discussed in

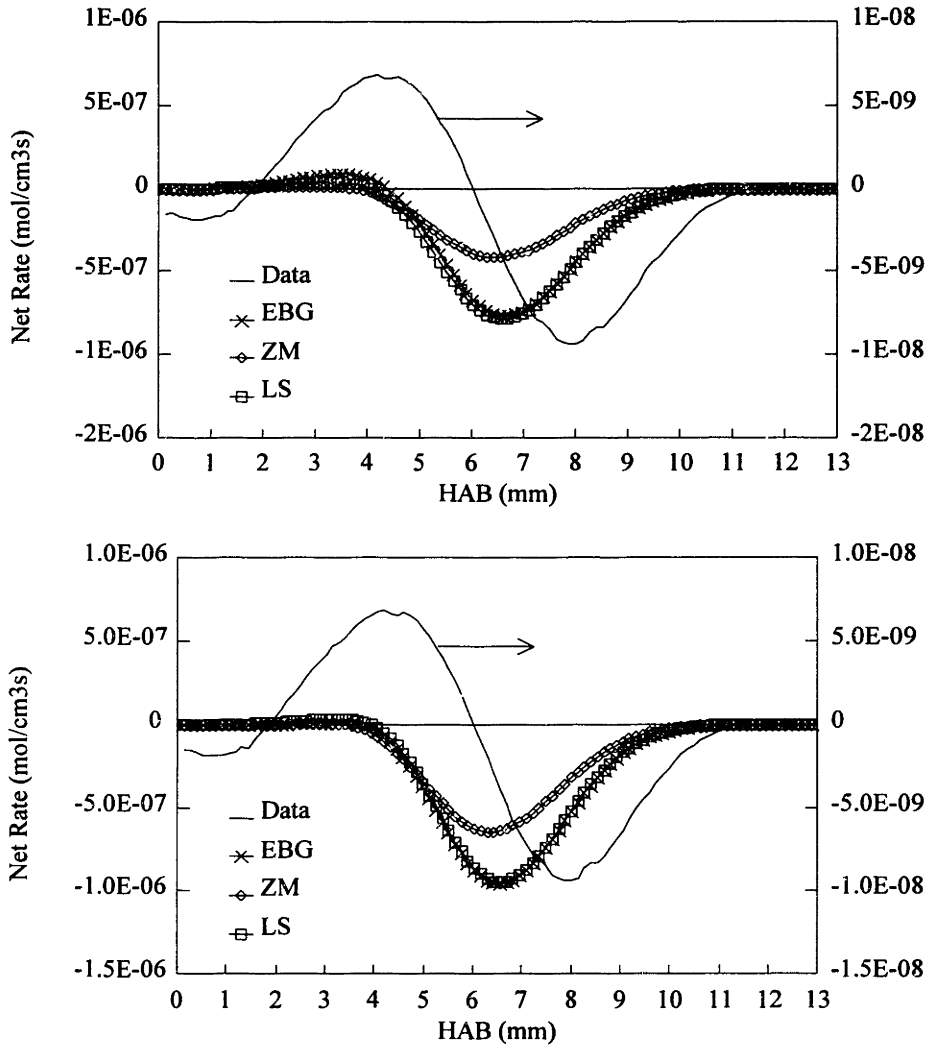

Figure 7.2 Data and model-predicted net rates for phenol. Top: Sandia thermochemistry. Bottom: modified Sandia thermochemistry.

Section 7.7.

All of the mechanisms overpredict phenol consumption rate by one to two orders of magnitude, relative to measurements. Phenol formation is better modeled, being within an order of magnitude when modified Sandia thermochemistry is used. Detailed analysis of C_6H_5OH chemistry is given in Section 7.3.

The third species for which individual rate constants were analyzed was C_6H_5. The phenyl mole fraction profile was extremely noisy, the magnitude being probably no more accurate than a factor of 3, and the shape and location being very uncertain. Nevertheless, the net

rate derived from smoothing and differentiation can be used as a rough guide for comparison with model predictions. The data and model net rates, using modified Sandia thermochemistry, are plotted in Figure 7.3. The results for Sandia thermochemistry are nearly the same, the only

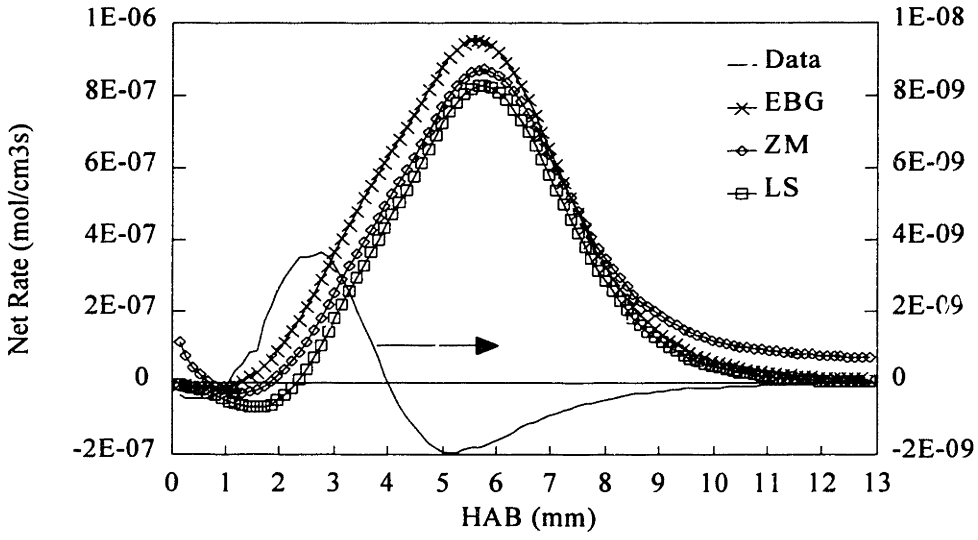

Figure 7.3 Data and model-predicted net rates for phenyl, using modified Sandia thermochemistry.

difference being that the predicted magnitude of the formation rate in each case is about 50% higher with the Sandia set.

It was empirically observed that the maximum experimental net rate scaled well with the maximum mole fraction. For example, see Table 7.1, where the ratios of mole fractions and (absolute value of) net rates for various combinations of species are listed. In most cases, the scaling is excellent, and the greatest deviation of mole fraction ratio from the net rate ratio is a factor of four. The relationship holds for comparison to broad peaks (e.g., C_6H_6 vs. O_2 or OH) and

Table 7.1 Ratios of maximum mole fractions and net rates for various pairs of species.

Species, j and k	$(x_j)_{max}/(x_k)_{max}$	$\lvert(rate_j)_{max}/(rate_k)_{max}\rvert$	Comments
C_6H_6, O_2	$2x10^{-2}$	$2x10^{-2}$	Destruction rate for both
C_6H_5OH, C_2H_2	$7x10^{-2}$	$6x10^{-2}$	Formation rate for both
H_2CO, CH_3	1.3	0.8	Formation rate for both
C_6H_6, OH	2	0.8	Destruction of benzene, production of OH
H, H_2O	$3x10^{-2}$	0.11	Formation rate for both
H, OH	5	7	Formation rate for both
C_6H_6, C_2H_2	12	8	Destruction of benzene, production of C_2H_2
C_6H_6, mass 42	5	13	Destruction of C_6H_6, production of mass 42

narrow peaks (e.g., C_6H_6 vs. mass 42 and H_2CO vs. CH_3) alike. It is important in such comparisons to use the maximum destruction rate for feed gases and the maximum formation rate for product gases. In support of this observation, the error analysis described in Appendix A revealed that varying the mole fraction has a proportional effect on the net rate then derived. It must be acknowledged though, that this phenomenon is has not been shown on a theoretical basis, and could be incorrect for specific cases.

The maximum mole fraction of phenyl is about 10^{-3} that of benzene and about 10^{-1} that of phenol. Therefore, although the measured net rate of C_6H_5 has a high degree of uncertainty, comparison with the mole fraction and net rate of phenol support a conclusion that the scale of the data net rate shown for phenyl, about $1x10^{-9}$ mol/cm^{3}s, is correct. The model predictions, that the formation rate of phenyl is nearly equal to the consumption rate of benzene, thus point to a probable lack of effective destruction pathways for C_6H_5. The good fit of model predictions for the net rate of benzene destruction is shown below to hinge entirely on a phenyl formation rate of the same magnitude. If the fit of the C_6H_6 destruction rate modeling is not coincidental, then, there must be a large consumption channel or channels for C_6H_5 to balance formation. Such strong production and destruction pathways must just balance in a way which results in a small but measureable mole fraction. Phenyl chemistry is discussed in more depth in Section 7.4.

Detailed reaction path analysis, presented in the following sections, demonstrates that phenoxy radical is another intermediate of great importance. As documented in Chapter 4, the

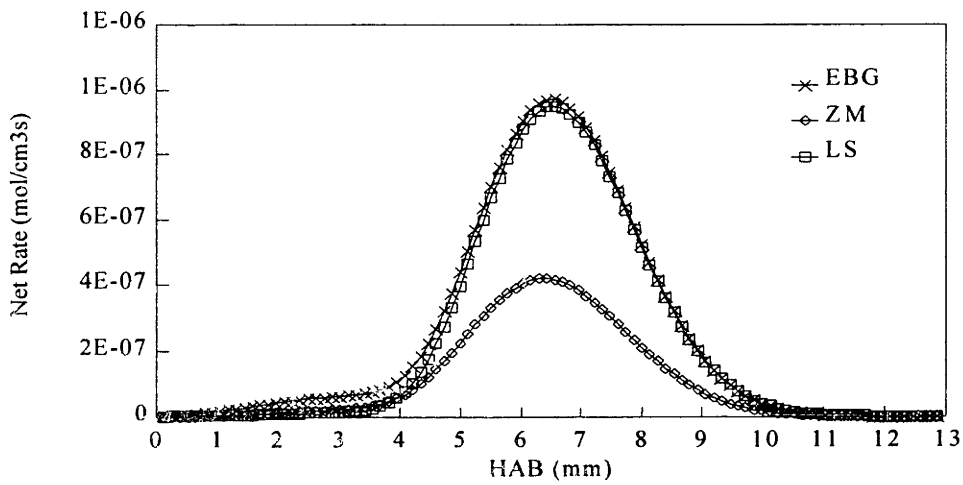

Figure 7.4 Data and model-predicted net rates for C_6H_5O, using modified Sandia thermochemistry.

mole fraction of C_6H_5O is below or just at the detection limit in this flame. Yet, Figure 7.4 shows that as with C_6H_5, the models predict the phenoxy net formation rate to be approximately equal to the destruction rate of C_6H_6. The mechanism for this phenomenon in all three models is the reaction $C_6H_5O+H \rightleftharpoons C_6H_5OH$, which clearly runs backwards in this case. Phenoxy chemistry is reviewed in Section 7.5.

Finally, the net rate of the intermediate C_5H_6 is graphed in Figure 7.5. This species has been postulated to arise from phenol pyrolysis to C_5H_6 and CO (Spielmann and Cramers (1972); Cyprès and Bettens (1974)), though only the ZM model contains this reaction. Cyclopentadiene is also related to C_5H_5, which is also an important species because it is the product of phenoxy decomposition (also producing CO in the process). The mass 65 signal, which includes

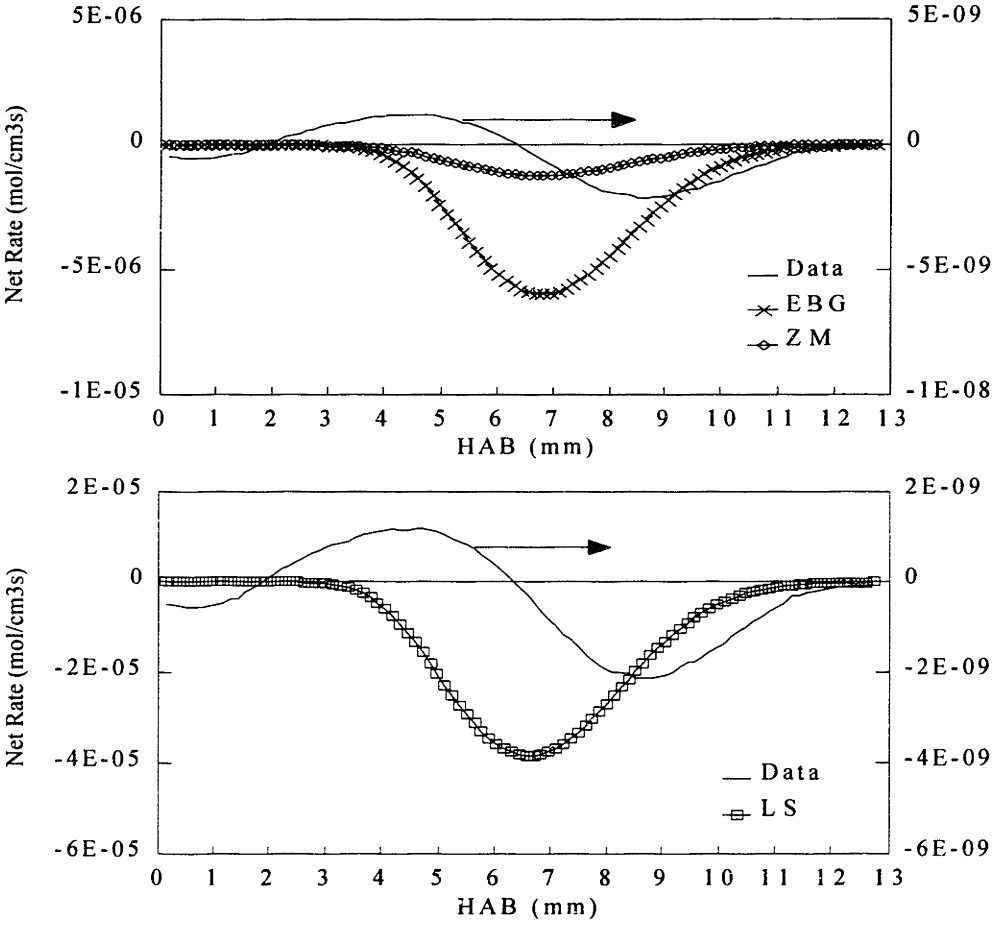

Figure 7.5 Data and model-predicted net rates for C_5H_6, using modified Sandia thermochemistry. Top: ZM and EBG models. Bottom: LS model.

cyclopentadienyl, was too noisy to estimate more than the general shape and magnitude of the mole fraction profile accurately. All of the models severely overpredict the destruction of C_5H_6, though none worse than the LS model, which has an exceedingly fast decyclization reaction, uncorrected for falloff effects. None of the models other than ZM has a reaction that produces cyclopentadiene.

7.2 C_6H_6 Net Rate Analysis

Two of the three models are shown above to do a good job of predicting the net rate of C_6H_6, above 2 mm, provided modified Sandia thermochemistry is used. The LS model overpredicts benzene destruction with either set of themochemical parameters. The first step in analysis of the benzene submechanisms was to perform a reaction path analysis relative to the net rate calculation for the entire submechanism. In this section, the net rate analysis will be extended to the level of individual reaction rates.

From the analysis shown in Section 7.1 and a review of the nature of elementary steps, specific reactions were identified as candidates for further analysis by consideration of falloff and reaction pathway assumptions (Section 7.2.1). In some cases, rates were appropriately modified or identified as inappropriate. The resulting revised mechanism was tested via net rate comparison (Section 7.2.2). Other reactions, present in the literature but not in the original models, were then considered (Section 7.2.3).

Unless specifically mentioned otherwise, the modified Sandia thermochemical data was used in the following calculations.

7.2.1 Model Reaction Sets for C_6H_6

Because of the low C/H environment of the additive H_2-O_2 flame, a number of reactions involving C_6H_6, e.g., $C_6H_6+C_2H \rightleftharpoons C_8H_6+H$, were removed from consideration. A complete list of reactions considered is given, in reaction path analysis form, in Table 7.2. For each reaction in a mechanism, the "reaction path ratio" $\frac{R_{rxn}}{R_{bnz}}$ is given, where R_{rxn} is the maximum net benzene destruction rate (reverse reaction included) by the reaction in question, anywhere in the flame. R_{bnz} refers to the maximum experimental net rate of C_6H_6 destruction in the flame. It can be seen that for the EBG and ZM models, three reactions — all involving production of C_6H_5 — account for

Table 7.2 C_6H_6 reactions in the mechanisms under review, and the reaction path ratio $\left(\frac{R_{rxn}}{R_{bnz}}\right)$ for each. "0" ≡ <0.01.

Rxn No.	Reaction	EBG†	ZM†	LS†
B1	$C_6H_5+H \rightleftharpoons C_6H_6$	0.53	0.53	0.53
B2	$C_6H_6+OH \rightleftharpoons C_6H_5+H_2O$	0.41	0.29	0.26
B3	$C_6H_5O+H \rightleftharpoons C_6H_6+O$	0.06*	0*	
B4	$C_6H_6+H \rightleftharpoons C_6H_5+H_2$	0.49	0.49	0.49
B5	$C_6H_6+O_2 \rightleftharpoons C_6H_5+HO_2$	0.00	0.00	0.00
B6	$C_6H_5OH+H \rightleftharpoons C_6H_6+OH$	0.04	0.03	0.03
B7	$C_6H_5CH_3+H \rightleftharpoons C_6H_6+CH_3$	0.00	0.00	
B8	$C_6H_5+C_6H_5OH \rightleftharpoons C_6H_6+C_6H_5O$	0.00	0.00	
B9	$C_6H_5+C_6H_5CH_3 \rightleftharpoons C_6H_6+C_6H_5CH_2$	0.00	0.00	
B10	$C_6H_5+C_6H_6 \rightleftharpoons C_{12}H_{10}+H$		0.00	
B11	$C_6H_5+CH_2O \rightleftharpoons C_6H_6+HCO$		0.00	
B12	C_3H_4(allene)$+C_3H_2 \rightleftharpoons C_6H_6$		0*	
B13	C_3H_4P ($CH_3C{\equiv}CH$)$+C_3H_2 \rightleftharpoons C_6H_6$		0*	
B14	C_3H_4(allene)$+H_2CC{\equiv}CH \rightleftharpoons C_6H_6+H$		0.00	
B15	$CH_2{=}CHCH{=}CH+C_2H_2 \rightleftharpoons C_6H_6+H$		0.00	
B16	$CH_2{=}CHCH{=}CH+C_2H_3 \rightleftharpoons C_6H_6+H_2$		0.00	
B17	$C_4H_4+C_2H_2 \rightleftharpoons C_6H_6$		0.01	
B18	'C_6H_6D'§ ($HC{\equiv}CCH_2CH_2C{\equiv}CH$) $\rightleftharpoons C_6H_6$			0.11
B19	C_6H_6F (fulvene) $\rightleftharpoons C_6H_6$			1.82
B20	$C_6H_6+O \rightleftharpoons C_6H_5OH$			0.02
B21	$C_6H_6+O \rightleftharpoons C_6H_5+OH$			0.00
B22	$C_6H_6+CH_3 \rightleftharpoons C_6H_5+CH_4$			0.00
B23	$C_6H_6+H \rightleftharpoons C_6H_7$			1.53‡
	Total for each model:	1.52	1.35	4.79

* Falloff effects were included for the reaction in the original model.

† Mole fraction assumptions were made for the following species:
O, HCO, HO_2, C_2H_3, C_3H_2, C_3H_3, C_3H_4, C_3H_4P, C_4H_4, C_4H_5, 'C_6H_6D', C_6H_6F, C_6H_7, C_6H_5O, $C_6H_5CH_2$, $C_6H_5CH_3$, $C_{12}H_{10}$
The assumptions and their rationale are found in Section 7.7.

‡ Reaction displays complex behavior; refer to Section 7.6.

[§] This l-C_6H_6 species is is called C_6H_6D by Lindstedt and Skevis (1995). Here it is labeled 'C_6H_6D' so that it will not be confused with C_6H_6D, the mass 80 isotope of C_6H_7.

nearly all of the destruction of benzene.

Several of the reactions are unimolecular decompositions or bimolecular recombinations for which falloff corrections are needed, if the most accurate rate constant is desired. On the other hand, the contribution of certain reactions to the overall rate is quite small, and correction of these reactions would cause no significant change to the end result — especially for those reactions in which the net rate would be reduced even further by the falloff correction. Reactions sufficiently important to merit a falloff calculation include B1, B18, B19 and B23. Reactions B3, B6, and B20 are not important to benzene, but play a major role in phenol formation and are considered in Section 7.3.

Another reason for selecting a reaction for further consideration was a possible discrepancy in pathway or an indication in the literature that a different elementary mechanism should be operative. Reaction B20 falls into this category.

7.2.2 Falloff and Mechanistic Analyses of C_6H_6 Reactions

Falloff calculation methods used.

Three computer programs were used to calculate pressure effects: CHEMACT, UQRRK and RRKM. The last of the three programs was based on the program FALLOFF (Gilbert, 1983) distributed by the Quantum Chemistry Program Exchange. FALLOFF calculates pressure effects of unimolecular reactions using RRKM theory (Robinson and Holbrook, 1972), with a direct count algorithm for the density of states (Beyer and Swinehardt, 1973; and Astholz et al., 1979). The program was revised by Shandross and Howard (1987 and 1988-1995) to incorporate the Waage-Rabinovitch (1970) treatment of adiabatic rotations, and to implement the collision efficiency and weak collision broadening factor treatments of Gilbert et al. (1983). The program code and a detailed discussion of the program modifications are found in Appendix B.

RRKM calculations require vibrational frequencies and moment of inertia for the transition state of the reaction. The geometry and moment of inertia of the transition state may be estimated by the methods of Benson (1976). Vibrational frequencies are more difficult to calculate, but it has been found that the results of the calculation are insensitive to the choice of frequencies so long as the resulting computed A-factor is correct (Robinson and Holbrook, 1972).

Therefore, a method similar to that used by Kiefer et al. (1985) was used here: the frequencies of the reactant (usually excepting the lowest or several lowest) were modified by addition or subtraction of a constant amount, until the pre-exponential factor calculated by the program agreed with the known high-pressure limit at some mean temperature or temperature range. Occasionally, for better fit of the A-factor, the lowest frequency was modified as well.

The CHEMACT program, which calculates chemical activation effects by the bimolecular QRRK formalism of Dean (1985), was written by Dean, Bozzelli and Ritter (Dean et al., 1991). It was modified in two ways for use in this work: (1) substituting the Forst (1973) approximation for the reduced collision integral ($\Omega^{(2,2)*}$ — used in calculating the Lennard-Jones collision rate) with that proposed by Troe (1977), to be consistent with the modified FALLOFF program, and (2) allowing the collision efficiency $ß_c$ to be input by the user as a 5-parameter polynomial fit with temperature. The general procedure used for chemical activation calculations was to compute $ß_c$ by the more accurate method of Gilbert et al. (1983), using the modified FALLOFF program for the reaction in the reverse direction, then fit it to the form required by the modified CHEMACT program using curve fitting software (TableCurve™ by Jandel Scientific).

The UQRRK program (Westmoreland, 1992a) was used for unimolecular isomerization with branched decompositions. The "Q-formalism" used by that program is described in Westmoreland (1992b).

Analyses of model reactions.

The two most important reactions, in terms of their effect on the predicted net rate, are isomerization of benzene to fulvene and H addition to form cyclohexadienyl. In this Section, as in Section 7.1, the C_6H_7-formation reaction (B23) is excluded from calculations. The reaction is significant for its ability to open up a pathway to more hydrogenated cyclic compounds, and is discussed in Section 7.6. The isomerization to fulvene is a unimolecular reaction which should be corrected for falloff effects. Details of all falloff calculations are given in Appendix C.

C_6H_6F (fulvene) $\rightleftharpoons C_6H_6$ (Rxn B19; LS) - Lindstedt and Skevis give no information on the rate constant used by them. Also, there are no entries in the NIST database for this reaction, nor any recommendation by Baulch et al. (1992). However, there is a VLPP measurement over 1050-1150 K by Gaynor et al. (1981), extrapolated to the high-pressure limit by an RRKM analysis. The data are quite noisy. The LS rate constant is 2.5 times that of the Gaynor et al.

high-pressure limit at the temperatures where the reaction would be important.

In the reverse direction some authors have postulated a species called "prefulvene" as a (meta-) stable intermediate. In their theoretical paper, Oikawa et al. (1984) performed a 3-21G level UHF *ab initio* calculation for the path benzene → prefulvene (→ fulvene). The difference in total energies of benzene and prefulvene is calculated to be 91.3 kcal/mole, about 25 kcal higher than the Gaynor et al. E_∞, so that pathway was deemed to be minor for the present purposes.

An RRKM calculation was performed for both k_∞'s. The revised rate constant reduces $\frac{R_{rxn}}{R_{bnz}}$ from 1.82 to 0.07 (Gaynor et al. k_∞) and 0.10 (LS k_∞), removing the large discrepancy between the LS and data net rates.

In order to gauge the possible effect of the presence of fulvene in the mass 78 signal, a steady-state analysis was performed. The LS model gives three destruction reactions for fulvene, all of which are isomerizations to other C_6H_6 species. Under the assumption that the only reactions involving fulvene are formation from benzene and destruction by isomerizations to other species without reverse reaction, the steady-state analysis gives:

$$\frac{(\text{fulvene})}{(C_6H_6)} = \frac{k_{bnz\rightarrow fulv}}{(k_{fulv\rightarrow bnz} + \Sigma k_{isom})}$$

From this formula and the mole fraction of C_6H_6, the mole fraction of fulvene was estimated. The LS high-pressure limits were used throughout. No oxidation reactions were included in this treatment. Such reactions would lower the steady-state mole fraction and bring the result closer to the original assumption that $x_{fulvene} = 0.0$ throughout the flame.

The resulting fulvene profile was no more than 1.2% of the mole fraction of benzene anywhere in the flame. Using the estimated mole fraction of fulvene, the net rate reaction B19 is only 10^{-1} that of the case where $x_{fulvene}$ is estimated as 0.0, in the region of the flame where this reaction contributes most. The importance of the reaction would be reduced even further.

$C_6H_5+H \rightleftharpoons C_6H_6$ (Rxn B1; EBG, ZM, LS) - The falloff candidate of next highest importance is this pyrolysis reaction of benzene. All three models use the Ackermann et al. (1990) recombination rate of 2.2×10^{14} cm^3/(mol-s). That value was measured at room temperature, in contrast to the estimate of Frenklach et al. (1985) (1.0×10^{13} for 1500-2000 K) and measurements of Braun-Unkhoff et al. (1989) (7.8×10^{13} for 1380-1700 K) listed in Baulch et al. The Baulch et

al. recommendation for the pyrolysis direction — a fit to existing literature data — was listed with an error of log k = ±0.4 (factor of 2.5). That recommendation is $9.0x10^{15}exp(-107,428/RT)$ s^{-1}, for the range 1200-2500 K. No data were given for lower temperatures in the compilation (nor in the NIST database). They note that a contribution from the fragmentation channel $C_6H_6 \rightleftharpoons C_4H_4+C_2H_2$ could not be eliminated from the rate constants listed, though it should be a minor channel.

Because of the smaller scatter, the greater number of studies, the more direct nature of those studies, and the ability to use RRKM theory instead of QRRK, falloff computations for reaction B1 were performed in the pyrolysis (H elimination) direction. The Baulch et al. recommendation was used for the high-pressure limit. The falloff correction reduces $\frac{R_{rxn}}{R_{bnz}}$ from 0.53 to 0.03, which drops the model net rate from just above to just below the measured curve. Near the burner (0-2 mm) the models then predict net formation of benzene. In the case of Sandia thermochemistry, the ratio drops from 1.22 to 0.03. Falloff correction then brings the net rates predicted by the models much closer to data than without the correction. Net production at low HAB's is still seen.

While this thesis was being written, a review of and new value for the heat of formation of phenyl radical was published (Davico et al., 1995). Reaction B1 is the only one in the models for which the change in $\Delta H^0_f(C_6H_5)$ changes the fit of the models to data: the net rate below 3 mm becomes positive and large. The temperature in that region is below that recommended for the rate constant, and the data net rate is of course less reliable there as well. Furthermore, in that temperature range, extrapolation of the pyrolysis rate is inconsistent with the measured recombination rate and the equilibrium constant. Use of the Kiefer et al. (1985) high-pressure limit rate constant for B1 removes the net production, but does not eliminate the inconsistency between forward and reverse reaction. More low-temperature data on this reaction are needed.

'C_6H_6D' ($HC\equiv CCH_2CH_2C\equiv CH$) $\rightleftharpoons C_6H_6$ (Rxn B18; LS) - This reaction is proposed without documentation or reference by Lindstedt and Skevis (1994). No other reference to this reaction was found in the literature.

A steady-state analysis on $HC\equiv CCH_2CH_2C\equiv CH$ was performed to examine the possible importance of this species to the reverse rate. The LS model gives five destruction reactions for this species, two of which are isomerizations to fulvene and to $CH_2=CCHCH_2C\equiv CH$, the other

three being bimolecular. Assuming that the reactions involving $HC{\equiv}CCH_2CH_2C{\equiv}CH$ are formation from benzene, and destruction by isomerizations to other species without reverse reaction, the steady-state analysis gives:

$$\frac{(HC \equiv CCH_2CH_2C \equiv CH)}{(C_6H_6)} = \frac{k_{decycl}}{(k_{cycl} + k_{\rightarrow fulvene} + k_{\rightarrow CH2CCHCH2CCH})}$$

The mole fraction of $HC{\equiv}CCH_2CH_2C{\equiv}CH$ was estimated from this equation and $x_{benzene}$. Using the LS high-pressure limits throughout, linear C_6H_6 would be no more than $1x10^{-3}$ of the mole fraction of benzene anywhere in the flame. With this estimated value for the linear isomer, the maximum net rate of reaction B18 is only $-9x10^{-11}$ mol/cm^{3}s. The reaction path ratio is then only $1.0x10^{-4}$.

Being a unimolecular decomposition reaction, a falloff computation would be needed for the most accurate rate constant. The analysis would be rather complex, as molecular rearrangements are required either before or after decyclization, and intermediate rate constants would have to be estimated. With or without the steady-state $HC{\equiv}CCH_2CH_2C{\equiv}CH$ mole fraction, the reaction is relatively unimportant in this flame. Therefore, under the present conditions, the additional work is not warranted.

$C_6H_6+OH \rightleftharpoons C_6H_5OH+H$ (Rxn -B6; EBG, ZM, LS) - Discussed in Section 7.3.

$C_6H_6+O \rightleftharpoons C_6H_5OH$ (Rxn B20; LS); C_6H_5O+H (Rxn -B3; EBG, ZM) - Discussed in Section 7.3.

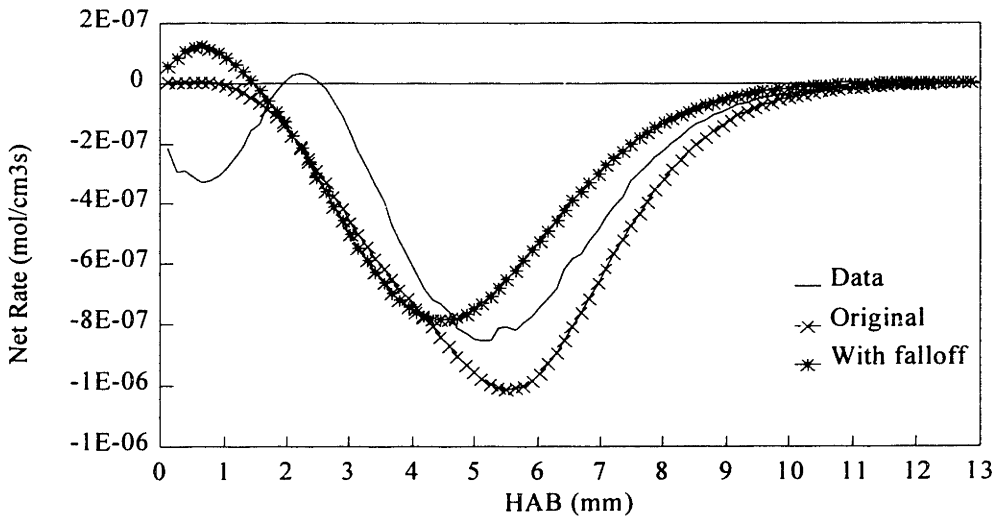

Figure 7.6 EBG model net rate predictions for C_6H_6, original model and as revised by falloff calculations.

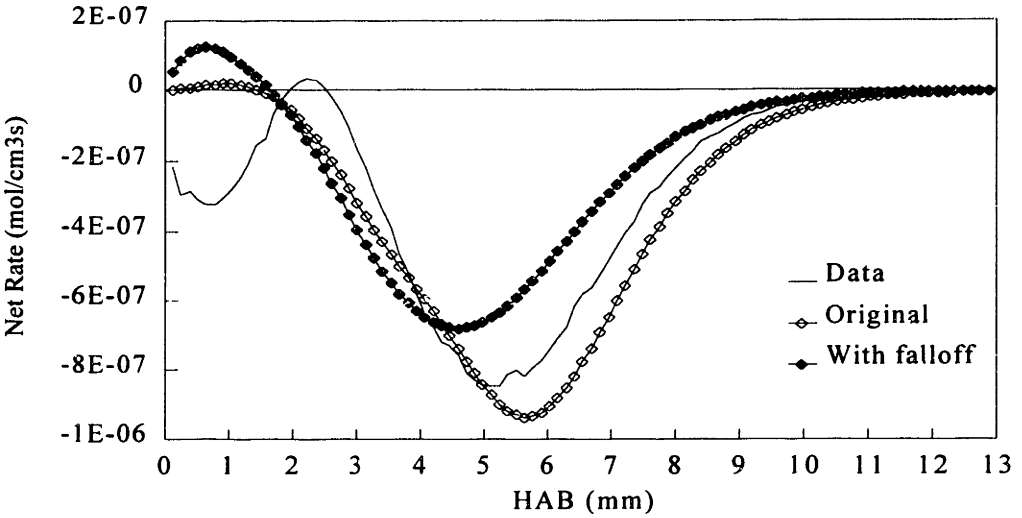

Figure 7.7 ZM model net rate predictions for C_6H_6, original model and as revised by falloff calculations

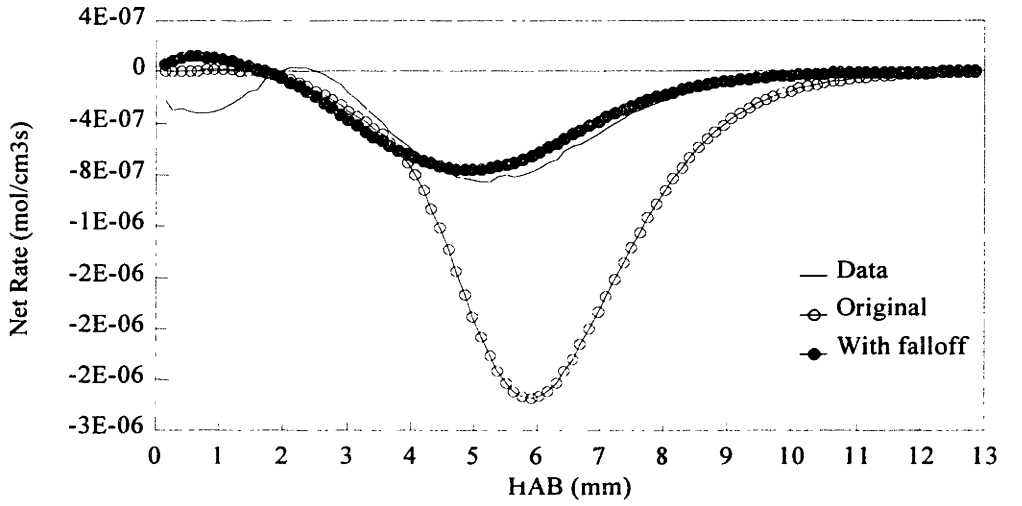

Figure 7.8 LS model net rate predictions for C_6H_6, original model and as revised by falloff calculations.

Net result of improvements to C_6H_6 chemistry.

Figures 7.6-7.8 show the predictions of the three models as revised by the above falloff calculations, contrasted with the original model results. Only those reactions originally in each reaction mechanism were considered for that model. For example, the isomerization of benzene to fulvene was only included in the LS model. Considering the error present in measurements

and rate constants, the fit of model to data should be considered unchanged for the EBG and ZM models, but much improved for the LS model.

The revised H elimination reaction drops the predicted rates below the measured net rate, however the isomerizations to fulvene and linear C_6H_6 (LS model only) replace some of that lost consumption rate. A comprehensive mechanism should contain the fulvene reaction; further work to identify the decyclization reaction (and to determine its rate) is needed.

7.2.3 Other C_6H_6 Reactions

A search of databases and other literature sources has uncovered several additional reactions which could be important in a benzene destruction model. Table 7.3 lists these reactions, with their rate constants, references and a reaction path analysis.

Table 7.3 Additional benzene destruction reactions found in the literature. "0" ≡ <0.01.

Rxn No.	Reaction	n	A (cm^3, sec)	E (cal)	Ref.	R_{rxn}/R_{bnz} †
B'1	$OH+C_6H_6 \rightleftharpoons C_6H_6OH$	-3.48	$9.33x10^{17}$	6430	a	0
B'2	$1,3\text{-}C_6H_8 \rightleftharpoons C_6H_6+H_2$	-7.26	$4.39x10^{37}$	71949	b	-0.04‡
B'3	$1,4\text{-}C_6H_8 \rightleftharpoons C_6H_6+H_2$	-4.94	$1.28x10^{28}$	49309	c	-0.25‡
B'3	$C_2H_3+CH_2CHCHCH \rightleftharpoons C_6H_6+H_2$	5.63	$2.80x10^{-7}$	1890	d	0
B'4	$C_2H_2+CH_2CHCHCH \rightleftharpoons C_6H_6+H$	1.47	$1.90x10^{7}$	4910	d	0
B'5	$2C_6H_7 \rightleftharpoons 1,3\text{-}C_6H_8+C_6H_6$	0	$2.82x10^{13}$	0	e	0
B'6	$2C_6H_7 \rightleftharpoons 1,4\text{-}C_6H_8+C_6H_6$	0	$1.39x10^{13}$	0	e	0
B'7	$C_6H_7+H \rightleftharpoons C_6H_6+H_2$	0	$1.00x10^{13}$	0	f	0
B'8	$C_6H_7+C_6H_5 \rightleftharpoons 2C_6H_6$	0	$1.00x10^{12}$	0	f	0

† Mole fraction assumptions were made for the following species:
C_2H_3, C_4H_5, C_6H_7, $1,3\text{-}C_6H_8$, $1,4\text{-}C_6H_8$, C_6H_6OH
The assumptions and their rationale are found in Section 7.7.

‡ Negative value means net consumption was negligible, and net *production* was used in ratio.

a - Witte et al. (1986), QRRK (CHEMACT computation performed).
b - Orchard and Thrush (1974), RRKM computation performed.
c - Ellis & Frey (1966), RRKM computation performed.
d - Westmoreland et al. (1989) QRRK 20 torr analysis performed by authors.
e - Tsang (1986), derived at 425 K (Written as unspecified C_6H_8, assumed 0.67 of rate is 1,3).
f - Louw and Lucas (1973).

The reaction path analysis shows that none of the reactions is important in the H_2-O_2-C_6H_6-Ar flame, except for concerted elmination of H_2 from C_6H_8 (B'2 and B'3). Those two

reactions are analyzed in Section 7.6. Their impact depends a great deal on the assumptions regarding mass 80 isomers. For example, if one assumes that there is no C_5H_4O, and all of the mass 80 signal is 1,4-C_6H_8, the ratio of maximum production from H_2 elimination to the maximum measured consumption is 0.49 instead of 0.29 (0.04+0.25). On the other hand, if all of the mass 80 signal is 1,3-C_6H_8, the ratio is only 0.07. The overall ratio is proportionally decreased by the percentage of mass 80 which is linear C_6H_8 and C_5H_4O; for example, if only 50% is cyclic C_6H_8, the latter ratio would be 0.036.

Because of the uncertainty about the exact nature of mass 80, it is impossible to evaluate the real effect of the H_2 elimination reactions on the model predictions.

7.3 C_6H_5OH Net Rate Analysis

The reaction mechanisms under review seriously miss the mark with respect to phenol's net rate, expecially for consumption, as Figure 7.2 shows. Phenol's reactions were analyzed in the same way as benzene's. Unless specifically mentioned otherwise, modified Sandia thermochemistry was used in the following calculations.

7.3.1 Model Reaction Sets for C_6H_5OH

The C_6H_5OH reaction path analysis, for reactions in the models, is given in Table 7.4. In this case, there are two comparisons: the net formation rate and the net destruction rate. Therefore, two $\frac{R_{rxn}}{R_{PhOH}}$ ratios are needed for the reaction path analysis.

Destruction is overpredicted by the full networks by a factor of 4-100. The most important reactions causing that problem are H elimination from phenol (-PhOH3) and decomposition to CO and C_5H_6 (-PhOH12). The only reactions resulting in net production are O+C_6H_6 (B20 — LS model only) and OH+C_6H_6 (-B6).

Interestingly, in a model-model or "MM" reaction path analysis[34] of the ZM model, the latter reaction is primarily seen to *destroy* phenol. In the MM analysis the primary producer of C_6H_5OH would be the reverse of H elimination, that is, recombination of hydrogen with phenoxy. Decomposition into CO and cyclopentadiene would be a relatively minor reaction. The

[34] A reaction path analysis using model reactions and model-predicted mole fractions (see. Chapter 6). A model-data analysis would be one which uses model reactions and *experimental* mole fractions.

Table 7.4 C_6H_5OH reactions in the mechanisms under review, and the fractions $\frac{R_{rxn}}{R_{PhOH}}$ for production and destruction, respectively. "0" ≡ <0.01.

Rxn No.	Reaction	EBG†	ZM†	LS†
B6	$C_6H_5OH+H \rightleftharpoons C_6H_6+OH$	4.43, 0	3.66, 0	4.23, 0
B8	$C_6H_5+C_6H_5OH \rightleftharpoons C_6H_6+C_6H_5O$	0, 0	0, 0	
PhOH1	$C_6H_5OH+C_6H_5CH_2 \rightleftharpoons C_6H_5O+C_6H_5CH_3$	0, 0	0, 0	
PhOH2	$HOC_6H_4CH_3+H \rightleftharpoons C_6H_5OH+CH_3$	0, 0	0, 0	
PhOH3	$C_6H_5O+H \rightleftharpoons C_6H_5OH$	0, 100.5	0, 42.2*	0, 100.5**
PhOH4	$C_6H_5OH+OH \rightleftharpoons C_6H_5O+H_2O$	0, 0.75	0, 0.88	0, 0.75
PhOH5	$C_6H_5OH+H \rightleftharpoons C_6H_5O+H_2$	0, 1.55	0, 1.55	0, 1.55
PhOH6	$C_6H_5OH+O \rightleftharpoons C_6H_5O+OH$	0, 0.03	0, 0.03	0, 0.03
PhOH7	$C_5H_6+C_6H_5O \rightleftharpoons C_5H_5+C_6H_5OH$	0, 0	0, 0.06	0, 0
PhOH8	$C_2H_3+C_6H_5OH \rightleftharpoons C_2H_4+C_6H_5O$	0, 0	0, 0	
PhOH9	$C_4H_5+C_6H_5OH \rightleftharpoons C_4H_6+C_6H_5O$	0, 0	specific isomers -- see below	
PhOH10	$C_6H_5OH+CH_2=CHCH=CH \rightleftharpoons C_4H_6+C_6H_5O$		0, 0	
PhOH11	$C_6H_5OH+CH_2=CHC=CH_2 \rightleftharpoons C_4H_6+C_6H_5O$		0, 0	
PhOH12	$CO+C_5H_6 \rightleftharpoons C_6H_5OH$		0, 25.0*	
PhOH13	$C_6H_5OH+OH \rightleftharpoons C_6H_4OH+H_2O$		0, 0.75	
PhOH14	$C_6H_5OH+HO_2 \rightleftharpoons C_6H_5O+H_2O_2$		0, 0	
B20	$C_6H_6+O \rightleftharpoons C_6H_5OH$‡			2.85, 0
	Total for each model:	4.43, 102.9	3.66, 70.5	7.08, 102.9

* Falloff effects were calculated for the reaction in the original model.

** The LS value reported for PhOH3 is that supplied by Lindstedt (1994, 1995). Using the rate constant of Lindstedt and Skevis (1995) would give a reaction path ratio of 2.3, for a model total of 4.62.

† Mole fraction assumptions were made for the following species:
O, HO_2, H_2O_2, C_4H_5, C_4H_6, CH_2=CHCH=CH, CH_2=CHC=CH_2, C_5H_5, C_5H_6, C_6H_5O, $C_6H_5CH_2$, $C_6H_5CH_3$, C_6H_4OH, $HOC_6H_4CH_3$
The assumptions and their rationale are found in Section 7.7.

‡ In the revised model recieved from Lindstedt (1995), this reaction was removed and replaced by $C_6H_6+O \rightleftharpoons C_6H_5O+H$, with the Ko et al. (1991) rate constant.

conclusions drawn from the MM analysis would be entirely different from those of the more realistic model-data ("MD") interpretation of this chapter. These differences occur because of the ill-predicted mole fractions involved, illustrating the difficulty in analyzing a model from the results of a flame code simulation.

Using criteria similar to those applied in the section on C_6H_6, several of the listed reactions were chosen for additional consideration, given below.

7.3.2 Falloff and Mechanistic Analyses of C_6H_5OH Reactions

Specific details of all falloff calculations are given in Appendix C.

$C_6H_6+O \rightleftharpoons C_6H_5OH$ (Rxn B20; LS); C_6H_5O+H (Rxn -B3; EBG, ZM) - As noted in Chapter 2, the branching ratio of this addition reaction has not been definitively determined, particularly at higher temperatures (higher energy content of the adduct). It would appear, though, that phenoxy formation is generally dominant at lower temperatures.

The only data from which one might be able to calculate the branching ratio are the relative intensities of masses 65, 66, 93 and 94, measured by Sibener et al. (1980). As those data were taken with a crossed supersonic molecular beams apparatus, one would need to perform a deconvolution with the energy distributions and reconvolute the result with a Boltzmann distribution, to determine an equivalent temperature for each collision energy used in the experiment. The usefulness of such a calculation is negated by the lack of calibration information. In particular one would need energy distributions for the excited phenol and phenoxy in their ionizer, plus ionization cross-sections for fragmentation to cyclic C_5 species for both species. In addition, the internal energy of the C_6H_6 in the beam is unspecified or unknown, leaving the true energy distibution of collided molecules in question. Depending on how much vibrational energy was converted to translational energy in the adiabatic isentropic expansion of molecular beam formation, as much as an additional 1.36 kcal/mol could have contributed to the reaction. It is also important to note that the identification of mass 94 as phenol by Sibener et al. was an assumption. That species could be triplet C_6H_6O, or a different (stable) singlet species such as oxepin (see Chapter 2). The possibility of formation of a C_5H_6 species from one of these isomers is unknown. Finally, the data were taken under single-collision conditions, preventing the energized adduct from being stabilized. Therefore, the Sibener et al. results may not be reliably used to determine a useful branching ratio, but are rather better suited as an indication of the effect of increasing reaction energy.

In spite of the above limitations, the signal ratio of C_6H_5O-derived to C_6H_5OH-derived species might be used as a *very* crude guideline for examining the effect of a contribution from an addition/isomerization channel. First, however, a temperature equivalent to the molecular

beam data must be determined for the case of a Maxwell-Boltzmann distribution. One way of doing so is to equate the sum of average energy contributions from translation and vibration, i.e. $\langle E \rangle = 1.5RT + \langle E \rangle_{vib}$ (Levine and Bernstein, 1974), with the most probable energy of collision in the experiment. Because of the high $\langle E \rangle_{vib}$ component of benzene, the resulting temperatures are quite low: 335 K for the Sibener et al. 2.5 kcal/mol collision energy experiment, and 510 K for the 6.5 kcal/mol results. (If all of the internal energy of the feedstock benzene remained as vibrational energy in the experiment, the temperatures would be 405 K and 550 K.)

With equivalent temperatures estimated, the branching ratio must then be approximated. Let the amount of phenol produced in the reaction be estimated by (I_{94}+I_{66}), and the amount of phenoxy by (I_{93}+I_{65}). Then at a collision energy of 2.5 kcal/mol, 7% of the products are phenol and 93% phenoxy+H. For the 6.5 kcal/mol experiment, 17% goes to phenol and 83% to C_6H_5O+H. This is an increase of 270% in $\left(\frac{\text{phenol}}{\text{phenoxy}}\right)$ over about 160 K temperature rise. However, in light of the results of Bajaj and Fontijn (1994) (see Chapter 2), these estimates of phenol production may be high for the estimated temperature. Several factors may be responsible for this:

1. As Sibener et al. point out, the most probable energy of the excited triplet adduct in their experiment was probably greater than the nominal collision energy, because the ~4 kcal/mol activation energy of the reaction is above the 2.5 kcal/mol collision energy and close to the 6.5 kcal/mol collision energy. In the former case, only molecules on the high side of the distribution could get excited, and in the latter case energies on the low side that were below the activation energy did not contribute, thus changing the effective distribution.
2. At the high mass spectrometer electron energy used by Sibener et al. (200 eV vs. the 20 eV of Bajaj and Fontijn), it is likely that some isomerization of excited C_6H_6O to phenol occurred in the ionizer, producing more of both C_6H_5OH and C_5H_6.
3. Under the single-collision conditions of the experiment, more phenol would be produced because the energized biradical adduct would not lose energy in collisions.

Because of these factors and the question of differing calibrations and fragmentation cross-sections for phenol and phenoxy radical, the estimations from Sibener et al. data were only used to estimate the temperature dependence of the branching ratio. For an absolute low-

temperature value of the branching ratio $\frac{k_{C6H5OH}}{k_{C6H5O}}$, the 405 K ratio $\frac{I_{94}}{I_{93}}$ measured by Bajaj and Fontijn (~0.0025) at 3-12 torr was used instead.

Assuming then the same relative increase in this ratio with temperature as calculated for the Sibener et al. data, one gets a rate constant for the phenol-producing pathway of $1.8x10^{12} * \exp(-7380/RT)$ cm^3/mol-s. With this estimated rate constant, the phenol channel is never more than 4% of the phenoxy pathway. The net formation ratio $\frac{R_{rxn}}{R_{PhOH}}$ for the reaction $C_6H_6+O \rightleftharpoons C_6H_5OH$ is reduced to 0.10 from 2.85.

Emdee et al. (1992) performed a bimolecular QRRK calculation for this reaction at one atmosphere, using an estimated rate constant for the isomerization channel of $3.3x10^{12} * \exp(-31000/RT)$ (cf. the *ab initio* estimated energy of Sloane (1977) for the crossing of triplet and singlet states: 38.2 kcal/mol). The barrier for adduct formation used was about 2.2 kcal/mol higher than the experimental E_a of Ko et al. (1991). It is not clear what rate constant was used for H elimination from the adduct. They found that at 1100 K almost all of the products predicted for the reaction were phenoxy and H atom. Using the Ko et al. rate for the overall reaction as k_∞, the Emdee et al. estimate for isomerization to phenol, and assuming the A-factor for H elimination to be $1x10^{13}$ and the activation energy to be 4 kcal/mol (Sibener et al. (1980)), one finds from a QRRK analysis that at 22 torr and 400-1900 K phenol production is never more than 0.05% that of C_6H_5O+H. This is much lower than the estimate based on Sibener et al. and Bajaj and Fontijn data.

The great uncertainty in the isomerization rate was motivation for a different kind of scrutiny of the reaction. Noting that Ko et al. find a good fit of experimental results to the Arrhenius expression over a wide range of temperature and pressure, it is possible to determine what sort of rate for the second half of the reaction would reproduce such behavior, and whether a reasonable rate for the H elimination pathway would satisfy the observed limitation. A description of that analysis is found in Appendix C. When $C_6H_6CH_3$ and C_6H_6OH were used as models for C_6H_6O, they were unable to predict the 405 K findings of Bajaj and Fontijn. The C_6H_7 analogy was in agreement, however, and if similar the C_6H_5O+H channel would be sufficiently fast at all temperatures to explain experimental observations. The biradical chemistry is probably not well-modeled by non-biradical analogies, though. Furthermore, a contribution from the phenol-producing pathway would not be eliminated by such an analysis.

$CO+C_5H_6 \rightleftharpoons C_6H_5OH$ (Rxn PhOH12; ZM) - The experimental evidence regarding this pathway clearly points to the conclusion that it is insignificant, at least up to 1175 K — just above the maximum temperature of the studies which suggest it as dominant in phenol pyrolysis. There is no information about this reaction above that temperature.

As discussed in Chapter 2, the authors from whom ZM borrowed this rate constant assumed inappropriately that the entire pyrolysis rate was a result of reaction PhOH12, without experimental evidence to suggest any specific pathway being operative. Until such time as a high-temperature study of this reaction is performed, it should be omitted from the model.

$C_6H_6+OH \rightleftharpoons C_6H_5OH+H$ (Rxn -B6; EBG, ZM, LS); C_6H_6OH - Formation of a stabilized adduct at low temperatures is a well documented pathway, but it was not found in any of the models. Proceeding via a chemically activated $[C_6H_6OH]^*$ intermediate, the pressure of the current experiment puts the addition reaction in the early part of the falloff curve. The addition/elimination reaction exhibits essentially no falloff except at very low temperatures. Because it was measured at the high-pressure limit, the addition/elimination rate constant of He et al. was used in this work as the basis of a chemical activation calculation. (The rate constant of Manion and Louw (1989) was also examined.) The measured low-temperature rate constant for adduct formation and dissociation (Witte et al., 1986) had to be extrapolated to higher temperature, a possible source of error in general, and additionally because the precise activation energy for addition varies widely in the literature (cf. Chapter 2).

Although EBG and ZM used the same rate constant for this reaction, they wrote the reaction in opposite directions in the models. Small differences in the thermochemistry used here and by EBG account for the variance in reaction path importance between models seen in Table 7.4. While falloff did not improve the overprediction of this reaction, use of the Manion and Louw rate constant did reduce the reaction path ratio from about 4 to about 2.

The main difference between the analysis in this work and the previous models is the inclusion of an addition/stabilization channel. That pathway does not contribute significantly to benzene destruction under these conditions and could probably be left out of any intermediate- or high-temperature model.

$C_6H_5O+H \rightleftharpoons C_6H_5OH$ (Rxn PhOH3; EBG, ZM, LS) - The rate parameters used by ZM were not based on experimental data *apropos* of this reaction, and they should not be part of a revised model. The values in the EBG model are from He et al. That rate constant was chosen as

the high-pressure limit for an RRKM analysis as the Lovell et al. (1989) and Manion and Louw (1989) values are estimates. The falloff correction greatly improved the contribution from the reaction, from 100.5 (He et al. k_∞) to 6.6. The benefit derives mainly from the large amount of falloff above 1500 K. However, it should be noted that above 1150 K, the rate constant is extrapolated.

Use of the value reported in Lindstedt and Skevis (1995) for this reaction would improve things even more. However, as noted in Chapter 2 and Table 7.4, LS report one value for this rate constant in the literature, but in fact that of He et al. in the model. In any event, the source of the "better" rate constant is an analogy to H elimination from toluene. The experimental value of He et al. is more reliable, and is recommended here and by Baulch et al. (1992).

$C_6H_5OH+OH \rightleftharpoons C_6H_5O+H_2O$ (Rxn PhOH4; EBG, ZM, LS); $C_6H_4OH+H_2O$ (Rxn PhOH13; ZM) - The rate constant used by Zhang and McKinnon ($6.00x10^{12}$ cm^3/mol-s) for the ring abstraction reaction is cited by them to have come from Chevalier and Warnatz (1991), but is in reality twice the latter's value. Tracing the rate constant back further, Chevalier and Warnatz cite Baulch et al. (1992), who assign the rate constant of He et al. (1988) to the combination of ring extraction and extraction from hydroxyl, $k_{abstr} = k_{ring}+k_{PhO\text{-}H}$. However, Baulch et al. do not speculate as to the branching ratio and He et al. interpret the rate constant to apply exclusively to $k_{PhO\text{-}H}$ on the basis of the known ring extraction rate. Chevalier and Warnatz split the He et al. value evenly between the two channels. While this might seem to be unfounded, there is a certain logic to this in that at temperatures above 1700 K, where most of the benzene destruction occurred in Bittner's rich benzene flame, the abstraction of H from benzene by OH is approximately constant at $(3.5\text{-}4.5)x10^{12}$ cm^3/mol-s. The rate constant for ring abstraction from phenol should be about two-thirds that for benzene, if one subtracts one-sixth for the loss of an abstraction site and one-sixth for steric hindrance from phenolic H. At high temperatures, this would be $(2.3\text{-}3.0)x10^{12}$, consistent with Chevalier and Warnatz.

In their evaluation of ring abstraction versus OH abstraction, He et al. state that the ring abstraction rate constant of Tully et al. (1981) results in a value that is only one-tenth of their rate constant for abstraction from phenolic H. On the contrary, even when adjusted to two-thirds of the Tully et al. $k_{ring,C6H6}$, in the temperature range of the He et al. experiment the rate constant is about $1.8x10^{12}$ — about one-third of the value that He et al. assigned to the phenolic H channel. The He et al. rate constant is therefore more appropriately a measure of the combined channels,

rather than only phenolic H abstraction. However, since the fate of phenoxy radicals produced by abstraction of phenolic H was part of the modeling scheme they used to derive their rate constants, their experimental rate constant is not equal to $k_{ring}+k_{PhO-H}$ to the degree of accuracy they claim for their estimate of k_{PhO-H} (and assumed by Baulch et al.). On the other hand, given the already high error limits He et al. imply for $OH+C_6H_5OH$, the stated rate constant is probably nearly as valid for estimation purposes as a revised rate constant would be.

A factor not considered by either Chevalier and Warnatz or Zhang and McKinnon is the temperature dependence of the rate constant. While it is true that at high temperatures the rate constant for abstraction of the ring H is nearly constant, the limiting value is more than twice that calculated for the temperature range of the He et al. experiment. Abstraction is an activated process, and He et al. admit that the nature of their technique did not allow them to measure the temperature dependence of the reaction.

Estimates of the rate constants for both channels in the temperature range 298-1032 K, including the temperature dependence, is possible thanks to the low-temperature work of Knispel et al. (1990). In their study of adduct formation in the reaction $OH+C_6H_5OH$, they determined k_{abstr} over the temperature range 298-374 K. They combined their results with those of He et al. at 1032 K to derive a rate constant of $2.95\text{x}10^{6}T^{2}\exp(+1312/RT)$ $cm^3/mol\text{-}s$ for both channels combined. Zhang and McKinnon erroneously assigned this rate constant to the phenolic H abstraction pathway, compounding their mistake regarding ring abstraction[35]. To separate the two channels in this work, the rate constant for ring abstraction was assumed to be two-thirds of that for reaction with benzene as discussed above. The recent value of Madronich and Felder (1985) for $k_{ring,C6H6}$ was used. The resulting rate constant was $k_{ring,C6H5OH} = 1.41\text{x}10^{13}\exp(-4571/RT)$ $cm^3/mol\text{-}s$. Subtraction of $k_{ring,C6H5OH}$ from the Knispel et al. k_{abstr} over the range 316-1149 K results in an expression for k_{PhO-H} of $1.4\text{x}10^{8}T^{1.43}\exp(+962/RT)$ $cm^3/mol\text{-}s$. Use of the rate constant at higher temperatures is admittedly hazardous, but was done for lack of a better value. High-temperature study of these reactions is warranted.

Little effect is achieved with the revisions; the revised reaction path ratios for destruction are 0.7 and 1.4 for the ring and phenolic H abstraction pathways, respectively.

$C_6H_5OH+H \rightleftharpoons C_6H_4O+H_2$ - In their study of reaction of H with phenol, He et al. (1988) comment that at the temperatures of their experiments (1000-1150 K) abstraction of a ring

[35] They inadvertently reversed the sign of the activation energy as well.

hydrogen by H atom is predicted to be one-fifth of the rate constant they measure, possibly affecting their rate expression to some extent. Westmoreland (1995) has pointed out that the abstraction reaction,

$$C_6H_5OH+H \rightleftharpoons C_6H_4O+H_2 \qquad \text{(PhOH'1)}$$

should be more important than the similar abstraction reaction by OH, in the present flame. As with abstraction by OH, the rate constant for this reaction was assumed to be two-thirds that for the same reaction with benzene. The Kiefer et al. (1985) rate constant for H abstraction of H from benzene was used for $k_{ring,\,C6H6}$. The resulting rate constant was $k_{ring,C6H5OH} = 1.67x10^{14} * \exp(-16000/RT)$. The reaction path ratios for phenol production and destruction, respectively, are 0.0 and 1.75.

Net result of improvements to C_6H_5OH chemistry.

Rather than producing revised versions of each of the three subnetworks under review, a single revised C_6H_5OH subnetwork was developed. Included in the proposed subnetwork are all of the ZM reactions listed in Table 7.4 except for PhOH12, with reactions B6, PhOH3, PhOH4 and PhOH13 revised as noted above. In addition, the reactions PhOH'1 and the crude estimate of $O+C_6H_6 \rightleftharpoons C_6H_5OH$ were included. The only effect of the latter was to slightly increase the formation rate.

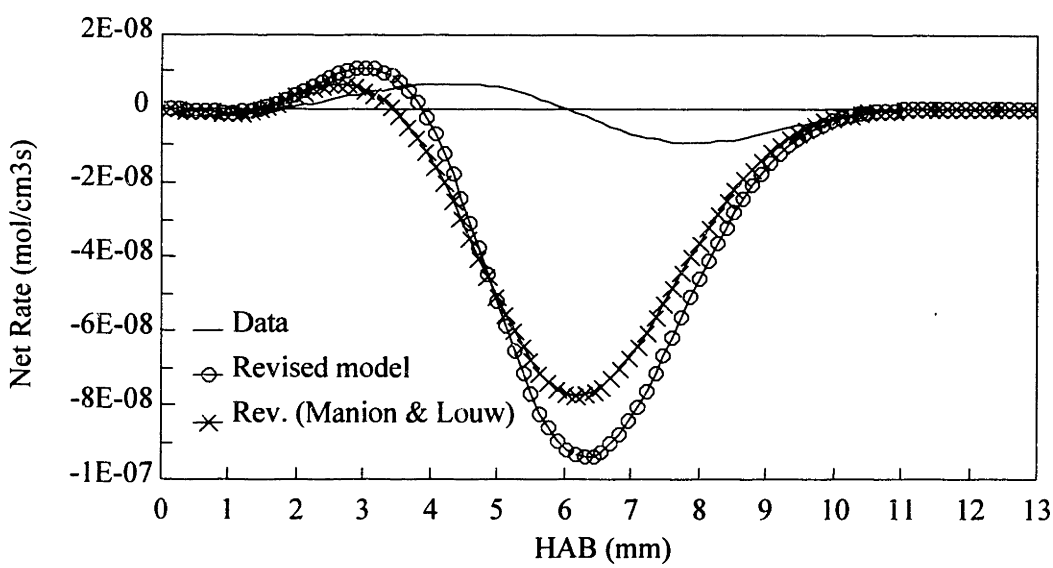

Figure 7.9 Revised phenol submechanism, compared to data net rate.

The results are shown in Figure 7.9. Recalling that the original model predictions of net destruction were between about 70 and 100 times the measurements, and net production about 4 to 7 times the data, it is clear that the revised submechanism is a significant improvement over the previous state of the art. This is principally due to correction of the H elimination reaction, with a strong contribution from removal of direct C_5H_6+CO production as well.

The source of the excessive destruction prediction could be one or more of three factors: (a) error in one or more consumption rate constants, (b) a reaction currently predicting destruction should predict formation, or (c) a missing formation reaction. The first two possibilities deal with error in rate constants. The reaction which contributes most to the models' destruction rate is -PhOH3. Its rate constant was derived from experiments at temperatures below 1200 K, whereas temperature in the region where the model net rate disagrees with data is 1500-1940 K. Extrapolation to that range could be responsible for some portion of the overprediction. Reactions PhOH4 and PhOH'1 together account for only half as much phenol destruction as predicted by -PhOH3, but three times the measured destruction. Again, the rate constants are extrapolated in the high-temperature region (T > 1150 K) of the flame.

As for the third case, one situation where the error might be ameliorated is by reactions PhOH13 and PhOH'1, if a different (yet still reasonable) assumption were made regarding x_{C6H4OH}. The effect of such a change coult bring the revised model much closer to an accurate prediction. Unfortunately, another reasonable assumption about x_{C6H4OH} could throw off the prediction to the point where the calculation results only in formation, with a reaction path ratio of 23. This situation is discussed in detail in Section 7.7.

7.3.3 Other C_6H_5OH Reactions

The only new reaction found for phenol was the abstraction reaction, $C_6H_5OH+H \rightleftharpoons C_6H_4O+H_2$, which was discussed in the previous subsection.

7.4 C_6H_5 Net Rate Analysis

Not only do the three models overpredict C_6H_5 production, but the analysis of the net rate is probably constrained by the relationship of phenyl formation to the well-predicted benzene destruction rate. Furthermore, the large amount of scatter and uncertainty in the mole fraction profile result in a sizable uncertainty in the net rate curve. In all other respects though, phenyl was

also analyzed in the same way as C_6H_6 and C_6H_5OH. Unless specifically mentioned otherwise, modified Sandia thermochemistry was used in the following calculations.

7.4.1 Model Reaction Sets for C_6H_5

A summary of reactions in the EBG, ZM and LS models, along with a reaction path analysis, is given in Table 7.5. As with phenol, there are two reaction path comparisons, net formation rate and net destruction rate.

Table 7.5 C_6H_5 reactions from the mechanisms under review, and the fractions $\frac{R_{rxn}}{R_{Ph}}$ for production and destruction, respectively. "0" ≡ <0.01.

Rxn No.	Reaction	EBG†	ZM†	LS†
B1	$C_6H_5+H \rightleftharpoons C_6H_6$	123, 59	123, 59	123, 59
B2	$C_6H_6+OH \rightleftharpoons C_6H_5+H_2O$	94, 0	66, 0	59, 0
B4	$C_6H_6+H \rightleftharpoons C_6H_5+H_2$	113, 0.01	113, 0.01	113, 0.01
B5	$C_6H_6+O_2 \rightleftharpoons C_6H_5+HO_2$	0, 0.05	0, 0.05	0, 0.05
B8	$C_6H_5+C_6H_5OH \rightleftharpoons C_6H_6+C_6H_5O$	0, 0	0, 0	
Ph1	$C_6H_5+O_2 \rightleftharpoons C_6H_5O+O$	0, 3.5	0, 3.5	0, 3.5
Ph2	$C_6H_5+CH_3 \rightleftharpoons C_6H_5CH_3$	0, 0	6.5, 0.14*	
B9	$C_6H_5+C_6H_5CH_3 \rightleftharpoons C_6H_6+C_6H_5CH_2$	0, 0	0, 0	
Ph3	$C_6H_5CH_2+O \rightleftharpoons C_6H_5+CH_2O$	0.25, 0		
Ph4	$C_6H_5CH_2+HO_2 \rightleftharpoons C_6H_5+CH_2O+OH$	40, 0	40, 0	
Ph5	$C_6H_5CO \rightleftharpoons C_6H_5+CO$	0, 9.7		
B10	$C_6H_5+C_6H_6 \rightleftharpoons C_{12}H_{10}+H$		0, 0.05	
B11	$C_6H_5+CH_2O \rightleftharpoons C_6H_6+HCO$		0, 0	
Ph6	$C_6H_5+O_2 \rightleftharpoons 2CO+C_2H_2+C_2H_3$		0, 9.0	
Ph7	$C_6H_5 \rightleftharpoons$ l-C_6H_5 (unspecified isomer)		0, 7.5	
Ph8	$2C_6H_5 \rightleftharpoons C_{12}H_{10}$		0, 0*	
Ph9	$C_6H_5+C_4H_6 \rightleftharpoons C_8H_8+C_2H_3$		0, 0	
Ph10	$C_6H_5+CH_3 \rightleftharpoons C_7H_7+H$		13, 0*	
Ph11	$C_6H_5+OH \rightleftharpoons C_6H_5O+H$		0, 3.8	
Ph12	$C_4H_4+C_2H_2 \rightleftharpoons C_6H_5+H$		0, 0	
Ph13	$C_6H_5 \rightleftharpoons C_2H_2+HC{=}CHC{\equiv}CH$		0, 17	
B21	$C_6H_6+O \rightleftharpoons C_6H_5+OH$			0.24, 0

Rxn No.	Reaction	EBG†	ZM†	LS†
B22	$C_6H_6+CH_3 \rightleftharpoons C_6H_5+CH_4$			0.76, 0
Ph14	$C_6H_5 \rightleftharpoons HC{\equiv}CCH{=}CHCH{=}CH$			0, 15
Ph15	$C_6H_5 \rightleftharpoons C_6H_4+H$			0, 0.13
Ph16	$C_6H_5+H \rightleftharpoons C_6H_4+H_2$			0, 40
Ph17	$C_6H_5+O \rightleftharpoons C_6H_4+OH$			0, 0.08
Ph18	$C_6H_5+OH \rightleftharpoons C_6H_4+H_2O$			0, 1.5
Ph19	$C_6H_5+HO_2 \rightleftharpoons C_6H_5O+OH$			0, 0.46
	Total for each model:	370, 72	362, 104	296, 119

* Falloff effects were calculated for the reaction in the original model.

† Mole fraction assumptions were made for the following species:
O, HCO, HO_2, C_2H_3, $HC{=}CHC{\equiv}CH$, C_4H_4, C_6H_4, l-C_6H_5, C_6H_5O, $C_6H_5CH_2$, $C_6H_5CH_3$, C_6H_5CO, C_8H_8, $C_{12}H_{10}$
The assumptions and their rationale are found in Section 7.7.

Since the C_6H_5 mole fraction is about 10^{-3} that of C_6H_6, one of the following must be true:

1. Phenyl production reactions result in a net formation rate on the scale of 10^{-3} of the benzene destruction rate.
2. There is a large amount of net formation, delicately balanced by a large amount of net destruction.
3. The phenyl production rate is large, but for an extremely short time (i.e., distance).

Table 7.5 shows that three reactions dominate the predicted phenyl production rate:

$$C_6H_5+H \rightleftharpoons C_6H_6 \quad \text{(B1)}$$

$$C_6H_6+OH \rightleftharpoons C_6H_5+H_2O \quad \text{(B2)}$$

$$C_6H_6+H \rightleftharpoons C_6H_5+H_2 \quad \text{(B4)}$$

These are the same reactions that control the destruction of benzene. Since one C_6H_5 is produced per C_6H_6 destroyed, the net production rate from these reactions is nearly as large as the benzene destruction rate, and is spread over the whole reaction zone. That is, the second of the three cases above must be true for the model to be consistent with data. Unfortunately, the model network results in much less consumption than production, and that consumption occurs in the preheat zone instead of the region of greatest net formation. Hence, the large predicted phenyl formation rate in the reaction zone goes unbalanced.

Using criteria similar to those applied in the sections on C_6H_6 and C_6H_5OH, several of the listed reactions were chosen for additional consideration, given below. Because a decrease in phenyl formation or increase in destruction are most needed, the falloff corrections most likely to improve the fit to data are those which:

- result in C_6H_5 formation,
- open up new destruction pathways, and
- result in phenyl destruction, but are addition/decomposition pathways.

7.4.2 Falloff and Mechanistic Analyses of C_6H_5 Reactions

General considerations.

One possible explanation for the discrepancy between models and data would be that the phenyl mole fraction profile was greatly in error, and the magnitude should be much larger. The relative peak heights of C_6H_5 and C_6H_6 in the present flame are, however, quite comparable with those measured by MBMS by Bittner (1981) in a rich C_6H_6-O_2-Ar flame, as verified by Hausmann et al. (1992) with their molecular beam radical scavenging technique[36]. Therefore, if the fit of the benzene destruction submechanism to data is not coincidental, the goal of any attempt at improving the phenyl subnetwork should be to find legitimate destruction pathways which would properly complement the high production rate from C_6H_6.

Another way to compare the two flames with respect to phenyl chemistry is by examining the three C_6H_6-C_6H_5 reactions qualitatively in each flame. Since the flames are so different, the rate-temperature profile is a more logical means to compare reactions than a rate-HAB plot.

The only reaction with a significant reverse rate at any point is the pyrolysis reaction $C_6H_6 \rightleftharpoons C_6H_5+H$ (B1). For that reaction, the relative ratios of C_6H_6, C_6H_5 and H, and temperature control the shape of the curve at any point. As illustrated in Figure 7.10, the only region of similarity between flames in the rate-temperature relationship of this reaction is the region above 1800 K. This is a result of the early location of the phenyl peak in the H_2-O_2 flame. After inclusion of falloff, reaction B1 is seen to be the least important of the three reactions, in both flames.

The rate-temperature plots for the other two reactions, which depend on temperature and

[36] The Hausmann et al. peak appears to be about 2 mm closer to the burner than Bittner's. If they shifted the measured profiles to account for probe effects, their phenyl profile would be in agreement with Bittner's with respect to location. It is not clear, however, if this is the case.

the relative ratios of species in the forward direction, are very similar. Therefore, there is nothing significantly different about the H_2-O_2 flame in regard to the behavior of the phenyl formation reactions.

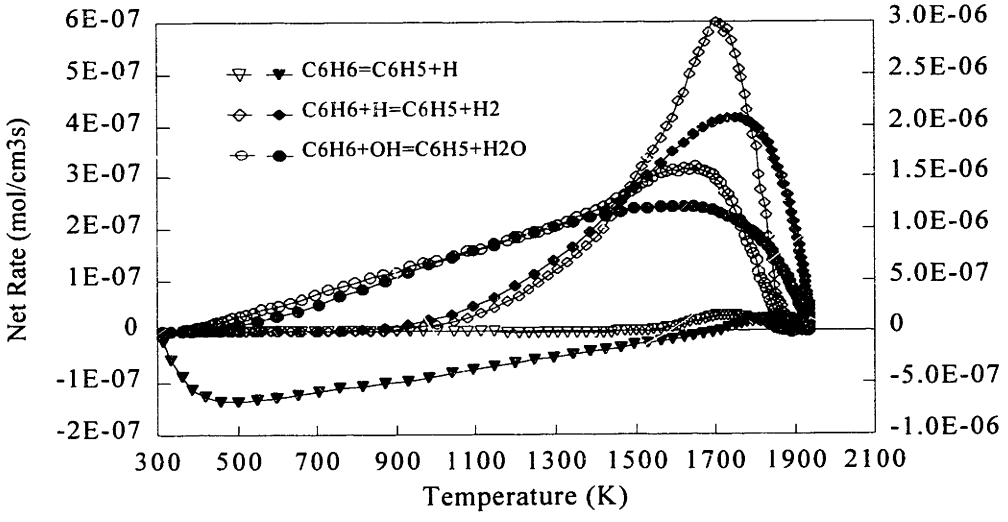

Figure 7.10 Rate-temperature relationship of the three major C_6H_6-C_6H_5 reactions in the H_2-O_2 (black symbols, left scale) and C_6H_6-O_2 (open symbols, right scale) flames. Positive means C_6H_5 formation. For the benzene pyrolysis reaction, a falloff correction has been applied.

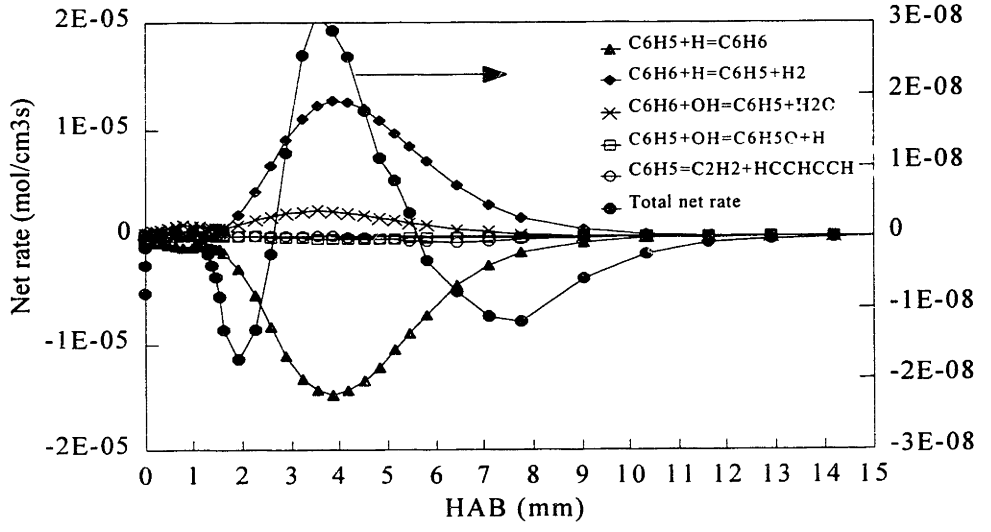

Figure 7.11 Model-model reaction path analysis for C_6H_5; ZM model, H_2-O_2-C_6H_6-Ar flame. Positive means C_6H_5 formation, regardless of which direction that would be with the reaction as written.

The EBG and ZM models do not predict an excessively high C_6H_5 mole fraction for the H_2-O_2 flame, leading one to wonder what reactions might have produced the necessary balance. Indeed, Figure 7.11 shows that the small phenyl MM total net rate is caused by balance of the same three reactions, two of them being about *three orders of magnitude* larger.

It might appear from the rate-temperature graph that a shift in the location and magnitude of the phenyl profile could bring the pyrolysis reaction in balance with the other two. To test this hypothesis, fabricated C_6H_5 profiles of Gaussian shape and various peak locations and magnitudes were substituted for the data profile, using the ZM submechanism. Improvement could be achieved with respect to the magnitude of the formation and destruction peaks. However, in every case where the predicted net rate was not completely formation or completely destruction, a destruction peak was predicted in the vicinity of the maximum mole fraction. This is unrealistic, as a net formation peak is expected close to the highest mole fraction. The best reduction of overall magnitude for a case where the integrated net rate was reasonably small (as it would be for an intermediate species) was to a factor of around 20.

In the ZM prediction of the Bittner rich benzene flame, different reactions establish the balance. A MM analysis shows that within the context of model reactions combined with model-predicted mole fractions, the net consumption of C_6H_5 is primarily due to these three reactions:

$$C_6H_5+H \rightleftharpoons C_6H_6 \qquad \text{(B1)}$$

$$C_6H_5 \rightleftharpoons C_2H_2+\text{n-}C_4H_3 \qquad \text{(Ph13)}$$

$$C_6H_5+O_2 \rightleftharpoons 2CO+C_2H_2+C_2H_3. \qquad \text{(Ph6)}$$

As seen in Figure 7.10, however, when using *data* mole fractions with the reaction network there would be no net destruction due to reaction B1. Also, reaction Ph13 is now known to be incorrect as written, in reality taking place by a two-step mechanism of decyclization followed by β-scission (cf. Chapter 2; further evidence is presented in Section 7.7). The third reaction, Ph6, is a semi-global reaction for a pathway which is now understood on an elementary basis, as discussed below. Using the 20 torr rate constant for -Ph13 calculated by Westmoreland et al. (1989) using QRRK, the MD net rate predicted for these three reactions produces no phenyl at all and the maximum destruction rate is three times the maximum measured formation rate. Therefore, neither of the mechanisms by which the ZM model achieves a fine balance of

production and destruction — in H_2-O_2-C_6H_6 or C_6H_6-O_2 flames — are viable.

One might therefore expect that in a flame code simulation the high phenyl mole fraction would have a strong impact on the benzene prediction. By compensation of errors, benzene chemistry is not much affected by the overprediction of x_{C6H5} in the model solution of H_2-O_2-C_6H_6 mole fractions. The excessive H and OH mole fractions predicted by the H/O chemistry drive reactions B2 and B4 to a much higher level of benzene consumption. The exaggerated rate of recombination by reaction B1 due to increased phenyl serves to balance the overpredicted consumption rate, rather than strongly reducing the benzene destruction level or creating net benzene production. The net result is a reasonable net reaction rate for benzene. In the rich C_6H_6-O_2-Ar flame, the net result of excessive phenyl is lowering of the benzene consumption rate, because recombination of C_6H_5 with H is predicted. However, the contribution of reaction B1 is not large compared to the other two reactions. In addition, those reactions are driven forward enough so that the overprediction of phenyl only makes a small difference. Benzene destruction via -B3, which is overpredicted because the O atom mole fraction prediction is too large, compensates for the production from B1 as well.

Specific reactions.

Detailed descriptions of all falloff calculations are given in Appendix C.

$C_6H_5+H \rightleftharpoons C_6H_6$ (Rxn B1; EBG, ZM, LS) - This reaction was discussed in Section 7.2.2. Correcting for falloff reduces the reaction path ratio for formation from 123 to 7.5.

$C_6H_5+O_2 \rightleftharpoons C_6H_5O+O$ (Rxn Ph1; EBG, ZM, LS); $2CO + C_2H_2 + C_2H_3$ (Rxn Ph6; ZM); $C_6H_5O_2$, $C_6H_4O_2+H$ - Oxygen reaction with phenyl appears to be a plausible bimolecular candidate, because of the high concentration of O_2. The RRKM analysis of Yu and Lin (1994) was used as the basis for a bimolecular QRRK calculation, in order to derive rate constants for the three channels

$$C_6H_5+O_2 \rightleftharpoons C_6H_5O+O \qquad \text{(Ph1)}$$

$$C_6H_5+O_2 \rightleftharpoons C_6H_4O_2+H \qquad (4)$$

$$C_6H_5+O_2 \rightleftharpoons C_6H_5O_2 \qquad (5)$$

at 22 torr. The addition/stabilization calculations agree with Yu and Lin within about a factor of three at 1 torr and 40 torr. With respect to their higher pressure (≥975 torr — the exact pressure is unclear) Arrhenius plot though, the CHEMACT results for the addition/elimination reactions

only agree with RRKM above 900 K. Below that temperature, QRRK predicts those rate constants to be smaller than the RRKM results. For example, at 600 K the QRRK rate constant for reaction Ph1 is 10 times smaller than the RRKM value, and $k_{rxn\,4,QRRK} \cong k_{rxn\,4,\,RRKM}/20$.

At the pressure of the Yu and Lin curve, the low-temperature discrepancy would not cause a problem since between 600 K and 900 K the error is not great, and below 600 K the two channels would be insignificantly small compared with stabilization anyway. To study whether this situation would also hold at 22 torr, QRRK rate constants were compared for each reaction at 22 and 975 torr. At 1 mm, or about 600 K, the 22 torr predictions for $\frac{k_{elim}}{k_{stab}}$ for both elimination channels are three times higher than at 975 torr. If the same trend were true of the RRKM calculation, this would bring the elimination channels up to ~$3x10^{-2}$ (rxn Ph1) and ~$3x10^{-3}$ (rxn 4) that of the stabilization channel at 22 torr and 600 K. At 300 K, the increase due to falloff is slightly greater, but the amount that those channels are less than the stabilization channel is significantly less, resulting in ratios relative to k_{stab} of about $1x10^{-4}$ and $6x10^{-6}$. In the 600-900 K region, falloff should bring the ratio close to one; lower for reaction 4 than reaction Ph1.

Therefore below 1 mm, error in the QRRK analysis should not affect the qualitative predictions of the elimination channels. Between 1-1.75 mm (600-900 K), the predictions for the elimination channels are somewhat in question, lower than they should be. Above 1.75 mm, QRRK results can be considered to be equivalent to RRKM. As mentioned above, the rate constant for reaction 5 is valid at all temperatures.

The adjusted Yu and Lin $C_6H_5+O_2 \rightleftharpoons C_6H_5O+O$ rate constant has a reaction path ratio for destruction of 89, up from 3.5. The narrow peak occurs early relative to the maximum C_6H_5 production rate (2.6 mm vs. 5.8 mm), and so brings the net rate to a large negative value from 1.5 to 2.5 mm, instead of balancing production. Additional destruction reactions for $C_6H_5O_2$ could not correct the early destruction problem because they would not affect the predicted C_6H_5 net rate, except for reactions of $C_6H_5O_2$ with C_6H_5. An artificial profile of the type discussed above with a peak located higher than about 4 mm would reduce or eliminate the large negative spike near the burner. However, all of the problems attendant to predictions with such profiles remain.

Including the H elimination pathway introduces little change, as expected. The reaction 5 channel introduces a sharp destruction peak at 1 mm, with $\frac{R_{rxn}}{R_{Ph}} = 240$. With the revised artificial profile instead of the measured mole fraction, though, the H elimination pathway reduces the

ratio to 40, and there is no addition/stabilization 'spike.'

The semi-global reaction to CO and other products (Ph6), while resulting in an apparent phenyl destruction, is not an elementary reaction. In fact, since reaction of C_6H_5 with O_2 is already accounted for on an elementary level, Ph6 should not be included in a model. In the present flame, reaction Ph6 is several times as fast as the Lin and Lin rate, but about 0.1-0.5 that Yu and Lin's. As a global reaction, its rate would be expected to be of the same order as the elementary reactions which replace it.

$C_6H_5CO \rightleftharpoons C_6H_5+CO$ (Rxn Ph5; EBG) - This reaction was not initially considered important enough to merit a falloff calculation. However, the sensitivity analysis (Section 7.7) revealed that with the high-pressure limit a very large phenyl production rate in the reaction zone would result if the benzoyl radical mole fraction were even $1/50^{th}$ of the detection limit. After correction for falloff using RRKM, excessive formation is no longer predicted.

$C_6H_5 \rightleftharpoons HC\equiv CCH=CHCH=CH$ (Rxns Ph7, Ph14; ZM, LS); $C_2H_2+HC=CHC\equiv CH$ (Rxn Ph 13; ZM) - As mentioned above the concerted pathway should be eliminated from the phenyl subnetwork. There are two measurements for the decyclization channel, that of Rao and Skinner (1988) and that of Braun-Unkhoff et al. (1989). The former investigators performed an RRKM calculation to derive the high-pressure limit. Another RRKM calculation was performed in this work, to calculate a rate constant for 22 torr. A falloff calculation was also done using the Braun-Unkhoff value as k_∞, even though it was measured at about 1.5-7.7 atm. Interestingly enough, while the two "high-pressure limits" differ by a factor of 3, the 22 torr rate constants are about identical above 1400 K.

Elimination of the inappropriate reaction channel removes a needed $\frac{R_{rxn}}{R_{Ph}}$ of 17. Correcting the decyclization rate constant for falloff lowers the ratio to 2 from 7.5-15 (depending on the model). Unfortunately, neither change improves the fit of model to data.

QRRK calculations of the Westmoreland (1986) and Westmoreland et al. (1989) network for phenyl decomposition (cf. Chapter 2) were performed at the pressures of the Rao and Skinner and Braun-Unkhoff et al. experiments, using the Q-formalism program of Westmoreland (1992a). The resulting rate constants for phenyl disappearance were a factor of 2.3 larger than Rao and Skinner's. At 1.5 bar, the QRRK rate constants ranged from 0.33 to 0.77 of the Braun-Unkhoff et al. value. In deriving their rate constant, Rao and Skinner modeled the reaction

sequence as

$$C_6H_5 \rightleftharpoons l\text{-}C_6H_5$$
$$l\text{-}C_6H_5 \rightarrow \text{products}$$

and derived high-pressure limits for the first reaction from the falloff curve, whereas Braun-Unkhoff et al. saw the network as

$$C_6H_5 \rightleftharpoons l\text{-}C_6H_5$$
$$l\text{-}C_6H_5 \rightleftharpoons [l\text{-}C_6H_5]^* \rightarrow C_4H_3+C_2H_2$$
$$l\text{-}C_6H_5 \rightleftharpoons [l\text{-}C_6H_5]^* \rightarrow l\text{-}C_6H_4+H$$

with estimated rate constants for the activated pathways at the pressure of measurement. Neither group considered that the energized linear species might be formed from the first decomposition step.

The theoretical network of Westmoreland (1986) and Westmoreland et al. (1989) agrees well enough with the experimental studies to consider the possibility that the differences are due to how the data were modeled. Since the former mechanism is more realistic about the mechanism by which energized $l\text{-}C_6H_5$ is formed and destroyed, it was tested in the present flame as well.

A QRRK computation was performed at 22 torr and appropriate bath gas conditions. According to those calculations, above about 1350 K the channel $[l\text{-}C_6H_5]^* \rightarrow l\text{-}C_6H_4+H$ is greater than stabilization pathway. Above about 1500 K the $[l\text{-}C_6H_5]^* \rightarrow 1\text{-}C_4H_3+C_2H_2$ channel is also predicted to be greater than stabilization. In spite of the differences in detail, above 1600 K the total decomposition rate predicted is within a factor of four of the two RRKM values. At 1300 K, where stabilization of the $l\text{-}C_6H_5$ is clearly preferred, the total Westmoreland et al. rate constant for phenyl disappearance is only 12% that of Rao and Skinner decyclization and 7% of the Braun-Unkhoff rate constant. The two rate constants meet at between 800 K and 900 K (Rao and Skinner) or 600 K and 700 K (Braun-Unkhoff et al.), and below that temperature the Westmoreland et al. prediction is significantly higher than that either of the other two. With the QRRK-computed reaction network, the reaction path ratio for unimolecular decomposition of phenyl is only 1.0, offsetting the large production from benzene decomposition even less than before.

Use of a falloff-corrected rate constant for decyclization of phenyl enhances the decomposition channel relative to cyclization back to c-C_6H_5. The two pathways would be equal at 1150 K (using the decomposition rate constant of Colket (1986b)), and the ratio of the two rate constants drops to $1.4x10^{-3}$ in the temperature range of the present flame. A steady-state analysis on (stabilized) l-C_6H_5 gives the following expression, under the assumption that the reactions involving it are formation from phenyl, recyclization, reaction with H atom to from l-C_6H_4+H_2, and unimolecular decomposition to C_2H_2+C_4H_3, 1-C_4H_3+C_2H_2, and l-C_6H_4+H:

$$\frac{(l-C_6H_5)}{(C_6H_5)} = \frac{k_{decycl}}{(k_{cycl} + k_{l-C6H4+H2}[H] + k_{C2H2+1-C4H3} + k_{l-C6H4+H})}$$

Using this relationship, the mole fraction of linear C_6H_5 never rises above 10^{-9} that of phenyl. This is too small to result in any change to the decyclization rate constants.

$C_6H_5CH_2+HO_2 \rightleftharpoons C_6H_5+CH_2O+OH$ (Rxn Ph4; EBG, ZM) - While this reaction has a somewhat large formation rate, the profiles used for both of the reactants have a very high degree of uncertainty. This reaction was assigned a rather high rate constant by EBG, on the basis of analogy with reaction of benzyl and O atom, and in spite of a measurement of the overall reaction by Hippler et al. (1991) that was two orders of magnitude lower. The basis for not using the Hippler et al. rate constant was the notation in the source that the rate is quite tentative and not independent of two other estimated rates. Given the uncertainty in this rate constant, and the lack of adequate profiles for both reactants and the relative low importance of the reaction, no falloff calculation was done.

Net result of improvements to C_6H_5 chemistry.

As with C_6H_5OH, a single revised submechanism was created from the reactions in Table 7.5. Reaction Ph6 was eliminated, and reactions B1, Ph1, and Ph7 (=Ph14) were modified as discussed above. Reaction Ph13 was revised to reflect a non-concerted pathway in two ways: decyclization with stabilization and subsequent decomposition (Colket, Rao and Skinner), and decyclization without stabilization (Westmoreland and Westmoreland et al.). Also, reactions 4, 5, and Ph'1, Ph'2 and B'8 from Table 7.6 below were added.

The results are plotted in Figure 7.12, along with the prediction of the revised ZM model, and the amended model using an artificial phenyl profile which provides a good reduction in production and destruction. There is little improvement for all the effort, and the early destruction

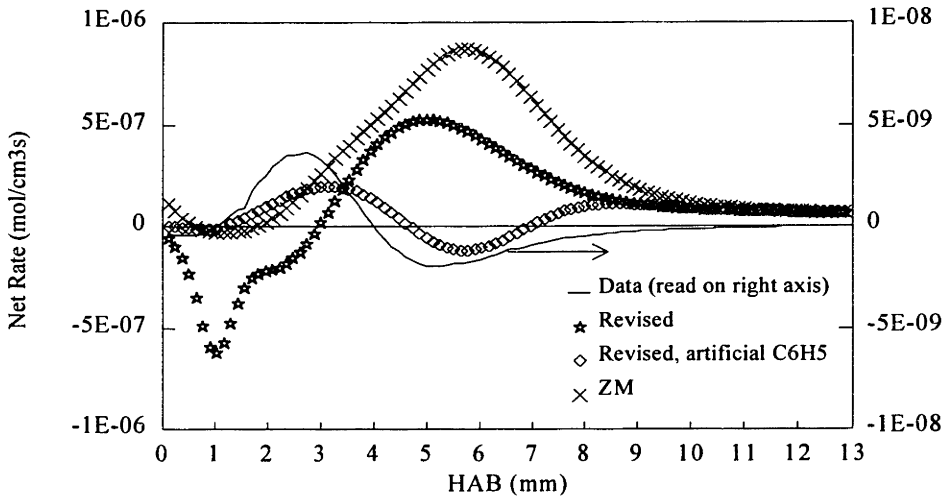

Figure 7.12 Revised C_6H_5 submechanism, compared to data net rate. "Revised, artificial C_6H_5" — see text.

spike — caused by formation of $C_6H_5O_2$ — is an unwelcome feature. Substitution of the Rao and Skinner decyclization rate constant caused only a barely perceptible change.

The shape and magnitude of the computed C_6H_5 net rate are very sensitive to the characteristics of the phenyl mole fraction. The artificial profile used, optimized to the revised model, had a peak height 2.4 times the data and a peak location of 5.25 mm. The maximum predicted formation and destruction rates were about 25 times those of the data profile, when the latter is adjusted by a factor of 2.4 to account for the larger x_{C6H5} being input to the mechanism. While the large destruction peak near the burner is eliminated with the modified profile, the formation peak is still off by 2 mm from its expected location, 5.3 mm. The magnitude change of the artificial profile is within reasonable limits of error for C_6H_5, but the different peak location is more difficult to justify experimentally[37]. Relative to the distribution of other species, though, a peak at about 5 mm makes sense because: (a) even discounting the recombination predicted by $C_6H_5+H \rightleftharpoons C_6H_6$, the region of greatest predicted phenyl production from C_6H_6 is from about 2.5-6 mm, and (b) such a peak location would be more consistent with that of the C_6H_6-O_2 flame of Bittner. In any event, even with the best substitute C_6H_5 profile, the model subnetwork does

[37] As noted in Chapter 4, some fraction of the mass 77 signal close to the burner (i.e., where the peak is located) could theoretically be due to fragmentation from linear C_6H_6, should there be any significant amount in that part of the flame. The steady state analysis of Section 7.2.2 predicts the mole fraction of l-C_6H_6 to be no more than $4x10^{-7}$ anywhere in the flame, far below what would be necessary to significantly affect the phenyl profile.

poorly with respect to data.

7.4.3 Other C_6H_5 Reactions

Other reactions found in the literature for C_6H_5 are listed in Table 7.6. Relative to other reactions in the phenyl subnetwork, these are unimportant in the present flame.

Table 7.6 Additional phenyl reactions found in the literature.

Rxn No.	Reaction	A (cm^3, sec)	n	E (cal)	Ref.	R_{rxn}/R_{Ph} †
Ph'1	$C_6H_5+O \rightleftharpoons C_5H_5+CO$	$1x10^{14}$	0	0	a	0, 0.4
Ph'2	$C_6H_5+C_2H_2 \rightleftharpoons C_6H_5C_2H+H$	$3.69x10^{30}$	-4.99	20927	b	0, 0.01
B'8	$C_6H_7+C_6H_5 \rightleftharpoons 2C_6H_6$	$1.00x10^{12}$	0	0	c	0, 0

† Mole fraction assumptions were made for the following species:
O, C_5H_5, C_6H_7, $C_6H_5CH_2$
The assumptions and their rationale are found in Section 7.7.
a - Frank et al. (1995); at 975-1875 torr.
b - Yu, Lin and Melius (1994), RRKM at 20 torr. Fit to 500-1500 K.
c - Louw and Lucas (1973).

7.5 C_6H_5O Net Rate Analysis

As the concentration of phenoxy is just at or below detection limit, there is neither a mole fraction profile nor a net rate curve for comparison. Therefore, only a reaction path analysis was performed, first on the original C_6H_5O subnetworks, then on the subnetworks as already revised with the falloff and mechanistic improvements made above. No other reactions were analyzed.

7.5.1 Model Reaction Sets for C_6H_5O

For each model, the sum of maximum net formation rates all reactions was used as an estimate of the magnitude of the model's maximum net formation rate; likewise for destruction. Recalling that $R_{rxn,formation}$ is the maximum net (that is, including the reverse reaction) formation rate of a particular reaction, define $R_{submech}$ as:

$$R_{submech,\ formation(destruction)} \equiv \Sigma R_{rxn,\ formation(destruction)}.$$

Since the maxima of individual reactions occur at different places in the flame, $R_{submech}$ is not necessarily equal to R_{PhO} (the true maximum net rate of phenoxy). Given the above definition, the (approximate) reaction path ratio $\left(\frac{R_{rxn}}{R_{submech}}\right)_{formation/destruction}$ is always positive. For formation,

the predicted $R_{submech}$'s are $1.02x10^{-6}$, $4.4x10^{-7}$ and $9.7x10^{-7}$ mol/cm^{3}s for the EBG, ZM, and LS models respectively. The totals for destruction are $-6.6x10^{-9}$, $-2.5x10^{-9}$, and $-1.2x10^{-8}$ mol/cm^{3}s.

Table 7.7 lists all of the phenoxy reactions relevant to the present flame, and the initial reaction path analysis, given as percentages of $R_{submech}$.

Table 7.7 C_6H_5O reactions from the mechanisms under review, and the ratios $\frac{R_{rxn}}{R_{submech}}$ (expressed as percentage) for production and destruction, respectively. "0" ≡ <1%.

Rxn	Reaction	EBG†	ZM†	LS†
B3	$C_6H_5O+H \rightleftharpoons C_6H_6+O$	5.0, 0	1.4, 0*	
B8	$C_6H_5+C_6H_5OH \rightleftharpoons C_6H_6+C_6H_5O$	0, 0	0, 0	
Ph1	$C_6H_5+O_2 \rightleftharpoons C_6H_5O+O$	1.2, 0	1.6, 0	0.7, 0
PhOH1	$C_6H_5OH+C_6H_5CH_2 \rightleftharpoons C_6H_5O+C_6H_5CH_3$	0, 0	0, 0	
PhOH3	$C_6H_5O+H \rightleftharpoons C_6H_5OH$	92.1, 0	89.9, 0*	96.9, 0
PhOH4	$C_6H_5OH+OH \rightleftharpoons C_6H_5O+H_2O$	0.7, 0	1.9, 0	0.7, 0
PhOH5	$C_6H_5OH+H \rightleftharpoons C_6H_5O+H_2$	1.4, 0	3.3, 0	1.5, 0
PhOH6	$C_6H_5OH+O \rightleftharpoons C_6H_5O+OH$	0, 0	0, 0	0, 0
PhOH9	$C_4H_5+C_6H_5OH \rightleftharpoons C_4H_6+C_6H_5O$	0, 0	specific isomers -- see below	
PhOH7	$C_5H_6+C_6H_5O \rightleftharpoons C_5H_5+C_6H_5OH$	0, 0	0.1, 0	0, 0
PhO1	$C_6H_5O \rightleftharpoons CO+C_5H_5$	0, 100	0, 98.5	0, 100
PhOH8	$C_2H_3+C_6H_5OH \rightleftharpoons C_2H_4+C_6H_5O$	0, 0	0, 0	
Ph11	$C_6H_5+OH \rightleftharpoons C_6H_5O+H$		1.7, 0	
PhOH14	$C_6H_5OH+HO_2 \rightleftharpoons C_6H_5O+H_2O_2$		0, 0	
PhOH10	$C_6H_5OH+CH_2=CHCH=CH \rightleftharpoons C_4H_6+C_6H_5O$		0, 0	
PhOH11	$C_6H_5OH+CH_2=CHC=CH_2 \rightleftharpoons C_4H_6+C_6H_5O$		0, 0	
PhO2	$C_6H_5O+CH_3 \rightleftharpoons C_7H_8O$		0, 0	
PhO3	$H+C_6H_5O \rightleftharpoons C_5H_6+CO$		0, 1.4*	
Ph19	$C_6H_5+HO_2 \rightleftharpoons C_6H_5O+OH$			0, 0

* Falloff effects were calculated for the reaction in the original model.

† Mole fraction assumptions were made for the following species:
O, HO_2, H_2O_2, C_2H_3, C_4H_5, C_4H_6, CH_2=CHCH=CH, CH_2=CHC=CH_2, C_5H_5, C_5H_6, C_6H_5O, $C_6H_5CH_2$, $C_6H_5CH_3$, $HOC_6H_4CH_3$
The assumptions and their rationale are found in Section 7.7.

7.5.2 Falloff and Mechanistic Analyses of C_6H_5O Reactions

$C_6H_6+O \rightleftharpoons C_6H_5O+H$ (Rxn -B3; EBG, ZM) - This reaction was analyzed in Section 7.3. The maximum rate calculated using the Ko et al. (1991) rate constant is about 3 times that of the ZM model. This only makes matters worse as far as excessive C_6H_5O production is concerned. However, as this reaction was not very significant to begin with, the difference is not more than a few percent of the total rate predicted by the models.

$C_6H_5O+H \rightleftharpoons C_6H_5OH$ (Rxn PhOH3; EBG, ZM, LS) - Also discussed in Section 7.3, accounting for falloff effects improves the contribution of reaction PhOH3 significantly. The revised rate maximum is 6.1×10^{-8} mol/cm^{3}s, as opposed to the high-pressure limit of 2.1×10^{-7}. As PhOH3 for about 90% of the high phenoxy creation rate, the overall rate is reduced about three-fold.

$C_6H_5OH+OH \rightleftharpoons C_6H_5O+H_2O$ (Rxn PhOH4; EBG, ZM, LS) - As with the first two reactions, this was discussed in Section 7.3, where the rate constant in the ZM model was revised to remove the contribution of abstraction from aromatic ring. With the corrected rate constant the maximum rate is 9.7×10^{-9} mol/cm^{3}s, slightly larger than the original Zhang and McKinnon value. The revised maximum rate would be expected to be *smaller* than the original, since the modified rate constant is smaller without ring abstraction. However, since ZM accidentally reversed the sign of the activation energy in the Knispel et al. (1990) rate constant, the corrected rate is larger. With the proper sign, the revised rate is 58% of the original rate.

The rate constant used by Emdee et al. and Lindstedt and Skevis was that of He et al. (1988), which predicts a maximum phenoxy formation rate that is 73% of the present value.

The impact of the change on the quality of the model prediction is very small.

$C_6H_5+O_2 \rightleftharpoons C_6H_5O+O$ (Rxn Ph1; EBG, ZM, LS) - This reaction was analyzed in Section 7.4. With the phenyl profile as measured, the maximum rate is 1.8×10^{-7} mol/cm^{3}s, peaking at 2.6 mm (1250 K). This would bring the bring total producion rate back up a great deal. Using an artificial C_6H_5 mole fraction profile (the same one as for Figure 7.12) brings no change to the size of the contribution, but moves the maximum to 4 mm (1635 K). In both cases, the peak occurs at a temperature above the region of uncertainty for the QRRK calculation ($T < 900$ K; see Section 7.4).

Net result of improvements to C_6H_5O chemistry.

With the the above four changes the sums $R_{submech}$ become 28% (EBG), 66% (ZM) and 29% (LS) of the original model amounts. With only the first three, the sums are 10%, 26% and 11% of the unmodified values. As the phenoxy mole fraction was near or below the detection limit, the maximum net rate would be expected to be about $1x10^{-9}$ mol/cm^{3}s, by comparison with phenyl. Therefore, with either scenario the revised models — while an improvement — are not good enough to be considered accurate.

7.6 C_6H_7 and C_6H_8 Chemistry

The potential for formation of C_6H_7, cyclohexadienyl radical, arises with benzene being in the presence of significant quantities of H atoms. An early "quasi-global" model of benzene oxidation, proposed by Jackson and Laurendeau (1987), contained the reaction

$$H+C_6H_6 \rightleftharpoons C_6H_7, \qquad (6)$$

but it was found to be unimportant for most of their lean H_2-O_2-C_6H_6(additive) flame. No destruction pathway other than back to reactants was included.

In the present work, species at masses 80-86 were found at the 1-60 ppm level, when calibrated as cyclic C_6H_x. Cyclohexadienyl radical, which would be mass 79, was found to be below the isotopic contribution from benzene. As the mass 79 isotopes of benzene, $^{13}CC_5H_6$ and C_6H_5D, are about 270 ppm near the burner, the upper limit on x_{C6H7} was probably about 25 ppm. This is the same order of magnitude as the more hydrogenated species.

The region of their flame where Jackson and Laurendeau found a noticeable effect from reaction 6 in their model calculation was from 415-775 K. This is due to the fact that the adduct is only stable at low temperatures. In the present flame, the peaks of mass 80-85 species were all located so close to the burner that their exact locations could not be determined. However, there was a clear trend of rapid decay that started in the 1-2 mm range, 600-1000 K. Therefore, it seems plausible from the locations and shapes of the mole fraction profiles that these species could be cyclic C_6H_x's, and some reactions which could produce and destroy such species were preliminarily investigated. The early appearance of C_2H_4 could be a result of unimolecular decomposition reactions of such species by sequential β-scission.

Of the three models fully reviewed in this work, only the LS model contains any reactions

which produce or involve C_6H_7. The two reactions found there,

$$H+C_6H_6 \rightleftharpoons C_6H_7 \quad (6')$$

$$C_6H_6 \rightleftharpoons CH_2=CHCH=CHCH=CH \quad (7)$$

are provided at the high-pressure limit, but in contrast to Jackson and Laurendeau a destruction pathway is provided. The model has no channels for further H addition, though.

The remainder of this section is devoted to an analysis of C_6H_7 and C_6H_8 reactions found in the literature, with the aim of developing a preliminary submechanism involving those species. In the following discussion, "C_6H_8" refers to the cyclic isomers, 1,3-C_6H_8 and/or 1,4-C_6H_8, unless otherwise specified.

$H+C_6H_6 \rightleftharpoons C_6H$- (Rxn 6; LS); l-$C_6H$- (LS); $C_5H_4CH_3$; $C_5H_4CH_2+H$ - As mentioned in

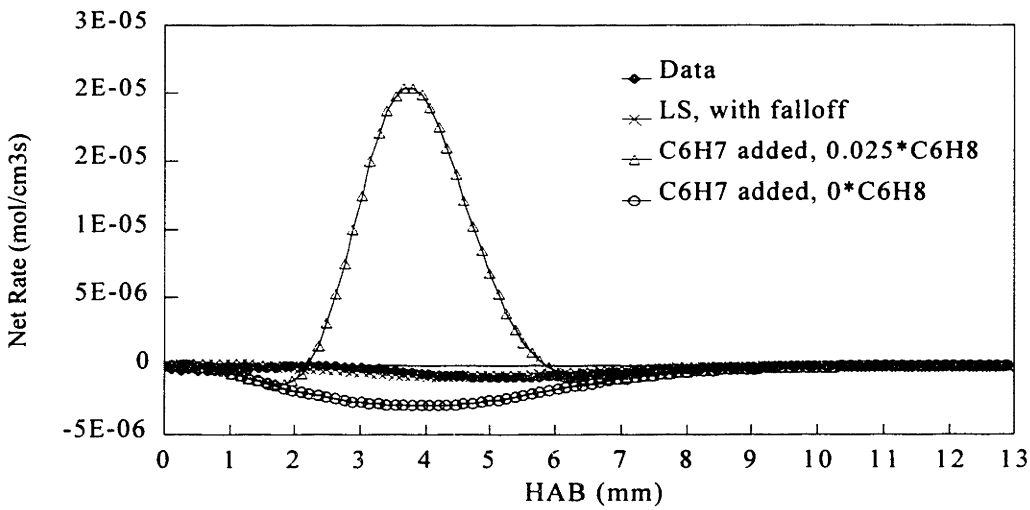

Figure 7.13 C_6H_6 net rate, LS model (revised for falloff) vs. data, with and without C_6H_7 formation reaction at high-pressure limit. Two assumptions on the cyclohexadienyl radical concentration profile are shown.

Section 7.1, the high-pressure addition/stabilization reaction produces a significant deviation in the model fit to data. Figure 7.13 shows the LS net rate for benzene, revised for falloff, before and after addition of reaction 6'. The $\Delta H_f^0(C_6H_7)$ and high-pressure rate constant used were those of Tsang (1986), rather than Nicovich and Ravishankara (1984). Two assumptions about the C_6H_7 mole fraction profile were tested: (a) the profile was set to $0.025*x_{C6H8}$, where x_{C6H8} is

the mass 80 profile as calibrated for cyclohexadiene, and (b) the mole fraction was set to 0.0 throughout the flame.

Case (a) has the feature that x_{C6H7} follows the shape and location of the mass 80-85 species, which were probably derived from mass 79. Also, the highest mole fraction of cyclohexadienyl radical under that scenario is 0.22% of the isotopic contribution of C_6H_6 to mass 79. This would put it well within the undetectable range. If the mole fraction were made just detectable, the huge production peak of Figure 7.13 would be about 20 times higher. Case (b) was simply used as an alternate, limiting situation. No assumption for x_{C6H7} between the two limits was found that could both remove or significantly dampen the oscillation and get the predicted rate within reasonable agreement with data.

After adjusting for the falloff effect of chemical activation on the reaction, the situation is much better. In Figure 7.14 one can see the result for the case (a) assumption on x_{C6H7}. The case (b) profile would be roughly the same, however increasing the x_{79}/x_{80} ratio by more than a factor

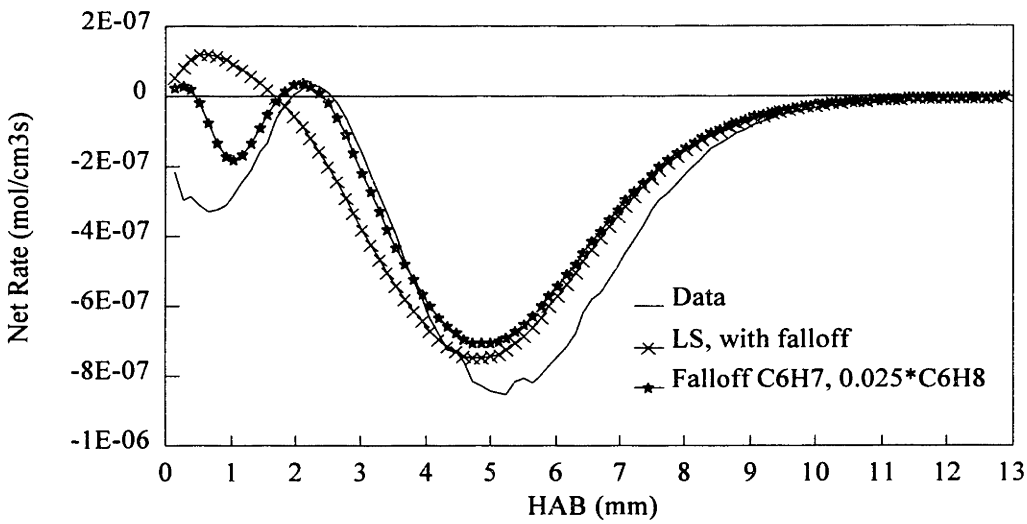

Figure 7.14 C_6H_6 net rate, LS model (revised for falloff) vs. data, with and without C_6H_7 formation reaction. In this case, the C_6H_7 reaction has been corrected for falloff. $x_{C6H7} = 0.025 * x_{C6H8}$.

of 2 would result in a production peak in the 1.5-3 mm range larger than 2×10^{-7} mole/cm^{3}s. It is tempting to view the reproduction of the small hump near the burner as significant, but the experimental hump may in fact be an artifact for two reasons. First, the benzene mole fraction profile was estimated below 1.2 mm. Second, nonidealities in gas flow and probe-burner

interactions probably affect the flux profiles negatively in the first several millimeters from the burner. What the predicted hump does indicate is that a pathway to more hydrogenated species is opened up in the model by the $H+C_6H_6$ addition reaction, as hoped for.

Other pathways for the cyclohexadienyl were investigated. In particular, the rate parameters of Ritter et al. (1990) were used for a chemical activation calculation of outlet channels to linear C_6H_7, $C_5H_4CH_3$ and $C_5H_4CH_2+H$ (as well as stabilization of cyclic C_6H_7, of course). None of the alternative pathways had a rate above $5.4x10^{-9}$ mol/cm^{3}s, about 10^{-2} as much as stabilization of the adduct.

This result is for assumed mole fractions of alternative products of 0.0 throughout the flame. A mole fraction of l-C_6H_7 above $10^{-3}*x_{cyclohexadienyl}$ would affect the importance of its channel, especially in the HAB region of 1-3 mm. The highest that the predicted rate of formation of the linear species gets is 0.7% of the maximum cyclohexadienyl formation rate (absent reaction back to benzene and hydrogen), and that not until 5.25 mm. Therefore, the mole fraction at 1-3 mm should be much lower than $7x10^{-3}*x_{cyclohexadienyl}$. Given the likelihood of l-C_6H_7 to further react by β-scission and bimolecular reactions, its mole fraction near the burner is probably low enough to have little impact on the reverse reaction there.

The effect that $C_5H_4CH_2$ (fulvene) could have on the reverse of the $H+C_6H_6 \rightleftharpoons$ fulvene+H reaction was tested in a similar way, by assuming that its profile would be shaped and located identically to cyclohexadienyl. The maximum fulvene formation rate from the forward direction is $1.4x10^{-2}$ as much as the maximum C_6H_7 formation rate, also occuring at 5 mm but being a wider peak. Therefore, the fulvene mole fraction was set to 0.014 that of cyclohexadienyl; the highest that the reverse rate would then get is $\sim10^{-12}$ mol/cm^{3}s, an insignificant magnitude. The reverse reaction is therefore unimportant to the benzene net rate.

Finally, the ratio of maximum formation rates for $C_5H_4CH_3$ and c-C_6H_7 is only 0.7%, though the peak for methylcyclopentadienyl is closer to the burner than the other species, at 3.5 mm. Assuming $x_{C5H4CH3}$ to be $0.01*x_{cyclohexadienyl}$ caused no change in the rate constant for its formation reaction.

$H+C_6H_7 \rightleftharpoons C_6H_8$ - The questions then arise as to whether sequential H addition occurs, and how important such a pathway to C_6H_8 might be. The high-pressure limit of this reaction was given by Benson and Shaw (1967b), for 1,3-C_6H_8 formation, to be $10^{13.6}$exp(-71000/RT) s^{-1}. However Dean (1985), in his generic rate constant table, gives $10^{15.7}$exp(-72600/RT) s^{-1}. Dean's

value was derived by assuming the radical recombination rate to be 10^{14} cm^3/mol-s. Benson and Shaw apparently assumed (ekT/h) for the forward A-factor. Both used thermochemistry to derive the reverse rate constant.

By applying Dean's method, but with Tsang's thermochemistry for C_6H_7 and the THERM (Ritter and Bozzelli, 1990) estimate for $\Delta H_f^0(1,3-C_6H_8)$, one gets $1.47x10^{16}T^{-0.316}$ * exp(-76501/RT). This value is intermediate between that of Dean and that of Benson and Shaw — much closer to the latter above about 420 K, and at most a factor of 8 higher than it. Using the "$0.025*x_{C6H8}$" profile for cyclohexadienyl, the Benson and Shaw value predicts considerable formation of 1,3-C_6H_8 from this reaction in the first couple of millimeters above the burner ($1x10^{-6}$ mol/cm^3-sec, greater than the measured benzene net rate). Dean's k_∞ would predict even more formation ($1x10^{-5}$ mol/cm^3s). The revised estimate with Tsang's thermochemistry gives a rate 2.5 times higher than the maximum seen for phenyl. The maximum C_6H_8 mole fraction — if all of mass 80 is cyclic with no oxygenated species — is about 10 times that of C_6H_5. The maximum recombination rate is completely unaffected by the assumptions made for mass 80, but is sensitive to those of mass 79.

The rate constant for formation of 1,4-C_6H_8 can be estimated from that of 1,3-C_6H_8. Benson and Shaw (1967a) estimate the two to be identical, as the heats of formation are within 1kcal/mol of each other. They are in fact only about 600 cal/mol apart, according to an estimate using THERM. On an Evans-Polyani plot, this would indeed give them about identical activation energies. The A-factor for formation of 1,3-C_6H_8 should be twice that of the other reaction because of reaction path degeneracy, though. In any event, the total formation from C_6H_7 should be about 3-6 times that of the maximum phenyl formation seen in the data.

It appears that this reaction could be important, but it should be adjusted for falloff. Dean (1990) published a QRRK value for 0.58 atm, however the amount of falloff at that pressure appears to be very high (k/k_∞ = 0.0174 at 600 K), if one assumes that the high-pressure limit came from Dean (1985). The source for k_∞ in that paper was not given, though. Therefore, an RRKM analysis was performed, which showed much less falloff, dropping the maximum only about 20%. Therefore, this reaction is worthy of consideration for a reaction network for production of cyclohexadiene.

$H_2+C_6H_6 \rightleftharpoons C_6H_8$ (Rxns -B'2 and -B'3) - In the present flame with such a high concentration of H_2, these reactions, mentioned in Section 7.2.3, could be important. RRKM calculations

were done for the elimination direction, based on the high-pressure limits of Ellis and Frey (1966) (1,4 isomer) and Orchard and Thrush (1974) (1,3 isomer). The effect of these reactions depends on the assumptions concerning how much of the mass 80 signal is C_6H_8, and how much

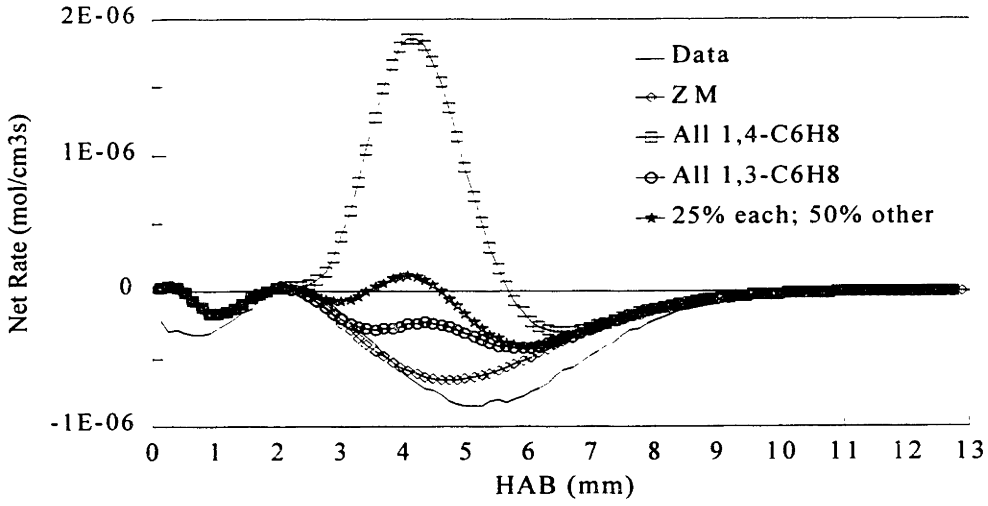

Figure 7.15 Effect of adding $H_2+C_6H_6 \rightleftharpoons C_6H_8$ in the high-pressure limit to the ZM model prediction (as revised by falloff calculations and the cyclohexadienyl-producing reaction). The results of various assumptions regarding the mass 80 signal are shown.

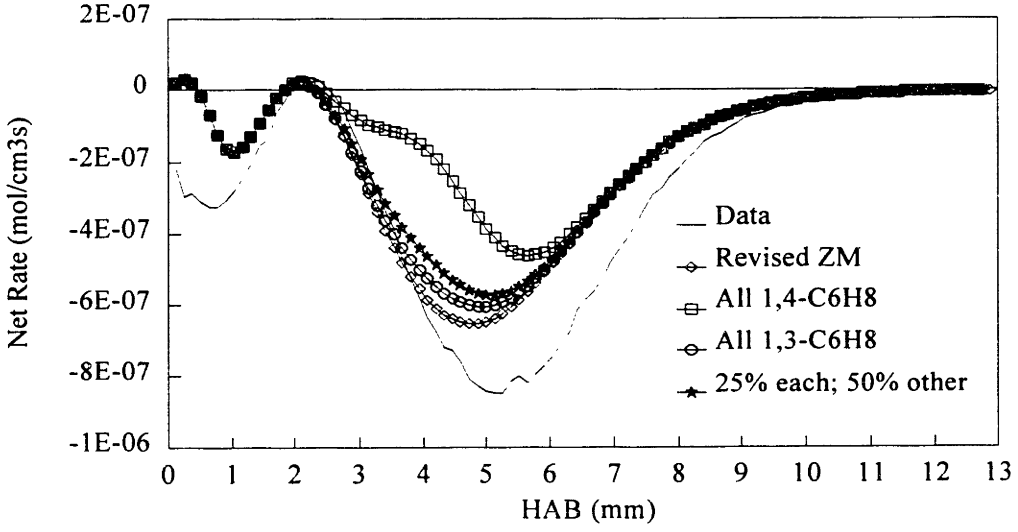

Figure 7.16 Effect of adding $H_2+C_6H_6 \rightleftharpoons C_6H_8$ with falloff to the ZM model prediction (as revised by falloff calculations and the cyclohexadienyl-producing reaction). The results of various assumptions regarding the mass 80 signal are shown.

is C_5H_4O; on how much of the C_6H_8 is linear and how much cyclic; and how much is 1,3-C_6H_8 vs. 1,4-C_6H_8. Because H_2 elimination from the 1,4 isomer is much faster than from 1,3-C_6H_8, the more mass 80 is 1,4-C_6H_8 the greater the effect on the net rates of benzene destruction and C_6H_8 formation.

Without falloff, most of the mass 80 would have to be linear or C_5H_4O in order for the model fit of C_6H_6 destruction to continue being reasonable (Figure 7.15). After accounting for falloff, the model fit is much less degraded with the signal being completely 1,4-C_6H_8, as shown in Figure 7.16. If any of the mass 80 is 1,3-C_6H_8, or it is not linear of C_6H_8 at all, then the prediction tends to go back toward what it previously was. For example, under a condition where the mass 80 signal is entirely 1,3-C_6H_8, with no linear compounds or C_5H_4O, there is practically no change at all to the fit. For equal amounts of 1,4- and 1,3-C_6H_8 with no linear or oxygenated species (not shown in Figure 7.16), there is about as much reduction of C_6H_6 consumption as the predicted net rate already differs from the data curve. If 50% of the mass 80 curve is then considered to be species other than C_6H_8, the amount of change to the calculated net rate is half as much.

Over the possible range of mass 80 compositions, the net formation rate of *cyclohexadiene* by reaction with H_2 is never more than $4x10^{-13}$ mol/cm^{3}s, about 4 orders of magnitude lower than the lowest measured phenol net rate. Therefore, this reaction is very minor in the production of mass 80 — rather, it is much more a consumer — and as such the relative amount of each isomer formed in this reaction is not really relevant.

Therefore, sequential H-addition to benzene may well be the primary route of C_6H_8 formation. Other factors to consider in the formation of C_6H_8, and the effect of the H_2 elimination reaction on the benzene net rate prediction, are:

1. A considerable amount of error is likely in the mass 80 profile and curve fit, and even more for mass 79.
2. If C_6H_8 is formed by addition of a second H-atom to *hot* C_6H_7, there could be enough energy in the molecule to open up alternative pathways for C_6H_8 destruction. That is, the chemically activated branching ratios would be different from the thermalized case. More of the mass 80 signal would then be a linear product of ring opening, reducing the C_6H_6 production rate from the H_2 elimination reaction.

3. Error in the rate constants and thermochemistry (estimated with THERM).

$C_6H_8+H \rightleftharpoons H_2+C_6H_7$ - The 1,4-C_6H_8 rate constant was measured by Furukawa et al. (1974) in the reaction system H+1,4-C_6H_8, and was found to be $1x10^{12}$ cm^3/mol-sec. If the reaction has the same activation energy as the 1,3 case measured by Benson and Shaw (1967b), then $k_{1,4} = 8.58x10^{14}exp(-4000/RT)$. Dean (1990) estimated the rate constant for the similar reaction $H+C_5H_6 \rightleftharpoons H_2+C_5H_5$ to be $4x10^{13}exp(-3000/RT)$. Table 7.8 shows the maximum net production of cyclohexadienyl from 1,4- and 1,3-cyclohexadiene for these rate constants, given different

Table 7.8 Maximum cyclohexadienyl radical formation rates from $C_6H_8+H \rightleftharpoons H_2+C_6H_7$, for various rate constants and assumptions regarding mass 80. $x_{C6H7} = 0.025*x_{80,\ as\ C6H8}$.

% mass 80 = 1,4-C_6H_8 (remainder is 1,3-C_6H_8)	Max $R_{est\ 1,4}$ Furukawa	Max $R_{est\ 1,4}$ Dean, C_5H_6+H	Max $R_{est\ 1,3}$ Benson and Shaw
0	(goes backward)	(goes backward)	$3x10^{-9}$
25	$7x10^{-8}$	$5x10^{-9}$	$2x10^{-9}$
50	$1x10^{-7}$	$1x10^{-8}$	$2x10^{-9}$
75	$2x10^{-7}$	$1x10^{-8}$	$8x10^{-10}$
100	$3x10^{-8}$	$2x10^{-8}$	(goes backward)

amounts of the mass 80 signal assigned to 1,4-C_6H_8. All of the rates are roughly constant at the maximum in the range 2-3 mm. Note that the maximum net rate of phenyl formation is only $4x10^{-9}$ mol/cm^3s.

The Furukawa et al. rate is quite high. They give the ratio of rate constants for 1,4 to 1,3 as about 7:1 at 296 K. However, using their value of $1x10^{12}$ for the 1,4 reaction, the ratio to Benson and Shaw's 1,3 rate constant is 91:1. The ratio of the cyclopentadiene-based rate constant to Benson and Shaw's is 22:1. It would therefore seem that there may be some inconsistencies in the Furukawa et al. work. For example, in that study they begin with a large excess of hydrocarbon, yet they do not consider any reactions between hydrocarbon radicals and the feedstock olefin.

Even using the C_5H_6 analog rate constant instead of Furukawa et al.'s, and granting the fact that this estimate assumes no linear C_6H_8 or C_5H_4O, this reaction is probably responsible for significant conversion from C_6H_8 back to C_6H_7.

$C_6H_7+H \rightleftharpoons H_2+C_6H_6$ (Rxn B'8) - Furukawa et al. (1974), in their system at 3.5-22 torr

and 296 K, calculate that the ratio of "disproportionation" to addition (to 1,3 and 1,4 combined) rate constants is 1.8:1. This of course is only for the single temperature of measurement, but it shows another possible pathway back to benzene, from cyclohexadiene.

Louw and Lucas (1973) give $1x10^{13}$ cm^3/mol-s as an estimate for this rate constant. Reactions such as $H+C_2H_3 \rightleftharpoons H_2+C_2H_2$ and $H+CHO \rightleftharpoons H_2+CO$, which proceed via a chemically activated adduct, have rate constants which are similar to the Louw and Lucas estimate. For those reactions, $k = 1.2x10^{13}$ and $9x10^{12}$ cm^3/mol-s. Using the Louw and Lucas value for abstraction and the RRKM prediction for addition at 3.5-22 torr, $\frac{k_{disprop}}{k_{addn}}$ at 296 K is $\sim 1x10^{13}/(9.8x10^{13}*(1+0.5)) = 0.07$, rather than 1.8. Abstraction would have to be $2.6x10^{14}$ cm^3/mol-s to produce the Furukawa et al. ratio. As mentioned above, there are other discrepancies with respect to the Furukawa et al. study.

In the present flame and including the reverse reaction, the ratio of this reaction (Louw and Lucas rate constant) to addition is ≤ 0.15 until 2.5 mm, both consuming cyclohexadienyl. In the range 2.5-3 mm, they are the same order of magnitude, about $4x10^{-10}$ mol/cm^3s. Above 3 mm abstraction destroys C_6H_7, whereas C_6H_8 decomposes back. However, decomposition is much faster. Apparently then, this pathway is at most secondary, and best characterized in most places in this flame as a minor pathway.

$C_6H_-+H_2 \rightleftharpoons C_6H_9$ - Louw et al. (1984) estimate the activation energy of this reaction to be 20 kcal/mol, based on the reaction cyclopentenyl+H_2 = cyclopentyl. If the A-factor is the same as for H_2 plus benzene, the maximum rate is extremely small, about $2x10^{-12}$ mol/cm^3s. Even if a looser A' = A·10^2 = $5x10^{13}$ cm^3/mol-s is used, the maximum rate is still small at $2x10^{-10}$ mol/cm^3s.

$2C_6H_6 \rightleftharpoons C_6H_5+C_6H_-$ (Rxn -B'9) - This is another Louw and Lucas (1973) rate constant, estimated at log k = 14.5-84/θ, or the reverse at 10^{12} cm^3/mol-s. The contribution of this reaction is insignificant to all species involved.

$CH_3+C_5H_5 \rightleftharpoons C_6H_-+H$ - The rate constant for this reaction was estimated by Dean (1990). He does not give a high-pressure limit value, only the results of a QRRK computation for 0.58 atm. Using the published rate constant as is, the maximum cyclohexadienyl production rate from this reaction is small, only $4.5x10^{-9}$ mol/cm^3-s.

Net rates of preliminary submechanism.

To check for internal consistency between the above set of reactions and the mole fraction profiles of C_6H_7 and C_6H_8, the net rates of those species as predicted by the preliminary submechanism were examined. Both cyclohexadienyl radical and cyclohexadiene are correctly predicted to be formed in the first two millimeters of the flame. However, the maximum predicted formation rate of C_6H_7 is more than ten times that of C_6H_8, in contrast to the assumption that $x_{C6H7,max} < x_{C6H8,max}$. Also, at least 80% of the mass 80 signal would have to be linear species or C_5H_4O for the cyclohexadiene destruction rate from 2-6 mm to be about equal to the production rate close to the burner. Otherwise, destruction would be far greater. As the amount of the 1,4 isomer of C_6H_8 is assumed to increase relative to 1,3-C_6H_8, more consumption is predicted.

7.7 Sensitivity Analysis

The following analysis applies to the reactions involved in the submechanisms for C_6H_6, C_6H_5OH, C_6H_5, C_6H_5O, C_6H_7 and C_6H_8, and their contributions to the predicted net rates of those species.

Mole fraction assumptions and rationale.

O - assumptions and rationale are given in Chapter 6.

HO_2, H_2O_2 - assumptions and rationale are given in Chapter 6.

C_4H_5, CH_2=CCH=CH_2, C_4H_6, CH_2=CHCH=CH, CH_2=CHC=CH_2, C_5H_5, C_5H_6 - entire signal for appropriate mass number, calibrated as the isomer in question for the reaction. Signals were measured for species of these mass numbers, but the particular isomers were not positively identified. As it is possible that the signal for a particular species *could* be entirely due to the proposed isomer, the reaction was tested under this assumption. In some cases, while the identity was not known for certain, the most probable isomer was the one in question.

As a test of the sensitivity of the results to this assumption, the mole fractions were set in turn to 0.0 throughout the flame. There was no significant effect on any rate involving the species in question.

C_6H- - 0.025*(mass 80 signal, calibrated as 1,3-C_6H_8). As discussed in Section 7.6 the magnitude, shape and positioning of the profiles for masses 80-85 are consistent with sequential addition of H atom to benzene. In order for this to be the case, a C_6H_7 profile of approximately the same location and form as both benzene and mass 80 is needed. Both species look

approximately the same, so mass 80 was chosen as a model. This is also consistent with the early production and early disappearance predicted by reaction 6 (or 6'). The magnitude assigned was half the amount that would begin to predict significant production of benzene from 1.5-2.5 mm. That level was also within the range of concentrations that were consistent with the lack of a signal above that expected for C_6H_5D.

1,3- and 1,4-C_6H_8 - one half of mass 80 signal each, calibrated as 1,3-C_6H_8 (except where otherwise specified). No information was available on the distribution of mass 80. While this was the default assumption for these species, other (limiting) cases were also studied. These are discussed in Section 7.6.

C_6H_5O - Gaussian shape, same position and height relative to phenol as found for $\phi = 1.8$ C_6H_6 flame, in Hausmann et al.(1992): $x/x_{phenol} = 6.5 \times 10^{-4}$, peak at 6.5 mm, width at half height 1.3 mm. This is the only phenoxy profile measured for a rich benzene flame. It was related to the C_6H_5OH profile because of their close relationship through $H+C_6H_5O \rightleftharpoons C_6H_5OH$.

$C_6H_5CH_2$ - 3.2×10^{-6} throughout flame. Upper limit estimate for benzyl.

$C_6H_5CH_3$ - 7.1×10^{-6} throughout flame. Upper limit estimate for toluene.

HCO, C_2H_3, C_3H_2, C_3H_3, C_3H_4, C_3H_4P, HC=CHC≡CH, C_4H_4, C_6H_4, l-C_6H_5, C_6H_6D ($HC{\equiv}CCH_2CH_2C{\equiv}CH$), C_6H_6F (fulvene), C_6H_4OH, C_6H_6OH, C_6H_6OH, $HOC_6H_4CH_3$, $C_6H_4O_2$, $C_6H_5O_2$, C_6H_5CO, C_8H_8, $C_{12}H_{10}$ - 0.0 throughout flame. These species were all found to be below the detection limit, hence the mole fractions were set to 0.0. For isomers of important species already measured (e.g., l-C_6H_6), steady-state analyses were performed to estimate mole fractions, as discussed in sections above. For other species, the sensitivity of the results to the $x_i = 0.0$ assumption was tested by setting in turn the mole fraction of each species to the approximate detection limit (7.0×10^{-7}) throughout the flame. Several reactions were significantly affected by the changes; these are given below.

Sensitivity to species below detection limit.

Although for the purposes of rate calculations the mole fractions of these species were set to 0.0 throughout the flame, the sensitivity to this assumption was examined by computing the rates with a flat mole fraction profile set at 7×10^{-7}, the estimated detection limit. Six reactions were altered greatly enough by this change to require further study:

$$C_6H_5CO \rightleftharpoons C_6H_5+CO \qquad \text{(Ph5)}$$

$$C_6H_5 \rightleftharpoons C_2H_2+HC{=}CHC{\equiv}CH \quad \text{(Ph13)}$$

$$C_6H_5+O_2 \rightleftharpoons C_6H_5O_2 \quad \text{(5)}$$

$$C_6H_5OH+OH \rightleftharpoons C_6H_4OH+H_2O \quad \text{(PhOH13)}$$

$$C_6H_5OH+H \rightleftharpoons C_6H_4OH+H_2 \quad \text{(PhOH'1)}$$

$$C_6H_5O+CH_3 \rightleftharpoons C_7H_8O \quad \text{(PhO2)}$$

$C_6H_5CO \rightleftharpoons C_6H_5+CO$ - With a detection-limit profile for C_6H_5CO this reaction in the high-pressure limit would cause an enormous production of phenyl radical, with a broad peak from 7 mm to 12 mm. Substitution of a fabricated Gaussian-shaped profile sharpens the predicted phenyl formation peak and moves it to the range 3-7 mm, depending on the location of the assumed x_{C6H5CO} peak. In the EBG model solution the mole fraction peak is only $1.6x10^{-8}$, located at 0.8 mm. With a similar artificial profile the reaction would still result in a formation peak, at 3.4 mm, that is $3x10^3$ times the maximum measured net formation rate and 13 times that of the ZM model.

After an RRKM calculation to account for the unimolecular pressure effect, this behavior is no longer predicted. With a flat C_6H_5CO profile at the detection limit, the formation rate prediction of the revised model is only increased to the point where it looks similar to the ZM net rate, except for the destruction spike near the burner from $C_6H_5O_2$ production. Use of an artificial profile with a peak mole fraction of $7x10^{-7}$ results in no improvement if the maximum is located at 3.5 mm or higher. At lower heights the improvement is no better than a return to the $x_{C6H5CO} = 0.0$ profile. With a benzoyl profile like that predicted by the EBG model, there is also only an imperceptible change from the original case. There is no change to the conclusion that further improvements are needed in the phenyl network.

$C_6H_5 \rightleftharpoons C_2H_2+HC{=}CHC{\equiv}CH$ - Reaction Ph13 is the direct decomposition pathway for phenyl. With the rate constant for this reaction, setting $x_{n\text{-}C4H3}$ to $7x10^{-7}$ causes the C_6H_5 formation rate in the first millimeter from the burner to become enormous ($1x10^{-3}$-$2x10^8$ mol/cm^{3}s!). The same behavior is observed for this reaction in the rich C_6H_6 flame of Bittner, using a measured mole fraction of C_4H_3. Therefore, the problem is not due to the flat profile assumption. If the thermochemistry for i-C_4H_3 were substituted for that of n-C_4H_3, substitution of the detection limit profile would cause no significant change in the reaction. Therefore, the Sandia thermochemistry was tested by replacement with values estimated by thermochemical kinetics

(THERM, Ritter and Bozzelli, 1990). Only a slight improvement was seen. In the temperature range of the problem region, falloff would not be extensive enough to improve the situation much. This pathway for phenyl was shown in Chapter 2 to take place indirectly, via l-C_6H_5, rather than directly as in Ph13. The unrealistically high phenyl production rate predicted in the present and rich C_6H_6 flames reinforces the conclusion that a direct decomposition pathway is not occurring.

$C_6H_5+O_2 \rightleftharpoons C_6H_5O_2$ - Substitution of the detection-limit profile for $C_6H_5O_2$ results in an increase in predicted phenyl formation rate at about 3 mm, to the point where it is 60% higher than the ZM prediction. If a Gaussian-shaped profile with a peak at 1 mm (where the $C_6H_5O_2$ formation spike occurs in the C_6H_5 net rate prediction) is used instead, that increase is damped and the net rate is only increased in the 2-4 mm region to the level of the original maximum at 5 mm. There is no change to the conclusion that further work is needed for the phenyl network.

$C_6H_5OH+OH \rightleftharpoons C_6H_4OH+H_2O$ *and* $C_6H_5OH+H \rightleftharpoons C_6H_4OH+H_2$ - With a detection-limit mole fraction profile for C_6H_4OH, the revised model prediction shows only production, with a peak at 4.3 mm and another from 9-13 mm. The reaction path ratio for the entire submechanism, $\frac{R_{submech,rev.}}{R_{PhOH}}$, for production, is 26 for the earlier formation peak (which is right on the data formation peak). The reaction path ratio for the later peak is 35. (Compare to 1.6 for formation and 10 for consumption, with the mole fraction of C_6H_4OH set to 0.0.)

The only other reaction in the ZM model involving C_6H_4OH is an analogue to PhOH12, $CO+C_5H_5 \rightleftharpoons C_6H_4OH$. This reaction should proceed with about the same rate as PhOH12, which was concluded to be too slow to be of importance. Therefore, reactions PhOH13 and PhOH'1 should control the production and destruction of C_6H_4OH absent any other consumption reactions. With a flat detection-limit mole fraction profile, the net rate of C_6H_4OH would only result in production, which is not a realistic scenario for a hydrocarbon intermediate similar in structure to phenyl, phenol and benzene. A fabricated Gaussian-shaped C_6H_4OH mole fraction profile was therefore substituted for the flat one, with a peak height left at $7x10^{-7}$ and a peak location of 5.5 mm. With a full-width at half maximum of 3.6 mm the net rate predicted still was all production, but the flat production rate from 5 mm onward sharpened into a peak at 5.5-6.0 mm, which would be the expected location. With some experimentation it was found that if the amplitude of the artificial profile were one-eleventh of the detection limit, the net production and destruction

would about balance throughout the flame. In such a case, the reaction path ratios would be 2 for production and 8 for destruction. That is, there would be little change to the original prediction.

In reality, oxidation and/or other consumption reactions could help to balance production from these two reactions. Therefore, a second test was performed by varying the height of the fabricated peak up to a maximum of the detection limit. The worst prediction occurred at the detection limit, where the reaction path ratios for production and destruction were, respectively, 23 and 0.1. The best prediction was seen with an amplitude of 30% of the detection limit (only three times the balancing case), where the ratios were 4 for both production and destruction. With the Manion and Louw rate constants for reactions B6, PhOH3 and PhOH5, the ratios are 2.8 and 2.4, rather good fits to data.

The result of the sensitivity analysis for PhOH13 and PhOH'1, then, is the discovery of the potential importance of those reactions, and the mole fraction of C_6H_4OH, to the revised model. The quantity of C_6H_4OH, and its reactions, in flames are important subjects for further study.

$C_6H_5O+CH_3 \rightleftharpoons C\text{-}H_8O$ - The last reaction to be affected by the test of the zero mole fraction assumption is PhO2. With the flat detection limit profile, a large phenoxy production rate of $3.9\text{x}10^{-7}$ mol/cm^{3}s is predicted, at 9.7 mm. From the reaction set involving cresol in the ZM model, the two species in the present flame which could be precursors of C_7H_8O are phenol and phenoxy. Phenol peaks at 3.6-6.5 mm, and phenoxy is predicted to peak at 5.5-7.5 mm. An artificial mole fraction profile for C_7H_8O similar to the one used for C_6H_4OH was tested, but with a peak at 6.75 mm. The only change resulting from using that profile was the location of maximum phenoxy production predicted by the reaction, from 9.7 mm to 7.2 mm.

Two factors could reduce the possible impact of this reaction. First, the phenoxy profile used was also guessed, and could easily be higher without being detectable. A larger phenoxy mole fraction would increase the forward rate of the reaction, and result in a lower *net* rate. Also, a (needed) falloff correction for this chemical activation process would reduce the rate as well.

Sensitivity to species not positively identified. As described above, the limiting cases of $x_i = 0.0$ and x_i = {entire signal for the mass number} were tested, and no change in results was found.

Sensitivity to O atom assumptions. The result of O profile variations was studied. Three major cases are considered. In the first, the position and shape are identical to the OH profile (the default assumption); in the second, they are the same as the original ZM model prediction; in the third, they are the same as the methane profile. In the first case, the base-case magnitude was that noted at the beginning of this section; it was varied from 0 to 20 times the base magnitude. In the second case the base height is 8% of the ZM model's prediction, and in the last it was 8% of the CH_4 peak mole fraction; magnitude variations from 0.5 to 12.5 times the base case were made. Analysis of the reaction network for phenyl shows it to be totally insensitive to O atom.

The main results of having a model- or CH_4-based O profile are enhanced reactions B3 (ZM/EBG) and B20 (LS model, determined to be based on an incorrect mechanism). The two profile variations behaved the same. The effect is most pronounced with respect to phenol formation for the LS model, with the production increase proportional to the O increase. The impact on the falloff-corrected model is less than that of the original models, because agreement for C_6H_5OH production starts out in good agreement in the former case. The model-based O profile would have to be 5 times the base magnitude for the falloff formation rate to be as high as that for the uncorrected model with the default O profile. At that point, the unrevised model would predict a formation rate 25 times higher.

The benzene net rate is only affected adversely when the magnitude is twice or more that of the base case for the model- and CH_4-based O profile. Then, there is significantly increased destruction below about 4 mm, except for the original ZM model prediction. With the OH-based profile for O atom, the magnitude would have to be increased more than 20 times the base case in order for there to be significant degradation of the fit of model to data, occurring principally from 1-5 mm. Even with the magnitude set to the height of the model-predicted O profile, though, the fit is reasonable in light of uncertainties in the rate constants and measurements.

The model-based profile variation is probably not a reasonable one in light of the problems seen with the width of the H_2-O_2 reaction zone (see Chapter 6) and O data from other flames. Even using that profile, or the CH_4-based one, the revised model performs better than the original.

Sensitivity to phenyl profile. Peak height variations for two cases were examined, the

original profile and an artificial Gaussian-shaped profile. The fabricated profile had a width at half-height of 2.9 mm, and the peak was put at the same location in the flame where the ZM model predicted it to be (4.5 mm). The magnitude was varied from 0 to 5 times the original, which was taken as the maximum of the measured profile in both cases.

The sensitivity analysis for changes in the peak height of the measured profile will be described first. This variation has only a small effect overall on the C_6H_6 net rate profile, until the phenyl magnitude is about 3 times the original. The primary effect is to cause a formation hump in the first 2.5 mm, because of reaction B1, which is slightly more pronounced for the revised submechanism. The effect is quite strong at 5 times the original height. The uncertainty in the extrapolation of the B1 rate constant to low temperatures (see Section 7.2) could be responsible for this situation. Similar results occur with respect to the phenyl net rate itself, except of course that net destruction instead of formation is enhanced near the burner. The reaction of phenyl with O_2 is also increased, resulting in even more consumption, particularly for the pathways added in this work. The variations caused no change to the phenol predictions, and little change to phenoxy as well.

With a fabricated C_6H_5 mole fraction profile, the revised benzene submodel predictions were quite tolerant to peak height increases, with only about 20% decrease in the main net consumption region. The original models do not fare so well. With an increase of about 3 times the original magnitude or more, a crimp is seen in the predicted net rate at about 3.3-4.3 mm. At the greatest x_{C6H5} increase, the wave goes so far as to become a net production, for the ZM model. Naturally, the effect is mirrored in the phenyl net rate prediction. For R_{ph} predictions of the original models, a large increase in phenyl mole fraction causes a net destruction peak to occur from about 3-6 mm, the region where maximum production would be expected for consistency with the mole fraction profile. For the falloff-corrected prediction a smaller increase in assumed phenyl mole fraction produces the same effect . Phenol and phenoxy were insensitive to the variations.

In summary, with either C_6H_5 profile, a height increase of more than a factor of three or more was needed to cause problems with the benzene prediction, and then not in the main reaction zone except for the fabricated profile with the unaltered models. The submechanism revisions proposed here are less affected by variations than the originals in most cases. Therefore, the conclusions drawn in this chapter are relatively insensitive to error in the phenyl

measurement. The large spike at 1 mm caused by the formation of $C_6H_5O_2$ is the only feature to argue in favor of a phenyl peak being farther from the burner, if not a second look at the rate constant.

Sensitivity to thermochemistry of phenoxy radical.

To examine the sensitivity of results to the phenoxy heat of formation, calculations were performed with a second modified Sandia thermochemistry set where the Burcat et al. (1985) values for phenoxy were replaced with BAC-MP4 computations. Benzene predictions were unaffected. The revised phenol and phenoxy submechanisms are unchanged, but the destruction rates predicted by the original models increase by a factor of about 2.5. The increase is due to reactions B3 and PhOH3. No effect was observed on phenyl.

Sensitivity to smoothing of C_6H_5OH profile. In the case of a species with a noisy mole fraction profile, such as C_6H_5OH, several choices are possible for a smoothed curve which can be drawn through the data points. The net rate derived from that curve is dependent on the choice made. Of the species compared to model submechanisms here, the phenol and phenyl curves are sufficiently noisy that the net rate could be strongly affected by the smoothing curve. Since the phenyl profile is not relied upon for its accuracy in this work, only the C_6H_5OH mole fraction profile was tested.

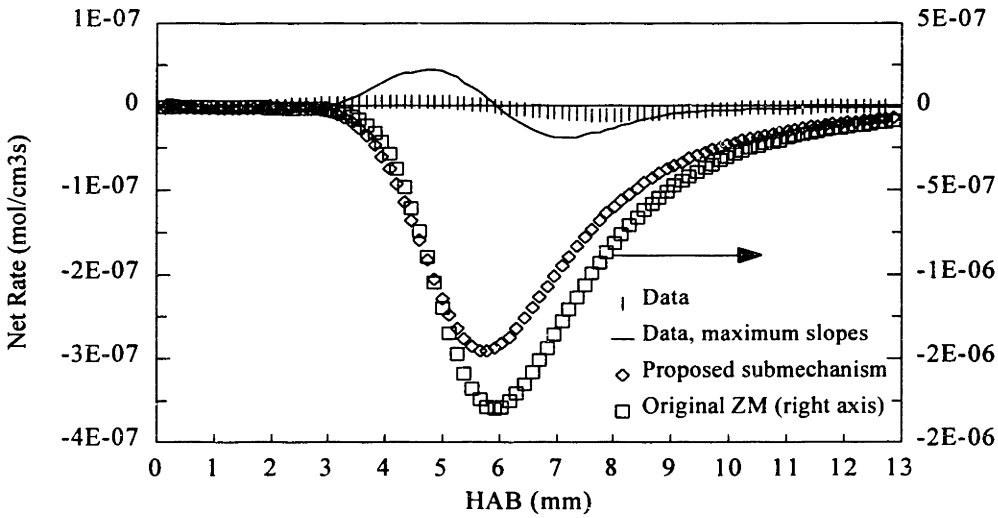

Figure 7.17 C_6H_5OH net rates, original and as derived from a smoothing curve with maximum slopes. Shown as well are the predictions of the revised phenol submechanism derived in this thesis and the original ZM submechanism.

The alternate, maximum-slope smoothing shown in Figure 4.48 was used to derive a net rate, which is shown in Figure 7.17 along with the net rate from optimum smoothing. Also plotted are the predictions of the original ZM phenol submechanism and the improved submechanism derived here, in both cases using the alternate phenol profile. The model and data net destruction rates are about 35% closer than before, but formation disappears. It is not impossible to imagine, though, that the optimum smoothing curve could be slightly modified to incorporate a greater slope from 6 mm onward, and still look good with respect to the data. This would increase the destruction rate and have no effect on production. In any event, the revised phenol submechanism is still acceptable within the range of slopes one would encounter in fitting the data to a smoothed curve.

Sensitivity to temperature profile. The temperature profile is subject to error in two primary ways: magnitude, and alignment with respect to mole fractions. Both of these features were varied within the expected maximum limits, and the resulting effect on the model predictions was gauged. To test alignment, the profile was shifted forward and back with respect to the burner, by 0.5 mm. To account for magnitude error, the profile was multiplied by 0.948 and 1.052, which in both cases resulted in a maximum difference of 100 K from the original profile. The modified temperature profiles were used as the basis for recalculating both the model predictions and data net rates of C_6H_6, C_6H_5OH and C_6H_5.

Table 7.9 Effect of temperature profile variations on conclusions of C_6H_6, C_6H_5OH and C_6H_5 net rate analyses. "No change" means the relative merits of the original and revised submechanisms remain the same.

	C_6H_6	C_6H_5OH	C_6H_5
Shifted back	No change.	No change.	No change.
Shifted forward	No change. Hump due to $C_6H_6 \rightleftharpoons C_6H_5+H$ near burner is a bit larger for revised models.	No change.	No change. $C_6H_5+O_2$ spike is even more pronounced.
Increased	No change. *All* unrevised models now greatly overpredict destruction in main reaction zone.	No change. Destruction more overpredicted; original models change more for the worse than the revised.	No change. Production more overpredicted; original models change more for the worse than the revised.
Decreased	No change. LS prediction's fulvene hump is gone.	No change. Unrevised models improve some, but are still less accurate.	Original and revised mechanisms perform about the same now.

Table 7.9 summarizes the effects of varying the temperature profile in these different ways. While certain specific features of the original and modified submechanism calculations may change, in no case was there a reversal of the conclusion that the modifications made here result in significant improvement. Therefore, errors in the temperature profile are not significant with respect to the overall results of this work.

7.8 Tests in Rich C_6H_6-O_2-Ar Flame

The revisions and falloff corrections developed in this chapter for benzene, phenyl and phenol were tested by modifying and running a revised version of the ZM model. The conditions of the $\phi = 1.8$, C_6H_6-O_2-Ar flame of Bittner (1981) were used because of their excellent predictions of H, OH and O_2. The ZM model was chosen as a base model because it is optimized for falloff to the greatest degree.

Based on the above mechanistic analysis, two reactions were removed from the original model, PhOH12 and Ph6. Reaction Ph13 was modified to reflect a pathway which proceeds via an excited linear C_6H_5 intermediate. A number of other reactions were added. The reactions in Table 7.10 were present in the original model, but the rate constants required modification. Those listed in Table 7.11 are new to the ZM model, though a couple of them appeared in the LS model. As with benzene decyclization, unimolecular benzyne decyclization (from the LS model) was included at the high-pressure limit because the reaction as written is not elementary. Inclusion of benzyne chemistry, with and without unimolecular decyclization, resulted in very little difference in the mole fraction solutions of the species examined here. Reaction networks for C_6H_7 and C_6H_8 were also included in the revised model, though they should be considered quite preliminary.

Figure 7.18 shows the results of the computations for C_6H_6. The original and revised model mole fraction predictions are equally good at predicting the benzene data. On the other hand, in Figure 7.19 one can see that the unrevised model — especially with modified Sandia thermochemistry — appears to do a much better job of describing phenol chemistry. The same is true of C_6H_5O, although *all* of the predictions are two or more orders of magnitude high. The ZM model predicts the phenyl mole fraction to be about 7 times data, and the revised model 4 times data. Benzyne chemistry does affect the phenyl profile; without it, the proposed model would be about equivalent to the ZM model. H atom and OH are accurate with both models.

Table 7.10 Revisions to the ZM model, for testing in rich benzene flame: replacement rate constants. Suitable for 22 torr and H_2-O_2-Ar flame bath gas environment.

Reaction	A	n	E_a	Comments
$C_6H_6=C_6H_5+H$	4.18E+60	-13.008	132988	Baulch et al. (1992), RRKM
$OH+C_6H_6=C_6H_5+H_2O$	2.11E+13	0	4571	Madronich & Felder (1985) — newest
$OH+C_6H_6=C_6H_5OH+H$	8.94E+19	-2.027	13310	He et al. (1988), QRRK
$OH+C_6H_5OH=H_2O+C_6H_5O$	1.39E+08	1.43	-962	This work
$OH+C_6H_5OH=H_2O+C_6H_4OH$	1.41E+13	0	4571	This work
$O+C_6H_6=C_6H_5O+H$	2.40E+13	0	4668	Ko et al. (1991)
$C_2H_2+CH_2CHCHCH=C_6H_6+H$	1.90E+07	1.47	4910	Westmoreland et al. (1989) QRRK 20 torr
$C_6H_5=l\text{-}C_6H_5$	7.22E+29	-5.762	72258	Westmoreland (1986), Westmoreland et al. (1989), QRRK
$C_6H_5=HCCHCCH+C_2H_2$	4.31E+73	-16.563	136003	Westmoreland (1986), Westmoreland et al. (1989), QRRK
$C_6H_5+O_2=C_6H_5O+O$	1.91E+37	-6.779	22070	Yu and Lin (1994), QRRK
$C_6H_5CH_2+HO_2=C_6H_5+CH_2O+OH$	5.00E+12	0	0	Hippler et al. (1991)
$C_6H_5OH=H+C_6H_5O$	5.65E+47	-9.765	98847	He et al. (1988), RRKM

Table 7.11 Revisions to the ZM model, for testing in rich benzene flame: reactions added to model. Suitable for 22 torr and H_2-O_2-Ar flame bath gas environment.

Reaction	A	n	E_a	Comments
$C_6H_6=C_6H_6D$	5.00E+11	0	47769	Lindstedt and Skevis (1994) model
$C_6H_6+O=C_6H_5+OH$	2.00E+13	0	14694	Lindstedt and Skevis (1994) model
$C_6H_5=c\text{-}C_6H_4+H$	3.00E+13	0	8894	Lindstedt and Skevis (1994) model
$C_6H_5+H=c\text{-}C_6H_4+H_2$	1.50E+14	0	0	Lindstedt and Skevis (1994) model
$C_6H_5+O=c\text{-}C_6H_4+OH$	2.00E+13	0	0	Lindstedt and Skevis (1994) model
$C_6H_5+OH=c\text{-}C_6H_4+H_2O$	2.00E+13	0	0	Lindstedt and Skevis (1994) model
$c\text{-}C_6H_4=l\text{-}C6H4$	1.00E+12	0	32978	Lindstedt and Skevis (1994) model
$C_6H_5+HO_2=C_6H_5O+OH$	5.00E+13	0	1000	Lindstedt and Skevis (1994) model
$C_6H_5+O=C_5H_5+CO$	1.00E+14	0	0	Frank et al, 25th Symp
$C_6H_6F=C_6H_6$	9.84E+37	-7.401	76979	Gaynor et al. (1981), RRKM
$C_6H_5+CH_4=C_6H_6+CH_3$	7.94E+11	0.00	11099	Duncan and Trotman-Dickenson (1962)
$OH+C_6H_6=C_6H_6OH$	9.33E+17	-3.475	6430	Witte et al. (1986), QRRK
$H+C_6H_5OH=H_2+C_6H_4OH$	1.67E+14	0	16000	This work
$C_6H_5=l\text{-}C_6H_4+H$	1.07E+58	-12.342	118977	Westmoreland (1986), Westmoreland et al. (1989), QRRK
$C_6H_5+C_2H_2=C_8H_6+H$	3.69E+30	-4.99	20927	Yu, Lin, and Melius (1994), RRKM 20 torr
$C_6H_813=C_6H_6+H_2$	4.39E+37	-7.257	71949	Orchard and Thrush (1974), RRKM
$C_6H_814=C_6H_6+H_2$	1.28E+28	-4.941	49309	Ellis and Frey (1966), RRKM
$C_6H_7=C_6H_6+H$	6.64E+46	-11.137	34478	Tsang (1986), RRKM
$CH_2CHCHCH+C_2H_2=C_6H_7$	1.96E+19	-3.35	4910	Westmoreland et al. (1989) QRRK 20 torr
$C_6H_813=C_6H_7+H$	2.42E+59	-13.316	96147	This work, RRKM

$C_6H_814=C_6H_7+H$	1.21E+59	-13.316	96147	This work, RRKM
$CH_3+C_5H_5=C_6H_7+H$	2.44E+41	-7.989	39259	Dean (1990) QRRK 0.58 atm
$C_6H_813+O_2=C_6H_7+HO_2$	8.13E+11	0	24840	Mulder (1987) thesis
$2C_6H_7=C_6H_813+C_6H_6$	2.82E+13	0	0	Tsang (1986), 425K (assumed 0.67 is 1,3)
$2C_6H_7=C_6H_814+C_6H_6$	1.39E+13	0	0	Tsang, 425K (assumed 0.67 is 1,3)
$C_6H_814+H=C_6H_7+H_2$	4.000E+13	0	3000	Same as Dean (1990) CPD+H=CPD.+H2 (=est)
$C_6H_7+H=C_6H_6+H_2$	1.00E+13	0	0	Louw and Lucas (1973)
$C_6H_7+C_6H_5=2C_6H_6$	1.00E+12	0	0	Louw and Lucas (1973)
$C_2H_3+CH_2CHCHCH=C_6H_813$	5.50E+15	-1.67	1470	Westmoreland et al. QRRK 20 torr
$C_2H_3+C_4H_6=C_6H_813+H$	1.14E+12	-0.24	9920	Westmoreland et al. QRRK 20 torr (half to 13, 14)
$C_2H_3+C_4H_6=C_6H_814+H$	1.14E+12	-0.24	9920	Westmoreland et al. QRRK 20 torr (half to 13, 14)
$C_4H_6+C_2H_2=C_6H_814$	2.30E+12	0	35000	Westmoreland et al. k_∞

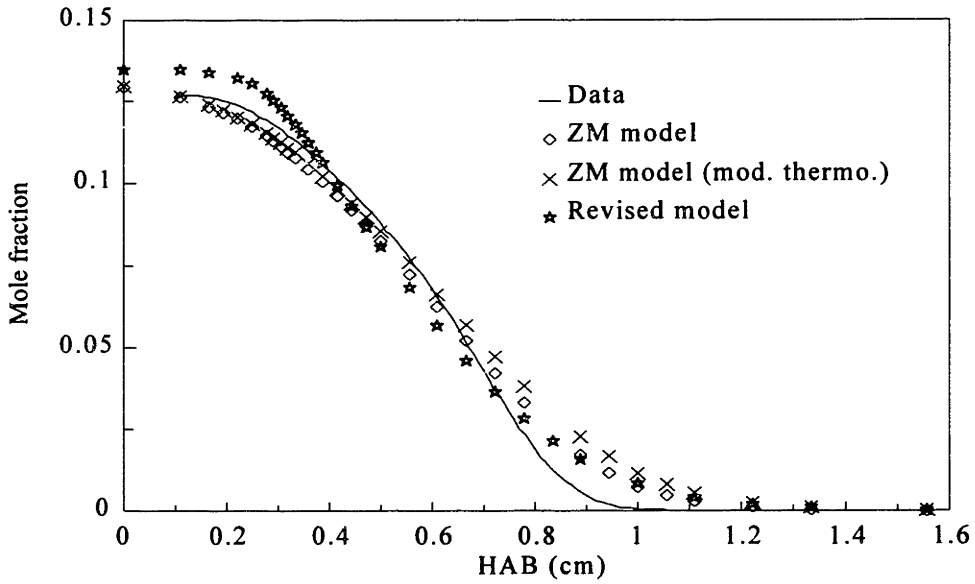

Figure 7.18 Measurement and calculations of C_6H_6 mole fraction in rich C_6H_6-O_2-Ar flame. Revised ZM model (modified Sandia thermochemistry) and original ZM model predictions (both thermochemical sets) are compared.

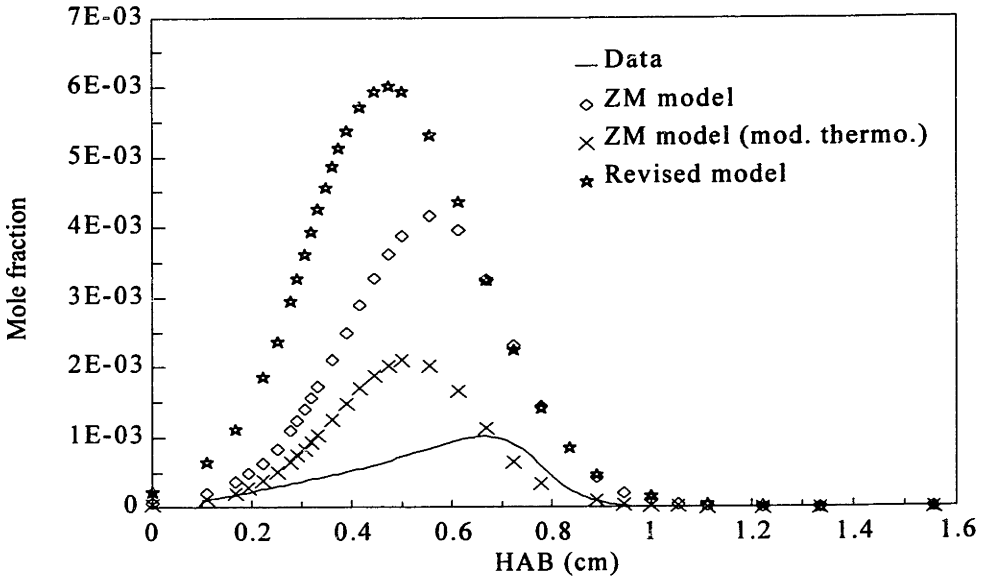

Figure 7.19 Measurement and calculations of C_6H_5OH mole fraction in rich C_6H_6-O_2-Ar flame. Revised ZM model (modified Sandia thermochemistry) and original ZM model predictions (both thermochemical sets) are compared.

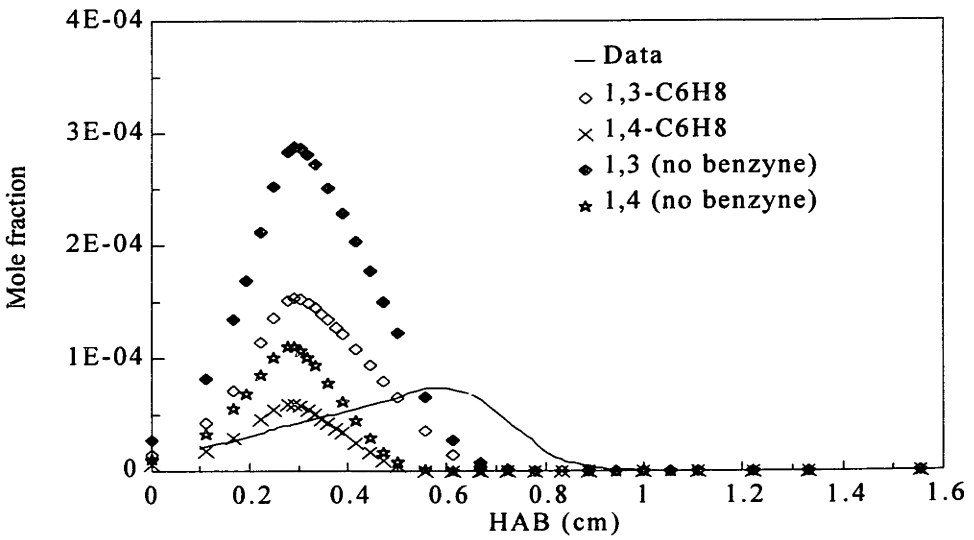

Figure 7.20 Measurement and calculations of C_6H_8 mole fractions in rich C_6H_6-O_2-Ar flame. Revised ZM model (modified Sandia thermochemistry) predictions are compared to data.

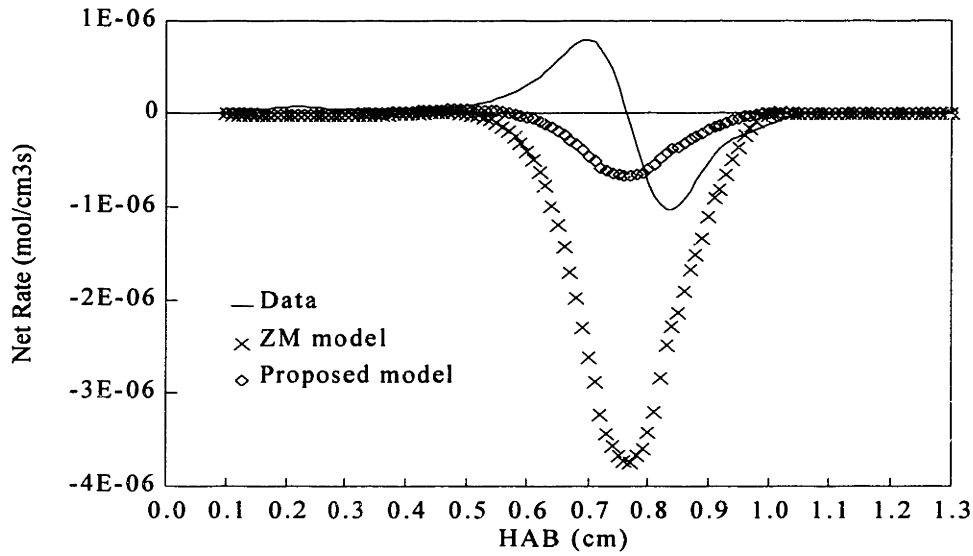

Figure 7.21 Measurement and calculations of C_6H_5OH in rich C_6H_6-O_2-Ar flame. Original and revised ZM model predictions (modified Sandia thermochemistry for both) are compared to data.

Only the revised version contained C_6H_8 reactions; the predictions are shown in Figure 7.20 to be good for a preliminary cyclohexadiene reaction network. The presence of benzyne chemistry improves the magnitude of the prediction from 6 times data to a factor of 3, because of its impact on the H atom profile in first few millimeters of the flame where C_6H_8 is formed. While there are no data to compare with the cyclohexadienyl radical prediction, it should be noted that the model prediction for C_6H_7 never goes above 2% of the isotopic contribution of benzene to mass 79. This is consistent with Bittner's inability to detect the species after subtraction of the isotopic contribution.

On the surface it would appear that the original ZM model "outperforms" the version proposed here, in regard to phenol and phenoxy. It must be understood, however, that the chemistries of C_6H_6, C_6H_5, C_6H_5O and C_6H_5OH are so interrelated that a model which predicts one or two, but not all, of them well is probably modeling the relationships between the species poorly. In particular, a MM reaction path analysis shows that phenol production is predicted to be dominated by the phenoxy mole fraction through reaction PhOH3. Since the C_6H_5O mole fraction is badly predicted, the C_6H_5OH mole fraction should be as well — yet the ZM model does reasonably well with phenol, especially when experimentally-based thermochemistry is used.

Because of this, even in the rich benzene flame where *most* important species are

accurately computed, an inaccurate mole fraction can lead to the impression that a reaction subnetwork is good. A more revealing way of studying the model is net rate analysis with measured mole fractions (MD analysis). This is shown for phenol in Figure 7.21, where it is seen with the more accurate data mole fractions that the revised subnetwork is indeed an improvement over the original. For several mass numbers, the ZM model had more than one isomer but the species was not specifically identified by Bittner. In those cases, the measured mole fraction was divided equally among the several species listed by Zhang and McKinnon. The phenoxy profile used was that of Hausmann et al. (1992). The O atom profile was an extrapolation of Table 8-2 of Bittner (1981).

According to the MD calculation, reaction -PhOH3 is responsible for the majority of the phenol destruction net rate prediction, as was the case for the H_2-O_2-C_6H_6 flame. Unlike the latter case, destruction is not overpredicted. Nevertheless, a high-temperature measurement of PhOH3 would be helpful to ensure that extrapolation is not causing significant error.

In Section 7.4 the high uncertainty in the C_6H_5 profile in the hydrogen flame raised some questions about the true level of performance of the phenyl submechanism. The phenyl reaction network can be tested in the rich benzene flame as well, and Figure 7.22 shows that the original and revised models still overpredict the net rate, by a factor of about 30. The off-scale

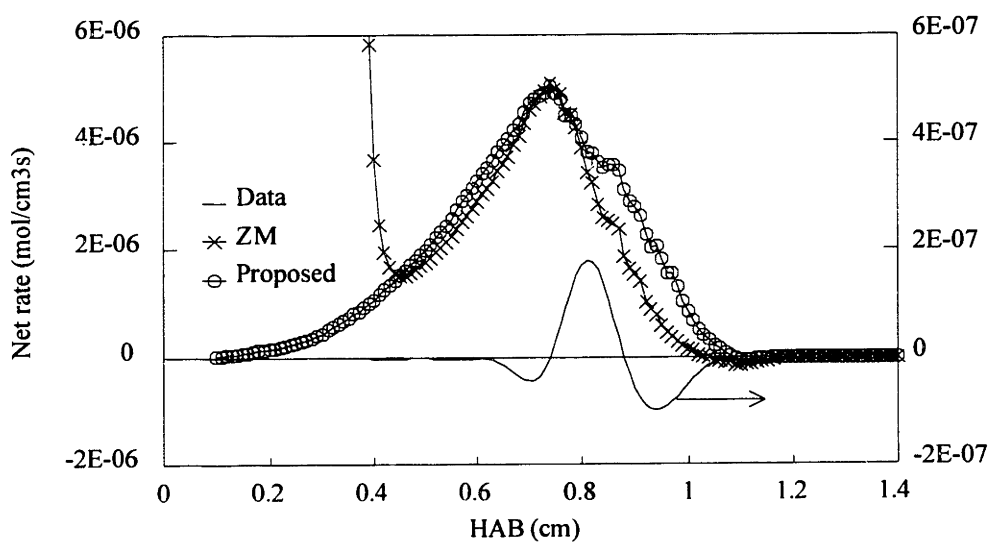

Figure 7.22 Measurement and calculations of C_6H_5 net rate in rich C_6H_6-O_2-Ar flame. Original and revised ZM model predictions (modified Sandia thermochemistry for both) are compared to data.

production rate of the ZM below 0.4 cm is caused by the low-temperature behavior of the reverse of the concerted dissociation pathway, -Ph13, discussed above in the sensitivity section. As in the present flame, the two reactions contributing most to phenyl formation are abstraction from benzene by H and OH.

The large overprediction seen with both mechanisms confirms the original C_6H_5 sub-mechanism evaluation.

7.9 Summary

Benzene destruction chemistry.

1. The currently-accepted submechanisms for C_6H_6 destruction do an excellent job of predicting the rate of benzene decomposition in a $\phi = 1.79$, H_2-O_2-C_6H_6-Ar flame. For uni-molecular decompositions and chemically activated reactions, pressure effects must be accounted for to achieve the best results.

2. Despite the accuracy of the benzene destruction mechanisms in hydrogen and benzene flames, no adequate destruction mechanism exists for large amounts of phenyl produced by the models. Therefore the possibility that agreement with data is fortuitous, and that a different mechanism which does not involve as much phenyl production is operative, is not ruled out. No such alternative reactions are currently proposed in the literature at this time.

3. The new reactions proposed by LS, in particular isomerization to fulvene and addition of H atom to form cyclohexadienyl, belong in the benzene submechanism — but only if corrected for falloff.

Phenol chemistry.

1. Subnetworks involving phenol in current models are less accurate than those for benzene.

2. The reaction of $O+C_6H_6$ to various products seems to be most in question. While the overall rate of benzene disappearance is well-documented, channels and branching ratios vary among the several modeling groups. The evidence points to $H+C_6H_5O$ as the primary products, with other channels being relatively insignificant.

3. Other important changes needed are elimination of the unimolecular decomposition of phenol to $CO+C_5H_6$, and accounting for falloff in the recombination of $H+C_6H_5O$ to phenol.

4. The C_6H_5OH submechanism with these changes is quite a bit better at predicting the net rate, in both the present H_2-O_2 flame and the rich benzene flame studied by Bittner.

5. Reactions involving C_6H_4OH are potentially important to the phenol submechanism, and merit further work.

Phenyl chemistry.

1. The chemistry of C_6H_5 is closely knit to that of benzene. Current phenyl submechanisms do not provide an adequate "outlet" for all of the C_6H_5 formed from C_6H_6 via reactions B1, B2 and B4.

2. This situation is true for both the present flame and the rich C_6H_6-O_2-Ar flame of Bittner. In neither case can existing C_6H_5 chemistry explain the low mole fractions and low net rates experimentally observed.

3. Accounting for falloff and duplicative or incorrect reaction channels cannot resolve the discrepancy.

4. In the model predictions of the present flame the benzene mole fraction is not adversely affected by the overprediction of x_{C6H5} because errors in the H/O and phenyl chemistries interact in a compensatory fashion.

5. One feature of the measured C_6H_5 curve that is particularly perplexing is the location of the peak early in the reaction zone. Even if this aspect of the mole fraction profile conformed more to expectations, the conclusions regarding phenyl chemistry listed above would still hold.

Phenoxy chemistry.

1. In spite of being undetectable (or just at the detection limit) in the present experiment, the models predict phenoxy to be produced in quantities comparable to C_6H_6. It is formed primarily by unimolecular decomposition of phenol, and secondarily from $O+C_6H_6$ and other reactions.

2. Some adjustments were made to account for falloff, including the most important formation reaction. The improvement was small.

3. Assuming its formation chemistry to be reasonably accuracte, phenoxy destruction chemistry would be the source of the discrepancy.

Chemistry of C_6H_7 and C_6H_8.

1. Inclusion of H atom addition to benzene is important for opening up a pathway to

more hydrogenated cyclic C_6 species. Only one of the current models has this reaction.

2. Without considering chemical activation, this reaction wreaks havoc on C_6H_6 destruction chemistry in the H_2-O_2 flame environment.

3. A preliminary C_6H_7-C_6H_8 mechanism was developed, including corrections for pressure effects. The results were tested for Bittner's rich benzene flame, and are promising.

4. Knowing the relative amounts of 1,3 and 1,4 isomers of C_6H_8 is important, as the chemistries of the two differ.

Specific mechanism changes made:

1. *Falloff calculations performed or revised* - Reactions B1, B3, B6, B19, B20, B23, PhOH3, Ph1, Ph5 and Ph7/Ph14.

2. *Redundant reactions removed* - Ph6, Ph13 (as a concerted reaction).

3. *Inappropriate pathway reactions removed* - B20[38], PhOH12.

4. *Inappropriate rate constant source corrected* - PhOH3 (ZM, LS models).

5. *Misinterpretation of literature rate constant corrected* - Ph13, PhOH4 and PhOH13.

Other conclusions.

1. Analysis of aromatics chemistry supports the conclusion that judging the performance of a kinetic model solely on the basis of the quality of its mole fraction predictions can be misleading. Net rate analysis, using measured mole fractions for input to the reaction submechanism (MD), is more direct and accurate. The advantage derives from the fact that in MD analysis errors in prediction of the net rate of chemical reaction for a species cannot propagate into the mole fractions used to calculate reaction rates.

2. Another unique feature of net rate analysis is that the *direction* in which the subnetwork needs to be mended (i.e., more consumption or formation) can often be determined.

3. The fact that a species has a low mole fraction, or may even be undetectable, does not mean that that it is unimportant. In the present flame, C_6H_5 and C_6H_5O have such profiles, yet are crucial to the chemistries of benzene and phenol.

4. A sensitivity analysis was performed to assess possible negative effects of assumptions made in the net rate analyses. For the most part, conclusions were shown to be insensitive

[38] Further study of this reaction could result in it being placed back in the mechanism, albeit at a much smaller rate.

to those assumptions within reasonable limits. Areas where conclusions were less strong were pointed out.

5. Sensitivity analysis was also shown to be helpful in learning more about certain reactions and their possible effects on predicted net rates. For example, through this medium: (a) the unlikelihood of a direct concerted destruction pathway for phenyl was reinforced, (b) the need for falloff computations for reactions Ph5 and PhO2 was discovered, and (c) the possibility that the reverse of reactions PhOH13 and PhOH'1 could be important to C_6H_5OH chemistry was recognized.

Chapter 8: Conclusions and Recommendations.

Temperature and mole fraction data for fourty-four species were collected in a 22 torr, $\phi = 1.79$, $(x_{C6H6}/x_{H2})_0 = 0.01$, $v_0 = 101$ cm/sec, H_2-O_2-C_6H_6-Ar flame, using the molecular-beam mass spectometry ("MBMS") technique. The data and analysis presented here are unique contributions to combustion chemistry, in the areas of aromatics destruction and H_2-O_2 flames.

Three literature models were reviewed by comparisons of mole fraction predictions and predicted net rates to data. Those models are: Emdee et al. (1992) ("EBG"), Lindstedt and Skevis (1994) ("LS"), and Zhang and McKinnon (1995) ("ZM"). Some analysis of the model of Jackson and Laurendeau (1987) ("JL") was also performed. In addition to the H_2-O_2 submechanisms of these four models, the mole fraction predictions of Miller et al. (1982) and Warnatz (1984) (as modified by Westmoreland, 1986) were tested.

8.1 Conclusions

The most important conclusions from this work are presented below. Secondary findings may also be found in the summaries presented in Chapters 5, 6 and 7.

8.1.1 Experimental Methods

An improved thermocouple coating technique has been developed and tested, for protection against catalytic heating in low pressure flames (Shandross et al., 1991). Modification of the shape of the support wires was also implemented to reduce heat conduction to the junction wire. A preliminary test showed a reduction in measured temperature in the region of highest gradient.

Regarding species identification techniques in MBMS systems, a noted discrepancy (Bittner, 1981) in experimental values of the ionization potential for benzene has been explained as being a consequence of fine structure in the ionization efficiency curve. The type of behavior causing the discrepancy may be common to aromatic species. Methods of determining ionization potentials which are more accurate than the thermal electron impact method used here are needed.

Calibration of stable species for MBMS experiments in H_2-O_2 flames was found to be considerably more complicated, because mass discrimination factors are a function of the flame temperature (or burner chamber density, in the cold gas experiment) and the gas composition. A second order approximation method which accounts for both effects was developed, from measurements of the factors for two gas compositions and a range of flame temperatures.

The Relative Ionization Cross-Section ("RICS") calibration method, for species which cannot be directly calibrated, is reviewed in Chapter 3. It is pointed out that the best type of electron impact ionization cross-sections to be used are those for single ionization, at the electron energy of the measurement. Some cross-section data of this sort are available, for H, O and H_2O. Low energy total cross-sections are also available for H_2 and certain other species. When using the best available cross-sections, H_2-O_2 partial equilibria are better met in the post-flame zone. This is also true for the stoichiometric benzene flame of Bittner (1981). Both of these observations support the use of more appropriate cross-section information in RICS calibrations.

Species which could not be identified in the present flame were calibrated and reported as though they were a particular assumed molecule. Calibration conversion factors were worked out for readjustment of mole fraction profiles to change from one assumption to another. Some help in species identification could be found by using a fragmentation magnitude analysis method developed here.

An extensive data reduction program was written to compute fluxes, net rates and reaction path analyses. The program is compatible with the CHEMKIN interpreter, and output from the PREMIX flat flame reactor code.

8.1.2 Data and Model Analysis Methods

The study of H/O and aromatics chemistries performed in this work supports the conclusion that judging the performance of a kinetic model solely on the basis of the quality of its mole fraction predictions can be misleading. Net rate analysis, when measured mole fractions are used for input to the reaction submechanism (the model-data, or "MD" method), is more direct and accurate. The advantage derives from the fact that in MD analysis errors in prediction of the net rate of chemical reaction for a species do not propagate into the mole fractions used to calculate total reaction rates. Another important feature of MD net rate analysis is that the *direction* in which the subnetwork needs to be mended (e.g., more consumption) can often be determined.

This type of net rate analysis was pioneered by Cole (1982), Cole et al. (1984a,b), Westmoreland (1986), and Westmoreland et al. (1989), and has been extended here to include predictions of entire model subnetworks involving a specified species.

In the more traditional form of rate or reaction path analysis, the rates of individual reactions computed in a model simulation when it solves for mole fractions are studied, independent of measured net rates. These individual reaction rates are calculated with model rate constants and model mole fractions, and so the method is referred to here as model-model ("MM") analysis. Although the MM method can yield some useful insights into the workings of a reaction mechanism, incorrect conclusions can be drawn from it, as examples presented in Chapters 6 and 7 demonstrate.

Differences between MD results and model predictions revealed that species (O, C_6H_5 and C_6H_5O in particular in the present flame) whose mole fractions are small, or even undetectable, can have extremely important roles as intermediates. For example, because of the significant error in the consumption chemistry of these species, the models overpredict their mole fractions. As a result, the reverse rate of crucial reactions is greatly increased, and the predictions of other species such as O_2, benzene and phenol are negatively affected.

8.1.3 H/O Chemistry

The following reactions from the H_2-O_2 system were found to be partially equlibrated at 28.5 mm:

$$H_2+OH \rightleftharpoons H+H_2O \quad (1)$$

$$H+O_2 \rightleftharpoons OH+O \quad (3)$$

When H and OH are recalibrated so that partial equilibrium ratios K/K_{eq} are equal to 1.0, a steady-state estimate of O atom at 28.5 mm agrees better with the measurement made there. Therefore, partial equilibrium calibration is probably more accurate than the RICS method.

While H_2-O_2 models have been found by others to perform well at temperatures below 1500 K, in the present flame (T_{max} = 1937 K) the burnout zone is predicted to be half the width seen experimentally, and radical mole fractions — particularly O atom — are severely overpredicted. There is some evidence of this behavior in other high-temperature experiments reported in the literature.

The problems are due in part to an imbalance in the rate constants of reactions (1)-(3),

$$O+H_2 \rightleftharpoons OH+H \quad (2)$$

which are responsible for the entire production and consumption rate predictions of H, OH, O, O_2, H_2, and H_2O. Reactions (1) and (3) predict equal and opposite quantities of H and OH to be produced/consumed. Since the measured net rates are not mirror images of each other, to achieve net rate predictions which agree even remotely with data, the rates of reactions (1) and (3) must be balanced so that the net result is small H and OH rates, on the order of the rate of reaction (2). Because of the directions in which these reactions run, with H produced in (1) being consumed by (3) and with OH produced in (3) being consumed in (1), this can be achieved without much trouble by adjustments in k_1 and k_3 that are within the literature limits of error. The accepted values of the two rate constants were independently found to be consistent with the H_2, H_2O and O_2 net rate measurements as well.

This picture, while resulting in more satisfactory net rate fits for other species, leaves a prediction of O atom production rate which is very much higher than data would support. Such a high rate is also inconsistent with the balance described above, in the sense that a mole fraction profile which would result from so much O atom formation would throw off the predictions of H and OH. A slowdown of reactions (1)-(3) could solve most of the problems, but this is ruled out for two reasons. First, k_1 and k_3 are well-studied rate constants. Secondly, the other way to have slower reactions, assumption that the temperature profile was in error from catalytic heating and appropriate modifications, causes the hydrocarbon chemistry to be nearly completely halted. This is a much more serious and unlikely condition than that seen without changing of the temperature profile. Therefore, the evidence points to a missing high-temperature pathway (or pathways) for O consumption.

From comparisons of model predictions to data published by others, it appears that the burnout rate error is a function of how much H/O chemistry is occurring relative to other types. The problem with overprediction of radical magnitudes seems to depend on the complexity of the chemistry (that is, the size of the reaction set), perhaps because of compensation of errors or the relative lack of importance of H/O reactions. Since there are few reported high-temperature H_2-O_2 flame measurements, the problem has gone unnoticed by many.

In summary, except for fine tuning of k_1 and k_3, the results support the literature values of three major H/O reactions, within their limits of error and those of the data. Such adjustment is crucial mainly in high-temperature situations. O atom chemistry was identified as a second

probable source of error at high temperatures; specifically, some heretofore unidentified consumption pathway appears to be missing from the reaction set.

8.1.4 General Hydrocarbons Chemistry

Unlike for H/O species predictions, mole fraction predictions for hydrocarbons agree well with the observed reaction (burnout) zone. However, the models need improvement with regard to their balance of more- to less-hydrogenated species. Furthermore, many species present in the flame, such as those with molecular weights of 67-69 and 80-86, are not even considered in the model reaction sets. The LS model did the best overall job of predicting hydrocarbon chemistry.

8.1.5 Benzene Destruction Chemistry

The chemistry of benzene and related aromatics was studied by (1) applying net rate analysis to the overall predictions of the various submechanisms of the three models under review, and (2) examining the MD reaction path contributions of various reactions, both before and after any modifications found to be necessary. Five types of changes were made to individual rate constants:

- falloff corrections,
- removal of redundant reactions[39],
- removal of reactions for incorrect pathways,
- correction of inappropriately assigned rate constants, and
- other corrections or reinterpretations of rate constants.

Most of the rate constants found in the literature for oxidation reactions have only been measured experimentally at low and intermediate temperatures. Few have been measured above 1000 K and even fewer still above 1400 K. Some of the inaccuracy of the model predictions remaining after these corrections were made could be due to extrapolation of oxidation rate constants above their measured temperature range.

Benzene and phenyl radical.

[39] "Redundant reactions" are those for which two (or more) different pathways are used to describe the same reaction. The several rate constants are approximately equal, but only one of the pathways is a true description of the elemental reaction that is occurring.

The mechanisms for C_6H_6 destruction tested here were shown to do an excellent job of predicting the rate of benzene decomposition. Certain reactions only seen in the LS model, in particular isomerization to fulvene and addition of H atom to form cyclohexadienyl, belong in the benzene submechanism — but only if corrected for falloff. Accounting for the pressure effects of unimolecular decompositions and chemically activated reactions was generally found to be necessary to achieve the best agreement of model net rate predictions with data.

Despite the accuracy of the benzene mechanisms in hydrogen and benzene flames, no adequate destruction mechanism exists for large amounts of phenyl produced by the model reaction network. Therefore the possibility is not excluded that agreement with C_6H_6 data is fortuitous, and that a different mechanism which does not involve as much phenyl production is operative. However, no such alternative reactions could be found at this time.

The chemistry of C_6H_5 was found to be closely knit to that of benzene, via reactions B1, B2 and B4[40]:

$$C_6H_5+H \rightleftharpoons C_6H_6 \quad \text{(B1)}$$

$$C_6H_6+OH \rightleftharpoons C_6H_5+H_2O \quad \text{(B2)}$$

$$C_6H_6+H \rightleftharpoons C_6H_5+H_2 \quad \text{(B4)}$$

Current phenyl submechanisms do not provide an adequate "outlet" for all of the C_6H_5 formed from C_6H_6 via these reactions. This situation was found to be true for both the present flame and the rich C_6H_6-O_2-Ar flame of Bittner (1981): existing C_6H_5 chemistry could not explain the low mole fractions and low net rates experimentally observed. Neither falloff corrections nor consideration of duplicative or incorrect reaction channels (all of which are discussed in detail in Chapter 7) were found to be adequate to bring production and consumption into the proper balance.

That benzene chemistry is not adversely affected by the overprediction of x_{C6H5} in the model solution of H_2-O_2-C_6H_6 mole fractions appears to be due to good fortune. The excessive H and OH mole fractions predicted by the H/O chemistry drive reactions B2 and B4 to a much-increased level of benzene consumption. Instead of reducing the benzene destruction level to below acceptable levels, or creating net benzene production, the exaggerated rate of recombination

[40] Those three reactions also account for almost the entire benzene net rate prediction in the present flame. Interestingly, B1 and B4, which are reduction reactions, have been measured at high temperatures.

by reaction B1 due to increased phenyl serves to balance the overpredicted consumption rate. The net result is a reasonable net reaction rate for benzene. In the rich C_6H_6-O_2-Ar flame, the net result of excessive phenyl is lowering of the benzene consumption rate, because recombination of C_6H_5 with H is predicted. However, the contribution of reaction B1 is not great compared to the other two reactions, which are themselves driven forward to the extent that the overprediction of phenyl makes only a small difference. Benzene destruction via -B3, which is overpredicted because O atom is too large, compensates for the production from B1 as well.

One other feature of the measured C_6H_5 curve that cannot be explained by the models is the location of the peak early in the reaction zone. The mole fraction profile data for this species were among the most noisy collected, and care was taken to avoid contribution from benzene fragmentation. However, a later peak would be more consistent with data taken in a rich benzene flame (Bittner, 1981), and production via benzene. Nevertheless, even if this aspect of the mole fraction profile conformed more to expectations, other conclusions regarding phenyl chemistry would still hold.

Phenol and phenoxy radical.

Subnetworks involving phenol in the models reviewed were found to be less accurate than those for benzene, though considerably better than the phenyl chemistry.

Of the benzene destruction reactions in the literature, that of $O+C_6H_6$ to various products seems to be most in question. While the overall rate of benzene disappearance by this reaction is well-documented, channels and branching ratios vary among the several modeling groups. The evidence points to $H+C_6H_5O$ as the primary products, with other channels being relatively insignificant. The assignment by Lindstedt and Skevis of phenol as the only product of $O+C_6H_6$ is therefore incorrect.

The unimolecular decomposition of phenol to $CO+C_5H_6$, found in the ZM model, was determined to be another inappropriate pathway. Also, accounting for falloff in the reaction

$$H+C_6H_5O \rightleftharpoons C_6H_5OH \qquad \text{(PhOH3)}$$

was shown to improve the reaction network.

The C_6H_5OH submechanism with these changes is much better at predicting the net rate, in both the present H_2-O_2 flame and the rich benzene flame studied by Bittner. Even so, destruction is still quite a bit overpredicted in the main part of the reaction zone. This is probably due in

part to the extrapolation of the rate constants of reaction PhOH3, PhOH4 and PhOH'1 above 1200 K.

A lack of knowledge of the true mole fraction of C_6H_4OH is an important uncertainty in assessing the quality of the fit of the improved model to data. The concentration of this species cannot be determined from the data, as mass 93 was determined to be just at the detection limit and phenoxy is also be present at that peak. Assumed mole fraction profiles of Gaussian shape with heights from 9% to 100% of the detection limit would result variously in improvement, partial improvement or worsening of the predicted net rate. The worst case of overprediction is a factor of 23, compared with 70-100 for the original models.

While phenoxy radical is undetectable (or just at the detection limit) in the present experiment, the models predict it to be produced in quantities comparable to C_6H_6. It is formed primarily by unimolecular decomposition of phenol, and secondarily from $O+C_6H_6$ and other reactions. Some adjustments were made to account for falloff, including the most important formation reaction; little improvement was seen. Assuming the predicted formation rate to be reasonably accurate, phenoxy destruction chemistry would be the source of the error.

C_6H_7 and C_6H_8.

It was determined that H atom addition to benzene should be included in models which will be applied to flames high in H, because it opens up a pathway to more hydrogenated cyclic C_6 species. Only one of the current models (LS) has this reaction. Without consideration of chemical activation, though, this reaction causes the C_6H_6 prediction to deviate strongly from data in the preheat and early reaction zones of the H_2-O_2 flame environment. With a proper falloff correction this was seen not to occur.

A preliminary C_6H_7-C_6H_8 mechanism was developed, including corrections for pressure effects. The submechanism was tested for Bittner's rich benzene flame, resulting in a C_6H_8 mole fraction prediction which is several times the measurements and about 3 mm early in the flame. The presence of benzyne chemistry improves the magnitude of the prediction from 6 times data to a factor of 3, because of its impact on the H atom profile in first few millimeters of the flame where C_6H_8 is formed. The results are encouraging, but the mechanism requires further work.

In summary, benzene and phenol chemistry are the most accurate of the aromatic species, after corrections for falloff, redundant and inappropriate pathways, and assignments of rate

constants. Phenyl and phenoxy radical chemistries have been identified as problem areas. In rich flames, H addition to benzene and subsequent further additions — all with falloff corrections — should be present.

Based on the above conclusions, a significantly improved benzene destruction mechanism has been proposed, suitable the H_2-O_2-Ar flame environment at 22 torr, in Tables 7.10 and 7.11. As implied in the above discussion, the revised mechanism could benefit from further work. Recommendations for improvement are given later in this chapter.

8.1.6 Other Conclusions

Sensitivity analysis was shown to be helpful in learning more about reactions in which one or more species is below the detection limit, and the possible effects of those reactions on predicted net rates. For example, through this medium: (a) the unlikelihood of a direct concerted destruction pathway for phenyl was reinforced, (b) the need for falloff calculations for reactions Ph5 and PhO2 was discovered, and (c) the possibility that reactions

$$C_6H_5OH+OH \rightleftharpoons C_6H_4OH+H_2O \qquad \text{(PhOH13)}$$

$$C_6H_5OH+H \rightleftharpoons C_6H_4OH+H_2 \qquad \text{(PhOH'1)}$$

could improve C_6H_5OH chemistry was recognized.

8.2 Recommendations for Future Work

8.2.1 Experimental Recommendations

1. Further tests of the modified thermocouple shape should be performed to verify the preliminary indication that it reduces conduction heating effects.

2. Improvements in species determinations by ionization efficiency curves should be implemented. Several possible methods are:

- use of an ionizer with monoenergetic electrons, or photo/chemi-ionization,
- use of an ionizer with a quasi-monoenergetic electron distribution, such as the retarding potential difference ionizer of Fox et al. (1955), and

- application of an analytical interpretation technique for simulating monoenergetic distributions, such as the energy-distribution difference method[41] of Winters et al. (1966).

3. Help in identification of unknown species in MBMS experiments can be obtained in some cases with the well-planned use of the fragmentation magnitude analysis technique developed here.

4. The existing database of electron impact ionization cross-sections should be expanded with measurements of more species important to combustion experiments. These cross-sections should be for single positive ionization, rather than total ionization and fragmentation, and should be measured at energies from the ionization potential to about 30 eV. If possible, more combustion-related radicals should be measured.

8.2.2 H/O Chemistry

1. The few high-temperature experiments found in the literature in which H/O chemistry was predominant show behavior consistent with that seen in the present flame. There are few such data overall, however, and all of the temperature measurements for those flame were made with thermocouples. Because of the disagreements of models with data, further study of high-temperature H_2-O_2 flames *per se* is warranted. A complete set of laminar, premixed flame mole fraction profiles should be obtained, the radicals preferably measured by several types of instruments (e.g., MBMS and laser-induced fluorescence ["LIF"]) so that the results of one technique can be verified by the other. Temperature measurements should not be performed with thermocouples (or thermocouples alone) so that data from a method in which there is no possibility of catalytic heating interference will be added to those already collected. Experiments with several flame conditions, from lean to rich, would provide a more comprehensive set of results with which to probe the flame chemistry.

2. Further experiments on individual reactions at high temperatures might reveal some insights into the mechanistic problems observed here. Specific areas requiring attention are O atom consumption chemistry, and more accurate values of k_1-k_3 above 1500 K.

[41] This technique requires an ionizer with good (say, 0.05 or 0.1 eV) and reproducible energy resolution.

8.2.3 General Hydrocarbon Chemistry

To develop models which are more applicable to rich flame, reaction sets should be improved with respect to hydrogen addition reactions. Chemical species resulting from multiple additions should be included.

8.2.4 Benzene Destruction Chemistry

1. The additive technique used here was shown to be very useful for the study of aromatics with non-hydrocarbon oxidants and reducing agents. Measurements of benzene additive in lean (and perhaps stoichiometric) H_2-O_2 flames could yield further insights into the remaining problematic areas of C_6H_6 destruction chemistry. In particular, the $O+C_6H_6$ reaction and the fate of phenoxy radical might be studied with a very lean flame. The high-temperature chemistries of toluene, styrene, vinylbenzene, chlorobenzene, or other aromatics could be fruitfully investigated with this technique.

2. Quantitative work on H addition reactions to c-C_6H_7 and other cyclic C_6's — including addition to already vibrationally hot species — would help to clarify the role of this reduction pathway in benzene destruction. It would also be important to the development of models applicable to flames with high levels of H atom. Direct measurment of c-C_6H_7 (and possibly $C_5H_4CH_3$ and $C_5H_4CH_2$) in flames would help in this regard. Also, microprobe sampling to determine the relative amounts of 1,3 and 1,4 isomers of C_6H_8 would be needed, as the chemistries of the two differ.

3. The rate constant of the benzene decyclization reaction (B18) should be measured experimentally so that it might be properly included in pyrolysis research and work in rich flames. Should the reaction be found to be potentially important under some combustion conditions of interest, falloff parameters should be determined as well.

4. Phenyl and phenoxy radical chemistries should be studied further, especially destruction reactions and especially to temperatures as high as 2000 K. Studies of individual reactions, and/or other additive-flame experiments, could be used. Alternative radical measurement techniques, such as the molecular-beam scavenging method of Hausmann et al. (1992), are needed to support MBMS measurements of critical radical species, and any discrepancies between them

should be resolved. In any event, a sampling and analysis system with high sensitivity and low signal/noise are needed to measure these important low-level transient species.

5. Should the early appearance of phenyl radical in the present or similar flames be verified by independent measurements, the chemistry of $C_6H_5O_2$ would merit further study because of the large amounts predicted to be formed at low temperatures.

6. Reactions of phenol are also in need of further investigation, particularly to extend the current work to temperatures as high as 2000 K. For example, the postulated phenol pyrolysis reaction (PhOH12) to form $CO+C_5H_6$ — which in this work was determined not to be important at temperatures studied thus far ($T < 1175$ K) — might play a larger role in the hottest regions of a flame. The $O+C_6H_6$ reaction should also be better characterized with regard to branching ratio at various temperatures and pressures.

7. The chemistry of C_6H_4OH should be studied because of that species' potential importance to phenol destruction. Efforts should also be made to quantify the mole fraction of this species in flames with large quantities of H and OH.

8. A detection method such as LIF should be used to measure O atom in any rich hydrocarbon flame, so that quantification of the relative amounts of CH_4 and O atom can be made. With this information, better MD analyses can be performed, and the H_2-O_2 chemistry environment will be better known.

8.2.5 Other Recommendations

Tatang (1995) has recently developed a method for systematically examining of the effects of uncertainties in rate constants on a reaction network prediction. Application of this method to net rate analysis would be a useful extention of the sensitivity and error analyses developed in this thesis, in that it would determine the contribution of the model itself to the overall uncertainty.

Appendix A. Error Analysis.

Level of error.

An analysis similar to that of Bittner (1981) was performed:

1. *Sensitivities.* The limits on deviation of $S_{i,Ar}$ (mass spectrometer sensitivity) were found to be ±6% (a little conservative, but not much).

2. *Signal deviations of major stable species.* The CO_2 and C_6H_6 data sets were examined for deviation from average signal at each height above burner ("HAB"). For CO_2, an average of 5.6% deviation was found. For Ar on that date, the deviation 0.9%. For C_6H_6 it was 11% for all signals, but only 4.2% for signals above 100 counts; in that set, Ar had an average deviation of 1.2%. So, it was assumed that for a particular species being measured the deviation was 5%, and for argon, 1%.

3. *Mass discrimination factors.* Reproducibility of $\alpha_{i,Ar}$ was about 6% (10% for H_2). For the accuracy of the second order approximation of the dependence of $\alpha_{i,Ar}$ on temperature and composition (cf. Chapter 3), a factor of 25% of the total variation in α was estimated . That would be 8% for H_2, about 3% for O_2, 4.4% for CO, 5% for CH_4, and 6.5% for C_6H_6, 1.6% for C_2H_2 (est), and 4% for CO_2 (est).

The formula $(\text{reproducibility}^2 + \text{accuracy}^2)^{0.5}$ was used to account for both factors.

4. *Overall reproducibility.* Day-to-day reproducibility was estimated, perhaps conservatively, at ±15%.

H_2 suffered from greater variability, which is a common problem with that species. However, there was a significant variation between the early and (two years) later profiles: in the latter measurements, the x_{H2}/x_{Ar} varied between the order of magnitude of the early set and 2-3 times that amount. The source of the problem was not determined, but was probably due to tuning or MS (electronics or electron multiplier) factors. The profile from the early set was chosen because of the apparent general stability of the H_2 signal at that time. As was noted, variations between the early set and later sets were greater than that within the later sets, so ±30% reproducibility error is assigned to hydrogen. Incidentally, with the exception of measurements made on one date, the I_H/I_{H2} measurements stayed within ±30% as well, regardless of the variation of H_2.

5. *Total error due to component measurements.* Using Bittner's formula K-3,

$$\frac{\Delta(x_i/x_{Ar})}{x_i/x_{Ar}} = \left[\left(\frac{\Delta\alpha_{i,Ar}}{\alpha_{i,Ar}} \right)^2 + \left(\frac{\Delta S_{i,Ar}}{S_{i,Ar}} \right)^2 + \left(\frac{\Delta(I_i/I_{Ar})}{I_i/I_{Ar}} \right)^2 \right]^{1/2} \tag{A-1}$$

one gets the following estimates, exclusive of overall reproducibility considerations:

Table A.1 Error of major species mole fractions, due to deviations in components.

Species, i	% error in $S_{i,Ar}$	% error in $\alpha_{i,Ar}$	% error in I_i/I_{Ar}	Total % for x_i/x_{Ar}
C_6H_6	6	8.8	5	11.8
O_2	6	6.7	5	10.3
H_2	6	12.8	5	15
CO	6	7.5	5	10.8
CO_2	6	7.2	5	10.6
C_2H_2	6	6.2	5	10
CH_4	6	7.8	5	11

6. *Total error, including reproducibility.* Now, accounting for general reproducibility by the same square root of the sum of squares formula, one gets:

Table A.2 Error of major species mole fractions, due to deviations in components.

Species, i	Overall error for x_i/x_{Ar}, %
C_6H_6	19.1
O_2	18.2
H_2	33.5
CO	18.5
CO_2	18.4
C_2H_2	18
CH_4	18.6

That is, the general reproducibility (a function of the mass spectrometer and its electronics, in the greatest part) as currently estimated overshadows the rest of the error. In all likelihood, among major species the largest variability is limited to H_2, O_2, and CO; the latter two because of background interferences or small leaks in the calibration system.

7. *Relative ionization cross-section error, for radicals.* For the relative ionization cross-section, the previously-cited error of from 30% to a factor of two is not changed in this experiment.

8. *Partial equilibrium calibration error, for H and OH.* The radicals H and OH were re-calibrated so that the reactions

$$H_2+OH \rightleftharpoons H+H_2O \quad (1)$$

$$O+H_2 \rightleftharpoons OH+H \quad (2)$$

were equilibrated in the post-flame zone of the flame (cf. Chapter 6). To estimate the error in this form of calibration, the partial equilibrium ratio

$$\frac{K_{exp}}{K_{eq}} = \left[\frac{\Pi\left(C_i^{\upsilon_i}\right)_{products}}{\Pi\left(C_i^{\upsilon_i}\right)_{reactants}} \right] / K_{eq}, \quad (A\text{-}2)$$

which is set to 1.0 for the calibration, is used. C_i refers to concentration of species *i*, and ν_i is the stoichiometric coefficient. The mole fraction of O atom has a large limit of error because of the RICS calibration, so equation 2 is preferable for the estimate since most of the error from species other than H and OH resides in O and H_2. Since partial equilibrium of reaction 2 is assumed,

$$\frac{K_{2,exp}}{K_{2,eq}} = \frac{[H][OH]}{[O][H_2]} / K_{2,eq} = 1.0,$$

and the errors in H and OH must offset those of H_2, O and the equilibrium constant. Therefore,

$$2 \times \left(E_{peqm\ cal}\right)^2 = (E_O)^2 + (E_{H2})^2 + \left(E_{Keq}\right)^2, \quad (A\text{-}3)$$

where

$E_{peqm\ cal}$ = fractional error of partial equilibrium calibration,

E_O = fractional error of O atom,

E_{H2} = fractional error of H_2, and

E_{Keq} = fractional error of the equilibrium constant.

Tsang and Hampson (1986) note that the maximum error in equilibrium constants for species with well-known thermochemistry is 2%. However, if one assumes the temperature profile to be known within ±100 K, the error due to K_{eq} is approximately 30%. Allowing for a full factor of two deviation in O atom, $E_{peqm\ cal} = 0.5*(1^2+(0.34)^2+(0.3)^2)^{1/2} = 0.55$, that is, 55%. (Had the error in O atom been designated as a factor of two too *low*, the first term would have been $((1\text{-}0.5)/1)^2 = 0.5^2$, and the error would be estimated as 34%. The conservative figure is more likely, since the recalibration of OH to a partial equilibrium basis required a factor of 1.84.)

Meaning of the error limits to computations in this research: sensitivity analysis.

How significant this level of error is can be considered by a test in which the H_2 and O_2 profiles are modified by their limits of error: there was virtually no effect on the net rates of benzene or H atom. The effect on the net rate profile of the species being varied is fractionally equal to the change in that species.

The final item checked was the sensitivity of the net rate (benzene was used as a sample case) to variation in other parameters which could affect it:

- Temperature alignment, ± 0.4mm (the amount of the bead wake correction).
- Temperature ± 75K (ramped up/down as $\pm 10\%$ until $10\% \geq 75$K).
- Benzene profile $\pm 30\%$.
- Mixture-averages vs. multicomponent diffusivity.
- Various smoothing parameter changes.

The benzene net rate suffers little deviation from the above variations. Use of mixture-averaging the diffusion coefficients results in a positive net rate near the burner that roughly mirrors the negative hump normally seen. The most sensitivity is to the benzene profile itself, and is a simple magnitude change of the same fractional amount.

The net rates of H_2, O_2, and H were checked for the effect of variations in diffusivity type and temperature profile features. There were no significant changes, except for H_2 under mixture-averaged diffusivity. The net rate profile looks inverted below 7 mm in that case.

Appendix B. RRKM Program.

Modifications made to program FALLOFF.

Adiabatic degrees of freedom. The program as originally written by Gilbert (1983) used the original treatment of Marcus (1952) for adiabatic degrees of freedom. This formalism gives the proper centrifugal correction at high pressures, but not in the falloff region or the low-pressure limit (Robinson and Holbrook, 1972; Waage and Rabinovitch, 1970). The revised version of this program incorporates a method based on the result of Waage and Rabinovitch. They found that

$$F_w \equiv \left(\frac{I}{I^+}\right)\left(\frac{(k_0)_{ad}}{k_0}\right) = \left(\frac{I}{I^+}\right)\left[1 + \frac{\int_0^{E_a} \rho^*(E)f(E)\exp(\frac{-E}{RT})dE}{Q_2^*}\right] \qquad \text{(B-1)}$$

where:

k_0 = low-pressure limit rate coefficient (1st or 2nd order),

$(k_0)_{ad}$ = same as above, but including two adiabatic degrees of freedom,

I, I^+ = moments of inertia for molecule and activated complex, respectively,

$\rho^*(E)$ = density of states of excited reactants (counting only active modes),

$Q_2^* = \int_{E_a}^{\infty} \rho^*(E)\exp(\frac{-E}{RT})dE$ = active-mode partition function of excited reactant (as a species), relative to ground state of reactant,

E_a = activation energy, and

$f(E)$ = fraction of molecules for which the difference in rotational energy between the reactant and complex (E_J-E_J^+) is greater than E_a-E.

The RRKM integral is then identical to equation (4.38) of Robinson and Holbrook; $k_a(E)$ is calculated by equation (4.18) of the same source, without the factor $\frac{Q_1^+}{Q_1}$. This treatment is, strictly speaking, applicable to molecules with two adiabatic dimensions. There is no simple way of rigorously applying it to the three-dimensional adiabatic rotations allowable in FALLOFF. For example, simply applying the correction factor of 3/2 to E_J, as Marcus (1965 and 1970) did in his calculation of $\langle E_J \rangle$, produces an incorrect result for the partition function and a result for f(E) which is identical to the two-dimensional case. The simplest three-dimensional case, that of a

spherical top, is easy to evaluate if $\frac{h^2}{8\pi^2 IRT}$ is not small, but other cases are considerably harder. Rather than using an approximate three-dimensional equation, the revised program was written so that F_w is the same for either two or three dimensions, as Robinson and Holbrook seem to have done. The expression for f(E) in two dimensions is, according to Waage and Rabinovitch,

$$f(E) = \exp\left(\frac{-(E_a - E)(\eta + 1)}{\eta RT}\right) \tag{B-2}$$

where $\eta = \frac{I}{I^+} - 1$.

The equation for F_w is simple to evaluate in the framework of the program using this expression. The results are very close to the approximate formula given by Waage and Rabinovitch. The user of the program is given the option of using the Waage-Rabinovitch formalism or that of Wieder and Marcus (1962).

Collision efficiency and broadening factor. RRKM is inherently a "strong collision" method, in that only a single collision is necessary to energize or de-energize a molecule with enough energy that reaction might take place. "Weak collision" treatments, known as master equation solutions, consider energy transfer to and from all energy levels of the molecule. That is, collisions can remove (or add) a small enough amount of energy that the molecule stays energized. Because of the complexity of the master equation, uncertainty in the probability of energy transfer between states, and lack of adequate knowledge about the amount of energy transfer for various combinations of molecules, many workers have striven to provide simpler solutions for unimolecular reactions which are neither strictly strong collision nor weak collision. These hybrid formalisms are essentially modified strong collision approximations. The most popular is perhaps that of Troe (1979 and 1983), in which the falloff equation is written with a modified Lindemann (1922) switching function:

$$k = \frac{k_\infty k_0[M]F}{k_\infty + k_0[M]} = k_\infty\left(\frac{P_r}{1 + P_r}\right)F \; ; \; P_r \equiv \frac{k_0[M]}{k\infty} \tag{B-3}$$

Here, P_r is defined as the reduced pressure to show the pressure dependence explicitly. F is a "broadening factor" made up of two parts, $F = F^{SC}F^{WC}$.

The first part, F^{SC}, is a strong collision broadening factor meant to account for spread, or broadening, of the falloff curve because of the energy dependence of the decomposition rate constant. Application of $F = F^{SC}$ to the switching function should result in a solution (approximately) equal to that achieved with an RRKM calculation. Troe (1983) gives an empirical

equation for F^{SC} as a function of P_r and modified versions of the RRK parameters (Emanuel, 1972) S and B. This factor is not needed for the current program, because the calculation is done by the RRKM method itself.

The second factor is a weak collision multiplier which introduces additional broadening due to the lack of de-energization for every collision. That parameter was given an empirical form by Gilbert et al. from comparison with master equation solutions. Those expressions are a function of the collision efficiency (β_c), F_E, and the internal vibrational energy of the activated complex.

The broadening factors primarily affect the width and sharpness of the falloff region, but not the slope of the low-pressure limit. To account for weak collisions in that region, the collision frequency used in calculating k_0 is multiplied a collision efficiency β_c[42]. Troe (1977a,b) gives an approximation for the collision efficiency as

$$\frac{\beta_c}{1-\sqrt{\beta_c}} = \frac{-<\Delta E>_{all}}{F_E kT} \qquad \text{(B-4)}$$

where:

$<\Delta E>_{all}$ = average energy transferred in collisions, in both directions, and

$$F_E = \frac{\int_{E_a}^{\infty} \rho_{vib}(E)\exp\left(\frac{-E}{kT}\right)dE}{\rho_{vib}(E_a)\exp\left(\frac{-E_a}{kT}\right)kT} = \text{"energy dependence of the density of states."}$$

This approximation is widely used, but is only valid at low temperatures where certain assumptions in its derivation hold. Gilbert et al. (1983) derived a more general version of β_c, namely:

$$\beta_c = \beta_{c,Troe} \div \int_0^{E_a} \frac{\rho_{vib}(E)}{Q_{vib}} \exp\left(\frac{-E}{kT}\right)\left[1-\left(\frac{E_a}{<\Delta E>_{down}+F_E kT}\right)\exp\left(-\frac{E_a-E}{F_E kT}\right)\right] \qquad \text{(B-5)}$$

where $<\Delta E>_{down}$ is the average energy transferred in the *downward* direction, from collisions. This expression still involves approximations, in particular for the so-called "non-equilibrium factor" which is applied to calculate the actual population of states from the equilibrium population (Gilbert et al., 1983). Gilbert et al. show that for a molecule as large as C_7H_8, and with an activation energy of 50.3 kcal/mol, the formula is accurate at least up to 1900 K. The difference

[42] Many investigators modify the collision efficiency in this way, but do not apply the broadening factors. Naturally, this is a lower-level approximation than the full Troe expression.

between this collision efficiency and that of Troe began to appear at 900 K in that case, and by 1500 K was more than an order of magnitude.

In the present RRKM program, it is easy to compute the more accurate formula, since the density of states is calculated precisely. For the downward energy transfer, the Troe (1977a) relationship

$$< \Delta E >_{all} = \frac{- < \Delta E >^2_{down}}{< \Delta E >_{down} + F_E kT} \tag{B-6}$$

was solved. With this accurate collision efficiency, calculation of the weak collision broadening factor is straightforwardly performed. The program gives k_{uni} as $k_{uni,RRKM}$*F^{WC}. The result of the calculation, then, is quite close to a master equation solution.

Instructions for program usage:

Input file format:

RRKM Program Input File Format: (No spaces between lines in the input file.)
Title (up to 80 characters)
N_{max} ΔE g_{BS} #P #T #chan #atom
#freq$^+$ #freq
$E_{0,1}$ [$E_{0,2}$]
(sig$^+$/n$^+$)$_1$ [(sig$^+$/n$^+$)$_2$] sig/n
B^+_1 [B^+_2] B
#int rot$^+_1$ [#int rot$^+_2$] #int rot
B^+ sig$^+$ dim$^+$ ← rotor 1, complex 1
.
.
B^+ sig$^+$ dim$^+$ ← rotor n, complex 1
[Same as above for m rotors of complex 2.]
Same as above for k rotors of reactant
sig_{AB} mw mw_{BATH} eps/K betaflg |<ΔE>|
freq$^+$#1 degen$^+$#1 freq$^+$#2 degen$^+$#2 ... ← complex 1
As many lines as needed to get all freqs
[Freqs and degens for complex 2.]
Freqs and degens for reactant
Pressures (torr).
Temperatures (K).

Glossary of terms:

N_{max} - number of terms in the numerical integration. Refers to terms of energy ABOVE E_0, not above E=0. Each term is separated from the previous by an energy of ΔE, so the energy you are at for term n is $E = E_0 + n*\Delta E$. (To be sure you have converged the integration, increase this and see if there is a change to k_∞. 800 is a good starting value for this parameter.)

ΔE - energy increment (cm^{-1}; each cm^{-1} = 2.8572 cal) for RRKM integration, and for values of E for which $\rho(E)$ and $k_a(E)$ are computed. (A good value to use is 100 cm^{-1}, but you might need to decrease this if you can't get the numerical A factor to agree with the thermo A factor. Remember to increase N_{max} so as not to unduly lower E_{max}, if you decrease this parameter.)

g_{BS} - Beyer-Swinehart direct count algorithm grain size. Must be an integer. (A good value to start with is one between 5 and 30, being as close to an integral factor of the lowest frequency as you can get. For example, if the lowest frequency is 217 cm^{-1}, use a g_{BS} of 7, because 7 is an integral factor of 217. (217 = 7*31) The closer you are to having the frequency be an exact multiple of the grain size, the more exact is the algorithm, and the percentage error will be greatest for the smallest frequency. The array sizes in the program have been increased so that for E_0 and N_{max} not too high, g_{BS} can be as low as 1 cm^{-1}. (This normally won't be necessary, and takes extra computation time, so it isn't recommended.)

#P - number of input pressures given.

#T - number of input temperatures given.

#chan - number of reaction channels, 1 or 2.

#atom - number of atoms in reactant.

$\#freq^+$, #freq - number of *different* frequencies given for activated complex ($^+$) and reactant. Total # freqs = $\Sigma(degen_i * freq_i)$, where i = 1,2,...,#freq.

$E_{0,1}$, $[E_{0,2}]$ - critical energy for complex 1 [and complex 2]. The reaction channels must be given in order of increasing E_0. Values in the format specification given in parentheses are the values you would have to supply if you had a second rxn channel.

$(sig^+/n^+)_1$, etc. - sig = symmetry number, n = no. of optical isomers. Here is where you flag the program to run the Wieder and Marcus (1962) treatment for adiabatic rotations instead of the default Waage-Rabinovitch: to do that, make $(sig^+/n^+)_1$ negative.

B^+_1, etc. - rotational constant. Here's where the moments of inertia are input: $B = 16.7364/I_m$ (in cm^{-1}) for I in amu-angstrom^2. $B = 2.7993 \times 10^{-39}/I_m$ for I_m in g-cm^2.

The default treatment is all three external rotations being adiabatic. It's common to have the moment of inertia with respect to the rxn coordinate axis not change (but that's not necessary). If so, $I_m = (I_a I_b)^{333}$, where a and b are the axes which change. Else, use $I_m = (I_a I_b I_c)^{333}$.

If the molecule is linear or you want to consider one external mode to contribute to the reaction, make B for the molecule (not the complex(ex)) negative. The third dimension must show up as a vibration or internal rotation.

#int_rot$^+_1$, etc. - no. of internal rotations for complex(ϵ) and reactant.

B^+, sig^+, dim^+ - rotational constant, internal symmetry no., and dimension of internal rotation. Note that each internal rotation must have a dimension of one, but if you have n identical internal rots, you can group them together and give them a dim^+ value of n (up to 3). (The program can handle up to 9 theoretically, but it won't calculate the partition function of a 9-dimensional rotation properly!)

sig_{AB} - average collision diameter, reactant and bath gas. You don't need to specify if A = B because for purposes of the deactivation rate constant A* is a different species than A.

mw, mw_{BATH} - molecular wt. of reactant and bath gas.

eps/K - Lennard-Jones well depth, units of K.

betaflg, $|\langle\Delta E\rangle|$ - betaflg indicates to the program the collision efficiency calculation to do:

0 - strong collision calculation.
1 - use collision efficiency, $|\langle\Delta E\rangle|_{down}$ supplied.
2 - use collision efficiency, $|\langle\Delta E\rangle|_{all}$ supplied.

$|\langle\Delta E\rangle|$ is the average energy transfer per collision, in cm^{-1}, in the downward direction or all directions, as required. This is also a flag parameter: the default efficiency calculation is that of Gilbert, Luther and Troe (1983), but if this number is made negative, the original Troe method will be used $[beta/(1\text{-}beta^5)] = |\langle\Delta E\rangle|_{all}/[F_E k_B T]$. Putting in a negative value does not otherwise affect the calculation, only the positive (i.e., absolute value) is used.

freq$^+$#1, degen$^+$#1, etc. - list of frequencies and degeneracies. Frequencies in cm^{-1}. List looks like "1020 3 980 2 450 3 220 1"...

To avoid artificial bumps in $k_a(E)$ and $\rho(E)$, which arise in the direct count procedure if one had degenerate frequencies, the program splits degenerate frequencies into spacings of 10 cm^{-1} around the original frequency; this makes no practical difference to the computed results. If you don't wish to use this procedure, feed in degenerate frequencies as individual frequencies with the same value and degeneracy 1.

If you are being careful with g_{BS} (usually because you aren't getting agreement between the numerical and thermo-derived A factor) as discussed above, remember that there will be splitting if the lowest frequency has a degeneracy other than 1.

Source code:

```
C ***** WARNING!  FOR  BETA_C CALCULATIONS WITH MORE THAN ONE
C ***** REACTION CHANNEL, USES THE MINIMUM E0 TO CALC. BETA_C
C 460   FALL OFF PGM.  Part I:  the main program
        PROGRAM RRKM
C RRKM MULTIPLE-REACTION PROGRAM, WITH PROVISION FOR OUTPUTTING
C MICROSCOPIC RATES,K(E), AND DENSITY OF STATES, RHO(E), ONTO UNIT 10,
C SUITABLE FOR INPUT TO MASTER EQUATION PROGRAM.
C METHOD USED IS BEYER-SWINEHART ALGORITHM, WITH TROE MODIFICATION
C FOR COMPUTING EFFECTS OF FREE INTERNAL ROTORS.
C
C UPDATES:  JULY 5 1985
C         FEB 25 1987  (BY R. SHANDROSS AND J.B. HOWARD (MIT))
C1         APR 07 1987 (BY R. SNIHUR AND R. SHANDROSS (MIT))
C         APR 10 1987  (BY R. SNIHUR AND R. SHANDROSS (MIT))
C         June 1987; July 24, 1988; Aug. 30, 1988; Oct. 14, 1988:
C                         (By R. Shandross and J.B. Howard (MIT))
C         Jul 24 1988    (By R. Shandross and J.B. Howard (MIT))
C         Aug 30 1988   (By R. Shandross and J.B. Howard (MIT))
C         Feb  7 1990    (By R. Shandross and J.B. Howard (MIT))
C         Mar 10 1990   (By R. Shandross and J.B. Howard (MIT))
C         Apr  3 1990    (By R. Shandross and J.B. Howard (MIT))
C         Jan 17 1995    (By R. Shandross and J.B. oward (MIT))
C
C2 Re: Update of Apr 10, 1987
C2 Purpose: Handle dbl. precision math.  All comment lines for this update
C2        begin with "C2".
C
C3 Re: Update of ~June 1987
C3 Purpose: Allow Marcus treatment again, print part'n. fcn. ratio
C
C4 Re: Update of July 24, 1988
C4 Purpose: Readability of output, notify user which adiabatic trtmt.
C
C5 Re: Update of August 30, 1988
C5 Purpose: Implement option to use Beta_c collision efficiency, per
C5        1) J. Troe, J. Chem. Phys., 66, 4758 (1977), or
C5        2) R.G. Gilbert, K. Luther, and J. Troe, Ber. Bunsenges. Phys.
C5          Chem., 87, 169 (1983)
C5     Also, change IF...GO TO statements to IF...THEN.
C5     And, remove "float" conversions where the result would be REAL*8 by
C5   Microsoft Fortran rules anyway.
C
C ***** WARNING!  FOR  BETA_C CALCULATIONS WITH MORE THAN ONE
```

```
C ***** REACTION CHANNEL, USES THE MINIMUM E0 TO CALC. BETA_C
C
C6 Re: Update of October 14, 1988
C6 Purpose: To fix the printing of OMEGA in the output, and the
C6       Waage-Rabinovitch treatment for more than one channel.
C
C7 Re: Update of February 7, 1990
C7 Purpose: Compatibility with Definicon coprocessor, add weak collision
C7       broadening factor calculation, print both <E>dn and <E>tot,
C7       produce a less verbose output file (.SUM), write B in .MAS
C7       file, put actual <E>dn in .MAS file, change some default
C7       .MAS parameters, correct lack of initialization of g.
C
C8 Re: Update of March 10, 1990
C8 Purpose: Print Waage-Rabinovitch factor. Check for I+ < I, go to
C8       Marcus treatment if so. Change to 1962 version of Marcus
C8       treatment. Force # dimensions of adiabatic modes of
C8       complexes and reactant to all be equal.
C
C9 Re: Update of April 3, 1990
C9 Purpose: Fix bug with reduced pressure calculation. All Pred for
C9       previous calcs too high if more than one pressure calc'ed.
C9       Also, make K array double precision. Finally, set Fwr to
C9       1.0 if it should stray above that value (as I+ -> I).
C
C10  Re: Update of Dec. 31, 1990
C10  Purpose: Calculate reduced pressure even if Fwc not calc'd.
C10        Before, it was not calc'd but still printed (as -INF).
C
C11  Re: Update of Jan. 17, 1995
C11  Purpose: Fix bug with low pressure limit. Add more verbiage to
C11        output about k0 and Pred.
C
C2 FORTRAN METACOMMAND IDENTIFYING LARGE ARRAYS OF DATA
C $LARGE: T,K,RHO,RVIB,AK
C $DEBUG
C2 SET DEFAULT VARIABLE TYPES
       IMPLICIT DOUBLE PRECISION(A-H,O-Z)
       IMPLICIT INTEGER(I-N)
C9
       double precision K
C2 TO SAVE SPACE, INPUT VARIABLES READ IN FROM UNIT 5 ARE TO BE
C2 OF TYPE "REAL".
       REAL EOK,SRC,SRM,BCMPLX,BMOLEC,AM,A,SGMA,WT1
      1 ,WT2,EPS,PRESS,TEMP,BVECM,BVEC,SIGVCM,BVEC1,SIGVC1
       character ibl,fname*20,fnamei*20,fnameo*20,fnamem*20,fnames*20,
      1 title*80
       DIMENSION TITLE(20), NM(100),JM(100),RHO(2499),IEXRTD(3),NRV(3)
      1        ,NC(3,100),JC(3,100),K(3,2500),BVEC(3,10),BVECM(10),SRC(3)
      2        ,SIGVC(3,10),SIGVCM(10),PRESS(30),TEMP(30),BCMPLX(3),JF(3),EOK(3)
      3        ,N(3),RATIO(3),ALNA(3),ALNAE(3),EAC(3),RATE(3),EJ(3),A(3),NCHK(3)
```

```
     4          ,NC1(100),JC1(100),BVEC1(10),SIGVC1(10),AK(2499),KKC(3),RATTH(3)
     5          ,AKG(3),RATHP(3),EKG(3),IRTDMC(3,10),IRTDMM(10),ISPARE(10)
     6          ,CPC(3),SVC(3),SROTC(3),STC(3),STOTC(3),QROTC(3),QVC(3),STLP(3)
     7          ,BRATIO(3),ADRAT(3),FRATIO(3),fwc(3),sk(3),pred(3),prbase(3)
      LOGICAL REORD, TEST1D, CHEKSZ, BTEST(3), ADFLAG, gltflg,wrnflg
      COMMON /ROTF/GAMON2(20),/UNSC/REORD,TEST1D,gltflg
      COMMON /BS/ FRE(200),IR(200),T(50000),
     1          DELTAE,IS,M
      common /bci/ibflg,inc,ni,nintr,nf,nreact,QV,RT,IT
      common /bcr/betac,energ,fexp,fofe
      DATA NC/300*0/,JC/300*0/,NM/100*0/,JM/100*0/,IRTDMM/10*0/,
     2          BVEC/30*0./,BVECM/10*0./,IRTDMC/30*0/,
     3          SIGVC/30*0./,SIGVCM/10*0./,STC/3*0./
     4          ,H/0.333566D-10/,R/0.69550184/,WKA/349.99086/,IEXMD/3/
     5          ,IEXRTD/3*3/,FRATIO/3*0./,wrnflg/.false./
C     DATA IBL/' '/
C Some formats:
 100    FORMAT(20A4)
 155    FORMAT(20X,'Beyer-Swinehart grain size',T50,F10.2)
 156    FORMAT(' Number of atoms in rxt.',T35,I12)
 220    FORMAT(' Frequencies and degeneracies')
 211    FORMAT(1H1,10X,'RRKM calculation',/,1X,
     1          20A4,///)
 701    FORMAT(//,38X,'Molecule',T49,'Complex(es)',I2,2I15)
 212    FORMAT(' External symmetry numbers',T35,F12.3,T50,F12.3,T65,
     1          F12.3,F15.3)
 213    FORMAT(' Critical energy(kcal/mol)',T50,F12.3,T65,F12.3,F15.3)
1213    FORMAT(10X,'(kJ/mol)',T50,F12.3,T65,F12.3,F15.3)
 214    FORMAT(/,' No. of frequencies',T35,I12,T50,I12,T65,I12,I15)
 215    FORMAT(T35,2I6,T50,2I6,T65,2I6,3X,2I6)
 716    FORMAT(/,1H1,1X,20A4,/)
 715    format(/,30x,'********************',/,10X,'Temperature',
     1          T40,F6.1,' Kelvin',/)
9716    FORMAT(33X,'Channel(s)',I2,T56,I2,I8)
 717    FORMAT(' Critical energies'
     2          ,' (kcal/mol)',T36,F8.2,T51,2F8.2)
1716    FORMAT(' High pres. actvn. energy (kcal/mol)'
     4          ,T38,F7.3,T51,2F8.2)
2716    FORMAT(10X, ' (kJ/mol)',
     5          T36,F8.2,T51,2F8.2)
3716    FORMAT(' High pressure log A',T36,F8.2,T51,2F8.2)
4716    FORMAT(' High pressure rate coefficient (from numerical integ',
     1          'ration)',/,25X,'(s-1)',T34,D10.3,T50,
     1          2D10.3)
5716    FORMAT(//,' Low-pressure rate coefficient:',/,'  = lim',
     1          ' (kuni/[M]), as [M]->0',/,'    (cm3/mol-s)',T34,D10.3,T50,
     1          2D10.3)
 571    format(/,' --> Includes beta and rotational corrections',/)
 718    FORMAT(//,12X,'Rate Constant Calculation, k = k_SC * F_WC:',//,
     1          5X,'Pressure',T24,'Omega',T35,'k1',T43,'k1/k1 inf',
     2          T58,'k2',T65,'k2/k2 inf',/,6X,'(torr)',T24,'(s-1)',T33,'(s-1)')
```

```
7181    FORMAT(D12.3,T20,D10.3,T31,3(D10.3,1X,D10.3,1X))
7200    format(a80)
        ibl=' '
        REORD=.TRUE.
        DO 7281 I=1,3
                DO 7282 J=1,2500
                        K(I,J)=0.
7282            CONTINUE
7281    CONTINUE
C7 Argument reading routine, to get root of file names for input,
C7 output, master, and summary files.
        print *, 'Name for .dat, .out, .sum (summary), and .mas files: '
        read '(A)', fname
        nnnn=0
        do 324 nnn=1,len(fname)
                if(fname(nnn:nnn).eq.' ') goto 325
                nnnn=nnnn+1
324     continue
325     continue
        fnamei=fname(1:nnnn)//'.dat'
        fnameo=fname(1:nnnn)//'.out'
        fnamem=fname(1:nnnn)//'.mas'
        fnames=fname(1:nnnn)//'.sum'
        open(7,status='old',form='formatted',file=fnamei)
        open(8,status='unknown',form='formatted',file=fnameo)
        open(10,status='unknown',form='formatted',file=fnamem)
C7 Unit 11 is for summary file.
        open(11,file=fnames,status='unknown')
C Read input cards:
        READ(7,100) TITLE
        READ(7,*)NN,INC,DELTAE,NP,NT,NCHAN,NUMATM
        NCHP=MAX0(NCHAN,2)
        READ(7,*) (JF(I),I=1,NCHAN),NF
        READ(7,*) (EOK(I),I=1,NCHAN)
        READ(7,*) (SRC(I),I=1,NCHAN),SRM
        READ(7,*) (BCMPLX(I),I=1,NCHAN),BMOLEC
C3 If (sigma/n)complex1 < 0, then use Marcus treatment for adiab. rot.
        ADFLAG=SRC(1).LT.0.
        SRC(1)=ABS(SRC(1))
C  Test for 2-D adiabatic rotation.
        TEST1D=BMOLEC.LT.0.
        if(test1d) iexmd=2
        BMOLEC=ABS(BMOLEC)
        READ(7,*) (N(I),I=1,NCHAN),NINTR
        DO 8709 I=1,NCHAN
                IF(I.LE.1) GO TO 80
C  CHECK THAT CRITICAL ENERGIES ARE IN INCREASING ORDER
                IF(EOK(I).GT.EOK(I-1)) GO TO 80
                WRITE(8,81)
                write(11,81)
 81             FORMAT('  Critical energies must be in increasing order; abort')
```

```
                STOP
 80             CONTINUE
C8 Force # dim of complex(es) to be equal to that of reactant.
                IF(test1d) IEXRTD(I)=2
C8 Disallow Waage-Rabinovitch treatment if I+ < I.
                if((.not.adflag).and.(bmolec.lt.bcmplx(i))) then
                        adflag=.true.
                        wrnflg=.true.
                endif
C  Get info about rotations, if any.
                IF(N(I).gt.0)then
                        J=N(I)
                        READ(7,*) (BVEC(I,II),SIGVC(I,II),IRTDMC(I,II),II=1,J)
                endif
 8709   continue
        IF(NINTR.GT.0) READ(7,*) (BVECM(I),SIGVCM(I),IRTDMM(I),I=1,NINTR)
C5 Card 11 mod.: ibflg = flag for beta_c calc., energ = <E>dn or |<E>tot|.
C5 ibflg=0, then DON'T use beta_c; =1, then <E>down supplied; =2, <E>total
C5 supplied.  Default is Gilbert, et al. treatment; but if energ<0, then
C5 original Troe treatment is used. (|energ| is always used in calcs.)
        READ(7,*) SGMA,WT1,WT2,EPS,ibflg,energ
        DO 8710 IN=1,NCHAN
                JF1=JF(IN)
                READ(7,*) (NC(IN,I),JC(IN,I),I=1,JF1)
 8710   CONTINUE
        READ(7,*)  (NM(I),JM(I),I=1,NF)
        READ(7,*)  (PRESS(I),I=1,NP)
        READ(7,*)  (TEMP(I),I=1,NT)
C  Parrot back input info. into output file.
        WRITE(8,211) TITLE
        WRITE(11,211) TITLE
 5010 FORMAT(//,20X,'Number of terms in integration',T55,I5,
       1        /,20X,'Energy spacing (cm-1)',T50,I10)
        WRITE(8,701) (I,I=1,NCHAN)
        WRITE(8,212) SRM, (SRC(I),I=1,NCHAN)
        WRITE(8,218) BMOLEC,(BCMPLX(I),I=1,NCHAN)
        WRITE(11,701) (I,I=1,NCHAN)
        WRITE(11,212) SRM, (SRC(I),I=1,NCHAN)
        WRITE(11,218) BMOLEC,(BCMPLX(I),I=1,NCHAN)
 218    FORMAT(' Overall rotation: B (cm-1)',T35,F12.3,T50,F12.3,
       1        T65,F12.3,F15.3)
C  SET UP GAMMA FUNCTION: GAMON(I)=GAMMA(2*I), I=1/2, 1, 3/2, ...
        GAMON2(1)=1.772454
        GAMON2(2)=1.
        DO 43 NG=2,10
                NG2=2*NG
                GAMON2(NG2)=(NG-1)*GAMON2(NG2-2)
                N2L1=NG2-1
                GAMON2(N2L1)=(NG-1.5)*GAMON2(N2L1-2)
 43     CONTINUE
        DO 8039 I8039=1,NCHAN
```

```
            A(I8039)=16.7364/BCMPLX(I8039)
8039    CONTINUE
        AM=16.7364/BMOLEC
        WRITE(8,6029) AM,(A(I),I=1,NCHAN)
        WRITE(8,3) IEXMD,(IEXRTD(I),I=1,NCHAN)
        WRITE(11,6029) AM,(A(I),I=1,NCHAN)
        WRITE(11,3) IEXMD,(IEXRTD(I),I=1,NCHAN)
3       FORMAT(' Dimensions of adiabatic rotations',T45,I2,T50,I12,
     1          T65,I12,I15)
        IF(TEST1D) then
                WRITE(8,4)
                write(11,4)
        endif
4       FORMAT(/,' (Having a 2-dimensional adiabatic (inactive) rotor',
     1          ' requires an',/,' additional 1-dimensional non-adiabatic',
     2          ' free internal rotor.)',/)
6029    FORMAT(' Corresponding moments of inertia (amu-A**2)',/,T35,F12.3,
     1          T50,F12.3,T65,F12.3,F15.3)
        DO 6125 I6124=1,NCHAN
                EJ(I6124)=4.1868*EOK(I6124)
6125    CONTINUE
        WRITE(8,213) (EOK(I),I=1,NCHAN)
        WRITE(8,1213) (EJ(I),I=1,NCHAN)
        WRITE(8,214) NF,(JF(I),I=1,NCHAN)
        WRITE(8,156) NUMATM
        WRITE(8,220)
        WRITE(11,213) (EOK(I),I=1,NCHAN)
        WRITE(11,1213) (EJ(I),I=1,NCHAN)
        WRITE(11,214) NF,(JF(I),I=1,NCHAN)
        WRITE(11,156) NUMATM
        WRITE(11,220)
        NL=NF
        NR=NINTR
        DO 6124 I6124=1,NCHAN
                NL=MAX0(NL,JF(I6124))
                NR=MAX0(NR,N(I6124))
6124    CONTINUE
        DO 1 I1=1,NL
                WRITE(8,215) NM(I1),JM(I1),(NC(J,I1),JC(J,I1),J=1,NCHAN)
                WRITE(11,215) NM(I1),JM(I1),(NC(J,I1),JC(J,I1),J=1,NCHAN)
1       CONTINUE
        IF(NR.gt.0)then
                WRITE(8,6122)
                write(11,6122)
                I=NCHAN+1
                WRITE(8,6022) (IBL,J=1,I)
                WRITE(8,6023) (IBL,J=1,I)
                WRITE(11,6022) (IBL,J=1,I)
                WRITE(11,6023) (IBL,J=1,I)
6022            FORMAT(T25,4(A1,'  B Symmetry Dimen-'))
6023            FORMAT(T25,4(A1,'(cm-1)  no.  sion '))
```

```
6122          FORMAT(/,' Free internal rotations:')
              DO 6121 I6=1,NR
                    WRITE(8,6120) BVECM(I6),SIGVCM(I6),IRTDMM(I6),(BVEC(J,I6),
     1                    SIGVC(J,I6),IRTDMC(J,I6),J=1,NCHAN)
                    WRITE(11,6120) BVECM(I6),SIGVCM(I6),IRTDMM(I6),(BVEC(J,I6),
     1                    SIGVC(J,I6),IRTDMC(J,I6),J=1,NCHAN)
6120                FORMAT(24X,2(2F7.3,I5,2X),3X,2(2F7.3,I5,2X))
6121          CONTINUE
      endif
CHECK ON NUMBER OF FREQUENCIES
      DO 6130 I6130=1,NCHAN
              IN=N(I6130)
              NCHK(I6130)=IEXRTD(I6130)
              IF(IN.ne.0)then
                    DO 6400 J6400=1,IN
                          NCHK(I6130)=NCHK(I6130)+IRTDMC(I6130,J6400)
6400                CONTINUE
              endif
6130  CONTINUE
      NCHKM=IEXMD
      IF(NINTR.nE.0)then
              DO 6901 J6901=1,NINTR
                    NCHKM=NCHKM+IRTDMM(J6901)
6901          CONTINUE
      endif
      DO 4924 I4924=1,NL
              DO 6134 J6134=1,NCHAN
                    IF(I4924.LE.JF(J6134)) NCHK(J6134)=NCHK(J6134)+JC(J6134,I4924)
6134          CONTINUE
              IF(I4924.LE.NF)  NCHKM=NCHKM+JM(I4924)
4924  CONTINUE
137   FORMAT(//,' Degree of freedom error for reactant.',
     1        I3,' (input) vs. ',I3,' (calc)')
      NUMTOT=3*NUMATM-3
      IF(NCHKM.nE.NUMTOT) then
              WRITE(8,137) NCHKM,NUMTOT
              WRITE(11,137) NCHKM,NUMTOT
      endif
      DO 6139 I=1,NCHAN
              IF(NCHK(I).nE.NCHKM-1)then
                    WRITE(8,4926) I
                    WRITE(11,4926) I
4926                FORMAT(//,' Incorrect number of frequencies for channel ',
     1                    I3,'. Abort.')
                    STOP
              endif
6139  continue
C  END OF CHECK.
      if(wrnflg) then
              write(8,779)
              write(11,779)
```

```
      endif
      If(adflag)then
            write(8,2212)
            write(11,2212)
      else
            write(8,2213)
            write(11,2213)
      endif
      WRITE(8,5010) NN,INC
      WRITE(8,155) DELTAE
      WRITE(8,200) SGMA,WT1,WT2
      WRITE(11,5010) NN,INC
      WRITE(11,155) DELTAE
      WRITE(11,200) SGMA,WT1,WT2
      IF(EPS.LE.0.) then
            WRITE(8,2210)
            WRITE(11,2210)
      endif
2210  FORMAT(20X,'Hard sphere collision frequency used')
      IF(EPS.GT.0.) then
            WRITE(8,2211) EPS
            WRITE(11,2211) EPS
      endif
2211  FORMAT(20X,'Lennard-Jones collision frequency used',/,
     1      20X,'  Well depth =',T50,F10.1,' K')
C5 If energ<0, then use original Troe beta_c, else Gilbert, et al.
      gltflg=.true.
      if(energ.lt.0) gltflg=.false.
      energ=abs(energ)
      if(ibflg.ne.0)then
            write(8,510)
            write(11,510)
            if(ibflg.eq.1)then
                  write(8,511) energ
                  write(11,511) energ
            else
                  write(8,512) energ
                  write(11,512) energ
            endif
      endif
510   format(20x,'Weak collision efficiency (beta) used,')
511   format(20x,'  <deltaE>down = ',T50,F10.1,' (cm-1)')
512   format(20x,'  <deltaE>total = ',T50,F10.1,' (cm-1)')
200   FORMAT(/,20X,'Collision diameter (Angstrom)',T50,F10.2,/,
     1      20X,'Weight of reactant (amu)   ',T50,F10.2,/,20X,
     2      'Weight of bath gas (amu)   ',T50,F10.2)
779   format(/,20x,'I+ < I ; Waage-Rabinovitch treatment disallowed.')
2212  format(/,20x,'Marcus (1962) treatment for adiabatic rotations')
2213  format(/,20x,'Waage-Rabinovitch treatment for adiabatic',
     1      ' rotations')
C
```

```
C  COMMENCE GENERATION OF MICROSCOPIC RATES, K(E).
C  Inc= no. of grains in integration step.
C  Incrou= rounded integration step.
        INC=INT(INC/DELTAE+0.5)
        INCROU=INT(INC*DELTAE+0.5)
        DO 3310 IN=1,NCHAN
                JF1=JF(IN)
                DO 3311 I=1,JF1
C Symmetry no. ratio, L+
                        STC(IN)=SRM/SRC(IN)
                        NC1(I)=NC(IN,I)
                        JC1(I)=JC(IN,I)
 3311           CONTINUE
                N1=N(IN)
                N11=MAX0(N1,1)
                DO 3312 I=1,N11
                        BVEC1(I)=BVEC(IN,I)
                        SIGVC1(I)=SIGVC(IN,I)
                        ISPARE(I)=IRTDMC(IN,I)
 3312           CONTINUE
                KK=INT((EOK(IN)-EOK(1))*WKA/INCROU+0.5)
                KKC(IN)=KK
                NN2=NN-KK
C  Get sum of states of complex, in AK.
                CALL BSWINE(NC1,JC1,AK,NN2,JF1,INC,BVEC1,SIGVC1,ISPARE,N1,.TRUE.)
                JF(IN)=JF1
                DO 7711 I=1,JF1
                        NC(IN,I)=NC1(I)
 7711           CONTINUE
                DO 3319 I=1,NN2
                        K(IN,I)=AK(I)
 3319           CONTINUE
C  USING TRAPEZOIDAL RULE, TAKE HALF OF FIRST VALUE IN SUM
                K(IN,1)=0.5*K(IN,1)
 3310   CONTINUE
        DELT=FLOAT(INCROU)
C  nreact,nrv = no. of steps in the activation energy
        NREACT=INT((EOK(1)*WKA/DELT))
        DO 83 IN=1,NCHAN
                NRV(IN)=INT((EOK(IN)*WKA/DELT))
 83     CONTINUE
C  ni = total # steps (E0+Eexcess)
        NI=NREACT+NN
C  TEST FOR EXCEEDING ARRAY SIZE
        IF(NI.gt.2499)then
                WRITE(8,14)
                WRITE(11,14)
  14            FORMAT(' Array exceeded, reduce NN or increase INC')
                STOP
        endif
C  NOW FIND DENSITY OF STATES OF REACTANT.
```

```
      CALL BSWINE(NM,JM,RHO,NI,NF,INC,BVECM,SIGVCM,IRTDMM,NINTR,.FALSE.)
C  FREQUENCIES ARE RE-ARRANGED BY DIRECT COUNT.
      STEM=STC(1)/H
      DO 5972 I5972=1,NN
C  Microscopic rate constant, ka(E)
            K(1,I5972)=K(1,I5972)*STEM/(RHO(I5972+NREACT))
 5972 CONTINUE
      DO 3320 IN=2,NCHP
            STEM=STC(IN)/H
            ICC=0
            DO 72 I72=1,NN
                  AK(I72)=0.
                  IF(I72.gt.KKC(IN).and.NCHAN.ne.1)then
                        ICC=ICC+1
C  ka(E) for other channels.
                        AK(I72)=K(IN,ICC)*STEM/(RHO(I72+NREACT))
                  endif
 72         continue
            DO 172 I172=1,NN
                  K(IN,I172)=AK(I172)
 172        CONTINUE
 3320 CONTINUE
C  COMPUTATION OF DENSITY OF STATES AND MICROSCOPIC RATES NOW COMPLETE.
C
C  NOTE THE DIRECT COUNT SUBROUTINE UNSCRAMBLES DEGENERATE FREQUENCIES
C  TO AVOID BUNCHING CAUSED BY DIRECT COUNT ALGORITHM.
C
C  COMMENCE INTEGRATION TO FIND RATE COEFFICIENTS,ETC.
      DO 5 IT=1,NT
            TT=TEMP(IT)
            RT=R*TT
            DO 3361 IN=1,NCHAN
                  STLP(IN)=0.
                  RATE(IN)=0.
                  EKG(IN)=0.
                  AKG(IN)=0.
                  FRATIO(IN)=0.
C  Ratio of moments of inertia  (I+)**(dim+/2) / I**(dim/2)  and
C  I+ / I.
C8 Since dim+ = dim now, just have (I+ / I)**(dim/2) and I+ / I.
                  BRATIO(IN)=BMOLEC/BCMPLX(IN)
                  ADRAT(IN)=Bratio(in)**IEXMD
                  ADRAT(IN)=ADRAT(IN)**0.5
C3 BTEST checks for the numerically intractable condition of Bmolec.=
C3  Bcomplex
                  BTEST(IN)=BMOLEC.EQ.BCMPLX(IN)
 3361       CONTINUE
            EGI=0.
            GI=0.
C  fexp = dE/RT
            FEXP=DELT/RT
```

```
C  THE FOLLOWING LOOP (8) FINDS HIGH-PRESSURE PARAMETERS.
                DO 8 I=1,NI
                        E=I*INCROU/WKA
C7 Correction:  initialize g so you don't just add the last value.
                        g=0
                        IF(RHO(I).GT.0) G=EXP(LOG(RHO(I))-I*FEXP)
                        GI=GI+G
                        EGI=EGI+G*E
C FEWR = f(E), Whitten-Rabinovitch treatment
                        DO 999 IN=1,NCHAN
C3 Following implements Waage-Rabinovitch treatment.
C6 FEWR initiation for each channel.
                                FEWR=1.
                                IF((.NOT.BTEST(IN)).AND.(I.LE.NRV(IN))) FEWR=
     1                           EXP((I-NRV(IN))*FEXP*BRATIO(IN)/(BRATIO(IN)-1.))
                                STLP(IN)=STLP(IN)+FEWR*G
999                     CONTINUE
                        IF(I.gt.NREACT)then
                                DO 3365 IN=1,NCHAN
                                        EKG(IN)=EKG(IN)+G*E*K(IN,I-NREACT)
                                        AKG(IN)=AKG(IN)+G*K(IN,I-NREACT)
                                        IF(I.GT.NRV(IN)) FRATIO(IN)=FRATIO(IN)+G
3365                            CONTINUE
                        endif
 8              continue
                DO 3366 IN=1,NCHAN
C  Eac = Ea,hi-press.  Rate = kinf.  Alna = log10(kinf)+Eac/RT =
C  log10(A).
                        EAC(IN)=(EKG(IN)/AKG(IN))-(EGI/GI)
                        RATE(IN)=ADRAT(IN)*AKG(IN)/GI
                        ALNA(IN)=log10(RATE(IN))+(EAC(IN)/(TT*2.30259E-3*1.9872))
                        RATHP(IN)=RATE(IN)
                        EJ(IN)=EAC(IN)*4.1868
C3 If Marcus treatment, make some adjustments; STLP=k0 and
C3  FRATIO=Q1+/Q1.  Otherwise, STLP=(k0)ad and FRATIO=1/Fw.
C8
C8 **** CHANGE:
C8 **** Go to Marcus (1962) treatment:  FRATIO=1 if Marcus.
C8 **** and STLP=Q1+/Q1 * k0.
                        IF(ADFLAG.OR.BTEST(IN)) STLP(IN)=adrat(in)*FRATIO(IN)
C7,C9  Get the eqm pop for the reduced pressure calculation.
                        prbase(in)=fratio(in)/gi
                        FRATIO(IN)=BRATIO(IN)*FRATIO(IN)/STLP(IN)
C8     IF(ADFLAG) FRATIO(IN)=ADRAT(IN)
C9 If FRATIO (=1/Fwr) < 1 (which can happen as I+ -> I), set it
C9 to 1.0, so Fwr is never > 1.0.
                        if(adflag.or.(fratio(in).lt.1.0)) fratio(in)=1.0
3366            CONTINUE
C  Report high pressure info.
                WRITE(8,716) TITLE
                write(8,715) TT
```

```
                write(11,715) TT
                if(nchan.gt.1) then
                        WRITE(8,9716) (I,I=1,NCHAN)
                        WRITE(11,9716) (I,I=1,NCHAN)
                endif
                WRITE(8,717) (EOK(I),I=1,NCHAN)
                WRITE(8,1716) (EAC(I),I=1,NCHAN)
                WRITE(11,1716) (EAC(I),I=1,NCHAN)
                WRITE(8,2716) (EJ(I),I=1,NCHAN)
                WRITE(8,3716) (ALNA(I),I=1,NCHAN)
                WRITE(8,4716) (RATE(I),I=1,NCHAN)
C  CALCULATE AND PRINT OUT THERMODYNAMIC PARAMETERS
                DO 4971 IN=1,NCHAN
                        BCPLX1=BCMPLX(IN)
                        N1=N(IN)
                        BVEC(IN,N1+1)=BCPLX1
                        SIGVC(IN,N1+1)=SRC(IN)
                        IRTDMC(IN,N1+1)=IEXRTD(IN)
                        IF(IN.eq.1)then
C  Append adiabatic rot. info. to the other info.
                                BVECM(NINTR+1)=BMOLEC
                                SIGVCM(NINTR+1)=SRM
                                IRTDMM(NINTR+1)=IEXMD
                        endif
 4971           continue
C  INCLUDE EXTERNAL AND INTERNAL ROTATIONS TOGETHER FOR THERMODYNAMICS.
                NRTOT=NINTR+1
C7  uvkt = vibrational internal energy / KT
                CALL THERM(uvkt,QV,QROT,RT,NM,JM,NF,CP,SV,SROT,ST,STOT,WT1,NRTOT,
       1                BVECM,SIGVCM,IRTDMM,TT)
                CHEKSZ=.TRUE.
                DO 4040 IN=1,NCHAN
                        JF1=JF(IN)
                        DO 5311 I=1,JF1
                                NC1(I)=NC(IN,I)
                                JC1(I)=JC(IN,I)
 5311                   CONTINUE
                        N1=N(IN)+1
                        DO 5312 I=1,N1
                                BVEC1(I)=BVEC(IN,I)
                                SIGVC1(I)=SIGVC(IN,I)
                                ISPARE(I)=IRTDMC(IN,I)
 5312                   CONTINUE
C7  uvkt = vibrational internal energy / KT
                        CALL
THERM(uvkt,V1,R1,RT,NC1,JC1,JF1,CP1,SV1,SROT1,ST1,STOT1,WT1,
       1                N1,BVEC1,SIGVC1,ISPARE,TT)
C7  Calculate S_K for F_WC computation.
                        sk(in)= 1. + dble(n(in))/2. + uvkt
                        DELTAS=STOT1-STOT
                        ALNAE(IN)=(2.71828*RT/H)*EXP(DELTAS/8.3144)
```

```
                        ALNAE(IN)=log10(ALNAE(IN))
                        IF(ABS(ALNAE(IN)-ALNA(IN)).GT.0.05) then
                              WRITE(8,6)
                              WRITE(11,6)
                        endif
 6                      FORMAT(/,' WARNING: Difference between exact and numerically',
     1                        /,' integrated log A is > 5% ; increase number of terms in',/,
     2                        ' integration and/or decrease grain size.')
                        CPC(IN)=CP1
                        QROTC(IN)=R1
                        QVC(IN)=V1
                        SVC(IN)=SV1
                        SROTC(IN)=SROT1
                        STC(IN)=ST1
                        STOTC(IN)=STOT1
                        RATTH(IN)=2.08364E10*TT*(QVC(IN)/QV)*(QROTC(IN)/QROT)
     1                        *EXP(-EOK(IN)*503.2206/TT)
                        IF(ABS(1.-(RATTH(IN)/RATE(IN))).GT.0.10) CHEKSZ=.FALSE.
4040              CONTINUE
                  WRITE(8,9) (RATTH(IN),IN=1,NCHAN)
C  RE-GENERATE THERMODYNAMICS WITHOUT INACTIVE ROTORS
C7  uvkt = vibrational internal energy / KT
                  CALL THERM(uvkt,QX,QROX,RT,NM,JM,NF,CX,SXY,SROX,SX,STOX,WT1,
     1                  NINTR,BVECM,SIGVCM,IRTDMM,TT)
C  corrat = Qcalc/Qthermo w/o the inactive rotors.
                  CORRAT = GI*INCROU/(QX*QROX)
                  IF(.not.CHEKSZ)then
                        WRITE(8,16) CORRAT
                        WRITE(11,16) CORRAT
 16                     FORMAT(' WARNING: Numerical and exact rates differ by more than',
     1                        /,' 10 percent, these rates and rates from MASTER should be',/,
     2                        ' corrected by partition function ratio (at this temperature)'
     3                        ,' =',F10.3)
                        DO 17 IN=1,NCHAN
                              RATE(IN)=RATE(IN)*CORRAT
 17                     CONTINUE
                        WRITE(8,18) (RATE(IN),IN=1,NCHAN)
                        WRITE(11,18) (RATE(IN),IN=1,NCHAN)
 18                     FORMAT(' Numerically integrated high pressure rates with',
     1                        ' this correction are',/
     1                        ,T20,'(S-1)',T34,D10.3,T50,2D10.3)
                  endif
                  WRITE(8,4000) (I,I=1,NCHAN)
4000              FORMAT(/,10X,'Thermodynamics',/,30X,
     1                  'Molecule  Complex(es):',I1,2I10)
 9                FORMAT(' High pressure rate coefficient (from thermodynamics)',
     1                  /,25X,'(s-1)',T34,D10.3,T50,2D10.3)
                  WRITE(8,4020) CP,(CPC(IN),IN=1,NCHAN)
4020              FORMAT(' Spec. heat (kJ/mol-K)',T30,F10.2,5X,3F10.2)
                  WRITE(8,4021) SV, (SVC(IN),IN=1,NCHAN)
4021              FORMAT(' Vibration entropy (J/mol-K)',T30,F10.2,5X,3F10.2)
```

```
                WRITE(8,4022) SROT, (SROTC(IN),IN=1,NCHAN)
4022            FORMAT(' Rotation entropy (J/mol-K)',T30,F10.2,5X,3F10.2)
                WRITE(8,2)
 2              FORMAT(' (Internal and external rotations included together)')
                WRITE(8,4023) ST,(STC(IN),IN=1,NCHAN)
4023            FORMAT(' Translational entropy (J/mol-K)',T33,F7.2,5X,3F10.2)
                WRITE(8,4024) STOT,(STOTC(IN),IN=1,NCHAN)
4024            FORMAT(' Total entropy (J/mol-K)',T30,F10.2,5X,3F10.2)
                WRITE(8,4025) (ALNAE(IN),IN=1,NCHAN)
                WRITE(11,4026) (ALNAE(IN),IN=1,NCHAN)
4025            FORMAT(/,' Log A from thermodynamics',T45,3F10.3)
4026            format(/,' Log A from thermodynamics',t35,f10.3,t51,2f10.3)
                WRITE(8,4028) QV,(QVC(IN),IN=1,NCHAN)
4028            FORMAT(' Vib. partition function',T30,D10.3,5X,3D10.3)
                WRITE(8,4029) QROT,(QROTC(IN),IN=1,NCHAN)
                WRITE(8,2)
4029            FORMAT(' Rotnl partition function',T30,D10.3,5X,3D10.3)
                IF(CHEKSZ) WRITE(8,4019) CORRAT
4019            FORMAT(' Q_numerical/Q_thermo',T45,F10.3)
C  HAVING FINISHED COMPUTATION OF HIGH PRESSURE PARAMETERS, FIND FALL-OF
C  REACTION RATES.
                WRITE(8,718)
                WRITE(11,718)
                betac=1.0
C5 If required, calculate beta here.
                if(ibflg.ne.0) call bcalc(bvecm,irtdmm,jm,nm,rho,sigvcm)
                DO 12 J=1,NP

OMEGA2=(4.39826E+07)*PRESS(J)*(SGMA**2)/SQRT(TT*WT1*WT2/(WT1+WT2))
                        IF(EPS.GT.0.)then
                                OM22=0.636+0.567*log10(TT/EPS)
                                OMEGA2=OMEGA2/OM22
                        endif
                        omega=omega2*betac
                        DO 3367 IN=1,NCHAN
                                RATE(IN)=0.
3367                    CONTINUE
C  Loops 10 and 3370 are the actual RRKM integration.
                        DO 10 II=nreact+1,NI
                                G=0.
                                IF(RHO(II).GT.0.) G=EXP(LOG(RHO(II))-II*FEXP)
                                AKTOT=0.
                                DO 3368 IN=1,NCHAN
                                        AKTOT=AKTOT+FRATIO(IN)*K(IN,II-NREACT)
3368                            CONTINUE
                                G=G*OMEGA/(OMEGA+AKTOT)
                                DO 3369 IN=1,NCHAN
                                        RATE(IN)=RATE(IN)+G*K(IN,II-NREACT)
3369                            CONTINUE
 10                     CONTINUE
                        DO 3370 IN=1,NCHAN
```

```
C7  If not strong coll., calculate F_wc; need reduced pressure for
C7  that.  Otherwise, use F_wc=1.  Remember that pred holds
C7  sum(rho*exp(-E/RT))/Q...we want to be careful to define k0 the
C7  same way Gilbert, et al. do:  no Waage-Rabinovitch correction,
C7  yes beta_c.
                                    fwc(in)=1.
C9  Was multiplying in pred_previous here.
c10 Calc pred even if fwc not calc'd.
                                    pred(in)=prbase(in)*OMEGA/rathp(in)
                                    if(.not.cheksz) pred(in)=pred(in)*corrat
                                    if(ibflg.ne.0) then
                                        call fcalc(pred(in),sk(in),fwc(in))
C7  Just don't use F_wc if the equation predicts it to be greater
C7  than 1.
                                        if(fwc(in).gt.1.) fwc(in)=1.
                                    endif
C7  Now, the rate is k_rrkm*F_wc.
                                    RATE(IN)=fwc(in)*ADRAT(IN)*RATE(IN)/GI
                                    RATIO(IN)=RATE(IN)/RATHP(IN)
 3370                           CONTINUE
C6  Output results.  Print original omega, not beta-modified one.
                               WRITE(8,7181) PRESS(J),OMEGA2,(RATE(IN),RATIO(IN),IN=1,NCHAN)
                               WRITE(11,7181) PRESS(J),OMEGA2,(RATE(IN),RATIO(IN),IN=1,NCHAN)
                               IF(.not.CHEKSZ)then
                                    WRITE(8,7182) (RATE(IN)*CORRAT,RATIO(IN),IN=1,NCHAN)
                                    WRITE(11,7182) (RATE(IN)*CORRAT,RATIO(IN),IN=1,NCHAN)
 7182                               FORMAT(' (Corrected from partn. fcn.)',T31,3(D10.3,1X,D10.3,1X))
                               endif
  12                 CONTINUE
C  Show beta, if used.
                     if(ibflg.eq.0) then
                               write(8,516)
                               write(11,516)
                     else
                               if(gltflg) then
                                    write(8,513)
                                    write(11,513)
                               else
                                    write(8,514)
                                    write(11,514)
                               endif
                               write(8,515) betac,fofe
                               write(11,515) betac,fofe
C7  Print F_WC.
                               write(8,5517) (fwc(i),i=1,nchan)
                               write(11,5517) (fwc(i),i=1,nchan)
C7  Warn user if out of GLT range of validity.
                               iwarn=0
                               do 9000 i=1,nchan
                                    if(sk(i).gt.25.) iwarn=1
 9000                          continue
```

```
                        if((iwarn.ne.0).or.(fofe.gt.70.).or.(betac.lt.1.e-3)) then
                                write(8,9001) (sk(i),i=1,nchan)
                                write(11,9001) (sk(i),i=1,nchan)
                        endif
 9001                   format(/,' *** Warning.  Out of range of validity to use F_WC.',
     1                          ' ***',/,' ***  S_K = ',3f8.2,//)
C Print <deltaE>'s; convert if needed.
C Edn^2-Edn*Etot-FKT*Etot=0; need positive root.
                        Edn=energ
                        if(ibflg.eq.2) then
                                Edn=0.5*(energ+sqrt(energ*(energ+4*fofe*RT)))
                                Etot=-energ
                        else
                                Edn=energ
                                Etot=-Edn**2/(Edn+fofe*RT)
                        endif
                        write(8,517) Edn,Etot
                        write(11,517) Edn,Etot
                endif
 516                    format(/,' Strong collision calculation. F_WC set to 1.')
 513                    format(//,' Beta given by Gilbert, et al., Ber. Buns. Phys.'
     1                          ' Chem., 87, 169-177 (1983)')
 514                    format(//,' Beta given by Troe, J. Chem. Phys., 66,',
     1                          ' 4745-4757 (1977)')
 515                    format(/,5X,'Beta = ',D10.4,/,5X,'Energy dependence of density',
     1                          ' of states, F-E = ',f10.2)
 517                    format(5x,'<deltaE>down = ',t22,f8.1,' cm-1',/,5x,
     1                          '<deltaE>total = ',t22,f8.1,' cm-1',/)
5517                    format(5x,'F_WC (each channel) = ',t28,3f6.3)
 5720                   format(/,' Log(reduced pressure): ',t34,f10.3,t50,2f10.3)
 572                    format(/,' --> Includes beta but not rotational corrections')
C  Calculate and output k0.
                DO 5717 I=1,NCHAN
C                       STLP(I)=STLP(I)*OMEGA*6.23633E4*TT/PRESS(NP)
C11  Forgot partition function.  Correct that error...
                        STLP(I)=STLP(I)/GI*OMEGA*6.23633E4*TT/PRESS(NP)
C  Add that third dimension if 3-D adiabatic rot.
C8  Only one dimension needed, because dim+ = dim.
                        IF(.NOT.ADFLAG) STLP(I)=STLP(I)*(BRATIO(I)**((IEXMD-2.)/2.))
 5717           CONTINUE
C8  Print Waage-Rabinovitch Fwr, if that method is being used.
                if(.not.adflag) then
                        write(8,777) (1/fratio(i),i=1,nchan)
                        write(11,777) (1/fratio(i),i=1,nchan)
                endif
 777            format(/,' Waage-Rabinovitch factor, Fwr = ',t34,f10.3,t50,
     1                  2f10.3)
                WRITE(8,5716) (STLP(I),I=1,NCHAN)
                WRITE(11,5716) (STLP(I),I=1,NCHAN)
                IF(.NOT.CHEKSZ) then
                        WRITE(8,5718) (STLP(I)*CORRAT,I=1,NCHAN)
```

```
                        WRITE(11,5718) (STLP(I)*CORRAT,I=1,NCHAN)
                        write(8,571)
                        write(11,571)
C7  Print reduced pressure.  Correction factor is already in if
C7  needed
                        write(8,5720) (log10(pred(i)/corrat),i=1,nchan)
                        write(8,5721) (log10(pred(i)),i=1,nchan)
                        write(11,5720) (log10(pred(i)/corrat),i=1,nchan)
                        write(11,5721) (log10(pred(i)),i=1,nchan)
                        write(8,572)
                        write(11,572)
                else
C7  ...and it's not there if it isn't needed.
                        write(8,571)
                        write(11,571)
                        write(8,5720) (log10(pred(i)),i=1,nchan)
                        write(11,5720) (log10(pred(i)),i=1,nchan)
                        write(8,572)
                        write(11,572)
                endif
                write(8,5719)
                write(11,5719)
5718            format(' (Corrected with partn. fcn.)',t34,d10.3,t50,2d10.3)
5721            format(' (Corrected with partn. fcn.)',t34,f10.3,t50,2f10.3)
5719            format(/,30x,'********************',/)
 5      CONTINUE
        REWIND 10
C  PREPARE INPUT FILE FOR MASTER EQUATION PROGRAM
        IDM=2
        IDELT=400
        REWIND 10
C7  Default convergence parameter B of 0.1
        b=0.1
        WRITE(10,5000) TITLE,IDM,IDELT,NCHAN,INCROU,b
5000    FORMAT(20A4,/,I1,I6,5X,2I5,5x,d10.3)
        ERR1=1.E-3
        ERR2=1.E-3
        ITMAX=800
        WRITE(10,7109) ERR1,ERR2,ERR1,ITMAX
7109    FORMAT(3D10.3,/,I4)
C7  If a beta is calculated, print actual <deltaE>dn, if not, assume
C7  the given energ is <deltaE>dn and print it.
        if(ibflg.eq.0) then
                WRITE(10,5002) EOK(1),energ,NP
5002            FORMAT(F12.3,/,'1',/,f10.1,/,I1)
        else
                write(10,5003) eok(1),Edn,np
5003            format(f12.3,/,'1',/,f10.1,/,i1)
        endif
        WRITE(10,1207) (PRESS(IP),IP=1,NP)
        WRITE(10,5004) SGMA,WT1,WT2,EPS,NN
```

```
5004    FORMAT(4F12.3,/,I4)
1207    FORMAT(8D10.3)
        DO 3371 IN=1,NCHP
              WRITE(10,1207) (ADRAT(IN)*K(IN,I),I=1,NN)
3371    CONTINUE
        WRITE(10,5005) NI
5005    FORMAT(I4)
        WRITE(10,1207) (RHO(I),I=1,NI)
        WRITE(10,5004) TT
        IOPTHT=0
        IOPTPR=NCHAN
        WRITE(10,7190) IOPTHT,IOPTPR
7190    FORMAT(2I3)
C7 Change default ALMT1 to 0.25
        ALMT1=0.25
        WRITE(10,7929) ALMT1
7929    FORMAT(F6.2)
        close(7)
        close(8)
        close(11)
        close(10)
        STOP
        END
C Part II of RRKM:  the subroutines.
C2 MICROSOFT FORTRAN METACOMMAND IDENTIFYING LARGE ARRAYS OF DATA
C $DEBUG
C $LARGE: T, RHO
        SUBROUTINE BSWINE(NM,JM,RHO,NI,NF,INC,BVEC,SIGVC,IROT,NINTR,SUM)
C  SUBROUTINE FOR DIRECT COUNT TO GIVE  DENSITY OF STATES
C  OR SUM OF STATES.
C2 SET DEFAULT VARIABLE TYPES
        IMPLICIT DOUBLE PRECISION(A-H,O-Z)
        IMPLICIT INTEGER(I-N)
C2 KEEP ALL VARIABLES THE SAME TYPE AS IN MAIN PROGRAM.
        REAL EOK,SRC,SRM,BCMPLX,BMOLEC,AM,A,SGMA,WT1
      1         ,WT2,EPS,PRESS,TEMP,BVECM,BVEC,SIGVCM,SIGVC
        DIMENSION NM(100),JM(100),RHO(2499),BVEC(10),SIGVC(10),IROT(10)
        LOGICAL SUM,REORD,TEST1D,gltflg
        COMMON /ISTP/ ISTEP
        COMMON /UNSC/REORD,TEST1D,gltflg
        COMMON /BS/ FRE(200),IR(200),T(50000),
      1         DELTAE,IS,M
        DO 30 I=1,50000
30      T(I)=0
        IS=0
        ISTEP=INC
        INCROU=INT(INC*DELTAE+0.5)
        EMAX=FLOAT(NI*INCROU)
        IF(REORD)then
              SPACE=DELTAE*0.5
C  SEPARATE ANY DEGENERATE FREQUENCIES TO AVOID BEYER-SWINEHART
```

```
C  BUNCHING PROBLEMS.
                DO 100 I=1,NF
                        NTEMP=JM(I)
                        J=INT(NTEMP*0.5)
                        JR=NTEMP-2*J
                        VAL=FLOAT(NM(I))
                        IF(JR.nE.0)then
                                IS=IS+1
                                FRE(IS)=VAL
                        endif
                        IF(J.ge.1)then
                                DO 6 IX=1,J
                                        IS=IS+1
                                        BIT=SPACE*IX
                                        FRE(IS)=VAL+BIT
                                        IS=IS+1
                                        FRE(IS)=VAL-BIT
 6                              CONTINUE
                        endif
100             continue
C  HAVING UNSCRAMBLED FREQUENCIES, REPLACE THE OLD WITH THE NEW VALUES.
                NF=IS
                DO 3 I3=1,NF
                        NM(I3)=INT(FRE(I3))
 3              CONTINUE
        else
                DO 51 I51=1,NF
                FRE(I51)=FLOAT(NM(I51))
 51             CONTINUE
                IS=NF
        endif
        CALL GRAIN
        M=1.+EMAX/DELTAE
        IF(M.GT.50000) WRITE(6,7722) M
7722    FORMAT('  Maximum energy too great for direct count',
       1        ' array, M=  ',I8)
        IF(M.GT.50000) STOP
        CALL TNONH(BVEC,SIGVC,IROT,NINTR)
        CALL COUNT
        IF(SUM)then
                SUMS=0.
                DO 11 I11=1,M
                        SUMS=SUMS+T(I11)
                        T(I11)=DELTAE*SUMS
 11             CONTINUE
        endif
        ISUM=0
        DO 720 I720=1,M,ISTEP
                ISUM=ISUM+1
                IP=I720+ISTEP-1
                AV=0.
```

```
                DO 721 J721=I720,IP
                        AV=AV+T(J721)
721             CONTINUE
                RHO(ISUM)=AV/INCROU
720     CONTINUE
C5  Correction: Isum >= ni, return... if less, then fill up remaining
C5  space w/0 (instead of whatever happens to be there).
        IF(ISUM.gE.NI) RETURN
        ISUM=ISUM+1
        DO 20 I20=ISUM,NI
                RHO(I20)=0.
20      CONTINUE
        RETURN
        END
        SUBROUTINE GRAIN
C    GRAIN CALCULATES FREQUENCIES IN GRAIN UNITS
C2 SET DEFAULT VARIABLE TYPES
        IMPLICIT DOUBLE PRECISION(A-H,O-Z)
        IMPLICIT INTEGER(I-N)
C2 KEEP ALL VARIABLES THE SAME TYPE AS IN MAIN PROGRAM.
        REAL EOK,SRC,SRM,BCMPLX,BMOLEC,AM,A,SGMA,WT1
      1         ,WT2,EPS,PRESS,TEMP,BVECM,BVEC,SIGVCM
        COMMON /BS/ FRE(200),IR(200),T(50000),
      1         DELTAE,IS,M
        DO 752 I752=1,IS
                FFR=FRE(I752)/DELTAE
                IR(I752)=NINT(FFR)
752     CONTINUE
        RETURN
        END
        SUBROUTINE COUNT
C  CALCULATES DENSITY OF STATES USING BEYER-SWINEHART ALGORITHM
C
C2 SET DEFAULT VARIABLE TYPES

        IMPLICIT DOUBLE PRECISION(A-H,O-Z)
        IMPLICIT INTEGER(I-N)
C2 KEEP ALL VARIABLES THE SAME TYPE AS IN MAIN PROGRAM.
        REAL EOK,SRC,SRM,BCMPLX,BMOLEC,AM,A,SGMA,WT1
      1         ,WT2,EPS,PRESS,TEMP,BVECM,BVEC,SIGVCM
        COMMON /BS/ FRE(200),IR(200),T(50000),
      1         DELTAE,IS,M
        DO 750 I750=1,IS
                IR750=1+IR(I750)
                DO 751 I751=IR750,M
                        II751=I751-IR750+1
                        T(I751)=T(I751)+T(II751)
751             CONTINUE
750     CONTINUE
        RETURN
        END
```

```
      SUBROUTINE TNONH(BVEC,SIGVC,IROT,NINTR)
C  INITIALIZES ARRAY FOR BEYER-SWINEHART ALGORITHM, INCLUDING SEMI-CLASS
C  FORM FOR FREE INTERNAL ROTORS, AS SUGGESTED BY TROE.
C
C
C2 SET DEFAULT VARIABLE TYPES
      IMPLICIT DOUBLE PRECISION(A-H,O-Z)
      IMPLICIT INTEGER(I-N)
C2 KEEP ALL VARIABLES THE SAME TYPE AS IN MAIN PROGRAM.
      REAL EOK,SRC,SRM,BCMPLX,BMOLEC,AM,A,SGMA,WT1
     1     ,WT2,EPS,PRESS,TEMP,BVECM,BVEC,SIGVCM,SIGVC
      DIMENSION BVEC(10),SIGVC(10),IROT(10)
      COMMON /BS/ FRE(200),IR(200),T(50000),
     1     DELTAE,IS,M
      COMMON /ROTF/ GAMON2(20)
      IIR=0
      Q=1.
      IF(NINTR.gt.0)then
            DO 1 I=1,NINTR
                  IRX=IROT(I)
                  IIR=IIR+IRX
                  HD=0.5*IRX
                  Q=Q*GAMON2(IRX)/(SIGVC(I)*(BVEC(I)**HD))
                  IF(IRX.EQ.3) Q=Q*2
 1          CONTINUE
            HR=0.5*IIR
            EROT=0.
            Q=DELTAE*Q/GAMON2(IIR)
            DO 753 I753=1,M
                  EROT=EROT+DELTAE
                  T(I753)=Q*(EROT**HR)/EROT
753         continue
      endif
      IF(NINTR.LE.0) T(1)=1.
      RETURN
      END
C7 Modify to calc (vibrational internal energy / kT)
      SUBROUTINE THERM(uvkt,QV,QR,RT,NM,JM,NF,CP,SV,SROT,ST,STOT,WT1,
     1     NINTR,BVEC,SVECM,IRDIM,T)
C  CALCULATES ALL THERMODYNAMIC QUANTITIES.
C
C2 SET DEFAULT VARIABLE TYPES
      IMPLICIT DOUBLE PRECISION(A-H,O-Z)
      IMPLICIT INTEGER(I-N)
C2 KEEP ALL VARIABLES THE SAME TYPE AS IN MAIN PROGRAM.
      REAL EOK,SRC,SRM,BCMPLX,BMOLEC,AM,A,SGMA,WT1
     1     ,WT2,EPS,PRESS,TEMP,BVECM,BVEC,SIGVCM,SVECM
      DIMENSION NM(100),JM(100),BVEC(10),SVECM(10),IRDIM(10)
      COMMON /ROTF/ GAMON2(20)
      CV=0.
      QV=1.
```

```
      uvkt=0.
      SV=0.
      DO 126 I=1,NF
            X=NM(I)/RT
            EX=EXP(X)
            REX=1./EX
            uvkt = uvkt + x/(ex - 1.)
            QV=QV/(1.-REX)
            EXL1=EX-1
            CV=CV+X*X*EX/(EXL1*EXL1)
            SV=SV+(-LOG(1.-REX)+(X/EXL1))
126   CONTINUE
      SV=SV*8.3144
      ST=6.8635*log10(WT1)+11.4392*log10(T)-2.314
      ST=ST*4.1868
      SROT=0.
      QR=1.
      IIR=0
      IF(NINTR.nE.0)then
            DO 5 I=1,NINTR
                  IND=IRDIM(I)
                  IIR=IIR+IND
                  PWR=0.5*IND
                  QR=QR*((RT/BVEC(I))**PWR)*GAMON2(IND)/SVECM(I)
                  IF(IND.EQ.3) QR=QR*2
5           CONTINUE
            SROT=8.3144*(LOG(QR) + 0.5*IIR)
      endif
      STOT=SROT+ST+SV
      CP=8.3144*(2.5+CV+IIR*0.5)
      RETURN
      END
C5  Collision efficiency calculation.
C $debug
C $large: T, RHO, RVIB
      subroutine bcalc(bvecm,irtdmm,jm,nm,rho,sigvcm)
      implicit double precision(a-h,o-z)
      implicit integer(i-n)
      real bvecm,sigvcm
      logical reord, test1d, gltflg
      dimension nm(100),jm(100),rho(2499),rvib(2499),bvecm(10),
     1      sigvcm(10),irtdmm(10)
      common /unsc/reord,test1d,gltflg
      common /bs/ fre(200),ir(200),t(50000),
     1      deltae,is,m
      common /bci/ibflg,inc,ni,nintr,nf,nreact,QV,RT,IT
      common /bcr/betac,energ,fexp,fofe
      save rvib
C5 Calculate Troe's F_E (="energy dependence of the vibrational density of
C5 states")
      if(IT.eq.1)then
```

```
                if(nintr.eq.0)then
                        do 51 I=1,NI
 51                     rvib(I)=rho(I)
                else
                        reord=.false.
                        call bswine(nm,jm,rvib,ni,nf,inc,bvecm,sigvcm,irtdmm,
     1                          0,.false.)
                endif
        endif
C5 Trapezoidal rule. Slightly inconsistent with main program, which
C5 starts integration at E0+dE.
        fofe=0.0
        if(rvib(nreact).gt.0.0)then
                fofe=0.5*exp(log(rvib(nreact))-nreact*fexp)
        endif
C write (*,*) fexp,RT
        do 50 I=nreact+1,NI
C write(*,*) I,rvib(I),fofe
 50     if(rvib(I).gt.0.0) fofe=fofe+exp(log(rvib(I))-I*fexp)
        fofe=fofe*fexp/exp(log(rvib(nreact))-nreact*fexp)
        FKT=fofe*RT
C5 energ=Etot. Convert via Edn^2-Edn*Etot-FKT*Etot=0; need positive root.
        Edn=energ
        if(ibflg.eq.2) Edn=0.5*(energ+sqrt(energ*(energ+4*FKT)))
        EplusF=Edn+FKT
        betac=(Edn/EplusF)**2.
        if(gltflg)then
C5 Calculate normalization integral = integral(0-Eo){f(E)-FKT/(Edn+FKT)
C5 *f(E)*exp((E-Eo)/FKT)} using trapezoidal rule. Assumes rhovib(E=0)=0.
                Eratio=FKT/EplusF
                fnorm=exp(log(rvib(nreact))-nreact*fexp)*(1.0-Eratio)/2.0
                if(nreact.gt.1)then
                        do 500 I=1,nreact-1
 500                    if(rvib(I).gt.0.0) fnorm=fnorm+exp(log(rvib(I))-I*fexp)-
     1                          Eratio*exp(log(rvib(I))-fexp*(I+(nreact-I)/fofe))
                endif
                fnorm=fnorm*(fexp*RT)/QV
                betac=betac/fnorm
        endif
 501    format(8D10.3)
 502    format(8I10)
        return
        end
C7 F_WC calculation subroutine. Gilbert, Luther, and Troe weak
C7 collision broadening factor. Eqns. 5.1 and 5.6-5.9.
        subroutine fcalc(pred,sk,fwc)
        implicit double precision(a-h,o-z)
        implicit integer(i-n)
        common /bci/ibflg,inc,ni,nintr,nf,nreact,QV,RT,IT
        common /bcr/betac,energ,fexp,fofe
        fwc=0
```

```
C7 fwcc=log(F_WCcent), bclog=log(betac), xnwc=N_WC
        bclog=log10(betac)
        fwcc=(0.16*bclog+0.04*(bclog**2))*(1.+(log10(fofe))**2.2)
        xnwc=1.-(0.086*sk+1.7)*fwcc-0.3*bclog
        c=1.5*(fwcc**2)*(1.-0.5*bclog)
        d=-0.03*sk+0.45*(1.-exp(-0.3*sk))
        tmp = (log10(pred)+c)/(xnwc-d*(log10(pred)+c))
        fwc=fwcc/(1.+ tmp*tmp)
        fwc=10.**fwc
C  write(*,*)bclog,fwcc,xnwc,c,d,fwc
        return
        end
```

Appendix C. Falloff Calculations.

C.1 General Procedures

Three computer programs were used to calculate pressure effects: CHEMACT, UQRRK and RRKM. The last of the three was based on the program FALLOFF (Gilbert, 1983) distributed by the Quantum Chemistry Program Exchange. FALLOFF calculates pressure effects of unimolecular reactions using RRKM theory (Robinson and Holbrook, 1972), with a direct count algorithm for the density of states (Beyer and Swinehardt, 1973; and Astholz et al., 1979). The program was revised by Shandross and Howard (1987 and 1988-1995) to incorporate the Waage-Rabinovitch (1970) treatment of adiabatic rotations, and to implement the collision efficiency and weak collision broadening factor treatments of Gilbert et al. (1983). The program code and a detailed discussion of the program modifications are found in Appendix B.

RRKM calculations require vibrational frequencies and moment of inertia for the transition state of the reaction. The geometry and moment of inertia of the transition state may be estimated by the methods of Benson (1976). Vibrational frequencies are more difficult to calculate, but it has been found that the results of the calculation are insensitive to the choice of frequencies so long as the resulting computed A-factor is correct (Robinson and Holbrook, 1972). Therefore, a method similar to that used by Kiefer et al. (1985) was used here: the frequencies of the reactant (usually excepting the lowest or several lowest) were modified by addition or subtraction of a constant amount, until the pre-exponential factor calculated by the program agreed with the known high-pressure limit at some mean temperature or temperature range. Occasionally, for better fit of the A-factor, the lowest frequency was modified as well.

The CHEMACT program, which calculates chemical activation effects by the bimolecular QRRK formalism of Dean (1985), was written by Dean, Bozzelli and Ritter (Dean et al., 1991). It was modified in two ways for use in this work: (1) substituting the Forst (1973) approximation for the reduced collision integral ($\Omega^{(2,2)*}$ — used in calculating the Lennard-Jones collision rate) with that proposed by Troe (1977), to be consistent with the modified FALLOFF program, and (2) allowing the collision efficiency $ß_c$ to be input by the user as a 5-parameter polynomial fit with respect to temperature:

$$\beta_c = \sum_{i=1}^{5} a_i T^{b_i} \qquad \text{(C-1)}$$

The general procedure used for chemical activation calculations was to compute β_c by the more accurate method of Gilbert et al. (1983), using the modified FALLOFF program for the reaction in the reverse direction, then fit it to the form required[43] by the modified CHEMACT program using curve fitting software (TableCurve™ by Jandel Scientific).

The UQRRK program (Westmoreland, 1992a) was used for unimolecular isomerization with branched decompositions. The "Q-formalism" used by that program is described in Westmoreland (1992b).

In the flame studied here, several species were present in high concentrations: H_2, O_2, H_2O, and argon. For the RRKM and QRRK calculations documented in this chapter, a hypothetical collision partner with weighted average properties ($[prop] = \Sigma (x_i)_{ave}[prop]_i$ for molecular weight and collision diameter, and $[prop] = \Pi [prop]_i^{(x_i)_{ave}}$ for well depth) was used, rather than assuming the bath gas to be one of those species[44] (e.g., argon). The average mole fractions used were estimated from measured flame data. Based on the values in Table C.1, the molecular weight of the hypothetical bath gas was 19.4 amu, the collision diameter 3.046 Å., and the Lennard-Jones potential well depth 145.8 K.

Table C.1 Parameters used for calculation of average bath gas properties. Lennard-Jones parameters from Kee et al. (1986).

	Ar	H_2	H_2O	O_2
x_i	0.416	0.238	0.271	0.075
σ (Å)	3.33	2.92	2.61	3.46
ε/k_B (K)	136.5	38	572.4	107.4
$\langle \Delta E \rangle_{all}$ (cal/mol)	1,260	700	1,250	780

Average values for $\langle \Delta E \rangle_{all}$ were only used for revisions of the QRRK calculations of the Zhang and McKinnon (1995) model (cf. Section 5.1). The literature data used to calculate the average $\langle \Delta E \rangle_{all}$ for each bath gas are listed in Table C.2. The starting point for energy transfer for most of the calculations in this appendix was 70 cm^{-1}, the value used by Kiefer et al. (1985)

[43] Typical values used for $b_{i,i=1,5}$ were 0, 1, 2, -1, and -2.

[44] A slightly different averaging method was used to revise the QRRK calculations in the Zhang and McKinnon (1995) model for 22 torr and an appropriate bath gas environment. For those calculations, QRRK results were computed for each of the bath gases, then the rate constant weighted as $k = \Sigma (x_i)_{ave} k_i$.

for -$\langle\Delta E\rangle_{all}$ for benzene pyrolysis. This low value is consistent with other literature values for benzene, as the information in Table C.2 shows. In some cases, constant $\langle\Delta E\rangle_{down}$ was used

Table C.2 Literature collision energy transfer values used for derivation of average bath gas $\langle\Delta E\rangle_{all}$.

	$\langle\Delta E\rangle_{all}$, cm^{-1}				
Bath gas →	H_2	Ar	H_2O	O_2	Reference
Species or Reaction:					
azulene	129	155	394	156	b
toluene	92	130	480	160	b
cycloheptatriene		130			b
benzene		45		66	b
C_6F_6		360		343	b
CF_3I		40			b
H_2C=CHCl		210			b
1,1,2,2-tetrafluorocyclopropane		1,196			b
CH_3CO_2Et		248			b
cyclobutane-t		456			b
I+NO_2	67	276		501	a
CH_3CF_3	309	254			a,g
C_7H_8 isom	230	313		376	a,c
ClNO		100			c
NO_2		251		301	c
methylhexyls	400				d
NO_2Cl	215	365			e
CH_3NC	238	280			a,e
C_2H_5NC	201				a
C_2H_4+CH_2		1,886			f
$2CH_2Cl$		1,541			f
trans-hexene-3+H	270				f
cis-butene+H	281	606			f
hexene-1+H	298				f
octene-1+H	298				f
pentene-1+H	314				f
2,4-dimethylpentene-1+H	360				f
Average:	247	442	437	272	
	H_2	Ar	H_2O	O_2	
In kcal/mole:	0.7	1.26	1.25	0.78	
In kJ/mole:	2.95	5.29	5.23	3.25	

a - Quack and Troe (1977).
b - Oref and Tardy (1990).
c - Gardiner and Troe (1984).
d - Larson and Rabinovitch (1969).
e - Tardy and Malins (1979).
f - Tardy and Rabinovitch (1977); converted to $\langle\Delta E\rangle_{all}$ by Troe formula with F_E=1.15.
g - Marcoux and Setser (1978).

instead of constant $\langle\Delta E\rangle_{all}$, since it would give more reasonable-appearing results. Generally a value of $\langle\Delta E\rangle_{down} = 409$ cm^{-1} was used, which is the downward energy transfer in benzene pyrolysis at about 1350 K, when $\langle\Delta E\rangle_{all}$ is -70 cm^{-1}.

One case where downward energy transfer was preferred was cyclohexadienyl decomposition. The frequencies and activation energy were such that F_E, the energy dependence of the density of states (see Appendix B), soared above the range of validity of the Gilbert et al. (1983) approximation for the weak collision broadening factor (F^{WC}) at temperatures above 1500 K. Using a constant $\langle\Delta E\rangle_{all}$, $\langle\Delta E\rangle_{down}$ as calculated from Equation B-6 is 12,200 cm^{-1} at 2100 K. On the other hand, with a constant $\langle\Delta E\rangle_{down}$, $\langle\Delta E\rangle_{all}$ would be -0.1 cm^{-1}, a much more reasonable value.

There were also other molecules for which F_E rapidly increased with temperature, above the approximation range for F^{WC}. In all such cases, when F_E was outside that range (i.e., above 75) F^{WC} was set to its value just before F_E became too high.

Other instances for which one or the other energy assumption was preferred were when β_c would exceed 1.0 or would drop rapidly and dramatically as temperature increased. The latter behavior is more characteristic of the crude collision efficiency approximation formula, Equation B-4. Naturally, the energy assumption which resulted in more realistic behavior was chosen.

Most of the QRRK results were easily fit to the 3-parameter modified Arrhenius form, $k = AT^n\exp(-E_a/RT)$. However, the RRKM output was usually not well-behaved in this regard. For internal calculation purposes, the RRKM rate constants were fit to the 5-parameter modified Landau-Teller form used by the CHEMKIN II programs (Kee et al., 1991):

$$k_i = A_i T^{n_i} \exp\left(\frac{-E_i}{RT} + \frac{B_i}{T^{1/3}} + \frac{C_i}{T^{2/3}}\right) \qquad \text{(C-2)}$$

In almost every case, the resulting parameters were computationally unwieldy for computer systems with average precision. For the revised model of Chapter 7, the rate constants were fit to the more convenient 3-parameter form over the temperature range in which k was greater than 1×10^{-14} cm^3/mol-s. This was found to be an acceptable compromise between the accuracy of the fit and the impact of the range of lowest accuracy.

C.2 Specific Reactions

The high-pressure limit and Lennard-Jones parameters used in RRKM and QRRK calculations are summarized in Tables C.3 and C.4.

Table C.3 High-pressure limit parameters for RRKM and QRRK calculations. The direction for k_∞ is for the reaction as written, unless noted otherwise. Reverse rate constants, when needed, were computed from microscopic reversibility.

Reaction	Comments	A (mol-cm-s)	n	E (cal/mol)	Source
$C_6H_6 \rightleftharpoons C_6H_5+H$	RRKM	9.0×10^{15}	0	1 7,430	a
$C_6H_6+O \rightleftharpoons$ products	QRRK, minimum exit channel calculation	2.4×10^{13}	0	4,668	b
$C_6H_6OH \rightleftharpoons C_6H_6+OH$	RRKM, to get β_c	3.0×10^{12}	0	16,300	c
$C_6H_6+OH \rightleftharpoons C_6H_6OH$	QRRK	1.39×10^{12}	0	378	c
$C_6H_6+OH \rightleftharpoons C_6H_5OH+H$	Overall rate constant used to get H elimination channel	1.34×10^{13}	0	10,592	d
$C_6H_6+OH \rightleftharpoons C_6H_5OH+H$	Overall rate constant used to get H elimination channel; k_∞ for reverse direction	7.08×10^{12}	0	5,387	e
$HC\equiv CCH_2CH_2C\equiv CH \rightleftharpoons C_6H_6$	RRKM	5.00×10^{11}	0	47,769	f
fulvene $\rightleftharpoons C_6H_6$	RRKM, average of A, E given	3.16×10^{13}	0	66,390	g
$C_6H_7 \rightleftharpoons C_6H_6+H$	RRKM, for model and β_c; QRRK	2.0×10^{13}	0	26,030	h
$C_6H_6+H \rightleftharpoons C_6H_7$	QRRK, for mech. testing	4.0×10^{13}	0	4,300	i
$C_6H_7 \rightleftharpoons$ l-C_6H_7	QRRK, for mech. testing	2.0×10^{13}	0	48,900	i
$C_6H_7 \rightarrow C_5H_4CH_3$	QRRK, for mech. testing	5.0×10^{12}	0	38,100	i
$C_5H_4CH_3 \rightarrow C_6H_7$	QRRK, for mech. testing	8.0×10^{11}	0	40,000	i
$C_5H_4CH_3 \rightarrow C_5H_4CH_2+H$	QRRK, for mech. testing	1.2×10^{13}	0	50,500	j (A), i (E)
1,3-$C_6H_8 \rightleftharpoons C_6H_6+H_2$	RRKM	1.7×10^{13}	0	61,622	k
1,4-$C_6H_8 \rightleftharpoons C_6H_6+H_2$	RRKM	1.05×10^{12}	0	42,690	l
$C_6H_5O+H \rightleftharpoons C_6H_5OH$	RRKM	2.5×10^{14}	0	0	m
$C_6H_5+O_2 \rightleftharpoons C_6H_5O_2$	QRRK	6.02×10^{12}	0	-320	n
$C_6H_5 \rightleftharpoons HC\equiv CCH=CHCH=CH$	RRKM	1.3×10^{15}	0	81,300	o
$C_6H_5 \rightleftharpoons HC\equiv CCH=CHCH=CH$	QRRK (unimolecular)	1.2×10^{14}	0	70,900	p
$HC\equiv CCH=CHCH=CH \rightleftharpoons C_6H_5$	QRRK (unimolecular)	4.0×10^{10}	0	7,000	p
$HC\equiv CCH=CHCH=CH \rightleftharpoons$ l-C_6H_4+H	QRRK (unimolecular)	8.0×10^{12}	0	36,700	p

Reaction	Comments	A (mol-cm-s)	n	E (cal/mol)	Source
$HC{\equiv}CCH{=}CHCH{=}CH \rightleftharpoons 1\text{-}C_4H_3{+}C_2H_2$	QRRK (unimolecular)	5.5×10^{14}	0	45,800	p
$C_6H_7{+}H \rightleftharpoons C_6H_8$	RRKM performed in the reverse direction; k_∞ is for recombination	1.0×10^{14}	0	0	q
$C_6H_5CO \rightleftharpoons C_6H_5{+}CO$	RRKM	4.0×10^{14}	0	29,400	r

a - Baulch et al. (1992).
b - Ko et al. (1991).
c - Witte et al. (1986).
d - He et al. (1988).
e - Manion and Louw (1989).
f - Lindstedt and Skevis (1995).
g - Gaynor et al. (1981).
h - Tsang (1986).
i - Ritter et al. (1990).
j - Estimated from generic A factors of Dean (1985).
k - Orchard and Thrush (1974).
l - Ellis and Frey (1966). High-pressure limit around 600 K, as noted by Benson and Shaw (1967).
m - He et al. (1988).
n - Yu and Lin (1994).
o - Rao and Skinner (1988).
p - Westmoreland (1986) and Westmoreland et al. (1989).
q - Dean (1985).
r - Solly and Benson (1971).

Table C.4 Lennard-Jones parameters for RRKM and QRRK calculations.

Species	Reaction	σ (Å)	ε/k_B (K)	Based on
C_6H_6	$C_6H_5{+}H \rightleftharpoons C_6H_6$	5.35	412.3	Kee et al. (1991)
C_6H_6O	$C_6H_6{+}O \rightleftharpoons C_6H_5OH$; $C_6H_5O{+}H$	5.5	450	C_6H_5OH
C_6H_6OH	$C_6H_6{+}OH \rightleftharpoons C_6H_6OH$; $C_6H_5OH{+}H$	5.5	450	C_6H_5OH
C_6H_6	$HC{\equiv}CCH_2CH_2C{\equiv}CH \rightleftharpoons C_6H_6$	5.35	412.3	Kee et al. (1991)
C_6H_6	fulvene $\rightleftharpoons C_6H_6$	5.35	412.3	Kee et al. (1991)
c-C_6H_7; $C_5H_4CH_3$	$C_6H_6{+}H \rightleftharpoons C_6H_7$; l-C_6H_7; $C_5H_4CH_3$; $C_5H_4CH_2$	5.35	412.3	C_6H_6
1,3-C_6H_8	1,3-$C_6H_8 \rightleftharpoons C_6H_6{+}H_2$	5.35*	412.3	C_6H_6
1,4-C_6H_8	1,4-$C_6H_8 \rightleftharpoons C_6H_6{+}H_2$	5.35*	412.3	C_6H_6
C_6H_5OH	$C_6H_5O{+}H \rightleftharpoons C_6H_5OH$	5.5	450	Kee et al. (1991)
$C_6H_5O_2$	$C_6H_5{+}O_2 \rightleftharpoons C_6H_5O{+}O$; $C_6H_5O_2$; $C_6H_4O_2{+}H$	5.75	450	Larger than C_6H_5OH
C_6H_5	$C_6H_5 \rightleftharpoons HC{\equiv}CCH{=}CHCH{=}CH$	5.35	412.3	Kee et al. (1991)
C_6H_8 (generic)	$C_6H_8 \rightleftharpoons C_6H_7{+}H$	5.35*	412.3	C_6H_6
C_6H_5CO	$C_6H_5CO \rightleftharpoons C_6H_5{+}CO$	5.5	593	Emdee et al. (1992)

* A slightly larger value (5.50 Å) was used in flame code calculations.

$C_6H_5+H \rightleftharpoons C_6H_6$ (Rxn B1; EBG, ZM, LS)

RRKM parameters. The calculation was performed in the reverse direction, i.e., unimolecular decomposition of benzene. Vibrational frequencies for benzene were taken from Shimanouchi (1972). The moment of inertia, 88 amu-Å^2, was taken to be that of phenyl from Benson (1976). The exact value is unimportant, because it changes little in the reaction. That is, the relevant ratio, I/I^+, remains approximately constant. The moment of inertia was in fact assumed to be constant in the present calculation.

Comments. The fit to high-pressure parameters was made at 1500 K. One problem which arises is that the RRKM calculation as described above doesn't reproduce the high-pressure limit well at low temperatures. The high-pressure limit value of the original rate constant was used below 900K because (a) the RRKM prediction of k_∞ is excellent above that temperature, and (b) the falloff calculation predicts that $k/k_\infty \approx 1$ for 300-900K.

RRKM input file:

```
Benzene pyrolysis.  Baulch et al. (1992).  beta_GLT
900  150  5   1  7  1  12
20  20
102.44
-2  12
0.190  0.190
0  0
4.20  78.11  19.4  245.2  2  70
2954 1   884 1  1218 1   565 1  2960 1  902 1   887 1   595 1
1202 1 1042 1   741 2  2955 1  1378 2  930 2  2939 2  1488 2
1070 2   498 2   867 2   302 2
3062 1   992 1  1326 1   673 1  3068 2  1010 1   995 1   703 1
1310 1  1150 1   849 2  3063 1  1486 2  1038 2  3047 2  1596 2
1178 2   606 2   975 2   410 2
22.
300. 600. 900. 1200. 1500. 1800. 2100.
```

$C_6H_5+O \rightleftharpoons C_6H_5OH$ (Rxn B20; LS); C_6H_5O+H (Rxn -B3; EBG, ZM)

Chapter 2 contains an extensive review of this reaction, including a reaction network describing possible outlet channels for adduct. The reader is referred to that discussion.

Unfortunately, Arrhenius parameters for the various channels are not so easy to determine. What is available is the overall k_∞, and $E_{0,add}$, the potential energy barrier for addition (from a study of reactive scattering of fast, but vibrationally not activated, molecules). The latter was measured by Gonzalez Ureña et al. (1986).

Noting that Ko et al. found a good fit of experimental results to the same Arrhenius expression over a wide range of temperatures and pressures[45], the approach taken here is to model the reaction to determine whether the observed behavior is reproduced under reasonable limiting assumptions. Attempts to estimate the rate constant for addition, using the available information and analogies to other radical additions to benzene, were not successful in reproducing the Ko et al. fit to better than within an order of magnitude. Furthermore, the amount of falloff estimated in the direction of dissociation of the adduct is as large as $k/k_\infty = 10^{-2}$ at 1500K, unlike the literature experiments for overall reaction. Therefore, addition with stabilization is not sufficient to model the reaction.

Because the rate of decomposition of the adduct is unknown, the questions investigated became (1) what minimum rates of reaction of the adduct (other than back to reactants) would predict the observed lack of pressure dependence, and (2) whether reasonable estimates for the rate of dissociation of the adduct to C_6H_5O+H meet the criteria.

In the determining the answer to the first question, the highest and lowest pressures in the literature data considered by Ko et al., 1.8 torr and 518 torr, were used as limiting cases. Since the Ko et al. rate constant was evaluated to be good to ± 23%, a limit of 23% falloff was considered to satisfy the criterion of a *minimum* rate for adduct decomposition channels. QRRK calculations were performed for an addition channel and a nondescript ("products") decomposition channel.

Falloff calculation parameters. THERM (Ritter et al. 1990) gives an average heat of formation (from routes via 1,3 and 1,4 diene) of 62.50 kcal/mol for the biradical C_6H_6O. MOPAC (Stewart, 1990) predicts the energy of C_6H_6O to be 9.89 kcal/mol greater than that of C_6H_7, which

[45] In a review of the NIST database (Mallard et al., 1993) information on this reaction at 298K, there is a pretty clear (though certainly noisy) trend towards lower k with higher pressure, consistent with the expectation for an addition/decomposition reaction. The trend is only seen at low temperature. The only exceptions to this are the Colussi et al. (1975) data and the Tabares et al. (1983) data. Ko et al. did not use much of this low temperature information in their fit of literature data.

would be 59.75 kcal/mol. The agreement is good. The heat capacities predicted by the MOPAC vibrational frequencies are also quite close to those predicted by THERM. Those frequencies were therefore used to estimate the mean frequency of 1050 cm^{-1}.

The collision efficiency was calculated using RRKM. For that calculation, the MOPAC vibrational frequencies and moment of inertia were used for C_6H_6O. The moment of inertia product was calculated to be $[(17.056) \times (31.239) \times (45.702)]^{1/3} = 29.98$ g-cm^2, making B = 0.0966. The transition state was approximated as simply an increase in the C-O bond of a factor of 2.2 (Benson, 1976, pp. 91 and 100, using T_m = 900K). Ignoring the change in H atom position at that carbon, the moment of inertia of the transition state is $[(19.01) \times (54.92) \times (67.42)]^{1/3} = 41.29$ ($B^+ = 0.0678$). In the analysis of Amano et al., *Int. J. Chem. Kinet.*, **8**, 321 (1976), for $C_6H_6CH_3 = CH_3+C_6H_6$, the "dissociation complex" was assumed to be tight. The present assumption is most likely better for C_6H_6O, being more in line with Benson's method and the observations of Gonzalez Ureña et al. that the barrier for association in the reverse reaction is early.

The RRKM input file is given below:

```
C6H6O decomposition to O+C6H6.  B_GLT.
900  150  5   1  7  1  13
32  33
18.37
1  1
0.0678 0.0966
0  0
4.27  94.11  19.4  256  1  409
 144 1  376 1  466 1  525 1  552 1  642 1  668 1  861 1
 896 1  933 1  980 1  906 1  916 1  942 1 1013 1 1040 1
1144 1 1181 1 1190 1 1201 1 1296 1 1345 1 1380 1 1387 1
1498 1 1519 1 2780 1 3067 1 3068 1 3079 1 3079 1 3089 1
 144 1  321 1  411 1  470 1  497 1  587 1  613 1  806 1
 841 1  878 1  925 1  851 1  861 1  887 1  958 1  985 1
1089 1 1126 1 1135 1 1146 1 1241 1 1290 1 1325 1 1332 1
1412 1 1443 1 1464 1 2725 1 3012 1 3013 1 3024 1 3024 1
3034 1
22.
300. 600. 900. 1200. 1500. 1800. 2100.
```

Minimum rates for reaction channel(s). By systematically varying the rate of the "products" channel over a range of temperatures and the two noted pressures, k_{min} for additional (decomposition) exit channels was found to be $1.17x10^{-7}T^{5.84}exp(-2521/RT)$ for the low-pressure case and $8.05x10^{-13}T^{7.11}exp(4941/RT)$ for the high-pressure case. While these expressions are odd looking, they were only derived for the purpose of a *minimum* exit channel rate, and so would not be expected to be chemically meaningful as a rate constant.

Investigation of C_6H_5O+H channel. For the answer to the second question posed above, several assumptions or analogies were made to test the possible rate of H elimination channel against the minimum exit rate. The first of those analogies was comparison of the present reaction to the branching ratio of H to CH_3 loss from methylcyclohexadienyl radical; second, comparison to loss of H from c-C_6H_7; third, loss of H from C_6H_6OH.

Ejection of H atom from C_6H_6O is thermoneutral with Sandia thermochemistry (Kee et al., 1994) or 1 kcal/mol endothermic with Burcat et al. (1985) thermochemistry. Since the reverse process should have no activation energy, the forward process has no activation energy, or 1 kcal/mol. The rate of reaction for the H elimination is then approximately equal to the A-factor.

Methylcyclohexadienyl analogy: The branching ratio of H/CH_3 loss from $C_6H_6CH_3$ estimated by Robaugh and Tsang (1986) was used to calculate a rate of phenoxy production, by assuming (a) that the H/O branching ratio was the same, and (b) the rate of O loss from C_6H_6O is equal to the reverse rate constant calculated from the equilibrium constant and assignment of the Ko et al. rate constant to the reaction $O+C_6H_6 \rightleftharpoons C_6H_6O$. The H elimination rate constant thus estimated is orders of magnitude lower than the minimum requirement, even at 400 K where the experiments of Bajaj (1994) shows the products to be primarily phenoxy+H. Since the toluene analogy (and/or the assumptions involved) did not describe the known 400 K situation even reasonably well, it was considered inadequate for description of the H elimination channel. This could be related to the tightness of the $C_6H_5CH_3$ transition state relative to that of C_6H_6O.

Cyclohexadienyl analogy: Both substituents in cyclohexadienyl are H atoms, leaving some question as to how appropriate the comparison might be. By assuming the A factors to be equal in the c-C_6H_7 and C_6H_6O cases, one can get what is probably an upper limit on loss of H from the adduct .

If the pre-exponential factors are assumed to be equal, $k_{PhO+H} \approx 1.8x10^{13}/2 = 9x10^{12}$ (on a per-H basis), which would be more than adequate to explain the lack of pressure dependence, with or without a 1 kcal/mol barrier. That is, it is greater than k_{min} at all temperatures. If the reverse pre-exponential is expressed in the more accurate AT^n form, $k_{PhO+H} \approx 1.13x10^{13}T^{0.16}/2 = 5.65x10^{12}T^{0.16}$ (per-H basis), which still meets the criterion, always being greater than $1.4x10^{13}$ cm^3/mol-s.

(It is worth noting that if one assigned the A factor to that of the reverse of the Ko et al. rate constant — assuming it applied to the process $O+C_6H_6 = C_6H_6O$ — the rate would be $1.42x10^{13}$ cm^3/mol-s (or $7.0x10^{17}T^{-1.36}$ in AT^n form), which is larger than the minimum. On the other hand, if the reverse Ko et al. rate constant applied to $O+C_6H_6 = C_6H_5O+H$, the rate would be $3.96x10^{12}$ [$1.46x10^{13}$ Burcat et al. thermo] or $8.7x10^{16}T^{-1.26}$, still very adequate for the phenoxy pathway to explain the data.)

Hydroxycyclohexadienyl analogy: To get a lower limit estimate, we can look at the case of addition and elimination of OH. The rate of elimination of OH from C_6H_6OH must be estimated. He et al. (1988) point out that the elimination of H is much less likely than OH, at higher temperatures. In that system, He et al. also note that if the reaction is written as

$$OH+C_6H_6 \underset{k_f}{\overset{k_{OH}}{\rightleftarrows}} C_6H_6OH \xrightarrow{k_H} C_6H_5OH+H,$$

then $k_{overall} = \dfrac{k_f k_H}{k_{OH} + k_H}$. Rearranging, one gets $k_H = \dfrac{k_{overall} k_f / K_{eq,add}}{k_f - k_{overall}}$, where $K_{eq,add} \equiv \dfrac{k_f}{k_{OH}}$. With $k_{overall}$ from He et al., and either the Tully et al. (1981) value or that of Witte et al. (1986) for the addition (k_f) step, the calculated k_H is always less than k_{min}. At 405 K, where the H elimination step is known to dominate, the calculated k_H is more than six orders of magnitude lower than the minimum rate constant. Therefore, as with $C_6H_6CH_3$, this analogy is not valid for description of the phenoxy-producing channel.

Conclusion. The only analogy to correctly predict the measurements at 405 K also predicts that the C_6H_5O+H channel would be sufficiently fast at all temperatures to explain experimental observations. However, the failure of the other two analogies emphasizes the difficulty in modeling the biradical chemistry of the C_6H_6O adduct with other, non-biradical systems. Other channels, such as isomerization of the adduct to phenol, are not ruled out by this analysis either.

$C_6H_6+OH \rightleftharpoons C_6H_5OH+H$ (Rxn -B6; EBG, ZM, LS); C_6H_6OH

As noted in the literature review of Chapter 2, He et al. (1988) measured the reverse rate constant, that of H+phenol, at 2.5-5 atm and 1000-1150 K. Their rate constant was used as the basis for a QRRK calculation for a low-pressure value. The addition/stabilization rate constant was measured by Witte et al. (1986). With $k_{a/s}$ and the overall value of He et al., a rate for H elimination from the adduct was determined.

A comparison with the abstraction rate was then made, to confirm the conclusion of He et al. and Madronich and Felder (1985) that abstraction is the dominant mechanism above about 400 K. Lin and Lin (1984) concluded otherwise on the basis of an RRKM calculation.

Falloff calculation parameters. THERM was used to estimate the heat of formation of the adduct, at 10.29 kcal/mol. From MOPAC, by comparison with c-C_6H_7 calculations and the experimental heat of formation for that species of Tsang (1986), $\Delta_f H^0_{298}(C_6H_6OH)$ = 9.63 kcal/mol. The two predictions are therefore rather close, and the vibrational frequencies and moment of inertia estimated by MOPAC were considered to be valid for the RRKM calculation of the collision efficiency.

In previous measurements, Witte et al. found the bond dissociation energy ("BDE") of C_6H_6-OH to be 16.5±1.4 kcal/mol; Perry et al. (1977) measured 18.4±3.1 kcal/mol and Lorenz and Zellner (1983) 18.4±1.4 kcal/mol; Manion and Louw (1989) estimated 19.6 kcal/mol. From the thermodynamics estimations in this work, one derives 18.8 kcal/mol. This should not be considered far off from experimental values, considering the noise of all the data in all studies. That is, the activation energies in various studies disagree quite a bit in spite of apparent good fit in all cases, because E_a itself is very low in relation to the noise. It should be noted that the $K_{eq,exp}$ from Witte et al. is in substantial agreement (within 25%) with K_{eq} calculated from the thermochemistry used in this thesis above 650K, but below that the two differ by as much as 87%. The Witte et al. equilibrium constant is consistently below the present estimate in that range. This is within the limits of error they place on their reverse rate constant. In the present flame the location of the low temperature region in which there is disagreement is only 0-1.2 mm, where comparison to experimental net rates is not considered reasonable.

Unfortunately, the only RRKM parameter given by Lin and Lin is the barrier for the decomposition channel, which they asserted to be 1 kcal/mol. This does not seem plausible, given

that the heat of reaction from the adduct to phenol+H is roughly 16.8-18.8 kcal/mol, depending on the thermochemistry used for phenol. In their estimation, the bond dissociation energy of C_6H_6-OH is 17 kcal/mol, close to that of Witte et al. but 1.8 kcal/mol lower than the estimate in the present work. Also, they report $\Delta_f H^0_{298}(C_6H_6OH)$ = 12.7 kcal/mol for the adduct, in contrast to the values given above. (Interestingly, Manion and Louw derived a heat of formation of 4.5 kcal/mol, from Tsang's heat of formation of c-C_6H_7 and an estimated group additivity contribution from comparison of cyclohexanol and cyclohexane.)

With regard to the moment of inertia, the factor of 2.2 used for the increase in O-C length to form the transition state in the C_6H_6O case above was also used for hydroxycyclohexadienyl. The fit of Arrhenius parameters to $k_{rev,\infty}$ of Witte et al., by adjustment of transition state frequencies, was done at 300K. For $\langle\Delta E\rangle_{all}$ constant (70 cm^{-1}), β_c goes above 1.0 above 1200 K, so a constant $\langle\Delta E\rangle_{dn}$ of 409 cm^{-1} was used.

Using CHEMACT with a mean frequency of 1060 cm^{-1} from the MOPAC calculation, a falloff curve was calculated at 300K and compared to that measured by Witte et al. There is not as much falloff in the calculated curve with $\langle\Delta E\rangle_{dn}$ = 409 cm^{-1}. A revised downward energy transfer of 83 cm^{-1} results in a good fit to experimental data. The RRKM file is shown below:

```
C6H6OH decomposition to OH+C6H6.  B_GLT.
1300  100  4   1  7  1  14
35  36
16.8
1  1
0.0647 0.0938
0  0
4.27  95.12  19.4  256  1  83
 138 1   531 1   552 1   643 1   694 1   727 1   817 1   853 1
1034 1 1075 1 1107 1 1157 1 1080 1 1088 1 1116 1 1196 1
1216 1 1336 1 1367 1 1375 1 1416 1 1480 1 1529 1 1553 1
1558 1 1645 1 1674 1 1690 1 3008 1 3242 1 3243 1
3252 1 3252 1 3264 1 3844 1
 138 1   301 1   322 1   413 1   464 1   497 1   587 1   623 1
 804 1   845 1   877 1   927 1   850 1   858 1   886 1   966 1
 986 1 1106 1 1137 1 1145 1 1186 1 1250 1 1299 1 1323 1
1328 1 1386 1 1415 1 1444 1 1460 1 2778 1 3012 1 3013 1
3022 1 3022 1 3034 1 3614 1
22.
300. 600. 900. 1200. 1500. 1800. 2100.
```

To derive rate parameters for the exit channel, a simple variation of the high-pressure limit A and E_a was performed, until the CHEMACT prediction fit the He et al. measurement.

A good fit is found with $k_{decomp} = 2.4x10^{14}exp(-26100/RT)$ s^{-1} [or $4.25x10^{13}exp(-26300/RT)$ s^{-1}, Burcat et al. thermochemistry]. Manion and Louw estimated the intrinsic barrier for H addition to phenol to be 5.4 kcal/mol, which in combination with the estimated heat of formation for the adduct would result in an activation energy of 24.4 kcal/mol, not far from the fitted value.

Then checking the falloff curve, one finds at the lowest pressure a bit more falloff now than experimentally observed (Sandia thermo case only), but the calculated falloff overall still compares very well.

Results. Performing a calculation at 1000K, within the range of both the He et al. measurements and the high Tully et al. measurements, one gets $k_{C6H6+OH=C6H5OH+H} = 3.6x10^{11}$ cm^3/mol-s at 100 torr (Tully et al experiments). This is about a factor of $1/6^{th}$ of Tully's measurements of $k_{C6H6+OH=products}$, confirming the likelihood that abstraction is the dominant channel. The confirmation is even stronger if Burcat et al. thermochemistry is used: $k_{C6H6+OH=C6H5OH+H} = 9.0x10^{10}$ cm^3/mol-s at 100 torr, a factor of about 15 less (as found by He et al. at 2.5-5 atm).

Interestingly, there is no pressure effect between 100 torr and 5 atm for this channel, and this holds true for all temperatures above about 700K. The Burcat et al. thermochemistry case is similar, with slightly less pressure effect at lower temperatures.

A comparison of the predicted $k_{a/d}$ vs. $k_{abstraction}$ (as determined by Madronich and Felder, 1985, 790-1410K) at high temperatures look like this:

T (K)	$k_{a/d}$ (cm^3/mol-s) (fit to He et al, Sandia thermo.)	$k_{a/d}$ (cm^3/mol-s) (fit to He et al, NASA thermo.)	$k_{abstraction}$ (cm^3/mol-s) (extrapolated if needed)
1,300	$7x10^{11}$	$2.5x10^{11}$	$3.6x10^{12}$
1,600	$9x10^{11}$	$4.4x10^{11}$	$5.0x10^{12}$
1,900	$1x10^{12}$	$6x10^{11}$	$6.3x10^{12}$

So the factor of 5-6 holds about constant in the high temperature range, in the Sandia case. In the Burcat case, a factor of 10-15 is found over the temperature range.

<u>C_6H_6F (fulvene) $\rightleftharpoons$ C_6H_6 (Rxn B19; LS)</u>

RRKM parameters. The reaction was calculated in the direction the reaction was written. Gaynor et al. (1981) performed an RRKM analysis, and reported most of the parameters they

used. The Gaynor et al. frequencies were used for fulvene and the complex, with $I^+/I = 1$ and rxn path degeneracy = 1, as in their analysis. Calculations with a range of I^+/I were also performed to determine the sensitivity to that factor. A MOPAC calculation was run to determine the moment of inertia of fulvene, which is $I_m = (10.21*22.72*32.93)^{333} \times 10^{-39} = 19.69 \times 10^{-39}$ g-cm^2, i.e. B = 0.142.

Comments. There is a noticeable difference in results, but not a large one, with respect to moment of inertia. A calculation was also performed using the Lindstedt and Skevis high-pressure limit. The effect on model predictions was essentially the same for the two rate constants.

RRKM input file:

```
Fulvene Isomerization to Benzene. Gaynor et al. (1981). beta_GLT
900  150  5   1  8  1  12
12 12
65.157
-1   1
0.142  0.142
0  0
4.20  78.11  19.4  245.2  2  70
3025 6  1665 2  1480 1  1300 8  1240 1  1000 2
  929 1   890 1   765 4   670 1   613 1   261 1
3025 6  1665 3  1480 2  1380 2  1300 4  1000 3
  929 2   890 1   765 4   670 1   450 1   350 1
22.
300. 600. 900. 1100. 1200. 1500. 1800. 2100.
```

$C_6H_6+H \rightleftharpoons C_6H_7$ (Rxn B23; LS); l-C_6H_7 (LS); $C_5H_4CH_3$; $C_5H_4CH_2+H$

Two types of calculations were performed. The first was RRKM computation using the high-pressure limit for various unimolecular decompositions. A β_c was chosen from those results, which was then used for a QRRK calculation of the mechanism as written above, with Ritter et al. (1990) rate coefficients.

Falloff calculation parameters. Vibrational frequencies for C_6H_7 were taken from Tsang (1986), as corrected by Tsang (1995). The transition state frequencies were adjusted to match the pre-exponential factor at 550 K. Frequencies for $C_6H_5CH_3$ were calculated with MOPAC.

For the high-pressure limit of $C_6H_5CH_3 \rightleftharpoons C_6H_5CH_2+H$, $E_a = \Delta H_r+2.5$ kcal/mol and $A = 1.2x10^{13}$ were used, as suggested by Dean (1985). Moments of inertia were assumed not to change during the reaction.

Collision efficiencies were calculated under both energy assumptions (constant $<\Delta E>_{down}$ and constant $<\Delta E>_{all}$), and for dissociation channels of (1) c-C_6H_7 to benzene and H atom, (2) c-C_6H_7 to l-C_6H_7, and (3) $C_5H_4CH_3$ to $C_5H_4CH_2$+H. In some cases, using $<\Delta E>_{all}$ produced β_c's greater than 1.0, so that energy assumption was eliminated. The collision efficiency for H elimination from c-C_6H_7, with constant downward energy transfer, was approximately a median value of the results from all computations, so the β_c from that calculation used for the QRRK analysis.

The mean frequency used for QRRK purposes, from c-C_6H_7 frequencies, was 1170 cm^{-1}.

RRKM input files:

```
Cyclohexadienyl decomposition to H+C6H6. Tsang (1986). B_GLT
900  150 5   1  8  1  13
26  27
25.97
1  2
0.142  0.142
0  0
4.20  79.12  19.4  245.2  1  409
 106 1   483 1   703 1   713 1   723 1 1108 1   993 2 1029 1
1431 1 1693 2 1723 1   773 1   779 1 1023 4 1173 1
1203 1 1223 1 1232 1 1270 1 1493 1 1523 1
2895 1 2948 1 3150 1 3092 1 3105 2
 106 1   410 1   630 1   640 1   650 1 1035 1   920 2
 956 1 1358 1 1620 2 1650 1    700 1   706 1
1100 1 1130 1 1150 1 1159 1 1197 1    950 4
1420 1 1450 1 2822 1 2875 1 2877 1 3077 1
3019 1 3032 2
22.
550. 300. 600. 900. 1200. 1500. 1800. 2100.
```

```
C5H4CH3 decomposition to C5H4CH2+H. Ritter et al (1990). B_GLT
900  150  5   1  8  1  13
32 33
47.5
2  1
0.134  0.134
0  0
4.20  79.12  19.4  245.2  1  409
131 1 196 1 325 1 414 1 537 1 603 1 689 1 801 1
855 1 800 1 824 1 827 1 872 1 913 1 966 1 972 1
1032 1 1069 1 1162 1 1227 1 1285 1 1295 1 1339 1 1362 1
1388 1 1439 1 2829 1 2839 1 2915 1 3041 1 3043 1 3050 1
131 1 231 1 360 1 449 1 572 1 638 1 724 1 836 1
890 1 835 1 859 1 862 1 907 1 948 1 1001 1 1007 1
1067 1 1104 1 1197 1 1262 1 1320 1 1330 1 1374 1 1397 1
1423 1 1474 1 2864 1 2874 1 2950 1 3076 1 3078 1 3085 1
3092 1
22.
550. 300. 600. 900. 1200. 1500. 1800. 2100.
```

```
Cyclohexadienyl decomposition to l-C6H7. Ritter et al (1990). B_GLT
900  150  5   1  8  1  13
26  27
48.5
1  2
0.142  0.142
0  0
4.20  79.12  19.4  245.2  1  409
 106 1  483 1  703 1  713 1  723 1 1108 1  993 2  1029 1
1431 1 1693 2 1723 1  773 1  779 1 1023 4 1173 1
1203 1 1223 1 1232 1 1270 1 1493 1 1523 1
2895 1 2948 1 3150 1 3092 1 3105 2
 106 1  410 1  630 1  640 1  650 1 1035 1  920 2
 956 1 1358 1 1620 2 1650 1  700 1  706 1
1100 1 1130 1 1150 1 1159 1 1197 1  950 4
1420 1 1450 1 2822 1 2875 1 2877 1 3077 1
3019 1 3032 2
22.
550. 300. 600. 900. 1200. 1500. 1800. 2100
```

<u>1,3-$C_6H_8 \rightleftharpoons C_6H_6+H_2$ and 1,4-$C_6H_8 \rightleftharpoons C_6H_6+H_2$</u>

RRKM parameters. Vibrational frequencies for the 1,3- and 1,4- isomers are given by Di Lauro et al. (1969) and Stidham (1965) respectively. For 1,4-C_6H_8 there were three frequencies not measured, all CH_2-related (rock, wag and twist). For the purpose of the calculations here,

Stidham's value for the other CH_2 rock, wag and twist modes were simply set to be degenerate to account for the missing vibrations.

The reaction coordinate in both cases was assumed to be a C-H stretch, and it was assumed that there was no change of moment of inertia. For the 1,3- decomposition, the energy transfer parameter was calculated by fitting the Orchard and Thrush (1973) data, and was found somewhat insensitive to the exact value; $\langle\Delta E\rangle_{all} = 70$ cm^{-1} gives an excellent fit to their measurements. The same energy transfer assumptions were initially used for 1,4-C_6H_8. No problem was observed with F_E in the 1,3- case, but it gets too large at 2100K for the 1,4- calculation. Setting $\langle\Delta E\rangle_{all} = 50$ cm^{-1} prevents this, with little change to the rate constant (maximum about 20% at 1800K), so this was done. Indeed, falloff for the 1,3 reaction only begins close to 1200K.

The heats of formation for 1,3- and 1,4-C_6H_8 given in Orchard and Thrush (1974) are those of Benson (1968), and are very close to those estimated by THERM; within 0.5 kcal/mol for each. The heat capacities from THERM agree extremely well with those from the vibrational frequencies.

RRKM input files:

```
1,3-c-C6H8 = benzene+H2.  Orchard & Thrush et al. (1973)
1300  70  4  1  7  1  14
31 31
60.5
1  2
0.0875  0.0875
0  0
4.20  80.11  19.4  245.2  2  70
221 1 318 1 488 1 526 1 579 1 678 1 765 1 773 1
870 1 947 1 965 1 1014 1 1036 1 1060 1 1079 1 1131 1
1170 1 1185 1 1198 2 1243 1 1263 1 1350 1 1397 1 1455 1
1460 1 1597 1 1622 1 2858 2 2904 1 2959 1 3070 3
201 1 298 1 468 1 506 1 559 1 658 1 745 1 753 1
850 1 927 1 945 1 994 1 1016 1 1040 1 1059 1 1111 1
1150 1 1165 1 1178 2 1223 1 1243 1 1330 1 1377 1 1435 1
1440 1 1577 1 1602 1 2838 2 2884 1 2939 1 3050 4
22.
300. 600. 900. 1200. 1500. 1800. 2100.
```

```
1,4-c-C6H8 = benzene+H2. Ellis & Frey (1966).
1300  84  4  1  7  1  14
30 30
44.2
2  4
0.0875  0.0875
0  0
4.20  80.11  19.4  245.2  2  50
 210 1  495 1  648 1  775 1  819 1  867 1  951 1 1099 1
1132 1 1201 3 1230 1 1245 1 1280 1 1345 2 1404 1 1438 1
1442 1 1603 2 1622 1 1650 1 1671 1 1675 1 1884 1 1925 1
3067 1 3070 1 3120 1 3122 1 3264 2 3277 1
 210 1  250 1  403 1  530 1  574 1  622 1  706 1  854 1
 887 1  956 3  985 1 1000 1 1035 1 1100 2 1159 1 1193 1
1197 1 1358 2 1377 1 1405 1 1426 1 1430 1 1639 1 1680 1
2822 1 2825 1 2875 1 2877 1 3019 2 3032 2
22.
300. 600. 900. 1200. 1500. 1800. 2100.
```

$C_6H_5O+H \rightleftharpoons C_6H_5OH$ (Rxn PhOH3; EBG, ZM, LS)

RRKM parameters. Vibrational frequencies and moments of inertia for phenol were taken from Burcat (1985). The moment of inertia of the transition state was assumed to be equal to that of the reactant, but an internal rotation was included ($B_{int} = 20.95$, $\sigma = 2$ from Burcat et al.). For the moment of inertia of the rotation, the following equation was derived from the formula for coaxial symmetrical rotors in Benson (1976), by equating $\frac{1}{I_{C6H5}}$ for the cases of phenol and its transition state:

$$\frac{1}{I_{r,ts}} = \frac{1}{I_r} - \frac{1}{I_{OH}} + \frac{1}{I_{OH,ts}} \qquad \text{(C-3)}$$

Given an OH bond distance of 0.96 Å, the moment of inertia for OH is 0.867 amu-Å^2 (0.145 g-cm^2). If the factor of 2.2 for bond increase to form the transition state is applied, as assumed in reactions documented above, the moment is 4.198 amu-Å^2 (0.701 g-cm^2). Therefore, $1/I_{r\_ts} = 7.485 - 6.897 + 1.427 = 2.015$, or $I_{r\_ts} = 0.496$ and $B_{int\_ts} = 5.64$. The rotation was assumed to replaced the C-O-H bend in phenol, with a frequency of approximately 1200 cm^{-1} (per Benson). Using the internal rotation resulted in virtually no difference in results.

The RRKM input file is shown below:

```
C6H5OH decomposition to H+C6H5O.  B_GLT.
1300  75  4   1  8  1  13
31  32
80.15
1  1
0.0993 0.0993
1  1
5.64  2  1
20.95  2  1
4.27  94.11  19.4  256  2  70
225 1 223 1 317 1 323 1 417 1 440 1 533 1 600 1
665 1 731 1 737 1 795 1 872 1 887 1 913 1 939 1
984 1 1064 1 1082 1 1090 1 1191 1 1257 1 1386 1
1415 1 1517 1 1524 1 2941 1 2963 1 2977 1 2984 1 3001 1
225 1 309 1 403 1 409 1 503 1 526 1 619 1 686 1
751 1 817 1 823 1 881 1 958 1 973 1 999 1 1025 1
1070 1 1150 1 1168 1 1176 1 1277 1 1343 1 1472 1
1501 1 1603 1 1610 1 3027 1 3049 1 3063 1 3070 1 3087 1
3656 1
22.
1100. 300. 600. 900. 1200. 1500. 1800. 2100.
```

Choosing either constant $\langle\Delta E\rangle_{down}$ or constant $\langle\Delta E\rangle_{all}$ has some effect on the results, but not much. With its high activation energy, the energy dependence of the density of states for phenol is well-behaved. Constant $\langle\Delta E\rangle_{all}$ was chosen, since that assumption was used by Kiefer et al. for benzene pyrolysis.

The calculation was also performed with the high-pressure limit rate constant of Manion and Louw (1989).

$C_6H_5+O_2 \rightleftharpoons C_6H_5O+O$ (Rxn Ph1; EBG, ZM, LS); $C_6H_5O_2$, $C_6H_4O_2$+H

This reaction is discussed in some depth in Chapters 2 and 7. The reader is referred to those locations for background information. Yu and Lin (1994) performed an RRKM calculation, and report some of the parameters used. They also presented falloff curves for addition/ stabilization at 760, 40 and 1 torr, plus the rate constants calculated for each channel at 975 torr or greater (the pressure of the experiments of Frank et al., in press).

Yu and Lin's parameters are somewhat incomplete, as they give heats of formation at 0 K (unclear as to what the standard state is), and no stabilization parameters. Zero Kelvin heats of formation are useful for RRKM calculations, but high-pressure limits are needed for a QRRK

analysis. Because of the ambiguity of the standard state, such rate constant cannot easily be computed from $\Delta H^0_{f,0K}$. Fortunately, Yu and Lin give k_∞ for the addition/stabilization reaction, so with an RRKM calculation to determine the high-pressure limit for the decomposition of the adduct back to reactants a QRRK calculation to fit the remaining parameters is feasible.

Falloff calculation parameters. From microscopic reversibility, the pre-exponential factor for decomposition of the adduct is calculated to be $1.99 \times 10^{21} T^{-1.355}$ s^{-1}, or $4.27 \times 10^{22} T^{-1.887}$ s^{-1} with Burcat et al. (1985) thermochemistry for phenyl radical. The activation energy depends on the heat of formation of the adduct at 298 K, and would be expected to range from 41,177 cal/mol ($\Delta H_{f,298} = \Delta H_{f,0}$-4.5 kcal/mol[46]) to 32,177 cal/mol ($\Delta H_{f,298} = \Delta H_{f,0}$+4.5 kcal/mol). (With Burcat et al. thermochemistry, the activation energy range would be 40492 to 31492 cal/mol — about 0.7 kcal/mol less than the Sandia thermochemistry case.)

The vibrational frequecies and moments of inertia are found in the Yu and Lin article, and the critical energy E_0 is taken as 40 kcal/mol, the difference in 0 K heats of formation. The energy transfer are irrelevant, since high-pressure results are desired. Nevertheless, the Troe formalism was chosen for the β_c calculation, and $\langle \Delta E \rangle_{all}$ = -1 kcal/mol was used, to be consistent with the Yu and Lin methods. There was little sensitivity to the symmetry number of the internal

```
C6H5OO decomposition to O2+C6H5. Yu and Lin (1994)
1300  75  4  4  7  1  13
7  32
40.00  32.5
1  1
0.062 0.073
1  1
0.88 1 3
1.69 1 1
4.61  109.11  32.0  220  2  -350
90 1 374 2 600 4 880 8 1170 4
1450 5 3029 5
227 1 261 1 409 1 433 1 493 1 598 1 602 1 680 1
758 1 788 1 842 1 918 1 974 1 981 1 1000 1 1004 1
1053 1 1090 1 1128 1 1148 1 1192 1 1220 1 1315 1
1453 1 1488 1 1609 1 1611 1 3004 1 3014 1 3026 1
3035 1 3064 1
1.  22.  40.  760.
300. 600. 900. 1200. 1500. 1800. 2100.
```

[46] 4.5 kcal/mol is the difference in energy between the heats of formation 0 K and 298 K, if the standard state for both were 298 K.

rotations (not given by Yu and Lin) and the type of treatment of external rotations. The RRKM input file is shown above.

The best fit of the high-pressure limit from the RRKM calculation gives $1.33x10^{17}T^{-0.199}$ exp(-41349/RT) s^{-1}, with E_a apparently within the range cited. The A factors are quite different, though, so k_∞ was refit so that A = $1.99x10^{21}T^{-1.355}$. In that case, the best value for E_a was 44,500 cal/mol. For this to be true, the 298 K heat of formation for the adduct would have to be 35.2 kcal/mol, which is actually only 1.8 kcal/mol less than THERM predicts. For the Burcat et al. thermochemistry case, setting A = $4.27x10^{22}T^{-1.887}$ gives E_a = 43,350 cal/mol, which would imply that the 298 K heat of formation for the adduct is 35.6 kcal/mol. A good fit to the RRKM high-pressure limit for adduct decomposition can be made with the simple equation $2.87x10^{17}$ * exp(-41091/RT). This expression was used for the QRRK analysis.

The mean vibrational frequency was 1026 cm^{-1}, from Yu and Lin frequencies. The remaining parameters to be determined were the rate constants for the adduct decomposition channels to C_6H_5O+O and $C_6H_4O_2$+H. Those were obtained empirically by fitting the results for all three channels to the falloff and 975$^+$ torr curves. The collision efficiencies calculated in the RRKM analysis were found to be too low to enable good reproduction of the Yu and Lin results. Rather, the Troe (1977) formalism with F_E = 1.15, CHEMACT's standard collision efficiency formula, was used to better results. The fitted high-pressure limits for the phenoxy and $C_6H_4O_2$ channels were found to be $1.8x10^{19}$exp(-55400/RT) s^{-1} and $3.5x10^{19}$exp(-58500/RT) s^{-1} respectively. These are on the order of 20 kcal/mol above the difference in 0 K heats of formation for each channel given by Yu and Lin. In any event, the results are reasonable, with agreement to a factor of three for the addition/stabilization calculations at 1 torr and 40 torr. With respect to their higher pressure Arrhenius plot though, the CHEMACT results for the addition/elimination reactions only agree with RRKM above 900 K. Below that temperature, QRRK predicts those rate constants to be smaller than the RRKM results. This seems reasonable, since the Frank et al. measurements to which the Yu and Lin calculation was optimized for elimination reactions were made in the range 900-1800K. It is probably satisfactory to consider the 22 torr prediction made here as an adequate first order approximation to these rate constants. It is not clear whether use of more realistic collision efficiencies would improve results, since Yu and Lin derived their transition state properties by fitting to data with a computation that did not use such β_c's.

$C_6H_5 \rightleftharpoons HC{\equiv}CCH{=}CHCH{=}CH$ (Rxns Ph7, Ph14; ZM, LS), $1\text{-}C_4H_3+C_2H_2$ (Rxn 13; ZM); $1\text{-}C_6H_4+H$

Decyclization: RRKM parameters. The vibrational frequencies of phenyl were taken from Rao and Skinner (1988). In that source, however, an extra phenyl frequency was included and a transition state frequency was missing. The 1150 cm^{-1} frequency of phenyl was removed, since that was close to the geometric mean frequency and also resulted in a revised mean frequency close to that one would obtain with the frequencies of Burcat et al. (1985). The 934 cm^{-1} frequency of the transition state was doubled, since that kept the mean frequency constant. For the transition state, the reaction coordinate was assumed to be the ring bending or puckering at 369 cm^{-1}. The ratios of moments of inertia for molecule and transition state were assumed to be the same as those Dewar et al. (1987) give for the reaction ($B^+/B = I/I^+ = 181.47/208.88 = 0.87$), with no internal rotations.

The energy dependence of the density of states and the collision efficiency were well-behaved.

RRKM input file:

```
Phenyl decyclization; Rao and Skinner (1988). B_GLT
1300  75  4   2  8  1  11
22  20
78.3
1  2
0.096  0.154
0  0
4.20  77.11  19.4  245.2  2  70
3193 1 3188 1 3187 1 3172 2 919 1 1318 1 731 1 250 1
1020 1 687 1 1160 1 889 2 350 1 1314 1 1059 2 665 1
925 1 1402 1 755 1 485 2 1003 1 328 1
3068 1 3063 1 3062 1 3047 2 1596 2 1486 2 1038 1 1326 1
1310 1 600 2 1010 1 995 1 992 1 975 1 849 2 410 2
703 1 700 1 606 2 673 1
304. 22.
1700. 300. 600. 900. 1200. 1500. 1800. 2100.
```

Network via [HC≡CCH=CHCH=CH]: QRRK parameters.*

Rate constants for the reaction network

$$C_6H_5 \rightleftharpoons [HC{\equiv}CCH{=}CHCH{=}CH]^* \begin{array}{l} \xrightarrow[k_{stab}]{} HC{\equiv}CCH{=}CHCH{=}CH \\ \xrightarrow[k_{C-C}]{} 1\text{-}C_4H_3{+}C_2H_2 \\ \xrightarrow[k_{C-H}]{} 1\text{-}C_6H_4{+}H \end{array}$$

were calculated using the unimolecular QRRK program of Westmoreland (1992a). The parameters of Westmoreland (1986) and Westmoreland et al.(1989) were used, except for the mean frequency for phenyl and the energy difference between C_6H_5 and HC≡CCH=CHCH=CH. The mean frequency was calculated from the frequencies used in the RRKM calculation. The heat of formation for HC≡CCH=CHCH=CH was taken from Kee et al. (1993); athough it was derived from an *ab initio* calculation, it was within 0.4 kcal/mol of an estimation using THERM. The heat of formation of phenyl used was that of Burcat et al. (1985).

QRRK input file:

```
Thermal rxns of: C6H5
Sequential isomerization - no branching
 Number of sequential isomers, reactant to last isomer 2
   No. of dissociation channels from 1= 0
 Stabilization product -     Isomer 2: l-C6H5
   No. of dissociation channels from 2= 2
          Dissociation channel 1: 1-C4H3+C2H2
          Dissociation channel 2: l-C6H4+H
Mean freq of isomer=   1103.0 wavenumbers,s=  27 oscillators
Complex: MW=  77.11, L-J diam. =  5.350 angstroms, L-J well =  412.30 K
Bath gas: ALL
 MW=  19.40, d= 3.046, e/K= 229.00, E(coll)=  200.0
 Isomerization reaction 2:  C6H5              -> l-C6H5
  .....A=  1.200D+14, E=  70.90
 Reverse isomerization 2:  l-C6H5            -> C6H5
  .....A=  4.000D+10, E=   7.00
 E(isomer 2)-E(isomer 1)=  61.6, isomer freq=  990. wavenumbers
       Dissociation 1: l-C6H5           -> 1-C4H3+C2H2
       .....A=  5.500D+14, E=  45.80
       Dissociation 2: l-C6H5           -> l-C6H4+H
       .....A=  8.000D+12, E=  36.70
```

$C_6H_7+H \rightleftharpoons C_6H_8$ (Chapter 7)

Using the recombination rate constant listed in Table C.3 and microscopic reversibility, the high-pressure limit for the unimolecular direction (for 1,3-C_6H_8) is $1.47x10^{16}T^{-0.316}$ * exp(-76501/RT) cm^3/mol-s. The frequencies of 1,3-C_6H_8 were those Di Lauro et al. (1969). As was typical for H eliminations from large molecules, the moment of inertia was assumed to be constant. While F_E and β_c were well-behaved, it was very difficult to get good agreement for the pre-exponential factor using several methods of varying transition state frequencies. It was found that k_{uni}/k_∞ as a function of temperature was reasonably constant, regardless of the method used for the frequencies. Because of this, k_{uni} was calculated as $\left(\frac{k_{uni}}{k_\infty}\right) \times k_\infty$.

The RRKM input file for this reaction is shown below.

```
1,3-c-C6H8 = C6H7+H.  Addition rate = 1E14 mol/cm3/s
1300  70  4  1  7  1  14
31 31
74.
1  2
0.0875  0.0875
0  0
4.20  80.11  19.4  245.2  2  70
101 1 198 1 368 1 406 1 459 1 558 1 645 1 653 1
750 1 827 1 845 1 894 1 916 1 940 1 959 1 1011 1
1050 1 1065 1 1078 2 1123 1 1143 1 1230 1 1277 1 1335 1
1340 1 1477 1 1502 1 2738 2 2784 1 2839 1 2950 3
201 1 298 1 468 1 506 1 559 1 658 1 745 1 753 1
850 1 927 1 945 1 994 1 1016 1 1040 1 1059 1 1111 1
1150 1 1165 1 1178 2 1223 1 1243 1 1330 1 1377 1 1435 1
1440 1 1577 1 1602 1 2838 2 2884 1 2939 1 3050 4
22.
300. 600. 900. 1200. 1500. 1800. 2100.
```

$C_6H_5CO \rightleftharpoons C_6H_5+CO$ (Rxn Ph5; EBG)

RRKM parameters. All falloff parameters except for <ΔE> were taken from Solly and Benson (1971). The high-pressure limit rate constant was verified at 640 K. Constant $\langle\Delta E\rangle_{down}$ was chosen over constant $\langle\Delta E\rangle_{all}$ because with the latter assumption extremely large $\langle\Delta E\rangle_{down}$ values were calculated at high temperatures. With the downward energy constant, the total

average energy transfer approached 0 cm^{-1}, not an unreasonable situation. Above a temperature of 1500 K, the energy dependence of the density of states exhibited the acceleration noted above for certain other reactions. Correction to the F^{WC} at 1500 K was performed.

The input file is shown below:

```
C6H5CO decomposition to CO+C6H5. Solly and Benson (1971).
1600  80  5  1  8  1  13
14  14
27.9
2  1
0.057 0.072
1  0
0.93  3  1
4.27  105.12  19.4  294  1  400
  80 1  175 2  310 1  440 3  695 1  785 3  940 3
1035 3 1160 2 1290 2 1483 1 1600 3 1950 1 3060 5
  80 1  154 1  350 2  440 3  655 2  785 3  940 3
1035 3 1160 2 1260 3 1483 1 1600 3 1700 1 3060 5
22.
640. 300. 600. 900. 1200. 1500. 1800. 2100.
```

Over the range 300-2000 K, k_{uni} never drops below $2x10^{-7}$ cm^3/mol-s. A fit of the calculated 22 torr rate constant to modified Arrhenius format from 300 to 1600 K produces the expression $4.52x10^{52}T^{-12.854}exp(-36947/RT)$ cm^3/mol-s. The error of the fit is -36% at 2000 K, 96% at 400 K and 257% at 300 K. With the alternative method of fitting over the entire temperature range, the rate constant of $4.08x10^{47}T^{-11.373}exp(-34303/RT)$ produces good results above 500 K. However, at 400 K the fit error is 250% and at 300 K it is 1200%.

Appendix D. FBR — Data Reduction Program.

Instructions for program usage:

FBR: A FORTRAN PROGRAM FOR FLUX AND RATE ANALYSES OF
EXPERIMENTAL DATA AND FLAME CODE SOLUTIONS
VERSION 1.12

Abstract

This program reads a text file of steady laminar one-dimensional premixed flame data, or the binary solution output file produced by the Sandia flame code Version 2.5b (Kee et al., 1985), and analyzes it with respect to flux and reaction rate. In doing so, it reads information from chemical kinetics and transport properties link files, and optionally prints the data (or solution) and the chemical mechanism from the CHEMKIN II link file. Calculated at each height above the burner are: rates and partial equilibrium ratios for those reactions in the mechanism which contain a specified species, molar fluxes for each species in the flame, net rates of reaction calculated from the flux profiles, an elemental flux balance for three elements of choice, diffusion coefficients for each species, and various flame properties (density, viscosity, etc). The data and molar flux profiles can be smoothed by the Savitsky-Golay method. The method of calculating diffusion coefficients (multicomponent or mixture-averaged, with or without thermal diffusion) can be specified by the user.

Table of Contents

Introduction

The flame code of Kee, Grcar, Smooke, and Miller, published by Sandia National Laboratories (Kee et al., 1985) as an adjunct to the CHEMKIN II package of Kee et al. (1991), is an invaluable tool for those who model laminar, premixed flames. The output of that program is concentration profiles and sensitivities, but not reaction rate and flux information. Researchers wishing to know the contributions of individual reactions to the net rate of a species, and experimentalists analyzing their data to produce net rates or check internal consistency, have to write separate programs for those purposes. FBR combines the analyses required for experimentalists and modelers, using the CHEMKIN II subroutine library to calculate the necessary molecular properties. The TRANLIB transport properties subroutine library (Kee et al., 1986) is also used.

The program also calculates the basic physical properties of the flame: gas velocity, mass density, viscosity, heat capacity, and thermal conductivity. This is useful information for those who might be running a model to predict those properties, or for experimentalists who need to better characterize their flames.

Anyone who uses CHEMKIN frequently for modelling purposes eventually runs into the situation where he or she encounters a link or binary solution file whose origin has been forgotten. The user may have forgotten the name of a link or solution file for a valuable mechanism. It could even happen that the interpreter or flame code text file has been lost, but the binary file remains. FBR reads and prints the information in binary solution and CHEMKIN link files, solving the modeler's dilemma. The program also creates a flame code binary file from the text file information. By having FBR read a binary file and create a text file on one system, then create a new binary file from that text file on a second system, one can transfer a flame code calculation between the different systems.

Installation

Simply compile file "fbr.f", then link with the CHEMKIN II, TRANLIB, and DMATH libraries. Sample input and output files are included in this manual so that it can be checked to see that the program runs correctly on your computer system.

Governing Equations

1. Reaction rates

The chemical reaction rate expressions for reaction path analysis are those given by Kee et al. in the CHEMKIN II manual, equations 48-78. In contrast, though, FBR separates the forward and reverse rates, and itemizes them by reaction, according to the formalism $\dot{w}_{ki,f} = \upsilon_{ki} q_{i,f}$, where

$\dot{w}_{ki,f}$ = forward rate for species k and reaction i, mol/cm^{3}s
υ_{ki} = stoichiometric coefficient from routine CKNU
$q_{i,f}$ = forward portion of the rate of progress variable (a la CKKFKR),

and also $\dot{w}_{ki,r} = -\upsilon_{ki} q_{i,r}$. In this manner, the traditional $\dot{w}$ of equation 49 (CHEMKIN II manual) and subroutine CKWC is $\dot{w} = \sum_{i=1}^{I} (\dot{w}_{ki,f} + \dot{w}_{ki,r})$.

The total positive and negative rates are calculated by summing over the reactions all of the terms of $\dot{w}_{ki,f}$ and $\dot{w}_{ki,r}$ with positive and negative sign, respectively. Thus, the positive rate is the net formation rate and the negative rate the net destruction rate.

The more traditional method of defining the directional rate is simply to use the appropriate part of the rate of progress variable (cf. CHEMKIN II routine CKKFKR). The advantage of the present formalism is that the specified rate for a given species and reaction is the NET production or destruction of the species caused by that reaction in that direction, as opposed to the total moles produced or destroyed. Artificial production or destruction arising from writing the equation with a species as an explicit third body or as part of a complicated or unreduced reaction mechanism is eliminated. For example, one can write

$$C_6H_6 + C_6H_6 + H \rightleftharpoons C_6H_6 + C_6H_5 + H_2$$

or

$$2H_2 + 2O_2 \rightleftharpoons 2OH + H_2 + O_2$$

and not suffer an inflated destruction rate for the forward reaction.

For the net rate calculation performed on experimental data, the flame equation

$$\dot{w}_k = \frac{1}{A}\frac{dF_k}{dz}$$

is used, with

$\dot{w}_k$ = as above, net molar chemical production rate of species k
A = area expansion ratio (cross-sectional area of flame stream tube)
F_k = molar flux of species k, mol/cm^{2}s
z = height above burner (HAB), cm.

2. Partial equilibrium.

A common way of exploring partial equilibrium is to compare the concentration product ratio, K, to that ratio at equilibrium, K_{eq}. Hsu (1992) expresses the partial equilibrium ratio K/K_{eq} simply, as the ratio of the reverse rate to the forward rate, R_r/R_f. For example, for the reaction $H + O_2 \rightleftharpoons OH + O$ one writes:

$$R_r/R_f = \frac{k_r[OH][O]}{k_f[H][O_2]} = \frac{[OH][O]/([H][O_2])}{(k_f/k_r)} = \frac{K}{K_{eq}}$$

noting that $K_{eq} = k_f/k_r = \left(\frac{[OH][O]}{[H][O_2]}\right)_{eq}$.

Then, noting the fact that $R_f = q_f$ and $R_r = q_r$, it is easily seen that $K/K_{eq} = -\frac{\dot{w}_{ki,r}}{\dot{w}_{ki,f}}$. This is the formula used by FBR for the partial equilibrium ratio.

3. *Flux and elemental flux balance.*

The molar flux is defined as $F_k = AX_k(P/RT)(v + V_k)$, where:

X_k = mole fraction of species k
P = pressure, atm
R = gas constant, cc-atm/mol/K
T = temperature, K
v = mass average velocity, cm/sec
V_k = diffusion velocity (flame code manual, eqns. 6-9; multicomponent diffusion coefficient is given in Fickian form when used), cm/sec.

In this program though, the molar flux is calculated from the mass flux fraction from the relationship $F_k = G_k\dot{M}/MW_k$, with

G_k = mass flux fraction of species k
MW_k = molecular weight of species k, g/mol
$\dot{M}$ = (total) mass flow rate, g/cm^{2}s.

The mass flux fraction is therefore $G_k = \frac{MW_k}{\dot{M}} Ax_k \frac{P}{RT}(v + V_k)$, which reduces to this computationally convenient equation in mass fraction Y_k:

$$G_k = Y_k + (Y_k V_k) / v$$

A subroutine from the flame code (MDIFV) calculates the YV product. From the mass flux fraction, the element flux balance is then performed, by calculating

$$PD_m = \sum_{k=1}^{K} \left(\frac{G_k f_{mk}}{e_{init,m}} - 1\right) \times 100\%$$

where

PD_m = % deviation of the total mass flux fraction of element m
f_{mk} = fraction of mass of species k due to element m
$e_{init,m}$ = mass flux fraction of element m in unburnt gas mixture.

4. Savitsky-Golay smoothing

The species and molar flux profiles may be smoothed by the simplified least squares procedure known as the Savitsky-Golay procedure (Savitsky and Golay, 1964 and Steinier et al., 1972). In that method, the profile is fit to a polynomial, at each point using just the points within

a moving window of fixed size. The formalism used in FBR is that of Steinier et al. (1972). That is, the smoothed profile is the convolution of the original profile with the first row of the matrix $T = (X_t X)^{-1} X$, with:

m = integer defining the convolution window size; number of points on each side of the point being smoothed to be convolved

k = 1 + (degree of the polynomial weighting function)

$$X = \begin{bmatrix} 1 & (-m)^{-1} & \dots & \dots & (-m)^{k-1} \\ . & . & & & . \\ . & . & & & . \\ . & . & & & . \\ 1 & 0 & \dots & \dots & 0 \\ . & . & & & . \\ . & . & & & . \\ . & . & & & . \\ 1 & (+m)^{1} & \dots & \dots & (+m)^{k-1} \end{bmatrix}$$

= coefficient matrix which gives the least square estimation D of the data within the window (Y) as $D = X(X_t X)^{-1} X_t Y$

X_t = transpose of X

Because the product matrix $X_t X$ is by definition symmetric, the simple Doolittle algorithm (Bargmann, 1973) is used to invert it.

One of the weaknesses of the procedure is its handling of points close to the "edges" of a profile; that is points 1,...,m and jj-m+1,..,jj. (jj is the total number of points in the profile.) For those points, one end of the window extends past the edge. One is tempted to just shrink the window as one approaches an edge, but the loss of smoothing then becomes significant because the noise starts to look like a reasonably-shaped polynomial. A satisfactory alternative is to use a simple moving average in the edge regions. FBR allows one to choose either method.

In this implementation of the moving average treatment of the edge region, the edge point itself is smoothed by a weighted average which accounts for the window size:

$$Y_{1,sm} = (1 - 0.01m)Y_1 + 0.01mY_2$$

The point just inside the edge is assigned the average of itself and the two points to either side of it, $Y_{2,sm} = (Y_1 + Y_2 + Y_3)/3$, and points 3,...,m and jj-m+3,...,jj are smoothed to the average of themselves and the four points on either side, or $Y_{j,sm} = (Y_{j-2} + Y_{j-1} + Y_j + Y_{j+1} + Y_{j+2})/5$.

5. Numerical considerations

The method of differentiation used in FBR is the same as that used in the flame code, i.e., the finite difference approximation. However, FBR does not refine the mesh, so it is important that the initial data or solution be on a sufficiently fine mesh. A good flame code solution — one with sufficiently low values for the adaptive mesh parameters — should cause no problems.

The Savitsky-Golay method of data smoothing is intended for data with a fixed, uniform abscissa interval. Having a non-uniform interval may cause a significant degradation in the quality of results, though not in all circumstances. It is strongly recommended that the smoothed profiles be checked if the mesh is not uniform. The best results are achieved when the profiles

are pre-processed onto a uniform, fine mesh.

The fluxes are evaluated at the mesh midpoints because the diffusion velocity is computed there; it is important to realize this when using the results in conjunction with other quantities measured or computed at the mesh points themselves. Net reaction rates are calculated in a manner analagous to the second order central difference method used in the flame code to calculate the conduction term of the energy equation. The area expansion ratio outside of the derivative is calculated at the midpoints of the flux mesh. This is only the same as the initial mesh if the original points are evenly spaced. Again, the user should keep this in mind when plotting the computed net rates or considering them in light of other quantities (such as mole fractions or fluxes).

When transferring a flame code calculation from one computer system to another via a text file, it should also be borne in mind that some precision is lost when the text file is created from the initial binary solution file.

The CGS system of units is used throughout, except for pressure (atm instead of dynes/cm^2) and energy (cal instead of erg).

Program Operation

1. Required files.

- CONTROL FILE. File that contains information needed to run and control operation of the program. This file is fed to the program via redirection. For example, if the control file is called "fbr.dat", the command line would be 'fbr < fbr.dat'.
- CHEMICAL REACTION LINK FILE. This is the standard link file produced by the CHEMKIN II interpreter, Version 3.1. In the case of a binary (flame code produced) species profile file, the link information may be read from that file. The link file name is not restricted.
- TRANSPORT INFORMATION LINK FILE. Produced by program TRANFIT, Version 1.7, though the link file version is called Version 1.9. This information is taken from the binary file when chemical reaction link data is also read from that file. The transport link file name is not restricted.
- SPECIES PROFILE FILE. A binary or text file containing temperature and species concentration profiles as a function of HAB. The source of either type file is irrelevant; experimental data put in binary file format is indistinguishable from flame code output of the same format, and vice versa. The species profile file does not need to contain data for every species found in the link file, *but* the link file must have every species found in the species profile file. The file name is not restricted.

2. File formats.

The formats of the two linking files are fixed by the interpreter and transport fitting programs; standard linking files of the versions noted will work.

The format of a binary solution file is that produced by the Sandia flame code, Version 2.5b; both 'recover' and 'save' files will work. The format of a text species profile file is given in Appendix A. The data must be given as mole fractions.

The format of the control file is shown below.

FORMAT OF CONTROL FILE:

```
arglink
atplink
ftype
solfile
numsmth ipoly numpts
nsmflux ipolfx nptflx
edge
spec
iignore
ignorxn(1) ... ignorxn(iignore)
ihablo ihabhi
method
multi thdif
fmmwt
el(1) elflux(1)
el(2) elflux(2)
el(3) elflux(3)
pcontrol(1) pcontrol(2)
areab areac
```

The meanings of the control variables are described in the next section. Except for file names, the control variables can be either upper or lower case.

3. Control variables.

arglink — CHARACTER*80. Name of CHEMKIN link file. If 'nolink', the program gets all link contents from the binary solution file.

atplink — CHARACTER*80. Name of transport link file.

ftype — CHARACTER*16. 'text' if solution file is a text file; anything else means solution file is a flame code binary file.

solfile — CHARACTER*80. Name of solution file; must include path if not in the same directory as the executables.

numsmth ipoly numpts — INTEGER. Number of times to smooth data or solution; polynomial degree (2-6); number of points to each side of the point being smoothed, in the window.

nsmflux ipolfx nptflx — INTEGER. Smoothing parameters for the flux profiles.

edge — CHARACTER*3. Method of handling edge regions in Savitsky-Golay smoothing. 'ave' means a simple moving average is used until there is room for the full-sized window. 'SG ' means gradually increasing windows are used near the edges.

spec — CHARACTER*16. Name of species to be analyzed in reaction path analysis.

iignore — INTEGER. Number of reactions which should not be printed in the reaction path printout. A value of -1 means print no reactions.

ignorxn(1) ... ignorxn(iignore) — INTEGER. The reaction numbers of all iignore reactions which will not be printed in reaction path analysis.

ihablo ihabhi — INTEGER. Endpoints of the range of HAB's to be printed out, in all types of analysis. Refers to the number of the HAB, not the HAB itself. For example, "5" would be the fifth HAB given, not an HAB of 5 cm.

method — CHARACTER*16. Method of rate calculation desired for reaction path analysis. 'absol' means the absolute rates will be printed; 'ratio' means the ratio of the rate to the total positive or negative rate, as appropriate, will be printed.

multi thdif — CHARACTER*16. Control method of diffusion coefficient calculation. For multi, 'mxave' sets the method to be mixture averaging; anything else results in multi-component calculation. For thdif, 'ntdif' means that thermal diffusion ratio should not be calculated; anything else means that thermal diffusion will be included.

fmmwt — DOUBLE PRECISION. Mean molecular weight of unburnt gas mixture.

el(1) elflux(1) — CHARACTER*16, DOUBLE PRECISION. Name and initial (unburnt gas) mass flux fraction for first element.

el(2) elflux(2) — CHARACTER*16, DOUBLE PRECISION. ...for second element

el(3) elflux(3) — CHARACTER*16, DOUBLE PRECISION. ...for third element

pcontrol(1) pcontrol(2) — CHARACTER*3. Program control variables: "OK " - no control
"NSL" - don't print solution or link files
"NRP" - don't do reaction path analysis
"NFN" - don't do flux/net-rate analysis
"LDP" - only print soln and link, check for duplicate reactions in link file (default - no checking)

areab areac — DOUBLE PRECISION. Area expansion ratio fit parameters for the expression: $A = 1 / (1 + areab*HAB + areac*HAB^2)$

SAMPLE CONTROL FILE:

```
'cklink'
'tplink'
'text'
'/workn/xyza/chemkin/inp/fbr/jl22arh2.txt'
0 4 4
4 4 4
'ave'
'OH'
1
8
1 26
'absol'
'mxave' 'tdif'
19.062
'H'  5.455E-02
'AR' 6.667E-01
'O'  2.787E-01
'ok ' 'ok '
-1.1600E-01  0.0000E+00
```

This control file specifies the names of the link files to be "cklink" and "tplink". The solution file is a text file, named "jl22arh2.atx" and located in directory "/workn/xyza/chemkin/inp/fbr". The input profiles will not be smoothed (numsmth = 0), but the flux profiles will be smoothed four times by a fourth degree polynomial, with a window size of 9 points (2 * 4 + 1).

Species OH will be analyzed by reaction path analysis. The results for all reactions containing OH except reaction 8 will be printed in the output file for that analysis. HAB numbers 1-26 will be analyzed upon. The absolute rate will be printed.

For flux and net rate analysis, thermal diffusion will be accounted for, but the diffusion coefficients will be calculated as mixture averages. The elements H, C, and Ar will be checked in the flux balance. All types of analyses will be performed, because the only pcontrol variable is "ok".

The area expansion ratio fits the equation A = 1 / (1 - 0.116 * HAB).

4. Program output.

Sample output generated with the above "fbr.dat" file may be found in Appendix B.

The standard output (unit 6) receives a running account of what the program is doing. If discrepancies are found between species in the solution and link files, these are noted. There shouldn't be a problem when the link file has all the species in the solution file, but a warning is given anyway to alert the user to the differences. A list of reactions which are part of the reaction path analysis is printed, along with some of the essential control variables.

Other output is to files. What files are created depends on the portions of the program one allows to run. All files are written to the directory which contains the executable. One file is always written, "solnhead.out".

- If the keyword "NSL" is not specified, files named "soln.out" and "link.out" are written. "soln.out" contains a mirror of the solution file; that is, the HABs, temperatures, and mole fractions of all species. An extra column containing the sum of mole fractions is included for the user to check data consistency. This file is written in a format which is easily importable into a spreadsheet program; no text is present in the file except some identification information at the bottom. The headers for the columns in "soln.out" are written to a file called "solnhead.out" instead.

  As mentioned above, all solution information is sorted into the order of species found in the link file. Mole fractions for species in the link file but not the data are set to 0.00. For reference, a list of the species as found in the solution file are printed at the end of "solnhead.out".

  The identification information at the bottom of the file is intended to assist the user in keeping track of the source of the information in the file.

  The file "link.out" is the listing of the reaction mechanism as found in the link file (or binary if "nolink" is specified).
- If the keyword "NRP" is not specified, the files "rates.out" and "parteqm.out" are written. The results of the reaction path analysis are writtten to "rates.out". Each column is headed by a number identifying which reaction number corresponds to the information printed below it. The total positive, total negative and total (net) rates are the last numbers printed. Below that is identifying information to help the user keep track of which files were used and how the analysis was performed.

  File "parteqm.out" contains the partial equilibrium ratios (K/K_{eq}) for each

reaction at each HAB. Column headers refer to the reaction number. Identifying information is given at the end.

- If the keyword "NFN" is not specified, five files are written: "flux.out", "fluxbal.out", "netrate.out", "diffusion.out" and "props.out". The files "flux.out", "netrate.out" and "diffusion.out" are written as spreadsheet-importable files; the appropriate headers in file "solnhead.out" apply to them as well. The molar fluxes are written to "flux.out" and the profile-calculated net rates are written to "netrate.out". The third file contains the results of the element flux balance analysis. As mentioned above, the fluxes and flux balance are calculated at the midpoints of the initial mesh, and the net rate is calculated at the midpoints of the flux mesh. The file "diffusion.out" contains the diffusion coefficients for each species, at the mesh midpoints . For multicomponent diffusivity, the coefficient is for the diffusion equation written in an equivalent Fickian form. Finally, the "props.out" file contains a listing of the gas velocity, mass density, viscosity, heat capacity, and thermal conductivity, at every HAB.

  In all of the files resulting from flux/net-rate analysis, identifying information is printed at the bottom.
- If the species profile file is a text file, the program writes a file called "binary.fbr" containing the data and link information in flame code solution file format.

Note that when the program opens a file for output, it overwrites any existing file with the same name in the directory containing the executable file. To avoid this, change all STATUS = 'UNKNOWN' specifiers in OPEN statements to STATUS = 'NEW' before compiling the program.

Appendix A

FORMAT OF TEXT DATA FILE:

aaa x.xxxEsxx ← *3 characters of text, then PRESSURE; s = +/-*
aaa x.xxxEsxx ← *3 characters of text, then FLOW RATE; s = +/-*

(Blank lines are permitted here)

HAB	TEMP	sp_1	sp_2	sp_3	sp_4
x.xxxx	x.xxxE+xx	x.xxxE-xx	x.xxxE-xx	x.xxxE-xx	x.xxxE-xx
.	.	.	.	.	.
.	.	.	.	.	.
.	.	.	.	.	.
-1.0000	0.000E-00	0.000E-00	0.000E-00	0.000E-00	0.000E-00

(Blank lines are permitted here)

sp_5	sp_6	sp_7	sp_8	sp_9	sp_{10}
x.xxxE-xx	x.xxxE+xx	x.xxxE-xx	x.xxxE-xx	x.xxxE-xx	x.xxxE-xx
.	.	.	.	.	.
.	.	.	.	.	.
.	.	.	.	.	.

(Blank lines are permitted here)

More sets of 6 species; blank lines allowed between each set

sp_{kk-2}	sp_{kk-1}	sp_{kk}
x.xxxE-xx	x.xxxE+xx	x.xxxE-xx
.	.	.
.	.	.
.	.	.

Notes on text data file format:

1. There must be no blank lines at the top of the file.
2. The characters allowed at the beginning of the first to lines are for user convenience; for example to write "P = 2.011E-01".
3. Only the first set of species — the one with HAB and TEMP — ends with a line that has -1.0000 as the first entry. That first set defines the number of HAB entries, and all other sets must have the same number of data points as the first (not including the -1.0000 as a data point).
4. TEMP must precede all species data, i.e. it immediately follows HAB.

5. HAB is given in cm, TEMP in K.
6. "sp_k" referred to species k, above. The order is irrelevant because FBR will sort the profiles according to the order that species are found in the link file.
7. Blank lines are permitted, but not required, between sets of six profiles. Blank lines are not permitted between the species names and the data.
8. The field width for pressure and flow rate is 10 (e10.3e2). The column width for species data is 12 (f12.3 for HAB and e12.3e2 for the rest).

Appendix B

SAMPLE RUN

1. Control file ("fbr.dat"). See above.

2. Species profile file. The flame was H_2-O_2-Ar. The solution was generated by the Sandia flame code, and manually translated into a text file. While the calculation which produced this solution converged properly, the adaptive mesh and tolerance parameters were very loose. That is, this is not a particularly good solution, only meant for illustrative purposes.

P = 2.895E-02
M = 2.340E-03

HAB	TEMP	AR	H	H2
0.0000	3.500e+02	4.201e-01	1.116e-03	3.086e-01
0.0187	3.767e+02	4.210e-01	1.163e-03	3.010e-01
0.0374	4.045e+02	4.216e-01	2.216e-03	2.926e-01
0.0561	4.395e+02	4.212e-01	4.432e-03	2.843e-01
0.0747	4.745e+02	4.207e-01	7.831e-03	2.750e-01
0.0934	5.354e+02	4.177e-01	1.237e-02	2.680e-01
0.1121	5.966e+02	4.148e-01	1.726e-02	2.608e-01
0.1495	7.390e+02	4.077e-01	2.729e-02	2.481e-01
0.1869	8.945e+02	4.005e-01	3.681e-02	2.368e-01
0.2242	1.052e+03	3.937e-01	4.559e-02	2.263e-01
0.2616	1.202e+03	3.877e-01	5.345e-02	2.165e-01
0.2990	1.343e+03	3.825e-01	6.031e-02	2.080e-01
0.3737	1.567e+03	3.749e-01	7.072e-02	1.945e-01
0.4485	1.714e+03	3.702e-01	7.708e-02	1.862e-01
0.5232	1.811e+03	3.673e-01	8.072e-02	1.817e-01
0.5980	1.880e+03	3.652e-01	8.280e-02	1.798e-01
0.7475	1.953e+03	3.627e-01	8.440e-02	1.794e-01
0.8970	1.990e+03	3.611e-01	8.503e-02	1.802e-01
1.0465	2.008e+03	3.599e-01	8.544e-02	1.811e-01
1.1960	2.003e+03	3.592e-01	8.581e-02	1.813e-01
1.3455	1.972e+03	3.593e-01	8.614e-02	1.807e-01

1.4950	1.945e+03	3.593e-01	8.649e-02	1.802e-01
1.6445	1.917e+03	3.594e-01	8.682e-02	1.796e-01
1.7940	1.890e+03	3.594e-01	8.713e-02	1.791e-01
1.9435	1.863e+03	3.594e-01	8.741e-02	1.787e-01
2.0930	1.835e+03	3.594e-01	8.741e-02	1.787e-01
-1.0000	0.000e+00	0.000e+00	0.000e+00	0.000e+00

O	OH	H2O	O2	HO2
1.653e-06	4.726e-04	9.762e-02	1.720e-01	7.340e-05
1.819e-06	5.193e-04	1.102e-01	1.661e-01	8.378e-05
2.143e-06	5.870e-04	1.233e-01	1.597e-01	7.859e-05
8.033e-06	6.532e-04	1.368e-01	1.526e-01	6.441e-05
3.777e-05	6.853e-04	1.505e-01	1.451e-01	4.936e-05
1.876e-04	6.615e-04	1.641e-01	1.369e-01	3.298e-05
4.693e-04	6.146e-04	1.774e-01	1.287e-01	2.219e-05
1.244e-03	5.751e-04	2.030e-01	1.120e-01	1.043e-05
2.100e-03	8.146e-04	2.273e-01	9.568e-02	5.332e-06
2.969e-03	1.413e-03	2.501e-01	8.000e-02	2.970e-06
3.736e-03	2.366e-03	2.707e-01	6.549e-02	1.775e-06
4.307e-03	3.622e-03	2.886e-01	5.266e-02	1.109e-06
4.824e-03	6.622e-03	3.156e-01	3.287e-02	4.963e-07
4.949e-03	9.423e-03	3.316e-01	2.051e-02	2.572e-07
5.031e-03	1.167e-02	3.403e-01	1.327e-02	1.526e-07
5.147e-03	1.341e-02	3.446e-01	9.149e-03	1.046e-07
5.397e-03	1.540e-02	3.467e-01	6.038e-03	7.745e-08
5.568e-03	1.640e-02	3.466e-01	5.080e-03	7.338e-08
5.658e-03	1.687e-02	3.463e-01	4.784e-03	7.378e-08
5.636e-03	1.678e-02	3.466e-01	4.670e-03	7.177e-08
5.488e-03	1.604e-02	3.477e-01	4.591e-03	6.600e-08
5.333e-03	1.537e-02	3.488e-01	4.504e-03	6.185e-08
5.173e-03	1.470e-02	3.499e-01	4.414e-03	5.858e-08
5.013e-03	1.404e-02	3.510e-01	4.329e-03	5.619e-08
4.872e-03	1.341e-02	3.520e-01	4.270e-03	5.475e-08
4.872e-03	1.341e-02	3.520e-01	4.270e-03	5.475e-08

H2O2
3.052e-05
3.487e-05
3.544e-05
3.365e-05
3.071e-05
2.721e-05
2.386e-05
1.793e-05
1.320e-05

9.553e-06
6.797e-06
4.725e-06
2.080e-06
8.264e-07
3.693e-07
2.227e-07
1.647e-07
1.473e-07
1.400e-07
1.422e-07
1.561e-07
1.694e-07
1.838e-07
1.991e-07
2.151e-07
2.151e-07

("jl22arh2.atx")

3. *Link contents output file ("link.out").* Thermodynamics and transport data from Sandia databases ("thermdat" and "trandat").

Contents of Link File cklink

ELEMENTS CONSIDERED

1. H
2. O
3. AR

SPECIES CONSIDERED

1. AR
2. H
3. O
4. OH
5. H2O
6. O2
7. H2
8. HO2
9. H2O2

```
     REACTIONS CONSIDERED
                                                PRE EXP     TEMP EXP     ACT ENG

  1. H2O2+M<=>2OH+M                            1.200E+17    0.00000      45500.0
  2. H2O2+H<=>HO2+H2                           4.790E+13    0.00000       7950.0
  3. H2O2+H<=>OH+H2O                           1.000E+13    0.00000       3590.0
  4. H2O2+O<=>OH+HO2                           9.550E+06    2.00000       3970.0
  5. H2O2+O<=>O2+H2O                           9.550E+06    2.00000       3970.0
  6. HO2+H<=>H2O+O                             3.000E+13    0.00000       1070.0
  7. HO2+H<=>H2+O2                             6.610E+13    0.00000       2130.0
  8. HO2+H<=>2OH                               1.400E+14    0.00000       1073.0
  9. HO2+OH<=>H2O+O2                           7.500E+12    0.00000          0.0
 10. 2HO2<=>H2O2+O2                            2.000E+12    0.00000          0.0
 11. H2+OH<=>H2O+H                             2.140E+08    1.51000       3430.0
 12. H2+O2<=>2OH                               1.700E+13    0.00000      47780.0
 13. H+O2<=>OH+O                               1.910E+14    0.00000      16440.0
 14. H+O2+M<=>HO2+M                            3.610E+17   -0.72000          0.0
                                H2O          Enhanced by   18.600
                                H2           Enhanced by    2.900
 15. 2H+M<=>H2+M                               1.000E+18   -1.00000          0.0
 16. 2H+H2<=>2H2                               9.200E+16   -0.60000          0.0
 17. 2H+H2O<=>H2+H2O                           6.000E+19   -1.25000          0.0
 18. H+OH+M<=>H2O+M                            2.240E+22   -2.00000          0.0
 19. H+O+M<=>OH+M                              6.020E+16   -0.60000          0.0
                                H2O          Enhanced by    5.000
 20. OH+H2O2<=>H2O+HO2                         7.080E+12    0.00000       1430.0
 21. 2OH<=>O+H2O                               1.230E+04    2.62000      -1878.0
 22. O+HO2<=>OH+O2                             1.740E+13    0.00000       -400.0
 23. O+H2<=>OH+H                               5.130E+04    2.67000       6290.0
 24. 2O+M<=>O2+M                               6.170E+15   -0.50000          0.0
 25. O+OH+M<=>HO2+M                            1.000E+17    0.00000          0.0

^^^^^^^^^^^^^^^^^^^^^^^^^^^^^^^^^^^^^^^^^^^^^^^^^^^^^^^^^^^^^^^^^^^^^^^^^^^^^^^^^^^^
^^^^^^^^^^^^^^^^^^^^^^^^^^^^^^^^^^("link.out")^^^^^^^^^^^^^^^^^^^^^^^^^^^^^^^^^^^^^^
```

4. Data/solution headers file ("solnhead.out"):

```
^^^^^^^^^^^^^^^^^^^^^^^^^^^^^^^^^^^^^^^^^^^^^^^^^^^^^^^^^^^^^^^^^^^^^^^^^^^^^^^^^^^^
 X  T     AR     H     O     OH     H2O
 X  O2     H2     HO2    H2O2
```

Headers for flux, net rate and diffusion:

```
X AR   H    O    OH    H2O   O2
X H2   HO2   H2O2
```

Species found in original data/solution file:

```
   T    AR    H    H2    O    OH
  H2O   O2    HO2   H2O2
```

Contents of input file inp/fbr/jl22arh2.atx
Sorted by the link file species list.
Smoothed 0 times.

^^^

^^^^^^^^^^^^^^^^^^^^^^^^^^^^^^^^^^^("solnhead.out")^^

5. *Data/solution contents output file ("soln.out").* Generated for spreadsheet input.

^^^

1	0.0000	3.500E+02	4.201E-01	1.116E-03	1.653E-06	4.726E-04	9.762E-02
2	0.0187	3.767E+02	4.210E-01	1.163E-03	1.819E-06	5.193E-04	1.102E-01
3	0.0374	4.045E+02	4.216E-01	2.216E-03	2.143E-06	5.870E-04	1.233E-01
4	0.0561	4.395E+02	4.212E-01	4.432E-03	8.033E-06	6.532E-04	1.368E-01
5	0.0747	4.745E+02	4.207E-01	7.831E-03	3.777E-05	6.853E-04	1.505E-01
6	0.0934	5.354E+02	4.177E-01	1.237E-02	1.876E-04	6.615E-04	1.641E-01
7	0.1121	5.966E+02	4.148E-01	1.726E-02	4.693E-04	6.146E-04	1.774E-01
8	0.1495	7.390E+02	4.077E-01	2.729E-02	1.244E-03	5.751E-04	2.030E-01
9	0.1869	8.945E+02	4.005E-01	3.681E-02	2.100E-03	8.146E-04	2.273E-01
10	0.2242	1.052E+03	3.937E-01	4.559E-02	2.969E-03	1.413E-03	2.501E-01
11	0.2616	1.202E+03	3.877E-01	5.345E-02	3.736E-03	2.366E-03	2.707E-01
12	0.2990	1.343E+03	3.825E-01	6.031E-02	4.307E-03	3.622E-03	2.886E-01
13	0.3737	1.567E+03	3.749E-01	7.072E-02	4.824E-03	6.622E-03	3.156E-01
14	0.4485	1.714E+03	3.702E-01	7.708E-02	4.949E-03	9.423E-03	3.316E-01
15	0.5232	1.811E+03	3.673E-01	8.072E-02	5.031E-03	1.167E-02	3.403E-01
16	0.5980	1.880E+03	3.652E-01	8.280E-02	5.147E-03	1.341E-02	3.446E-01
17	0.7475	1.953E+03	3.627E-01	8.440E-02	5.397E-03	1.540E-02	3.467E-01
18	0.8970	1.990E+03	3.611E-01	8.503E-02	5.568E-03	1.640E-02	3.466E-01
19	1.0465	2.008E+03	3.599E-01	8.544E-02	5.658E-03	1.687E-02	3.463E-01
20	1.1960	2.003E+03	3.592E-01	8.581E-02	5.636E-03	1.678E-02	3.466E-01
21	1.3455	1.972E+03	3.593E-01	8.614E-02	5.488E-03	1.604E-02	3.477E-01
22	1.4950	1.945E+03	3.593E-01	8.649E-02	5.333E-03	1.537E-02	3.488E-01
23	1.6445	1.917E+03	3.594E-01	8.682E-02	5.173E-03	1.470E-02	3.499E-01
24	1.7940	1.890E+03	3.594E-01	8.713E-02	5.013E-03	1.404E-02	3.510E-01
25	1.9435	1.863E+03	3.594E-01	8.741E-02	4.872E-03	1.341E-02	3.520E-01

26	2.0930	1.835E+03	3.594E-01	8.741E-02	4.872E-03	1.341E-02	3.520E-01

1	0.0000	1.720E-01	3.086E-01	7.340E-05	3.052E-05
2	0.0187	1.661E-01	3.010E-01	8.378E-05	3.487E-05
3	0.0374	1.597E-01	2.926E-01	7.859E-05	3.544E-05
4	0.0561	1.526E-01	2.843E-01	6.441E-05	3.365E-05
5	0.0747	1.451E-01	2.750E-01	4.936E-05	3.071E-05
6	0.0934	1.369E-01	2.680E-01	3.298E-05	2.721E-05
7	0.1121	1.287E-01	2.608E-01	2.219E-05	2.386E-05
8	0.1495	1.120E-01	2.481E-01	1.043E-05	1.793E-05
9	0.1869	9.568E-02	2.368E-01	5.332E-06	1.320E-05
10	0.2242	8.000E-02	2.263E-01	2.970E-06	9.553E-06
11	0.2616	6.549E-02	2.165E-01	1.775E-06	6.797E-06
12	0.2990	5.266E-02	2.080E-01	1.109E-06	4.725E-06
13	0.3737	3.287E-02	1.945E-01	4.963E-07	2.080E-06
14	0.4485	2.051E-02	1.862E-01	2.572E-07	8.264E-07
15	0.5232	1.327E-02	1.817E-01	1.526E-07	3.693E-07
16	0.5980	9.149E-03	1.798E-01	1.046E-07	2.227E-07
17	0.7475	6.038E-03	1.794E-01	7.745E-08	1.647E-07
18	0.8970	5.080E-03	1.802E-01	7.338E-08	1.473E-07
19	1.0465	4.784E-03	1.811E-01	7.378E-08	1.400E-07
20	1.1960	4.670E-03	1.813E-01	7.177E-08	1.422E-07
21	1.3455	4.591E-03	1.807E-01	6.600E-08	1.561E-07
22	1.4950	4.504E-03	1.802E-01	6.185E-08	1.694E-07
23	1.6445	4.414E-03	1.796E-01	5.858E-08	1.838E-07
24	1.7940	4.329E-03	1.791E-01	5.619E-08	1.991E-07
25	1.9435	4.270E-03	1.787E-01	5.475E-08	2.151E-07
26	2.0930	4.270E-03	1.787E-01	5.475E-08	2.151E-07

		Sum Xi
1	0.0000	1.000E+00
2	0.0187	1.000E+00
3	0.0374	1.000E+00
4	0.0561	1.000E+00
5	0.0747	9.999E-01
6	0.0934	1.000E+00
7	0.1121	1.000E+00
8	0.1495	9.999E-01
9	0.1869	1.000E+00
10	0.2242	1.000E+00
11	0.2616	1.000E+00
12	0.2990	1.000E+00
13	0.3737	1.000E+00
14	0.4485	1.000E+00
15	0.5232	1.000E+00
16	0.5980	1.000E+00

17	0.7475	1.000E+00
18	0.8970	1.000E+00
19	1.0465	1.000E+00
20	1.1960	1.000E+00
21	1.3455	1.000E+00
22	1.4950	1.000E+00
23	1.6445	1.000E+00
24	1.7940	1.000E+00
25	1.9435	1.000E+00
26	2.0930	1.000E+00

Pressure (atm): 0.028950
Flowrate (g/cm2/sec): 2.340E-03

Contents of input file inp/fbr/jl22arh2.atx
Sorted by the link file species list.
Smoothed 0 times.

^^
^^^^^^^^^^^^^^^^^^^^^^^^^^^^^^^^^^("soln.out")^^^^^^^^^^^^^^^^^^^^^^^^^^^^^^^^^^

6. Reaction path analysis output file ("rates.out"):

^^

		1	3	4	9	11	12
1	0.0000	2.870E-28	1.983E-09	1.990E-13	-2.644E-07	-1.588E-06	2.665E-30
2	0.0187	2.924E-26	2.939E-09	3.749E-13	-2.862E-07	-2.329E-06	2.823E-28
3	0.0374	1.681E-24	6.863E-09	6.464E-13	-2.632E-07	-3.386E-06	1.840E-26
4	0.0561	1.227E-22	1.576E-08	3.409E-12	-2.034E-07	-4.938E-06	1.646E-24
5	0.0747	4.483E-21	2.952E-08	2.046E-11	-1.403E-07	-6.448E-06	7.350E-23
6	0.0934	7.552E-19	5.004E-08	1.453E-10	-7.106E-08	-8.648E-06	1.692E-20
7	0.1121	4.290E-17	6.970E-08	4.675E-10	-3.577E-08	-1.032E-05	1.249E-18
8	0.1495	3.423E-14	9.674E-08	1.776E-09	-1.025E-08	-1.445E-05	1.591E-15
9	0.1869	3.758E-12	1.003E-07	3.531E-09	-5.068E-09	-2.670E-05	2.534E-13
10	0.2242	9.082E-11	8.795E-08	5.047E-09	-3.540E-09	-5.457E-05	8.191E-12
11	0.2616	7.486E-10	6.963E-08	5.727E-09	-2.714E-09	-1.005E-04	8.516E-11
12	0.2990	3.081E-09	5.123E-08	5.465E-09	-2.079E-09	-1.628E-04	4.305E-10
13	0.3737	1.140E-08	2.354E-08	3.333E-09	-1.250E-09	-3.100E-04	2.386E-09
14	0.4485	1.325E-08	9.406E-09	1.516E-09	-7.702E-10	-4.443E-04	4.443E-09
15	0.5232	1.085E-08	4.172E-09	7.328E-10	-5.069E-10	-5.516E-04	5.327E-09
16	0.5980	9.660E-09	2.484E-09	4.708E-10	-3.705E-10	-6.377E-04	5.490E-09
17	0.7475	1.044E-08	1.799E-09	3.799E-10	-2.920E-10	-7.423E-04	5.403E-09
18	0.8970	1.118E-08	1.588E-09	3.573E-10	-2.837E-10	-7.998E-04	5.529E-09
19	1.0465	1.157E-08	1.502E-09	3.482E-10	-2.882E-10	-8.296E-04	5.728E-09

20	1.1960	1.148E-08	1.536E-09	3.514E-10	-2.802E-10	-8.253E-04	5.460E-09
21	1.3455	1.086E-08	1.722E-09	3.698E-10	-2.542E-10	-7.817E-04	4.570E-09
22	1.4950	1.031E-08	1.904E-09	3.845E-10	-2.346E-10	-7.429E-04	3.880E-09
23	1.6445	9.699E-09	2.106E-09	3.986E-10	-2.188E-10	-7.040E-04	3.257E-09
24	1.7940	9.113E-09	2.324E-09	4.123E-10	-2.062E-10	-6.666E-04	2.739E-09
25	1.9435	8.501E-09	2.557E-09	4.263E-10	-1.975E-10	-6.313E-04	2.308E-09
26	2.0930	7.264E-09	2.597E-09	4.194E-10	-2.036E-10	-6.271E-04	1.953E-09

		13	18	19	20	21	22
1	0.0000	2.017E-12	-9.880E-08	4.707E-12	-1.328E-08	-3.847E-07	3.813E-09
2	0.0187	9.361E-12	-7.834E-08	4.293E-12	-1.665E-08	-4.015E-07	3.969E-09
3	0.0374	6.729E-11	-1.182E-07	7.729E-12	-1.891E-08	-4.512E-07	3.667E-09
4	0.0561	5.554E-10	-1.737E-07	4.453E-11	-1.950E-08	-4.883E-07	9.173E-09
5	0.0747	3.209E-09	-2.195E-07	2.907E-10	-1.808E-08	-4.810E-07	2.741E-08
6	0.0934	2.730E-08	-1.830E-07	1.527E-09	-1.443E-08	-3.851E-07	6.809E-08
7	0.1121	1.408E-07	-1.381E-07	3.726E-09	-1.087E-08	-2.966E-07	8.881E-08
8	0.1495	1.827E-06	-7.005E-08	7.658E-09	-6.284E-09	-2.185E-07	6.757E-08
9	0.1869	1.006E-05	-5.151E-08	9.239E-09	-5.298E-09	-3.952E-07	3.796E-08
10	0.2242	3.009E-05	-4.919E-08	9.454E-09	-5.424E-09	-1.122E-06	2.090E-08
11	0.2616	5.903E-05	-4.958E-08	8.987E-09	-5.391E-09	-3.056E-06	1.175E-08
12	0.2990	8.837E-05	-4.919E-08	8.111E-09	-4.893E-09	-7.063E-06	6.664E-09
13	0.3737	1.146E-04	-4.877E-08	6.420E-09	-3.123E-09	-2.349E-05	2.401E-09
14	0.4485	1.025E-04	-4.830E-08	5.345E-09	-1.535E-09	-4.775E-05	1.055E-09
15	0.5232	8.054E-05	-4.757E-08	4.737E-09	-7.783E-10	-7.358E-05	5.666E-10
16	0.5980	6.251E-05	-4.652E-08	4.377E-09	-5.078E-10	-9.755E-05	3.672E-10
17	0.7475	4.593E-05	-4.501E-08	4.093E-09	-4.054E-10	-1.293E-04	2.631E-10
18	0.8970	4.057E-05	-4.396E-08	3.976E-09	-3.745E-10	-1.470E-04	2.473E-10
19	1.0465	3.914E-05	-4.344E-08	3.928E-09	-3.607E-10	-1.557E-04	2.479E-10
20	1.1960	3.817E-05	-4.394E-08	3.967E-09	-3.660E-10	-1.540E-04	2.415E-10
21	1.3455	3.642E-05	-4.558E-08	4.109E-09	-3.940E-10	-1.404E-04	2.234E-10
22	1.4950	3.479E-05	-4.698E-08	4.221E-09	-4.190E-10	-1.287E-04	2.095E-10
23	1.6445	3.311E-05	-4.850E-08	4.338E-09	-4.452E-10	-1.175E-04	1.984E-10
24	1.7940	3.152E-05	-4.991E-08	4.448E-09	-4.713E-10	-1.070E-04	1.900E-10
25	1.9435	3.013E-05	-5.139E-08	4.575E-09	-4.978E-10	-9.745E-05	1.855E-10
26	2.0930	2.902E-05	-5.543E-08	4.832E-09	-5.100E-10	-9.729E-05	1.915E-10

		23	25
1	0.0000	1.947E-11	-8.003E-11
2	0.0187	4.168E-11	-7.762E-11
3	0.0374	8.921E-11	-8.349E-11
4	0.0561	6.406E-10	-2.715E-10
5	0.0747	5.217E-09	-1.064E-09
6	0.0934	5.848E-08	-3.551E-09
7	0.1121	2.807E-07	-5.966E-09
8	0.1495	2.272E-06	-7.785E-09
9	0.1869	8.759E-06	-1.050E-08

10	0.2242	2.241E-05	-1.583E-08
11	0.2616	4.294E-05	-2.235E-08
12	0.2990	6.755E-05	-2.829E-08
13	0.3737	1.099E-04	-3.646E-08
14	0.4485	1.363E-04	-4.067E-08
15	0.5232	1.548E-04	-4.341E-08
16	0.5980	1.714E-04	-4.563E-08
17	0.7475	1.959E-04	-4.901E-08
18	0.8970	2.119E-04	-5.089E-08
19	1.0465	2.208E-04	-5.178E-08
20	1.1960	2.190E-04	-5.169E-08
21	1.3455	2.051E-04	-5.041E-08
22	1.4950	1.926E-04	-4.893E-08
23	1.6445	1.801E-04	-4.741E-08
24	1.7940	1.684E-04	-4.579E-08
25	1.9435	1.578E-04	-4.438E-08
26	2.0930	1.522E-04	-4.644E-08

		-1	-3	-4	-9	-11	-12
1	0.0000	-5.091E-07	-4.363E-50	-4.543E-21	4.176E-44	1.840E-15	-1.087E-25
2	0.0187	-2.911E-07	-6.946E-47	-4.031E-20	4.755E-41	1.378E-14	-2.205E-24
3	0.0374	-1.865E-07	-5.505E-44	-2.494E-19	2.660E-38	1.557E-13	-3.544E-23
4	0.0561	-1.073E-07	-7.025E-41	-1.529E-18	2.380E-35	2.089E-12	-6.660E-22
5	0.0747	-6.033E-08	-2.988E-38	-6.249E-18	7.700E-33	1.881E-11	-7.364E-21
6	0.0934	-2.082E-08	-1.437E-34	-4.131E-17	2.803E-29	2.890E-10	-1.813E-19
7	0.1121	-7.868E-09	-1.201E-31	-1.669E-16	1.917E-26	2.500E-09	-2.098E-18
8	0.1495	-1.584E-09	-1.050E-26	-1.736E-15	1.060E-21	8.514E-08	-1.384E-16
9	0.1869	-1.011E-09	-6.167E-23	-1.289E-14	2.732E-18	1.074E-06	-6.115E-15
10	0.2242	-1.283E-09	-4.016E-20	-6.653E-14	6.625E-16	6.534E-06	-1.594E-13
11	0.2616	-1.891E-09	-4.500E-18	-2.213E-13	2.954E-14	2.365E-05	-2.006E-12
12	0.2990	-2.704E-09	-1.520E-16	-5.176E-13	4.434E-13	6.098E-05	-1.392E-11
13	0.3737	-4.812E-09	-1.205E-14	-1.278E-12	9.571E-12	1.951E-04	-1.693E-10
14	0.4485	-6.941E-09	-1.187E-13	-1.676E-12	3.637E-11	3.546E-04	-6.546E-10
15	0.5232	-8.726E-09	-4.417E-13	-1.715E-12	6.538E-11	4.945E-04	-1.443E-09
16	0.5980	-1.011E-08	-1.030E-12	-1.677E-12	8.681E-11	6.074E-04	-2.405E-09
17	0.7475	-1.169E-08	-2.351E-12	-1.765E-12	1.080E-10	7.332E-04	-3.975E-09
18	0.8970	-1.245E-08	-3.467E-12	-1.972E-12	1.226E-10	7.981E-04	-5.019E-09
19	1.0465	-1.278E-08	-4.156E-12	-2.142E-12	1.329E-10	8.312E-04	-5.586E-09
20	1.1960	-1.275E-08	-3.965E-12	-2.044E-12	1.249E-10	8.271E-04	-5.450E-09
21	1.3455	-1.228E-08	-2.907E-12	-1.652E-12	9.622E-11	7.814E-04	-4.560E-09
22	1.4950	-1.181E-08	-2.197E-12	-1.375E-12	7.586E-11	7.430E-04	-3.867E-09
23	1.6445	-1.135E-08	-1.630E-12	-1.149E-12	5.884E-11	7.036E-04	-3.248E-09
24	1.7940	-1.087E-08	-1.210E-12	-9.720E-13	4.574E-11	6.663E-04	-2.722E-09
25	1.9435	-1.043E-08	-8.908E-13	-8.334E-13	3.549E-11	6.293E-04	-2.275E-09
26	2.0930	-1.100E-08	-6.727E-13	-7.637E-13	2.737E-11	5.881E-04	-2.071E-09

		-13	-18	-19	-20	-21	-22
1	0.0000	-1.231E-08	1.226E-69	-3.368E-64	5.255E-26	6.669E-17	-3.475E-36
2	0.0187	-1.239E-08	1.859E-64	-1.016E-59	1.795E-24	4.026E-16	-6.576E-34
3	0.0374	-1.384E-08	8.546E-60	-1.138E-55	3.585E-23	2.216E-15	-7.545E-32
4	0.0561	-4.718E-08	8.854E-55	-2.555E-51	7.770E-22	4.338E-14	-1.209E-29
5	0.0747	-1.937E-07	1.651E-50	-1.244E-47	9.705E-21	8.453E-13	-8.562E-28
6	0.0934	-6.994E-07	1.906E-44	-1.991E-42	3.277E-19	3.076E-11	-3.362E-25
7	0.1121	-1.268E-06	1.298E-39	-2.694E-38	5.040E-18	3.854E-10	-3.663E-23
8	0.1495	-1.962E-06	1.644E-31	-2.471E-31	4.468E-16	1.589E-08	-9.611E-20
9	0.1869	-3.143E-06	1.177E-25	-4.052E-26	1.008E-14	2.059E-07	-3.928E-17
10	0.2242	-5.571E-06	1.590E-21	-2.682E-22	8.145E-14	1.279E-06	-3.433E-15
11	0.2616	-9.069E-06	1.269E-18	-1.498E-19	3.197E-13	4.689E-06	-8.339E-14
12	0.2990	-1.298E-05	1.662E-16	-1.611E-17	7.888E-13	1.202E-05	-8.350E-13
13	0.3737	-1.998E-05	5.913E-14	-5.033E-15	1.852E-12	3.634E-05	-1.189E-11
14	0.4485	-2.478E-05	1.164E-12	-9.834E-14	2.224E-12	6.256E-05	-3.803E-11
15	0.5232	-2.825E-05	6.263E-12	-5.374E-13	2.114E-12	8.539E-05	-6.297E-11
16	0.5980	-3.105E-05	1.844E-11	-1.606E-12	1.954E-12	1.054E-04	-7.966E-11
17	0.7475	-3.493E-05	5.251E-11	-4.676E-12	1.923E-12	1.320E-04	-9.535E-11
18	0.8970	-3.712E-05	8.618E-11	-7.749E-12	2.080E-12	1.478E-04	-1.062E-10
19	1.0465	-3.818E-05	1.088E-10	-9.818E-12	2.224E-12	1.561E-04	-1.141E-10
20	1.1960	-3.800E-05	1.021E-10	-9.223E-12	2.128E-12	1.539E-04	-1.077E-10
21	1.3455	-3.636E-05	6.809E-11	-6.136E-12	1.760E-12	1.405E-04	-8.455E-11
22	1.4950	-3.470E-05	4.732E-11	-4.246E-12	1.500E-12	1.289E-04	-6.764E-11
23	1.6445	-3.304E-05	3.206E-11	-2.868E-12	1.283E-12	1.175E-04	-5.336E-11
24	1.7940	-3.137E-05	2.177E-11	-1.938E-12	1.112E-12	1.071E-04	-4.211E-11
25	1.9435	-2.988E-05	1.459E-11	-1.296E-12	9.756E-13	9.769E-05	-3.324E-11
26	2.0930	-3.070E-05	9.483E-12	-8.835E-13	8.691E-13	9.103E-05	-2.752E-11

		-23	-25
1	0.0000	-1.302E-10	1.030E-39
2	0.0187	-2.461E-10	8.381E-37
3	0.0374	-8.353E-10	2.904E-34
4	0.0561	-3.050E-09	1.392E-31
5	0.0747	-8.660E-09	2.415E-29
6	0.0934	-2.446E-08	3.662E-26
7	0.1121	-5.233E-08	1.161E-23
8	0.1495	-1.841E-07	1.645E-19
9	0.1869	-6.767E-07	1.425E-16
10	0.2242	-2.356E-06	1.477E-14
11	0.2616	-6.584E-06	3.420E-13
12	0.2990	-1.487E-05	3.052E-12
13	0.3737	-4.471E-05	3.311E-11
14	0.4485	-8.303E-05	8.587E-11
15	0.5232	-1.196E-04	1.264E-10
16	0.5980	-1.511E-04	1.554E-10

17	0.7475	-1.895E-04	2.032E-10
18	0.8970	-2.102E-04	2.524E-10
19	1.0465	-2.207E-04	2.883E-10
20	1.1960	-2.196E-04	2.708E-10
21	1.3455	-2.050E-04	1.992E-10
22	1.4950	-1.924E-04	1.528E-10
23	1.6445	-1.800E-04	1.168E-10
24	1.7940	-1.681E-04	9.047E-11
25	1.9435	-1.569E-04	7.072E-11
26	2.0930	-1.526E-04	5.586E-11

		Tot Pos	Tot Neg	Total
1	0.0000	4.988E-06	-2.871E-06	2.117E-06
2	0.0187	5.714E-06	-3.415E-06	2.299E-06
3	0.0374	9.774E-06	-4.439E-06	5.335E-06
4	0.0561	1.510E-05	-5.980E-06	9.122E-06
5	0.0747	1.924E-05	-7.571E-06	1.167E-05
6	0.0934	1.830E-05	-1.005E-05	8.249E-06
7	0.1121	1.576E-05	-1.214E-05	3.620E-06
8	0.1495	1.312E-05	-1.691E-05	-3.786E-06
9	0.1869	2.493E-05	-3.099E-05	-6.058E-06
10	0.2242	6.299E-05	-6.369E-05	-7.021E-07
11	0.2616	1.319E-04	-1.193E-04	1.258E-05
12	0.2990	2.299E-04	-1.978E-04	3.210E-05
13	0.3737	4.564E-04	-3.983E-04	5.805E-05
14	0.4485	6.562E-04	-5.999E-04	5.623E-05
15	0.5232	8.154E-04	-7.731E-04	4.230E-05
16	0.5980	9.467E-04	-9.176E-04	2.914E-05
17	0.7475	1.107E-03	-1.096E-03	1.104E-05
18	0.8970	1.199E-03	-1.194E-03	4.297E-06
19	1.0465	1.247E-03	-1.244E-03	2.931E-06
20	1.1960	1.238E-03	-1.237E-03	1.259E-06
21	1.3455	1.163E-03	-1.164E-03	-6.476E-08
22	1.4950	1.099E-03	-1.099E-03	5.157E-07
23	1.6445	1.034E-03	-1.035E-03	-3.258E-07
24	1.7940	9.733E-04	-9.732E-04	9.211E-08
25	1.9435	9.150E-04	-9.157E-04	-7.287E-07
26	2.0930	8.604E-04	-9.078E-04	-4.737E-05

Link file: cklink
Input file: inp/fbr/jl22arh2.atx
Species analyzed: OH
Reactions not printed: 8
Beginning HAB no: 1 Ending HAB no: 26

Absolute rate, or ratio (normalized): ABSOL

^^

^^^^^^^^^^^^^^^^^^^^^^^^^^^^^^^^^^^^^("rates.out")^^^^^^^^^^^^^^^^^^^^^^^^^^^^^^^^^^^^^

7. Partial equilibrium ratio file ("parteqm.out").

^^

		1	3	4	9	11	12
1	0.0000	1.774E+21	2.200E-41	2.283E-08	1.580E-37	1.159E-09	4.078E+04
2	0.0187	9.958E+18	2.363E-38	1.075E-07	1.661E-34	5.919E-09	7.811E+03
3	0.0374	1.109E+17	8.021E-36	3.859E-07	1.011E-31	4.599E-08	1.926E+03
4	0.0561	8.747E+14	4.459E-33	4.485E-07	1.170E-28	4.230E-07	4.045E+02
5	0.0747	1.346E+13	1.012E-30	3.055E-07	5.489E-26	2.917E-06	1.002E+02
6	0.0934	2.757E+10	2.872E-27	2.842E-07	3.945E-22	3.342E-05	1.071E+01
7	0.1121	1.834E+08	1.723E-24	3.569E-07	5.359E-19	2.422E-04	1.680E+00
8	0.1495	4.627E+04	1.086E-19	9.779E-07	1.034E-13	5.893E-03	8.701E-02
9	0.1869	2.691E+02	6.148E-16	3.652E-06	5.390E-10	4.025E-02	2.413E-02
10	0.2242	1.413E+01	4.567E-13	1.318E-05	1.871E-07	1.197E-01	1.946E-02
11	0.2616	2.526E+00	6.463E-11	3.864E-05	1.089E-05	2.353E-01	2.356E-02
12	0.2990	8.778E-01	2.966E-09	9.471E-05	2.133E-04	3.746E-01	3.233E-02
13	0.3737	4.222E-01	5.119E-07	3.834E-04	7.659E-03	6.293E-01	7.093E-02
14	0.4485	5.237E-01	1.262E-05	1.106E-03	4.721E-02	7.983E-01	1.473E-01
15	0.5232	8.041E-01	1.059E-04	2.340E-03	1.290E-01	8.966E-01	2.710E-01
16	0.5980	1.046E+00	4.146E-04	3.562E-03	2.343E-01	9.524E-01	4.381E-01
17	0.7475	1.120E+00	1.307E-03	4.645E-03	3.700E-01	9.879E-01	7.358E-01
18	0.8970	1.113E+00	2.183E-03	5.521E-03	4.322E-01	9.980E-01	9.077E-01
19	1.0465	1.105E+00	2.767E-03	6.151E-03	4.612E-01	1.002E+00	9.753E-01
20	1.1960	1.111E+00	2.581E-03	5.818E-03	4.456E-01	1.002E+00	9.983E-01
21	1.3455	1.130E+00	1.689E-03	4.467E-03	3.786E-01	9.996E-01	9.977E-01
22	1.4950	1.145E+00	1.154E-03	3.576E-03	3.233E-01	1.000E+00	9.965E-01
23	1.6445	1.170E+00	7.738E-04	2.883E-03	2.689E-01	9.994E-01	9.974E-01
24	1.7940	1.193E+00	5.205E-04	2.358E-03	2.218E-01	9.995E-01	9.938E-01
25	1.9435	1.227E+00	3.484E-04	1.955E-03	1.797E-01	9.967E-01	9.860E-01
26	2.0930	1.514E+00	2.590E-04	1.821E-03	1.345E-01	9.378E-01	1.060E+00

		13	18	19	20	21	22
1	0.0000	6.100E+03	1.241E-62	7.156E-53	3.958E-18	1.734E-10	9.112E-28
2	0.0187	1.323E+03	2.373E-57	2.367E-48	1.078E-16	1.003E-09	1.657E-25
3	0.0374	2.057E+02	7.230E-53	1.472E-44	1.896E-15	4.912E-09	2.057E-23
4	0.0561	8.495E+01	5.097E-48	5.738E-41	3.984E-14	8.883E-08	1.318E-21
5	0.0747	6.036E+01	7.520E-44	4.279E-38	5.369E-13	1.757E-06	3.123E-20
6	0.0934	2.562E+01	1.042E-37	1.304E-33	2.271E-11	7.989E-05	4.938E-18
7	0.1121	9.011E+00	9.397E-33	7.232E-30	4.638E-10	1.299E-03	4.124E-16
8	0.1495	1.074E+00	2.347E-24	3.227E-23	7.111E-08	7.271E-02	1.422E-12

9	0.1869	3.124E-01	2.285E-18	4.386E-18	1.902E-06	5.209E-01	1.035E-09
10	0.2242	1.851E-01	3.232E-14	2.837E-14	1.502E-05	1.139E+00	1.643E-07
11	0.2616	1.536E-01	2.559E-11	1.667E-11	5.930E-05	1.535E+00	7.094E-06
12	0.2990	1.469E-01	3.379E-09	1.986E-09	1.612E-04	1.702E+00	1.253E-04
13	0.3737	1.743E-01	1.213E-06	7.839E-07	5.930E-04	1.547E+00	4.952E-03
14	0.4485	2.418E-01	2.410E-05	1.840E-05	1.449E-03	1.310E+00	3.604E-02
15	0.5232	3.507E-01	1.317E-04	1.134E-04	2.716E-03	1.161E+00	1.111E-01
16	0.5980	4.968E-01	3.963E-04	3.670E-04	3.847E-03	1.080E+00	2.169E-01
17	0.7475	7.605E-01	1.167E-03	1.142E-03	4.743E-03	1.021E+00	3.623E-01
18	0.8970	9.149E-01	1.960E-03	1.949E-03	5.553E-03	1.006E+00	4.296E-01
19	1.0465	9.755E-01	2.505E-03	2.500E-03	6.165E-03	1.002E+00	4.602E-01
20	1.1960	9.955E-01	2.324E-03	2.325E-03	5.815E-03	9.995E-01	4.458E-01
21	1.3455	9.986E-01	1.494E-03	1.493E-03	4.469E-03	1.000E+00	3.784E-01
22	1.4950	9.976E-01	1.007E-03	1.006E-03	3.581E-03	1.001E+00	3.229E-01
23	1.6445	9.980E-01	6.611E-04	6.611E-04	2.883E-03	1.000E+00	2.690E-01
24	1.7940	9.952E-01	4.362E-04	4.358E-04	2.360E-03	1.001E+00	2.216E-01
25	1.9435	9.917E-01	2.840E-04	2.833E-04	1.960E-03	1.003E+00	1.792E-01
26	2.0930	1.058E+00	1.711E-04	1.828E-04	1.704E-03	9.357E-01	1.437E-01

		23	25
1	0.0000	6.684E+00	1.287E-29
2	0.0187	5.903E+00	1.080E-26
3	0.0374	9.364E+00	3.479E-24
4	0.0561	4.762E+00	5.127E-22
5	0.0747	1.660E+00	2.270E-20
6	0.0934	4.183E-01	1.031E-17
7	0.1121	1.864E-01	1.946E-15
8	0.1495	8.104E-02	2.113E-11
9	0.1869	7.726E-02	1.357E-08
10	0.2242	1.051E-01	9.331E-07
11	0.2616	1.533E-01	1.530E-05
12	0.2990	2.201E-01	1.079E-04
13	0.3737	4.069E-01	9.081E-04
14	0.4485	6.093E-01	2.111E-03
15	0.5232	7.726E-01	2.911E-03
16	0.5980	8.818E-01	3.405E-03
17	0.7475	9.674E-01	4.146E-03
18	0.8970	9.922E-01	4.959E-03
19	1.0465	9.997E-01	5.568E-03
20	1.1960	1.003E+00	5.238E-03
21	1.3455	9.992E-01	3.952E-03
22	1.4950	9.989E-01	3.123E-03
23	1.6445	9.994E-01	2.463E-03
24	1.7940	9.986E-01	1.976E-03
25	1.9435	9.942E-01	1.594E-03
26	2.0930	1.002E+00	1.203E-03

Link file: cklink
Input file: inp/fbr/jl22arh2.atx
Species analyzed: OH
Reactions not printed: 8
Beginning HAB no: 1 Ending HAB no: 26

RATIO OF +/- 9.999E+99 MEANS FORWARD RATE WAS ZERO

^^

^^("parteqm.out")^^

8. *Flux balance output file ("fluxbal.out").* These numbers are percent deviations. Because the balance is done at the mesh midpoints, there is one fewer HAB reported than are found in the species profile file. Note that the balance is not nearly-perfect, as one would expect from a flame code solution. This is because the flame code analysis was done with multicomponent diffusion coefficients, but this run was done with mixture-averaged coefficients.

^^

	HAB	H	AR	O
1	0.0094	-49.41	3.92	0.31
2	0.0281	-48.33	4.01	-0.12
3	0.0468	-58.70	4.78	0.08
4	0.0654	-55.42	4.62	-0.19
5	0.0840	-95.12	7.49	0.72
6	0.1027	-91.79	7.49	0.06
7	0.1308	-102.58	8.56	-0.39
8	0.1682	-106.15	9.43	-1.76
9	0.2055	-103.11	9.83	-3.30
10	0.2429	-94.21	9.54	-4.35
11	0.2803	-86.25	9.11	-4.90
12	0.3363	-66.81	7.56	-5.00
13	0.4111	-43.88	5.14	-3.70
14	0.4858	-29.22	3.38	-2.35
15	0.5606	-21.80	2.33	-1.30
16	0.6727	-13.04	1.20	-0.30
17	0.8222	-8.13	0.58	0.23
18	0.9718	-5.47	0.30	0.36
19	1.1212	-1.90	0.02	0.35
20	1.2707	2.12	-0.37	0.48
21	1.4202	1.63	-0.31	0.43
22	1.5697	2.08	-0.36	0.46
23	1.7192	1.88	-0.32	0.42
24	1.8687	1.93	-0.34	0.46
25	2.0182	2.24	-0.41	0.57

Element flux balances for input file inp/fbr/jl22arh2.atx

Area expansion ratio = 1 / (1 + -1.1600E-01 * HAB + 0.0000E+00 * HAB**2)

Transport parameters: MXAVE TDIF

^^
^^^^^^^^^^^^^^^^^^^^^^^^^^^^^^^^^^^^("fluxbal.out")^^^^^^^^^^^^^^^^^^^^^^^^^^^^^^^^^^^^

9. *Flux analysis output file ("flux.out"):*

^^

1	0.0094	4.061E-05	-8.622E-07	-1.921E-09	-1.236E-09	-3.947E-08	2.046E-05
2	0.0281	4.083E-05	-5.694E-06	-4.069E-08	1.538E-08	-3.606E-08	2.045E-05
3	0.0468	4.111E-05	-1.116E-05	-1.044E-07	4.479E-08	-2.977E-08	2.047E-05
4	0.0654	4.140E-05	-1.664E-05	-1.796E-07	7.169E-08	-2.105E-08	2.048E-05
5	0.0840	4.170E-05	-2.226E-05	-2.455E-07	1.168E-07	1.317E-09	2.050E-05
6	0.1027	4.206E-05	-2.800E-05	-3.811E-07	1.333E-07	1.216E-08	2.051E-05
7	0.1308	4.242E-05	-3.368E-05	-5.515E-07	6.041E-08	-1.803E-08	2.051E-05
8	0.1682	4.273E-05	-3.888E-05	-6.973E-07	-1.642E-07	7.646E-09	2.044E-05
9	0.2055	4.289E-05	-4.278E-05	-7.257E-07	-5.477E-07	5.550E-07	2.008E-05
10	0.2429	4.284E-05	-4.389E-05	-5.878E-07	-1.018E-06	2.484E-06	1.904E-05
11	0.2803	4.251E-05	-4.076E-05	-2.998E-07	-1.424E-06	6.597E-06	1.693E-05
12	0.3363	4.191E-05	-3.305E-05	4.248E-08	-1.597E-06	1.295E-05	1.372E-05
13	0.4111	4.117E-05	-2.231E-05	3.182E-07	-1.422E-06	2.052E-05	9.901E-06
14	0.4858	4.045E-05	-1.129E-05	4.569E-07	-9.125E-07	2.764E-05	6.278E-06
15	0.5606	3.990E-05	-2.408E-06	4.815E-07	-2.028E-07	3.296E-05	3.503E-06
16	0.6727	3.953E-05	3.381E-06	4.712E-07	5.307E-07	3.606E-05	1.779E-06
17	0.8222	3.930E-05	6.541E-06	4.924E-07	1.158E-06	3.734E-05	9.211E-07
18	0.9718	3.914E-05	8.113E-06	5.537E-07	1.622E-06	3.756E-05	5.919E-07
19	1.1212	3.903E-05	8.936E-06	6.241E-07	1.927E-06	3.736E-05	5.164E-07
20	1.2707	3.896E-05	9.396E-06	6.648E-07	2.062E-06	3.717E-05	5.227E-07
21	1.4202	3.893E-05	9.679E-06	6.663E-07	2.049E-06	3.716E-05	5.303E-07
22	1.5697	3.892E-05	9.871E-06	6.317E-07	1.905E-06	3.740E-05	5.097E-07
23	1.7192	3.891E-05	1.010E-05	6.054E-07	1.789E-06	3.757E-05	4.979E-07
24	1.8687	3.890E-05	1.032E-05	5.739E-07	1.651E-06	3.779E-05	4.812E-07
25	2.0182	3.889E-05	1.057E-05	5.369E-07	1.493E-06	3.803E-05	4.653E-07

1	0.0094	3.219E-05	1.948E-09	6.193E-10
2	0.0281	3.032E-05	6.253E-09	1.977E-09
3	0.0468	2.737E-05	9.226E-09	3.131E-09
4	0.0654	2.434E-05	1.147E-08	4.143E-09
5	0.0840	2.077E-05	1.422E-08	5.285E-09
6	0.1027	1.720E-05	1.278E-08	5.580E-09

7	0.1308	1.520E-05	8.938E-09	5.242E-09
8	0.1682	1.585E-05	4.585E-09	4.503E-09
9	0.2055	1.878E-05	1.938E-09	3.752E-09
10	0.2429	2.248E-05	8.406E-10	3.027E-09
11	0.2803	2.534E-05	5.838E-10	2.307E-09
12	0.3363	2.629E-05	4.251E-10	1.569E-09
13	0.4111	2.499E-05	2.447E-10	8.946E-10
14	0.4858	2.215E-05	9.431E-11	3.889E-10
15	0.5606	1.907E-05	2.813E-11	1.057E-10
16	0.6727	1.706E-05	1.158E-11	7.266E-12
17	0.8222	1.677E-05	1.249E-11	4.900E-12
18	0.9718	1.790E-05	1.030E-11	1.964E-11
19	1.1212	1.959E-05	8.976E-12	2.157E-11
20	1.2707	2.088E-05	8.342E-12	1.606E-11
21	1.4202	2.140E-05	8.578E-12	1.313E-11
22	1.5697	2.112E-05	7.828E-12	1.586E-11
23	1.7192	2.106E-05	7.319E-12	1.760E-11
24	1.8687	2.089E-05	6.615E-12	1.991E-11
25	2.0182	2.066E-05	6.017E-12	2.256E-11

Fluxes for input file inp/fbr/jl22arh2.atx
Fluxes smoothed 4 times. Poly order 4, window size 9, edge method AVE.
Species names found in file "solnhead.out"

Area expansion ratio = 1 / (1 + -1.1600E-01 * HAB + 0.0000E+00 * HAB**2)

Transport parameters: MXAVE TDIF

^^

^^^^^^^^^^^^^^^^^^^^^^^^^^^^^^^^^^^^^^^("flux.out")^^^^^^^^^^^^^^^^^^^^^^^^^^^^^^^^^^^^^^

10. Diffusion coefficients file ("diffusion.out")

^^

2	0.0187	1.051E+01	8.226E+01	2.319E+01	2.276E+01	1.790E+01	1.464E+01
3	0.0374	1.198E+01	9.443E+01	2.645E+01	2.596E+01	2.080E+01	1.672E+01
4	0.0561	1.372E+01	1.089E+02	3.032E+01	2.976E+01	2.426E+01	1.918E+01
5	0.0747	1.631E+01	1.303E+02	3.604E+01	3.537E+01	2.940E+01	2.283E+01
6	0.0934	1.992E+01	1.600E+02	4.396E+01	4.314E+01	3.658E+01	2.790E+01
7	0.1168	2.658E+01	2.152E+02	5.861E+01	5.752E+01	5.005E+01	3.728E+01
8	0.1495	3.772E+01	3.079E+02	8.311E+01	8.156E+01	7.301E+01	5.301E+01
9	0.1869	5.109E+01	4.200E+02	1.126E+02	1.105E+02	1.011E+02	7.197E+01
10	0.2242	6.577E+01	5.443E+02	1.451E+02	1.424E+02	1.326E+02	9.292E+01
11	0.2616	8.102E+01	6.744E+02	1.790E+02	1.757E+02	1.659E+02	1.148E+02
12	0.3083	1.019E+02	8.545E+02	2.256E+02	2.215E+02	2.122E+02	1.450E+02

13	0.3737	1.251E+02	1.056E+03	2.776E+02	2.727E+02	2.645E+02	1.787E+02
14	0.4485	1.414E+02	1.199E+03	3.142E+02	3.088E+02	3.017E+02	2.026E+02
15	0.5232	1.530E+02	1.300E+03	3.403E+02	3.346E+02	3.280E+02	2.196E+02
16	0.6167	1.634E+02	1.389E+03	3.634E+02	3.574E+02	3.511E+02	2.346E+02
17	0.7475	1.717E+02	1.460E+03	3.819E+02	3.756E+02	3.693E+02	2.467E+02
18	0.8970	1.760E+02	1.496E+03	3.914E+02	3.851E+02	3.786E+02	2.529E+02
19	1.0465	1.772E+02	1.505E+03	3.940E+02	3.876E+02	3.810E+02	2.546E+02
20	1.1960	1.746E+02	1.483E+03	3.882E+02	3.819E+02	3.755E+02	2.509E+02
21	1.3455	1.703E+02	1.447E+03	3.788E+02	3.726E+02	3.665E+02	2.448E+02
22	1.4950	1.663E+02	1.414E+03	3.699E+02	3.639E+02	3.580E+02	2.390E+02
23	1.6445	1.623E+02	1.380E+03	3.612E+02	3.552E+02	3.495E+02	2.333E+02
24	1.7940	1.585E+02	1.348E+03	3.526E+02	3.468E+02	3.414E+02	2.278E+02
25	1.9435	1.546E+02	1.315E+03	3.441E+02	3.384E+02	3.330E+02	2.223E+02

2	0.0187	6.339E+01	1.463E+01	1.453E+01
3	0.0374	7.180E+01	1.670E+01	1.659E+01
4	0.0561	8.168E+01	1.917E+01	1.903E+01
5	0.0747	9.634E+01	2.281E+01	2.266E+01
6	0.0934	1.166E+02	2.787E+01	2.768E+01
7	0.1168	1.538E+02	3.724E+01	3.698E+01
8	0.1495	2.155E+02	5.293E+01	5.258E+01
9	0.1869	2.887E+02	7.184E+01	7.136E+01
10	0.2242	3.684E+02	9.271E+01	9.210E+01
11	0.2616	4.505E+02	1.145E+02	1.137E+02
12	0.3083	5.621E+02	1.445E+02	1.435E+02
13	0.3737	6.850E+02	1.779E+02	1.768E+02
14	0.4485	7.710E+02	2.016E+02	2.003E+02
15	0.5232	8.323E+02	2.184E+02	2.170E+02
16	0.6167	8.872E+02	2.333E+02	2.318E+02
17	0.7475	9.316E+02	2.452E+02	2.437E+02
18	0.8970	9.549E+02	2.514E+02	2.499E+02
19	1.0465	9.611E+02	2.531E+02	2.515E+02
20	1.1960	9.469E+02	2.494E+02	2.478E+02
21	1.3455	9.237E+02	2.433E+02	2.418E+02
22	1.4950	9.019E+02	2.376E+02	2.361E+02
23	1.6445	8.803E+02	2.320E+02	2.305E+02
24	1.7940	8.594E+02	2.265E+02	2.251E+02
25	1.9435	8.385E+02	2.210E+02	2.196E+02

Diffn. coeffs. for input file inp/fbr/jl22arh2.atx
Fluxes smoothed 4 times. Poly order 4, window size 9, edge method AVE.
Species names found in file "solnhead.out"

Area expansion ratio = 1 / (1 + -1.1600E-01 * HAB + 0.0000E+00 * HAB**2)

Transport parameters: MXAVE TDIF

^^
^^^("diffusion.out")^^

11. Flame properties file ("props.out"):

^^

	HAB	VEL	RHO	VISC	Cp	COND
1	0.0000	9.406E+01	2.488E-05	2.311E-04	6.252E+00	1.360E-04
2	0.0187	1.008E+02	2.317E-05	2.432E-04	6.285E+00	1.414E-04
3	0.0374	1.078E+02	2.161E-05	2.556E-04	6.318E+00	1.472E-04
4	0.0561	1.169E+02	1.988E-05	2.709E-04	6.355E+00	1.553E-04
5	0.0747	1.261E+02	1.839E-05	2.858E-04	6.390E+00	1.636E-04
6	0.0934	1.428E+02	1.621E-05	3.117E-04	6.447E+00	1.800E-04
7	0.1121	1.597E+02	1.446E-05	3.368E-04	6.505E+00	1.966E-04
8	0.1495	2.000E+02	1.150E-05	3.922E-04	6.646E+00	2.361E-04
9	0.1869	2.447E+02	9.355E-06	4.488E-04	6.826E+00	2.796E-04
10	0.2242	2.908E+02	7.837E-06	5.030E-04	7.034E+00	3.239E-04
11	0.2616	3.353E+02	6.766E-06	5.523E-04	7.233E+00	3.662E-04
12	0.2990	3.775E+02	5.983E-06	5.970E-04	7.417E+00	4.062E-04
13	0.3737	4.445E+02	5.036E-06	6.655E-04	7.695E+00	4.698E-04
14	0.4485	4.874E+02	4.552E-06	7.090E-04	7.866E+00	5.116E-04
15	0.5232	5.139E+02	4.277E-06	7.373E-04	7.971E+00	5.391E-04
16	0.5980	5.312E+02	4.100E-06	7.572E-04	8.039E+00	5.588E-04
17	0.7475	5.446E+02	3.924E-06	7.780E-04	8.101E+00	5.797E-04
18	0.8970	5.462E+02	3.838E-06	7.883E-04	8.129E+00	5.908E-04
19	1.0465	5.418E+02	3.795E-06	7.932E-04	8.143E+00	5.968E-04
20	1.1960	5.304E+02	3.800E-06	7.917E-04	8.141E+00	5.965E-04
21	1.3455	5.116E+02	3.860E-06	7.827E-04	8.122E+00	5.890E-04
22	1.4950	4.941E+02	3.914E-06	7.749E-04	8.106E+00	5.826E-04
23	1.6445	4.767E+02	3.973E-06	7.667E-04	8.089E+00	5.758E-04
24	1.7940	4.598E+02	4.030E-06	7.588E-04	8.072E+00	5.693E-04
25	1.9435	4.433E+02	4.089E-06	7.508E-04	8.054E+00	5.628E-04
26	2.0930	4.268E+02	4.151E-06	7.426E-04	8.032E+00	5.559E-04

Miscellaneous properties, input file inp/fbr/jl22arh2.atx

Area expansion ratio = 1 / (1 + -1.1600E-01 * HAB + 0.0000E+00 * HAB**2)

Transport parameters: MXAVE TDIF

^^
^^^("props.out")^^

12. Profile-calculated net rates output file ("netrate.out"). Here there are two fewer HABs than the species profile file because this calculation is done at the midpoints of the flux mesh.

2	0.0187	1.172E-05	-2.578E-04	-2.069E-06	8.868E-07	1.819E-07	-8.629E-08
3	0.0374	1.507E-05	-2.911E-04	-3.394E-06	1.566E-06	3.349E-07	7.133E-07
4	0.0561	1.563E-05	-2.916E-04	-4.004E-06	1.433E-06	4.642E-07	6.338E-07
5	0.0747	1.607E-05	-2.990E-04	-3.503E-06	2.397E-06	1.189E-06	8.869E-07
6	0.0934	1.897E-05	-3.038E-04	-7.172E-06	8.721E-07	5.737E-07	6.446E-07
7	0.1168	1.269E-05	-1.995E-04	-5.992E-06	-2.562E-06	-1.062E-06	-1.760E-08
8	0.1495	7.929E-06	-1.366E-04	-3.832E-06	-5.903E-06	6.746E-07	-1.858E-06
9	0.1869	4.304E-06	-1.021E-04	-7.433E-07	-1.004E-05	1.434E-05	-9.259E-06
10	0.2242	-1.304E-06	-2.914E-05	3.596E-06	-1.225E-05	5.030E-05	-2.709E-05
11	0.2616	-8.541E-06	8.135E-05	7.466E-06	-1.055E-05	1.066E-04	-5.471E-05
12	0.3083	-1.027E-05	1.326E-04	5.888E-06	-2.968E-06	1.093E-04	-5.527E-05
13	0.3737	-9.511E-06	1.374E-04	3.529E-06	2.242E-06	9.686E-05	-4.889E-05
14	0.4485	-9.075E-06	1.398E-04	1.759E-06	6.459E-06	9.031E-05	-4.595E-05
15	0.5232	-7.008E-06	1.116E-04	3.087E-07	8.918E-06	6.689E-05	-3.487E-05
16	0.6167	-3.064E-06	4.792E-05	-8.496E-08	6.073E-06	2.566E-05	-1.427E-05
17	0.7475	-1.412E-06	1.930E-05	1.292E-07	3.830E-06	7.829E-06	-5.243E-06
18	0.8970	-9.216E-07	9.425E-06	3.674E-07	2.783E-06	1.308E-06	-1.973E-06
19	1.0465	-6.509E-07	4.832E-06	4.138E-07	1.792E-06	-1.212E-06	-4.436E-07
20	1.1960	-4.019E-07	2.653E-06	2.345E-07	7.747E-07	-1.091E-06	3.578E-08
21	1.3455	-1.890E-07	1.596E-06	8.263E-09	-6.812E-08	-1.556E-08	4.315E-08
22	1.4950	-2.016E-08	1.062E-06	-1.912E-07	-8.010E-07	1.284E-06	-1.139E-07
23	1.6445	-7.001E-08	1.263E-06	-1.424E-07	-6.281E-07	9.536E-07	-6.401E-08
24	1.7940	-4.502E-08	1.168E-06	-1.669E-07	-7.272E-07	1.131E-06	-8.831E-08
25	1.9435	-4.450E-08	1.270E-06	-1.914E-07	-8.212E-07	1.253E-06	-8.240E-08

2	0.0187	-9.963E-05	2.297E-07	7.245E-08
3	0.0374	-1.574E-04	1.583E-07	6.145E-08
4	0.0561	-1.613E-04	1.196E-07	5.387E-08
5	0.0747	-1.895E-04	1.462E-07	6.071E-08
6	0.0934	-1.888E-04	-7.635E-08	1.561E-08
7	0.1168	-7.043E-05	-1.351E-07	-1.188E-08
8	0.1495	1.706E-05	-1.144E-07	-1.943E-08
9	0.1869	7.674E-05	-6.935E-08	-1.967E-08
10	0.2242	9.647E-05	-2.861E-08	-1.891E-08
11	0.2616	7.417E-05	-6.657E-09	-1.864E-08
12	0.3083	1.629E-05	-2.731E-09	-1.270E-08
13	0.3737	-1.655E-05	-2.309E-09	-8.629E-09
14	0.4485	-3.606E-05	-1.907E-09	-6.414E-09
15	0.5232	-3.873E-05	-8.315E-10	-3.558E-09
16	0.6167	-1.666E-05	-1.371E-10	-8.152E-10
17	0.7475	-1.745E-06	5.586E-12	-1.445E-11
18	0.8970	6.776E-06	-1.315E-11	8.830E-11

```
 19  1.0465  9.946E-06 -7.773E-12  1.137E-11
 20  1.1960  7.420E-06 -3.652E-12 -3.175E-11
 21  1.3455  2.910E-06  1.331E-12 -1.655E-11
 22  1.4950 -1.519E-06 -4.144E-12  1.511E-11
 23  1.6445 -3.214E-07 -2.757E-12  9.427E-12
 24  1.7940 -9.376E-07 -3.726E-12  1.223E-11
 25  1.9435 -1.192E-06 -3.102E-12  1.375E-11

Net rates for input file inp/fbr/jl22arh2.atx
Fluxes smoothed  4 times.  Poly order  4, window size  9, edge method AVE.
Area expansion ratio = 1 / (1 + -1.1600E-01 * HAB +  0.0000E+00 * HAB**2)

Transport parameters:  MXAVE  TDIF

^^^^^^^^^^^^^^^^^^^^^^^^^^^^^^^^^^^^^^^^^^^^^^^^^^^^^^^^^^^^^^^^^^^^^^^^^^^^^^^^
^^^^^^^^^^^^^^^^^^^^^^^^^^^^^^^^^^^^^^("netrate.out")^^^^^^^^^^^^^^^^^^^^^^^^^^^^
```

13. Screen (unit 6) output.

```
^^^^^^^^^^^^^^^^^^^^^^^^^^^^^^^^^^^^^^^^^^^^^^^^^^^^^^^^^^^^^^^^^^^^^^^^^^^^^^^^

 FBR:  Data/Model Analysis Program
     Version 1.12, personal use, August 1994
     DOUBLE PRECISION

     Massachusetts Institute of Technology
     Chemical Engineering Department


     Reading control file
     Initializing CHEMKIN from link file cklink
     Opening text data file inp/fbr/jl22arh2.atx
      for data input
     Opening "link.out"
     Printing link file contents...
     Opening transport link file, tplink
     Initializing transport from file tplink

TRANLIB:  Multicomponent transport library,
       CHEMKIN-II Version 1.7, October 1992
       DOUBLE PRECISION

Diffusion/flux/rate calculation working space requirements:

                PROVIDED      REQUIRED
```

LOGICAL	500	0
INTEGER	12000	555
REAL	1500000	44460
CHARACTER	500	13

Creating a flame code binary file ("binary.fbr")
Writing file "soln.out"
Writing file "solnhead.out"
Finding reactions with species to be analyzed

Reactions which contain species to be analyzed (OH) by rxn path analysis:

1. H2O2+M<=>2OH+M	1.200E+17	0.00000	45500.0
3. H2O2+H<=>OH+H2O	1.000E+13	0.00000	3590.0
4. H2O2+O<=>OH+HO2	9.550E+06	2.00000	3970.0
8. HO2+H<=>2OH	1.400E+14	0.00000	1073.0
9. HO2+OH<=>H2O+O2	7.500E+12	0.00000	0.0
11. H2+OH<=>H2O+H	2.140E+08	1.51000	3430.0
12. H2+O2<=>2OH	1.700E+13	0.00000	47780.0
13. H+O2<=>OH+O	1.910E+14	0.00000	16440.0
18. H+OH+M<=>H2O+M	2.240E+22	-2.00000	0.0
19. H+O+M<=>OH+M	6.020E+16	-0.60000	0.0
20. OH+H2O2<=>H2O+HO2	7.080E+12	0.00000	1430.0
21. 2OH<=>O+H2O	1.230E+04	2.62000	-1878.0
22. O+HO2<=>OH+O2	1.740E+13	0.00000	-400.0
23. O+H2<=>OH+H	5.130E+04	2.67000	6290.0
25. O+OH+M<=>HO2+M	1.000E+17	0.00000	0.0

Calculating rates of each reaction
Opening "rates.out"
Opening "parteqm.out"
Writing reaction rates in "rates.out"
Writing partial equilibrium ratios in "parteqm.out"

Reactions not printed: 8
Beginning HAB no: 1 Ending HAB no: 26
Absolute rate, or ratio (normalized): ABSOL

Calculating transport coefficients
Calculating diffusion velocities
Calculating fluxes, flux balances, and net rates

Area expansion ratio = 1 / (1 + -1.1600E-01 * HAB + 0.0000E+00 * HAB**2)

Smoothing soln 4 times, polynomial order 4, window size 9, edge method AVE

```
Writing file "flux.out"
Writing file "netrate.out"
Writing file "diffusion.out"
Writing file "fluxbal.out"
Writing file "props.out"

END of program FBR

** Send comments, questions, and bug reports to ras@mit.edu **
```

(screen output)

(End of program instructions)

Source code:

```
ccccccccccccccccccccccccccccccccccccccccccccccccccccccccccccccccccccccccccc
C*********************************************************************
C
C
C                      **** Main program ****
C
C
C
C*********************************************************************
ccccccccccccccccccccccccccccccccccccccccccccccccccccccccccccccccccccccccccc
C
C  Program to:
C
C     1.  Perform reaction path analysis of model pathways, using model
C          output or experimental data.
C     2.  Calculate flux, perform an elemental flux balance, and calculate
C          net reaction rate, given experimental data or model output.
C
C    (Uses Chemkin II.)
C    R. Shandross, MIT Chemical Engineering Dept., January 1995.
C
C/////////////////////////////////////////////////////////////////////////
C
C    Version 1.1
C
C  Changes from Version 1.0
C
C     1.  Implement partial equilibrium calculation.
C     2.  Move control file to standard input.
C     3.  Put area expansion ratio fit parameters in control file.
C
ccccccccccccccccccccccccccccccccccccccccccccccccccccccccccccccccccccccccccc
c    Version 1.11
c
c  Changes from version 1.1
c
c     1.  Prints path in files names, can handle big path.
c     2.  New keyword, 'LDP', means only print soln and link, and link
c          with duplicate-checking (default - no checking)
c     3.  Improved duplicate reaction checking.
c     4.  Larger workspaces, more reactions and species.
c
ccccccccccccccccccccccccccccccccccccccccccccccccccccccccccccccccccccccccccc
c    Version 1.12
c
c  Changes from version 1.11
c
c     1.  Print out diffusion coefficients in Fickian form.
C
ccccccccccccccccccccccccccccccccccccccccccccccccccccccccccccccccccccccccccc
        program fbr
        implicit double precision (a-h,o-z)
        implicit integer (i-n)
        parameter (lniwk=12000, lnrwk=1500000, lncwk=500, lnlwk=500)
        parameter (kdm=100, jdm=175, krx=550)
CC
C ...These parameters (above) are only for the main program.  The same
C    parameters are defined for all subroutines in the BLOCK DATA program.
C    Changes to kdim, jdim, krxn, leniwk, lenrwk, lencwk, and lenlwk
C    must be made both here and in the BLOCK DATA subprogram at the end.
CC
```

```
      character*80  arglink, atplink, solfile, sname(krx), str,
     +              lnkused
      character*16  cwork, isolut, icklnk, imclnk, spname, spec, fn,
     +              method, multi, el, cwb, thdif, ftype
      character*3   pcontrol(3), edge
      logical       kerr, lmulti, discrep1(kdm), discrep2(kdm),
     +              ltdif
      dimension     mhol(2,10), s(kdm+2,jdm), x(jdm), cwb(lncwk),
     +              iwork(lniwk), rwork(lnrwk), cwork(lncwk),
     2              aki(kdm,krx), ithb(krx), nuki(kdm,krx),
     3              irev(krx), ra(krx), rb(krx), re(krx), w(kdm),
     4              irxntab(krx), spname(kdm), ispectab(kdm),
     5              wdotf(krx,jdm), wdotr(krx,jdm), wdot(jdm),
     6              y(kdm+2,jdm), nelem(3), xmf(kdm), wneg(jdm),
     7              wpos(jdm), xsg(7,25), asg(7,14), rsg(7,7),
     8              convol(25,25), swork(jdm)
      common /ckstrt/ nmm , nkk , nii , mxsp, mxtb, mxtp, ncp , ncp1,
     +     ncp2, ncp2t,npar, nlar, nfar, nlan, nfal, nrev,
     2     nthb, nrlt, nwl,  icmm, ickk, icnc, icph, icch,
     3     icnt, icnu, icnk, icns, icnr, iclt, icrl, icrv,
     4     icwl, icfl, icfo, ickf, ictb, ickn, ickt, ncaw,
     5     ncwt, nctt, ncaa, ncco, ncrv, nclt, ncrl, ncfl,
     6     nckt, ncwl, ncru, ncrc, ncpa, NcKF, NcKR, nck1, nck2, nck3,
     7     nck4, nci1, nci2, nci3, nci4
      common /fileinfo/ nnnn, jj, p, dmflrt, kk, natj
      common /rxprxp/ nckw, nmcw, nsch, nd, ndkj, ntdr, nyv,
     +                nomeg, nki, ngflx, nflux, nfbal, nvel, ickw,
     2                imcw, ielk, ncnc, nsum, nprt
      common /lenprm/ leniwk, lenrwk, lencwk, lenlwk, kdim, jdim, krxn
      common /locs/ nt, nm, nys, ny, nx, nxs
      common /mach/ small, big, exparg
      common /fbrrd/  elflux(3), fmmwt, iignore, ignorxn(100), ihablo,
     +       ihabhi, numsmth, ipoly, numpts, nsmflux, ipolfx, nptflx,
     2       areab, areac, arglink, solfile, spec, method, multi,
     3       thdif, el(3), pcontrol, edge
      data iout/6/, ilkout/7/, irate/9/, link/12/, linktp/14/
      data isolout/8/, ibinary/10/, ifbrdat/5/
      data icklnk/'CKLINK          '/
      data isolut/'SOLUTION        '/
      data imclnk/'MCLINK          '/
CC
C  ...Print header.
CC
       write (iout,5)
 5     format (/,2x,'FBR:  Data/Model Analysis Program',/,
     +     8x,'Version 1.12, personal use, January 1995',
     2     /,8x,'DOUBLE PRECISION',//,8x,
     3     'Massachusetts Institute of Technology',/,8x,
     4     'Chemical Engineering Department',//)
CC
C  ...Read the control file, which has params needed for operation, and
C     get the parameters.
C
C
C  ...Format of control file:
C
C    arglink    {character*80}     # name of link file; 'nolink' to read link
C                                                    contents from binary sol'n file
C    atplink        "              # name of transport link file
C    ftype      {character*16}     # 'text' or 'bin' - refers to sol'n file
C    solfile    {character*80}     # name of data/solution file
C    numsmth  ipoly  numpts {int}  # number of times to smooth data/solution;
C                                    polynomial order (2-6);
C                                    number of points (to each side) to use in
```

```
C                                     Savitsky-Golay smoothing.  (numsmth = 0
C                                     means don't smooth data/solution)
C    nsmflux  ipolfx  nptflx  "     # Savitsky-Golay params for flux profiles
C    edge       {character*3}       # method of handling smoothing near edges:
C                                     'ave' - average of 5 pts til full window
C                                     'SG ' - increasing window size til full
C    spec       {character*16}      # species name to analyze
C    iignore    {integer}           # no. rxns to ignore; -1 means ignore all
C                                                          (for print out only)
C    ignorxn(1)...ignorxn(iignore) # rxn. nos. to ignore; based on link file
C    ihablo  ihabhi                # HAB range to analyze on; sol'n file based
C                                                          (for print out only)
C    method     {character*16}     # method of rate calculation desired:
C                                     'absol' - absolute rate of
C                                                       forward/reverse
C                                     'ratio' - ratio to sum(>0) or sum (<0)
C    multi  thdif      "           # 'mxave' for mixture averaged diffusion
C                                     'ntdif' for no thermal diffusion
C                                     Multicomponent, w/thermal diffusion =
C                                     default.
C    fmmwt      {double}           # mean molecular wt. of feedstock
C    el  elflux {char*16},{double} # name and initial mass flux of element;
C                                     one line each for H, C, O.
C    pcontrol(2){character*3}      # program control:
C                                     OK - no control
C                                     NSL - don't print "soln.out" or
C                                           "link.out"
C                                     NRP - don't do reaction path analysis
C                                     NFN - don't do flux/net-rate analysis
C                                     LDP - print "soln.out" and "link.out"
C                                           only; do duplicate rxn check
C    areab  areac  {double}        # area expansion ratio fit parameters for
C                                  # expression:
C                                  #  A = 1 / (1 + areab * HAB + areac * HAB^2)
C
C
C  (End format of control file)
C
CC
C        read (*,*) fn
C        open (unit=ifbrdat, status='old', form='formatted', file=fn)
         call fbrread (atplink, ftype)
CCCCCCCCCCCCCCCCCCCCCCCCCCCCCCCCCCCCCCCCCCCCCCCCCCCCCCCCCCCCCCCCCCCCCCCCCCCCCCC
CC                                                                            CC
CC                      **** CONTROL BLOCK ****                               CC
CC                                                                            CC
CCCCCCCCCCCCCCCCCCCCCCCCCCCCCCCCCCCCCCCCCCCCCCCCCCCCCCCCCCCCCCCCCCCCCCCCCCCCCCC
CC
C  1. Get data/solution from file.  For a text file, the data is assumed
C     to be in the form of mole fractions.  The routine 'openbin' will
C     convert to mass fraction, into array y.  For a binary file, the
C     solution is in the form of mass fractions.  'openbin' will convert
C     to mole fraction, so s will contain mole fractions and y will
C     contain mass fractions when returning from either 'openbin' or
C     'opentext'.
C
C     For a text file, open link file, initialize CHEMKIN and print file
C     contents first; but for a binary file get the link information from
C     the binary file if 'arglink' is set to "nolink" in fbr.dat
C
C     In either case, the data returned from the file-opening routines
C     will be sorted according to the order of species found in the link
C     information.  Only the profiles for species in the link file will
C     be included in the data array which is returned.
```

```
C
C     If there are species in the species profile file that are not found in
C     the link file, the mole fractions of the data array returned will not
C     fulfill a mass balance because some species will have been
C     eliminated.  The run will be aborted in this case.
CC
        nkk = 0
CC
C ...The variable 'nkk' (number of species) will be the flag for the sub-
C    routine 'openbin':  if it is still 0 when the binary solution file
C    is opened, then the link file was not initialized, and link info
C    should be read from the binary solution file.  The variable "lnkused"
C    keeps track of the source of link information.
CC
        lnkused = arglink
        if ((arglink .eq. 'nolink') .or. (arglink .eq. 'NOLINK')) then
           lnkused = solfile
           goto 22
        endif
CC
C ...The "no link" flag was not set, so open link file and initialize
C    CHEMKIN from it.
CC
        open (unit=link, status='old', form='unformatted', file=arglink)
        call ckinit (leniwk, lenrwk, lencwk, link, ilkout, iwork, rwork,
     +               cwork)
        call strip (arglink, str)
        write (iout,20) str
 20     format (8x,'Initializing CHEMKIN from link file ',a28)
 22     continue
CC
C ...Get Savitsky-Golay parmameters, if needed.
CC
        if (numsmth .ne. 0) call sgparam (ipoly, xsg, asg, rsg, convol)
        if (ftype(1:4).eq.'TEXT') then
CC
C ...The data is in a text file; open it.
CC
           call opentext (convol, swork, discrep1, discrep2, ispectab,
     +                    xmf, iwork, rwork, cwork(IcKK), spname, x, s,
     2                    y)
        else
CC
C ...The solution is in a binary file; open it.
CC
         call openbin (convol, swork, discrep1, discrep2, ispectab,
     +                 xmf, iwork, rwork, cwork, cwb, spname, x, s, y)
        endif
CC
C ...Print the link information, whatever the source.
CC
        call printlnk (lnkused, pcontrol, iwork, rwork, cwork, sname,
     +                 aki, ra, rb, re, nuki, ruc)
        write (iout,*)
CC
C ...Set up internal work pointers above the CHEMKIN workspace.
CC
        if ((arglink .ne. 'nolink') .and. (arglink .ne. 'NOLINK')) then
           open (linktp, status='old', form='unformatted', file=
     +          atplink)
           call strip (atplink, str)
           write (iout,16) str
 16        format (8x,'Opening transport link file, ', a28)
        endif
```

```
        call fbrptr (link, linktp, iout, iwork, rwork, cwork,
     +               arglink, atplink)
CC
C  2. If the species profile file was a text file, write a binary flame
C     code file from it.
CC
        if (ftype(1:4).eq.'TEXT') call svsoln(x, y, iwork, rwork, cwork)
CC
C  3. Print out data/solution in the form of spreadsheet-importable files
C     ("soln.out" and "solnhead.out").  rwork(nsum) is workspace for sum
C     of mole fractions.
CC
        call printit (x, s, cwork(IcKK), spname, rwork(nsum), iwork,
     +                rwork)
        if ((pcontrol(1).ne.'NRP').and.(pcontrol(2).ne.'NRP')) then
CC
C  4. Get a list of rxns which involve species 'spec', in array irxntab.
CC
           call speclist (cwork, iwork, rwork, ispec, irxntab, kerr)
           if (kerr) then
              write (iout,7200)
 7200         format (//, 'ABORT RUN',//)
              stop
           endif
CC
C ...Print reactions which have the species to be analyzed.
CC
           ll = index(spec,' ') - 1
           write (iout, 6100)
           write (iout, 6110) (spec(jjj:jjj),jjj=1,ll)
           write (iout, 6120)
 6100      format (/,1x, 'Reactions which contain species to be ',
     +          'analyzed (',$)
 6110      format (a1,$)
 6120      format (') by rxn path analysis:',/)
           do 3100 i = 1, nii
              if (irxntab(i).ne.0) write (iout,6000) i, sname(i), ra(i),
     +             rb(i), ruc*re(i)
 6000         format (1x,i3,'. ',a32,t40,1pe10.3,3x,0pf10.5,3x,0pf10.1)
 3100      continue
           write (iout, 7140)
 7140      format (/)
CC
C  5. Process forward and reverse rates of the species 'spec' for each
C     reaction containing the species to be analyzed, and every HAB.
C     The data sent to subroutine rates must be sorted so that the species
C     are in the order found in the link file.
CC
           write (iout,30)
 30        format (8x,'Calculating rates of each reaction')
           do 3200 j = 1, jj
              wdot(j) = 0.0
CC
C ... rwork(ncnc) is work space for concentrations.
CC
              call rates (s(nt,j), s(nx,j), iwork, rwork, irxntab,
     +             rwork(ncnc), ispec, nuki, w, wdotf(1,j),
     2             wdotr(1,j), wdot(j), kerr)
              if (kerr) write (iout,160) j, w(ispec), wdot(j)
 160          format (1x,'WDOT discrepancy at HAB no. ',i3,4x,
     +             'CHEMKIN: ',1pe10.2,/,t45,'FBR: ',1pe10.2)
 3200      continue
CC
C  6. Print out rates for reaction path analysis.
```

```
CC
           if (iignore.eq.-1) then
              write (iout, 7210)
 7210         format (/, ' Per instructions, no reaction path'
     +             ,' analysis file was written.',/)
           else
              call printrate (x, wneg, wpos, wdotf, wdotr, wdot,
     +                        rwork(nprt), irxntab, ispec, iwork,
     2                        rwork)
           endif
CC
C  7. Print out contents of control file.
CC
           if (iignore.gt.0) write (iout,140) (ignorxn(i),i=1,iignore)
 140       format (//,3x,'Reactions not printed:  ',100(i4))
           write (iout,150) ihablo,ihabhi,method
 150       format (3x,'Beginning HAB no:  ',i4,3x,'Ending HAB no:  ',i4,
     +          /,3x,'Absolute rate, or ratio (normalized):  ',a5,/)
        endif
        if ((pcontrol(1).ne.'NFN').and.(pcontrol(2).ne.'NFN')) then
CC
C  8. Calculate diffusion velocity for flux analysis.
C
C ...First, evaluate and store the transport coefficients.  Default is
C    multi-component diffusion, thermal diffusion, correction velocity
C    method.  Correction diffusion velocity is always used.  Various work-
C    spaces are sent to the two diffusion routines.  See subroutine fbrptr.
CC
           lmulti = .TRUE.
           ltdif = .TRUE.
           if (multi(1:5).eq.'MXAVE') lmulti = .FALSE.
           if (thdif(1:5).eq.'NTDIF') ltdif = .FALSE.
           write (iout, 145)
 145       format (8x,'Calculating transport coefficients')
           call mtrnpr (lmulti, ltdif, x, y, rwork(ncwt),
     1          rwork(nsch), iwork(ickw), rwork(nckw), iwork(imcw),
     2          rwork(nmcw), rwork(nd), rwork(ntdr), rwork(ndkj))
CC
C ...Finally, evaluate and store the diffusion velocities.
CC
           write (iout, 155)
 155       format (8x,'Calculating diffusion velocities')
           call mdifv (lmulti, .TRUE., ltdif, x, y, rwork(ncwt),
     1          rwork(nsch), rwork(nd), rwork(ntdr), iwork(ickw),
     2          rwork(nckw), rwork(ndkj), rwork(nyv), cwork(1))
CC
C  9. Now calculate the flux, do a flux balance, and calculate the net
C     reaction rate Ki at the mesh midpoints.  Use some of the
C     workspace for these calcs:
C                                   VARIABLE          WORKSPACE
C                                  womega(nkk,3)        nomeg
C                                  vel(jdim)            nvel
C                                  gflux(nkk,jdim)      ngflx
C                                  flux(nkk,jdim)       nflux
C                                  fluxbal(jdim,3)      nfbal
C                                  rate(nkk,jdim)       nki
C                                  nelk(nmm,nkk)        ielk
C     Fluxbal is the percent deviation of the element flux balance at a
C     particular HAB.
C
C     Get a new  convolution matrix if the polynomial order is different
C     than it was for the data smoothing.
CC
           if ((numsmth .eq. 0) .and. (nsmflux .ne. 0)) then
```

```
            call sgparam (ipolfx, xsg, asg, rsg, convol)
         else
            if ((nsmflux .ne. 0) .and. (ipolfx .ne. ipoly))
     +              call sgparam (ipolfx, xsg, asg, rsg, convol)
         endif
         write (iout, 165)
 165     format (8x,'Calculating fluxes, flux balances, and net ',
     +           'rates')
         call fbrcalc (convol, swork, x, y, rwork(nsch), rwork(nyv),
     +        rwork(ncwt), cwork(IcMM), iwork(ielk), rwork(nomeg),
     2        rwork(NcAW), iwork(ickw), rwork(nckw), rwork(nvel),
     3        rwork(nflux), rwork(ngflx), rwork(nfbal), nelem,
     4        rwork(nki))
CC
C  10. Print the results of the flux/rate analysis.
CC
         call printfbr (x, cwork(IcMM), cwork(IcKK), rwork(nflux),
     +        rwork(nfbal), rwork(nd), nelem, rwork(nki))
CC
C  11. Calculate and print some flame properties (vel, viscosity, Cp, rho,
C      k).
CC
         call properties (x, s, rwork, iwork)
       endif
CC
C  12. Make a pretty exit.
CC
       write(iout,170)
 170   format(/,8x,'END of program FBR',//,' ** Send comments, ques',
     +        'tions, and bug reports to ras@mit.edu **',//)
CCCCCCCCCCCCCCCCCCCCCCCCCCCCCCCCCCCCCCCCCCCCCCCCCCCCCCCCCCCCCCCCCCCCCCCCCCCCCCC
CC                    **** END CONTROL BLOCK ****                           CC
CC                                                                          CC
CCCCCCCCCCCCCCCCCCCCCCCCCCCCCCCCCCCCCCCCCCCCCCCCCCCCCCCCCCCCCCCCCCCCCCCCCCCCCCC
       stop
       end
CCCCCCCCCCCCCCCCCCCCCCCCCCCCCCCCCCCCCCCCCCCCCCCCCCCCCCCCCCCCCCCCCCCCCCCCCCCCCCC
C*************************************************************************
C                                                                        C
C                     **** End of main program ****                      C
C                                                                        C
C*************************************************************************
CCCCCCCCCCCCCCCCCCCCCCCCCCCCCCCCCCCCCCCCCCCCCCCCCCCCCCCCCCCCCCCCCCCCCCCCCCCCCCC
CXXXXXXXXXXXXXXXXXXXXXXXXXXXXXXXXXXXXXXXXXXXXXXXXXXXXXXXXXXXXXXXXXXXXXXXXXXXX
C#########################################################################
C#########################################################################
CXXXXXXXXXXXXXXXXXXXXXXXXXXXXXXXXXXXXXXXXXXXXXXXXXXXXXXXXXXXXXXXXXXXXXXXXXXXX
      subroutine strip (str1, str2)
C
C**** Strip a file name string of the substring '/work2/u2170/chemkin/'
C
      character*80   str1, str2
      if (str1(1:21).eq.'/work2/u2170/chemkin/') then
         str2 = str1(22:80)
      else
         str2 = str1
      endif
C
C**** End "Strip file name string"
C
      return
      end
CXXXXXXXXXXXXXXXXXXXXXXXXXXXXXXXXXXXXXXXXXXXXXXXXXXXXXXXXXXXXXXXXXXXXXXXXXXXX
C#########################################################################
```

```
C###########################################################################
CXXXXXXXXXXXXXXXXXXXXXXXXXXXXXXXXXXXXXXXXXXXXXXXXXXXXXXXXXXXXXXXXXXXXXXXXXXX
        subroutine printlnk (arglink, pcontrol, iwork, rwork, cwork,
     +                          sname, aki, ra, rb, re, nuki, ruc)
c
C****  Print link file contents.
c
        implicit double precision (a-h,o-z)
        implicit integer (i-n)
        character*80  arglink, solfile, sname, str
        character*16  cwork
        character*3   pcontrol(3)
        integer       pp
        logical       kerr
        dimension     iwork(*), rwork(*), cwork(*), sname(*),
     +                aki(kdim,*), ra(*), rb(*), re(*), nuki(kdim,*)
        common /lenprm/ leniwk, lenrwk, lencwk, lenlwk, kdim, jdim, krxn
        common /mach/ small,big,exparg
        common /ckstrt/ nmm , nkk , nii , mxsp, mxtb, mxtp, ncp , ncp1,
     1      ncp2, ncp2t,npar, nlar, nfar, nlan, nfal, nrev,
     2      nthb, nrlt, nwl,  icmm, ickk, icnc, icph, icch,
     3      icnt, icnu, icnk, icns, icnr, iclt, icrl, icrv,
     4      icwl, icfl, icfo, ickf, ictb, ickn, ickt, ncaw,
     5      ncwt, nctt, ncaa, ncco, ncrv, nclt, ncrl, ncfl,
     6      nckt, ncwl, ncru, ncrc, ncpa, NcKF, NcKR, nck1, nck2, nck3,
     7      nck4, nci1, nci2, nci3, nci4
        data ifbrdat/5/, iout/6/, ilkout/7/, irate/9/, link/12/
cc
c  ...Some initializations.
cc
        call ckrp (iwork, rwork, ru, ruc, pa)
        nm = nkk + 2
cc
c  ...Get species and reaction information.
c
c     nmm - total # of elements in mech.
c     nkk - total # of species in mech.
c     nii - total # of reactions in mech.
cc
        kerr = .false.
cc
c  ...Arrhenius coefficients:
cc
        call ckabe (iwork, rwork, ra, rb, re)
cc
c  ...Third body coefficients:
c
c     Don't call CKTHB because of an error; some users may not
c     have corrected it.
c
c         call ckthb (kdim, iwork, rwork, aki)
c
c    The following is from CKTHB in CHEMKIN II, but corrected:
cc
        do 152 iii = 1, nii
           do 140 kkk = 1, nkk
              aki(kkk,iii) = 1.0
 140       continue
 152    continue
c
        do 252 nnn = 1, nthb
           iii = iwork(IcTB+nnn-1)
           do 252 l = 1, iwork(IcKN+nnn-1)
cc
```

```
C     k = iwork(IcKT + (n-1)*mxsp + 1 - 1)
C     ak = rwork(NcKT + (n-1)*mxsp + 1 - 1)
C
C     Correction, R. Shandross, 5/14/93:  Should be MXTB, not MXSP
CC
              kkk = iwork(IcKT+(nnn-1)*mxtb+1-1)
              ak = rwork(NcKT+(nnn-1)*mxtb+1-1)
              aki(kkk,iii) = ak
 252        continue
CC
C  ...Flags for reversibility and arbitrary 3rd bodies:
C     ITHB, IREV  contain "how many" species.
CC
        call ckitr (iwork, rwork, ithb, irev)
CC
C  ...Stoichiometric coefficients:
CC
        call cknu (kdim,iwork,rwork,nuki)
        if ((pcontrol(1).ne.'NSL').and.(pcontrol(2).ne.'NSL')) then
CC
C  ...Document contents of link file in file "link.out".
CC
           open (unit=ilkout, status='unknown', form='formatted', file=
     +           "link.out")
           write (iout,15)
 15        format (8x,'Opening "link.out"')
           write (iout,25)
 25        format (8x,'Printing link file contents',$)
           call strip (arglink, str)
           write (ilkout,7000) str
           write (ilkout,7005)
           do 50 m=1,nmm
              write (ilkout,7010) m, cwork(IcMM+m-1)
 50        continue
           write (iout,8000)
           write (ilkout,7020)
           do 75 k=1,nkk
              write (ilkout,7010) k, cwork(IcKK+k-1)
 75        continue
           write (iout,8000)
           write (ilkout,7060)
CC
C  ...Reaction descriptions:
C
C  (1) Get reaction description.
CC
           do 100 i = 1, nii
              call cksymr (i, ilkout, iwork, rwork, cwork, lt, sname(i),
     +                     kerr)
              if (kerr) then
                 write (ilkout,*) 'Character length error in CKSYMR,',
     +                ' reaction ',i
                 stop
              endif
CC
C  (2) Notify if description longer than 32 chars, then print rxn info,
C      including description and Arrhenius parameters.
CC
              if(lt.gt.32) write (ilkout,7015)
              write (ilkout,6000) i, sname(i), ra(i), rb(i), ruc*re(i)
 CC
C  (3) Print any falloff parameters for this rxn.
CC
              do 85 pp = 1, nfal
```

```
                if (iwork(IcFL+(pp-1)).eq.i) then
                   failflag = iwork(IcFO+pp-1)
                   indx = NcFL + (pp-1)*nfar
                   write (ilkout,3050) (rwork(indx+(l-1)),l=1,2),
     +                  rwork(indx+2)*ruc
                   if (fallflag.eq.2) then
                      write (ilkout,3070) (rwork(indx+l-1),l=4,6)
                      write (ilkout,3075) (rwork(indx+l-1),l=7,8)
                   elseif (fallflag.eq.3) then
                      write (ilkout,3080) (rwork(indx+l-1),l=4,6)
                   elseif (fallflag.eq.4) then
                      write (ilkout,3090) (rwork(indx+l-1),l=4,7)
                   endif
                endif
 85          continue
CC
C  (4) Print any third body efficiencies and hv freqencies for this rxn.
CC
             do 80 pp = 1, nthb
                if (iwork(IcTB+(pp-1)).eq.i) then
                   do 175 k=1,nkk
                      if (aki(k,i).ne.1.0) write (ilkout,7090)
     +                                        cwork(IcKK+k-1), aki(k,i)
 175                  continue
                endif
 80          continue
             do 87 pp = 1, nwl
                if(iwork(IcWL+(pp-1)).eq.i) then
                   write (ilkout,3020) rwork(NcWL+(pp-1))
                endif
 87          continue
CC
C  (5) Print any Landau-Teller info for this rxn.
CC
             do 90 pp = 1, nlan
                if (iwork(IcLT+(pp-1)).eq.i) then
                   write (ilkout,3000) (rwork(NcLT+(pp-1)*nlar+(l-1)),
     +                                  l=1,2)
                endif
 90          continue
CC
C  (6) Identify given reverse reactions, and any reverse L-T info.
CC
             do 93 pp = 1, nrev
                if (iwork(IcRV+(pp-1)).eq.i) then
                   write (ilkout,4100) (rwork(NcRV+(pp-1)*(npar+1)+
     +                 (l-1)),l=1,2),ruc*rwork(NcRV+(pp-1)*(npar+1)+2)
                endif
 93          continue
             do 95 pp = 1, nrlt
                if (iwork(IcRL+(pp-1)).eq.i) then
                   write (ilkout,3000) (rwork(NcRL+(pp-1)*nlar+(l-1)),
     +                    l=1,2)
                endif
 95          continue
CC
C  (7) Identify duplicate reactions.  This CKDUP is from CKINTERP.F.
CC
c1
c1  Skip this step now, unless the keyword LDP was used.
c1
             if (pcontrol(3).ne.'LDP') goto 160
C1             do 97 pp = 1, nii
                call ckdup (i, MXSP, iwork(IcNS), iwork(IcNR),
```

```
     +                iwork(IcNU), iwork(IcNK), NFAL, iwork(IcFL),
     1                iwork(IcKF), ISAME)
                   if (isame .gt. 0) then
                      n1 = 0
                      n2 = 0
                      if (nthb .gt. 1) then
                         do 150 n = 1, nthb
                            IF (iwork(IcTB+N-1) .EQ. ISAME) N1 = 1
                            IF (iwork(IcTB+N-1) .EQ. pp)    N2 = 1
 150                     continue
                      endif
                      IF (N1 .EQ. N2) WRITE (ilkout, 4000) i,isame
                   endif
C  97              continue
 160             continue
 100          continue
              write (iout,8000)
              close (ilkout)
           else
              do 20 i = 1, nii
                 call cksymr (i, ilkout, iwork, rwork, cwork, lt, sname(i),
     +                        kerr)
                 if (kerr) then
                    write (ilkout,*) 'Character length error in CKSYMR,',
     +                               ' reaction ',i
                    stop
                 endif
 20           continue
           endif
CC
C  ...End reaction descriptions
CC
CC
C  ...Format statements:
CC
 3000 FORMAT (9X,'Landau-Teller parameters:  B =',1pe12.4,', C =',
     +        1pe12.4)
 3010 FORMAT (9X,A10,' Enhanced by ',1PE12.3)
 3020 FORMAT (9X,'Radiation wavelength (A): ',F8.2,'  [<0 means react'
     +        ,'ant]')
C 1900 FORMAT (6X,A,T51,E10.3,F7.3,F11.3)
 1900 FORMAT (9X, A, T53, 1PE8.2, 2X, 0PF5.1, 2X, F9.1)
 3040 FORMAT (9X,'Reverse Landau-Teller parameters:  B =',1pe12.4,
     +           ', C =',1pe12.4)
 3050 FORMAT (9X,'Low pressure limit:',3(1pe13.4))
 3060 FORMAT (9X,'SRI centering:     ',3(1pe13.4))
 3070 FORMAT (9X,'SRI centering:     ',3(1pe13.4))
 3075 format (t29,2(1pe13.4))
 3080 FORMAT (9X,'TROE centering:    ',3(1pe13.4))
 3090 FORMAT (9X,'TROE centering:    ',4(1pe13.4))
 4000 FORMAT (9X,'Note:  reaction ',I4,' is the same as reaction ',I4)
 4100 FORMAT (9x,'Reverse reaction...',T40,1pe10.3,3X,0pf10.5,3X,
     +        0pf10.1)
 5000 format (a80)
 6000 FORMAT (1x,I3,'. ',A32,T40,1pe10.3,3X,0pf10.5,3X,0pf10.1)
 7000 FORMAT (1H1//5X,'Contents of Link File ',a28)
 7005 FORMAT (////,10X,19HELEMENTS CONSIDERED//)
 7010 FORMAT (10X,I3,1H.,2X,A16)
 7015 format (10x, 'The following reaction description is over ',
     +        '32 characters long:')
 7020 FORMAT (////,10X,18HSPECIES CONSIDERED//)
 7030 FORMAT(10X,I3,1H.,2X,10A1)
 7060 FORMAT (////,10X,20HREACTIONS CONSIDERED/
     +        T43,7HPRE EXP,5X,8HTEMP EXP,
```

```
     2        6X,7HACT ENG/)
 7090 FORMAT (20X,a16,2X,11HEnhanced by,f12.3)
 7140 FORMAT (/)
 8000 format ('.',$)
      return
      end
C
C**** End "Print link file contents"
CXXXXXXXXXXXXXXXXXXXXXXXXXXXXXXXXXXXXXXXXXXXXXXXXXXXXXXXXXXXXXXXXXXXXXXXXXX
C##########################################################################
C##########################################################################
CXXXXXXXXXXXXXXXXXXXXXXXXXXXXXXXXXXXXXXXXXXXXXXXXXXXXXXXXXXXXXXXXXXXXXXXXXX
subroutine opentext (convol, swork, ldiscrep, sdiscrep,
     +                     ispectab, xmf, iwork, rwork, kname,
     2                     spname, x, s, y)
C
C****  Read from a data (text) file.
C      Get X, T info from file.
C
        implicit double precision (a-h,o-z)
        implicit integer (i-n)
        character*80  solfile, arglink, str
        character*16  kname(*), spname(*), spec, method, multi, el,
     +                thdif
        character*12  name(5)
        character*3   nothing, pcontrol(3), edge
        logical       ldiscrep(*), sdiscrep(*), lflag, sflag
        dimension     s(kdim+2,*), x(*), ispectab(*), xmf(*),
     +                y(kdim+2,*), convol(25,25), swork(*)
        common /lenprm/ leniwk, lenrwk, lencwk, lenlwk, kdim, jdim, krxn
        common /locs/ nt, nm, nys, ny, nx, nxs
        common /fileinfo/ nnnn, jj, p, dmflrt, kk, natj
        common /rxprxp/ nckw, nmcw, nsch, nd, ndkj, ntdr, nyv,
     +                  nomeg, nki, ngflx, nflux, nfbal, nvel, ickw,
     2                  imcw, ielk, ncnc, nsum, nprt
        common /fbrrd/  elflux(3), fmmwt, iignore, ignorxn(100), ihablo,
     +          ihabhi, numsmth, ipoly, numpts, nsmflux, ipolfx, nptflx,
     2          areab, areac, arglink, solfile, spec, method, multi,
     3          thdif, el(3), pcontrol, edge
        common /ckstrt/ nmm , nkk , nii , mxsp, mxtb, mxtp, ncp , ncp1,
     +      ncp2, ncp2t,npar, nlar, nfar, nlan, nfal, nrev,
     2      nthb, nrlt, nwl,  icmm, ickk, icnc, icph, icch,
     3      icnt, icnu, icnk, icns, icnr, iclt, icrl, icrv,
     4      icwl, icfl, icfo, ickf, ictb, ickn, ickt, ncaw,
     5      ncwt, nctt, ncaa, ncco, ncrv, nclt, ncrl, ncfl,
     6      nckt, ncwl, ncru, ncrc, ncpa, NcKF, NcKR, nck1, nck2, nck3,
     7      nck4, nci1, nci2, nci3, nci4
        data iout/6/, itextdata/10/
CC
C ...Open the text file.
CC
        open(unit=itextdata, status='old', form='formatted',
     +      file=solfile, err=5)
        call strip (solfile, str)
        write (iout,10) str
 10     format (8x,'Opening text data file ',a40,/,8x,
     +          ' for data input')
CC
C ...Initializations.
CC
        lflag = .FALSE.
        sflag = .FALSE.
        do 15 i = 1, kdim + 2
           if (i .le. kdim) then
```

```
               ispectab(i) = 0
               xmf(i) = 0.0
               ldiscrep(i) = .FALSE.
               sdiscrep(i) = .FALSE.
               name(i)   = '            '
               spname(i) = '                '
            endif
            do 20 j = 1, jdim
               s(i,j) = 0.0
               y(i,j) = 0.0
 20         continue
 15      continue
CC
C ...Read pressure and flow rate.  They must be in the form x.xxxE-xx or
C    x.xxxE+xx  The field width is 10, and the field starts in the fourth
C    column so that the line can start "P =" or "M =", for ease of viewing.
C    P must be in atm and dmflrt in g/cm^2/sec.  P will be immediately
C    converted to dyne/cm^2.
CC
        read (itextdata,160) nothing, p
        p = p * 1.01325e6
        read (itextdata,160) nothing, dmflrt
 170    format ("Pressure = ",e10.4e2,"  Flow rate = ",e10.4e2)
CC
C ...Get the first set of data.  HAB and TEMP must be the first two columns.
C    Stop when HAB < 0.00.  There can only be five columns; the HAB data is
C    in the form x.xxx and the species profiles are in the form x.xxxE-xx
C    or x.xxxE+xx  The width of each field, numeric and character, is 12.
C    NOTE:  HAB must be in cm units, not mm.
C
C    Species names first:
CC
        numhab = 0
        numspec = 0
 5      read (itextdata,100,end=25) (name(i), i = 1, 5)
 25     if (name(1).eq.' ') goto 5
CC
C ...Write 'name' string to variable 'spname', removing leading blanks and
C    converting to uppercase.  Then check for end of species input.  For
C    now, the variable 'numspec' will be (number of species + 1).  The +1
C    is for temperature.
CC
        do 400 i = 3,5
           ii = i - 2
           spname(ii) = name(i)
           call rmblank(spname(ii))
           call upcase(spname(ii))
           if (spname(ii).eq.' ') goto 410
 400    continue
        numspec = 4
        goto 420
 410    numspec = i - 2
 420    continue
CC
C ...Next, the data:
CC
 11     numhab = numhab + 1
        read (itextdata,110)  x(numhab),(s(i,numhab), i = 1, numspec)
        if (x(numhab).lt.(0.00)) goto 150
        goto 11
 150    continue
CC
C ...Set the correct HAB index, accounting for HAB < 0 end-of-HABs flag
C    entry.
```

```
CC
        jj = numhab - 1
CC
C ...Now get the rest of the species data.
CC
 45     read (itextdata,100,end=300) (name(i), i = 1, 5)
        if (name(1) .eq. ' ') goto 45
        do 500 i = 1, 5
           numsp = numspec + i - 1
           spname(numsp) = name(i)
           call rmblank(spname(numsp))
           call upcase(spname(numsp))
           if (spname(numsp) .eq. ' ') goto 510
 500    continue
        do 530 j = 1, jj
           read (itextdata,130) (s(i,j),i=numspec+1,numspec+5)
 530    continue
        numspec = numspec + 5
        goto 520
 510    do 535 j = 1, jj
           read (itextdata,130) (s(ii,j),ii=numspec+1,numspec+i-1)
 535    continue
        numspec = numspec + i - 1
 520    continue
        goto 45
CC
C ...End of file.  Set kk to the number of species (one less than numspec
C    because of temperature profile) and get cross-reference array of
C    species w/r/t link file species.  Catch any species that are in the
C    link file but not in the data file with array ldiscrep.
CC
 300    continue
        close (itextdata)
        kk = numspec - 1
        nnnn = kk + 2
        do 430 k = 1, nkk
           do 440 iii = 1, kk
              if (spname(iii) .eq. kname(k)) then
                 ispectab(k) = iii
                 goto 430
              endif
 440       continue
           ldiscrep(k) = .TRUE.
           lflag = .TRUE.
 430    continue
CC
C ...Now catch any species in the species profile file which are not in the
C    link file, in array sdiscrep.
CC
        do 450 iii = 1, kk
           do 460 k = 1, nkk
              if (kname(k) .eq. spname(iii)) goto 450
 460       continue
           sdiscrep(iii) = .TRUE.
           sflag = .TRUE.
 450    continue
CC
C ...Document any species discrepancies.
CC
        if (kk.ne.nkk) write (iout,505) nkk, kk
 505    format (//,1x,'Discrepancy in number of species - USE ',
     +          'RESULTS WITH CAUTION !',//,5x,'Link file:      ',
     2          i3,/,5x,'Text data file: ',i3)
        if (lflag) then
```

```
            write (iout, 522)
 522        format (//,1x,'Species discrepancies, CAUTION !',//,5x,
     +              'Species unique to link file:')
            do 330 nn = 1, nkk
               if (ldiscrep(nn)) write (iout,*) kname(nn)
 330        continue
            write(iout,*)
         endif
         if (sflag) then
            write (iout, 512)
 512        format (//,1x,'Species discrepancies, CAUTION !',//,5x,
     +           'Species unique to text data file:')
            do 340 nn = 1, kk
               if (sdiscrep(nn)) write (iout,*) spname(nn)
 340        continue
            write(iout,*)
            write (iout, 565)
 565        format (//,'Link file must cover all species in ',
     +                 'data file:  ABORT RUN',//)
            stop
         endif

CC
C ...Sort data into the same order as the species are found in the link
C    file.  When done, the s array will contain only data for the species
C    found in the link file.  Profiles for other species will be set to
C    0.0, and the link file number-of-species index, nkk, is used instead
C    of nk.  No conversion to mole fractions is necessary for text file,
C    however for later computations convert to mass fractions into array
C    y.
CC
         nk = nkk
         if (kk .gt. nkk) nk = kk
         do 540 j = 1, jj
CC
C    (There are nkk species in the link file to be checked, and possibly
C     put in temporary holding array 'xmf'.  The value of xmf(k) remains
C     0.0 at every HAB if ispectab(k) is 0.)
CC
            do 550 k = 1, nkk
               if (ispectab(k) .ne. 0)  xmf(k) = s(nys+ispectab(k),j)
 550        continue
CC
C    (There are nk species profiles to finally end up being filled.  s must
C     be set to 0.0 first to avoid having a left-over value.)
C ..."Zeroize" any points less than zero.
CC
            do 560 k = 1, nk
               s(nys+k,j) = 0.0
               if (ispectab(k) .ne. 0) then
                  if(xmf(k) .ge. 0.0)  s(nys+k,j) = xmf(k)
               endif
 560        continue
CC
C ...Assign temperature and flow rate.
CC
            y(nt,j) = s(nt,j)
            y(nys+nkk+1,j) = dmflrt
            s(nys+nkk+1,j) = dmflrt
 540     continue
CC
C ...Convert to mass fraction, first performing any smoothing that is
C    needed.
CC
```

```
      if (numsmth .ne. 0) then
         write (iout, 600) numsmth, ipoly, 2*numpts+1, edge
 600     format (/,' Smoothing data ',i2,' times, polynomial order ',
     +           i2,', window size ',i2,', edge method ',a3,/)
         call smooth (numsmth, numpts, convol, kdim+2, ny, nkk, jj,
     +                .false., edge, swork, s)
      endif
      do 570 j = 1, jj
         call ckxty (s(ny,j), iwork, rwork, y(ny,j))
 570  continue
CC
C ...Formats
CC
 100  format (5a12)
 110  format (f12.4,4e12.3e2)
 130  format (5e12.3e2)
 160  format (a3,e10.3e2)
      return
      end
C
C****  End "get info from data (text) file."
C
CXXXXXXXXXXXXXXXXXXXXXXXXXXXXXXXXXXXXXXXXXXXXXXXXXXXXXXXXXXXXXXXXXXXXXX
C######################################################################
C######################################################################
CXXXXXXXXXXXXXXXXXXXXXXXXXXXXXXXXXXXXXXXXXXXXXXXXXXXXXXXXXXXXXXXXXXXXXX
      subroutine openbin (convol, swork, ldiscrep, bdiscrep, ispectab,
     +                    xmf, iwork, rwork, cwork, cwb, spname, x, s,
     2                    y)
C
C****  Read from a flame code output (binary) file.
C      Get X, T info from file.
C
      implicit double precision (a-h,o-z)
      implicit integer (i-n)
      character*80  solfile, arglink, str
      character*16  ichr, isolut, icklnk, imclnk, cwork(*), vers,
     +     prec, cwb(*), spname(*), pre, ver, spec, method, multi,
     2     thdif, el
      character*3 pcontrol(3), edge
      logical       iok, rok, cok, kerr, ldiscrep(*), lflag,
     +              bflag, bdiscrep(*), nolink
      dimension     s(kdim+2,*), x(*), xmf(*), iwork(*), swork(*),
     +              rwork(*), ispectab(*), y(kdim+2,*), convol(25,25)
CC
C    Data about the machine dependent constants is carried in
CC
      common /mach/ small, big, exparg
      common /lenprm/ leniwk, lenrwk, lencwk, lenlwk, kdim, jdim, krxn
      common /lenx/ lenick, lenrck, lencck
      common /locs/ nt, nm, nys, ny, nx, nxs
      common /fileinfo/ nnnn, jj, p, dmflrt, kk, natj
      common /fbrrd/  elflux(3), fmmwt, iignore, ignorxn(100), ihablo,
     +        ihabhi, numsmth, ipoly, numpts, nsmflux, ipolfx, nptflx,
     2        areab, areac, arglink, solfile, spec, method, multi,
     3        thdif, el(3), pcontrol, edge
      common /ckstrt/ nmm , nkk , nii , mxsp, mxtb, mxtp, ncp , ncp1,
     +     ncp2, ncp2t,npar, nlar, nfar, nlan, nfal, nrev,
     2     nthb, nrlt, nwl,  icmm, ickk, icnc, icph, icch,
     3     icnt, icnu, icnk, icns, icnr, iclt, icrl, icrv,
     4     icwl, icfl, icfo, ickf, ictb, ickn, ickt, ncaw,
     5     ncwt, nctt, ncaa, ncco, ncrv, nclt, ncrl, ncfl,
     6     nckt, ncwl, ncru, ncrc, ncpa, NcKF, NcKR, nck1, nck2, nck3,
     7     nck4, nci1, nci2, nci3, nci4
```

```
        data ibinary/10/, iout/6/, ilkout/7/
        data icklnk/'CKLINK          '/
        data isolut/'SOLUTION        '/
        data imclnk/'MCLINK          '/
CC
C      This statement will not compile, machine-dependent constants
C      Be sure these are consistent with CKLIB.F and TRANLIB.F
CC
c*****bigexp
        small = 10.0D0**(-300)
        big = 10.0D0**(+300)
c*****end bigexp
        exparg = log(big)
CC
C ...Initializations.
CC
        nolink = .FALSE.
        lflag = .FALSE.
        bflag = .FALSE.
        do 4000 i = 1, kdim
           ispectab(i) = 0
           ldiscrep(i) = .FALSE.
           bdiscrep(i) = .FALSE.
 4000   continue
CC
C ...Open the binary file.
CC
        call strip (solfile, str)
        write (iout,10) str
 10     format (8x,'Opening binary solution file ',a35,/,8x,
     +          ' for data input')
        open (unit=ibinary, status='old', form='unformatted', file=
     +       solfile, err=170)
        goto 175
 170    write (iout,500) solfile
 500    format (1x,'File ',a15,'doesn"t exist, opening "save"')
        solfile='./binary/save'
        open (unit=ibinary, status='old', form='unformatted', file=
     +       solfile, err=180)
        goto 175
 180    write (iout,*)'"save" doesn"t exist, opening "restart"'
        solfile='./binary/restart'
        open (unit=ibinary, status='old', form='unformatted', file=
     +       solfile, err=190)
        goto 175
 190    write (iout,*)'"restart" doesn"t exist, opening "recover"'
        solfile='./binary/recover'
        open (unit=ibinary, status='old', form='unformatted', file=
     +       solfile, err=200)
 200    write (iout,*)'"recover" doesn"t exist, abort!'
        stop
 175    continue
CC
C ...Read the binary file, whatever type it may be.
CC
 205    read(ibinary)ichr
        if (ichr.eq.isolut) goto 220
        if (ichr.eq.icklnk) then
          if (nkk.eq.0) then
CC
C ...nkk.eq.0:  Get link file info from binary file.  Replaces CKINIT.
CC
            nolink = .TRUE.
            call strip (solfile, str)
```

```
            write (iout,20) str
 20         format (8x,'Initializing CHEMKIN from solution file ',
     +              a28)
            write (ilkout,15)
 15         FORMAT (/1X,' CKLIB:  Chemical Kinetics Library',
     +              /1X,'         CHEMKIN-II Version 3.0, April 1991',
C*****double precision
     2              /1X,'         DOUBLE PRECISION')
C*****END double precision
C
            read (ibinary) npoint, vers,   prec,  lenick, lenrck,
     *          lencck, nmm , nkk , nii , mxsp, mxtb, mxtp, ncp , ncp1,
     1                  ncp2, ncp2t,npar, nlar, nfar, nlan, nfal, nrev,
     2                  nthb, nrlt, nwl,  IcMM, IcKK, IcNC, IcPH, IcCH,
     3                  IcNT, IcNU, IcNK, IcNS, IcNR, IcLT, IcRL, IcRV,
     4                  IcWL, IcFL, IcFO, IcKF, IcTB, IcKN, IcKT, NcAW,
     5                  NcWT, NcTT, NcAA, NcCO, NcRV, NcLT, NcRL, NcFL,
     6                  NcKT, NcWL, NcRU, NcRC, NcPA, NcKF, NcKR, NcK1,
     7                  NcK2, NcK3, NcK4, NcI1, NcI2, NcI3, NcI4
            iok = (leniwk .ge. lenick)
            rok = (lenrwk .ge. lenrck)
            cok = (lencwk .ge. lencck)
            if (.not. iok) write (iout, 305) lenick
            if (.not. rok) write (iout, 350) lenrck
            if (.not. cok) write (iout, 375) lencck
            if (.not.iok .or. .not.rok .or. .not.cok) stop
            read (ibinary) (iwork(l), l = 1, lenick)
            read (ibinary) (rwork(l), l = 1, lenrck)
            read (ibinary) (cwork(l), l = 1, lencck)
C
 305        format (8x,'iwork must be dimensioned at least ',i10)
 350        format (8x,'rwork must be dimensioned at least ',i10)
 375        format (8x,'cwork must be dimensioned at least ',i8)
 475      format (8x,'Character length of cwork must be at least 16')
CC
C ...Set cross-reference array to refer species to themselve and fill
C    array 'spname' with the species names from the solution file link
C    information.
CC
 114        do 245 k = 1, nkk
               ispectab(k) = k
               spname(k) = cwork(IcKK+k-1)
 245        continue
        else
CC
C ... nkk.ne.0 ; check species in solution file against the link file.
CC
           write (iout,25)
 25        format (8x,'Checking link file against solution file')
           read (ibinary) npoint, vers, prec, nn, nn, lencck,
     +                 nnmm, kk, nn, nn, nn, nn, nn, nn,
     2                 nn, nn, nn, nn, nn, nn, nn, nn,
     3                 nn, nn, nn, nn, IIcKK, nn, nn, nn,
     4                 nn, nn, nn, nn, nn, nn, nn, nn,
     5                 nn, nn, nn, nn, nn, nn, nn, nn,
     6                 nn, nn, nn, nn, nn, nn, nn, nn,
     7                 nn, nn, nn, nn, nn
           do 210 l = 1,2
             read (ibinary, end=205, err=215) what
 210       continue
           read (ibinary, end=205, err=215) (cwb(l),l=1,lencck)
CC
C ...Get a cross-reference array of species w/r/t link file species, and
C    fill array 'spname' with species from binary solution file, in the
```

```
C     order found there.  Catch any species that are in the link file but
C     not in the solution file with array ldiscrep.
CC
            do 250 k = 1, nkk
              do 260 iii = 1, kk
                if (cwb(IIcKK+iii-1).eq.cwork(IcKK+k-1)) then
                   ispectab(k) = iii
                   goto 250
                endif
 260          continue
              ldiscrep(k) = .TRUE.
              lflag = .TRUE.
 250        continue
            do 270 k = 1, kk
                spname(k) = cwb(IIcKK+k-1)
 270        continue
CC
C ...Now catch any species in the binary file which are not in the
C     link file, in array bdiscrep.
CC
            do 280 iii = 1, kk
               do 290 k = 1, nkk
                  if (cwork(IcKK+k-1).eq.cwb(IIcKK+iii-1)) goto 280
 290           continue
               bdiscrep(iii) = .TRUE.
               bflag = .TRUE.
 280        continue
CC
C ...Document any species discrepancies.
CC
            if (kk.ne.nkk) write (iout,505) nkk, kk
 505        format (//,1x,'Discrepancy in number of species - USE ',
     +              'RESULTS WITH CAUTION!',//,5x,'Link file:        ',
     2              i3,/,5x,'Binary soln file: ',i3)
            if (lflag) then
               write (iout, 520)
 520           format (//,1x,'Species discrepancies, CAUTION!',//,5x,
     +                 'Species unique to link file:')
               do 330 nn = 1, nkk
                  if (ldiscrep(nn)) write (iout,*) cwork(IcKK+nn-1)
 330           continue
               write (iout,*)
            endif
            if (bflag) then
               write (iout, 510)
 510           format (//,1x,'Species discrepancies, CAUTION!',//,5x,
     +                 'Species unique to binary solution file:')
               do 340 nn = 1, kk
                  if (bdiscrep(nn)) write (iout,*) cwb(IIcKK+nn-1)
 340           continue
               write (iout,*)
               write (iout, 565)
 565           format (//,'Link file must cover all species in ',
     +                    'solution file:  ABORT RUN',//)
               stop
            endif
          endif
CC
C         {ends section of nkk.eq/neq.0}
CC
          goto 205
CC
C         {ends section of ichr.eq.icklink}
CC
```

```
CC
C ...Get transport info from binary file if need be.
CC
        elseif (ichr.eq.imclnk) then
           if (nolink) then
             call mcpnt (ibinary, iout, npoint, ver, pre, lenimc,
     +                   lenrmc, kerr)
             call strip (solfile, str)
             write (iout, 1000) str, ver
 1000        format (8x,'Initializing transport from solution ',
     +            'file ', a28, /,/,
     2            '  TRANLIB:  Multicomponent trans',
     3            'port library, Version ',a4,/,
     4            '             DOUBLE PRECISION',/)
             if (kerr) then
                write (iout,*) 'Error reading transport.  ABORT'
                stop
             endif
             read (ibinary) (iwork(lenick+l), l = 1, lenimc)
                  read (ibinary) (rwork(lenrck+l), l = 1, lenrmc)
           else
             do 209 l = 1, 3
                read (ibinary, end=205, err=215) what
 209             continue
           endif
           goto 205
        endif
 215    write (iout,*) 'Error reading solution file...'
CC
C ...Read solution from file.
CC
 220    read (ibinary) nnnn, jj, p, dmflrt
        kk = nnnn - 2
        read (ibinary) (x(j), j=1, jj)
        read (ibinary) ((s(n,j), n = 1, nnnn), j = 1, jj)
        close (ibinary)
CC
C ...Sort data into the same order as the species are found in the
C    link file.  When done, the s array will contain only data for the
C    species found in the link file.  Profiles for other species will
C    be set to 0.0, and the link file number-of-species index, nkk, is
C    used instead of nk.  Conversion from mass to mole fractions cannot
C    be done until the species are sorted in link-file order.
CC
        nk = nkk
        if (kk.gt.nkk) nk = kk
        do 3110 j = 1, jj
           y(nt,j) = s(nt,j)
CC
C ...Sort and "zeroize" any points that are less than zero.
CC
           do 3120 k = 1, nk
              y(nys+k,j) = 0.0
              if (ispectab(k) .ne. 0) then
                 y(nys+k,j) = s(nys+ispectab(k),j)
                 if (y(nys+k,j) .lt. 0.0) y(nys+k,j) = 0.0
              endif
 3120      continue
 3110   continue
CC
C ...Smooth if required, and convert to mole fractions.
CC
        if (numsmth .ne. 0) then
           write (iout, 600) numsmth, ipoly, 2*numpts+1, edge
```

```
 600       format (/,' Smoothing soln ',i2,' times, polynomial order ',
     +             i2,', window size ',i2,', edge method ',a3,/)
           call smooth (numsmth, numpts, convol, kdim+2, ny, nkk, jj,
     +                  .false., edge, swork, y)
        endif
        do 3140 j = 1, jj
           call ckytx(y(ny,j), iwork, rwork, s(ny,j))
CC
C ...Clean rest of s array, and copy flow rate back into arrays.
CC
           if (kk.gt.nkk) then
              do 3130 k = nkk+1, kk
                 s(nys+k,j) = 0.0
 3130         continue
           endif
           y(nys+nkk+1,j) = dmflrt
           s(nys+nkk+1,j) = dmflrt
 3140   continue
        return
        end
C
C****  End "get info from flame code output (binary) file."
C
CXXXXXXXXXXXXXXXXXXXXXXXXXXXXXXXXXXXXXXXXXXXXXXXXXXXXXXXXXXXXXXXXXXXXXXXXXXXXXXXXXXXXX
C###############################################################################
C###############################################################################
CXXXXXXXXXXXXXXXXXXXXXXXXXXXXXXXXXXXXXXXXXXXXXXXXXXXXXXXXXXXXXXXXXXXXXXXXXXXXXXXXXXXXX
subroutine printit (x, s, kname, spname, sum, iwork, rwork)
C
C****  Write data/solution to files suitable for spreadsheet input.
C      The array 's' is in link-file order, and does not contain any
C      species which was not in the link file list of species.
C
        implicit double precision (a-h,o-z)
        implicit integer (i-n)
        character*3   pcontrol(3), edge
        character*80  solfile, arglink, str
        character*16  kname(*), spname(*), method, multi, el, spec,
     +                thdif
        dimension     s(kdim+2,*), x(*), iwork(*), rwork(*), sum(*)
        common /locs/ nt, nm, nys, ny, nx, nxs
        common /fbrrd/  elflux(3), fmmwt, iignore, ignorxn(100), ihablo,
     +         ihabhi, numsmth, ipoly, numpts, nsmflux, ipolfx, nptflx,
     2         areab, areac, arglink, solfile, spec, method, multi,
     3         thdif, el(3), pcontrol, edge
        common /fileinfo/ nnnn, jj, p, dmflrt, kk, natj
        common /mach/ small, big, exparg
        common /lenprm/ leniwk, lenrwk, lencwk, lenlwk, kdim, jdim, krxn
        common /ckstrt/ nmm , nkk , nii , mxsp, mxtb, mxtp, ncp , ncp1,
     +      ncp2, ncp2t,npar, nlar, nfar, nlan, nfal, nrev,
     2      nthb, nrlt, nwl,  icmm, ickk, icnc, icph, icch,
     3      icnt, icnu, icnk, icns, icnr, iclt, icrl, icrv,
     4      icwl, icfl, icfo, ickf, ictb, ickn, ickt, ncaw,
     5      ncwt, nctt, ncaa, ncco, ncrv, nclt, ncrl, ncfl,
     6      nckt, ncwl, ncru, ncrc, ncpa, NcKF, NcKR, nck1, nck2, nck3,
     7      nck4, nci1, nci2, nci3, nci4
        data isolout/8/, kperln/6/, iout/6/
CC
C  ...Open "soln.out" for printout, after setting some parameters.
CC
        nm = nkk + 2
        k2 = kperln - 1
        ls = k2 + 1
        if ((pcontrol(1).eq."NSL").or.(pcontrol(2).eq."NSL")) goto 1100
```

```
        open (unit=isolout, status='unknown', form='formatted', file=
     +       "soln.out")
        write (iout,100)
CC
C ...Write concentrations to file "soln.out".  Get and print sum of mole
C    fractions as well, in array sum.
CC
        do 300 j = 1, jj
           sum(j) = 0.0
           do 310 k = 1, nkk
              sum(j) = sum(j) + s(nys+k,j)
 310       continue
           write(isolout,7020) j, x(j), s(nt,j), (s(nys+k,j), k = 1, k2)
 300    continue

        write (isolout,7090)
        if (k2 .ne. nkk) then
          do 415 l = ls, nkk, kperln
             k1 = l
             k2 = l + kperln - 1
             if (k2 .gt. nkk) k2 = nkk
             do 400 j = 1, jj
                write (isolout,7020) j, x(j), (s(nys+k,j), k = k1, k2)
  400        continue
             write (isolout,7090)
  415        continue
        endif
CC
C  ...Print out sum of mole fractions.
CC
        write (isolout, 7100)
        do 425 j = 1, jj
           write (isolout, 7020) j, x(j), sum(j)
 425    continue
        write (isolout,7090)
CC
C  ...Print out pressure and flow rate.
CC
        patm = p / 1.01325e6
        write (isolout,1600) patm, dmflrt
CC
C  ...Identify binary file.
CC
        call strip (solfile, str)
        write (isolout,1500) str, numsmth
        if (numsmth .ne. 0) write (isolout,1550) ipoly, 2*numpts+1, edge
        close (isolout)
CC
C  ...Write the species header lines to file "solnhead.out".
CC
 1100   open (unit=isolout, status='unknown', form='formatted',
     +       file="solnhead.out")
        write (iout,110)
        k2 = kperln - 1
        ls = k2 + 1
        if (k2. gt. nkk) k2 = nkk
        write (isolout,7070) (kname(i), i = 1, k2)
        if (k2 .ne. nkk) then
                do 405 l = ls, nkk, kperln
                        k1 = l
                        k2 = l + kperln - 1
                        if (k2 .gt. nkk) k2 = nkk
                        write (isolout,7060) (kname(in), in = k1, k2)
 405            continue
```

```
       endif
CC
C ...Write the species headers for flux/netrate/diffusion.
CC
       k2 = kperln - 1
       if (k2. gt. nkk) k2 = nkk
       write (isolout, 7110)
 7110  format (//,' Headers for flux, net rate and diffusion:',//)
       do 445 l = 1, nkk, kperln
          k1 = l
          k2 = l + kperln - 1
          if (k2 .gt. nkk) k2 = nkk
          write (isolout,7060) (kname(in), in = k1, k2)
 445   continue
CC
C ...Write the species found in the original data/solution file.
CC
       k2 = kperln - 1
       ls = k2 + 1
       if (k2. gt. kk) k2 = kk
       write (isolout,7075) (spname(i), i = 1, k2)
       if (k2 .ne. kk) then
               do 435 l = ls, kk, kperln
                       k1 = l
                       k2 = l + kperln - 1
                       if (k2 .gt. kk) k2 = kk
                       write (isolout,7065) (spname(in), in = k1, k2)
 435           continue
       endif
CC
C  ...Identify data/solution file in header lines file, for safety.
CC
       call strip (solfile, str)
       write (isolout,1500) str, numsmth
       close (isolout)
CC
C**** FORMATS
CC
 100   format (8x,'Writing file "soln.out"')
 110   format (8x,'Writing file "solnhead.out"')
 1000  format (a60)
 1050  format (a80)
 1500  format (/,1x,'Contents of input file ',a40,/,
     +      ' Sorted by the link file species list.',/,
     2      ' Smoothed ',i2,' times.',$)
 1550  format ('  Polynomial order ',i2,', window size ',i2,
     +         ', edge method ',a3,'.')
 1600  format (/,5x,'Pressure (atm): ',f10.6,/,5x,
     +         'Flowrate (g/cm2/sec): ',1pe11.3,/)
 7020  format (i4,2x,f7.4,6(1pe11.3))
 7060  format (3x,1HX,3x,6(a8,1x))
 7065  format (7x,6(a8,1x))
 7070  format (3x,1HX,4x,1HT,7x,5(a8,1x))
 7075  format (//,' Species found in original data/solution file:',//,
     +         8x,1HT,7x,5(a8,1x))
 7080  format (///)
 7090  format (/)
 7100  format (13x,'    Sum Xi   ')
       return
       end
C
C**** End "Write data/solution to spreadsheet compatible files."
C
CXXXXXXXXXXXXXXXXXXXXXXXXXXXXXXXXXXXXXXXXXXXXXXXXXXXXXXXXXXXXXXXXXXXXXXXXXXX
```

```
C###############################################################################
C###############################################################################
CXXXXXXXXXXXXXXXXXXXXXXXXXXXXXXXXXXXXXXXXXXXXXXXXXXXXXXXXXXXXXXXXXXXXXXXXXXXX
subroutine fbrread (atplink, ftype)
C
C**** Subroutine to read parameters from "fbr.dat"
C
        implicit double precision (a-h,o-z)
        implicit integer (i-n)
        character*3   pcontrol(3), edge
        character*80  arglink, solfile, atplink
        character*16  spec, method, multi, thdif, el, ftype
        common /fbrrd/  elflux(3), fmmwt, iignore, ignorxn(100), ihablo,
     +         ihabhi, numsmth, ipoly, numpts, nsmflux, ipolfx, nptflx,
     2         areab, areac, arglink, solfile, spec, method, multi,
     3         thdif, el(3), pcontrol, edge
        data ifbrdat/5/, iout/6/

        write (iout,5)
CC
C ...Get some file names.
CC
        read (ifbrdat,*) arglink
        read (ifbrdat,*) atplink
        read (ifbrdat,*) ftype
        call upcase (ftype)
        read (ifbrdat,*) solfile
CC
C ...Get Savitsky-Golay smoothing parameters.
CC
        read (ifbrdat,*) numsmth, ipoly, numpts
        read (ifbrdat,*) nsmflux, ipolfx, nptflx
        read (ifbrdat,*) edge
        call upcase (edge)
CC
C ...Get species to analyze.
CC
        read (ifbrdat,*) spec
        call upcase (spec)
CC
C ...How many rxns to ignore?
CC
        read (ifbrdat,*) iignore
CC
C ...Read the rxns to be ignored, the HAB nos. to be analyzed upon,
CC
        if (iignore.gt.0) read (ifbrdat,*) (ignorxn(i), i=1,iignore)
        read (ifbrdat,*) ihablo, ihabhi
        read (ifbrdat,*) method
        call upcase (method)
CC
C ...Parameters for flux calculations, and program control variable.
CC
        read (ifbrdat,*) multi, thdif
        call upcase (multi)
        call upcase (thdif)
        read (ifbrdat,*) fmmwt
        do 10 i = 1, 3
           read (ifbrdat,*) el(i), elflux(i)
           call upcase (el(i))
 10     continue
        read (ifbrdat,*) pcontrol(1), pcontrol(2)
        call upcase (pcontrol(1))
        call upcase (pcontrol(2))
```

```
c1
c1  LDP, new keyword, means "soln.out" and "link.out" only, check
c1  duplicate reactions in link file.
c1
        if ((pcontrol(1).eq.'LDP').or.(pcontrol(2).eq.'LDP')) then
           pcontrol(1) = 'NFN'
           pcontrol(2) = 'NRP'
           pcontrol(3) = 'LDP'
        else
           pcontrol(3) = '   '
        endif
c1
c1  End LDP mod.
c1
CC                                                                    1.1
C ...If flux/rate analysis is specified, read area expansion ratio data.
CC                                                                    1.1
        areab = 0.0
        areac = 0.0
        if ((pcontrol(1).ne.'NFN').and.(pcontrol(2).ne.'NFN')) then
           read (ifbrdat,*) areab, areac
        endif
 5      format (8x,'Reading control file')
C 1.1        close (ifbrdat)
        return
        end
C
C**** End "read parameters from 'fbr.dat'"
C
CXXXXXXXXXXXXXXXXXXXXXXXXXXXXXXXXXXXXXXXXXXXXXXXXXXXXXXXXXXXXXXXXXXXXXXXXXXXXXXX
C##############################################################################
C##############################################################################
CXXXXXXXXXXXXXXXXXXXXXXXXXXXXXXXXXXXXXXXXXXXXXXXXXXXXXXXXXXXXXXXXXXXXXXXXXXXXXXX
subroutine speclist (cwork, iwork, rwork, ispec, irxntab, kerr)
C
C**** Get list of reactions which involve species 'spec'
C
        implicit double precision (a-h,o-z)
        implicit integer (i-n)
        character*3   pcontrol(3), edge
        character*80  arglink, solfile
        character*16  spec, cwork(*), method, el, multi, thdif
        logical       kerr
        dimension     iwork(*), rwork(*), irxntab(*)
        common /ckstrt/ nmm , nkk , nii , mxsp, mxtb, mxtp, ncp , ncp1,
     +      ncp2, ncp2t,npar, nlar, nfar, nlan, nfal, nrev,
     2      nthb, nrlt, nwl,  icmm, ickk, icnc, icph, icch,
     3      icnt, icnu, icnk, icns, icnr, iclt, icrl, icrv,
     4      icwl, icfl, icfo, ickf, ictb, ickn, ickt, ncaw,
     5      ncwt, nctt, ncaa, ncco, ncrv, nclt, ncrl, ncfl,
     6      nckt, ncwl, ncru, ncrc, ncpa, NcKF, NcKR, nck1, nck2, nck3,
     7      nck4, nci1, nci2, nci3, nci4
        common /fileinfo/ nnnn, jj, p, dmflrt, kk, natj
        common /fbrrd/  elflux(3), fmmwt, iignore, ignorxn(100), ihablo,
     +         ihabhi, numsmth, ipoly, numpts, nsmflux, ipolfx, nptflx,
     2         areab, areac, arglink, solfile, spec, method, multi,
     3         thdif, el(3), pcontrol, edge
        data iout/6/, ilkout/7/, irate/9/, link/12/
        data isolout/8/, ibinary/10/, idata/11/
        write (iout,1100)
CC
C   The following finds the species number of the species to be
C   analyzed.
CC
```

```
        ispec = 0
        do 1 k = 1, nkk
           if (cwork(IcKK+k-1).eq.spec) then
              ispec = k
              goto 5
           endif
 1      continue
        write (iout, 1000) spec
        kerr = .true.
        return
CC
C   The following finds the reactions involving species spec, and
C   stores the result in array irxntab.  Only the first occurence
C   is noted.
CC
 5      continue
        do 10 i = 1, nii
           irxntab(i) = 0
           do 15 j = 1, mxsp
              if (iwork(IcNK+(i-1)*mxsp+j-1).eq.ispec) then
                 irxntab(i) = j
                 goto 10
              endif
 15        continue
 10     continue
 1000   format (/,1x,'Species ',a10,' is not found in the link file',/)
 1100   format (8x,'Finding reactions with species to be analyzed')
        return
        end
C
C**** End "list of rxns involving species 'spec'"
C
CXXXXXXXXXXXXXXXXXXXXXXXXXXXXXXXXXXXXXXXXXXXXXXXXXXXXXXXXXXXXXXXXXXXXXXXXXXXXXXX
C###############################################################################
C###############################################################################
CXXXXXXXXXXXXXXXXXXXXXXXXXXXXXXXXXXXXXXXXXXXXXXXXXXXXXXXXXXXXXXXXXXXXXXXXXXXXXXX
       SUBROUTINE CKDUP (I, MAXSP, NS, NR, NU, NUNK, NFAL, IFAL, KFAL,
     1                   ISAME)
C
C     Checks reaction I against the (I-1) reactions for duplication
C     (Directly from CKINTERP.F - RS)
C-----------------------------------------------------------------------C
C*****precision > double
       IMPLICIT DOUBLE PRECISION (A-H,O-Z), INTEGER (I-N)
C*****END precision > double
C*****precision > single
C      IMPLICIT REAL (A-H,O-Z), INTEGER (I-N)
C*****END precision > single
C
      DIMENSION NS(*), NR(*), NU(MAXSP,*), NUNK(MAXSP,*), IFAL(*),
     1          KFAL(*)
C
      ISAME = 0
      NRI = NR(I)
      NPI = ABS(NS(I)) - NR(I)
C
      DO 500 J = 1, I-1
C
         NRJ = NR(J)
         NPJ = ABS(NS(J)) - NR(J)
C
         IF (NRJ.EQ.NRI .AND. NPJ.EQ.NPI) THEN
C
            NSAME = 0
```

```
            DO 20 N = 1, MAXSP
               KI = NUNK(N,I)
               NI = NU(N,I)
C
               DO 15 L = 1, MAXSP
                  KJ = NUNK(L,J)
                  NJ = NU(L,J)
                  IF (NJ.NE.0 .AND. KJ.EQ.KI .AND. NJ.EQ.NI)
     1               NSAME = NSAME + 1
   15             CONTINUE
   20          CONTINUE
C
            IF (NSAME .EQ. ABS(NS(J))) THEN
C
C           same products, reactants, coefficients, check fall-off
C           third body
C
               IF (NFAL.GT.0 .AND. IFAL(NFAL).EQ.I) THEN
                  DO 22 N = 1, NFAL-1
                     IF (J.EQ.IFAL(N) .AND. KFAL(N).EQ.KFAL(NFAL)) THEN
                        ISAME = J
                        RETURN
                     ENDIF
   22             CONTINUE
                  RETURN
               ENDIF
C
               ISAME = J
               RETURN
            ENDIF
         ENDIF
C
         IF (NPI.EQ.NRJ .AND. NPJ.EQ.NRI) THEN
C
            NSAME = 0
            DO 30 N = 1, MAXSP
               KI = NUNK(N,I)
               NI = NU(N,I)
C
               DO 25 L = 1, MAXSP
                  KJ = NUNK(L,J)
                  NJ = NU(L,J)
                  IF (NJ.NE.0 .AND. KJ.EQ.KI .AND. -NJ.EQ.NI)
     1               NSAME = NSAME + 1
   25             CONTINUE
   30          CONTINUE
C
            IF (NSAME.EQ.ABS(NS(J)) .AND.
     1           (NS(J).GT.0 .OR. NS(I).GT.0)) THEN
C
C           same products as J reactants, and vice-versa
C
               IF (NFAL.GT.0 .AND. IFAL(NFAL).EQ.I) THEN
                  DO 32 N = 1, NFAL-1
                     IF (J.EQ.IFAL(N) .AND. KFAL(N).EQ.KFAL(NFAL)) THEN
                        ISAME = J
                        RETURN
                     ENDIF
   32             CONTINUE
                  RETURN
               ENDIF
C
               ISAME = J
               RETURN
```

```
          ENDIF
        ENDIF
C
  500 CONTINUE
      RETURN
      END
C
C**** End CKDUP
C
C*****************************************************************************
CXXXXXXXXXXXXXXXXXXXXXXXXXXXXXXXXXXXXXXXXXXXXXXXXXXXXXXXXXXXXXXXXXXXXXXXXXXX
C###########################################################################
C###########################################################################
CXXXXXXXXXXXXXXXXXXXXXXXXXXXXXXXXXXXXXXXXXXXXXXXXXXXXXXXXXXXXXXXXXXXXXXXXXXX
      subroutine rates  (t, x, iwork, rwork, irxntab, c, ispec, nuki,
     +                   w, wdotf, wdotr, wdot, kerr)
C
C**** Calculate forward and reverse rates for reactions, species spec.
C     (Based on CHEMKIN II's CKWXP)
CC
c  Returns the molar production rates of the species, forward and
c  back, given the pressure, temperature and mass fractions.
c
c  output
c     wdotf    - forward chemical molar production rates of the species.
c                cgs units - moles/(cm**3*sec)
c                data type - double precision array
c                dimension wdot(*) at least nii, the total number of
c                reactions.
c     wdotr    - reverse chemical molar production rates of the species.
c                cgs units - moles/(cm**3*sec)
c                data type - double precision array
c                dimension wdot(*) at least nii, the total number of
c                reactions.
C     wdot     - net rate for all reactions, forward and back, at this
C                HAB.
CC
        implicit double precision (a-h, o-z), integer (i-n)
        logical     kerr
        dimension   iwork(*), rwork(*), x(*), wdotf(*), c(*),
     +              wdotr(*), irxntab(*), nuki(kdim,*), w(*)
        common /fileinfo/ nnnn, jj, p, dmflrt, kk, natj
        common /mach/ small, big, exparg
        common /lenprm/ leniwk, lenrwk, lencwk, lenlwk, kdim, jdim, krxn
        common /ckstrt/ nmm , nkk , nii , mxsp, mxtb, mxtp, ncp , ncp1,
     +                  ncp2, ncp2t,npar, nlar, nfar, nlan, nfal, nrev,
     2                  nthb, nrlt, nwl,  icmm, ickk, icnc, icph, icch,
     3                  icnt, icnu, icnk, icns, icnr, iclt, icrl, icrv,
     4                  icwl, icfl, icfo, ickf, ictb, ickn, ickt, ncaw,
     5                  ncwt, nctt, ncaa, ncco, ncrv, nclt, ncrl, ncfl,
     6                  nckt, ncwl, ncru, ncrc, ncpa, NcKF, NcKR, nck1,
     7                  nck2, nck3, nck4, nci1, nci2, nci3, nci4
        data toler/1.0E-4/
        call ckxtcp (p, t, x, iwork, rwork, c)
        call ckrat (rwork, iwork, nii, nkk, mxsp, mxtb, rwork(ncru),
     +              rwork(ncpa), t, c, iwork(icns),
     2              iwork(icnu), iwork(icnk), npar+1,rwork(ncco),
     3              nrev, iwork(icrv), rwork(ncrv), nfal, iwork(icfl),
     4              iwork(icfo), iwork(ickf), nfar, rwork(ncfl), nlan,
     5              nlar, iwork(iclt), rwork(nclt), nrlt, iwork(icrl),
     6              rwork(ncrl), nthb, iwork(ictb), iwork(ickn),
     7              rwork(nckt), iwork(ickt), rwork(nck2),
     8              rwork(nci1), rwork(nci2), rwork(nci3),
     9              rwork(nci4))
```

```
CC
C  Set:
C
C     wdot_fi =  (nu_ki_r - nu_ki_f) * (k_fi * prod([Xk]^nu_ki_f))
C     wdot_ri = -(nu_ki_r - nu_ki_f) * (k_ri * prod([Xk]^nu_ki_r))
C
C  This gives:  wdot_i = wdot_fi + wdot_ri
C
C  (nu here is the absolute value of what is in array iwork(IcNU).)
CC
       wdot = 0.0
       do 100 i = 1, nii
          wdotf(i) = 0.0
          wdotr(i) = 0.0
          if (irxntab(i) .ne. 0) then
             wdotf(i) = wdotf(i) + rwork(NcI1+i-1)*nuki(ispec,i)
             wdotr(i) = wdotr(i) - rwork(NcI2+i-1)*nuki(ispec,i)
             wdot = wdot + wdotf(i) + wdotr(i)
          endif
  100  continue
CC
C ...Double check on wdot.  Routine CKWC reassigns the workspace which con-
C    tains the concentrations, so use another array.
CC
       call ckwc(t, c, iwork, rwork, w)
       if (wdot .ge. small) then
          diff = abs((w(ispec)-wdot)/wdot)
       else
          diff = abs(w(ispec)- wdot)
       endif
       kerr = .false.
       if (diff .gt. toler) kerr = .true.
       return
       end
C
C**** End "Calculate forward and reverse rates for reactions"
C
CXXXXXXXXXXXXXXXXXXXXXXXXXXXXXXXXXXXXXXXXXXXXXXXXXXXXXXXXXXXXXXXXXXXXXXXXXXXXXXXXXXX
C###############################################################################
C###############################################################################
CXXXXXXXXXXXXXXXXXXXXXXXXXXXXXXXXXXXXXXXXXXXXXXXXXXXXXXXXXXXXXXXXXXXXXXXXXXXXXXXXXX
subroutine printrate (x, wneg, wpos, wdotf, wdotr, wdot, partl,
     +                      irxntab, ispec, iwork, rwork)
C
C****  Print rates for reaction path analysis.
C
        implicit double precision (a-h,o-z)
        implicit integer (i-n)
        character*3   pcontrol(3), edge
        character*16  method, spec, el, multi, thdif
        character*80  arglink, solfile, str1, str2
        logical       zeropos, zeroneg
        dimension     x(*), wdotf(krxn,*), wdotr(krxn,*), wdot(*),
     +                irxntab(*), iprnt(6), iwork(*), rwork(*),
     2                wpos(*), wneg(*), partl(krxn,*)
        common /mach/ small, big, exparg
        common /lenprm/ leniwk, lenrwk, lencwk, lenlwk, kdim, jdim, krxn
        common /fileinfo/ nnnn, jj, p, dmflrt, kk, natj
        common /fbrrd/  elflux(3), fmmwt, iignore, ignorxn(100), ihablo,
     +          ihabhi, numsmth, ipoly, numpts, nsmflux, ipolfx, nptflx,
     2          areab, areac, arglink, solfile, spec, method, multi,
     3          thdif, el(3), pcontrol, edge
        common /ckstrt/ nmm , nkk , nii , mxsp, mxtb, mxtp, ncp , ncp1,
     +       ncp2, ncp2t,npar, nlar, nfar, nlan, nfal, nrev,
```

```
     2      nthb, nrlt, nwl,  icmm, ickk, icnc, icph, icch,
     3      icnt, icnu, icnk, icns, icnr, iclt, icrl, icrv,
     4      icwl, icfl, icfo, ickf, ictb, ickn, ickt, ncaw,
     5      ncwt, nctt, ncaa, ncco, ncrv, nclt, ncrl, ncfl,
     6      nckt, ncwl, ncru, ncrc, ncpa, NcKF, NcKR, nck1, nck2, nck3,
     7      nck4, nci1, nci2, nci3, nci4
        data iout/6/, ilkout/7/, irate/9/, link/12/, iperln/6/
        data ipart/13/
CC                                                          1.1
C  ...Open "rates.out" and "parteqm.out" for printout.
CC                                                          1.1
        open (unit=irate, status='unknown', form='formatted', file=
     +       "rates.out")
        write (iout,110)
        open (unit=ipart, status='unknown', form='formatted', file=
     +       "parteqm.out")
        write (iout,115)
CC                                                                  1.1
C ...Calculate partial equilibrium ratios.  If forward rate is too small,
C    set ratio to 9.999E+99.
CC                                                                  1.1
        do 1000 j = 1, jj
           do 1010 i = 1, nii
              if (abs(wdotf(i,j)) .lt. small) then
                 partl(i,j) = 9.999E+99
              else
                 partl(i,j) = -wdotr(i,j) / wdotf(i,j)
              endif
 1010      continue
 1000   continue
CC
C  ...Now get the sum of positive and negative rates.
CC
        do 100 j = 1, jj
           wpos(j) = 0.0
           wneg(j) = 0.0
           do 3210 i = 1, nii
              if (wdotf(i,j).gt.0) then
                 wpos(j) = wpos(j) + wdotf(i,j)
              else
                 wneg(j) = wneg(j) + wdotf(i,j)
              endif
              if (wdotr(i,j).gt.0) then
                 wpos(j) = wpos(j) + wdotr(i,j)
              else
                 wneg(j) = wneg(j) + wdotr(i,j)
              endif
 3210      continue
CC
C     If this is the ratio method, replace the wdot arrays with the frac-
C     tion of the total rate.  Positive for positive rate, negative for
C     negative rate.
CC
           if (method(1:3).eq.'RAT') then
CC
C               Check for zero total rate.
CC
              zeropos = .false.
              zeroneg = .false.
              if ((wpos(j).lt.small).or.(abs(wneg(j)).lt.small)) then
                 if (wpos(j).lt.small) then
                    write (irate,3500) 'posi',j
                    zeropos = .true.
                 endif
```

```
                  if (abs(wneg(j)).lt.small) then
                     write (irate,3500) 'nega',j
                     zeroneg = .true.
                  endif
               endif
CC
C                Proceed with ratio calculation.  If total rate is
C                zero, replace partial rate with +/- 9.999E+99.
CC
               do 3220 i = 1, nii
                  if (wdotf(i,j).gt.0) then
                     if (zeropos) then
                        wdotf(i,j) = 9.999E+99
                     else
                        wdotf(i,j) = wdotf(i,j)/wpos(j)
                     endif
                  else
                     if (zeroneg) then
                        wdotf(i,j) = 9.999E+99
                     else
                        wdotf(i,j) = wdotf(i,j)/abs(wneg(j))
                     endif
                  endif
                  if (wdotr(i,j).gt.0) then
                     if (zeropos) then
                        wdotf(i,j) = 9.999E+99
                     else
                        wdotr(i,j) = wdotr(i,j)/wpos(j)
                     endif
                  else
                     if (zeropos) then
                        wdotf(i,j) = 9.999E+99
                     else
                        wdotr(i,j) = wdotr(i,j)/abs(wneg(j))
                     endif
                  endif
 3220          continue
            endif
 100     continue
CC
C  ...Protect against ill-defined HAB bounds.
CC
         if (ihabhi.gt.jj) ihabhi = jj
         if (ihablo.lt.1)  ihablo = 1
         if (ihablo.gt.ihabhi) ihablo = 1
         if (ihabhi.lt.ihablo) ihabhi = jj
CC                                                                    1.1
C  ...Now print out the forward rates for each reaction and HAB, and the
C     partial equilibrium ratios.
CC                                                                    1.1
         write (iout,120)
         write (iout,125)
         write (irate,*)
         write (ipart,*)
         next = 1
         do 3240 i = 1, nii
CC
C  1. Make sure it's in the reaction table.
CC
            if (irxntab(i) .eq. 0) then
               if (i .eq. nii) then
CC
C                  It was the last reaction; print.
CC
```

```
                write (irate,3300) (iprnt(n), n=1, next-1)
                write (ipart,3300) (iprnt(n), n=1, next-1)
                do 3270 j = ihablo, ihabhi
                   write (irate,3280) j, x(j), (wdotf(iprnt(n),j), n=1,
     +                                                          next-1)
                   write (ipart,3280) j, x(j), (partl(iprnt(n),j), n=1,
     +                                                          next-1)
 3270           continue
                write (irate,*)
                write (ipart,*)
              endif
C
              goto 3240
            endif
CC
C  2. Make sure it's not marked to be ignored.
CC
           do 3260 ii = 1,iignore
              if (ignorxn(ii) .eq. i) then
                if (i .eq. nii) then
CC
C                     It was the last reaction; print.
CC
                  write (irate,3300) (iprnt(n), n = 1, next - 1)
                  write (ipart,3300) (iprnt(n), n = 1, next - 1)
                  do 3290 j = ihablo, ihabhi
                     write (irate,3280) j, x(j), (wdotf(iprnt(n),j),n=1,
     +                                                          next-1)
                     write (ipart,3280) j, x(j), (partl(iprnt(n),j),n=1,
     +                                                          next-1)
 3290                continue
                     write (irate,*)
                     write (ipart,*)
                endif
C
                goto 3240
              endif
 3260       continue
CC
C  3. It's OK; add it to the list to be printed.
CC
         iprnt(next) = i
CC
C  4. If the page is full or it's the last reaction, print.
CC
         if ((next.eq.6).or.(i.eq.nii)) then
            write (irate,3300) (iprnt(n), n = 1, next)
            write (ipart,3300) (iprnt(n), n = 1, next)
            do 3230 j = ihablo, ihabhi
               write (irate,3280) j, x(j), (wdotf(iprnt(n),j), n=1,next)
               write (ipart,3280) j, x(j), (partl(iprnt(n),j), n=1,next)
 3230       continue
            write (irate,*)
            write (ipart,*)
CC
C                   Reset markers after page print.
CC
            next = 1
            goto 3240
         endif
CC
C  5. Next reaction.
CC
         next = next+1
```

```
 3240   continue
CC
C  ...Done with forward rates and partial equilibrium factors.
C
C  ...Now print out the reverse rates for each reaction and HAB.
CC
        write (irate, *)
        next = 1
        do 3340 i = 1,nii
CC
C  1. Make sure it's in the reaction table.
CC
          if (irxntab(i).eq.0) then
            if (i.eq.nii) then
CC
C                 It was the last reaction; print.
CC
              write (irate,3300) (-1*iprnt(n),n=1,next-1)
              do 3370 j = ihablo, ihabhi
                 write (irate,3280) j,x(j),(wdotr(iprnt(n),j),n=1,
     +                                                      next-1)
 3370         continue
              write (irate,*)
            endif
C
            goto 3340
          endif
CC
C  2. Make sure it's not marked to be ignored.
CC
          do 3360 ii = 1,iignore
             if (ignorxn(ii).eq.i) then
               if (i.eq.nii) then
CC
C                    It was the last reaction; print.
CC
                  write (irate,3300) (-1*iprnt(n),n=1,next-1)
                  do 3390 j = ihablo, ihabhi
                     write (irate,3280) j,x(j),(wdotr(iprnt(n),j),
     +                                                n=1,next-1)
 3390             continue
                  write (irate,*)
               endif
C
               goto 3340
             endif
 3360     continue
CC
C  3. There must be a reverse reaction.  Check irreversibility, reverse
C     parameters and reverse Landau-Teller parameters.
CC
          if (iwork(IcNS+i-1).lt.0) then
CC
C        No reverse reaction; if it was the last rxn, print.  Otherwise,
C        just skip to the end of the loop over reactions.
CC
             if (i.eq.nii) then
                write (irate,3300) (-1*iprnt(n),n=1,next-1)
                do 3490 j = ihablo, ihabhi
                  write (irate,3280) j,x(j),(wdotr(iprnt(n),j),
     +                                                n=1,next-1)
 3490             continue
                  write (irate,*)
             endif
```

```
            goto 3340
          endif
CC
C  4. It's OK; add it to the list to be printed.
CC
        iprnt(next) = i
CC
C  5. If the page is full or it's the last reaction, print.
CC
        if ((next.eq.6).or.(i.eq.nii)) then
           write (irate,3300) (-1*iprnt(n),n=1,next)
           do 3330 j = ihablo, ihabhi
              write (irate,3280) j,x(j),(wdotr(iprnt(n),j),n=1,next)
 3330      continue
           write (irate,*)
CC
C                 Reset markers after page print.
CC
           next = 1
           goto 3340
        endif
CC
C  6. Next reaction
CC
        next = next+1
 3340   continue
CC
C  7. Total rates.
CC
        write (irate,3450)
        do 3470 j = ihablo, ihabhi
           write (irate,3280) j,x(j),wpos(j),wneg(j),wdot(j)
 3470   continue
        call strip (arglink, str1)
        call strip (solfile, str2)
        write (irate,130) str1, str2, spec
        write (ipart,130) str1, str2, spec
        if (iignore .gt. 0) write (irate,140) (ignorxn(i),i=1,iignore)
        if (iignore .gt. 0) write (ipart,140) (ignorxn(i),i=1,iignore)
        write (irate,150) ihablo, ihabhi
        write (ipart,150) ihablo, ihabhi
        if (method(1:3) .eq. 'RAT') then
           write (irate, 160) method
        else
           write (irate, 170) method
        endif
        write (ipart,180)
        close (irate)
        close (ipart)
 110    format (8x,'Opening "rates.out"')
 115    format (8x,'Opening "parteqm.out"')
 120    format (8x,'Writing reaction rates in "rates.out"')
 125    format (8x,'Writing partial equilibrium ratios in ',
     +          '"parteqm.out"',/)
 130    format (///,3x,'Link file:  ',a30,/,3x,'Input file:  ',
     +          a40,/,3x,'Species analyzed:  ',a16)
 140    format (3x,'Reactions not printed:  ',100(i4))
 150    format (3x,'Beginning HAB no:  ',i4,3x,'Ending HAB no:  ',i4)
 160    format (3x,'Absolute rate, or ratio (normalized):  ',a5,//,
     +          13x,'RATIO OF +/- 9.999E+99 MEANS TOTAL RATE WAS ZERO',
     2          //)
 170    format (3x,'Absolute rate, or ratio (normalized):  ',a5,//)
 180    format (//,13x,'RATIO OF +/- 9.999E+99 MEANS FORWARD RATE WAS ',
     +          'ZERO')
```

```
 3300   format (10x,6(i11))
 3280   format (i4,2x,f7.4,6(1pe11.3))
 3450   format (/,16x,'Tot Pos',4x,'Tot Neg',5x,'Total')
 3500   format (' Total ',a4,'tive rate is zero at HAB number ',i3)
 3510   format (//,' Rerun with "method" set to "absol" in fbr.dat',//,
     +          ' ABORT ',//)
        return
        end
C
C**** End "Print rates for reaction path analysis"
C
CXXXXXXXXXXXXXXXXXXXXXXXXXXXXXXXXXXXXXXXXXXXXXXXXXXXXXXXXXXXXXXXXXXXXXXXXXXXXXXX
C###############################################################################
C###############################################################################
CXXXXXXXXXXXXXXXXXXXXXXXXXXXXXXXXXXXXXXXXXXXXXXXXXXXXXXXXXXXXXXXXXXXXXXXXXXXXXX
      subroutine rmblank (ch)
C
C**** Remove leading blanks from a character*16 variable.
C
      character*16  ch
      do 450 k = 1, 16
         if (ch(k:k).eq.' ') goto 450
         goto 460
 450  continue
 460  do 470 kk = 1, 17-k
         ch(kk:kk) = ch(kk+k-1:kk+k-1)
 470  continue
      return
      end
C
C**** End "Remove leading blanks from character*16 variable"
C
CXXXXXXXXXXXXXXXXXXXXXXXXXXXXXXXXXXXXXXXXXXXXXXXXXXXXXXXXXXXXXXXXXXXXXXXXXXXXXXX
C###############################################################################
C###############################################################################
CXXXXXXXXXXXXXXXXXXXXXXXXXXXXXXXXXXXXXXXXXXXXXXXXXXXXXXXXXXXXXXXXXXXXXXXXXXXXXX
      subroutine upcase(istr)
C
C**** Convert from lower to upper case.  From PREMIX.F.
C
      character   istr*(*), lcase(26)*1, ucase(26)*1
      data lcase /'a','b','c','d','e','f','g','h','i','j','k','l','m',
     1            'n','o','p','q','r','s','t','u','v','w','x','y','z'/,
     2     ucase /'A','B','C','D','E','F','G','H','I','J','K','L','M',
     3            'N','O','P','Q','R','S','T','U','V','W','X','Y','Z'/
C
      do 10 j = 1, len(istr)
         do 10 n = 1, 26
            if (istr(j:j) .eq. lcase(n)) istr(j:j) = ucase(n)
   10 continue
      return
      end
C
C**** End "Convert from lower case to upper case"
C
CXXXXXXXXXXXXXXXXXXXXXXXXXXXXXXXXXXXXXXXXXXXXXXXXXXXXXXXXXXXXXX
C###############################################################################
C###############################################################################
CXXXXXXXXXXXXXXXXXXXXXXXXXXXXXXXXXXXXXXXXXXXXXXXXXXXXXXXXXXXXXX
      subroutine fbrptr (linkck, linkmc, iout, i, r, c, arglink,
     1                  atplink)
C
C**** Set workspace pointers for flux/rate calculation.  Based on
C     PREMIX.F.
```

```
C
C
C*****double precision
c        implicit double precision (a-h, o-z), integer (i-n)
C*****END double precision
C
C*****double precision
        implicit double precision (a-h, o-z), integer (i-n)
C*****END double precision
C
      dimension i(*), r(*)
      character c(*)*(*)
      character*80 arglink, atplink, str
      common /ckstrt/ nmm , nkk , nii , mxsp, mxtb, mxtp, ncp , ncp1,
     1      ncp2, ncp2t,npar, nlar, nfar, nlan, nfal, nrev,
     2      nthb, nrlt, nwl,  icmm, ickk, icnc, icph, icch,
     3      icnt, icnu, icnk, icns, icnr, iclt, icrl, icrv,
     4      icwl, icfl, icfo, ickf, ictb, ickn, ickt, ncaw,
     5      ncwt, nctt, ncaa, ncco, ncrv, nclt, ncrl, ncfl,
     6      nckt, ncwl, ncru, ncrc, ncpa, NcKF, NcKR, nck1, nck2, nck3,
     7      nck4, nci1, nci2, nci3, nci4
      common /fileinfo/ nnnn, jj, p, dmflrt, kk, natj
      common /lenprm/ leniwk, lenrwk, lencwk, lenlwk, kdim, jdim, krxn
      common /lenx/ lenick, lenrck, lencck
CC
C ...Some of the names in the following common (mcmcmc) have been
C    modified to avoid conflict or make lines fit.  See tranlib.f for
C    the original names.
CC
      common /mcmcmc/ ru, patmos, small, nk, no, nlite, inlin, iktdif,
     1                ipvt, nw,  neps,  nsig, ndip, npol, nzrot, nlam,
     2                neta, ndf,  ntdif, nxx, nvis, nxi,  nc,  ncrot,
     3                ncint, npk, nbind, neok, nsgm, nast, nbst, ncst,
     4                nxl, nr, nwrk, k3
      common /rxprxp/ nckw, nmcw, nsch, nd, ndkj, ntdr, nyv,
     +                nomeg, nki, ngflx, nflux, nfbal, nvel, ickw,
     2                imcw, ielk, ncnc, nsum, nprt
      common /locs/ nt, nm, nys, ny, nx, nxs
CC
C ...Set the pointers into the solution vector.
CC
      nt  = 1
      nys = 1
      ny  = 2
      nm  = nkk + 2
      if ((arglink .ne. 'nolink') .and. (arglink .ne. 'NOLINK')) then
         call cklen (linkck, iout, lenick, lenrck, lencck)
         call mclen (linkmc, iout, lenimc, lenrmc)
      else
         lenimc = 4 * nk * nlite
         lenrmc = nk * (19 + 2*no + no*nlite) + (no + 15) * nk**2
      endif
CC
C ...Real chemkin work space.
CC
      nckw = 1
CC
c ...Real transport work space.
CC
      nmcw = nckw + lenrck
      ntot = nmcw + lenrmc
CC
c ...Integer chemkin work space.
CC
```

```
      ickw = 1
CC
c ...Integer transport work space.
CC
      imcw = ickw + lenick
      itot = imcw + lenimc
CC
C ...Character chemkin work space.
CC
      icc = 1
      ictot = icc + lencck
CC
C ...Initialize transport linking file, unit linkmc, unless that was done
C    in the binary file reading routine (openbin).
CC
      if ((itot.lt.leniwk .and. ntot.lt.lenrwk .and. ictot.lt.lencwk)
     + .and. ((arglink.ne.'nolink') .and. (arglink.ne.'NOLINK'))) then
         call strip (atplink, str)
         write (iout, 1000) str
 1000    format (8x,'Initializing transport from file ',a28,/)
         call mcinit (linkmc, iout, lenimc, lenrmc, i(imcw), r(nmcw))
      endif
      natj = nkk + 2
CC
C ...Apportion the balance of the floating point space.
CC
      ncnc = ntot
C  Concentration workspace for "rates"
      nprt = ncnc + nkk
C  Partial equilibrium space
      nsum = nprt + kdim*jdim
C  Sum of mole fractions, "printit"
      nsch = nsum  + jdim
C  Miscellaneous scratch space
      nd   = nsch + nkk*5
C  Diffusion coefficient
      ndkj = nd   + nkk*jdim
C  Multicomponent diffusion
      ntdr = ndkj + nkk*nkk*jdim
C  Thermal diffusion
      nyv  = ntdr + nkk*jdim
C  YV diffusion velocity product
      nomeg = nyv + nkk*jdim
C  Element mass fractions
      nki = nomeg + nkk*nmm
C  Net rates
      ngflx = nki + nkk*jdim
C  Element flux fractions
      nflux   = ngflx + nkk*jdim
C  Molar fluxes
      nfbal  = nflux  + nkk*jdim
C  Element flux balances
      nvel = nfbal  + 3*jdim
C  Gas velocity
      ntot = nvel + jdim
CC
C ...Apportion the balance of the integer space.
CC
      ielk  = itot
      itot  = ielk + nmm*nkk
CC
C ...Apportion the logical space.
CC
      ltot = 0
```

```
CC
C ...Check for enough space; stop if not.
CC
      write (iout, 7000) lenlwk, ltot, leniwk, itot, lenrwk, ntot,
     1     lencwk, ictot
 7000 format (/,' Diffusion/flux/rate calculation working space',
     +     ' requirements:',
     1     //,'                  PROVIDED        REQUIRED ',
     2     /,' LOGICAL  ' , 2I15,
     3     /,' INTEGER  ' , 2I15,
     4     /,' REAL     ' , 2I15,
     5     /,' CHARACTER' , 2I15,/)
      if ((ltot.gt.lenlwk) .or. (itot.gt.leniwk) .or.(ntot.gt.lenrwk)
     1     .or. (ictot.gt.lencwk)) then
          write (iout, *) '  FATAL ERROR, NOT ENOUGH WORK SPACE PROVIDED'
          stop
      endif
      return
      end
C
C**** End "Set workspace pointers for flux/rate calcs."
C
CXXXXXXXXXXXXXXXXXXXXXXXXXXXXXXXXXXXXXXXXXXXXXXXXXXXXXXXXXXXXXXXXXXXXXXXXXXXXXXX
C###############################################################################
C###############################################################################
CXXXXXXXXXXXXXXXXXXXXXXXXXXXXXXXXXXXXXXXXXXXXXXXXXXXXXXXXXXXXXXXXXXXXXXXXXXXXXXX
      subroutine mtrnpr (lmulti, ltdif, x, y, wt, scrchk,
     +                  ickwrk, rckwrk, imcwrk, rmcwrk, d, tdr, dkj)

C
C**** Subroutine to get diffusion coefficients.  Based on PREMIX.F.
C
C*****double precision
C        IMPLICIT DOUBLE PRECISION (A-H, O-Z), INTEGER (I-N)
C*****END double precision
C
C*****double precision
        IMPLICIT DOUBLE PRECISION (A-H, O-Z), INTEGER (I-N)
C*****END double precision
C
      common /fileinfo/ nnnn, jj, p, dmflrt, kk, natj
      common /locs/ nt, nm, nys, ny, nx, nxs
      common /lenprm/ leniwk, lenrwk, lencwk, lenlwk, kdim, jdim, krxn
      common /ckstrt/ nmm , nkk , nii , mxsp, mxtb, mxtp, ncp , ncp1,
     +       ncp2, ncp2t,npar, nlar, nfar, nlan, nfal, nrev,
     2       nthb, nrlt, nwl,  icmm, ickk, icnc, icph, icch,
     3       icnt, icnu, icnk, icns, icnr, iclt, icrl, icrv,
     4       icwl, icfl, icfo, ickf, ictb, ickn, ickt, ncaw,
     5       ncwt, nctt, ncaa, ncco, ncrv, nclt, ncrl, ncfl,
     6       nckt, ncwl, ncru, ncrc, ncpa, NcKF, NcKR, nck1, nck2, nck3,
     7       nck4, nci1, nci2, nci3, nci4
      dimension x(*), y(kdim+2,*), scrchk(nkk,*), ickwrk(*), rckwrk(*),
     1          imcwrk(*), rmcwrk(*), d(nkk,*), tdr(nkk,*),
     2          dkj(nkk,nkk,*), wt(*)
      logical ltdif, lmulti
      data eps/1.0e-30/
CC
C
C   KK     - NUMBER OF CHEMICAL SPECIES.
C   JJ     - NUMBER OF MESH POINTS.
C   NATJ   - NUMBER OF DEPENDENT VARIABLES AT EACH MESH POINT.  ALSO,
C            NATJ MUST BE THE EXACT FIRST DIMENSION OF several arrays.
C   LTDIF  - IF LTDIF=.TRUE. THEN EVALUATE THERMAL DIFFUSION RATIOS AS
C            WELL AS DIFFUSION COEFFICIENTS.
```

```
C   LMULTI - IF LMULTI=.TRUE. THEN MULTICOMPONENT FORMULAS USED
C            IF LMULTI=.FALSE. THEN MIXTURE-AVERAGED FORMULAS USED
C   P      - PRESSURE.
C              CGS UNITS - DYNES/CM**2
C   X      - THE ARRAY OF MESH POINT LOCATIONS.
C              DIMENSION X(*) AT LEAST JJ
C              CGS UNITS - CM
C   T      - DEPENDENT VARIABLE MATRIX.  THE TEMPERATURES ARE STORED IN
C            T(J)=y(NT,J), THE MASS FRACTIONS ARE IN Y(K,J)=y(NYS+K,J),
C            AND THE FLOW RATES ARE IN FLRT(J)=y(NM,J).
C              DIMENSION y(NATJ,*) EXACTLY NATJ FOR THE FIRST DIMENSION,
C              AND AT LEAST JJ FOR THE SECOND.
C
C WORK AND SCRATCH SPACE
C   YAV    - ARRAY OF MASS FRACTIONS AT MESH MIDPOINTS. ---> Replaced here
C            by scrchk(1,1).
C              DIMENSION Y(*) AT LEAST KK.
C   XAV    - ARRAY OF MOLE FRACTIONS AT MESH MIDPOINTS. ---> Replaced here
C            by scrchk(1,5)
C              DIMENSION X(*) AT LEAST KK
C   ICKWRK - INTEGER CHEMKIN WORK SPACE.
C              DIMENSIONING - SEE CHEMKIN DOCUMENTATION.
C   RCKWRK  - FLOATING POINT CHEMKIN WORK SPACE.
C              DIMENSIONING - SEE CHEMKIN DOCUMENTATION.
C   IMCWRK - INTEGER TRANSPORT PROPERTY WORK SPACE.
C              DIMENSIONING - SEE TRANSPORT DOCUMENTATION.
C   RMCWRK  - FLOATING POINT TRANSPORT PROPERTY WORK SPACE.
C              DIMENSIONING - SEE TRANSPORT DOCUMENTATION.
C OUTPUT-
C   COND   - ARRAY OF CONDUCTIVITIES AT THE MESH MID-POINTS.
C   D      - MATRIX OF DIFFUSION COEFFICIENTS AT THE MESH MID-POINTS.
C              DIMENSION D(KK,*) EXACTLY KK FOR THE FIRST DIMENSION,
C              AND AT LEAST JJ FOR THE SECOND.
C   TDR    - MATRIX OF THERMAL DIFFUSION RATIOS AT THE MESH MID-POINTS.
C              DIMENSION TDD(KK,*) EXACTLY KK FOR THE FIRST DIMENSION,
C              AND AT LEAST JJ FOR THE SECOND.
C   DKJ    - ARRAY OF MULTICOMPONENT DIFFUSION COEFFICIENTS AT THE
C             MESH MIDPOINTS. DIMENSION D(KK,KK,*) EXACTLY KK FOR THE
C             FIRST AND SECOND DIMENSION, AND AT LEAST JJ FOR THE THIRD.
C             CGS UNITS - CM**2/SEC
C
CC
      if (lmulti) then
CC
C-----------------Multicomponent formulas---------------------
C ...The xmf and xmfp arrays (scrchk(1,3) and scrchk(1,4) are obsolete
C    and have been commented out.
CC
C         call ckytx (y(ny,1), ickwrk, rckwrk, scrchk(1,3))
         do 200 j = 1, jj-1
            tav = 0.5 * (y(nt,j) + y(nt,j+1))
            xdif = x(j+1) - x(j)
CC
C ...Dimensional temperature at the grid points.
CC
            do 100 k = 1, nkk
               scrchk(k,1) = 0.5 * (y(nys+k,j) + y(nys+k,j+1))
C               scrchk(k,4) = scrchk(k,3)
 100        continue
            call ckytx (scrchk(1,1), ickwrk, rckwrk, scrchk(1,5))
C            call ckytx (y(ny,j+1), ickwrk, rckwrk, scrchk(1,3))
            call ckmmwx (scrchk(1,5), ickwrk, rckwrk, wtmav)
            call mcmdif(p, tav, scrchk(1,5), nkk, imcwrk, rmcwrk,
     +                  dkj(1,1,j))
```

```
            do 75 k = 1, nkk
               sumn = 0.0
               do 50 l = 1, nkk
                  sumn = sumn + dkj(k,l,j) *
     1                 (y(nys+l,j+1) - y(nys+l,j)) / xdif
    50          continue
               denom = - (y(nys+k,j+1) - y(nys+k,j)) / xdif
               d(k,j) = (sumn + eps) / ( wtmav * (denom + eps))
    75       continue
CC
C ...Determine the mixture conductivity and thermal diffusion
C    coefficient at j.
CC
            if (ltdif) call mcmcdt
     1         ( p, tav, scrchk(1,5), imcwrk, rmcwrk, ickwrk, rckwrk,
     2           tdr(1,j), cond)
200      continue
      else
CC
C-----------------Mixture-averaged formulas--------------------
CC
         do 400 j = 1, jj-1
            tav = 0.5 * (y(nt,j) + y(nt,j+1))
CC
C ...Dimensional temperature at the grid points.
CC
            do 300 k = 1, nkk
               scrchk(k,1) = 0.5 * (y(nys+k,j) + y(nys+k,j+1))
300         continue
            call ckytx (scrchk(1,1), ickwrk, rckwrk, scrchk(1,5))
            call mcadif(p, tav, scrchk(1,5), rmcwrk, d(1,j) )
CC
C ...Determine the mixture conductivity at j.
CC
            if (ltdif) then
               call mcatdr(tav, scrchk(1,5), imcwrk, rmcwrk, tdr(1,j))
               call ckrhoy (p, tav, scrchk(1,1), ickwrk, rckwrk, rhoav)
               call ckmmwy (scrchk(1,1), ickwrk, rckwrk, wtm)
               do 350 k = 1, nkk
                  tdr(k,j) = d(k,j) * tdr(k,j) * rhoav * wt(k)/wtm
 350           continue
            endif
400      continue
      endif
      return
      end
C
C**** End "Get diffusion coefficients."
C
CXXXXXXXXXXXXXXXXXXXXXXXXXXXXXXXXXXXXXXXXXXXXXXXXXXXXXXXXXXXXXXXXXXXXXXXXXXXXXXXXXXXXXXX
C###############################################################################
C###############################################################################
CXXXXXXXXXXXXXXXXXXXXXXXXXXXXXXXXXXXXXXXXXXXXXXXXXXXXXXXXXXXXXXXXXXXXXXXXXXXXXXXXXXXXXXX
       subroutine mdifv (imulti, lvcor, ltdif, x, y, wt, scrchk, d, tdr,
     +                  ickwrk, rckwrk, dkj, yv, cckwrk)
C
C***** Calculate diffusion velocity.  Based on PREMIX.F.
C
C*****double precision
C        IMPLICIT DOUBLE PRECISION (A-H, O-Z), INTEGER (I-N)
C*****END double precision
C
C*****double precision
        IMPLICIT DOUBLE PRECISION (A-H, O-Z), INTEGER (I-N)
```

```
C*****END double precision
C
      common /fileinfo/ nnnn, jj, p, dmflrt, kk, natj
      common /locs/ nt, nm, nys, ny, nx, nxs
      common /lenprm/ leniwk, lenrwk, lencwk, lenlwk, kdim, jdim, krxn
      common /ckstrt/ nmm , nkk , nii , mxsp, mxtb, mxtp, ncp , ncp1,
     +       ncp2, ncp2t,npar, nlar, nfar, nlan, nfal, nrev,
     2       nthb, nrlt, nwl,  icmm, ickk, icnc, icph, icch,
     3       icnt, icnu, icnk, icns, icnr, iclt, icrl, icrv,
     4       icwl, icfl, icfo, ickf, ictb, ickn, ickt, ncaw,
     5       ncwt, nctt, ncaa, ncco, ncrv, nclt, ncrl, ncfl,
     6       nckt, ncwl, ncru, ncrc, ncpa, NcKF, NcKR, nck1, nck2, nck3,
     7       nck4, nci1, nci2, nci3, nci4
      common /mach/ small, big, exparg
      dimension x(*), y(kdim+2,*), wt(*), scrchk(nkk,*), rckwrk(*),
     1          ickwrk(*), d(nkk,*), tdr(nkk,*), yv(nkk,*),
     2          dkj(nkk,nkk,*)
      character*16 spec, cckwrk(*)
      logical ltdif, lmulti, lvcor
CC
C
C   KK      - NUMBER OF CHEMICAL SPECIES.
C   JJ      - NUMBER OF MESH POINTS.
C   NATJ    - NUMBER OF DEPENDENT VARIABLES AT EACH MESH POINT, AND
C             THE EXACT FIRST DIMENSION OF several arrays.
C   LTDIF   - IF LTDIF=.TRUE. THEN EVALUATE THERMAL DIFFUSION RATIOS AS
C             WELL AS DIFFUSION COEFFICIENTS.
C               CGS UNITS - GM/(CM**2-SEC)
C   LMULTI  - IF LMULTI=.TRUE. THEN MULTICOMPONENT FORMULAS USED
C             IF LMULTI=.FALSE. THEN MIXTURE-AVERAGED FORMULAS USED
C   LVCOR   - IF LVCOR=.TRUE. THEN USE CORRECTION VELOCITY FORMULISM
C             IF LVCOR=.FALSE. THEN USE 'TRACE' APPROXIMATION, LUMPING
C             ALL TRANSPORT ERRORS INTO THE 'LAST' SPECIES.
C   X       - THE ARRAY OF MESH POINT LOCATIONS.
C               DIMENSION X(*) AT LEAST JJ
C               CGS UNITS - CM
C   S       - DEPENDENT VARIABLE MATRIX.  THE TEMPERATURES ARE STORED IN
C             T(J)=y(NT,J), THE MASS FRACTIONS ARE IN Y(K,J)=y(NYS+K,J),
C             AND THE FLOW RATES ARE IN FLRT(J)=y(NM,J).
C               DIMENSION y(NATJ,*) EXACTLY NATJ FOR THE FIRST DIMENSION,
C               AND AT LEAST JJ FOR THE SECOND.
C   WT      - THE ARRAY OF SPECIES MOLECULAR WEIGHTS.
C               CGS UNITS - GM/MOLE
C               DIMENSION WT(*) AT LEAST KK.
C
C WORK AND SCRATCH SPACE
C   YAV     - ARRAY OF MASS FRACTIONS AT MESH MIDPOINTS.  YAV(J) IS THE
C             MASS FRACTION BETWEEN J AND J+1. ---> Replaced here by
C             scrchk(1,1)
C               DIMENSION YAV(*) AT LEAST KK.
C   XMF     - ARRAY OF MOLE FRACTIONS AT MESH POINT J. ---> Replaced here
C             by scrchk(1,4)
C               DIMENSION XMF(*) AT LEAST KK.
C   XMFP    - ARRAY OF MOLE FRACTIONS AT MESH POINT J+1. ---> Replaced here
C             by scrchk(1,3)
C               DIMENSION XMFP(*) AT LEAST KK.
C   D       - MATRIX OF SPECIES DIFFUSION COEFFICIENTS AT THE MESH
C             MIDPOINTS.  IF LVARMC=.TRUE. THESE ARE COMPUTED EACH
C             TIME THE FUNCTION IS CALLED, OTHERWISE THE STORED VALUES
C             ARE USED.
C               CGS UNITS - CM**2/SEC
C               DIMENSION D(KK,*) EXACTLY KK FOR THE FIRST DIMENSION
C               AND AT LEAST JJ FOR THE SECOND.
C   TDR     - MATRIX OF SPECIES THERMAL DIFFUSION RATIOS AT THE MESH
```

```
C             MIDPOINTS.  IF LVARMC=.TRUE. THESE ARE COMPUTED EACH
C             TIME THE FUNCTION IS CALLED, OTHERWISE THE STORED VALUES
C             ARE USED.
C               CGS UNITS - NONE
C               DIMENSION TDR(KK,*) EXACTLY KK FOR THE FIRST DIMENSION
C               AND AT LEAST JJ FOR THE SECOND.
C   DKJ     - ARRAY OF MULTICOMPONENT DIFFUSION COEFFICIENTS AT THE
C              MESH MIDPOINTS. DIMENSION D(KK,KK,*) EXACTLY KK FOR THE
C              FIRST AND SECOND DIMENSION, AND AT LEAST JJ FOR THE THIRD.
C              CGS UNITS - CM**2/SEC
C   ICKWRK - INTEGER CHEMKIN WORK SPACE.
C               DIMENSIONING - SEE CHEMKIN DOCUMENTATION.
C   RCKWRK  - FLOATING POINT CHEMKIN WORK SPACE.
C               DIMENSIONING - SEE CHEMKIN DOCUMENTATION.
C OUTPUT-
C   YV      - MATRIX OF MASS FRACTIONS TIMES DIFFUSION VELOCITIES AT THE
C             MESH MIDPOINTS.  YV(K,J) IS THE FLUX OF KTH SPECIES BETWEEN
C             J AND J+1.
C               DIMENSION YV(KK,*) EXACTLY KK FOR THE FIRST DIMENSION
C               AND AT LEAST JJ FOR THE SECOND.
C
CC
      call ckytx (y(ny,1), ickwrk, rckwrk, scrchk(1,3))
CC
C ...Loop over all mesh points, computing the diffusion
C    velocity at the mid points.  the indexing is such that
C    yv(k,j) is the diffusion velocity of the kth species
C    midway between nodes j and j+1.
CC
      do 1000 j = 1, jj-1
         tav = 0.5 * (y(nt,j) + y(nt,j+1))
         do 300 k = 1, nkk
            scrchk(k,1) = 0.5 * (y(nys+k,j) + y(nys+k,j+1))
 300     continue
         do 400 k = 1, nkk
            scrchk(k,4) = scrchk(k,3)
 400     continue
         call ckmmwy (scrchk(1,1), ickwrk, rckwrk, wtm)
         call ckrhoy (p, tav, scrchk(1,1), ickwrk, rckwrk, rhoav)
         call ckytx (y(ny,j+1), ickwrk, rckwrk, scrchk(1,3))

         xdif = x(j+1) - x(j)
         if ( lmulti ) then
CC
C ...Evaluate the multicomponent diffusion velocity directly,
C    rather than use the mixture-averaged form for d(k,j).
CC
            do 475 k = 1, nkk
               sum = 0.0
               do 450 l = 1, nkk
                  sum = sum + wt(l) * dkj(k,l,j) *
     1                    (scrchk(l,3)-scrchk(l,4)) / xdif
 450           continue
               yv(k,j) = (wt(k)/wtm**2) * sum
 475        continue

CC
C    Calculate the equivalent Fickian diffusion coefficient for
C    information purposes.
CC
            do 480 k = 1, nkk
               d(k,j) = 0.0
               do 485 l = 1, nkk
                  d(k,j) = d(k,j) - wt(l) * dkj(k,l,j) *
```

```
     1                      (scrchk(l,3)-scrchk(l,4))
 485           continue
               dxk = (scrchk(k,3)-scrchk(k,4))
               if(abs(dxk).gt.small) then
                  d(k,j) = d(k,j) / wtm / dxk
               else
                  d(k,j) = -9.999E99
               endif
 480        continue
         else
CC
C ...Use mixture-averaged form for Fickian diffusion,
C    whether we are using the multicomponent formalism
C    or mixture-averaged.
CC
            do 500 k = 1, nkk
               yv(k,j) = - d(k,j) * (wt(k)/wtm) *
     1                     (scrchk(k,3)-scrchk(k,4)) / xdif
 500        continue
         endif
CC
C ...Add the thermal diffusion, if requested.
CC
         if (ltdif) then
            tdif = y(nt, j+1) - y(nt,j)
            do 600 k = 1, nkk
               yv(k,j) = yv(k,j) -
     1                   (tdr(k,j) / (tav*rhoav)) * tdif/xdif
 600        continue
         endif
CC
C ...Compute and add the correction velocity.
CC
         if (lvcor) then
            sum = 0.0
            do 700 k = 1, nkk
               sum = sum + yv(k,j)
 700        continue
            vc = - sum
            do 800 k = 1, nkk
               yv(k,j) = yv(k,j) + scrchk(k,1)*vc
 800        continue
         endif
 1000 continue
      return
      end
C
C**** End "Calculate diffusion velocity."
C
CXXXXXXXXXXXXXXXXXXXXXXXXXXXXXXXXXXXXXXXXXXXXXXXXXXXXXXXXXXXXXXXXXXXXXXXXXXXXXXXXXXXXXXX
C###############################################################################
C###############################################################################
CXXXXXXXXXXXXXXXXXXXXXXXXXXXXXXXXXXXXXXXXXXXXXXXXXXXXXXXXXXXXXXXXXXXXXXXXXXXXXXXXXXXXXXX
      subroutine fbrcalc (convol, swork, x, y, yav, yv, wt, ename, nelk,
     +                    womega, aw, iwork, rwork, vel, flux, gflux,
     2                    fluxbal, nelem, rate)
C
C**** Flux, flux balance, and net reaction rate.
C
        implicit double precision (a-h,o-z)
        implicit integer (i-n)
        character*3     pcontrol(3), edge
        character*16    el, ename(*), spec, method, multi, thdif
        character*80    solfile, arglink
```

```
      logical         deriv
      dimension x(*), y(kdim+2,*), yv(nkk,*), wt(*), womega(nkk,*),
     +          vel(*), flux(nkk,*), gflux(nkk,*), fluxbal(jdim,*),
     2          rate(nkk,*), nelk(nmm,*), nelem(3), yav(*), aw(*),
     3          rwork(*), iwork(*), convol(25,25), swork(jdim)
      common /ckstrt/ nmm , nkk , nii , mxsp, mxtb, mxtp, ncp , ncp1,
     +     ncp2, ncp2t,npar, nlar, nfar, nlan, nfal, nrev,
     2     ntab, nrlt, nwl,  icmm, ickk, icnc, icph, icch,
     3     icnt, icnu, icnk, icns, icnr, iclt, icrl, icrv,
     4     icwl, icfl, icfo, ickf, ictb, ickn, ickt, ncaw,
     5     ncwt, nctt, ncaa, ncco, ncrv, nclt, ncrl, ncfl,
     6     nckt, ncwl, ncru, ncrc, ncpa, NcKF, NcKR, nck1, nck2, nck3,
     7     nck4, nci1, nci2, nci3, nci4
      common /fileinfo/ nnnn, jj, p, dmflrt, kk, natj
      common /lenprm/ leniwk, lenrwk, lencwk, lenlwk, kdim, jdim, krxn
      common /rxprxp/ nckw, nmcw, nsch, nd, ndkj, ntdr, nyv,
     +                nomeg, nki, ngflx, nflux, nfbal, nvel, ickw,
     2                imcw, ielk, ncnc, nsum, nprt
      common /locs/ nt, nm, nys, ny, nx, nxs
      common /fbrrd/  elflux(3), fmmwt, iignore, ignorxn(100), ihablo,
     +        ihabhi, numsmth, ipoly, numpts, nsmflux, ipolfx, nptflx,
     2        areab, areac, arglink, solfile, spec, method, multi,
     3        thdif, el(3), pcontrol, edge
      data iout/6/, ilkout/7/, irate/9/, link/12/
      data isolout/8/, ibinary/10/, idata/11/
      data linktp/14/
      write (iout,120) areab, areac
 120  format (/,' Area expansion ratio = 1 / (1 + ',1pe11.4,
     +        ' * HAB + ',1pe11.4,' * HAB**2)',/)
CC
C ...Figure out womega_mk, the fraction of mass of species k that is
C    element m, for the three elements H, O and C.
CC
      call ckncf (nmm, iwork, rwork, nelk)
      do 100 lm = 1, 3
CC
C    (Scan the element list to be sure the element is present; no flux
C     balance will be done if it's not present.  Array "nelem" holds the
C     index for element lm, where lm is the order in which it was read
C     from file 'fbr.dat')
CC
         nelem(lm) = 0
         do 110 m = 1, nmm
            if (el(lm).eq.ename(m)) nelem(lm) = m
 110     continue
         if (nelem(lm).eq.0) then
            write(iout,200) el(lm)
 200        format(/,' FLUX BALANCE:  No counterpart to element ', a2,
     +          /,16x,'No mass flux balance will be done for it.',/)
         else
CC
C    (Finally, calculate the wt. fraction:
C          womega = #atoms(element m) * AW(element m) / MW(species)
CC    )
            do 130 k = 1, nkk
               womega(k,lm) = nelk(nelem(lm),k)*aw(nelem(lm))/wt(k)
 130        continue
         endif
 100  continue
      do 7220 j = 1, jj-1
CC
C ...Calculate gas velocity at mesh midpoints.
CC
         xav = 0.5 * (x(j) + x(j+1))
```

```
         A = 1.0 / (1.0 + areab * xav + areac * xav**2)
         tav = 0.5 * (y(nt,j) + y(nt,j+1))
         do 7200 k = 1, nkk
            yav(k) = 0.5 * (y(nys+k,j) + y(nys+k,j+1))
 7200    continue
         call ckmmwy (yav, iwork, rwork, wtm)
         vel(j) = (dmflrt / wtm) * (8.314e7 * tav / p) / A
CC
C ...Calculate Gi (mass flux fraction) and Fi (molar flux) for each
C    species at the mesh midpoints.
CC
         do 7230 k = 1, nkk
            gflux(k,j) = yav(k) + yv(k,j)/vel(j)
            flux(k,j) = gflux(k,j)* dmflrt / wt(k)
 7230    continue
CC
C ...Calculate the percent mass flux deviation for hyrogen, oxygen, and
C    carbon, at the mesh midpoints.
CC
         do 7240 lm = 1, 3
            fluxbal(j,lm) = 10000.00
            if (nelem(lm).ne.0) then
               sum = 0.00
               do 7250 k = 1, nkk
                  sum = sum + womega(k,lm) * gflux(k,j)
 7250          continue
               fluxbal(j,lm) = (sum /elflux(lm) - 1.0) * 100.
            endif
 7240    continue
 7220 continue
CC
C ...Finally, calculate the net reaction rate, at the midpoints of the
C    flux mesh.  That turns out to be the original mesh (midpoint of
C    midpoints) IF the original points are evenly spaced.  Only points
C    2,..,j-1 are valid.   Ki = 1/A * dFi/dx.  Smooth the flux profiles
C    before the differentiation.
CC
      deriv = .false.
      if (nsmflux .ne. 0) then
         write (iout, 600) nsmflux, ipolfx, 2*nptflx+1, edge
 600     format (/,' Smoothing soln ',i2,' times, polynomial order ',
     +              i2,', window size ',i2,', edge method ',a3,/)
         call smooth (nsmflux, nptflx, convol, nkk, 1, nkk, jj-1,
     +                 deriv, edge, swork, flux)
      endif
      do 7300 j = 2, jj - 1
         xav = 0.25 * (x(j-1) + 2.0*x(j) + x(j+1))
         A = 1.0 / (1.0 + areab * xav + areac * xav**2)
         xdif = 0.5 * (x(j+1) - x(j-1))
         do 7310 k = 1, nkk
            rate(k,j) = (flux(k,j) - flux(k,j-1)) / xdif / A
 7310    continue
 7300 continue
      return
      end
C
C**** End "Flux, flux balance, and net reaction rate."
C
CXXXXXXXXXXXXXXXXXXXXXXXXXXXXXXXXXXXXXXXXXXXXXXXXXXXXXXXXXXXXXXXXXXXXXXXXX
C#########################################################################
C#########################################################################
CXXXXXXXXXXXXXXXXXXXXXXXXXXXXXXXXXXXXXXXXXXXXXXXXXXXXXXXXXXXXXXXXXXXXXXXXX
      subroutine printfbr (x, ename, kname, flux, fluxbal, d,
     +                     nelem, rate)
```

```
C
C****  Print flux, flux balance, and net reaction rates.
C
        implicit double precision (a-h,o-z)
        implicit integer (i-n)
        character*3   pcontrol(3), edge
        character*16  method, spec, el, multi, ename(*), kname(*),
     +                thdif
        character*80  arglink, solfile, str
        dimension     x(*), flux(nkk,*), fluxbal(jdim,*), rate(nkk,*),
     +                d(nkk,*), nelem(3)
        common /lenprm/ leniwk, lenrwk, lencwk, lenlwk, kdim, jdim, krxn
        common /fileinfo/ nnnn, jj, p, dmflrt, kk, natj
        common /fbrrd/  elflux(3), fmmwt, iignore, ignorxn(100), ihablo,
     +         ihabhi, numsmth, ipoly, numpts, nsmflux, ipolfx, nptflx,
     2         areab, areac, arglink, solfile, spec, method, multi,
     3         thdif, el(3), pcontrol, edge
        common /ckstrt/ nmm , nkk , nii , mxsp, mxtb, mxtp, ncp , ncp1,
     +      ncp2, ncp2t,npar, nlar, nfar, nlan, nfal, nrev,
     2      nthb, nrlt, nwl,  icmm, ickk, icnc, icph, icch,
     3      icnt, icnu, icnk, icns, icnr, iclt, icrl, icrv,
     4      icwl, icfl, icfo, ickf, ictb, ickn, ickt, ncaw,
     5      ncwt, nctt, ncaa, ncco, ncrv, nclt, ncrl, ncfl,
     6      nckt, ncwl, ncru, ncrc, ncpa, NcKF, NcKR, nck1, nck2, nck3,
     7      nck4, nci1, nci2, nci3, nci4
        data iout/6/, ilkout/7/, irate/9/, link/12/
        data isolout/8/, kperln/6/, idiffn/15/
CC
C  ...Protect against ill-defined HAB bounds.
CC
        if (ihabhi.gt.jj) ihabhi = jj
        if (ihablo.lt.1)  ihablo = 1
        if (ihablo.gt.ihabhi) ihablo = 1
        if (ihabhi.lt.ihablo) ihabhi = jj
CC
C ...Some initializations.
CC
        nm = nkk + 2
        k2 = kperln - 1
        ls = k2 + 1
        ihabh = ihabhi
        if (ihabhi.eq.jj) ihabh = jj - 1
CC
C  ...Open "flux.out" for printout.
CC
        open (unit=isolout, status='unknown', form='formatted', file=
     +        "flux.out")
        write (iout,100)
 100    format (8x,'Writing file "flux.out"')
CC
C  ...Write fluxes to file "flux.out".  (The species names are in
C     "solnhead.out".)
CC
        do 415 l = 1, nkk, kperln
           k1 = l
           k2 = l + kperln - 1
           if (k2.gt.nkk) k2 = nkk
           do 400 j = ihablo, ihabh
              write (isolout,7020) j, 0.5*(x(j)+x(j+1)),
     +                             (flux(k,j), k = k1, k2)
 400       continue
           write (isolout,*)
 415    continue
CC
```

```
C  ...Identify data/solution file, for safety.
CC
        call strip (solfile, str)
        write (isolout,1500) str, nsmflux
        if (nsmflux.ne.0) write (isolout,2050) ipolfx, 2*nptflx+1, edge
        write (isolout,1540)
 1500   format (/,' Fluxes for input file ',a40,/,
     +          ' Fluxes smoothed ',i2,' times.',$)
 2050   format ('  Poly order ',i2,', window size ',i2,
     +          ', edge method ',a3,'.',$)
 1540   format (/,' Species names found in file "solnhead.out"',/)
        write (isolout,970) areab, areac
 970    format (' Area expansion ratio = 1 / (1 + ',1pe11.4,
     +          ' * HAB + ',1pe11.4,' * HAB**2)',/)
        write (isolout,1530) multi, thdif
        close (isolout)
CC
C  ...Repeat the process for "netrate.out"...
CC
        open (unit=isolout, status='unknown', form='formatted', file=
     +        "netrate.out")
        write (iout,120)
 120    format (8x,'Writing file "netrate.out"')
        ihabl = ihablo
        if (ihablo.eq.1) ihabl = 2

        do 425 l = 1, nkk, kperln
           k1 = l
           k2 = l + kperln - 1
           if (k2.gt.nkk) k2 = nkk
           do 430 j = ihabl, ihabh
              xav = 0.25 * (x(j-1) + 2.0*x(j) + x(j+1))
              write (isolout,7020) j, xav, (rate(k,j),k = k1, k2)
 430       continue
           write (isolout,*)
 425    continue
        write (isolout,1510) str, nsmflux
        if (nsmflux.ne.0) write (isolout,2060) ipolfx, 2*nptflx+1, edge
 1510   format (/,1x,'Net rates for input file ',a40,/,
     +          ' Fluxes smoothed ',i2,' times.',$)
 2060   format ('  Poly order ',i2,', window size ',i2,
     +          ', edge method ',a3,'.',$)
 1560   format (/,' Species names found in file "solnhead.out"',/)
        write (isolout,980) areab, areac
 980    format (/,' Area expansion ratio = 1 / (1 + ',1pe11.4,
     +          ' * HAB + ',1pe11.4,' * HAB**2)',/)
        write (isolout,1530) multi, thdif
        close (isolout)
CC
C  ...Repeat the process for "diffusion.out"...
CC
        open (unit=idiffn, status='unknown', form='formatted', file=
     +        "diffusion.out")
        write (iout,130)
 130    format (8x,'Writing file "diffusion.out"')
        ihabl = ihablo
        if (ihablo.eq.1) ihabl = 2
        do 735 l = 1, nkk, kperln
           k1 = l
           k2 = l + kperln - 1
           if (k2.gt.nkk) k2 = nkk
           do 740 j = ihabl, ihabh
              xav = 0.25 * (x(j-1) + 2.0*x(j) + x(j+1))
              write (idiffn,7020) j, xav, (d(k,j),k = k1, k2)
```

```
 740       continue
           write (idiffn,*)
 735     continue
         write (idiffn,710) str, nsmflux
         if (nsmflux.ne.0) write (idiffn,2060) ipolfx, 2*nptflx+1, edge
         write (idiffn, 1540)
 710     format (/,1x,'Diffn. coeffs. for input file ',a40,/,
     +          ' Fluxes smoothed ',i2,' times.',$)
         write (idiffn,980) areab, areac
         write (idiffn,1530) multi, thdif
         close (idiffn)
CC
C  ...SORT OF repeat the process for "fluxbal.out".  There are only four
C     columns, one for HAB and one for each element.
CC
         open (unit=isolout, status='unknown', form='formatted', file=
     +        'fluxbal.out')
         write (iout,110)
 110     format (8x,'Writing file "fluxbal.out"')
         write (isolout,7030) (el(lm),lm=1,3)
 7030    format (7x,'  HAB  ',3x,3(4x,a7))
         do 435 j = ihablo, ihabh
            write (isolout,7040) j, 0.5*(x(j)+x(j+1)), (fluxbal(j,lm),
     +                           lm = 1, 3)
 435     continue
 7040    format(i4,2x,f7.4,3(f11.2))
         write (isolout,*)
         write (isolout,1520) str
 1520    format (/,1x,'Element flux balances for input file ',a40)
         write (isolout,990) areab, areac
 990     format (/,' Area expansion ratio = 1 / (1 + ',1pe11.4,
     +          ' * HAB + ',1pe11.4,' * HAB**2)',/)
         write (isolout,1530) multi, thdif
         close (isolout)
 1530    format (1x,'Transport parameters:  ',2a7,/)
 7020    format (i4,2x,f7.4,6(1pe11.3))
         return
         end
C
C**** End "Print flux, flux balance, and net reaction rates."
C
CXXXXXXXXXXXXXXXXXXXXXXXXXXXXXXXXXXXXXXXXXXXXXXXXXXXXXXXXXXXXXXXXXXXXXXXXXXXXXXXXXXXXXXX
C###############################################################################
C###############################################################################
CXXXXXXXXXXXXXXXXXXXXXXXXXXXXXXXXXXXXXXXXXXXXXXXXXXXXXXXXXXXXXXXXXXXXXXXXXXXXXXXXXXXXXXX
      subroutine svsoln (x, y, iwork, rwork, cwork)
C
C**** Write a binary file of the text file data.
C
      implicit double precision (a-h, o-z), integer (i-n)
      dimension iwork(*), rwork(*), x(*), y(kdim+2,*)
      character*16 icklnk, isolut, imclnk, cwork(*)
      common /lenprm/ leniwk, lenrwk, lencwk, lenlwk, kdim, jdim, krxn
      common /ckstrt/ nmm , nkk , nii , mxsp, mxtb, mxtp, ncp , ncp1,
     +       ncp2, ncp2t,npar, nlar, nfar, nlan, nfal, nrev,
     2       nthb, nrlt, nwl,  icmm, ickk, icnc, icph, icch,
     3       icnt, icnu, icnk, icns, icnr, iclt, icrl, icrv,
     4       icwl, icfl, icfo, ickf, ictb, ickn, ickt, ncaw,
     5       ncwt, nctt, ncaa, ncco, ncrv, nclt, ncrl, ncfl,
     6       nckt, ncwl, ncru, ncrc, ncpa, NcKF, NcKR, nck1, nck2, nck3,
     7       nck4, nci1, nci2, nci3, nci4
      common /fileinfo/ nnnn, jj, p, dmflrt, kk, natj
      common /rxprxp/ nckw, nmcw, nsch, nd, ndkj, ntdr, nyv,
     +       nomeg, nki, ngflx, nflux, nfbal, nvel, ickw,
```

```
     2       imcw, ielk, ncnc, nsum, nprt
      data iout/6/, ibinary/10/
      data icklnk/'CKLINK          '/
      data isolut/'SOLUTION        '/
      data imclnk/'MCLINK          '/
      write (iout,100)
 100  format (8x,'Creating a flame code binary file ("binary.fbr")')
      open (unit=ibinary, status='unknown', form='unformatted',
     +      file='binary.fbr')
      write (ibinary) icklnk
      call cksave (iout, ibinary, iwork, rwork, cwork)
      write (ibinary) imclnk
      call mcsave (iout, ibinary, iwork(imcw), rwork(nmcw))
      write (ibinary) isolut
      write (ibinary) natj, jj, p, dmflrt
      write (ibinary) (x(j), j = 1, jj)
      write (ibinary) ((y(n,j), n = 1, natj), j = 1, jj)
      close (ibinary)
      return
      end
C
C**** End "Write a binary file of the text file data"
C
CXXXXXXXXXXXXXXXXXXXXXXXXXXXXXXXXXXXXXXXXXXXXXXXXXXXXXXXXXXXXXXXXXXXXXXXXXXXXXXX
C###############################################################################
C###############################################################################
CXXXXXXXXXXXXXXXXXXXXXXXXXXXXXXXXXXXXXXXXXXXXXXXXXXXXXXXXXXXXXXXXXXXXXXXXXXXXXXX
      subroutine properties (x, s, rwork, iwork)
C
C**** Calculate and print some flame properties.
C
      implicit double precision (a-h, o-z), integer (i-n)
      dimension iwork(*), rwork(*), x(*), s(kdim+2,*)
      character*3   pcontrol(3), edge
      character*16  method, spec, el, multi, thdif
      character*80  arglink, solfile, str
      common /fbrrd/  elflux(3), fmmwt, iignore, ignorxn(100), ihablo,
     +       ihabhi, numsmth, ipoly, numpts, nsmflux, ipolfx, nptflx,
     2       areab, areac, arglink, solfile, spec, method, multi,
     3       thdif, el(3), pcontrol, edge
      common /lenprm/ leniwk, lenrwk, lencwk, lenlwk, kdim, jdim, krxn
      common /ckstrt/ nmm , nkk , nii , mxsp, mxtb, mxtp, ncp , ncp1,
     +       ncp2, ncp2t,npar, nlar, nfar, nlan, nfal, nrev,
     2       nthb, nrlt, nwl,  icmm, ickk, icnc, icph, icch,
     3       icnt, icnu, icnk, icns, icnr, iclt, icrl, icrv,
     4       icwl, icfl, icfo, ickf, ictb, ickn, ickt, ncaw,
     5       ncwt, nctt, ncaa, ncco, ncrv, nclt, ncrl, ncfl,
     6       nckt, ncwl, ncru, ncrc, ncpa, NcKF, NcKR, nck1, nck2, nck3,
     7       nck4, nci1, nci2, nci3, nci4
      common /fileinfo/ nnnn, jj, p, dmflrt, kk, natj
      common /locs/ nt, nm, nys, ny, nx, nxs
      common /rxprxp/ nckw, nmcw, nsch, nd, ndkj, ntdr, nyv,
     +       nomeg, nki, ngflx, nflux, nfbal, nvel, ickw,
     2       imcw, ielk, ncnc, nsum, nprt
      data iout/6/, iprops/19/
CC
C ...Information message and file headers.
CC
      write (iout, 100)
 100  format (8x,'Writing file "props.out"')
      open (unit=iprops, status='unknown', form='formatted', file=
     +      'props.out')
      write (iprops, 200)
 200  format (7x,'  HAB  ',3x,' VEL   ',3x,'  RHO  ',3x,'  VISC ',
```

```
     +        5x,'   Cp  ',3x,'  COND ')
      do 150 j = 1, jj
CC
C ...Calculate velocity at the mesh points.
CC
         A = 1.0 / (1.0 + areab * x(j) + areac * x(j)**2)
         call ckmmwx (s(nx,j), iwork, rwork, wtm)
         vel = (dmflrt / wtm) * (8.314e7 * s(nt,j) / p) / A
CC
C ...Calculate density, viscosity, Cp, and thermal conductivity.
CC
         call ckrhox (p, s(nt,j), s(nx,j), iwork, rwork, rho)
         call mcavis (s(nt,j), s(nx,j), rwork(nmcw), vismix)
         call ckcpbl (s(nt,j), s(nx,j), iwork, rwork, cpbml)
         call mcacon (s(nt,j), s(nx,j), rwork(nmcw), conmix)
CC
C ...Convert Cp and conductivity from erg*[] to cal*[].
CC
         cpbml = cpbml * 1.987 / 8.314e7
         conmix = conmix * 1.987 / 8.314e7
CC
C ...Print it all out.
CC
         write (iprops, 250) j, x(j), vel, rho, vismix, cpbml, conmix
 150  continue
 250  format(i4,2x,f7.4,5(1pe11.3))
      write(iprops,*)
      call strip (solfile, str)
      write(iprops,1520) str
 1520 format(/,1x,'Miscellaneous properties, input file ',a40)
      write (iprops,990) areab, areac
 990  format (/,' Area expansion ratio = 1 / (1 + ',1pe11.4,
     +        ' * HAB + ',1pe11.4,' * HAB**2)',/)
      write(iprops,1530) multi, thdif
 1530 format (1x,'Transport parameters:  ',2a7,/)
      close (iprops)
      return
      end
C
C**** End "Calculate and print some flame properties"
C
CXXXXXXXXXXXXXXXXXXXXXXXXXXXXXXXXXXXXXXXXXXXXXXXXXXXXXXXXXXXXXXXXXXXXXXXXXXXXXXX
C##########################################################################
C##########################################################################
CXXXXXXXXXXXXXXXXXXXXXXXXXXXXXXXXXXXXXXXXXXXXXXXXXXXXXXXXXXXXXXXXXXXXXXXXXXXXXX
       subroutine smooth (nsm, npts, convol, ntot, nlow, npro, num,
     +                   deriv, edge, swork, sm)
C
C**** Savitsky-Golay smoothing, 2nd to 6th order polynomial.
C
CC
C ...Subroutine parameters:
C
C    nsm = number of smoothings to perform
C    npts = (2 * npts + 1) is the window width for convolution
C    convol = Savitsky-Golay coefficient matrix
C    ntot = leading dimension of array sm
C    nlow = starting index of leading dimension, array sm
C    npro = number of profiles to be smoothed
C    num = second dimension of array sm, number of points in the profile.
C          Smoothing starts at sm(*,1) and  ends at sm(*,num)
C    deriv = flag for last smoothing to be the derivative of the input
C            profile (true) or not (false)
C    swork = work array for smoothing
```

```
C     sm = array of profiles to be smoothed (ntot,num)
CC
      implicit double precision (a-h,o-z)
      implicit integer (i-n)
      dimension sm(ntot,*), swork(*), convol(25,25)
      character*3 edge
      logical deriv
CC
C ...The weights for averaging of the edge points are dependent on the
C     window size.
CC
      wt1 = (1.0 - 0.01 * npts)
      wt2 =        0.01 * npts
CC
C ...Loop over the leading dimension, i.e., from the first profile to the
C     last.  The (initial) range for the loop over the main body of points is
C     based on the treatment method for near-edge points.
CC
      nhi = nlow + npro - 1
      do 10 k = nlow, nhi
         if (edge .eq. 'SG ') then
            low = 3
         else
            low = npts + 1
         endif
CC
C ...Loop over the number of smoothings.
CC
         do 20 nn = 1, nsm
CC
C ...Loop from one end of the profile at hand to the other.  The edge
C     points and the points just inside (that is, until the window can be
C     full-sized) are either averages of neighboring points or SG convolutes
C     with smaller windows, depending on the variable 'edge'.  If derivative,
C     near-edge points are handled by the increasing window method; the edge
C     points should be considered undefined on return from this subroutine.
CC
            numpts = 1
            if (deriv .and. (nn .eq. nsm)) then
               swork(2)     = 0.5 * (sm(k,3) - sm(k,1))
               swork(num-1) = 0.5 * (sm(k,num) - sm(k,num-2))
               low = 3
            else
               swork(1)   =  wt1 * sm(k,1) + wt2 * sm(k,2)
               swork(num) =  wt1 * sm(k,num) + wt2 * sm(k,num-1)
               swork(2)     = (sm(k,1) + sm(k,2) + sm(k,3)) / 3.0
               swork(num-1) = (sm(k,num) + sm(k,num-1) + sm(k,num-2))
     +                                          / 3.0
CC
C ...Default edge treatment is averaging until the window is full-sized.
CC
               if (edge .ne. 'SG ') then
                  do 25 j = 3, npts
                     swork(j) = 0.0
                     swork(num-j+1) = 0.0
                     do 35 jj = j - 2, j + 2
                        swork(j) = swork(j) + 0.2 * sm(k,jj)
                        swork(num-j+1) = swork(num-j+1) +
     +                                   0.2 * sm(k,num-jj+1)
 35                  continue
 25                  continue
                     numpts = npts
                  endif
               endif
```

```
CC
C ...Loop over the main body of points. The first part is done to make a
C    gradually increasing window, but when the other treatment is being done,
C    'numpts' and the low and high ends of the loop have been set to avoid
C    this.
CC
            do 30 j = low, num - low + 1
               if ((num - j) .lt. numpts) then
                  numpts = num - j
               else
                  if (numpts .lt. npts) numpts = numpts + 1
               endif
CC
C ...Set the convolution matrix index based on numpts and whether smoothing or
C    smoothing plus derivative needed.
CC
               if (deriv .and. (nn .eq. nsm)) then
                  idx = 2 * numpts + 1
               else
                  idx = 2 * numpts
               endif
CC
C ...Do the convolution.  The subroutine gets the appropriate column from the
C    convolution matrix, and the profile to be smoothed starting at the bottom
C    of the window; as well as dimensions needed for the convolution.
CC
               call convolute (convol(1,idx), sm(1,j-numpts), ntot,
     +                         k, numpts, smthed)
CC
C ...Store the smoothed point in swork array.
CC
               swork(j) = smthed
 30         continue
C  {end loop over profile at hand}
CC
C ...Replace points with smoothed points.
CC
            do 40 j = 1, num
               sm(k,j) = swork(j)
 40         continue
 20      continue
C  {end loop over number of smoothings}
 10   continue
C  {end loop over all profiles}
      return
      end
C
C**** End "Savitsky-Golay smoothing, 2nd to 6th order polynomial."
C
CXXXXXXXXXXXXXXXXXXXXXXXXXXXXXXXXXXXXXXXXXXXXXXXXXXXXXXXXXXXXXXXXXXXXXXXXXXXXXXX
C###############################################################################
C###############################################################################
CXXXXXXXXXXXXXXXXXXXXXXXXXXXXXXXXXXXXXXXXXXXXXXXXXXXXXXXXXXXXXXXXXXXXXXXXXXXXXXX
      subroutine convolute (convo, smth, ntot, k, m, smthed)
C
C**** Do the convolution process for Savitsky-Golay smoothing.
C
      implicit double precision (a-h,o-z)
      implicit integer (i-n)
      dimension convo(25), smth(ntot,*)
      smthed = 0.0
      do 10 i = 1, 2 * m + 1
         smthed = smthed + smth(k,i) * convo(i)
 10   continue
```

```
C
C**** End "Do the convolution process for Savitsky-Golay smoothing."
C
      return
      end
CXXXXXXXXXXXXXXXXXXXXXXXXXXXXXXXXXXXXXXXXXXXXXXXXXXXXXXXX
C###########################################################################
C###########################################################################
CXXXXXXXXXXXXXXXXXXXXXXXXXXXXXXXXXXXXXXXXXXXXXXXXXXXXXXXX
      subroutine sgparam (ipoly, x, a, r, convol)
C
C**** Calculate coefficients for Savitsky-Golay smoothing.
C
      implicit double precision (a-h,o-z)
      implicit integer (i-n)
      dimension x(ipoly+1,25), r(ipoly+1,ipoly+1), convol(25,25),
     +          a(ipoly+1,2*(ipoly+1))
      iorder = ipoly + 1
      do 5 i = 1, 25
         do 7 j = 1, 25
            convol(i,j) = 0.0
 7       continue
 5    continue
CC
C ...Loop over all values of m from 2 to 12, representing 5 to 25 points for
C    smoothing.
CC
      do 100 m = 2, 12
         n = 2 * m + 1
CC
C ...Initialize coefficient matrix X.
CC
         do 10 i = 1, n
            x(1,i) = 1.0
            x(2,i) = i - m - 1
 10      continue
         do 20 j = 3, iorder
            do 30 i = 1, n
               x(j,i) = x(2,i)**(j-1)
 30         continue
 20      continue
CC
C ...Transpose times original matrix; R = XtX.
CC
         do 40 i = 1, iorder
            do 50 j = 1, iorder
               r(i,j) = 0.0
               do 60 mm = 1, n
                  r(i,j) = r(i,j) + x(i,mm) * x(j,mm)
 60            continue
 50         continue
 40      continue
CC
C ...Take inverse of R matrix.  Use A as a work matrix for Doolittle
C    computation.  The Doolittle algorithm gives the inverse of a symmetric
C    matrix.  R (hence A) is symmetric, being XtX.
CC
         do 110 i = 1, iorder
            do 120 j = 1, iorder
               a(i,j) = r(i,j)
 120        continue
 110     continue
         call doolittle (iorder, a, r)
CC
```

```
C ...Finally, compute T = (XtX)^-1*X matrix, here called 'convol'.  Store the
C    smoothing coefficients for 2m+1 points in locations convol(*,2m), and the
C    1st derivative coefficients in locations convol(*,2m+1).
CC
         do 80 j = 1, n
            do 90 mm = 1, iorder
               convol(j,2*m) = convol(j,2*m) + r(mm,1) * x(mm,j)
               convol(j,2*m+1) = convol(j,2*m+1) + r(mm,2) * x(mm,j)
 90         continue
 80      continue
 70      continue
 100   continue
       return
       end
C
C**** End "Calculate coefficients for Savitsky-Golay smoothing."
C
CXXXXXXXXXXXXXXXXXXXXXXXXXXXXXXXXXXXXXXXXXXXXXXXXXXXXXXXXXXXXXXXXXXXXXXXXXXXXXXXXXXXXXXX
C###############################################################################
C###############################################################################
CXXXXXXXXXXXXXXXXXXXXXXXXXXXXXXXXXXXXXXXXXXXXXXXXXXXXXXXXXXXXXXXXXXXXXXXXXXXXXXXXXXXXXXX
       subroutine doolittle (ndim, a, ainv)
C
C**** Doolittle method of inverting symmetric matrices, implemented here
C      for order up to 7.  From "Matrices and Determinants," Dr. R.E.
C      Bargmann, chapter in CRC Standard Mathematical Tables, 21st Edition,
C      1973, pp. 117-139.
C
       implicit double precision (a-h,o-z)
       implicit integer (i-n)
       dimension ainv(ndim,ndim), a(ndim,2*ndim), p(7,14), u(7,14)
CC
C ...Set up a and p matrices above ndim.
CC
       do 5 i = ndim + 1, ndim + ndim
          do 7 j = 1, ndim
             a(j,i) = 0.0
             p(j,i) = 0.0
 7        continue
          a(i-ndim,i) = 1.0
 5     continue
CC
C ...Forward solution.
CC
       do 10 m = 1, ndim
          do 20 i = m, ndim + m
             p(m,i) = a(m,i)
             do 30 j = 1, m - 1
                p(m,i) = p(m,i) - u(j,m) * p(j,i)
 30          continue
             u(m,i) = p(m,i) / p(m,m)
 20       continue
 10    continue
CC
C ...Backward solution.
CC
       do 40 j = 1, ndim
          ainv(ndim,j) = u(ndim,ndim+j)
          ainv(j,ndim) = ainv(ndim,j)
 40    continue
       do 50 k = 1, ndim - 1
          do 60 j = 1, ndim - k
             ainv(ndim-k,j) = u(ndim-k,ndim+j)
             do 70 i = 0, k - 1
```

```
                ainv(ndim-k,j) = ainv(ndim-k,j) -
     +                           u(ndim-k,ndim-i) * ainv(ndim-i,j)
 70          continue
             ainv(j,ndim-k) = ainv(ndim-k,j)
 60       continue
 50    continue
       return
       end
C
C**** End "Doolittle method of inverting symmetric matrices."
C
CXXXXXXXXXXXXXXXXXXXXXXXXXXXXXXXXXXXXXXXXXXXXXXXXXXXXXXXXXXXXXXXXXXXXXXXXXXXXXXXXXXXXX
C###############################################################################
C###############################################################################
CXXXXXXXXXXXXXXXXXXXXXXXXXXXXXXXXXXXXXXXXXXXXXXXXXXXXXXXXXXXXXXXXXXXXXXXXXXXXXXXXXXXXX
        BLOCK DATA names
        common /locs/ nt, nm, nys, ny, nx, nxs
        common /lenprm/ leniwk, lenrwk, lencwk, lenlwk, kdim, jdim, krxn
        data nt/1/,nys/1/,ny/2/,nxs/1/,nx/2/
        data leniwk/12000/, lenrwk/1500000/, lencwk/500/, lenlwk/500/
        data kdim/100/, jdim/175/, krxn/550/
        end
CXXXXXXXXXXXXXXXXXXXXXXXXXXXXXXXXXXXXXXXXXXXXXXXXXXXXXXXXXXXXXXXXXXXXXXXXXXXXXXXXXXXXX
C###############################################################################
C###############################################################################
CXXXXXXXXXXXXXXXXXXXXXXXXXXXXXXXXXXXXXXXXXXXXXXXXXXXXXXXXXXXXXXXXXXXXXXXXXXXXXXXXXXXXX
C  CHEMKIN work info:
C
C  The work arrays contain all the pertinent information about the
C  species and the reaction mechanism.  They also contain some work
C  space needed by various routines for internal manipulations.  If a
C  user wishes to modify a CKLIB subroutine or to write new routines,
C  he will probably want to use the work arrays directly.  The starting
C  adddresses for information stored in the work arrays are found in
C  the labeled common block, COMMON /CKSTRT/, and are explained below.
C
C  COMMON /CKSTRT/ NMM , NKK , NII , MXSP, MXTB, MXTP, NCP , NCP1,
C 1                NCP2, NCP2T,NPAR, NLAR, NFAR, NLAN, NFAL, NREV,
C 2                NTHB, NRLT, NWL,  IcMM, IcKK, IcNC, IcPH, IcCH,
C 3                IcNT, IcNU, IcNK, IcNS, IcNR, IcLT, IcRL, IcRV,
C 4                IcWL, IcFL, IcFO, IcKF, IcTB, IcKN, IcKT, NcAW,
C 5                NcWT, NcTT, NcAA, NcCO, NcRV, NcLT, NcRL, NcFL,
C 6                NcKT, NcWL, NcRU, NcRC, NcPA, NcKF, NcKR, NcK1,
C 7                NcK2, NcK3,NcK4, NcI1, NcI2, NcI3, NcI4
C
C  INDEX CONSTANTS.
C
C     NMM    - Total number of elements in problem.
C     NKK    - Total number of species in problem.
C     NII    - Total number of reactions in problem.
C     MXSP   - Maximum number of species (reactants plus products)
C              allowed for any reaction;  unless changed in the
C              interpreter, MXSP=6.
C     MXTB   - Maximum number of enhanced third-bodies allowed fo any
C              reaction;  unless changed in the interpreter, MXTB=10.
C     MXTP   - Maximum number of temperatures allowed in fits of
C              thermodynamic properties for any species;  unless
C              changed in the interpreter and the thermodynamic
C              database, MXTP=3.
C     NCP    - Number of polynomial coefficients to fits of CP/R for
C              a species;  unless changed in the interpreter and the
C              thermodynamic database, NCP=5.
C     NCP1   - NCP + 1
C     NCP2   - NCP + 2
```

```
C     NCP2T  - Total number of thermodynamic fit coefficients for the
C              species;  unless changed, NCP2T = (MXTP-1)*NCP2 = 14.
C     NPAR   - Number of parameters required in the rate expression
C              for the reactions;  in the current formulation NPAR=3.
C     NLAR   - Number of parameters required for Landau-Teller
C              reactions; NLAR=4.
C     NFAR   - Number of parameters allowed for fall-off reactions;
C              NFAR=8.
C     NLAN   - Total number of Landau-Teller reactions.
C     NFAL   - Total number of fall-off reactions.
C     NREV   - Total number of reactions with reverse parameters.
C     NTHB   - Total number of reactions with third-bodies.
C     NRLT   - Total number of Landau-Teller reactions with reverse
C              parameters.
C     NWL    - Total number of reactions with radiation wavelength
C              enhancement factors.
C
C  STARTING ADDRESSES FOR THE CHARACTER WORK SPACE, CCKWRK.
C
C     IcMM   - Starting address of an array of the NMM element names.
C              CCKWRK(IcMM+M-1) is the name of the Mth element.
C     IcKK   - Starting address of an array of the NKK species names.
C              CCKWRK(icKK+M-1) is the name of the Kth species.
C
C  STARTING ADDRESSES FOR THE INTEGER WORK SPACE, IWORK.
C
C     IcNC  - Starting address of an array of the elemental content
C             of the NMM elements in the NKK species.
C             IWORK(IcNC+(K-1)*NMM+M-1) is the number of atoms of the
C             Mth element in the Kth species.
C     IcPH  - Starting address of an array of phases of the NKK species.
C             IWORK(IcPH+K-1) = -1, the Kth species is a solid
C                             =  0, the Kth species is a gas
C                             = +1, the Kth species is a liquid
C     IcCH  - Starting address of an array of the electronic charges of
C             the NKK species.
C             IWORK(IcCH+K-1) = -2, the Kth species has two excess
C                                   electrons.
C     IcNT  - Starting address of an array of the number of temperatures
C             used to fit thermodynamic coefficients for the
C             NKK species.
C             IWORK(IcNT+K-1) = N, N temperatures were used in the fit
C                               for the Kth species.
C     IcNU  - Starting address of a matrix of stoichiometric
C             coefficients of the MXSP species in the NII reactions.
C             IWORK(IcNU+(I-1)*MXSP+N-1) is the coefficient of the Nth
C             participant species in the Ith reaction
C     IcNK  - Starting address of a matrix of species index numbers for
C             the MXSP species in the NII reactions.
C             IWORK(IcNK+(I-1)*MXSP+N-1) = K, the species number of
C             the Nth participant species in the Ith reaction.
C     IcNS  - Starting address of an array of the total number of
C             participant species for the NII reactions, and the
C             reversibility of the reactions.
C             IWORK(IcNS+I-1) = +N, the Ith reaction is reversible
C                                   and has N participant species
C                                   (reactants + products)
C                             = -N, the Ith reaction is irreversible
C                                   and has N participant species
C                                   (reactants + products)
C     IcNR  - Starting address of an array of the number of reactants
C             only for the NII reactions.
C             IWORK(IcNR+I-1) is the total number of reactants in the
C             Ith reaction.
```

```
C     IcLT  - Starting address of an array of the NLAN reaction numbers
C             for which Landau-Teller parameters have been given.
C             IWORK(IcLT+N-1) is the reaction number of the Nth
C             Landau-Teller reaction.
C     IcRL  - Starting address of an array of the NRLT reaction numbers
C             for which reverse Landau-Teller parameters have been
C             given.
C             IWORK(IcRL+N-1) is the reaction number of the Nth
C             reaction with reverse Landau-Teller parameters.
C     IcRV  - Starting address of an array of the NREV reaction numbers
C             for which reverse Arhennius coefficients have been given.
C             IWORK(IcRV+N-1) is the reaction number of the Nth
C             reaction with reverse coefficients.
C     IcWL  - Starting address of an array of the NWL reactions numbers
C             for which radiation wavelength has been given.
C             IWORK(IcWL+N-1) is the reaction number of the Nth
C             reaction with wavelength enhancement.
C     IcFL  - Starting address of an array of the NFAL reaction numbers
C             with fall-off parameters.
C             IWORK(IcFL+N-1) is the reaction number of the Nth
C             fall-off reaction.
C     IcFO  - Starting address of an array describing the type of
C             the NFAL fall-off reactions.
C             IWORK(IcFO+N-1) is the type of the Nth fall-off
C             reaction: 1 for 3-parameter Lindemann Form
C                       2 for 6- or 8-parameter SRI Form
C                       3 for 6-parameter Troe Form
C                       4 for 7-parameter Troe form
C     IcKF  - Starting address of an array of the third-body species
C             numbers for the NFAL fall-off reactions.
C             IWORK(IcKF+N-1) = 0: the concentration of the third-body
C                                  is the total of the concentrations
C                                  of all species in the problem
C                             = K: the concentration of the third-body
C                                  is the concentration of species K.
C     IcTB  - Starting address of an array of reaction numbers for the
C             NTHB third-body reactions.
C             IWORK(IcTB+N-1) is the reaction number of the Nth
C             third-body reaction.
C     IcKN  - Starting address of an array of the number of enhanced
C             third bodies for the NTHB third-body reactions.
C             IWORK(IcKN+N-1) is the number of enhanced species for
C             the Nth third-body reaction.
C     IcKT  - Starting address of an array of species numbers for the
C             MXTB enhanced 3rd bodies in the NTHB third-body reactions.
C             IWORK(IcTB+(N-1)*MXTB+L-1) is the species number of the
C             Lth enhanced species in the Nth third-body reaction.
C
C  STARTING ADDRESSES FOR THE REAL WORK SPACE, RWORK.
C
C     NcAW  - Starting address of an array of atomic weights of the
C             NMM elements (gm/mole).
C             RWORK(NcAW+M-1) is the atomic weight of element M.
C     NcWT  - Starting address of an array of molecular weights for
C             the NKK species (gm/mole).
C             RWORK(NcWT+K-1) is the molecular weight of species K.
C     NcTT  - Starting address of an array of MXTP temperatures used in
C             the fits of thermodynamic properties of the NKK species
C             (Kelvins).
C             RWORK(NcTT+(K-1)*MXTP+N-1) is the Nth temperature for the
C             Kth species.
C     NcAA  - Starting address of a three-dimensional array of
C             coefficients for the NCP2 fits to the thermodynamic
C             properties for the NKK species, for (MXTP-1) temperature
```

```
C            ranges.
C            RWORK(NcAA+(L-1)*NCP2+(K-1)*NCP2T+N-1) = A(N,L,K);
C            A(N,L,K),N=1,NCP2T = polynomial coefficients in the fits
C            for the Kth species and the Lth temperature range, where
C            the total number of temperature ranges for the Kth species
C            is IWORK(IcNT+K-1) - 1.
C     NcCO   - Starting address of an array of NPAR Arrhenius parameters
C            for the NII reactions.
C            RWORK(NcCO+(I-1)*NPAR+(L-1)) is the Lth parameter of the
C            Ith reaction, where
C               L=1 is the pre-exponential factor (mole-cm-sec-K),
C               L=2 is the temperature exponent, and
C               L=3 is the activation energy (Kelvins).
C     NcRV   - Starting address of an array of NPAR reverse Arrhenius
C            parameters for the NREV reactions.
C            RWORK(NcRV+(N-1)*NPAR+(L-1)) is the Lth reverse
C            parameter for the Nth reaction with reverse parameters
C            defined, where
C               L=1 is the pre-exponential factor (mole-cm-sec-K),
C               L=2 is the temperature exponent, and
C               L=3 is the activation energy (Kelvins).
C            The reaction number is IWORK(IcRV+N-1).
C     NcLT   - Starting location of an array of the NLAR parameters for
C            the NLAN Landau-Teller reactions.
C            RWORK(NcLT+(N-1)*NLAR+(L-1)) is the Lth Landau-Teller
C            parameter for the Nth Landau-Teller reaction, where
C               L=1 is B(I) (Eq. 72) (Kelvins**1/3), and
C               L=2 is C(I) (Eq. 72) (Kelvins**2/3).
C            The reaction number is IWORK(IcLT+N-1).
C     NcRL   - Starting location of an array of the NLAR reverse
C            parameters for the NRLT Landau-Teller reactions for which
C            reverse parameters were given.
C            RWORK(NcRL+(N-1)*NLAR+(L-1)) is the Lth reverse
C            parameter for the Nth reaction with reverse Landau-Teller
C            parameters, where
C               L=1 is B(I) (Eq. 72) (Kelvins**1/3), and
C               L=2 is C(I) (Eq. 72) (Kelvins**2/3).
C            The reaction number is IWORK(IcRL+N-1).
C     NcFL   - Starting location of an array of the NFAR fall-off
C            parameters for the NFL fall-off reactions.
C            RWORK(NcFL+(N-1)*NFAR+(L-1)) is the Lth fall-off
C            parameter for the Nth fall-off reaction, where the low
C            pressure limits are defined by
C               L=1 is the pre-exponential factor (mole-cm-sec-K),
C               L=2 is the temperature exponent, and
C               L=3 is the activation energy (Kelvins).
C            Additional parameters define the centering, depending on
C            the type of formulation -
C               Troe: L=4 is the Eq. 68 parameter a,
C                     L=5 is the Eq. 68 parameter T*** (Kelvins),
C                     L=6 is the Eq. 68 parameter T*   (Kelvins), and
C                     L=7 is the Eq. 68 parameter T**  (Kelvins).
C               SRI:  L=4 is the Eq. 69 parameter a,
C                     L=5 is the Eq. 69 parameter b (Kelvins),
C                     L=6 is the Eq. 69 parameter c (kelvins),
C                     L=7 is the Eq. 69 parameter d, and
C                     L=8 is the Eq. 69 parameter e.
C            The reaction number is IWORK(IcFL+N-1), and the type
C            of formulation is IWORK(IcFO+N-1).
C     NcWL   - Starting location of an array of wavelengths for the NWL
C            wavelength-enhanced reactions.
C            RWORK(NcWL+N-1) is the wavelength enhancement (angstrom)
C            for the Nth wavelength-enhanced reaction;
C            the reaction number is IWORK(IcWL+N-1).
```

```
C     NcKT  - Starting location of an array of MXTB enhancement factors
C             for the NTHB third-body reactions.
C             RWORK(NcKT+(N-1)*MXTB+(L-1)) is the enhancement factor
C             for the Lth enhanced species in the Nth third-body
C             reaction;
C             the reaction number is IWORK(IcTB+N-1), and the Lth
C             enhanced species index number is
C             IWORK(IcKT+(N-1)*MXTB+L-1).
C     NcRU  - RWORK(NcRU) is the universal gas constant (ergs/mole-K).
C     NcRC  - RWORK(NcRC) is the universal gas constant (cal/mole-K).
C     NcPA  - RWORK(NcPA) is the pressure of one standard atmosphere
C             (dynes/cm**2).
C     NcKF  - Starting address of an array of intermediate forward
C             temperature-dependent rates for the II reactions.
C     NcKR  - Starting address of an array of intermediate reverse
C             temperature-dependent rates for the II reactions.
C     NcK1  - Starting addresses of arrays of internal work space
C     NcK2
C     NcK3                  space of length NKK
C     NcK4
C     NcI1  - Starting addresses of arrays of internal work space
C     NcI2
C     NcI3                  space of length NII
C     NcI4
C
C  The linking file consists of the following binary records:
C
C
C   1) Information about the linking file:  VERS, PREC, KERR
C      Where VERS   = character*16 string representing the version
C                     number of the interpreter which created the
C                     the linking file.
C            PREC   = character*16 string representing the machine
C                     precision of the linking file (SINGLE, DOUBLE).
C            KERR   = logical which indicates whether or not
C                     an error occurred in the interpreter input.
C   2) Index constants:
C      LENI, LENR, LENC, NMM,  NKK,  NII,  MXSP, MXTB,
C      MXTP, NCP,  NPAR, NLAR, NFAR, NREV, NFAL, NTHB,
C      NLAN, NRLT, NWL, NCHRG
C      Where LENI = required length of IWORK.
C            LENR = required length of RWORK.
C            LENC = required length of CCKWRK.
C            NCHRG= total number of species with an electronic
C                   charge not equal to zero.
C
C  3) Element information:
C     ((CCKWRK(IcMM + M-1),                          !element names
C      RWORK(NcAW + M-1)),                          !atomic weights
C      M=1,NMM)
C
C  4) Species information:
C     ((CCKWRK(IcKK+K-1),                             !species names
C       (IWORK(IcNC+(K-1)*NMM+M-1),M=1,MMM),         !composition
C       IWORK(IcPH+K-1),                             !phase
C       IWORK(IcCH+K-1),                             !charge
C       RWORK(NcWT+K-1),                             !molec weight
C       IWORK(IcNT+K-1),                             !# of fit temps
C       (RWORK(NcTT+(K-1)*MXTP + L-1),L=1,MXTP),     !array of temps
C       ((RWORK(NcAA+(L-1)*NCP2+(K-1)*NCP2T+N-1),    !fit coeff'nts
C                N=1,NCP2), L=1,(MXTP-1))),
C       K = 1,NKK)
C
C  5) Reaction information (if NII>0):
```

```
C     (IWORK(IcNS+I-1),                              !# of species
C      IWORK(IcNR+I-1),                              !# of reactants
C      (RWORK(NcCO+(I-1)*NPAR+N-1), N=1,NPAR),       !Arr. coefficients
C      (IWORK(IcNU+(I-1)*MXSP+N-1),                  !stoic coef
C      IWORK(IcNK+(I-1)*MXSP+N-1), N=1,MXSP),        !species numbers
C      I = 1,NII)
C
C  6) Reverse parameter information (if NREV>0):
C     (IWORK(IcRV+N-1),                              !reaction numbers
C      (RWORK(NcRV+(N-1)*NPAR+L-1),L=1,NPAR),        !reverse coefficients
C      N = 1,NREV)
C
C  7) Fall-off reaction information (if NFAL>0):
C     (IWORK(IcFL+N-1),                              !reaction numbers
C      IWORK(IcFO+N-1),                              !fall-off option
C      IWORK(IcKF+N-1),                              !3rd-body species
C      (RWORK(NcFL+(N-1)*NFAR+L-1),L=1,NFAR),        !fall-off parameters
C      N=1,NFAL)
C
C  8) Third-body reaction information (if NTHB>0):
C     (IWORK(IcTB+N-1),                              !reaction numbers
C      IWORK(IcKN+N-1),                              !# of 3rd bodies
C      (IWORK(IcKT+(N-1)*MXTB+L-1),                  !3rd-body species
C      RWORK(NcKT+(N-1)*MXTB+L-1),L=1,MXTB),         !enhancement factors
C      N=1,NTHB)
C
C  9) Landau-Teller reaction information (if NLAN>0):
C     (IWORK(IcLT+N-1),                              !reaction numbers
C      (RWORK(NcLT+(N-1)*NLAR+L-1),L=1,NLAR),        !L-T parameters
C      N=1,NLAN)
C
C 10) Reverse Landau-Teller reaction information (if NRLT>0):
C     (IWORK(IcRL+N-1),                              !reaction numbers
C      (RWORK(NcRL+(N-1)*NLAR+L-1),L=1,NLAR),        !rev. L-T parameters
C      N=1,NRLT)
C
C 11) Photon radiation reaction information (if NWL>0):
C     (IWORK(IcWL+N-1),                              !reaction numbers
C      RWORK(NcWL+N-1),                              !wavelength factor
C      N=1,NWL)
C
C-----------------------------------------------------------------------
C
C   End CHEMKIN work space info.
C
```

Appendix E. Calibration Factors for Measured Species.

The purpose of this appendix is to (a) list all of the ionization cross-sections used for the Relative Ionization Cross-Section ("RICS") calibrations in this work, and (b) to provide calibration correction factors for translation of certain mole fraction profiles from one assumed identity to another.

The RICS method is spelled out in detail in Chapter 3. The calibration factor for conversion of the ratio of signals $\frac{I_j}{I_k}$ to the ratio of mole fractions $\frac{x_j}{x_k}$ is simply $\frac{Q_k}{Q_j} \times f_{EE}$, where Q is the ionization cross-section and f_{EE} is an energy correction factor, if needed[47] (Equation 3-15). This assumes that the identity of the species being measured is known, so that the amount that the electron energies used exceed the ionization potentials can be determined. It also assumes that the ionization potentials are known.

In calibrating for an unknown species according to an assumed identity, Equation 3-15 is used to adjust the signal to the correct electron energy basis. Equation 3-18 is then appropriate if one wishes to change the presumed identity. In combination with the difference in ionization cross-sections, the total correction or conversion factor by which a mole fraction profile should be multiplied in translating from an assumed species A to an assumed species B is then:

$$f_{A\to B} = \left(\frac{EE_{meas} - (IP_A + \Delta)}{EE_{meas} - (IP_B + \Delta)}\right)\left(\frac{Q_A}{Q_B}\right) \qquad \text{(E-1)}$$

where

EE_{meas} = electron energy at which the signal of the species being measured was taken,

IP = ionization potential,

Δ = energy scale correction = ICP - IP, and

ICP = intercept of linear portion of ionization efficiency curve.

Therefore, to compute a conversion factor the ionization potentials and ionization cross-sections must be known.

---

[47] The specific f_{EE}'s used in this work are not documented here, since unprocessed signal ratio data are not reported. The ionization cross-section information *is* given, however, because those are subject to revision as experimental cross-section data or estimation methods are improved.

Unless indicated otherwise, sources for literature ionization potentials were Field and Franklin (1970), Rosenstock et al. (1977), Levin and Lias (1982), and Lias et al. (1988). In most cases, when electron impact IP data were available they were preferred over those of some other measurement technique. The only ionization potential data listed here are the values used for the calculation; in some cases many other values can be found in the literature. "V" refers to a vertical (or adiabatic) ionization potential measurement, which is always greater than a non-adiabatic IP.

For some species, no literature IP was measured but the heat of formation of the positive ion was given in Lias et al. (1988). The ionization potential was then calculated as $\left(\Delta H_f^0(\text{ion}) - \Delta H_f^0(\text{neutral, est.})\right)$, with the estimation of the heat of formation of the neutral species performed by thermochemical kinetics (Appendix M).

Ionization cross-section estimations were also required at times. The general methodology used was explained in Chapter 3. In the following, TOTIXC refers to a computer (spreadsheet) program written for this research which estimates total ionization cross-sections by a combination of methods, as described in Section 3.4.2. It should be pointed out that some molecules fit more than one category under the estimation schemes of Harrison et al. (1966) and Beran and Kevan (1969). In such cases, the value used was generally the average of those predicted for the various applicable categories (e.g., alkene and aldehyde). Units for ionization cross-sections are 10^{-16} cm^2.

H, O and OH

H_2 was the reference species for the H atom measurements. As discussed in Chapter 3, the most accurate results are achieved in a RICS calibration when:

- the ionization cross-sections for the energy being measured are used, rather than 70 or 75 eV cross-sections, and
- the cross-sections used are for single positive ionization, without fragmentation, rather than total cross-sections.

Only total ionization data are available for H_2, but low-energy data for it and for H atom have been measured by Kieffer and Dunn (1966). Those were used for the RICS calculation of the H profile.

The reference species for OH was H_2O. While there are no low-energy cross-section data

for OH, there is total ionization information for H_2O. In addition, there are reliable data for both CH_4 and CH_3 (see the discussion of CH_3 below). Using the 20 eV CH_3-CH_4 data to compute an H atom additivity increment, the OH cross-section was estimated as $Q_{OH,\ 20eV} = Q_{H2O,\ 20\ eV} - \Delta Q_{H\ increment}$.

Finally, the partial (single-ionization) O atom cross-section measured by Fite and Brackmann (1959) at 36 eV[48] was used for computation of x_O in the post-flame zone, with H_2O as the reference species. Single positive ionization data for H_2O were measured by Mark and Egger (1976).

Table E.1 Ionization cross-sections used for RICS calibration of species in the H/O system.

Species	$Q_{Bittner}$	Source	$Q_{Present\ Work}$	Source
H, 25 eV			0.43	Kieffer and Dunn (1966)
H, 70 eV	0.68	Kieffer and Dunn (1966)		
OH, 20 eV			0.25	Estimated, see text.
OH, 70 eV	2.2	Bittner (1981)		
O, partial 36 eV			1.22	Fite and Brackmann (1959)
O, 70 eV	1.54	Kieffer and Dunn (1966)		
H_2, 25 eV			0.55	Kieffer and Dunn (1966)
H_2, 70 eV	1.0	Kieffer and Dunn (1966)		
H_2O, 20 eV			0.38	Djuric et al. (1988)*
H_2O, partial 36 eV			0.55	Mark and Egger (1976)
H_2O, 70 eV	2.96	Lampe et al. (1957)	2.41	Djuric et al. (1988)*
O_2	2.55	Kieffer and Dunn (1966)		

*Adjusted to the same energy basis as Harrison et al. (1966) and Fitch and Sauter (1983).

CH_3

Methyl was measured with respect to methane. Literature data for CD_3 is found in Deutsch et al. (1989). Near 20 eV, CH_4 was empirically found to fragment a great deal, most likely more than CH_3 though the appearance potential of CH and CH_2 is about that of CH_3 from CH_4. In fact, while Q_{CH4}/Q_{CH3} is approximately constant from 20 to 70 eV, it is a bit higher at 20eV, probably for the reason described. Therefore, $Q_{tot,CH4}$(20 eV) may be too high relative to Q_{CH3}(20 eV). Because there are no partial ionization data, the ratio Q_{CH4}/Q_{CH3} was chosen at 40 eV, where the ratio is 1.30 (= 3.0/2.3).

[48] The lowest electron energy reported.

H_2CO

CO was the reference species for formaldehyde. The program TOTIXC gives a value for Q_{CO} of 3.01, close to the experimental values of 3.11 (Harrison et al.) and 3.12 (Rapp and Englander-Golden, 1965). Therefore, the ratio of cross-sections estimated by TOTIXC was used, $\frac{Q_{CO}}{Q_{H_2CO}} = \frac{3.01}{3.95} = 0.76$.

Mass 42

Mass 42 was measured with respect to CO_2. For CO_2, the average of cross-sections from Harrison et al. (1966) and Margreiter et al. (1990) was used, $Q_{CO2,ave} = 4.11$. An adjustment of the latter to the same energy basis of the former was required. Mass 42 was assumed to be C_3H_6. Ionization cross-sections for c-C_3H_6 and C_3H_6 were taken from Harrison et al. (1966); those of HC≡COH and H_2C=CO were estimated with TOTIXC. To get a profile for one of these species, multiply the existing profile by $f_{A\to B}$ listed below.

Table E.2 Ionization cross-sections and conversion factors for RICS calibration of mass 42.

Species	Q	$f_{A\to B}$
c-C_3H_6	10.4	0.91
C_3H_6	8.97	1.00
HC≡COH	5.15	1.80
H_2C=CO	6.18	1.38

Mass 43

Mass 43 was quantified from species scans. The reported ionization potentials for each possible species varied over a large range, all of them overlapping at 8.0 eV. That energy was chosen to represent all of the candidate species. The ionization cross section for the chosen reference species, C_2H_2, was taken from Harrison et al. (1966). Cross-sections for other molecules were calculated with TOTIXC.

Table E.3 Ionization cross-sections for RICS calibration of mass 43.

Species	Q
C_2H_2	4.61
CH_3CO	5.95
C_3H_7	9.70

Mass 44, low electron energy species

As would be expected, the reference species was CO_2, whose cross-section was discussed above. The species being measured was assumed to be CH_3CHO.

TOTIXC was used to estimate ionization cross-sections.

Table E.4 Ionization potentials, ionization cross-sections and conversion factors for RICS calibration of mass 44.

Species	IP	Q	$f_{A\rightarrow B}$
CH_3CHO	10.24	6.2	1.00
C_3H_8	11.19	10.3	0.61
Ethylene oxide	10.61	7	0.89

Mass 53

The reference species was CO_2. Mass 53 was assumed to be $CH_2{=}CCH{=}CH_2$. Cross-sections were estimated with TOTIXC.

Table E.5 Ionization potentials, ionization cross-sections and conversion factors for RICS calibration of mass 53.

Species	IP	Q	$f_{A\rightarrow B}$
$CH{\equiv}CCHCH_3$ and $CH_3C{\equiv}CCH_2$	7.97, 7.95	9.19	1.11
$CH_2{=}CCH{=}CH_2$	8.08 (est)	10.48	1.00
c-$C_3H_2CH_3$	6.21 (est)	10.81	0.68
$HC{\equiv}CC.{=}O$	7.67 (est)	6.43	1.49

Mass 54

The reference species was CO_2. Mass 54 was assumed to be 1,3-C_4H_6. Cross-sections were estimated with TOTIXC, except for 1,3-C_4H_6 for which the source was Beran and Kevan.

Table E.6 Ionization potentials, ionization cross-sections and conversion factors for RICS calibration of mass 54.

Species	IP	Q	$f_{A\rightarrow B}$
1,3-C_4H_6	9.18	11.6	1.00
1,2-C_4H_6	9.57	10.95	1.19
$CH_3CH_2C{\equiv}CH$	10.2	9.53	1.72
$CH_3C{\equiv}CCH_3$	9.9	9.53	1.53
$HC{\equiv}CCHO$	10.8	6.83	3.16
$CH_2{=}C{=}C{=}O$	9.12	7.68	1.48
c-$C_3H_2{=}O$	9.47, 10.0	8.21	1.85

Mass 55

The reference species was CO_2. Mass 55 was assumed to be $CH_3CH{=}CHCH_2$. Cross-sections were estimated with TOTIXC.

Table E.7 Ionization potentials, ionization cross-sections and conversion factors for RICS calibration of mass 55.

Species	IP	Q	$f_{A\to B}$
$CH_3CH{=}CHCH_2$	7.71	11.54	1.00
$CH_2{=}C(CH_3)CH_2$	8.02	11.54	1.11
$CH_3CHCH{=}CH_2$	7.49	11.54	0.93
c-$C_3H_4CH_3$	7.23 (est)	12.65	0.79
c-C_4H_7	7.54, 7.88	12.65	0.86
$CH_2{=}CHCO$	7.0	8.22	1.14
$HC{\equiv}CCH_2O$	7.16 (est)	7.47	1.31

Mass 56

The reference species was CO_2. Mass 56 was assumed to be 2-C_4H_8. Cross-sections were estimated with TOTIXC, unless noted otherwise.

Table E.8 Ionization potentials, ionization cross-sections and conversion factors for RICS calibration of mass 56.

Species	IP	Q	$f_{A\to B}$
$CH_2{=}CHCHO$	10.2	8.63	2.07
$HC{\equiv}CCH_2OH$	10.48	7.81	2.67
$CH_3CH{=}C{=}O$	8.95	8.8***	1.25
c-$C_3H_4(=O)$	9.1	9.06	1.27
$HC{\equiv}COCH_3$	9.48	8.8	1.50
$CH_2{=}CHCH_2CH_3$	9.75	12.18**,11.91	1.20
$CH_3CH{=}CHCH_3$	9.3	12.31**,11.91	1.00
i-C_4H_8	9.25	13.2*,13.01	0.92
c-C_4H_8	10.58	13.01	1.70
c-$C_3H_5(CH_3)$	9.9	13.01	1.20

* Lampe, et al.
** Beran and Kevan
*** 'aldehyde'+'alkene'

Mass 57

The reference species was CO_2. Mass 57 was assumed to be s-C_4H_9. Cross-sections were estimated with TOTIXC.

Table E.9 Ionization potentials, ionization cross-sections and conversion factors for RICS calibration of mass 57.

Species	IP	Q	$f_{A\rightarrow B}$
t-C_4H_9	7.42	13.38	0.90
n-C_4H_9	8.64	13.38	1.17
s-C_4H_9	7.93	13.38	1.00
i-C_4H_9	8.35	13.38	1.09
C_2H_5CO	5.7	9.02	1.02
CH_2=CHCHOH	6.63*	9.72	1.09

*Alfassi et al. (1973) heat of formation used (0.0 kcal/mol). THERM gives 16.54 kcal/mol if a secondary carbon bond dissociation energy ("BDE") is used, or -1.38 kcal/mol if primary allyl is used, from CH_3CH=CHOH.

Mass 58

The reference species was CO_2. Mass 58 was assumed to be n-C_4H_{10}. Cross-sections were estimated with TOTIXC, unless otherwise noted.

Table E.10 Ionization potentials, ionization cross-sections and conversion factors for RICS calibration of mass 58.

Species	IP	Q	$f_{A\rightarrow B}$
n-C_4H_{10}	10.23-10.88	14.4**	1.00
i-C_4H_{10}	10.23-10.74	14.7***	0.95
C_2H_5CHO	9.95	9.38**	1.23
$(CH_3)_2CO$	9.7	10.2**	1.04
CH_2=$CHCH_2OH$	9.67	10.09	1.05
CH_3CH=CHOH	8.67	10.09	0.82
CH_2=C(OH)CH_3	8.67	10.09	0.82
CH_2=$CHOCH_3$	8.93	10.41*	0.84
c-C_3H_6O	9.67	11.05	0.96
c-$C_2H_3O(CH_3)$ (1,2-epoxypropane)	10.22	11.05	1.15
c-C_3H_5(OH)	9.1	10.91	0.84

* Ether and alkene averaged.
** Harrison et al.
*** Lampe et al.

Mass 59

The reference species was CO_2. Mass 59 was assumed to be C_2H_5CHOH (low electron energy species) and n- or i-C_3H_7O (high electron energy species). Cross-sections were estimated with TOTIXC.

Table E.11 Ionization potentials, ionization cross-sections and conversion factors for RICS calibration of mass 59.

Species	IP	Q	$f_{A\rightarrow B}$ (low EE species)	$f_{A\rightarrow B}$ (high EE species)
n,i-C_3H_7O	9.2	11.4	10.75	1.00
CH_3CHOCH_3	6.19 (est),≤6.50	11.4	0.91	0.54*
C_2H_5CHOH	6.47 (est)	11.4	1.00	0.57*
$C(CH_3)_2OH$	6.10 (est)	11.4	0.89	0.54*
$C_2H_5OCH_2$	6.63 (est)	11.4	0.99	0.56*

*Fragmentation would probably be present for these species, which would mean that the estimated factor is high.

Mass 60

The reference species was CO_2. Mass 60 was assumed to be n-C_3H_7OH. Cross-sections were estimated with TOTIXC, except for $C_2H_5OCH_3$ which was taken from Harrison et al.

Table E.12 Ionization potentials, ionization cross-sections and conversion factors for RICS calibration of mass 60.

Species	IP	Q	$f_{A\rightarrow B}$
n-C_3H_7OH	10-10.37	11.89	1.00
i-C_3H_7OH	10.27,10.41	11.89	1.06
$C_2H_5OCH_3$	9.62	12.8	0.76

Mass 65

Benzene was the reference species. Mass 65 was assumed to be c-C_5H_5. Cross-sections were estimated with TOTIXC.

Table E.13 Ionization potentials, ionization cross-sections and conversion factors for RICS calibration of mass 65.

Species	IP	Q	$f_{A\rightarrow B}$
c-C_5H_5	8.6	12.66	1.00
$HC\equiv CC=CO$	9.5 (est*)	8.62	2.66
$HC=C=C=CO$	9.5 (est*)	9.43	2.43
$HC\equiv CCHCH=CH_2$	7.88 (est)	11.61	0.80
c-$C_3H_2(CH=CH_2)$	5.41	12.66	0.39

*By analogy to HC=CO.

Mass 66

Benzene was the reference species. Mass 66 was assumed to be c-C_5H_6. Cross-sections were estimated with TOTIXC.

Table E.14 Ionization potentials, ionization cross-sections and conversion factors for RICS calibration of mass 66.

Species	IP	Q	$f_{A\rightarrow B}$
c-C_5H_6	8.56-9.00	13.03	1.00
$CH_3CH{=}CHC{\equiv}CH$	8.50,9.14	11.97	1.11
$CH_2{=}C{=}CHCH{=}CH_2$	8.88	12.8	1.06
Bicyclo[2.1.0]pent-2-ene	8.00,8.60	13.36	0.81
c-$C_3H_5C{\equiv}CH$	8.70, 9.58	11.52	1.09

Mass 68

Benzene was the reference species. Mass 68 was assumed to be c-C_5H_8. Cross-sections were estimated with TOTIXC, except where indicated.

Table E.15 Ionization potentials, ionization cross-sections and conversion factors for RICS calibration of mass 68.

Species	IP	Q	$f_{A\rightarrow B}$
c-C_4H_4O	8.8-9.04	9.1*,11.4	1.46
$CH_3CH{=}C{=}C{=}O$	8.68	10.7	1.17
$CH_2{=}C(OH)C{\equiv}CH$	8.92	10.2	1.30
1-CH_3-c-$C_3H(=O)$	9.15	8.92	1.59
c-$C_3H_4(=C=O)$	8.78	10.75	1.19
c-C_5H_8	9-9.27	14.09	1.00
$CH_2{=}CHCH{=}CHCH_3$	8.6-8.68	13.76	0.90
$CH_3CH{=}C{=}CHCH_3$	9.26	13.87	1.06
$CH_2{=}CHC(CH_3){=}CH_2$	8.85-9.04	13.76	0.97
$CH_2{=}C{=}C(CH_3)_2$	8.9	13.87	0.95
$CH_2{=}C{=}CHCH_2CH_3$	9.24	13.87	1.05
c-$C_4H_6{=}CH_2$	9.16-9.35	14.09	1.04
Bicyclo[2.1.0]pentane	8.7	15.19	0.82

* Turecek et al. (1990).

Mass 69

Benzene was the reference species. Mass 69 was assumed to be c-C_5H_9. Cross-sections were estimated with TOTIXC.

Table E.16 Ionization potentials, ionization cross-sections and conversion factors for RICS calibration of mass 69.

Species	IP	Q	$f_{A\rightarrow B}$
$C_2H_5CH=CHCH_2$	7.30,7.65	14.46	1.03
c-C_5H_9	7.47,7.79	15.56	1.00
$CH_2=CHCHCH_2CH_3$	7.3	14.46	0.98
$CH_3CHCH=CHCH_3$	7.07	14.46	0.92
$CH_3CH=CC_2H_5$	6.55 (est)	14.46	0.82
$(CH_3)_2CCH=CH_2$	7.13	14.46	0.94
$(CH_3)_2CHC=CH_2$	6.51 (est)	14.46	0.81
$CH_3CH=C(CH_3)CH_2$	7.4	14.46	1.01
c-$C_4H_6(CH_3)$	6.42 (est)	15.56	0.74
c-C_3H_5-(CH_2CH_2) or -$(CHCH_3)$	6.75 (est)	15.56	0.79
c-$C_3H_3(CH_3)_2$	7.32 (est)	15.56	0.92
$CH_2=C(C_2H_5)CH_2$	7.9	14.46	1.17
$CH_2CH(CH_3)CH=CH_2$	8	14.46	1.21
c-C_4H_7O (2-hydrofuran)	6.63 (est)	12.19	0.99

Mass 70

Benzene was the reference species. Mass 70 was assumed to be c-C_5H_{10}. Cross-sections were estimated with TOTIXC, unless otherwise specified.

Table E.17 Ionization potentials, ionization cross-sections and conversion factors for RICS calibration of mass 70.

Species	IP	Q	$f_{A\rightarrow B}$
$C_3H_7CH=CH_2$	9.67,9.82	16.1^{+}	0.72
$C_2H_5CH=CHCH_3$	9.1-9.32	16.1^{+}	0.61
$(CH_3)_2CHCH=CH_2$	9.6	16.1**	0.69
$C_2H_5C(CH_3)=CH_2$	9.28	16.1**	0.63
$(CH_3)_2C=CHCH_3$	8.86	16.1**	0.56
c-$C_3H_4(CH_3)_2$	9.08-9.77	16.9^{++}	0.62
c-C_5H_{10}	10.54,10.92	16.9*	1.00
c-$C_4H_7(CH_3)$	9.6	16.9^{++}	0.65
c-$C_3H_5(C_2H_5)$	9.5	16.9^{++}	0.64
$CH_3CH=CHCHO$	9.81	11.2***	1.06
3,4-epoxy-1-butene	9.7,9.94(V)	$(8.5,9.1)^{+++}$	1.35
c-$C_4H_6=O$	9.4,9.58	9.5***	1.13
$CH_2=CHCOCH_3$	9.66	10.4***,12.1***	1.02
$(CH_3)_2C=C=O$	8.38(V),8.45	11.6	0.73

Species	IP	Q	$f_{A\rightarrow B}$
HC4CCH(CH_3)OH	10.41(V),10.15	10.47	1.29
CH_2=C=CHOCH_3	8.75(V),8.64	12.2	0.72
2,5-dihydrofuran	9.16	8.5***,9.1***	1.14
3,4-dihydrofuran	9.14	(8.5,9.1)$^{+++}$	1.13
CH_2=C(CH_3)CHO	9.86,9.92	11.2°	1.10
C_2H_5CH=C=O	8.8	11.6	0.79
$CH_3C_4COCH_3$	8.79	11.5	0.79
CH_2=CHCH=CHOH	8.5	11.9	0.72
CH_2=C=CHCH_2OH	8.74	12.0	0.76
HC4CCH_2CH_2OH	9.66	10.47	1.10
CH_3C4CCH_2OH	9.78	10.47	1.14
CH_2=CHC(OH)=CH_2	8.68	11.9	0.75
HC4CCH_2OCH_3	9.78	11.5	1.04
CH_2=CHOCH=CH_2	8.7	12.2	0.73

* Harrison et al. (1966).
** Lampe et al. (1957). Normalized to Harrison et al. so that C_3H_6's are equal.
*** Turecek et al. (1990). No renormalization appears to be necessary.
$^{+}$ Set equal to $(CH_3)_2$CHCH=CH_2 experimental value, because TOTIXC would predict the two to be the same.
$^{++}$ Set equal to c-C_5H_{10} experimental value, see note just above.
$^{+++}$ Set equal to 2,5-dihydroxyfuran, as note above.
° Set equal to CH_3CH=CHCHO, as note above.

Mass 71

Benzene was the reference species. Mass 71 was assumed to be n-C_5H_{11}. Cross-sections were estimated with TOTIXC.

Table E.18 Ionization potentials, ionization cross-sections and conversion factors for RICS calibration of mass 71.

Species	IP	Q	$f_{A\rightarrow B}$
n-C_5H_{11}	7.7-8.6	16.3	1.00
n-$C_3H_7CHCH_3$	7.41,7.73	16.3	0.86
$(C_2H_5)_2$CH	7.86	16.3	0.92
i-C_5H_{11}	8.6	16.3	1.15
i-$C_3H_7CHCH_3$	8.09-8.2	16.3	1.00
C_2H_5CH(CH_3)CH_2	7.91	16.3	0.94
t-C_5H_{11}	6.85,7.12	16.3	0.76
neo-C_5H_{11}	8.33	16.3	1.05
CH_3CHCHCHOH	6.49 (est)	12.6	0.88
CH_2C(CH_3)CHOH	6.6 (est)	12.6	0.90
CH_2CHC(OH)CH_3	6.23 (est)	12.6	0.85
2,3,4-trihydrofuran	6.3 (est)	13.5	0.80
2,4,5-trihydrofuran	6.62 (est)	13.5	0.86

Mass 72

Benzene was the reference species. Mass 71 was assumed to be n-C_5H_{12}. Cross-sections were estimated with TOTIXC, except where indicated otherwise.

Table E.19 Ionization potentials, ionization cross-sections and conversion factors for RICS calibration of mass 72.

Species	IP	Q	$f_{A\to B}$
n-C_5H_{12}	10.59	17.7*	1.00
i-C_5H_{12}	10.50,10.60	17.1**	1.02
neo-C_5H_{12}	10.3	17.0*	0.95
n-C_3H_7CHO	9.86	12.1***	1.80
i-C_3H_7CHO	9.74	12.4*	1.11
$C_2H_5COCH_3$	9.58	12.9*,12.1*	1.06
c-$(CH_2)_4O$	9.3,9.45	11.9***	1.06
c-C_4H_7OH	9.25	9.8***	1.25
CH_2=$CHCH_2(OCH_3)$	9.84(V),9.56	11.8^{+}	1.12
CH_2=$CHCH(OH)CH_3$	10.05(V),9.50	$(10.4,9.9)^{++}$	1.28
CH_2=$C(CH_3)OCH_3$	8.64	11.8***	0.91
$C_2H_2O(CH_3)_2$ 2,2-dimethyl-oxirane 2,3-dimethyl,trans-oxirane	10.0(V)	10.8^{+++}	1.37
$C_2H_3OC_2H_5$ ethyl-oxirane	10.15(V)	10.8***	1.42
CH_2=$CHOC_2H_5$	8.8	11.8***	0.95
CH_3CH_2CH=$CHOH$	8.34	$(10.4,9.9)^{++}$	1.00
CH_3CH=$CHCH_2OH$	9.13	9.9***,10.4***	1.17
CH_2=$CHCH_2CH_2OH$	9.56	$(10.4,9.9)^{++}$	1.30
CH_3CHCH_2CHOH	6.15 (est)	14.1	0.51
CH_2=$C(CH_3)CH_2OH$	9.26	$(10.4,9.9)^{++}$	1.21
$(CH_3)_2C$=$CHOH$	8.27	$(10.4,9.9)^{++}$	0.98
$CH_2CH(CH_3)CHOH$	5.65 (est)	14.1	0.48
$CH_3CH_2C(OH)$=CH_2	8.36	$(10.4,9.9)^{++}$	1.00
$CH_3C(OH)$=$CHCH_3$	8.05 (est)	$(10.4,9.9)^{++}$	0.94
$CH_3C(OH)CH_2CH_2$	5.49 (est)	14.1	0.46

* Harrison et al. (1966)
** Lampe et al. (1957).
*** Turecek et al. (1990) No renormalization appears to be necessary.
$^{+}$ Set equal to CH_2=$C(CH_3)OCH_3$ experimental, as TOTIXC would predict them to be equal.
$^{++}$ Set equal to CH_3CH=$CHCH_2OH$ experimental; see note just above.
$^{+++}$ Set equal to ethyl-oxirane experimental, as above.

Phenyl

Phenyl was measured with respect to benzene. The cross-section for benzene predicted by Fitch and Sauter (1983) is 13.4, exactly that measured by Harrison et al. The ratio of cross-sections estimated by Fitch and Sauter was used, $\frac{Q_{C_6H_6}}{Q_{C_6H_5}} = \frac{13.4}{13.04} = 1.03$.

Mass 80

Benzene was the reference species. Mass 80 was assumed to be 1,3-c-C_6H_8. Cross-sections were estimated with TOTIXC.

Table E.20 Ionization potentials, ionization cross-sections and conversion factors for RICS calibration of mass 80.

Species	IP	Q	$f_{A\rightarrow B}$
2-c-$C_5H_5(CH_3)$	8.4	17.4	0.97
1-c-$C_5H_5(CH_3)$	8.4	17.4	0.97
1,2,trans-4-C_6H_8	8.32	15.7	1.02
2,3,5-C_6H_8	8.56	15.7	1.20
cis-CH_2=CHCH=CHCH=CH_2	8.31	15.6	1.03
trans-CH_2=CHCH=CHCH=CH_2	8.29	15.6	1.01
1,3-c-C_6H_8	8.3	15.9	1.00
1,3-c-$C_5H_5(CH_3)$	8.29-8.45	17.4	0.95
3-C_5H_6=CH_2	8.4	15.9	1.06
(E)-CH_2=C=CHCH=$CHCH_3$	8.32	15.7	1.02
CH_3CH=C=CHCH=CH_2	8.56	15.7	1.20

Mass 81

Benzene was the reference species. Mass 81 was assumed to be 3- or 4-c-C_6H_8. Cross-sections were estimated with TOTIXC.

Table E.21 Ionization potentials, ionization cross-sections and conversion factors for RICS calibration of mass 81.

Species	IP	Q	$f_{A\rightarrow B}$
3- or 4-c-C_6H_9	7.54,7.0est	16.6	1.00
$CH_3C{\equiv}CC(CH_3)_2$	6.97est	14.5	1.07
c-$C_5H_6(CH_3)$ [1-ene,2-CH_3]	5.8est	16.6	0.75
1,3-c-$C_4H_3(CH_3)_2$	6.4est	16.6	0.84
c-$C_3(CH_3)_3$	5.3est	16.6	0.69

Mass 82

Benzene was the reference species. Mass 82 was assumed to be c-C_6H_{10}. Cross-sections were estimated with TOTIXC, except where indicated otherwise.

Table E.22 Ionization potentials, ionization cross-sections and conversion factors for RICS calibration of mass 82.

Species	IP	Q	$f_{A\rightarrow B}$
CH_2=CHC(CH_3)=$CHCH_3$	8.37-8.46	16.7	0.74
CH_2=C(C_2H_5)CH=CH_2	8.81	16.7	0.82
CH_2=C(CH_3)CH_2CH=CH_2	9.16	16.7	0.91
CH_2=C(CH_3)CH=$CHCH_3$	8.45	16.7	0.74
(CH_3)$_2$C=CHCH=CH_2	8.26	16.7	0.71
CH_2=CHCH(CH_3)CH=CH_2	9.4	16.7	0.99
C_2H_5C(=CH_2)CH=CH_2	8.79	16.7	0.82
CH_2=C(CH_3)C(CH_3)=CH_2	8.54, 8.66	16.7	0.77
CH_2=C=C(CH_3)C_2H_5	8.74	16.8	0.80
CH_2=C=CHCH(CH_3)$_2$	9.06	16.8	0.88
(CH_3)$_2$C=C=$CHCH_3$	8.64	16.8	0.78
CH_2=C=$CHCH_2C_2H_5$	9	16.8	0.86
1,2-n-C_6H_{10}	9	16.8	0.86
1,3-n-C_6H_{10}	8.53	16.7	0.76
1,4-n-C_6H_{10}	8.98-9.04	16.7	0.87
1,5-n-C_6H_{10}	9.29	16.7	0.95
2,3-n-C_6H_{10}	8.76	16.8	0.80
2,4-n-C_6H_{10}	8.09-8.48	16.7	0.71
(CH_3)$_2$$CHCH_2$C≡CH	9.83	14.9	1.31
C_2H_5C≡CC_2H_5	9.34	14.9	1.09
C_3H_7C≡CCH_3	9.37, 9.97	14.9	1.23
CH_3CH_2CH(CH_3)C≡CH	9.79	14.9	1.29
(CH_3)$_2$CHC≡CCH_3	9.31	14.9	1.08
C_4H_9C≡CH	9.95, 10.52	14.9	1.57
HC≡CC(CH_3)$_3$	9.8-10.67	14.9	1.57
c-(C_3H_5)$_2$	8.80, 9.29	18.1	0.81
c-C_3H_5C(CH_3)=CH_2	8.66	17	0.77
c-C_3H(CH_3)$_3$	8.58	17	0.76
2-c-$C_4H_3O(CH_3)$	8.31	14.3	0.84
3-c-$C_4H_3O(CH_3)$	8.58	14.3	0.90
c-C_4H_6=$CHCH_3$	8.7	17	0.78
c-C_4H_7CH=CH_2	8.7	17	0.78
2-c-C_5H_6-1-one	8.47	13.8	0.90
3-c-C_5H_6-1-one	9.44(V)	13.8	1.22
c-C_5H_6O	8.38	14.3	0.85
c-C_5H_8=CH_2	7.2, 8.51-9.26	17	0.72
1-c-$C_5H_7CH_3$	9.12	17	0.89
3-c-$C_5H_7CH_3$	8.99	17	0.85
c-C_6H_{10}	8.85, 9.57	15.5*	1.00
bicyclo[3.1.0]hexane	9.16	18.1	0.84
bicyclo[2.2.0]hexane	9	18.1	0.80

Species	IP	Q	$f_{A\rightarrow B}$
bicyclo[2.1.1]hexane	9.7	18.1	1.02
spirohexane	9.66	18.1	1.01

* Harrison, et al.

Mass 83

Benzene was the reference species. Mass 83 was assumed to be c-C_6H_{11}. Cross-sections were estimated with TOTIXC.

Table E.23 Ionization potentials, ionization cross-sections and conversion factors for RICS calibration of mass 83.

Species	IP	Q	$f_{A\rightarrow B}$
c-C_6H_{11}	7.66	18.5	1.00
$CH_3CH{=}CHC(CH_3)_2$	6.62 (est)	17.4	0.87
$C_2H_5C(CH_3)CH{=}CH_2$	6.54 (est)	17.4	0.85
$(CH_3)_2CC(CH_3){=}CH_2$	6.86 (est)	17.4	0.91
$(CH_3)_2C{=}CHCO$	6.23 (est)	13.9	1.01
2-methyl,5-hydro-c-C_4H_3O	5.94 (est)	14.5	0.93
3-methyl,2-hydro-c-C_4H_3O	6.15 (est)	14.5	0.96
c-$C_3H_5C(CH_3)_2$	6.13 (est)	18.5	0.75
1,1-c-$C_3H_4(CH_3)$-CH_2CH_2	6.04 (est)	18.5	0.74
-$CHCH_3$	6.15 (est)	18.5	0.75
1,2-c-$C_4H_5(CH_3)_2$ H at CH3	6.21 (est)	18.5	0.76
H at H	6.30 (est)	18.5	0.77
c-$C_3H_2(CH_3)_3$ H at CH3	6.70 (est)	18.5	0.73
H at H	6.79 (est)	18.5	0.84
1-c-$C_5H_8CH_3$	6.45 (est)	18.5	0.79
2-c-$C_5H_8CH_3$	6.88 (est)	18.5	0.85

Mass 84

Benzene was the reference species. Mass 84 was assumed to be c-C_6H_{12}. Cross-sections were estimated with TOTIXC, except where indicated otherwise.

Table E.24 Ionization potentials, ionization cross-sections and conversion factors for RICS calibration of mass 84.

Species	IP	Q	$f_{A\rightarrow B}$
1-C_6H_{12}	9.33	17.7	0.72
2-C_6H_{12}	8.88-9.16	17.7	0.65
3-C_6H_{12}	8.83-9.12	17.7	0.64
$C_2H_5CH_2C(CH_3){=}CH_2$	9.08	17.7	0.67
$C_2H_5CH(CH_3)CH{=}CH_2$	9.44	17.7	0.75
$CH_3CH{=}C(CH_3)C_2H_5$	8.58	17.7	0.57
$(C_2H_5)_2C{=}CH_2$	9.06,9.21	17.7	0.68

Species	IP	Q	$f_{A\rightarrow B}$
$(CH_3)_2C=C(CH_3)_2$	8.3	17.7	0.53
$(CH_3)_2CHC(CH_3)=CH_2$	9.07	17.7	0.66
$(CH_3)_2CHCH=CHCH_3$	8.98	17.7	0.64
$(CH_3)_2CHCH_2CH=CH_2$	9.45	17.7	0.75
$(CH_3)_3CCH=CH_2$	9.62	17.7	0.80
$(CH_3)_4C=C$ **	9.07	17.7	0.66
$CH_2=C(OCH_3)CH=CH_2$	8.43	15.0	0.65
$CH_3OCH=CHCH=CH_2$	8.03	15.0	0.59
$CH_3CH=C(CH_3)CHO$	9.6	14.3	0.98
$CH_2=C(CH_3)C(=O)CH_3$	9.5	14.6	0.93
$CH_3CH_2CH=CHCHO$	9.7	14.3	1.02
$C_2H_5COCH=CH_2$	9.5	14.6	0.93
$CH_3CH=CHC(=O)CH_3$	9.39	14.6	0.89
$HC\equiv CC(CH_3)_2OH$	10.18(V)	13.1	1.38
$HC\equiv CCH_2CH(OH)CH_3$	10.24(V)	13.1	1.42
1-c-$C_3H_5(COCH_3)$	9.48(V)	14.5	0.93
1,2,2-c-$C_3H_3(CH_3)_3$	8.9	17.9***	0.62
2-c-C_5H_7OH	9.6	15.2	0.93
c-$C_5H_8=O$	9.26	14.5	0.86
c-C_5H_8O	8.34	15.4	0.62
c-$C_5H_9CH_3$	10.45	17.7	1.17
c-C_6H_{12}	9.83,10.50	17.9*	1.00

* Harrison et al. (1966)
** Assumed to be $(CH_3)_2C=C(CH_3)_2$.
*** Set equal to c-C_6H_{12}, as TOTIXC would predict them to be the same.

Mass 85

Benzene was the reference species. Mass 85 was assumed to be 1-C_6H_{13}. Cross-sections were estimated with TOTIXC.

Table E.25 Ionization potentials, ionization cross-sections and conversion factors for RICS calibration of mass 85.

Species	IP	Q	$f_{A\rightarrow B}$
1-C_6H_{13}	7.92	19.2	1.00
2-C_6H_{13}	7.38	19.2	0.90
n-$C_3H_7C(CH_3)_2$	6.82	19.2	0.76
$(CH_3)_2CHC(CH_3)_2$	6.49 (est)	19.2	0.65
$(C_2H_5)_2(CH_3)C$	6.51 (est)	19.2	0.65
$CH_3C(OH)=C(CH_2)CH_3$	6.07 (est)	15.6	0.72
$CH_3CH=CHC(OH)CH_3$	5.85 (est)	15.6	0.69
c-$C_3H_5C(OH)CH_3$	5.67 (est)	16.6	0.62
1-c-C_5H_8OH	5.99 (est)	16.6	0.66
2-c-C_5H_9O	6.10 (est)	16.3	0.69
2-c-C_4H_6O-CH_3- 2-yl	5.73 (est)	16.3	0.64
2-c-C_4H_6O-CH_3-3-yl	6.07 (est)	16.3	0.69

Mass 86

Benzene was the reference species. Mass 86 was assumed to be n-C_6H_{14}. Cross-sections were estimated with TOTIXC, except where indicated otherwise.

Table E.26 Ionization potentials, ionization cross-sections and conversion factors for RICS calibration of mass 86.

Species	IP	Q	$f_{A \to B}$
n-C_6H_{14}	10.18	20.8*	1.00
i-C_6H_{14}	10.12	20.8**	0.98
$(C_2H_5)_2CHCH_3$	10.08	20.8**	0.97
$C_2H_5C(CH_3)_2$	10.06	20.8**	0.96
$(CH_3)_2CHCH(CH_3)_2$	10.02	20.8**	0.95
$(CH_3)_3CCH_2CH_3$	10.06	20.8**	0.96
n-C_4H_9CHO	9.72,9.90	15	1.24
i-C_4H_9CHO	9.71	15	1.21
s-C_4H_9CHO	9.59	15	1.17
t-C_4H_9CHO	9.5	15	1.14
n-$C_3H_7COCH_3$	9.37-10.7	15	1.33
i-$C_3H_7COCH_3$	9.3	15	1.09
$(C_2H_5)_2CO$	9.37	15.2	1.09
CH_2=$CHOCH(CH_3)_2$	8.9	16.1	0.92
CH_2=$CHC(CH_3)_2OH$	9.90(V)	15.9	1.20
CH_2=$CHCH_2CH_2CH_2OH$	9.42	15.9	1.06
CH_2=$CHCH_2CH(OH)CH_3$	9.38	15.9	1.05
CH_2=$CHCH(OH)CH_2CH_3$	9.4	15.9	1.05
CH_3CH=$CHCH(OH)CH_3$	9.56(V)	15.9	1.10
CH_2=$C(CH_3)CH(OH)CH_3$	9.61(V)	15.9	1.11
c-C_5H_9OH	9.58	17	1.03
c-$(CH_2)_5O$	9.7	17	1.06

* Harrison et al. (1966).

** Set equal to n-C_6H_{14}, since TOTIXC would set the two equal.

Masses 91-93

Benzene and phenol were the reference species, and masses 91-93 were assumed to be $C_6H_5CH_2$, $C_6H_5CH_2$ and C_6H_5O respectively. Fitch and Sauter (1983) was used to compute cross sections for all species.

Table E.27 Ionization cross-sections for RICS calibration of mass 91-93 species .

Species	Q	Q_{C6H6}/Q_i	Q_{C6H5OH}/Q_i
mass 91	15.6	0.86	0.92
mass 92	16.1	0.83	0.90
mass 93	13.9	0.96	1.04
C_6H_5OH	14.4	----------	----------
C_6H_6	13.4	----------	----------

Mass 94

Mass 94, assumed to be phenol, was measured with benzene as a reference. No conversion factors were computed. Fitch and Sauter was used to estimate Q_{C6H6}, and TOTIXC was used for Q_{C6H5OH}. The RICS calibration factor was 0.96 (13.4/14.0).

Mass 95, 96 and 110

Benzene and phenol were the reference species, and the species were assumed to be C_6H_6OH, C_6H_7OH and $C_6H_4(OH)_2$, respectively. Although the signals of the first two were ultimately deemed to be due to isotopes of phenol (C_6H_4DOH and C_6H_5OD for mass 95, and $C_6H_3D_2OH$ and C_6H_4DOD for mass 96), RICS calibration was needed for those determinations. Fitch and Sauter (1983) was used to compute cross sections for all species.

Table E.28 Ionization cross-sections for RICS calibration of masses 95, 96 and 110.

Species	Q	Q_{C6H6}/Q_i	Q_{C6H5OH}/Q_i
mass 95	15.0	0.89	0.96
mass 96	15.5	0.86	0.93
mass 110	15.6	0.86	0.92
C_6H_5OH	14.4	----------	----------
C_6H_6	13.4	----------	----------

Appendix F. Purities of Liquid and Gaseous Fuels.

Chemical	Grade	Min. Purity†	Supplier	Comments
Ar	prepurified	99.998%	Middlesex	
CH_4	1.3	98.0%	Middlesex	
C_2H_2	prepurified	99.6%	Granite State‡	
C_2H_4	C.P.	99.5%	Matheson	
C_4H_6	C.P.	99.0%	Matheson	
C_6H_6	Resi-Analyzed	99.8%	Doe & Ingalls	J.T. Baker brand. Residue after evap. - 5 ppm
CO	C.P.	99.5%	Granite State	
CO_2	technical (2.0)	99.0%	Granite State	
H_2	prepurified	99.995%	Middlesex	
He	high purity	99.997%	Granite State	
O_2	extra dry	99.8%	Granite State	

†Supplier's specification.
‡Also known as US Airgas, and Northeast Airgas.

Appendix G. Thermocouple Coating Technique.

Improvements to thermocouple coating technique of Kent (1970): post-flame zone data.

The following was published as a Brief Communication in *Combustion and Flame*, **85**, 282 (1991). One minor correction has been made to that version: the temperature labels in Figure 1 were in error in the original source, Bittner (1981), and have been corrected.

The data shown in the article were taken in the post-flame zone of the flames cited, as that was originally considered to be the region of greatest susceptibility to catalytic effects: high temperature, H, O and OH. That was also the location whether Bittner performed tests for catalytic activity. Further research showed that greater activity was found in the reaction zone, as will be discussed in the section following this one.

Noncatalytic Thermocouple Coating for Low-Pressure Flames

R. A. SHANDROSS, J. P. LONGWELL, AND J. B. HOWARD*

Chemical Engineering Department, Massachusetts Institute of Technology, Cambridge, MA 02139

Ceramic-coated platinum- and iridium-rhodium thermocouples exhibit little catalytic heating in atmospheric-pressure flames [1,2], but can drift as much as 350 K in high temperature regions of stoichiometric low-pressure (20-30 torr) flat flames [2,3]. Figure 1 shows a typical

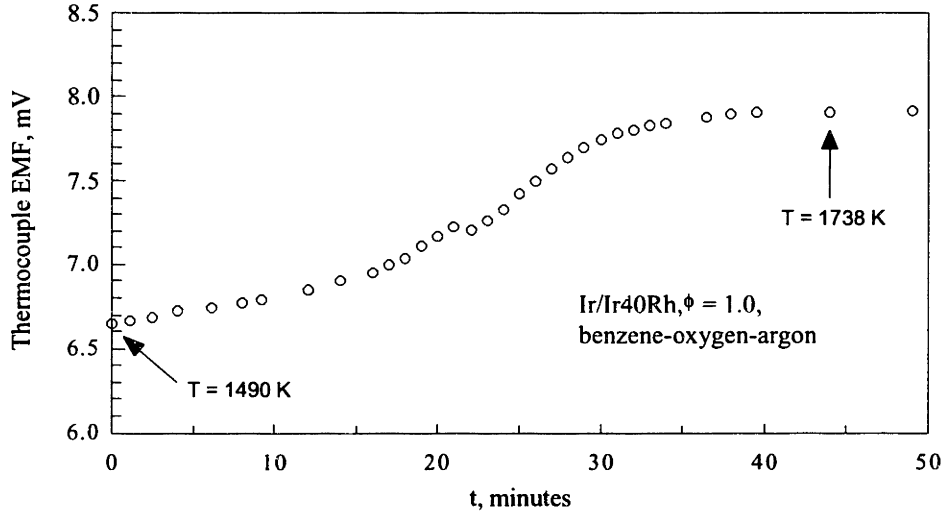

Fig. 1. Catalytic heating in 20-torr stoichiometric benzene-oxygen-Ar flame. Ir/Ir40Rh thermocouple. After Bittner [2].

drift curve for a 20 torr flame. Catalytic heating is less in rich flames — on the order of 60 K [2] — with their lower radical concentration. From an order-of-magnitude analysis, Bittner [2] hypothesized that the observed behavior is caused by a temperature-dependent property of the coating or metal, such as type, size, or number of grain boundaries, pores, cracks, and microfissures.

The coating method generally used for atmospheric-pressure flames is that of Kent, which uses the BeO-Y_2O_3 ceramic system [1]. We have developed a modification to the Kent procedure that significantly reduces the amount of catalytic heating in low-pressure flames.

To lower the probability of pore formation, the coating is heated electrically rather than in a flame. The coating is thus not exposed to H_2O, which reacts with BeO to form volatile $Be(OH)_2$ [4]. Heating is controlled so that the solvent evaporates slowly instead of boiling off. Because there is no oxidation, Y_2O_3 is used in place of YCl_3. Ethylene glycol is added to the solvent to increase viscosity and wetting ability [5].

To reduce phase-transition-related changes, 4.5 wt% BeO is used. No liquid phase is present at firing or measurement temperatures, lessening the amount of secondary crystallization. The ceramic is sintered below the phase-change temperature, rather than fused above it, so no phase transition occurs in coating[49]. To reduce fractures from elevated pressure of trapped gas, and to increase densification [7], the process is done at low pressures (150 torr in this work).

Because changes in the calibration curve used in the radiation compensation method [8] occur early in flame usage, the thermocouple was preconditioned in an atmospneric-pressure flame. In normal usage one should precondition the thermocouple in the flame being measured.

The wire should be cleaned thoroughly before coating. We washed the bare thermocouple wire five times with HCl, distilled water, and methylene chloride. A problem encountered because of the small-diameter wire is beading of the coating solution, resulting in periodic thin spots. To prevent this, the wire was coated by pulling it through a drop of coating solution suspended from an eyedropper [5].

Thermocouples were constructed and tested in 20 ± 2 torr hydrogen and acetylene flames. For simplicity and comparison with previous tests, temperature drift measurements were made without radiation compensation heating. If radiation compensation heating is used, coupling between electrical and catalytic heating causes an error greater than unheated thermocouple drift. For example, for a point in the post-flame zone of a stoichiometric benzene flame [2], we

[49] However, the phase transition temperature is only about 1725 K [6].)

estimate the amount of such error to be about twice the drift of an unheated thermocouple.

In H_2-O_2-Ar flames ($\phi \approx 0.6$, 1.0, and 1.8), ≤ 20 K of temperature drift was generally found, regardless of equivalence ratio. At the hottest positions, temperature *decreases* of the same magnitude were seen. Figure 2 shows typical drift curves for hydrogen at several equivalence ratios.

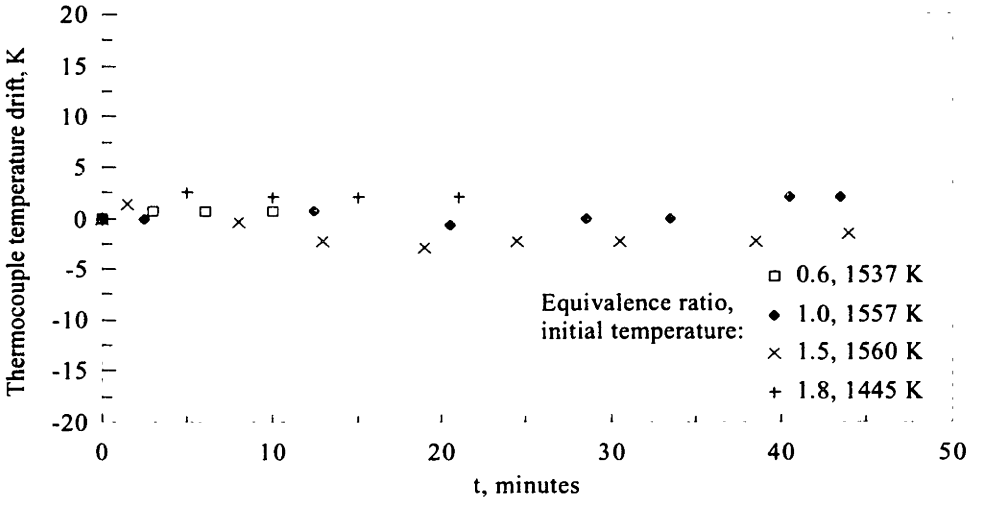

Fig. 2. Typical H_2 drift curves, Pt/Pt13Rh thermocouples constructed by new method.

In C_2H_2-O_2-Ar flames, ≤ 30 K of catalytic heating was generally found in rich and lean conditions ($\phi \approx 0.8$ and 1.5). Under very rich conditions, $\phi \approx 1.8$, only temperature decreases were found. Several minutes exposure to leaner conditions restored the original temperature. At

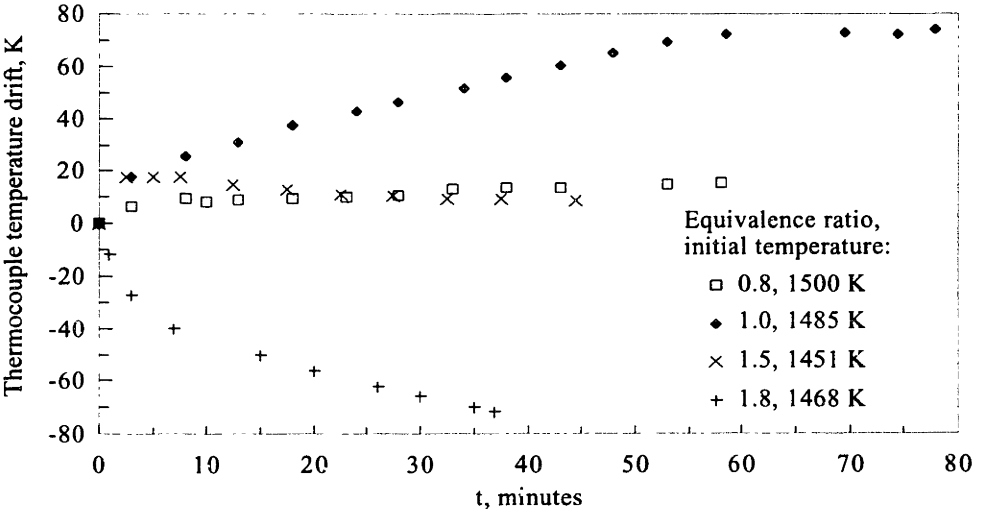

Fig. 3. Typical C_2H_2 drift curves, Pt/Pt13Rh thermocouples constructed by new method.

$\phi \approx 1.5$, rapid temperature rise was seen, followed by a slow decline. Drift curves for acetylene are given in Figure 3.

In stoichiometric acetylene, the thermocouple could also be brought back to the original temperature, by exposure to leaner conditions. A steady temperature was reached after 2 h, the overall drift being about 115 K, one third that seen by Bittner [2] in his stoichiometric hydrocarbon flame.

Two processes might explain the existence of a temperature drop: emissivity changes[50] and pore or microfissure "healing." In very rich hydrocarbon flames accurate measurements can probably be made by (a) recovering the original emissivity at leaner conditions before each measurement, or (b) allowing the thermocouple to reach a steady reading — if one occurs — at flame conditions before calibration. In either case, radiation compensation heating is not recommended. Further study at these conditions is warranted.

In summary, we have achieved significant reductions in catalytic heating of BeO-Y_2O_3-coated thermocouples by changing the ceramic composition and the coating methodology. This supports Bittner's picture that the amount of catalysis is dependent upon properties of the coating.

We are grateful to the Division of Chemical Sciences, Office of Basic Energy Sciences, Office of Energy Research, U.S. Department of Energy, for financial support under Grant No. DE-FG02-84ER13282.

REFERENCES

1. Kent, J. H., *Combust. Flame* 14:279-281 (1970).
2. Bittner, J. D., Ph.D. thesis, Department of Chemical Engineering, MIT, 1981.
3. Caddell, J. P., B.S. thesis, Department of Chemical Engineering, MIT, 1984.
4. Metal and Ceramics Information Center, Battelle, *Engineering Property Data on Selected Ceramics. Volume III, Single Oxides*, Battelle Columbus Laboratories, Columbus, 1981, p. 5.4.2-20.
5. Keselica, D. S., Final UROP Project Report, Department of Chemical Engineering, MIT, 1982.

[50] In particular for rich hydrocarbon flames. Switching to leaner conditions probably restores the original emissivity; hence the temperature reading. For the stoichiometric flame, temperature recovery is probably due to lessening of catalytic heating at lower ϕ.

6. Levin, E. M., Robbins, C. R., and McMurdie, H. F., in *Phase Diagrams for Ceramists* (M. K. Reser, Ed.), The American Ceramic Society, Westville, 1964, vol. I, p. 100.
7. Kingery, W. D., *Introduction to Ceramics*, Wiley, New York, 1960, p. 393.
8. Schmidt, H., *Annal. Phys.* 29:971-1028 (1909).

After the data reported in the above article were taken, measurements were made in the post-flame zone of C_6H_6-O_2-Ar flames for direct comparison with the Bittner experiments. For equivalence ratios from 0.4 to 1.2, in increments of 0.1, the drift was always less than 20 K over periods of 8-15 minutes. In most cases, including $\phi = 1.0$, the temperature peaked after a few minutes and dropped slightly thereafter. The temperature rise in the case documented in Figure 1 of the article was 52 K in 15 minutes.

Data taken in reaction zones.

A greater amount of catalytic heating was observed in reaction zones than the post-flame zones. Because of this observation, additional tests were performed in the reaction zones of several flames. Except for a lean C_2H_2+H_2 flame where the coating performed very poorly, the new

Table G.1 Reaction zone thermocouple drift experiments with revised coating technique.

Flame	ϕ	% Ar	T drift (K)	t (min)	Initial T_u (K)	Comments
H_2	1.0	0	90	55	1479	
C_2H_2	0.31	?	none	3	1288	Slight drop in T
C_2H_2	0.58	?	77	5	1538	Peaked at 77 K, then dropped over 10 min. more
C_2H_2	1.0	0	120	2	1596	Peaked at 120 K, then dropped over 14 min. more
C_2H_2	1.0	0	261	12	1405	End of reaction zone. Peaked at 261 K, then dropped over 14 min. more
C_2H_2 (ϕ=0.35) + H_2 (ϕ=0.28)	0.63	21	452	< 10	1366	T dropped after maximum
C_2H_2 (ϕ=0.35) + H_2 (ϕ=0.28)	0.63	21	483	~2	~1432	T dropped after maximum

method resulted in drifts equal to or less than the postflame zone data of Bittner, as can be seen from the data in Table G.1, below. The self-healing observed in post-flame zone experiments seems to be an important factor in the improved behavior.

Practical aspects of the thermocouple coating technique.

Mixing of coating liquid. No heating was performed in the mixing process. The ceramic powders used were allowed to unclump over time — hours or days — and with manual mixing with a paintbrush. The suspension ultimately formed would rapidly settle out, so mixing immediately before use was necessary.

Avoidance of boiling. Ethylene glycol has a boiling point of 198°C at one atmosphere, but only 142°C at 100 torr and 178°C at 400 torr (CRC, 1985, p. D-197). That of water also drops with pressure, but more gradually, being approximately 60°C at 150 mm (CRC, 1985, p. D-190). The presence of HCl and dissolved solids slightly raises the boiling point of water. To minimize boiling of the solvents:

1. The vacuum chamber was evacuated gradually, so as to effect an initial evaporation of the aqueous portion of the solvent.

2. The thermocouple temperature was then ramped up to about 50°C, and held at that temperature for a short while.

3. It was then ramped up again to 160°C, such that the time between the two temperatures was about 3.5 minutes. The temperature was held at 160°C for another 3.5 minutes, then gradually increased to the next level.

Protection of the junction wire. A great deal of experimentation (and patience) was necessary to develop a method of heating and cooling the thermocouples that would not result in segmentation of the platinum side, or breakage of the wire entirely. Wire segmentation has been noted in the literature. Anderson (1972) observed a "bamboo" structure on heating a platinum wire for 18 hours at 1673 K in air. He attributed this to the formation of large crystals, and points out how the crystals can slip along the grain boundaries. This is in accord with the offsetting of segments seen here in thermocouples, especially those which broke in the coating process. Zysk (1963) reported grains as long as 1 cm and the full diameter of a 0.5 mm diameter wire after only 15 minutes heating at 1723 K.

Annealing of platinum/platinum-rhodium thermocouples is a standard procedure for high

accuracy work (Zysk, 1963; Bedford, 1972), but it should also be useful for relieving strain due to cold working of the metal in handling. Bedford (1972) recommended a cold working anneal at 1673 K. For high accuracy purposes he also specified a second annealing at 1273 K after the thermocouple is sheathed (if applicable) and a long anneal at 723 K. According to Zysk, others recommend high-temperature annealing at temperatures ranging from 1373-1723 K, for various amounts of time from two minutes to an hour. Berry (1972) also discusses an anneal at 773 K, to reduce the effects of rapid thermocouple quenching.

Based on the above and empirical results, an annealing procedure was developed for the coating process. A large reduction in thermcouple failures due to "bamboo structure" was achieved with this method. Because it was developed with an eye towards usability rather than efficiency, it is possible that not every step in the following procedure is necessary to get good results.

1. After cleaning, but before coating, the thermcouple was annealed for about 10 minutes at 1470 K, with the junction wire slack.

2. The junction wire was then made taut, and a second annealing performed at 1635 K.

3. Every time the thermcouple was ramped down from high temperatures, it was kept at 775 K for several minutes, to offset any strain which might have been introduced in quenching.

Other procedures. The beads formed at the connection of the junction and support wires, as well as a few millimeters of support wire, were coated to reduce catalytic activity on the supports and concomitant conduction to the junction wire. Sintering of the ceramic coating was performed at 1685 K. The first coat was sintered for three minutes, and the second through fourth coats for four minutes. The intention of this practice was to allow approximately the same amount of sintering time for all of the coats, allowing for the fact that the second and later coats were heated through one or more layers of coating. The fifth and later coats were sintered for at least five, and up to ten, minutes, so that the later coats were not significantly "fresher" than the first several.

Appendix H. Temperature and Mole Fraction Data Points.

Note: "HAB" = height above burner.

Table H.1 Raw temperature data; raw H atom and H_2 data with respect to argon.

HAB (mm)	T (K)*	HAB (mm)	x_H/x_{Ar}	HAB (mm)	x_{H2}/x_{Ar}
0.70	476	1.03	2.234E-03	-0.18	8.300E-01
1.10	608	1.48	2.364E-03	0.23	8.203E-01
1.40	705	2.08	2.999E-03	0.58	7.800E-01
1.50	804	2.53	4.777E-03	1.08	7.327E-01
1.70	834	3.03	5.898E-03	1.53	6.793E-01
1.90	942	3.53	8.148E-03	1.98	6.949E-01
1.90	972	3.78	8.846E-03	2.53	6.346E-01
2.05	1009	4.63	1.308E-02	3.03	6.165E-01
2.15	1038	5.03	1.485E-02	3.53	5.758E-01
2.20	1092	5.53	1.837E-02	4.03	5.936E-01
2.30	1111	5.93	2.047E-02	4.53	5.561E-01
2.40	1174	6.63	2.369E-02	5.03	5.386E-01
2.60	1258	6.98	2.536E-02	5.53	5.370E-01
2.80	1308	7.03	2.720E-02	6.03	5.340E-01
2.90	1352	7.53	2.924E-02	6.58	5.438E-01
3.00	1409	7.98	3.315E-02	6.98	4.880E-01
3.15	1444	8.63	3.526E-02	7.53	5.210E-01
3.40	1505	9.07	3.660E-02	8.03	4.937E-01
3.45	1552	9.57	3.968E-02	8.53	5.206E-01
3.70	1613	10.03	3.797E-02	28.53	5.423E-03
3.90	1605	10.63	4.256E-02		
4.40	1688	10.98	4.285E-02		
5.00	1762	28.53	2.921E-02		
6.00	1844				
9.00	1937				
10.15	1938				
11.40	1935				
12.45	1925				
12.85	1923				
30.35	1642				

* Thermocouple emissivity: 0.54 (average, using optical pyrometry).
Diameter of coated thermocouple: 7.88×10^{-3} cm (500x light microscope).

Table H.2 Raw CH_3, CH_4 and OH data, with respect to argon.

HAB (mm)	x_{CH3}/x_{Ar}	HAB (mm)	x_{CH4}/x_{Ar}	HAB (mm)	x_{OH}/x_{Ar}
1.03	1.777E-04	1.03	4.394E-03	1.03	1.633E-04
1.03	1.932E-04	1.03	4.220E-03	2.03	1.735E-04
2.03	2.732E-04	2.03	4.651E-03	2.53	4.358E-04
2.88	4.272E-04	2.88	5.108E-03	3.18	5.215E-04
3.18	5.360E-04	3.18	5.560E-03	3.53	5.392E-04
4.03	6.157E-04	4.03	6.183E-03	4.08	1.044E-03
4.08	6.453E-04	4.08	6.126E-03	4.48	1.316E-03
5.08	6.502E-04	5.08	5.828E-03	5.08	1.587E-03
6.03	4.901E-04	6.03	4.728E-03	5.43	1.655E-03
8.03	1.029E-04	8.03	8.128E-04	6.08	2.285E-03
8.03	8.903E-05	8.03	1.245E-03	6.48	2.312E-03
10.98	-3.879E-05	10.98	3.718E-04	7.08	2.555E-03
28.53	0.000E+00	28.53	9.122E-05	8.03	2.662E-03
				9.03	2.894E-03
				9.43	2.555E-03
				9.98	2.485E-03
				10.98	2.534E-03
				28.53	8.010E-04

Table H.3 Raw H_2O, C_2H_2 and C_2H_4 data, with respect to argon.

HAB (mm)	x_{H2O}/x_{Ar}	HAB (mm)	x_{C2H2}/x_{Ar}	HAB (mm)	x_{C2H4}/x_{Ar}
1.13	1.840E-01	1.03	2.57E-04	1.03	2.067E-03
1.53	2.100E-01	2.03	4.12E-04	1.03	2.088E-03
1.93	2.299E-01	3.08	5.35E-04	2.03	1.544E-03
2.53	2.864E-01	3.53	6.44E-04	2.03	1.594E-03
3.03	3.135E-01	4.03	7.25E-04	2.58	9.763E-04
3.53	3.669E-01	4.98	8.00E-04	3.03	2.841E-03
3.93	4.147E-01	5.98	7.99E-04	3.03	2.859E-03
4.53	4.782E-01	6.53	8.17E-04	4.03	1.679E-03
4.93	5.104E-01	7.03	8.67E-04	4.03	1.789E-03
5.63	5.843E-01	8.03	7.21E-04	4.63	1.438E-03
6.03	6.262E-01	9.03	5.54E-04	5.03	1.102E-03
6.68	6.740E-01	10.03	3.78E-04	5.03	9.559E-04
6.98	7.045E-01	10.98	3.46E-04	6.03	1.288E-03
7.53	7.553E-01	28.53	8.82E-05	6.03	1.050E-03
7.93	8.056E-01			6.53	6.099E-04
8.53	8.434E-01			6.98	1.015E-03
9.03	8.527E-01			6.98	7.987E-04
9.53	9.042E-01			8.03	1.023E-04
9.98	8.588E-01			8.03	7.906E-05
10.48	9.242E-01			8.53	6.406E-05
11.03	8.733E-01			9.03	9.649E-06
28.53	8.648E-01			9.03	1.256E-05
				11.03	8.140E-05

HAB (mm)	x_{H2O}/x_{Ar}	HAB (mm)	x_{C2H2}/x_{Ar}	HAB (mm)	x_{C2H4}/x_{Ar}
				11.03	1.060E-04
				28.53	4.751E-04
				28.53	3.655E-04
				28.53	8.466E-05
				28.53	6.512E-05

Table H.4 Raw CO data, with respect to argon.

HAB (mm)	x_{CO}/x_{Ar}-11/7/91	HAB (mm)	x_{CO}/x_{Ar}-8/23/91	HAB (mm)	x_{CO}/x_{Ar}-5/11/93
0.18	2.571E-02	0.23	3.766E-02	1.03	2.130E-02
0.53	3.003E-02	0.58	4.494E-02	2.03	4.656E-02
1.03	3.372E-02	1.03	4.881E-02	3.03	4.120E-02
1.53	3.938E-02	1.53	5.599E-02	4.03	6.483E-02
2.03	4.344E-02	2.53	6.836E-02	5.03	1.033E-01
2.53	4.604E-02	3.53	8.409E-02	6.03	1.027E-01
3.08	5.165E-02	4.78	9.557E-02	6.98	1.040E-01
3.53	5.633E-02	5.98	8.713E-02	8.03	1.072E-01
4.08	5.940E-02	7.33	9.022E-02	9.03	1.348E-01
4.48	6.295E-02	8.57	8.792E-02	10.03	1.127E-01
5.03	6.624E-02	9.82	8.171E-02	11.03	1.167E-01
5.53	6.983E-02	11.08	8.191E-02		
6.08	7.062E-02	14.83	8.096E-02		
6.48	6.976E-02	18.28	7.364E-02		
7.08	7.081E-02	22.03	7.777E-02		
7.53	7.049E-02	25.63	7.093E-02		
8.13	7.174E-02	29.23	6.962E-02		
8.53	7.023E-02	32.88	6.963E-02		
28.53	6.195E-02				

Table H.5 Raw CO, H_2CO and O_2 data, with respect to argon.

HAB (mm)	x_{CO}/x_{Ar}-6/17/93	HAB (mm)	x_{H2CO}/x_{Ar}	HAB (mm)	x_{O2}/x_{Ar}-11/10/91
1.48	5.076E-02	2.58	8.142E-04	0.18	4.009E-01
2.58	4.820E-02	2.58	8.317E-04	0.58	3.936E-01
4.63	7.201E-02	4.63	8.792E-04	0.98	3.789E-01
5.58	8.430E-02	4.63	7.877E-04	1.53	3.551E-01
6.53	8.724E-02	6.53	2.384E-04	2.03	3.412E-01
8.53	9.228E-02	6.53	2.991E-04	2.53	3.142E-01
11.03	9.404E-02	8.53	6.123E-05	3.03	2.921E-01
28.53	7.287E-02	8.53	8.050E-05	3.53	2.557E-01
		11.03	1.066E-04	4.03	2.314E-01
		11.03	1.413E-04	4.48	1.738E-01
				5.08	1.517E-01
				5.58	1.256E-01
				6.03	1.063E-01
				6.58	8.373E-02
				7.08	6.188E-02
				7.58	4.874E-02
				8.03	3.824E-02
				8.48	3.162E-02
				28.53	0.000E+00

Table H.6 Raw O_2, mass 42 and CO_2 data, with respect to argon.

HAB (mm)	x_{O2}/x_{Ar}-7/19/93	HAB (mm)	x_{42}/x_{Ar} (as C_3H_6)	HAB (mm)	x_{CO2}/x_{Ar}
1.08	4.546E-01	1.03	5.569E-04	1.03	3.101E-03
1.83	4.232E-01	2.53	7.120E-04	2.13	3.595E-03
2.53	3.923E-01	4.03	2.874E-04	3.03	4.296E-03
3.53	3.131E-01	6.53	4.873E-05	3.88	6.224E-03
4.63	2.504E-01	8.57	1.296E-05	4.63	7.395E-03
5.63	1.806E-01			5.03	1.036E-02
6.48	1.338E-01			5.68	9.460E-03
7.58	6.754E-02			5.98	1.112E-02
8.63	3.950E-02			7.03	1.177E-02
9.57	2.164E-02			7.98	1.253E-02
10.53	1.607E-02			9.03	1.426E-02
				9.98	1.524E-02
				11.03	1.696E-02
				11.63	1.854E-02
				12.13	1.565E-02
				28.53	2.917E-02

Table H.7 Raw mass 44 (low electron energy), mass 53 and mass 54 data, with respect to argon.

HAB (mm)	x_{44low}/x_{Ar} (as CH_3CHO)	HAB (mm)	x_{53}/x_{Ar} (as CH_2=CCH=CH_2)	HAB (mm)	x_{54}/x_{Ar} (as 1,3-C_4H_6)
1.03	1.090E-04	1.03	2.919E-06	1.03	3.043E-05
2.13	8.056E-05	2.98	4.870E-06	2.98	5.113E-05
2.13	1.113E-04	5.03	3.631E-06	5.03	2.476E-05
2.48	1.890E-04	7.13	9.135E-08	7.13	9.862E-06
3.03	1.847E-04				
3.88	5.207E-05				
4.63	3.305E-05				

Table H.8 Raw mass 55-57 data, with respect to argon.

HAB (mm)	x_{55}/x_{Ar} (as CH3CH=$CHCH_2$)	HAB (mm)	x_{56}/x_{Ar} (as CH_3CH=$CHCH_3$)	HAB (mm)	x_{57}/x_{Ar} (as s-C_4H_9)
1.03	6.803E-06	1.03	5.553E-05	1.03	2.261E-05
2.98	1.168E-05	2.98	7.904E-05	2.98	2.269E-05
5.03	3.545E-06	5.03	2.034E-05	5.03	2.145E-06
7.13	0.000E+00	7.13	2.724E-06	7.13	3.214E-07

Table H.9 Raw mass 58, mass 59 and mass 59 (low electon energy) data, with respect to argon.

HAB (mm)	x_{58}/x_{Ar} (as n-C_4H_{10})	HAB (mm)	x_{59low}/x_{Ar} (as C_2H_5CHOH)	HAB (mm)	x_{59}/x_{Ar} (as n,i-C_3H_7O)
1.03	3.250E-05	1.03	4.717E-07	1.03	6.617E-06
2.98	3.534E-05			2.98	2.543E-06
5.03	1.029E-05			5.03	0.000E+00
7.13	0.000E+00			7.13	0.000E+00

Table H.10 Raw mass 60, mass 65 and mass 66 data, with respect to argon.

HAB (mm)	x_{60}/x_{Ar} (as n-C_3H_7O)	HAB (mm)	x_{65}/x_{Ar} (as c-C_5H_5)	HAB (mm)	x_{66}/x_{Ar} (as c-C_5H_6)
1.03	3.790E-06	1.38	-6.864E-07	1.53	1.434E-05
2.98	4.773E-06	3.48	2.370E-06	2.58	1.482E-05
5.03	1.716E-06	5.53	1.712E-06	3.53	1.587E-05
7.13	-2.111E-06	6.53	7.234E-07	4.03	1.724E-05
		7.03	9.340E-07	4.53	2.668E-05
		7.43	4.213E-06	5.13	1.648E-05
		8.03	4.691E-06	5.53	1.547E-05
		8.53	3.071E-06	6.53	1.318E-05
		9.07	1.718E-06	7.03	7.732E-06

HAB (mm)	x_{60}/x_{Ar} (as n-C_3H_7O)	HAB (mm)	x_{65}/x_{Ar} (as c-C_5H_5)	HAB (mm)	x_{66}/x_{Ar} (as c-C_5H_6)
		9.53	7.685E-07	7.53	8.413E-06
		10.53	5.496E-07	8.03	7.425E-06
				8.53	5.100E-06
				9.07	2.098E-06
				9.53	7.434E-07
				10.53	1.503E-06

Table H.11 Raw mass 68-70 data, with respect to argon.

HAB (mm)	x_{68}/x_{Ar} (as c-C_5H_8)	HAB (mm)	x_{69}/x_{Ar} (as c-C_5H_9)	HAB (mm)	x_{70}/x_{Ar} (as c-C_5H_{10})
1.03	3.241E-05	1.03	9.356E-06	1.03	3.018E-05
3.03	4.740E-05	3.03	5.665E-06	3.03	3.107E-05
5.03	1.343E-05	5.03	-4.616E-07	5.03	3.820E-06

Table H.12 Raw mass 71, mass 72 and C_6H_5 data, with respect to argon.

HAB (mm)	x_{71}/x_{Ar} (as n-C_5H_{11})	HAB (mm)	x_{72}/x_{Ar} (as n-C_5H_{12})	HAB (mm)	x_{C6H5}/x_{Ar}
1.03	4.795E-06	1.03	6.201E-06	1.53	8.795E-06
3.03	1.115E-05	3.03	-1.732E-06	1.68	3.798E-05
5.03	-1.486E-07	5.03	3.794E-07	1.83	4.444E-07
				2.08	1.943E-05
				2.53	8.879E-06
				3.03	1.555E-05
				3.83	6.415E-06
				4.38	8.306E-06
				4.48	4.870E-06
				4.83	-1.676E-05
				5.53	1.120E-05
				6.03	1.478E-07
				6.18	3.925E-06
				7.13	-9.412E-07
				8.07	-2.083E-06

Table H.13 Raw C_6H_6, mass 80 and mass 81 data, with respect to argon.

HAB (mm)	x_{C6H6}/x_{Ar}	HAB (mm)	x_{80}/x_{Ar} (as 1,3-c-C_6H_8)	HAB (mm)	x_{81}/x_{Ar} (as 3- or 4-c-C_6H_9)
1.23	9.400E-03	1.03	5.766E-05	1.03	9.428E-06
1.48	9.246E-03	2.53	4.121E-05	2.53	7.057E-06
1.48	8.736E-03	4.38	7.599E-06	4.58	9.437E-07
2.08	8.384E-03	4.58	5.269E-06	4.78	2.969E-06
2.08	8.043E-03	4.78	5.293E-06	6.53	5.673E-07
2.08	7.726E-03	6.53	-2.053E-07		
2.58	7.230E-03				
2.58	7.266E-03				
3.13	6.541E-03				
3.13	6.407E-03				
3.53	5.001E-03				
3.53	5.089E-03				
4.08	4.365E-03				
4.08	4.077E-03				
4.08	4.674E-03				
4.08	4.826E-03				
4.48	2.992E-03				
4.48	3.497E-03				
4.48	3.065E-03				
5.08	2.228E-03				
5.08	2.379E-03				
5.53	1.828E-03				
5.53	1.648E-03				
6.03	1.220E-03				
6.03	1.213E-03				
6.43	1.081E-03				
6.43	1.040E-03				
6.88	7.945E-04				
6.88	8.279E-04				
7.38	5.215E-04				
7.38	4.187E-04				
7.38	3.997E-04				
7.93	2.365E-04				
8.32	1.940E-04				
8.32	1.338E-04				
8.32	1.099E-04				
9.53	5.985E-05				
9.53	4.079E-05				
9.53	3.637E-05				
10.43	2.659E-05				
10.43	3.150E-05				
10.43	1.628E-05				
11.48	3.250E-05				

HAB (mm)	x_{C6H6}/x_{Ar}	HAB (mm)	x_{80}/x_{Ar} (as 1,3-c-C_6H_8)	HAB (mm)	x_{81}/x_{Ar} (as 3- or 4-c-C_6H_9)
11.48	4.946E-06				
11.48	1.245E-05				
11.48	4.999E-06				

Table H.14 Raw mass 82-84 data, with respect to argon.

HAB (mm)	x_{82}/x_{Ar} (as c-C_6H_{10})	HAB (mm)	x_{83}/x_{Ar} (as c-C_6H_{11})	HAB (mm)	x_{84}/x_{Ar} (as c-C_6H_{12})
1.03	2.535E-05	1.03	4.830E-06	1.03	1.124E-05
2.53	2.154E-05	2.53	3.245E-06	2.53	1.192E-05
4.58	2.807E-06	4.58	1.424E-06	4.58	1.226E-06
4.78	2.247E-06	4.78	4.058E-07	4.78	4.938E-07
6.53	-5.282E-06	6.53	-1.223E-06	6.53	4.145E-06

Table H.15 Raw mass 85, mass 86 and mass 91 data, with respect to argon.

HAB (mm)	x_{85}/x_{Ar} (as 1-C_6H_{13})	HAB (mm)	x_{86}/x_{Ar} (as n-C_6H_{14})	HAB (mm)	x_{91}/x_{Ar} (as $C_6H_5CH_2$)
1.03	1.950E-06	1.03	6.29E-07	3.03	0.000E+00
2.53	8.619E-07	2.53	1.47E-06	3.03	6.588E-06
4.58	0.000E+00	4.58	3.47E-07	3.03	1.398E-06
4.78	0.000E+00	4.78	1.04E-06	4.38	3.166E-06
6.53	-2.494E-06	6.53	4.17E-07	6.03	0.000E+00
				6.08	6.710E-07

Table H.16 Raw mass 92-94 data, with respect to argon.

HAB (mm)	x_{92}/x_{Ar} (as $C_6H_5CH_3$)	HAB (mm)	x_{93}/x_{Ar} (as C_6H_5O)	HAB (mm)	x_{94}/x_{Ar} (as C_6H_5OH)
3.03	-4.243E-06	1.68	7.273E-06	0.48	3.379E-05
3.03	0.000E+00	2.78	1.291E-06	1.03	3.980E-05
3.03	5.031E-06	3.03	-1.849E-06	1.53	3.575E-05
4.38	7.052E-06	3.03	5.640E-06	2.08	4.773E-05
6.03	1.784E-06	4.18	-1.370E-06	2.53	4.820E-05
6.08	5.182E-06	4.38	4.557E-07	3.03	4.540E-05
		5.53	4.244E-06	3.53	6.233E-05
		6.03	-2.208E-06	4.13	6.047E-05
		6.58	1.902E-07	4.48	5.822E-05
		7.48	2.717E-06	4.48	4.897E-05
		8.53	-5.622E-07	4.73	4.330E-05
		8.6	1.958E-07	5.08	7.124E-05
		9.53	2.287E-06	5.28	4.923E-05
		10.53	-3.760E-07	5.48	7.604E-05
				5.68	3.767E-05
				6.1	5.659E-05
				6.28	3.265E-05
				6.53	4.773E-05
				6.88	4.354E-05
				7.08	3.513E-05
				7.23	3.827E-05
				7.53	2.097E-05
				7.83	1.998E-05
				8.23	1.806E-05
				8.78	7.824E-06

Appendix I. Smoothed Curves of Temperature and Mole Fraction Data.

Table I.1 Smoothed temperature, argon, H atom, H_2, CH_3, CH_4 profiles.

HAB (mm)	TEMP (K)	x_{Ar}	x_H	x_{H2}	x_{CH3}	x_{CH4}
0.00	316	3.934E-01	1.525E-04	3.326E-01	5.272E-05	1.611E-03
0.13	335	3.957E-01	1.814E-04	3.282E-01	5.354E-05	1.628E-03
0.26	360	3.979E-01	2.125E-04	3.240E-01	5.515E-05	1.646E-03
0.39	389	4.000E-01	2.461E-04	3.199E-01	5.732E-05	1.664E-03
0.53	422	4.019E-01	2.823E-04	3.159E-01	6.005E-05	1.682E-03
0.66	460	4.038E-01	3.210E-04	3.119E-01	6.323E-05	1.701E-03
0.79	502	4.055E-01	3.625E-04	3.081E-01	6.690E-05	1.720E-03
0.92	548	4.071E-01	4.069E-04	3.044E-01	7.103E-05	1.741E-03
1.05	597	4.085E-01	4.542E-04	3.008E-01	7.566E-05	1.762E-03
1.18	648	4.099E-01	5.045E-04	2.973E-01	8.075E-05	1.784E-03
1.31	702	4.112E-01	5.580E-04	2.938E-01	8.635E-05	1.807E-03
1.44	758	4.123E-01	6.148E-04	2.905E-01	9.245E-05	1.831E-03
1.58	814	4.134E-01	6.748E-04	2.872E-01	9.901E-05	1.857E-03
1.71	871	4.143E-01	7.383E-04	2.840E-01	1.060E-04	1.883E-03
1.84	928	4.152E-01	8.053E-04	2.809E-01	1.135E-04	1.910E-03
1.97	985	4.159E-01	8.759E-04	2.779E-01	1.216E-04	1.939E-03
2.10	1041	4.165E-01	9.503E-04	2.750E-01	1.300E-04	1.969E-03
2.23	1095	4.170E-01	1.028E-03	2.721E-01	1.388E-04	2.001E-03
2.36	1149	4.175E-01	1.110E-03	2.693E-01	1.480E-04	2.034E-03
2.49	1200	4.178E-01	1.196E-03	2.665E-01	1.575E-04	2.068E-03
2.63	1249	4.180E-01	1.286E-03	2.639E-01	1.673E-04	2.103E-03
2.76	1297	4.182E-01	1.380E-03	2.613E-01	1.772E-04	2.140E-03
2.89	1342	4.183E-01	1.478E-03	2.587E-01	1.873E-04	2.179E-03
3.02	1385	4.182E-01	1.580E-03	2.563E-01	1.974E-04	2.218E-03
3.15	1425	4.182E-01	1.687E-03	2.539E-01	2.073E-04	2.259E-03
3.28	1464	4.180E-01	1.797E-03	2.515E-01	2.171E-04	2.301E-03
3.41	1500	4.177E-01	1.912E-03	2.492E-01	2.265E-04	2.342E-03
3.55	1533	4.174E-01	2.031E-03	2.469E-01	2.354E-04	2.384E-03
3.68	1565	4.170E-01	2.154E-03	2.447E-01	2.439E-04	2.425E-03
3.81	1594	4.165E-01	2.281E-03	2.426E-01	2.515E-04	2.464E-03
3.94	1622	4.160E-01	2.413E-03	2.405E-01	2.583E-04	2.501E-03
4.07	1648	4.154E-01	2.548E-03	2.385E-01	2.642E-04	2.536E-03
4.20	1672	4.148E-01	2.688E-03	2.365E-01	2.689E-04	2.565E-03
4.33	1694	4.141E-01	2.831E-03	2.345E-01	2.724E-04	2.589E-03
4.46	1714	4.134E-01	2.979E-03	2.326E-01	2.747E-04	2.606E-03
4.60	1733	4.126E-01	3.130E-03	2.308E-01	2.757E-04	2.614E-03
4.73	1751	4.118E-01	3.284E-03	2.290E-01	2.752E-04	2.611E-03
4.86	1767	4.110E-01	3.443E-03	2.272E-01	2.733E-04	2.595E-03
4.99	1782	4.102E-01	3.604E-03	2.255E-01	2.700E-04	2.566E-03
5.12	1796	4.093E-01	3.769E-03	2.239E-01	2.652E-04	2.522E-03
5.25	1809	4.084E-01	3.936E-03	2.223E-01	2.591E-04	2.463E-03
5.38	1821	4.076E-01	4.107E-03	2.208E-01	2.516E-04	2.387E-03
5.52	1832	4.067E-01	4.280E-03	2.193E-01	2.430E-04	2.296E-03
5.65	1842	4.058E-01	4.455E-03	2.178E-01	2.332E-04	2.191E-03
5.78	1851	4.049E-01	4.632E-03	2.164E-01	2.226E-04	2.074E-03
5.91	1859	4.040E-01	4.811E-03	2.150E-01	2.110E-04	1.946E-03

HAB (mm)	TEMP (K)	x_{Ar}	x_{H}	x_{H2}	x_{CH3}	x_{CH4}
6.04	1867	4.031E-01	4.991E-03	2.137E-01	1.988E-04	1.812E-03
6.17	1874	4.022E-01	5.172E-03	2.124E-01	1.862E-04	1.675E-03
6.30	1881	4.013E-01	5.354E-03	2.112E-01	1.732E-04	1.537E-03
6.43	1887	4.005E-01	5.536E-03	2.100E-01	1.600E-04	1.402E-03
6.57	1892	3.996E-01	5.718E-03	2.089E-01	1.469E-04	1.272E-03
6.70	1897	3.987E-01	5.900E-03	2.078E-01	1.339E-04	1.149E-03
6.83	1902	3.979E-01	6.080E-03	2.067E-01	1.212E-04	1.035E-03
6.96	1906	3.971E-01	6.260E-03	2.056E-01	1.090E-04	9.303E-04
7.09	1910	3.963E-01	6.438E-03	2.047E-01	9.732E-05	8.361E-04
7.22	1913	3.954E-01	6.615E-03	2.037E-01	8.625E-05	7.517E-04
7.35	1916	3.947E-01	6.788E-03	2.027E-01	7.589E-05	6.768E-04
7.48	1919	3.939E-01	6.960E-03	2.019E-01	6.629E-05	6.109E-04
7.62	1921	3.931E-01	7.128E-03	2.010E-01	5.748E-05	5.532E-04
7.75	1924	3.924E-01	7.293E-03	2.002E-01	4.945E-05	5.027E-04
7.88	1926	3.917E-01	7.454E-03	1.994E-01	4.223E-05	4.587E-04
8.01	1927	3.910E-01	7.611E-03	1.986E-01	3.578E-05	4.204E-04
8.14	1929	3.904E-01	7.764E-03	1.979E-01	3.009E-05	3.868E-04
8.27	1930	3.898E-01	7.913E-03	1.972E-01	2.510E-05	3.577E-04
8.40	1932	3.892E-01	8.057E-03	1.965E-01	2.077E-05	3.322E-04
8.54	1933	3.886E-01	8.196E-03	1.959E-01	1.706E-05	3.099E-04
8.67	1934	3.880E-01	8.329E-03	1.953E-01	1.389E-05	2.904E-04
8.80	1934	3.875E-01	8.458E-03	1.947E-01	1.122E-05	2.732E-04
8.93	1935	3.870E-01	8.581E-03	1.942E-01	8.986E-06	2.581E-04
9.06	1936	3.865E-01	8.698E-03	1.936E-01	7.139E-06	2.447E-04
9.19	1936	3.861E-01	8.810E-03	1.931E-01	5.625E-06	2.328E-04
9.32	1936	3.857E-01	8.916E-03	1.927E-01	4.393E-06	2.221E-04
9.45	1936	3.853E-01	9.016E-03	1.922E-01	3.403E-06	2.126E-04
9.59	1937	3.849E-01	9.111E-03	1.918E-01	2.613E-06	2.041E-04
9.72	1937	3.845E-01	9.199E-03	1.914E-01	1.989E-06	1.963E-04
9.85	1937	3.842E-01	9.282E-03	1.910E-01	1.501E-06	1.893E-04
9.98	1936	3.839E-01	9.359E-03	1.906E-01	1.122E-06	1.830E-04
10.11	1936	3.836E-01	9.430E-03	1.903E-01	8.320E-07	1.771E-04
10.24	1936	3.833E-01	9.496E-03	1.900E-01	6.110E-07	1.718E-04
10.37	1936	3.831E-01	9.556E-03	1.897E-01	4.451E-07	1.669E-04
10.51	1935	3.828E-01	9.611E-03	1.894E-01	3.210E-07	1.623E-04
10.64	1935	3.826E-01	9.660E-03	1.891E-01	2.295E-07	1.581E-04
10.77	1935	3.824E-01	9.704E-03	1.888E-01	1.625E-07	1.542E-04
10.90	1934	3.822E-01	9.743E-03	1.886E-01	1.140E-07	1.505E-04
11.03	1934	3.821E-01	9.777E-03	1.884E-01	7.928E-08	1.470E-04
11.16	1933	3.819E-01	9.807E-03	1.882E-01	5.458E-08	1.438E-04
11.29	1932	3.818E-01	9.832E-03	1.880E-01	3.724E-08	1.407E-04
11.42	1932	3.817E-01	9.852E-03	1.878E-01	2.516E-08	1.378E-04
11.56	1931	3.815E-01	9.869E-03	1.876E-01	1.683E-08	1.350E-04
11.69	1931	3.814E-01	9.881E-03	1.874E-01	1.116E-08	1.324E-04
11.82	1930	3.814E-01	9.889E-03	1.873E-01	7.322E-09	1.298E-04
11.95	1929	3.813E-01	9.894E-03	1.871E-01	4.758E-09	1.274E-04
12.08	1928	3.812E-01	9.895E-03	1.870E-01	3.062E-09	1.250E-04
12.21	1928	3.811E-01	9.892E-03	1.869E-01	1.951E-09	1.228E-04
12.34	1927	3.811E-01	9.887E-03	1.867E-01	1.231E-09	1.206E-04
12.47	1926	3.810E-01	9.879E-03	1.866E-01	7.685E-10	1.185E-04
12.61	1925	3.810E-01	9.867E-03	1.865E-01	4.751E-10	1.165E-04
12.74	1925	3.809E-01	9.853E-03	1.864E-01	2.909E-10	1.145E-04
12.87	1924	3.809E-01	9.836E-03	1.863E-01	1.762E-10	1.125E-04
13.00	1923	3.809E-01	9.817E-03	1.862E-01	1.057E-10	1.106E-04

Table I.2 Smoothed OH, H_2O, C_2H_2, C_2H_4, CO and H_2CO profiles.

HAB (mm)	x_{OH}	x_{H2O}	x_{C2H2}	x_{C2H4}	x_{CO}	x_{H2CO}
0.00	0.000E+00	6.122E-02	7.797E-05	5.721E-04	1.150E-02	2.822E-04
0.13	2.625E-06	6.328E-02	8.219E-05	6.006E-04	1.173E-02	2.855E-04
0.26	7.539E-06	6.538E-02	8.667E-05	6.289E-04	1.198E-02	2.889E-04
0.39	1.409E-05	6.766E-02	9.136E-05	6.566E-04	1.224E-02	2.923E-04
0.53	2.208E-05	7.006E-02	9.634E-05	6.837E-04	1.252E-02	2.956E-04
0.66	3.145E-05	7.259E-02	1.015E-04	7.100E-04	1.282E-02	2.989E-04
0.79	4.217E-05	7.526E-02	1.070E-04	7.353E-04	1.314E-02	3.022E-04
0.92	5.422E-05	7.809E-02	1.128E-04	7.594E-04	1.347E-02	3.055E-04
1.05	6.762E-05	8.105E-02	1.187E-04	7.823E-04	1.383E-02	3.087E-04
1.18	8.239E-05	8.415E-02	1.249E-04	8.037E-04	1.421E-02	3.119E-04
1.31	9.856E-05	8.741E-02	1.314E-04	8.235E-04	1.462E-02	3.151E-04
1.44	1.161E-04	9.081E-02	1.381E-04	8.415E-04	1.504E-02	3.183E-04
1.58	1.352E-04	9.437E-02	1.450E-04	8.577E-04	1.549E-02	3.214E-04
1.71	1.557E-04	9.811E-02	1.521E-04	8.718E-04	1.596E-02	3.245E-04
1.84	1.778E-04	1.020E-01	1.594E-04	8.838E-04	1.646E-02	3.276E-04
1.97	2.014E-04	1.060E-01	1.669E-04	8.936E-04	1.697E-02	3.306E-04
2.10	2.267E-04	1.102E-01	1.745E-04	9.012E-04	1.751E-02	3.336E-04
2.23	2.535E-04	1.145E-01	1.822E-04	9.065E-04	1.807E-02	3.365E-04
2.36	2.820E-04	1.190E-01	1.901E-04	9.094E-04	1.864E-02	3.393E-04
2.49	3.122E-04	1.236E-01	1.981E-04	9.099E-04	1.924E-02	3.421E-04
2.63	3.441E-04	1.284E-01	2.061E-04	9.081E-04	1.985E-02	3.447E-04
2.76	3.777E-04	1.333E-01	2.141E-04	9.039E-04	2.047E-02	3.472E-04
2.89	4.131E-04	1.384E-01	2.221E-04	8.974E-04	2.111E-02	3.496E-04
3.02	4.501E-04	1.435E-01	2.302E-04	8.886E-04	2.175E-02	3.519E-04
3.15	4.889E-04	1.487E-01	2.381E-04	8.777E-04	2.241E-02	3.539E-04
3.28	5.293E-04	1.541E-01	2.459E-04	8.647E-04	2.306E-02	3.557E-04
3.41	5.713E-04	1.596E-01	2.536E-04	8.497E-04	2.373E-02	3.572E-04
3.55	6.150E-04	1.652E-01	2.612E-04	8.328E-04	2.439E-02	3.584E-04
3.68	6.602E-04	1.708E-01	2.685E-04	8.141E-04	2.505E-02	3.592E-04
3.81	7.069E-04	1.765E-01	2.757E-04	7.939E-04	2.570E-02	3.595E-04
3.94	7.549E-04	1.822E-01	2.826E-04	7.722E-04	2.635E-02	3.594E-04
4.07	8.042E-04	1.880E-01	2.891E-04	7.492E-04	2.698E-02	3.585E-04
4.20	8.546E-04	1.938E-01	2.953E-04	7.250E-04	2.760E-02	3.569E-04
4.33	9.061E-04	1.997E-01	3.012E-04	6.999E-04	2.821E-02	3.545E-04
4.46	9.584E-04	2.056E-01	3.067E-04	6.740E-04	2.881E-02	3.511E-04
4.60	1.011E-03	2.114E-01	3.118E-04	6.474E-04	2.938E-02	3.465E-04
4.73	1.065E-03	2.173E-01	3.165E-04	6.203E-04	2.993E-02	3.406E-04
4.86	1.119E-03	2.231E-01	3.207E-04	5.929E-04	3.046E-02	3.334E-04
4.99	1.172E-03	2.289E-01	3.245E-04	5.653E-04	3.097E-02	3.245E-04
5.12	1.226E-03	2.347E-01	3.277E-04	5.376E-04	3.146E-02	3.140E-04
5.25	1.280E-03	2.404E-01	3.305E-04	5.101E-04	3.192E-02	3.017E-04
5.38	1.332E-03	2.460E-01	3.327E-04	4.828E-04	3.235E-02	2.875E-04
5.52	1.384E-03	2.516E-01	3.345E-04	4.558E-04	3.276E-02	2.714E-04
5.65	1.435E-03	2.571E-01	3.357E-04	4.293E-04	3.314E-02	2.536E-04
5.78	1.485E-03	2.625E-01	3.363E-04	4.034E-04	3.350E-02	2.343E-04
5.91	1.533E-03	2.679E-01	3.364E-04	3.781E-04	3.383E-02	2.137E-04
6.04	1.579E-03	2.731E-01	3.360E-04	3.535E-04	3.414E-02	1.922E-04
6.17	1.623E-03	2.782E-01	3.351E-04	3.298E-04	3.442E-02	1.705E-04
6.30	1.665E-03	2.832E-01	3.336E-04	3.068E-04	3.467E-02	1.490E-04
6.43	1.705E-03	2.880E-01	3.316E-04	2.848E-04	3.490E-02	1.283E-04
6.57	1.742E-03	2.928E-01	3.291E-04	2.637E-04	3.511E-02	1.090E-04
6.70	1.777E-03	2.974E-01	3.260E-04	2.435E-04	3.530E-02	9.143E-05
6.83	1.809E-03	3.018E-01	3.226E-04	2.243E-04	3.546E-02	7.592E-05

HAB (mm)	x_{OH}	x_{H2O}	x_{C2H2}	x_{C2H4}	x_{CO}	x_{H2CO}
6.96	1.838E-03	3.061E-01	3.186E-04	2.062E-04	3.561E-02	6.266E-05
7.09	1.864E-03	3.102E-01	3.143E-04	1.890E-04	3.574E-02	5.159E-05
7.22	1.888E-03	3.143E-01	3.094E-04	1.728E-04	3.585E-02	4.259E-05
7.35	1.908E-03	3.181E-01	3.042E-04	1.576E-04	3.594E-02	3.548E-05
7.48	1.926E-03	3.218E-01	2.987E-04	1.434E-04	3.602E-02	2.997E-05
7.62	1.941E-03	3.254E-01	2.928E-04	1.301E-04	3.609E-02	2.581E-05
7.75	1.953E-03	3.287E-01	2.866E-04	1.177E-04	3.614E-02	2.276E-05
7.88	1.962E-03	3.320E-01	2.801E-04	1.062E-04	3.618E-02	2.062E-05
8.01	1.969E-03	3.351E-01	2.734E-04	9.555E-05	3.621E-02	1.920E-05
8.14	1.974E-03	3.380E-01	2.664E-04	8.574E-05	3.624E-02	1.837E-05
8.27	1.976E-03	3.408E-01	2.593E-04	7.670E-05	3.625E-02	1.802E-05
8.40	1.976E-03	3.434E-01	2.520E-04	6.841E-05	3.626E-02	1.805E-05
8.54	1.974E-03	3.460E-01	2.446E-04	6.083E-05	3.627E-02	1.842E-05
8.67	1.970E-03	3.483E-01	2.371E-04	5.390E-05	3.627E-02	1.906E-05
8.80	1.964E-03	3.506E-01	2.294E-04	4.760E-05	3.626E-02	1.993E-05
8.93	1.957E-03	3.527E-01	2.218E-04	4.188E-05	3.625E-02	2.100E-05
9.06	1.948E-03	3.547E-01	2.141E-04	3.670E-05	3.624E-02	2.225E-05
9.19	1.938E-03	3.566E-01	2.065E-04	3.202E-05	3.622E-02	2.364E-05
9.32	1.926E-03	3.583E-01	1.989E-04	2.781E-05	3.621E-02	2.514E-05
9.45	1.913E-03	3.600E-01	1.914E-04	2.403E-05	3.619E-02	2.676E-05
9.59	1.899E-03	3.615E-01	1.839E-04	2.065E-05	3.617E-02	2.845E-05
9.72	1.885E-03	3.629E-01	1.765E-04	1.762E-05	3.615E-02	3.021E-05
9.85	1.869E-03	3.643E-01	1.693E-04	1.492E-05	3.614E-02	3.203E-05
9.98	1.853E-03	3.655E-01	1.622E-04	1.253E-05	3.612E-02	3.388E-05
10.11	1.837E-03	3.667E-01	1.552E-04	1.040E-05	3.610E-02	3.576E-05
10.24	1.819E-03	3.677E-01	1.485E-04	8.526E-06	3.608E-02	3.766E-05
10.37	1.802E-03	3.687E-01	1.419E-04	6.870E-06	3.606E-02	3.957E-05
10.51	1.784E-03	3.696E-01	1.355E-04	5.414E-06	3.605E-02	4.146E-05
10.64	1.765E-03	3.705E-01	1.293E-04	4.136E-06	3.603E-02	4.339E-05
10.77	1.747E-03	3.712E-01	1.233E-04	3.018E-06	3.602E-02	4.528E-05
10.90	1.728E-03	3.720E-01	1.176E-04	2.042E-06	3.600E-02	4.717E-05
11.03	1.709E-03	3.726E-01	1.121E-04	1.193E-06	3.599E-02	4.902E-05
11.16	1.690E-03	3.732E-01	1.068E-04	4.550E-07	3.597E-02	5.087E-05
11.29	1.671E-03	3.738E-01	1.017E-04	0.000E+00	3.596E-02	5.269E-05
11.42	1.653E-03	3.743E-01	9.690E-05	0.000E+00	3.595E-02	5.446E-05
11.56	1.634E-03	3.747E-01	9.230E-05	0.000E+00	3.594E-02	5.620E-05
11.69	1.615E-03	3.751E-01	8.796E-05	0.000E+00	3.594E-02	5.794E-05
11.82	1.596E-03	3.755E-01	8.382E-05	0.000E+00	3.593E-02	5.964E-05
11.95	1.578E-03	3.759E-01	7.991E-05	0.000E+00	3.592E-02	6.131E-05
12.08	1.559E-03	3.762E-01	7.624E-05	0.000E+00	3.591E-02	6.293E-05
12.21	1.541E-03	3.765E-01	7.276E-05	0.000E+00	3.590E-02	6.452E-05
12.34	1.523E-03	3.767E-01	6.951E-05	0.000E+00	3.590E-02	6.612E-05
12.47	1.505E-03	3.769E-01	6.645E-05	0.000E+00	3.590E-02	6.763E-05
12.61	1.488E-03	3.772E-01	6.362E-05	0.000E+00	3.589E-02	6.914E-05
12.74	1.470E-03	3.773E-01	6.095E-05	0.000E+00	3.589E-02	7.062E-05
12.87	1.453E-03	3.775E-01	5.847E-05	0.000E+00	3.588E-02	7.206E-05
13.00	1.436E-03	3.777E-01	5.618E-05	0.000E+00	3.588E-02	7.347E-05

Table I.3 Smoothed O_2, mass 42, mass 44 (low electron energy), CO_2, mass 53 and mass 54 profiles.

HAB (mm)	x_{O2}	x_{42}	$x_{44\ low}$	x_{CO2}	x_{53}	x_{54}
0.00	1.934E-01	1.855E-04	1.693E-05	8.064E-04	0.000E+00	5.389E-06
0.13	1.930E-01	1.872E-04	1.902E-05	8.576E-04	9.701E-08	6.065E-06
0.26	1.925E-01	1.901E-04	2.135E-05	9.103E-04	3.027E-07	6.807E-06
0.39	1.919E-01	1.941E-04	2.392E-05	9.643E-04	5.022E-07	7.618E-06
0.53	1.911E-01	1.992E-04	2.675E-05	1.020E-03	6.801E-07	8.497E-06
0.66	1.902E-01	2.053E-04	2.984E-05	1.076E-03	8.372E-07	9.444E-06
0.79	1.892E-01	2.123E-04	3.317E-05	1.134E-03	9.766E-07	1.046E-05
0.92	1.880E-01	2.203E-04	3.674E-05	1.193E-03	1.101E-06	1.152E-05
1.05	1.867E-01	2.291E-04	4.051E-05	1.253E-03	1.213E-06	1.264E-05
1.18	1.852E-01	2.386E-04	4.445E-05	1.314E-03	1.314E-06	1.379E-05
1.31	1.835E-01	2.487E-04	4.850E-05	1.376E-03	1.406E-06	1.495E-05
1.44	1.817E-01	2.592E-04	5.260E-05	1.439E-03	1.490E-06	1.611E-05
1.58	1.798E-01	2.697E-04	5.665E-05	1.503E-03	1.566E-06	1.724E-05
1.71	1.777E-01	2.798E-04	6.058E-05	1.568E-03	1.636E-06	1.830E-05
1.84	1.754E-01	2.890E-04	6.427E-05	1.634E-03	1.700E-06	1.929E-05
1.97	1.730E-01	2.966E-04	6.761E-05	1.700E-03	1.758E-06	2.015E-05
2.10	1.704E-01	3.020E-04	7.048E-05	1.767E-03	1.811E-06	2.088E-05
2.23	1.677E-01	3.046E-04	7.277E-05	1.835E-03	1.858E-06	2.145E-05
2.36	1.649E-01	3.037E-04	7.438E-05	1.903E-03	1.901E-06	2.185E-05
2.49	1.619E-01	2.992E-04	7.520E-05	1.972E-03	1.939E-06	2.207E-05
2.63	1.588E-01	2.909E-04	7.517E-05	2.041E-03	1.972E-06	2.210E-05
2.76	1.556E-01	2.792E-04	7.424E-05	2.110E-03	2.000E-06	2.197E-05
2.89	1.523E-01	2.646E-04	7.242E-05	2.180E-03	2.023E-06	2.168E-05
3.02	1.489E-01	2.478E-04	6.972E-05	2.251E-03	2.042E-06	2.124E-05
3.15	1.453E-01	2.297E-04	6.621E-05	2.321E-03	2.055E-06	2.069E-05
3.28	1.417E-01	2.110E-04	6.198E-05	2.392E-03	2.062E-06	2.005E-05
3.41	1.380E-01	1.925E-04	5.717E-05	2.463E-03	2.064E-06	1.932E-05
3.55	1.343E-01	1.746E-04	5.192E-05	2.534E-03	2.060E-06	1.855E-05
3.68	1.304E-01	1.577E-04	4.641E-05	2.605E-03	2.049E-06	1.774E-05
3.81	1.266E-01	1.421E-04	4.080E-05	2.676E-03	2.032E-06	1.691E-05
3.94	1.226E-01	1.278E-04	3.526E-05	2.747E-03	2.008E-06	1.608E-05
4.07	1.187E-01	1.148E-04	2.993E-05	2.818E-03	1.976E-06	1.525E-05
4.20	1.147E-01	1.032E-04	2.495E-05	2.889E-03	1.936E-06	1.444E-05
4.33	1.108E-01	9.277E-05	2.041E-05	2.961E-03	1.888E-06	1.366E-05
4.46	1.068E-01	8.349E-05	1.637E-05	3.031E-03	1.831E-06	1.290E-05
4.60	1.028E-01	7.524E-05	1.287E-05	3.102E-03	1.766E-06	1.217E-05
4.73	9.885E-02	6.791E-05	9.913E-06	3.173E-03	1.692E-06	1.148E-05
4.86	9.492E-02	6.141E-05	7.475E-06	3.244E-03	1.608E-06	1.083E-05
4.99	9.103E-02	5.564E-05	5.515E-06	3.314E-03	1.516E-06	1.021E-05
5.12	8.718E-02	5.051E-05	3.979E-06	3.385E-03	1.415E-06	9.621E-06
5.25	8.339E-02	4.594E-05	2.806E-06	3.455E-03	1.308E-06	9.070E-06
5.38	7.965E-02	4.188E-05	1.933E-06	3.526E-03	1.193E-06	8.552E-06
5.52	7.597E-02	3.825E-05	1.299E-06	3.596E-03	1.074E-06	8.065E-06
5.65	7.237E-02	3.501E-05	8.524E-07	3.666E-03	9.509E-07	7.609E-06
5.78	6.884E-02	3.210E-05	5.453E-07	3.736E-03	8.274E-07	7.182E-06
5.91	6.540E-02	2.950E-05	3.399E-07	3.806E-03	7.053E-07	6.781E-06
6.04	6.204E-02	2.715E-05	2.064E-07	3.876E-03	5.874E-07	6.407E-06
6.17	5.877E-02	2.504E-05	1.219E-07	3.946E-03	4.765E-07	6.056E-06
6.30	5.559E-02	2.314E-05	7.010E-08	4.016E-03	3.751E-07	5.728E-06
6.43	5.251E-02	2.142E-05	3.918E-08	4.085E-03	2.853E-07	5.421E-06
6.57	4.953E-02	1.986E-05	2.128E-08	4.155E-03	2.087E-07	5.133E-06

HAB (mm)	x_{O2}	x_{42}	$x_{44\ low}$	x_{CO2}	x_{53}	x_{54}
6.70	4.665E-02	1.844E-05	1.122E-08	4.224E-03	1.460E-07	4.864E-06
6.83	4.388E-02	1.715E-05	5.743E-09	4.293E-03	9.709E-08	4.611E-06
6.96	4.121E-02	1.598E-05	2.851E-09	4.362E-03	6.094E-08	4.375E-06
7.09	3.864E-02	1.491E-05	1.372E-09	4.432E-03	3.581E-08	4.153E-06
7.22	3.618E-02	1.393E-05	6.399E-10	4.501E-03	1.952E-08	3.946E-06
7.35	3.382E-02	1.303E-05	2.889E-10	4.569E-03	9.770E-09	3.750E-06
7.48	3.157E-02	1.221E-05	1.262E-10	4.638E-03	4.434E-09	3.567E-06
7.62	2.943E-02	1.145E-05	5.334E-11	4.707E-03	1.801E-09	3.395E-06
7.75	2.739E-02	1.075E-05	2.179E-11	4.776E-03	6.441E-10	3.234E-06
7.88	2.545E-02	1.011E-05	8.596E-12	4.844E-03	1.994E-10	3.082E-06
8.01	2.361E-02	9.520E-06	3.275E-12	4.913E-03	5.232E-11	2.939E-06
8.14	2.187E-02	8.974E-06	1.204E-12	4.982E-03	1.138E-11	2.805E-06
8.27	2.023E-02	8.468E-06	4.267E-13	5.050E-03	1.996E-12	2.678E-06
8.40	1.868E-02	7.999E-06	1.457E-13	5.119E-03	2.743E-13	2.559E-06
8.54	1.722E-02	7.564E-06	4.796E-14	5.187E-03	2.852E-14	2.446E-06
8.67	1.585E-02	7.160E-06	1.519E-14	5.256E-03	2.157E-15	2.340E-06
8.80	1.456E-02	6.785E-06	4.629E-15	5.324E-03	1.136E-16	2.240E-06
8.93	1.336E-02	6.435E-06	1.356E-15	5.393E-03	3.954E-18	2.145E-06
9.06	1.224E-02	6.109E-06	3.819E-16	5.461E-03	8.590E-20	2.056E-06
9.19	1.119E-02	5.804E-06	1.033E-16	5.530E-03	1.090E-21	1.971E-06
9.32	1.021E-02	5.520E-06	2.680E-17	5.598E-03	7.494E-24	1.891E-06
9.45	9.307E-03	5.254E-06	6.672E-18	5.667E-03	2.560E-26	1.815E-06
9.59	8.467E-03	5.005E-06	1.592E-18	5.735E-03	3.941E-29	1.743E-06
9.72	7.690E-03	4.771E-06	3.641E-19	5.804E-03	2.444E-32	1.675E-06
9.85	6.972E-03	4.552E-06	7.974E-20	5.872E-03	5.376E-36	1.610E-06
9.98	6.309E-03	4.346E-06	1.671E-20	5.940E-03	3.626E-40	1.548E-06
10.11	5.700E-03	4.153E-06	3.349E-21	6.009E-03	6.352E-45	1.490E-06
10.24	5.140E-03	3.971E-06	6.416E-22	6.077E-03	2.392E-50	1.435E-06
10.37	4.627E-03	3.799E-06	1.174E-22	6.145E-03	1.561E-56	1.382E-06
10.51	4.158E-03	3.638E-06	2.052E-23	6.213E-03	1.380E-63	1.332E-06
10.64	3.730E-03	3.485E-06	3.421E-24	6.280E-03	1.249E-71	1.284E-06
10.77	3.339E-03	3.341E-06	5.439E-25	6.348E-03	8.403E-81	1.238E-06
10.90	2.984E-03	3.205E-06	8.242E-26	6.416E-03	2.917E-91	1.195E-06
11.03	2.662E-03	3.076E-06	1.190E-26	6.483E-03	0.000E+00	1.154E-06
11.16	2.370E-03	2.955E-06	1.635E-27	6.550E-03	0.000E+00	1.114E-06
11.29	2.106E-03	2.839E-06	2.137E-28	6.617E-03	0.000E+00	1.076E-06
11.42	1.868E-03	2.730E-06	2.656E-29	6.684E-03	0.000E+00	1.040E-06
11.56	1.654E-03	2.626E-06	3.136E-30	6.750E-03	0.000E+00	1.006E-06
11.69	1.461E-03	2.527E-06	3.518E-31	6.817E-03	0.000E+00	9.729E-07
11.82	1.289E-03	2.434E-06	3.745E-32	6.883E-03	0.000E+00	9.414E-07
11.95	1.134E-03	2.345E-06	3.782E-33	6.948E-03	0.000E+00	9.113E-07
12.08	9.964E-04	2.260E-06	3.621E-34	7.014E-03	0.000E+00	8.824E-07
12.21	8.735E-04	2.179E-06	3.284E-35	7.079E-03	0.000E+00	8.547E-07
12.34	7.643E-04	2.103E-06	2.821E-36	7.144E-03	0.000E+00	8.282E-07
12.47	6.674E-04	2.029E-06	2.293E-37	7.208E-03	0.000E+00	8.028E-07
12.61	5.816E-04	1.959E-06	1.763E-38	7.272E-03	0.000E+00	7.783E-07
12.74	5.058E-04	1.893E-06	1.281E-39	7.336E-03	0.000E+00	7.549E-07
12.87	4.390E-04	1.829E-06	8.792E-41	7.399E-03	0.000E+00	7.324E-07
13.00	3.802E-04	1.768E-06	5.698E-42	7.462E-03	0.000E+00	7.108E-07

Table I.4 Smoothed mass 55-60 profiles.

HAB (mm)	x_{55}	x_{56}	x_{57}	x_{58}	$x_{59\ high\ EE}$	x_{60}
0.00	6.277E-07	1.682E-05	4.009E-07	1.128E-05	2.597E-06	1.222E-06
0.13	8.356E-07	1.746E-05	1.470E-06	1.155E-05	2.629E-06	1.262E-06
0.26	1.074E-06	1.813E-05	2.419E-06	1.181E-05	2.658E-06	1.303E-06
0.39	1.338E-06	1.883E-05	3.446E-06	1.207E-05	2.681E-06	1.344E-06
0.53	1.623E-06	1.956E-05	4.533E-06	1.232E-05	2.699E-06	1.386E-06
0.66	1.921E-06	2.033E-05	5.650E-06	1.258E-05	2.711E-06	1.428E-06
0.79	2.227E-06	2.113E-05	6.763E-06	1.283E-05	2.715E-06	1.470E-06
0.92	2.533E-06	2.197E-05	7.836E-06	1.308E-05	2.711E-06	1.513E-06
1.05	2.835E-06	2.285E-05	8.840E-06	1.332E-05	2.698E-06	1.556E-06
1.18	3.127E-06	2.376E-05	9.745E-06	1.355E-05	2.675E-06	1.598E-06
1.31	3.404E-06	2.470E-05	1.053E-05	1.377E-05	2.640E-06	1.640E-06
1.44	3.664E-06	2.567E-05	1.117E-05	1.399E-05	2.594E-06	1.682E-06
1.58	3.903E-06	2.665E-05	1.166E-05	1.419E-05	2.534E-06	1.723E-06
1.71	4.119E-06	2.765E-05	1.199E-05	1.438E-05	2.460E-06	1.762E-06
1.84	4.311E-06	2.865E-05	1.217E-05	1.455E-05	2.371E-06	1.801E-06
1.97	4.478E-06	2.962E-05	1.219E-05	1.470E-05	2.267E-06	1.837E-06
2.10	4.619E-06	3.055E-05	1.207E-05	1.482E-05	2.148E-06	1.871E-06
2.23	4.733E-06	3.140E-05	1.182E-05	1.492E-05	2.015E-06	1.903E-06
2.36	4.822E-06	3.215E-05	1.145E-05	1.499E-05	1.867E-06	1.931E-06
2.49	4.883E-06	3.276E-05	1.098E-05	1.503E-05	1.708E-06	1.955E-06
2.63	4.919E-06	3.317E-05	1.043E-05	1.502E-05	1.538E-06	1.974E-06
2.76	4.928E-06	3.336E-05	9.827E-06	1.497E-05	1.361E-06	1.988E-06
2.89	4.910E-06	3.327E-05	9.174E-06	1.487E-05	1.182E-06	1.995E-06
3.02	4.866E-06	3.289E-05	8.494E-06	1.472E-05	1.003E-06	1.996E-06
3.15	4.796E-06	3.218E-05	7.803E-06	1.451E-05	8.294E-07	1.988E-06
3.28	4.699E-06	3.115E-05	7.113E-06	1.423E-05	6.664E-07	1.971E-06
3.41	4.576E-06	2.982E-05	6.436E-06	1.387E-05	5.179E-07	1.944E-06
3.55	4.427E-06	2.822E-05	5.782E-06	1.345E-05	3.876E-07	1.906E-06
3.68	4.252E-06	2.641E-05	5.158E-06	1.294E-05	2.779E-07	1.856E-06
3.81	4.052E-06	2.444E-05	4.572E-06	1.236E-05	1.896E-07	1.794E-06
3.94	3.829E-06	2.240E-05	4.025E-06	1.169E-05	1.224E-07	1.718E-06
4.07	3.583E-06	2.033E-05	3.522E-06	1.095E-05	7.410E-08	1.630E-06
4.20	3.318E-06	1.831E-05	3.063E-06	1.013E-05	4.173E-08	1.529E-06
4.33	3.035E-06	1.636E-05	2.647E-06	9.253E-06	2.163E-08	1.416E-06
4.46	2.740E-06	1.454E-05	2.275E-06	8.321E-06	1.020E-08	1.292E-06
4.60	2.436E-06	1.285E-05	1.944E-06	7.355E-06	4.318E-09	1.159E-06
4.73	2.129E-06	1.131E-05	1.652E-06	6.374E-06	1.617E-09	1.021E-06
4.86	1.824E-06	9.924E-06	1.396E-06	5.400E-06	5.266E-10	8.800E-07
4.99	1.529E-06	8.683E-06	1.174E-06	4.460E-06	1.462E-10	7.401E-07
5.12	1.250E-06	7.582E-06	9.820E-07	3.577E-06	3.382E-11	6.052E-07
5.25	9.936E-07	6.610E-06	8.173E-07	2.775E-06	6.360E-12	4.794E-07
5.38	7.643E-07	5.757E-06	6.768E-07	2.072E-06	9.439E-13	3.662E-07
5.52	5.666E-07	5.010E-06	5.577E-07	1.482E-06	1.070E-13	2.684E-07
5.65	4.028E-07	4.358E-06	4.575E-07	1.009E-06	8.913E-15	1.876E-07
5.78	2.729E-07	3.789E-06	3.735E-07	6.492E-07	5.230E-16	1.242E-07
5.91	1.751E-07	3.295E-06	3.035E-07	3.918E-07	2.057E-17	7.738E-08
6.04	1.056E-07	2.865E-06	2.455E-07	2.198E-07	5.126E-19	4.494E-08
6.17	5.930E-08	2.492E-06	1.978E-07	1.134E-07	7.596E-21	2.409E-08
6.30	3.072E-08	2.167E-06	1.586E-07	5.321E-08	6.219E-23	1.179E-08
6.43	1.451E-08	1.886E-06	1.266E-07	2.240E-08	2.590E-25	5.203E-09
6.57	6.174E-09	1.641E-06	1.007E-07	8.332E-09	4.986E-28	2.039E-09
6.70	2.330E-09	1.429E-06	7.975E-08	2.692E-09	3.985E-31	6.981E-10

HAB (mm)	x_{55}	x_{56}	x_{57}	x_{58}	$x_{59\ high\ EE}$	x_{60}
6.83	7.670E-10	1.244E-06	6.290E-08	7.403E-10	1.168E-34	2.049E-10
6.96	2.161E-10	1.084E-06	4.941E-08	1.695E-10	1.091E-38	5.046E-11
7.09	5.098E-11	9.449E-07	3.866E-08	3.148E-11	2.768E-43	1.017E-11
7.22	9.823E-12	8.237E-07	3.013E-08	4.606E-12	1.587E-48	1.631E-12
7.35	1.503E-12	7.183E-07	2.339E-08	5.134E-13	1.669E-54	2.017E-13
7.48	1.767E-13	6.266E-07	1.809E-08	4.197E-14	2.538E-61	1.853E-14
7.62	1.538E-14	5.468E-07	1.394E-08	2.409E-15	4.257E-69	1.213E-15
7.75	9.515E-16	4.773E-07	1.070E-08	9.237E-17	5.778E-78	5.401E-17
7.88	3.984E-17	4.168E-07	8.184E-09	2.236E-18	4.459E-88	1.547E-18
8.01	1.069E-18	3.640E-07	6.238E-09	3.204E-20	1.308E-99	2.684E-20
8.14	1.726E-20	3.180E-07	4.737E-09	2.525E-22	0.000E+00	2.626E-22
8.27	1.563E-22	2.779E-07	3.585E-09	1.006E-24	0.000E+00	1.337E-24
8.40	7.314E-25	2.429E-07	2.704E-09	1.841E-27	0.000E+00	3.233E-27
8.54	1.613E-27	2.123E-07	2.032E-09	1.388E-30	0.000E+00	3.345E-30
8.67	1.508E-30	1.857E-07	1.522E-09	3.807E-34	0.000E+00	1.315E-33
8.80	5.301E-34	1.624E-07	1.136E-09	3.295E-38	0.000E+00	1.712E-37
8.93	6.103E-38	1.420E-07	8.453E-10	7.658E-43	0.000E+00	6.333E-42
9.06	1.969E-42	1.243E-07	6.268E-10	3.972E-48	0.000E+00	5.574E-47
9.19	1.488E-47	1.088E-07	4.633E-10	3.727E-54	0.000E+00	9.542E-53
9.32	2.151E-53	9.518E-08	3.414E-10	4.975E-61	0.000E+00	2.526E-59
9.45	4.711E-60	8.331E-08	2.507E-10	7.186E-69	0.000E+00	7.953E-67
9.59	1.200E-67	7.294E-08	1.835E-10	8.222E-78	0.000E+00	2.210E-75
9.72	2.629E-76	6.386E-08	1.339E-10	5.220E-88	0.000E+00	3.854E-85
9.85	3.510E-86	5.592E-08	9.745E-11	1.226E-99	0.000E+00	2.861E-96
9.98	1.929E-97	4.897E-08	7.068E-11	0.000E+00	0.000E+00	0.000E+00
10.11	0.000E+00	4.289E-08	5.110E-11	0.000E+00	0.000E+00	0.000E+00
10.24	0.000E+00	3.757E-08	3.684E-11	0.000E+00	0.000E+00	0.000E+00
10.37	0.000E+00	3.292E-08	2.648E-11	0.000E+00	0.000E+00	0.000E+00
10.51	0.000E+00	2.884E-08	1.897E-11	0.000E+00	0.000E+00	0.000E+00
10.64	0.000E+00	2.527E-08	1.355E-11	0.000E+00	0.000E+00	0.000E+00
10.77	0.000E+00	2.214E-08	9.655E-12	0.000E+00	0.000E+00	0.000E+00
10.90	0.000E+00	1.940E-08	6.858E-12	0.000E+00	0.000E+00	0.000E+00
11.03	0.000E+00	1.700E-08	4.856E-12	0.000E+00	0.000E+00	0.000E+00
11.16	0.000E+00	1.490E-08	3.429E-12	0.000E+00	0.000E+00	0.000E+00
11.29	0.000E+00	1.306E-08	2.415E-12	0.000E+00	0.000E+00	0.000E+00
11.42	0.000E+00	1.145E-08	1.695E-12	0.000E+00	0.000E+00	0.000E+00
11.56	0.000E+00	1.003E-08	1.187E-12	0.000E+00	0.000E+00	0.000E+00
11.69	0.000E+00	8.796E-09	8.288E-13	0.000E+00	0.000E+00	0.000E+00
11.82	0.000E+00	7.711E-09	5.771E-13	0.000E+00	0.000E+00	0.000E+00
11.95	0.000E+00	6.760E-09	4.007E-13	0.000E+00	0.000E+00	0.000E+00
12.08	0.000E+00	5.927E-09	2.774E-13	0.000E+00	0.000E+00	0.000E+00
12.21	0.000E+00	5.196E-09	1.916E-13	0.000E+00	0.000E+00	0.000E+00
12.34	0.000E+00	4.556E-09	1.319E-13	0.000E+00	0.000E+00	0.000E+00
12.47	0.000E+00	3.994E-09	9.061E-14	0.000E+00	0.000E+00	0.000E+00
12.61	0.000E+00	3.502E-09	6.206E-14	0.000E+00	0.000E+00	0.000E+00
12.74	0.000E+00	3.071E-09	4.240E-14	0.000E+00	0.000E+00	0.000E+00
12.87	0.000E+00	2.692E-09	2.889E-14	0.000E+00	0.000E+00	0.000E+00
13.00	0.000E+00	2.361E-09	1.963E-14	0.000E+00	0.000E+00	0.000E+00

Table I.5 Smoothed mass 65-71 profiles. (No mass 67 profile.)

HAB (mm)	x_{65}	x_{66}	x_{68}	x_{69}	x_{70}	x_{71}
0.00	1.305E-08	5.289E-06	9.439E-06	3.541E-06	1.020E-05	9.144E-07
0.13	1.588E-08	5.321E-06	9.880E-06	3.592E-06	1.048E-05	1.017E-06
0.26	1.888E-08	5.354E-06	1.034E-05	3.640E-06	1.076E-05	1.129E-06
0.39	2.207E-08	5.389E-06	1.080E-05	3.684E-06	1.103E-05	1.252E-06
0.53	2.546E-08	5.427E-06	1.129E-05	3.724E-06	1.131E-05	1.386E-06
0.66	2.906E-08	5.467E-06	1.178E-05	3.758E-06	1.158E-05	1.532E-06
0.79	3.288E-08	5.510E-06	1.229E-05	3.786E-06	1.185E-05	1.691E-06
0.92	3.694E-08	5.556E-06	1.281E-05	3.808E-06	1.212E-05	1.862E-06
1.05	4.125E-08	5.605E-06	1.333E-05	3.822E-06	1.237E-05	2.046E-06
1.18	4.584E-08	5.657E-06	1.387E-05	3.827E-06	1.262E-05	2.243E-06
1.31	5.072E-08	5.711E-06	1.441E-05	3.823E-06	1.285E-05	2.452E-06
1.44	5.592E-08	5.768E-06	1.496E-05	3.807E-06	1.307E-05	2.672E-06
1.58	6.146E-08	5.828E-06	1.550E-05	3.780E-06	1.327E-05	2.902E-06
1.71	6.736E-08	5.889E-06	1.604E-05	3.739E-06	1.344E-05	3.139E-06
1.84	7.366E-08	5.952E-06	1.658E-05	3.683E-06	1.360E-05	3.380E-06
1.97	8.038E-08	6.016E-06	1.709E-05	3.612E-06	1.372E-05	3.621E-06
2.10	8.758E-08	6.082E-06	1.760E-05	3.523E-06	1.381E-05	3.857E-06
2.23	9.526E-08	6.148E-06	1.807E-05	3.416E-06	1.386E-05	4.082E-06
2.36	1.035E-07	6.214E-06	1.851E-05	3.290E-06	1.386E-05	4.288E-06
2.49	1.123E-07	6.281E-06	1.890E-05	3.145E-06	1.382E-05	4.467E-06
2.63	1.218E-07	6.346E-06	1.924E-05	2.980E-06	1.372E-05	4.610E-06
2.76	1.320E-07	6.410E-06	1.952E-05	2.797E-06	1.355E-05	4.706E-06
2.89	1.430E-07	6.473E-06	1.972E-05	2.595E-06	1.332E-05	4.745E-06
3.02	1.548E-07	6.533E-06	1.982E-05	2.378E-06	1.301E-05	4.718E-06
3.15	1.676E-07	6.591E-06	1.982E-05	2.147E-06	1.262E-05	4.618E-06
3.28	1.815E-07	6.644E-06	1.971E-05	1.907E-06	1.215E-05	4.438E-06
3.41	1.965E-07	6.694E-06	1.946E-05	1.663E-06	1.160E-05	4.179E-06
3.55	2.127E-07	6.738E-06	1.906E-05	1.419E-06	1.096E-05	3.843E-06
3.68	2.304E-07	6.777E-06	1.851E-05	1.182E-06	1.024E-05	3.441E-06
3.81	2.497E-07	6.810E-06	1.780E-05	9.576E-07	9.442E-06	2.989E-06
3.94	2.707E-07	6.835E-06	1.692E-05	7.518E-07	8.581E-06	2.508E-06
4.07	2.937E-07	6.853E-06	1.588E-05	5.693E-07	7.669E-06	2.023E-06
4.20	3.188E-07	6.863E-06	1.468E-05	4.139E-07	6.725E-06	1.559E-06
4.33	3.464E-07	6.864E-06	1.335E-05	2.872E-07	5.771E-06	1.142E-06
4.46	3.768E-07	6.855E-06	1.191E-05	1.890E-07	4.831E-06	7.890E-07
4.60	4.101E-07	6.836E-06	1.040E-05	1.170E-07	3.932E-06	5.099E-07
4.73	4.469E-07	6.807E-06	8.852E-06	6.763E-08	3.100E-06	3.054E-07
4.86	4.875E-07	6.766E-06	7.328E-06	3.612E-08	2.356E-06	1.677E-07
4.99	5.322E-07	6.713E-06	5.875E-06	1.764E-08	1.718E-06	8.347E-08
5.12	5.817E-07	6.649E-06	4.540E-06	7.776E-09	1.194E-06	3.711E-08
5.25	6.362E-07	6.573E-06	3.365E-06	3.051E-09	7.866E-07	1.451E-08
5.38	6.963E-07	6.484E-06	2.378E-06	1.048E-09	4.871E-07	4.901E-09
5.52	7.623E-07	6.383E-06	1.592E-06	3.091E-10	2.812E-07	1.401E-09
5.65	8.346E-07	6.269E-06	1.002E-06	7.673E-11	1.498E-07	3.310E-10
5.78	9.132E-07	6.143E-06	5.872E-07	1.564E-11	7.285E-08	6.295E-11
5.91	9.979E-07	6.005E-06	3.177E-07	2.544E-12	3.192E-08	9.347E-12
6.04	1.088E-06	5.854E-06	1.568E-07	3.204E-13	1.242E-08	1.047E-12
6.17	1.183E-06	5.693E-06	6.969E-08	3.012E-14	4.219E-09	8.493E-14
6.30	1.280E-06	5.520E-06	2.749E-08	2.028E-15	1.228E-09	4.775E-15
6.43	1.377E-06	5.338E-06	9.465E-09	9.337E-17	2.998E-10	1.767E-16
6.57	1.470E-06	5.146E-06	2.791E-09	2.786E-18	5.986E-11	4.056E-18
6.70	1.554E-06	4.946E-06	6.893E-10	5.071E-20	9.506E-12	5.404E-20

HAB (mm)	x_{65}	x_{66}	x_{68}	x_{69}	x_{70}	x_{71}
6.83	1.625E-06	4.738E-06	1.392E-10	5.252E-22	1.162E-12	3.870E-22
6.96	1.677E-06	4.524E-06	2.232E-11	2.859E-24	1.055E-13	1.366E-24
7.09	1.706E-06	4.305E-06	2.754E-12	7.478E-27	6.821E-15	2.152E-27
7.22	1.709E-06	4.082E-06	2.519E-13	8.476E-30	2.993E-16	1.350E-30
7.35	1.687E-06	3.857E-06	1.638E-14	3.702E-33	8.442E-18	2.968E-34
7.48	1.641E-06	3.631E-06	7.219E-16	5.454E-37	1.439E-19	1.971E-38
7.62	1.574E-06	3.404E-06	2.042E-17	2.325E-41	1.381E-21	3.346E-43
7.75	1.492E-06	3.179E-06	3.482E-19	2.411E-46	6.888E-24	1.198E-48
7.88	1.399E-06	2.957E-06	3.335E-21	4.987E-52	1.627E-26	7.277E-55
8.01	1.301E-06	2.739E-06	1.654E-23	1.641E-58	1.640E-29	5.845E-62
8.14	1.201E-06	2.526E-06	3.877E-26	6.635E-66	6.261E-33	4.673E-70
8.27	1.104E-06	2.319E-06	3.861E-29	2.457E-74	7.894E-37	2.690E-79
8.40	1.010E-06	2.120E-06	1.450E-32	5.959E-84	2.815E-41	7.711E-90
8.54	9.216E-07	1.928E-06	1.790E-36	6.456E-95	2.378E-46	0.000E+00
8.67	8.397E-07	1.746E-06	6.217E-41	0.000E+00	3.888E-52	0.000E+00
8.80	7.644E-07	1.573E-06	5.083E-46	0.000E+00	9.770E-59	0.000E+00
8.93	6.957E-07	1.410E-06	7.984E-52	0.000E+00	2.902E-66	0.000E+00
9.06	6.334E-07	1.258E-06	1.912E-58	0.000E+00	7.546E-75	0.000E+00
9.19	5.770E-07	1.116E-06	5.362E-66	0.000E+00	1.221E-84	0.000E+00
9.32	5.260E-07	9.848E-07	1.303E-74	0.000E+00	8.330E-96	0.000E+00
9.45	4.800E-07	8.643E-07	1.946E-84	0.000E+00	0.000E+00	0.000E+00
9.59	4.385E-07	7.543E-07	1.208E-95	0.000E+00	0.000E+00	0.000E+00
9.72	4.010E-07	6.545E-07	0.000E+00	0.000E+00	0.000E+00	0.000E+00
9.85	3.672E-07	5.646E-07	0.000E+00	0.000E+00	0.000E+00	0.000E+00
9.98	3.366E-07	4.841E-07	0.000E+00	0.000E+00	0.000E+00	0.000E+00
10.11	3.089E-07	4.126E-07	0.000E+00	0.000E+00	0.000E+00	0.000E+00
10.24	2.837E-07	3.495E-07	0.000E+00	0.000E+00	0.000E+00	0.000E+00
10.37	2.609E-07	2.941E-07	0.000E+00	0.000E+00	0.000E+00	0.000E+00
10.51	2.401E-07	2.459E-07	0.000E+00	0.000E+00	0.000E+00	0.000E+00
10.64	2.211E-07	2.043E-07	0.000E+00	0.000E+00	0.000E+00	0.000E+00
10.77	2.038E-07	1.685E-07	0.000E+00	0.000E+00	0.000E+00	0.000E+00
10.90	1.879E-07	1.381E-07	0.000E+00	0.000E+00	0.000E+00	0.000E+00
11.03	1.733E-07	1.124E-07	0.000E+00	0.000E+00	0.000E+00	0.000E+00
11.16	1.600E-07	9.081E-08	0.000E+00	0.000E+00	0.000E+00	0.000E+00
11.29	1.477E-07	7.284E-08	0.000E+00	0.000E+00	0.000E+00	0.000E+00
11.42	1.363E-07	5.800E-08	0.000E+00	0.000E+00	0.000E+00	0.000E+00
11.56	1.259E-07	4.584E-08	0.000E+00	0.000E+00	0.000E+00	0.000E+00
11.69	1.162E-07	3.595E-08	0.000E+00	0.000E+00	0.000E+00	0.000E+00
11.82	1.072E-07	2.798E-08	0.000E+00	0.000E+00	0.000E+00	0.000E+00
11.95	9.884E-08	2.161E-08	0.000E+00	0.000E+00	0.000E+00	0.000E+00
12.08	9.110E-08	1.655E-08	0.000E+00	0.000E+00	0.000E+00	0.000E+00
12.21	8.388E-08	1.258E-08	0.000E+00	0.000E+00	0.000E+00	0.000E+00
12.34	7.716E-08	9.478E-09	0.000E+00	0.000E+00	0.000E+00	0.000E+00
12.47	7.088E-08	7.083E-09	0.000E+00	0.000E+00	0.000E+00	0.000E+00
12.61	6.500E-08	5.248E-09	0.000E+00	0.000E+00	0.000E+00	0.000E+00
12.74	5.951E-08	3.856E-09	0.000E+00	0.000E+00	0.000E+00	0.000E+00
12.87	5.435E-08	2.808E-09	0.000E+00	0.000E+00	0.000E+00	0.000E+00
13.00	4.952E-08	2.026E-09	0.000E+00	0.000E+00	0.000E+00	0.000E+00

Table I.6 Smoothed C_6H_5, C_6H_6, and mass 80-83 profiles.

HAB (mm)	x_{C6H5}	x_{C6H6}	x_{80}	x_{81}	x_{82}	x_{83}
0.00	1.823E-08	3.969E-03	2.340E-05	3.781E-06	1.025E-05	1.927E-06
0.13	6.275E-08	3.983E-03	2.353E-05	3.802E-06	1.027E-05	1.938E-06
0.26	1.323E-07	3.989E-03	2.365E-05	3.820E-06	1.030E-05	1.947E-06
0.39	2.344E-07	3.989E-03	2.375E-05	3.833E-06	1.032E-05	1.953E-06
0.53	3.763E-07	3.981E-03	2.382E-05	3.840E-06	1.033E-05	1.956E-06
0.66	5.637E-07	3.966E-03	2.385E-05	3.841E-06	1.034E-05	1.955E-06
0.79	7.999E-07	3.944E-03	2.384E-05	3.835E-06	1.035E-05	1.949E-06
0.92	1.085E-06	3.915E-03	2.377E-05	3.821E-06	1.034E-05	1.940E-06
1.05	1.415E-06	3.879E-03	2.364E-05	3.800E-06	1.033E-05	1.926E-06
1.18	1.784E-06	3.837E-03	2.345E-05	3.770E-06	1.031E-05	1.907E-06
1.31	2.181E-06	3.787E-03	2.318E-05	3.732E-06	1.027E-05	1.883E-06
1.44	2.594E-06	3.732E-03	2.284E-05	3.685E-06	1.022E-05	1.855E-06
1.58	3.011E-06	3.671E-03	2.241E-05	3.630E-06	1.016E-05	1.821E-06
1.71	3.417E-06	3.603E-03	2.191E-05	3.566E-06	1.008E-05	1.783E-06
1.84	3.800E-06	3.531E-03	2.132E-05	3.494E-06	9.973E-06	1.740E-06
1.97	4.148E-06	3.453E-03	2.065E-05	3.414E-06	9.847E-06	1.693E-06
2.10	4.455E-06	3.370E-03	1.990E-05	3.326E-06	9.695E-06	1.641E-06
2.23	4.711E-06	3.282E-03	1.907E-05	3.230E-06	9.514E-06	1.586E-06
2.36	4.914E-06	3.190E-03	1.817E-05	3.128E-06	9.301E-06	1.527E-06
2.49	5.062E-06	3.094E-03	1.722E-05	3.020E-06	9.054E-06	1.465E-06
2.63	5.154E-06	2.995E-03	1.621E-05	2.906E-06	8.770E-06	1.400E-06
2.76	5.195E-06	2.893E-03	1.516E-05	2.788E-06	8.446E-06	1.333E-06
2.89	5.186E-06	2.787E-03	1.407E-05	2.665E-06	8.082E-06	1.264E-06
3.02	5.132E-06	2.680E-03	1.298E-05	2.540E-06	7.676E-06	1.194E-06
3.15	5.040E-06	2.570E-03	1.187E-05	2.412E-06	7.228E-06	1.124E-06
3.28	4.913E-06	2.459E-03	1.078E-05	2.282E-06	6.739E-06	1.053E-06
3.41	4.759E-06	2.347E-03	9.704E-06	2.151E-06	6.213E-06	9.830E-07
3.55	4.582E-06	2.234E-03	8.663E-06	2.021E-06	5.655E-06	9.135E-07
3.68	4.387E-06	2.121E-03	7.666E-06	1.891E-06	5.072E-06	8.452E-07
3.81	4.180E-06	2.008E-03	6.722E-06	1.764E-06	4.473E-06	7.787E-07
3.94	3.965E-06	1.896E-03	5.838E-06	1.638E-06	3.870E-06	7.142E-07
4.07	3.746E-06	1.785E-03	5.022E-06	1.516E-06	3.276E-06	6.521E-07
4.20	3.525E-06	1.676E-03	4.276E-06	1.397E-06	2.704E-06	5.926E-07
4.33	3.306E-06	1.569E-03	3.604E-06	1.283E-06	2.169E-06	5.362E-07
4.46	3.090E-06	1.464E-03	3.005E-06	1.173E-06	1.683E-06	4.828E-07
4.60	2.881E-06	1.362E-03	2.478E-06	1.068E-06	1.259E-06	4.327E-07
4.73	2.678E-06	1.264E-03	2.020E-06	9.688E-07	9.021E-07	3.859E-07
4.86	2.484E-06	1.169E-03	1.628E-06	8.751E-07	6.158E-07	3.425E-07
4.99	2.299E-06	1.078E-03	1.297E-06	7.871E-07	3.976E-07	3.025E-07
5.12	2.123E-06	9.912E-04	1.020E-06	7.050E-07	2.409E-07	2.659E-07
5.25	1.958E-06	9.089E-04	7.925E-07	6.287E-07	1.358E-07	2.325E-07
5.38	1.801E-06	8.309E-04	6.078E-07	5.583E-07	7.048E-08	2.023E-07
5.52	1.655E-06	7.576E-04	4.600E-07	4.936E-07	3.329E-08	1.751E-07
5.65	1.519E-06	6.889E-04	3.435E-07	4.345E-07	1.412E-08	1.508E-07
5.78	1.392E-06	6.248E-04	2.530E-07	3.808E-07	5.297E-09	1.291E-07
5.91	1.273E-06	5.653E-04	1.837E-07	3.322E-07	1.728E-09	1.100E-07
6.04	1.164E-06	5.102E-04	1.315E-07	2.885E-07	4.803E-10	9.326E-08
6.17	1.063E-06	4.594E-04	9.276E-08	2.494E-07	1.113E-10	7.861E-08
6.30	9.690E-07	4.128E-04	6.445E-08	2.145E-07	2.095E-11	6.591E-08
6.43	8.828E-07	3.701E-04	4.409E-08	1.837E-07	3.112E-12	5.495E-08
6.57	8.034E-07	3.312E-04	2.970E-08	1.566E-07	3.527E-13	4.556E-08
6.70	7.305E-07	2.959E-04	1.968E-08	1.329E-07	2.936E-14	3.756E-08

HAB (mm)	x_{C6H5}	x_{C6H6}	x_{80}	x_{81}	x_{82}	x_{83}
6.83	6.635E-07	2.639E-04	1.283E-08	1.122E-07	1.720E-15	3.080E-08
6.96	6.020E-07	2.350E-04	8.230E-09	9.423E-08	6.744E-17	2.510E-08
7.09	5.458E-07	2.089E-04	5.189E-09	7.877E-08	1.674E-18	2.035E-08
7.22	4.942E-07	1.855E-04	3.215E-09	6.553E-08	2.465E-20	1.639E-08
7.35	4.471E-07	1.645E-04	1.957E-09	5.424E-08	2.002E-22	1.313E-08
7.48	4.041E-07	1.457E-04	1.171E-09	4.467E-08	8.248E-25	1.046E-08
7.62	3.647E-07	1.289E-04	6.874E-10	3.660E-08	1.567E-27	8.276E-09
7.75	3.288E-07	1.140E-04	3.963E-10	2.984E-08	1.232E-30	6.512E-09
7.88	2.961E-07	1.007E-04	2.241E-10	2.420E-08	3.538E-34	5.092E-09
8.01	2.662E-07	8.885E-05	1.244E-10	1.953E-08	3.224E-38	3.958E-09
8.14	2.390E-07	7.836E-05	6.768E-11	1.567E-08	7.934E-43	3.058E-09
8.27	2.141E-07	6.906E-05	3.611E-11	1.251E-08	4.387E-48	2.347E-09
8.40	1.915E-07	6.083E-05	1.888E-11	9.935E-09	4.421E-54	1.791E-09
8.54	1.710E-07	5.356E-05	9.670E-12	7.848E-09	6.392E-61	1.357E-09
8.67	1.522E-07	4.713E-05	4.851E-12	6.165E-09	1.010E-68	1.023E-09
8.80	1.352E-07	4.146E-05	2.383E-12	4.817E-09	1.277E-77	7.653E-10
8.93	1.196E-07	3.645E-05	1.146E-12	3.743E-09	9.076E-88	5.691E-10
9.06	1.055E-07	3.204E-05	5.391E-13	2.893E-09	2.419E-99	4.205E-10
9.19	9.267E-08	2.816E-05	2.481E-13	2.223E-09	0.000E+00	3.086E-10
9.32	8.098E-08	2.474E-05	1.116E-13	1.699E-09	0.000E+00	2.250E-10
9.45	7.034E-08	2.173E-05	4.910E-14	1.291E-09	0.000E+00	1.630E-10
9.59	6.067E-08	1.908E-05	2.111E-14	9.754E-10	0.000E+00	1.172E-10
9.72	5.188E-08	1.675E-05	8.853E-15	7.327E-10	0.000E+00	8.379E-11
9.85	4.388E-08	1.470E-05	3.635E-15	5.472E-10	0.000E+00	5.947E-11
9.98	3.660E-08	1.291E-05	1.455E-15	4.064E-10	0.000E+00	4.192E-11
10.11	2.999E-08	1.133E-05	5.687E-16	3.000E-10	0.000E+00	2.935E-11
10.24	2.397E-08	9.940E-06	2.168E-16	2.202E-10	0.000E+00	2.040E-11
10.37	1.850E-08	8.722E-06	8.061E-17	1.606E-10	0.000E+00	1.408E-11
10.51	1.352E-08	7.652E-06	2.922E-17	1.165E-10	0.000E+00	9.655E-12
10.64	8.999E-09	6.713E-06	1.033E-17	8.395E-11	0.000E+00	6.572E-12
10.77	4.885E-09	5.890E-06	3.556E-18	6.015E-11	0.000E+00	4.442E-12
10.90	1.144E-09	5.166E-06	1.193E-18	4.283E-11	0.000E+00	2.980E-12
11.03	0.000E+00	4.532E-06	3.895E-19	3.031E-11	0.000E+00	1.985E-12
11.16	0.000E+00	3.975E-06	1.238E-19	2.132E-11	0.000E+00	1.313E-12
11.29	0.000E+00	3.487E-06	3.831E-20	1.490E-11	0.000E+00	8.620E-13
11.42	0.000E+00	3.058E-06	1.153E-20	1.035E-11	0.000E+00	5.618E-13
11.56	0.000E+00	2.682E-06	3.374E-21	7.147E-12	0.000E+00	3.634E-13
11.69	0.000E+00	2.352E-06	9.601E-22	4.902E-12	0.000E+00	2.333E-13
11.82	0.000E+00	2.063E-06	2.655E-22	3.341E-12	0.000E+00	1.487E-13
11.95	0.000E+00	1.809E-06	7.133E-23	2.262E-12	0.000E+00	9.406E-14
12.08	0.000E+00	1.587E-06	1.861E-23	1.522E-12	0.000E+00	5.904E-14
12.21	0.000E+00	1.392E-06	4.716E-24	1.018E-12	0.000E+00	3.678E-14
12.34	0.000E+00	1.221E-06	1.160E-24	6.759E-13	0.000E+00	2.274E-14
12.47	0.000E+00	1.071E-06	2.768E-25	4.460E-13	0.000E+00	1.395E-14
12.61	0.000E+00	9.388E-07	6.406E-26	2.923E-13	0.000E+00	8.490E-15
12.74	0.000E+00	8.234E-07	1.438E-26	1.903E-13	0.000E+00	5.128E-15
12.87	0.000E+00	7.221E-07	3.128E-27	1.231E-13	0.000E+00	3.073E-15
13.00	0.000E+00	6.333E-07	6.594E-28	7.909E-14	0.000E+00	1.827E-15

Table I.7 Smoothed mass 84-86 and mass 94 profiles.

HAB (mm)	x_{84}	x_{85}	x_{86}	x_{94}
0.00	4.680E-06	8.136E-07	1.282E-07	1.364E-05
0.13	4.699E-06	8.182E-07	1.431E-07	1.374E-05
0.26	4.716E-06	8.221E-07	1.593E-07	1.387E-05
0.39	4.729E-06	8.244E-07	1.770E-07	1.403E-05
0.53	4.738E-06	8.246E-07	1.962E-07	1.421E-05
0.66	4.742E-06	8.222E-07	2.170E-07	1.443E-05
0.79	4.741E-06	8.165E-07	2.393E-07	1.468E-05
0.92	4.736E-06	8.070E-07	2.630E-07	1.495E-05
1.05	4.724E-06	7.932E-07	2.882E-07	1.524E-05
1.18	4.706E-06	7.749E-07	3.147E-07	1.556E-05
1.31	4.681E-06	7.518E-07	3.423E-07	1.590E-05
1.44	4.648E-06	7.238E-07	3.707E-07	1.627E-05
1.58	4.608E-06	6.911E-07	3.998E-07	1.666E-05
1.71	4.559E-06	6.538E-07	4.291E-07	1.706E-05
1.84	4.501E-06	6.124E-07	4.582E-07	1.749E-05
1.97	4.434E-06	5.676E-07	4.866E-07	1.792E-05
2.10	4.357E-06	5.202E-07	5.138E-07	1.838E-05
2.23	4.270E-06	4.711E-07	5.393E-07	1.884E-05
2.36	4.173E-06	4.211E-07	5.626E-07	1.931E-05
2.49	4.067E-06	3.714E-07	5.830E-07	1.979E-05
2.63	3.950E-06	3.229E-07	6.001E-07	2.028E-05
2.76	3.825E-06	2.766E-07	6.135E-07	2.076E-05
2.89	3.690E-06	2.332E-07	6.227E-07	2.123E-05
3.02	3.547E-06	1.934E-07	6.276E-07	2.170E-05
3.15	3.397E-06	1.577E-07	6.280E-07	2.216E-05
3.28	3.240E-06	1.263E-07	6.238E-07	2.260E-05
3.41	3.078E-06	9.927E-08	6.153E-07	2.302E-05
3.55	2.912E-06	7.653E-08	6.026E-07	2.341E-05
3.68	2.742E-06	5.783E-08	5.861E-07	2.376E-05
3.81	2.571E-06	4.279E-08	5.663E-07	2.409E-05
3.94	2.399E-06	3.099E-08	5.435E-07	2.437E-05
4.07	2.228E-06	2.195E-08	5.185E-07	2.460E-05
4.20	2.059E-06	1.519E-08	4.916E-07	2.478E-05
4.33	1.894E-06	1.027E-08	4.635E-07	2.490E-05
4.46	1.733E-06	6.773E-09	4.347E-07	2.496E-05
4.60	1.577E-06	4.356E-09	4.057E-07	2.496E-05
4.73	1.429E-06	2.730E-09	3.768E-07	2.488E-05
4.86	1.287E-06	1.666E-09	3.485E-07	2.474E-05
4.99	1.153E-06	9.888E-10	3.210E-07	2.452E-05
5.12	1.028E-06	5.708E-10	2.946E-07	2.422E-05
5.25	9.119E-07	3.201E-10	2.695E-07	2.385E-05
5.38	8.045E-07	1.743E-10	2.457E-07	2.341E-05
5.52	7.060E-07	9.207E-11	2.235E-07	2.288E-05
5.65	6.163E-07	4.715E-11	2.027E-07	2.229E-05
5.78	5.354E-07	2.339E-11	1.834E-07	2.163E-05
5.91	4.628E-07	1.123E-11	1.656E-07	2.090E-05
6.04	3.982E-07	5.218E-12	1.493E-07	2.010E-05
6.17	3.410E-07	2.343E-12	1.344E-07	1.926E-05
6.30	2.909E-07	1.016E-12	1.207E-07	1.837E-05
6.43	2.473E-07	4.253E-13	1.083E-07	1.743E-05
6.57	2.095E-07	1.717E-13	9.711E-08	1.647E-05
6.70	1.771E-07	6.681E-14	8.696E-08	1.548E-05

HAB (mm)	x_{84}	x_{85}	x_{86}	x_{94}
6.83	1.494E-07	2.504E-14	7.780E-08	1.447E-05
6.96	1.260E-07	9.028E-15	6.956E-08	1.346E-05
7.09	1.064E-07	3.131E-15	6.215E-08	1.246E-05
7.22	8.994E-08	1.043E-15	5.549E-08	1.146E-05
7.35	7.635E-08	3.338E-16	4.953E-08	1.048E-05
7.48	6.517E-08	1.025E-16	4.420E-08	9.534E-06
7.62	5.604E-08	3.017E-17	3.943E-08	8.618E-06
7.75	4.864E-08	8.511E-18	3.517E-08	7.742E-06
7.88	4.268E-08	2.298E-18	3.137E-08	6.911E-06
8.01	3.791E-08	5.938E-19	2.798E-08	6.130E-06
8.14	3.412E-08	1.467E-19	2.496E-08	5.401E-06
8.27	3.113E-08	3.460E-20	2.227E-08	4.726E-06
8.40	2.879E-08	7.794E-21	1.988E-08	4.108E-06
8.54	2.697E-08	1.675E-21	1.775E-08	3.545E-06
8.67	2.556E-08	3.429E-22	1.585E-08	3.037E-06
8.80	2.447E-08	6.689E-23	1.416E-08	2.582E-06
8.93	2.365E-08	1.242E-23	1.267E-08	2.179E-06
9.06	2.302E-08	2.193E-24	1.133E-08	1.825E-06
9.19	2.254E-08	3.680E-25	1.015E-08	1.517E-06
9.32	2.218E-08	5.864E-26	9.099E-09	1.250E-06
9.45	2.191E-08	8.869E-27	8.165E-09	1.022E-06
9.59	2.171E-08	1.272E-27	7.336E-09	8.287E-07
9.72	2.155E-08	1.728E-28	6.599E-09	6.663E-07
9.85	2.144E-08	2.224E-29	5.945E-09	5.310E-07
9.98	2.135E-08	2.708E-30	5.364E-09	4.196E-07
10.11	2.129E-08	3.117E-31	4.848E-09	3.285E-07
10.24	2.124E-08	3.389E-32	4.390E-09	2.549E-07
10.37	2.120E-08	3.479E-33	3.983E-09	1.960E-07
10.51	2.117E-08	3.370E-34	3.622E-09	1.493E-07
10.64	2.115E-08	3.077E-35	3.302E-09	1.126E-07
10.77	2.113E-08	2.646E-36	3.017E-09	8.410E-08
10.90	2.112E-08	2.142E-37	2.764E-09	6.221E-08
11.03	2.110E-08	1.631E-38	2.540E-09	4.555E-08
11.16	2.109E-08	1.167E-39	2.341E-09	3.302E-08
11.29	2.108E-08	7.844E-41	2.164E-09	2.369E-08
11.42	2.107E-08	4.948E-42	2.007E-09	1.681E-08
11.56	2.107E-08	2.927E-43	1.867E-09	1.181E-08
11.69	2.106E-08	1.622E-44	1.744E-09	8.205E-09
11.82	2.106E-08	8.421E-46	1.634E-09	5.638E-09
11.95	2.105E-08	4.090E-47	1.536E-09	3.832E-09
12.08	2.105E-08	1.857E-48	1.449E-09	2.575E-09
12.21	2.104E-08	7.881E-50	1.372E-09	1.710E-09
12.34	2.104E-08	3.122E-51	1.304E-09	1.123E-09
12.47	2.104E-08	1.154E-52	1.243E-09	7.288E-10
12.61	2.103E-08	3.976E-54	1.190E-09	4.674E-10
12.74	2.103E-08	1.276E-55	1.142E-09	2.961E-10
12.87	2.103E-08	3.813E-57	1.099E-09	1.853E-10
13.00	2.103E-08	1.060E-58	1.061E-09	1.146E-10

Appendix J. Species Fluxes and Element Flux Balances.

Molar fluxes for 18 important species were calculated from Equation 3-24 by the FBR program (documented in Appendix D). Units are mol/cm^{2}s. Mole fractions of H atom and OH were calibrated by the partial equilibrium method.

Elemental mass flux balances for C, H, O and Ar were also computed from these 18 species, plus argon, and are given in Table J.4. Details of the calculation method are also given in Appendix D.

Table J.1 Experimental molar fluxes for C_6H_6, mass 94 (as C_6H_5OH), C_6H_5, mass 66 (as C_5H_6), mass 54 (as 1,3-C_4H_6) and mass 42 (as C_3H_6).

HAB (mm)	F_{C6H6}	F_{94}	F_{C6H5}	F_{66}	F_{54}	F_{42}
0.07	3.776E-07	1.267E-09	-2.207E-11	4.939E-10	3.218E-10	1.650E-08
0.20	3.747E-07	1.253E-09	-2.546E-11	4.893E-10	3.245E-10	1.623E-08
0.33	3.708E-07	1.234E-09	-3.012E-11	4.829E-10	3.298E-10	1.589E-08
0.46	3.668E-07	1.214E-09	-3.470E-11	4.765E-10	3.360E-10	1.555E-08
0.60	3.625E-07	1.192E-09	-3.937E-11	4.694E-10	3.449E-10	1.522E-08
0.73	3.582E-07	1.168E-09	-4.346E-11	4.621E-10	3.574E-10	1.494E-08
0.86	3.539E-07	1.144E-09	-4.638E-11	4.546E-10	3.751E-10	1.475E-08
0.99	3.498E-07	1.119E-09	-4.736E-11	4.473E-10	3.999E-10	1.470E-08
1.12	3.460E-07	1.095E-09	-4.588E-11	4.403E-10	4.330E-10	1.482E-08
1.25	3.428E-07	1.072E-09	-4.127E-11	4.337E-10	4.761E-10	1.515E-08
1.38	3.400E-07	1.050E-09	-3.391E-11	4.277E-10	5.284E-10	1.567E-08
1.51	3.379E-07	1.031E-09	-2.232E-11	4.225E-10	5.934E-10	1.646E-08
1.65	3.361E-07	1.011E-09	-1.027E-11	4.173E-10	6.613E-10	1.733E-08
1.78	3.352E-07	1.000E-09	1.146E-11	4.143E-10	7.560E-10	1.868E-08
1.91	3.349E-07	9.936E-10	3.843E-11	4.126E-10	8.654E-10	2.029E-08
2.04	3.350E-07	9.929E-10	7.053E-11	4.123E-10	9.881E-10	2.212E-08
2.17	3.354E-07	9.983E-10	1.073E-10	4.133E-10	1.123E-09	2.411E-08
2.30	3.359E-07	1.010E-09	1.483E-10	4.158E-10	1.266E-09	2.621E-08
2.43	3.363E-07	1.029E-09	1.925E-10	4.196E-10	1.416E-09	2.834E-08
2.56	3.365E-07	1.055E-09	2.390E-10	4.247E-10	1.569E-09	3.043E-08
2.70	3.363E-07	1.087E-09	2.866E-10	4.311E-10	1.721E-09	3.239E-08
2.83	3.355E-07	1.126E-09	3.341E-10	4.387E-10	1.868E-09	3.416E-08
2.96	3.341E-07	1.172E-09	3.800E-10	4.473E-10	2.005E-09	3.565E-08
3.09	3.319E-07	1.224E-09	4.233E-10	4.569E-10	2.130E-09	3.680E-08
3.22	3.289E-07	1.281E-09	4.626E-10	4.673E-10	2.238E-09	3.757E-08
3.35	3.251E-07	1.345E-09	4.976E-10	4.787E-10	2.329E-09	3.794E-08
3.48	3.204E-07	1.414E-09	5.272E-10	4.909E-10	2.401E-09	3.789E-08
3.62	3.149E-07	1.488E-09	5.511E-10	5.038E-10	2.451E-09	3.743E-08
3.75	3.085E-07	1.567E-09	5.688E-10	5.174E-10	2.480E-09	3.656E-08
3.88	3.014E-07	1.650E-09	5.802E-10	5.317E-10	2.488E-09	3.532E-08
4.01	2.935E-07	1.736E-09	5.855E-10	5.466E-10	2.476E-09	3.375E-08
4.14	2.848E-07	1.826E-09	5.849E-10	5.619E-10	2.445E-09	3.191E-08

HAB (mm)	F_{C6H6}	F_{94}	F_{C6H5}	F_{66}	F_{54}	F_{42}
4.27	2.756E-07	1.917E-09	5.789E-10	5.777E-10	2.397E-09	2.985E-08
4.40	2.658E-07	2.011E-09	5.680E-10	5.938E-10	2.334E-09	2.764E-08
4.53	2.554E-07	2.104E-09	5.527E-10	6.102E-10	2.259E-09	2.533E-08
4.67	2.447E-07	2.197E-09	5.338E-10	6.266E-10	2.173E-09	2.300E-08
4.80	2.335E-07	2.289E-09	5.120E-10	6.429E-10	2.080E-09	2.069E-08
4.93	2.222E-07	2.377E-09	4.879E-10	6.591E-10	1.982E-09	1.846E-08
5.06	2.106E-07	2.462E-09	4.622E-10	6.748E-10	1.881E-09	1.635E-08
5.19	1.989E-07	2.541E-09	4.355E-10	6.900E-10	1.780E-09	1.439E-08
5.32	1.872E-07	2.613E-09	4.083E-10	7.046E-10	1.678E-09	1.259E-08
5.45	1.756E-07	2.678E-09	3.812E-10	7.182E-10	1.580E-09	1.099E-08
5.59	1.641E-07	2.734E-09	3.546E-10	7.308E-10	1.484E-09	9.572E-09
5.72	1.528E-07	2.779E-09	3.286E-10	7.421E-10	1.393E-09	8.343E-09
5.85	1.417E-07	2.814E-09	3.037E-10	7.520E-10	1.307E-09	7.293E-09
5.98	1.310E-07	2.838E-09	2.799E-10	7.603E-10	1.226E-09	6.408E-09
6.11	1.206E-07	2.849E-09	2.575E-10	7.669E-10	1.151E-09	5.670E-09
6.24	1.106E-07	2.847E-09	2.364E-10	7.715E-10	1.081E-09	5.060E-09
6.37	1.011E-07	2.831E-09	2.166E-10	7.741E-10	1.015E-09	4.560E-09
6.50	9.211E-08	2.803E-09	1.983E-10	7.745E-10	9.554E-10	4.150E-09
6.64	8.360E-08	2.761E-09	1.813E-10	7.726E-10	8.999E-10	3.812E-09
6.77	7.562E-08	2.706E-09	1.657E-10	7.684E-10	8.486E-10	3.531E-09
6.90	6.818E-08	2.638E-09	1.512E-10	7.617E-10	8.013E-10	3.293E-09
7.03	6.127E-08	2.559E-09	1.380E-10	7.526E-10	7.574E-10	3.086E-09
7.16	5.490E-08	2.468E-09	1.258E-10	7.411E-10	7.168E-10	2.902E-09
7.29	4.905E-08	2.368E-09	1.146E-10	7.271E-10	6.789E-10	2.734E-09
7.42	4.370E-08	2.259E-09	1.044E-10	7.108E-10	6.436E-10	2.578E-09
7.55	3.884E-08	2.142E-09	9.502E-11	6.923E-10	6.107E-10	2.429E-09
7.69	3.444E-08	2.019E-09	8.645E-11	6.717E-10	5.798E-10	2.287E-09
7.82	3.048E-08	1.892E-09	7.861E-11	6.491E-10	5.509E-10	2.151E-09
7.95	2.693E-08	1.762E-09	7.144E-11	6.247E-10	5.237E-10	2.022E-09
8.07	2.375E-08	1.630E-09	6.489E-11	5.988E-10	4.982E-10	1.898E-09
8.21	2.091E-08	1.498E-09	5.890E-11	5.715E-10	4.741E-10	1.780E-09
8.34	1.839E-08	1.367E-09	5.342E-11	5.431E-10	4.514E-10	1.669E-09
8.47	1.616E-08	1.239E-09	4.842E-11	5.137E-10	4.301E-10	1.566E-09
8.61	1.419E-08	1.115E-09	4.384E-11	4.837E-10	4.099E-10	1.469E-09
8.73	1.245E-08	9.952E-10	3.967E-11	4.533E-10	3.910E-10	1.380E-09
8.87	1.093E-08	8.815E-10	3.585E-11	4.228E-10	3.731E-10	1.298E-09
8.99	9.585E-09	7.743E-10	3.235E-11	3.923E-10	3.562E-10	1.223E-09
9.13	8.408E-09	6.741E-10	2.915E-11	3.621E-10	3.403E-10	1.153E-09
9.26	7.375E-09	5.813E-10	2.620E-11	3.325E-10	3.252E-10	1.089E-09
9.39	6.469E-09	4.963E-10	2.349E-11	3.035E-10	3.110E-10	1.030E-09
9.52	5.673E-09	4.190E-10	2.099E-11	2.755E-10	2.976E-10	9.754E-10
9.65	4.974E-09	3.496E-10	1.868E-11	2.485E-10	2.848E-10	9.245E-10
9.79	4.361E-09	2.878E-10	1.654E-11	2.228E-10	2.728E-10	8.770E-10
9.91	3.823E-09	2.334E-10	1.456E-11	1.984E-10	2.613E-10	8.325E-10
10.05	3.349E-09	1.859E-10	1.272E-11	1.753E-10	2.504E-10	7.908E-10
10.18	2.932E-09	1.451E-10	1.101E-11	1.537E-10	2.401E-10	7.515E-10
10.31	2.565E-09	1.103E-10	9.427E-12	1.336E-10	2.302E-10	7.145E-10
10.44	2.242E-09	8.124E-11	7.969E-12	1.152E-10	2.209E-10	6.796E-10
10.58	1.958E-09	5.735E-11	6.635E-12	9.838E-11	2.120E-10	6.467E-10
10.71	1.709E-09	3.817E-11	5.427E-12	8.326E-11	2.035E-10	6.158E-10
10.84	1.494E-09	2.321E-11	4.347E-12	6.983E-11	1.955E-10	5.869E-10
10.97	1.308E-09	1.199E-11	3.398E-12	5.808E-11	1.880E-10	5.600E-10
11.10	1.149E-09	4.005E-12	2.580E-12	4.795E-11	1.809E-10	5.350E-10
11.23	1.013E-09	-1.242E-12	1.891E-12	3.935E-11	1.743E-10	5.120E-10
11.36	8.992E-10	-4.264E-12	1.327E-12	3.219E-11	1.682E-10	4.907E-10

HAB (mm)	F_{C6H6}	F_{94}	F_{C6H5}	F_{66}	F_{54}	F_{42}
11.49	8.134E-10	-4.350E-12	9.667E-13	2.733E-11	1.625E-10	4.717E-10
11.63	7.313E-10	-4.584E-12	6.268E-13	2.255E-11	1.570E-10	4.532E-10
11.76	6.618E-10	-3.907E-12	3.833E-13	1.873E-11	1.518E-10	4.359E-10
11.89	5.998E-10	-2.932E-12	2.051E-13	1.552E-11	1.468E-10	4.194E-10
12.02	5.448E-10	-1.757E-12	9.385E-14	1.292E-11	1.419E-10	4.034E-10
12.15	4.941E-10	-6.839E-13	3.134E-14	1.076E-11	1.370E-10	3.877E-10
12.28	4.456E-10	9.071E-14	2.139E-15	8.928E-12	1.321E-10	3.720E-10
12.41	3.987E-10	5.391E-13	-7.549E-15	7.333E-12	1.272E-10	3.560E-10
12.54	3.529E-10	6.931E-13	-7.745E-15	5.906E-12	1.221E-10	3.398E-10
12.68	3.098E-10	6.502E-13	-5.125E-15	4.664E-12	1.170E-10	3.236E-10
12.81	2.668E-10	5.009E-13	-1.722E-15	3.462E-12	1.119E-10	3.071E-10
12.94	2.335E-10	3.312E-13	-9.690E-17	2.623E-12	1.075E-10	2.931E-10

Table J.2 Experimental molar fluxes for C_2H_4, C_2H_2, CH_4, CH_3, H_2CO and CO_2.

HAB (mm)	F_{C2H4}	F_{C2H2}	F_{CH4}	F_{CH3}	F_{H2CO}	F_{CO2}
0.07	4.366E-08	5.417E-09	1.526E-07	3.945E-09	2.627E-08	5.333E-08
0.20	4.393E-08	5.335E-09	1.535E-07	3.711E-09	2.624E-08	5.246E-08
0.33	4.455E-08	5.246E-09	1.546E-07	3.388E-09	2.620E-08	5.157E-08
0.46	4.525E-08	5.158E-09	1.557E-07	3.051E-09	2.616E-08	5.071E-08
0.60	4.619E-08	5.071E-09	1.568E-07	2.666E-09	2.613E-08	4.992E-08
0.73	4.735E-08	4.984E-09	1.578E-07	2.236E-09	2.609E-08	4.920E-08
0.86	4.875E-08	4.894E-09	1.586E-07	1.754E-09	2.605E-08	4.854E-08
0.99	5.039E-08	4.800E-09	1.591E-07	1.218E-09	2.600E-08	4.793E-08
1.12	5.225E-08	4.699E-09	1.592E-07	6.255E-10	2.596E-08	4.734E-08
1.25	5.433E-08	4.590E-09	1.588E-07	-2.089E-11	2.591E-08	4.676E-08
1.38	5.661E-08	4.470E-09	1.580E-07	-7.194E-10	2.587E-08	4.616E-08
1.51	5.912E-08	4.347E-09	1.566E-07	-1.459E-09	2.582E-08	4.560E-08
1.65	6.167E-08	4.208E-09	1.551E-07	-2.244E-09	2.578E-08	4.493E-08
1.78	6.468E-08	4.064E-09	1.522E-07	-3.037E-09	2.574E-08	4.457E-08
1.91	6.792E-08	3.999E-09	1.487E-07	-3.816E-09	2.571E-08	4.440E-08
2.04	7.137E-08	3.932E-09	1.447E-07	-4.551E-09	2.570E-08	4.444E-08
2.17	7.500E-08	3.903E-09	1.402E-07	-5.212E-09	2.571E-08	4.476E-08
2.30	7.878E-08	3.921E-09	1.354E-07	-5.763E-09	2.575E-08	4.539E-08
2.43	8.268E-08	3.996E-09	1.305E-07	-6.172E-09	2.583E-08	4.636E-08
2.56	8.664E-08	4.134E-09	1.258E-07	-6.402E-09	2.598E-08	4.769E-08
2.70	9.062E-08	4.343E-09	1.216E-07	-6.422E-09	2.619E-08	4.938E-08
2.83	9.456E-08	4.627E-09	1.181E-07	-6.198E-09	2.651E-08	5.144E-08
2.96	9.839E-08	4.990E-09	1.157E-07	-5.703E-09	2.694E-08	5.385E-08
3.09	1.021E-07	5.435E-09	1.148E-07	-4.913E-09	2.750E-08	5.657E-08
3.22	1.056E-07	5.963E-09	1.157E-07	-3.810E-09	2.823E-08	5.960E-08
3.35	1.088E-07	6.577E-09	1.188E-07	-2.378E-09	2.915E-08	6.293E-08
3.48	1.118E-07	7.276E-09	1.243E-07	-6.089E-10	3.027E-08	6.654E-08
3.62	1.144E-07	8.059E-09	1.325E-07	1.497E-09	3.161E-08	7.041E-08
3.75	1.167E-07	8.927E-09	1.437E-07	3.932E-09	3.319E-08	7.454E-08
3.88	1.186E-07	9.876E-09	1.579E-07	6.682E-09	3.501E-08	7.891E-08
4.01	1.202E-07	1.090E-08	1.753E-07	9.724E-09	3.707E-08	8.352E-08
4.14	1.213E-07	1.201E-08	1.958E-07	1.303E-08	3.934E-08	8.834E-08
4.27	1.220E-07	1.318E-08	2.191E-07	1.656E-08	4.182E-08	9.338E-08
4.40	1.223E-07	1.443E-08	2.451E-07	2.026E-08	4.446E-08	9.861E-08
4.53	1.222E-07	1.573E-08	2.734E-07	2.410E-08	4.722E-08	1.040E-07
4.67	1.216E-07	1.708E-08	3.035E-07	2.799E-08	5.004E-08	1.096E-07
4.80	1.207E-07	1.848E-08	3.346E-07	3.190E-08	5.285E-08	1.153E-07

HAB (mm)	F_{C2H4}	F_{C2H2}	F_{CH4}	F_{CH3}	F_{H2CO}	F_{CO2}
4.93	1.194E-07	1.991E-08	3.663E-07	3.574E-08	5.558E-08	1.211E-07
5.06	1.177E-07	2.137E-08	3.976E-07	3.946E-08	5.814E-08	1.271E-07
5.19	1.156E-07	2.286E-08	4.278E-07	4.298E-08	6.045E-08	1.332E-07
5.32	1.132E-07	2.435E-08	4.561E-07	4.626E-08	6.243E-08	1.394E-07
5.45	1.105E-07	2.585E-08	4.817E-07	4.922E-08	6.401E-08	1.456E-07
5.59	1.076E-07	2.734E-08	5.040E-07	5.183E-08	6.511E-08	1.520E-07
5.72	1.044E-07	2.882E-08	5.222E-07	5.402E-08	6.567E-08	1.585E-07
5.85	1.009E-07	3.027E-08	5.358E-07	5.578E-08	6.565E-08	1.650E-07
5.98	9.732E-08	3.169E-08	5.444E-07	5.706E-08	6.502E-08	1.716E-07
6.11	9.354E-08	3.308E-08	5.479E-07	5.785E-08	6.377E-08	1.783E-07
6.24	8.963E-08	3.441E-08	5.459E-07	5.815E-08	6.191E-08	1.851E-07
6.37	8.561E-08	3.569E-08	5.387E-07	5.795E-08	5.945E-08	1.920E-07
6.50	8.153E-08	3.691E-08	5.265E-07	5.728E-08	5.647E-08	1.990E-07
6.64	7.741E-08	3.806E-08	5.096E-07	5.615E-08	5.301E-08	2.060E-07
6.77	7.328E-08	3.913E-08	4.884E-07	5.460E-08	4.915E-08	2.130E-07
6.90	6.917E-08	4.011E-08	4.636E-07	5.265E-08	4.498E-08	2.201E-07
7.03	6.509E-08	4.100E-08	4.359E-07	5.037E-08	4.058E-08	2.273E-07
7.16	6.107E-08	4.180E-08	4.059E-07	4.779E-08	3.606E-08	2.345E-07
7.29	5.713E-08	4.250E-08	3.744E-07	4.497E-08	3.151E-08	2.417E-07
7.42	5.329E-08	4.311E-08	3.421E-07	4.196E-08	2.702E-08	2.490E-07
7.55	4.956E-08	4.361E-08	3.097E-07	3.883E-08	2.269E-08	2.563E-07
7.69	4.596E-08	4.400E-08	2.779E-07	3.563E-08	1.858E-08	2.635E-07
7.82	4.251E-08	4.429E-08	2.472E-07	3.240E-08	1.475E-08	2.708E-07
7.95	3.920E-08	4.448E-08	2.182E-07	2.921E-08	1.127E-08	2.780E-07
8.07	3.604E-08	4.456E-08	1.912E-07	2.609E-08	8.154E-09	2.853E-07
8.21	3.304E-08	4.454E-08	1.664E-07	2.308E-08	5.431E-09	2.925E-07
8.34	3.021E-08	4.442E-08	1.441E-07	2.021E-08	3.105E-09	2.998E-07
8.47	2.754E-08	4.420E-08	1.243E-07	1.752E-08	1.171E-09	3.070E-07
8.61	2.504E-08	4.388E-08	1.070E-07	1.502E-08	-3.891E-10	3.142E-07
8.73	2.270E-08	4.348E-08	9.220E-08	1.273E-08	-1.601E-09	3.215E-07
8.87	2.051E-08	4.298E-08	7.969E-08	1.065E-08	-2.500E-09	3.287E-07
8.99	1.849E-08	4.239E-08	6.927E-08	8.794E-09	-3.123E-09	3.360E-07
9.13	1.660E-08	4.173E-08	6.073E-08	7.151E-09	-3.511E-09	3.433E-07
9.26	1.486E-08	4.098E-08	5.382E-08	5.717E-09	-3.705E-09	3.505E-07
9.39	1.326E-08	4.017E-08	4.831E-08	4.481E-09	-3.745E-09	3.578E-07
9.52	1.178E-08	3.930E-08	4.394E-08	3.432E-09	-3.666E-09	3.651E-07
9.65	1.042E-08	3.837E-08	4.052E-08	2.555E-09	-3.501E-09	3.724E-07
9.79	9.169E-09	3.739E-08	3.783E-08	1.833E-09	-3.276E-09	3.796E-07
9.91	8.027E-09	3.636E-08	3.570E-08	1.251E-09	-3.013E-09	3.869E-07
10.05	6.981E-09	3.529E-08	3.398E-08	7.900E-10	-2.728E-09	3.942E-07
10.18	6.024E-09	3.418E-08	3.255E-08	4.344E-10	-2.436E-09	4.016E-07
10.31	5.151E-09	3.304E-08	3.133E-08	1.680E-10	-2.145E-09	4.090E-07
10.44	4.360E-09	3.188E-08	3.023E-08	-2.416E-11	-1.859E-09	4.164E-07
10.58	3.646E-09	3.070E-08	2.922E-08	-1.555E-10	-1.581E-09	4.239E-07
10.71	3.007E-09	2.951E-08	2.826E-08	-2.379E-10	-1.311E-09	4.314E-07
10.84	2.440E-09	2.832E-08	2.735E-08	-2.815E-10	-1.049E-09	4.389E-07
10.97	1.945E-09	2.714E-08	2.649E-08	-2.953E-10	-7.939E-10	4.463E-07
11.10	1.518E-09	2.597E-08	2.567E-08	-2.872E-10	-5.446E-10	4.537E-07
11.23	1.156E-09	2.483E-08	2.490E-08	-2.639E-10	-3.008E-10	4.608E-07
11.36	8.559E-10	2.373E-08	2.419E-08	-2.311E-10	-6.206E-11	4.678E-07
11.49	6.578E-10	2.265E-08	2.350E-08	-1.939E-10	1.822E-10	4.752E-07
11.63	4.666E-10	2.161E-08	2.290E-08	-1.570E-10	4.282E-10	4.823E-07
11.76	3.222E-10	2.060E-08	2.235E-08	-1.204E-10	6.767E-10	4.895E-07
11.89	2.094E-10	1.961E-08	2.183E-08	-8.679E-11	9.299E-10	4.968E-07
12.02	1.304E-10	1.865E-08	2.134E-08	-5.757E-11	1.191E-09	5.046E-07

HAB (mm)	F_{C2H4}	F_{C2H2}	F_{CH4}	F_{CH3}	F_{H2CO}	F_{CO2}
12.15	7.732E-11	1.770E-08	2.084E-08	-3.427E-11	1.465E-09	5.130E-07
12.28	4.356E-11	1.675E-08	2.032E-08	-1.795E-11	1.758E-09	5.224E-07
12.41	2.330E-11	1.580E-08	1.976E-08	-7.660E-12	2.075E-09	5.330E-07
12.54	1.166E-11	1.485E-08	1.917E-08	-2.109E-12	2.415E-09	5.448E-07
12.68	5.335E-12	1.391E-08	1.854E-08	2.749E-13	2.775E-09	5.577E-07
12.81	1.014E-12	1.295E-08	1.790E-08	1.188E-12	3.147E-09	5.712E-07
12.94	3.456E-14	1.215E-08	1.732E-08	9.015E-13	3.484E-09	5.839E-07

Table J.3 Experimental molar fluxes for CO, H_2O, H_2, H atom, OH and O_2.

HAB (mm)	F_{CO}	F_{H2O}	F_{H2}	F_{H}	F_{OH}	F_{O2}
0.07	9.620E-07	4.567E-06	6.093E-05	-1.059E-07	-6.500E-09	1.919E-05
0.20	9.513E-07	4.458E-06	6.403E-05	-1.216E-07	-7.841E-09	1.925E-05
0.33	9.380E-07	4.321E-06	6.753E-05	-1.413E-07	-9.643E-09	1.932E-05
0.46	9.243E-07	4.182E-06	7.088E-05	-1.612E-07	-1.148E-08	1.939E-05
0.60	9.095E-07	4.032E-06	7.399E-05	-1.825E-07	-1.352E-08	1.948E-05
0.73	8.934E-07	3.869E-06	7.672E-05	-2.048E-07	-1.570E-08	1.957E-05
0.86	8.756E-07	3.691E-06	7.898E-05	-2.288E-07	-1.807E-08	1.968E-05
0.99	8.559E-07	3.492E-06	8.072E-05	-2.547E-07	-2.064E-08	1.980E-05
1.12	8.339E-07	3.269E-06	8.197E-05	-2.832E-07	-2.344E-08	1.993E-05
1.25	8.093E-07	3.017E-06	8.274E-05	-3.149E-07	-2.652E-08	2.008E-05
1.38	7.824E-07	2.736E-06	8.316E-05	-3.497E-07	-2.988E-08	2.024E-05
1.51	7.530E-07	2.423E-06	8.316E-05	-3.886E-07	-3.358E-08	2.041E-05
1.65	7.219E-07	2.094E-06	8.316E-05	-4.287E-07	-3.741E-08	2.059E-05
1.78	6.887E-07	1.715E-06	8.233E-05	-4.770E-07	-4.185E-08	2.079E-05
1.91	6.548E-07	1.310E-06	8.120E-05	-5.303E-07	-4.666E-08	2.098E-05
2.04	6.212E-07	8.833E-07	7.983E-05	-5.884E-07	-5.180E-08	2.118E-05
2.17	5.887E-07	4.425E-07	7.826E-05	-6.512E-07	-5.725E-08	2.137E-05
2.30	5.584E-07	-5.515E-09	7.653E-05	-7.183E-07	-6.295E-08	2.156E-05
2.43	5.314E-07	-4.532E-07	7.467E-05	-7.894E-07	-6.886E-08	2.173E-05
2.56	5.085E-07	-8.927E-07	7.273E-05	-8.641E-07	-7.492E-08	2.189E-05
2.70	4.907E-07	-1.316E-06	7.074E-05	-9.418E-07	-8.106E-08	2.203E-05
2.83	4.787E-07	-1.717E-06	6.876E-05	-1.022E-06	-8.722E-08	2.214E-05
2.96	4.733E-07	-2.089E-06	6.680E-05	-1.104E-06	-9.333E-08	2.224E-05
3.09	4.749E-07	-2.426E-06	6.490E-05	-1.188E-06	-9.933E-08	2.231E-05
3.22	4.840E-07	-2.723E-06	6.308E-05	-1.274E-06	-1.051E-07	2.235E-05
3.35	5.009E-07	-2.978E-06	6.131E-05	-1.360E-06	-1.107E-07	2.237E-05
3.48	5.258E-07	-3.186E-06	5.960E-05	-1.447E-06	-1.160E-07	2.235E-05
3.62	5.589E-07	-3.343E-06	5.797E-05	-1.534E-06	-1.209E-07	2.230E-05
3.75	6.002E-07	-3.447E-06	5.641E-05	-1.621E-06	-1.254E-07	2.223E-05
3.88	6.496E-07	-3.494E-06	5.491E-05	-1.708E-06	-1.293E-07	2.212E-05
4.01	7.070E-07	-3.483E-06	5.347E-05	-1.794E-06	-1.326E-07	2.197E-05
4.14	7.720E-07	-3.413E-06	5.208E-05	-1.879E-06	-1.353E-07	2.180E-05
4.27	8.444E-07	-3.282E-06	5.075E-05	-1.962E-06	-1.372E-07	2.159E-05
4.40	9.235E-07	-3.092E-06	4.946E-05	-2.043E-06	-1.382E-07	2.135E-05
4.53	1.009E-06	-2.842E-06	4.823E-05	-2.122E-06	-1.384E-07	2.108E-05
4.67	1.100E-06	-2.535E-06	4.704E-05	-2.199E-06	-1.376E-07	2.078E-05
4.80	1.195E-06	-2.170E-06	4.590E-05	-2.273E-06	-1.359E-07	2.045E-05
4.93	1.295E-06	-1.748E-06	4.480E-05	-2.343E-06	-1.331E-07	2.010E-05
5.06	1.399E-06	-1.272E-06	4.375E-05	-2.410E-06	-1.292E-07	1.972E-05
5.19	1.504E-06	-7.433E-07	4.273E-05	-2.473E-06	-1.243E-07	1.932E-05
5.32	1.612E-06	-1.633E-07	4.176E-05	-2.532E-06	-1.183E-07	1.889E-05
5.45	1.721E-06	4.658E-07	4.083E-05	-2.585E-06	-1.112E-07	1.845E-05

HAB (mm)	F_{CO}	F_{H2O}	F_{H2}	F_{H}	F_{OH}	F_{O2}
5.59	1.831E-06	1.142E-06	3.994E-05	-2.633E-06	-1.030E-07	1.798E-05
5.72	1.940E-06	1.863E-06	3.908E-05	-2.676E-06	-9.368E-08	1.750E-05
5.85	2.049E-06	2.627E-06	3.825E-05	-2.712E-06	-8.337E-08	1.701E-05
5.98	2.156E-06	3.431E-06	3.746E-05	-2.742E-06	-7.209E-08	1.650E-05
6.11	2.261E-06	4.274E-06	3.669E-05	-2.765E-06	-5.990E-08	1.598E-05
6.24	2.364E-06	5.151E-06	3.596E-05	-2.781E-06	-4.687E-08	1.545E-05
6.37	2.464E-06	6.059E-06	3.524E-05	-2.789E-06	-3.310E-08	1.491E-05
6.50	2.560E-06	6.995E-06	3.456E-05	-2.790E-06	-1.869E-08	1.436E-05
6.64	2.652E-06	7.953E-06	3.389E-05	-2.783E-06	-3.763E-09	1.381E-05
6.77	2.740E-06	8.931E-06	3.326E-05	-2.769E-06	1.157E-08	1.326E-05
6.90	2.824E-06	9.924E-06	3.264E-05	-2.746E-06	2.718E-08	1.271E-05
7.03	2.903E-06	1.093E-05	3.204E-05	-2.716E-06	4.296E-08	1.216E-05
7.16	2.977E-06	1.194E-05	3.147E-05	-2.678E-06	5.879E-08	1.162E-05
7.29	3.046E-06	1.296E-05	3.092E-05	-2.632E-06	7.455E-08	1.108E-05
7.42	3.111E-06	1.398E-05	3.038E-05	-2.578E-06	9.014E-08	1.055E-05
7.55	3.170E-06	1.499E-05	2.986E-05	-2.518E-06	1.054E-07	1.002E-05
7.69	3.224E-06	1.599E-05	2.936E-05	-2.451E-06	1.204E-07	9.508E-06
7.82	3.274E-06	1.699E-05	2.888E-05	-2.377E-06	1.348E-07	9.004E-06
7.95	3.319E-06	1.797E-05	2.841E-05	-2.297E-06	1.487E-07	8.512E-06
8.07	3.360E-06	1.893E-05	2.796E-05	-2.212E-06	1.619E-07	8.034E-06
8.21	3.396E-06	1.988E-05	2.752E-05	-2.121E-06	1.745E-07	7.569E-06
8.34	3.428E-06	2.080E-05	2.710E-05	-2.025E-06	1.863E-07	7.118E-06
8.47	3.456E-06	2.171E-05	2.669E-05	-1.925E-06	1.974E-07	6.683E-06
8.61	3.481E-06	2.258E-05	2.629E-05	-1.821E-06	2.076E-07	6.263E-06
8.73	3.503E-06	2.343E-05	2.590E-05	-1.713E-06	2.170E-07	5.859E-06
8.87	3.521E-06	2.426E-05	2.552E-05	-1.603E-06	2.256E-07	5.472E-06
8.99	3.537E-06	2.505E-05	2.516E-05	-1.489E-06	2.333E-07	5.101E-06
9.13	3.550E-06	2.582E-05	2.481E-05	-1.373E-06	2.403E-07	4.746E-06
9.26	3.561E-06	2.656E-05	2.447E-05	-1.256E-06	2.464E-07	4.407E-06
9.39	3.569E-06	2.726E-05	2.414E-05	-1.136E-06	2.518E-07	4.085E-06
9.52	3.576E-06	2.794E-05	2.383E-05	-1.016E-06	2.565E-07	3.778E-06
9.65	3.581E-06	2.859E-05	2.353E-05	-8.951E-07	2.604E-07	3.488E-06
9.79	3.585E-06	2.922E-05	2.324E-05	-7.740E-07	2.637E-07	3.212E-06
9.91	3.588E-06	2.981E-05	2.296E-05	-6.530E-07	2.664E-07	2.953E-06
10.05	3.590E-06	3.037E-05	2.269E-05	-5.323E-07	2.685E-07	2.707E-06
10.18	3.591E-06	3.091E-05	2.244E-05	-4.124E-07	2.701E-07	2.475E-06
10.31	3.591E-06	3.142E-05	2.219E-05	-2.937E-07	2.711E-07	2.258E-06
10.44	3.590E-06	3.190E-05	2.196E-05	-1.766E-07	2.717E-07	2.054E-06
10.58	3.589E-06	3.236E-05	2.173E-05	-6.175E-08	2.718E-07	1.864E-06
10.71	3.587E-06	3.278E-05	2.152E-05	5.030E-08	2.714E-07	1.688E-06
10.84	3.585E-06	3.318E-05	2.131E-05	1.589E-07	2.707E-07	1.525E-06
10.97	3.583E-06	3.354E-05	2.112E-05	2.635E-07	2.697E-07	1.377E-06
11.10	3.581E-06	3.388E-05	2.094E-05	3.635E-07	2.683E-07	1.242E-06
11.23	3.579E-06	3.418E-05	2.077E-05	4.592E-07	2.668E-07	1.120E-06
11.36	3.576E-06	3.445E-05	2.062E-05	5.495E-07	2.651E-07	1.011E-06
11.49	3.574E-06	3.468E-05	2.048E-05	6.305E-07	2.628E-07	9.220E-07
11.63	3.571E-06	3.491E-05	2.035E-05	7.096E-07	2.607E-07	8.352E-07
11.76	3.569E-06	3.511E-05	2.023E-05	7.832E-07	2.583E-07	7.579E-07
11.89	3.567E-06	3.529E-05	2.011E-05	8.519E-07	2.558E-07	6.871E-07
12.02	3.564E-06	3.546E-05	2.000E-05	9.154E-07	2.530E-07	6.227E-07
12.15	3.562E-06	3.562E-05	1.990E-05	9.733E-07	2.498E-07	5.632E-07
12.28	3.560E-06	3.577E-05	1.979E-05	1.025E-06	2.461E-07	5.071E-07
12.41	3.558E-06	3.591E-05	1.968E-05	1.070E-06	2.417E-07	4.538E-07
12.54	3.557E-06	3.605E-05	1.956E-05	1.109E-06	2.367E-07	4.025E-07
12.68	3.555E-06	3.617E-05	1.943E-05	1.138E-06	2.311E-07	3.545E-07

HAB (mm)	F_{CO}	F_{H2O}	F_{H2}	F_{H}	F_{OH}	F_{O2}
12.81	3.553E-06	3.630E-05	1.930E-05	1.166E-06	2.251E-07	3.067E-07
12.94	3.552E-06	3.639E-05	1.918E-05	1.179E-06	2.194E-07	2.693E-07

Table J.4 Experimental elemental mass flux balance. Values are given as percentages of initial flux. See Appendix D for details of the calculation method.

HAB (mm)	H	C	O	Ar
0.07	1.90	-1.80	9.11	-3.98
0.20	11.74	-3.51	8.98	-4.71
0.33	17.53	-3.93	8.90	-5.15
0.46	19.23	-4.25	8.86	-5.27
0.60	28.76	-6.02	8.86	-6.02
0.73	32.90	-7.22	8.90	-6.35
0.86	36.00	-8.46	8.98	-6.61
0.99	38.40	-9.76	9.08	-6.82
1.12	39.79	-11.05	9.18	-6.94
1.25	40.35	-12.24	9.28	-6.99
1.38	40.21	-13.41	9.33	-6.97
1.51	33.67	-12.52	9.33	-6.44
1.65	37.81	-15.48	9.24	-6.66
1.78	35.17	-16.22	9.15	-6.38
1.91	32.35	-16.95	9.00	-6.06
2.04	29.37	-17.58	8.82	-5.71
2.17	25.15	-17.98	8.52	-5.22
2.30	22.90	-18.60	8.32	-4.93
2.43	18.11	-18.77	7.91	-4.34
2.56	10.34	-16.75	7.46	-3.55
2.70	11.44	-19.32	7.19	-3.46
2.83	7.02	-19.31	6.69	-2.87
2.96	3.56	-19.34	6.24	-2.39
3.09	-0.56	-19.17	5.70	-1.82
3.22	-2.90	-19.08	5.32	-1.46
3.35	-6.70	-18.70	4.75	-0.91
3.48	-12.38	-15.85	4.25	-0.30
3.62	-12.39	-17.70	3.73	-0.02
3.75	-15.81	-16.90	3.12	0.50
3.88	-17.60	-16.11	2.68	0.81
4.01	-20.02	-15.08	2.15	1.21
4.14	-22.31	-13.89	1.62	1.60
4.27	-24.48	-12.54	1.08	1.97
4.40	-26.53	-11.04	0.55	2.33
4.53	-28.19	-7.66	0.42	2.42
4.67	-28.87	-7.75	-0.30	2.79
4.80	-30.61	-5.90	-0.82	3.10
4.93	-31.52	-4.01	-1.22	3.29
5.06	-32.33	-2.08	-1.60	3.47
5.19	-33.05	-0.14	-1.97	3.63
5.32	-33.68	1.80	-2.33	3.78
5.45	-33.86	4.52	-2.21	3.66
5.59	-34.69	5.49	-2.97	4.03
5.72	-35.08	7.19	-3.27	4.14
5.85	-35.40	8.76	-3.54	4.23

HAB (mm)	H	C	O	Ar
5.98	-34.96	10.15	-3.65	4.20
6.11	-35.15	11.40	-3.87	4.28
6.24	-34.59	12.44	-3.93	4.22
6.37	-34.68	13.33	-4.11	4.28
6.50	-33.95	14.03	-3.72	4.03
6.64	-34.03	14.53	-4.24	4.25
6.77	-33.30	14.86	-4.20	4.16
6.90	-33.22	15.06	-4.28	4.18
7.03	-32.43	15.10	-4.19	4.07
7.16	-32.30	15.06	-4.24	4.08
7.29	-31.45	14.89	-4.10	3.96
7.42	-30.59	14.64	-3.95	3.83
7.55	-29.62	14.26	-3.43	3.54
7.69	-28.83	14.02	-3.61	3.55
7.82	-28.62	13.71	-3.58	3.53
7.95	-28.41	13.40	-3.54	3.51
8.07	-26.82	13.03	-3.16	3.22
8.21	-26.61	12.75	-3.11	3.19
8.34	-25.02	12.44	-2.71	2.89
8.47	-24.23	12.24	-2.20	2.62
8.61	-23.97	12.01	-2.41	2.69
8.73	-23.81	11.87	-2.34	2.65
8.87	-22.28	11.68	-1.92	2.35
8.99	-21.47	11.56	-1.67	2.18
9.13	-21.37	11.51	-1.60	2.14
9.26	-20.60	11.43	-1.35	1.98
9.39	-19.86	11.38	-1.10	1.81
9.52	-18.14	11.40	-0.34	1.34
9.65	-18.47	11.30	-0.61	1.48
9.79	-17.82	11.27	-0.36	1.32
9.91	-17.91	11.29	-0.31	1.31
10.05	-16.61	11.22	0.12	1.02
10.18	-16.05	11.20	0.36	0.87
10.31	-15.51	11.18	0.59	0.73
10.44	-15.50	11.36	0.89	0.59
10.58	-14.53	11.14	1.05	0.45
10.71	-14.09	11.13	1.27	0.32
10.84	-14.39	11.16	1.29	0.34
10.97	-13.31	11.11	1.68	0.08
11.10	-13.66	11.15	1.68	0.11
11.23	-13.35	11.15	1.87	0.00
11.36	-12.34	11.08	2.24	-0.24
11.49	-12.51	11.44	2.54	-0.36
11.63	-11.83	11.17	2.60	-0.43
11.76	-12.34	11.27	2.55	-0.38
11.89	-12.22	11.32	2.66	-0.43
12.02	-12.07	11.38	2.79	-0.50
12.15	-11.21	11.40	3.12	-0.71
12.28	-11.79	11.52	3.05	-0.64
12.41	-11.68	11.65	3.17	-0.70
12.54	-11.61	12.03	3.39	-0.81
12.68	-10.83	12.01	3.62	-0.98
12.81	-11.50	12.16	3.46	-0.86
12.94	-11.67	13.02	3.78	-1.01

Appendix K. Species Net Rates.

Net rates for 18 important species were calculated from Equation 3-25 by the FBR program (documented in Appendix D). Units are mol/cm^{3}s, and a positive rate signifies production of the species. Mole fractions of H atom and OH were calibrated by the partial equilibrium method.

Table K.1 Experimental net rates of C_6H_6, mass 94 (as C_6H_5OH), C_6H_5, mass 66 (as C_5H_6), mass 54 (as 1,3-C_4H_6) and mass 42 (as C_3H_6).

HAB (mm)	R_{C6H6}	R_{94}	R_{C6H5}	R_{66}	R_{54}	R_{42}
0.13	-2.144E-07	-1.103E-09	-3.167E-10	-3.597E-10	2.083E-10	-2.252E-08
0.26	-2.948E-07	-1.548E-09	-4.393E-10	-4.955E-10	3.746E-10	-2.951E-08
0.39	-2.852E-07	-1.517E-09	-4.180E-10	-4.823E-10	4.090E-10	-2.783E-08
0.53	-3.098E-07	-1.685E-09	-4.330E-10	-5.283E-10	5.819E-10	-2.806E-08
0.66	-3.258E-07	-1.832E-09	-4.066E-10	-5.654E-10	8.422E-10	-2.588E-08
0.79	-3.236E-07	-1.892E-09	-3.155E-10	-5.742E-10	1.224E-09	-1.964E-08
0.92	-3.071E-07	-1.886E-09	-1.561E-10	-5.620E-10	1.753E-09	-9.275E-09
1.05	-2.809E-07	-1.843E-09	4.791E-11	-5.379E-10	2.403E-09	4.270E-09
1.18	-2.445E-07	-1.742E-09	3.090E-10	-4.974E-10	3.203E-09	2.139E-08
1.31	-2.076E-07	-1.655E-09	5.423E-10	-4.607E-10	3.941E-09	3.790E-08
1.44	-1.545E-07	-1.392E-09	8.619E-10	-3.792E-10	4.800E-09	5.770E-08
1.58	-1.347E-07	-1.437E-09	9.082E-10	-3.808E-10	5.044E-09	6.524E-08
1.71	-6.332E-08	-8.600E-10	1.732E-09	-2.253E-10	7.400E-09	1.086E-07
1.84	-2.580E-08	-4.871E-10	2.157E-09	-1.303E-10	8.579E-09	1.302E-07
1.97	6.222E-09	-5.499E-11	2.568E-09	-2.565E-11	9.658E-09	1.490E-07
2.10	2.566E-08	4.033E-10	2.940E-09	7.856E-11	1.059E-08	1.631E-07
2.23	3.337E-08	8.893E-10	3.256E-09	1.833E-10	1.131E-08	1.718E-07
2.36	2.814E-08	1.390E-09	3.500E-09	2.853E-10	1.177E-08	1.742E-07
2.49	1.017E-08	1.828E-09	3.523E-09	3.693E-10	1.151E-08	1.637E-07
2.63	-1.808E-08	2.314E-09	3.583E-09	4.583E-10	1.137E-08	1.530E-07
2.76	-5.855E-08	2.895E-09	3.678E-09	5.615E-10	1.133E-08	1.411E-07
2.89	-1.073E-07	3.365E-09	3.527E-09	6.388E-10	1.053E-08	1.172E-07
3.02	-1.627E-07	3.816E-09	3.280E-09	7.094E-10	9.440E-09	8.837E-08
3.15	-2.232E-07	4.240E-09	2.943E-09	7.725E-10	8.098E-09	5.563E-08
3.28	-2.833E-07	4.675E-09	2.575E-09	8.391E-10	6.668E-09	2.246E-08
3.41	-3.329E-07	4.885E-09	2.062E-09	8.645E-10	4.886E-09	-1.167E-08
3.55	-3.925E-07	5.243E-09	1.611E-09	9.169E-10	3.285E-09	-4.427E-08
3.68	-4.682E-07	5.786E-09	1.187E-09	1.002E-09	1.739E-09	-7.782E-08
3.81	-5.265E-07	6.093E-09	7.027E-10	1.048E-09	1.098E-10	-1.065E-07
3.94	-5.815E-07	6.362E-09	2.347E-10	1.090E-09	-1.425E-09	-1.311E-07
4.07	-6.327E-07	6.585E-09	-2.031E-10	1.127E-09	-2.824E-09	-1.508E-07
4.20	-6.793E-07	6.755E-09	-6.009E-10	1.157E-09	-4.057E-09	-1.653E-07
4.33	-7.210E-07	6.862E-09	-9.512E-10	1.180E-09	-5.104E-09	-1.745E-07
4.46	-7.291E-07	6.643E-09	-1.204E-09	1.151E-09	-5.736E-09	-1.719E-07
4.60	-7.585E-07	6.603E-09	-1.440E-09	1.155E-09	-6.365E-09	-1.710E-07
4.73	-8.124E-07	6.733E-09	-1.686E-09	1.194E-09	-7.070E-09	-1.725E-07
4.86	-8.309E-07	6.524E-09	-1.823E-09	1.179E-09	-7.345E-09	-1.637E-07

Appendix K **Species Net Rates**

HAB (mm)	R_{C6H6}	R_{94}	R_{C6H5}	R_{66}	R_{54}	R_{42}
4.99	-8.434E-07	6.225E-09	-1.912E-09	1.151E-09	-7.457E-09	-1.522E-07
5.12	-8.498E-07	5.836E-09	-1.958E-09	1.112E-09	-7.427E-09	-1.387E-07
5.25	-8.502E-07	5.359E-09	-1.966E-09	1.060E-09	-7.279E-09	-1.241E-07
5.38	-8.134E-07	4.616E-09	-1.871E-09	9.593E-10	-6.776E-09	-1.050E-07
5.52	-8.028E-07	3.990E-09	-1.825E-09	8.849E-10	-6.476E-09	-9.080E-08
5.65	-8.175E-07	3.416E-09	-1.827E-09	8.286E-10	-6.367E-09	-8.031E-08
5.78	-7.968E-07	2.617E-09	-1.746E-09	7.254E-10	-5.983E-09	-6.752E-08
5.91	-7.720E-07	1.758E-09	-1.655E-09	6.099E-10	-5.590E-09	-5.620E-08
6.04	-7.435E-07	8.493E-10	-1.559E-09	4.828E-10	-5.200E-09	-4.648E-08
6.17	-7.118E-07	-9.492E-11	-1.461E-09	3.450E-10	-4.823E-09	-3.838E-08
6.30	-6.774E-07	-1.061E-09	-1.363E-09	1.974E-10	-4.467E-09	-3.181E-08
6.43	-6.171E-07	-1.960E-09	-1.220E-09	3.971E-11	-3.980E-09	-2.563E-08
6.57	-5.802E-07	-2.892E-09	-1.130E-09	-1.177E-10	-3.683E-09	-2.177E-08
6.70	-5.632E-07	-3.950E-09	-1.085E-09	-2.918E-10	-3.543E-09	-1.958E-08
6.83	-5.236E-07	-4.860E-09	-1.001E-09	-4.653E-10	-3.288E-09	-1.736E-08
6.96	-4.842E-07	-5.719E-09	-9.218E-10	-6.406E-10	-3.057E-09	-1.573E-08
7.09	-4.455E-07	-6.510E-09	-8.480E-10	-8.151E-10	-2.849E-09	-1.452E-08
7.22	-4.079E-07	-7.222E-09	-7.793E-10	-9.865E-10	-2.660E-09	-1.359E-08
7.35	-3.717E-07	-7.842E-09	-7.153E-10	-1.152E-09	-2.487E-09	-1.281E-08
7.48	-3.246E-07	-8.051E-09	-6.314E-10	-1.262E-09	-2.242E-09	-1.165E-08
7.62	-2.930E-07	-8.448E-09	-5.780E-10	-1.404E-09	-2.100E-09	-1.098E-08
7.75	-2.736E-07	-9.076E-09	-5.489E-10	-1.595E-09	-2.044E-09	-1.070E-08
7.88	-2.451E-07	-9.270E-09	-5.017E-10	-1.720E-09	-1.918E-09	-9.982E-09
8.01	-2.189E-07	-9.353E-09	-4.583E-10	-1.829E-09	-1.800E-09	-9.266E-09
8.14	-1.950E-07	-9.331E-09	-4.184E-10	-1.923E-09	-1.691E-09	-8.559E-09
8.27	-1.732E-07	-9.207E-09	-3.819E-10	-2.000E-09	-1.588E-09	-7.875E-09
8.40	-1.478E-07	-8.657E-09	-3.354E-10	-1.984E-09	-1.437E-09	-6.955E-09
8.54	-1.306E-07	-8.365E-09	-3.057E-10	-2.023E-09	-1.350E-09	-6.365E-09
8.67	-1.195E-07	-8.313E-09	-2.894E-10	-2.125E-09	-1.317E-09	-6.045E-09
8.80	-1.052E-07	-7.878E-09	-2.639E-10	-2.132E-09	-1.239E-09	-5.536E-09
8.93	-9.248E-08	-7.395E-09	-2.410E-10	-2.121E-09	-1.165E-09	-5.083E-09
9.06	-8.125E-08	-6.875E-09	-2.205E-10	-2.094E-09	-1.098E-09	-4.684E-09
9.19	-7.139E-08	-6.331E-09	-2.022E-10	-2.052E-09	-1.035E-09	-4.335E-09
9.32	-6.273E-08	-5.773E-09	-1.859E-10	-1.996E-09	-9.768E-10	-4.028E-09
9.45	-5.309E-08	-5.019E-09	-1.649E-10	-1.856E-09	-8.884E-10	-3.616E-09
9.59	-4.664E-08	-4.485E-09	-1.524E-10	-1.779E-09	-8.395E-10	-3.378E-09
9.72	-4.254E-08	-4.119E-09	-1.465E-10	-1.759E-09	-8.245E-10	-3.280E-09
9.85	-3.734E-08	-3.602E-09	-1.356E-10	-1.660E-09	-7.802E-10	-3.067E-09
9.98	-3.287E-08	-3.122E-09	-1.263E-10	-1.562E-09	-7.404E-10	-2.877E-09
10.11	-2.893E-08	-2.672E-09	-1.175E-10	-1.457E-09	-7.027E-10	-2.698E-09
10.24	-2.546E-08	-2.256E-09	-1.090E-10	-1.347E-09	-6.672E-10	-2.531E-09
10.37	-2.156E-08	-1.807E-09	-9.697E-11	-1.189E-09	-6.100E-10	-2.287E-09
10.51	-1.893E-08	-1.477E-09	-8.892E-11	-1.078E-09	-5.787E-10	-2.145E-09
10.64	-1.718E-08	-1.226E-09	-8.378E-11	-1.004E-09	-5.690E-10	-2.085E-09
10.77	-1.492E-08	-9.540E-10	-7.496E-11	-8.884E-10	-5.374E-10	-1.946E-09
10.90	-1.288E-08	-7.172E-10	-6.589E-11	-7.759E-10	-5.060E-10	-1.809E-09
11.03	-1.104E-08	-5.145E-10	-5.668E-11	-6.676E-10	-4.751E-10	-1.678E-09
11.16	-9.422E-09	-3.462E-10	-4.750E-11	-5.661E-10	-4.450E-10	-1.553E-09
11.29	-7.995E-09	-2.109E-10	-3.859E-11	-4.721E-10	-4.150E-10	-1.432E-09
11.42	-5.819E-09	-3.046E-11	-2.360E-11	-3.100E-10	-3.651E-10	-1.233E-09
11.56	-5.605E-09	-4.226E-11	-2.184E-11	-3.056E-10	-3.562E-10	-1.201E-09
11.69	-4.960E-09	1.044E-11	-1.584E-11	-2.552E-10	-3.501E-10	-1.167E-09
11.82	-4.446E-09	2.795E-11	-1.118E-11	-2.167E-10	-3.373E-10	-1.115E-09
11.95	-3.947E-09	4.135E-11	-6.581E-12	-1.766E-10	-3.264E-10	-1.070E-09
12.08	-3.614E-09	3.810E-11	-3.347E-12	-1.472E-10	-3.213E-10	-1.046E-09

HAB (mm)	R_{C6H6}	R_{94}	R_{C6H5}	R_{66}	R_{54}	R_{42}
12.21	-3.406E-09	2.421E-11	-1.280E-12	-1.256E-10	-3.211E-10	-1.040E-09
12.34	-3.231E-09	9.599E-12	-1.862E-13	-1.084E-10	-3.243E-10	-1.046E-09
12.47	-2.982E-09	-3.097E-12	2.277E-13	-9.218E-11	-3.166E-10	-1.017E-09
12.61	-2.759E-09	-1.007E-11	2.573E-13	-7.892E-11	-3.144E-10	-1.006E-09
12.74	-2.839E-09	-1.488E-11	2.328E-13	-7.857E-11	-3.312E-10	-1.059E-09
12.87	-2.150E-09	-1.168E-11	5.239E-14	-5.344E-11	-2.796E-10	-8.897E-10

Table K.2 Experimental net rates of C_2H_4, C_2H_2, CH_4, CH_3, H_2CO and CO_2.

HAB (mm)	R_{C2H4}	R_{C2H2}	R_{CH4}	R_{CH3}	R_{H2CO}	R_{CO2}
0.13	2.871E-08	-5.715E-09	6.843E-08	-1.938E-08	-2.056E-09	-5.609E-08
0.26	5.639E-08	-6.268E-09	8.950E-08	-2.642E-08	-2.315E-09	-5.755E-08
0.39	5.924E-08	-6.031E-09	8.323E-08	-2.625E-08	-2.265E-09	-5.384E-08
0.53	7.719E-08	-5.983E-09	8.375E-08	-2.959E-08	-2.320E-09	-4.924E-08
0.66	9.514E-08	-6.414E-09	7.723E-08	-3.374E-08	-2.560E-09	-4.847E-08
0.79	1.126E-07	-6.668E-09	6.225E-08	-3.733E-08	-2.689E-09	-4.516E-08
0.92	1.290E-07	-7.114E-09	3.940E-08	-4.105E-08	-2.826E-09	-4.326E-08
1.05	1.451E-07	-7.729E-09	1.156E-08	-4.499E-08	-2.881E-09	-4.300E-08
1.18	1.613E-07	-8.370E-09	-2.267E-08	-4.890E-08	-2.833E-09	-4.311E-08
1.31	1.751E-07	-9.142E-09	-5.317E-08	-5.277E-08	-2.710E-09	-4.477E-08
1.44	1.848E-07	-9.059E-09	-9.341E-08	-5.387E-08	-2.334E-09	-4.057E-08
1.58	1.879E-07	-1.023E-08	-9.622E-08	-5.714E-08	-1.999E-09	-4.768E-08
1.71	2.287E-07	-8.668E-09	-1.978E-07	-6.023E-08	-1.624E-09	-2.645E-08
1.84	2.458E-07	-7.229E-09	-2.456E-07	-5.958E-08	-8.758E-10	-1.265E-08
1.97	2.604E-07	-5.112E-09	-2.904E-07	-5.664E-08	1.550E-10	4.362E-09
2.10	2.740E-07	-2.230E-09	-3.277E-07	-5.146E-08	1.589E-09	2.526E-08
2.23	2.848E-07	1.334E-09	-3.551E-07	-4.373E-08	3.523E-09	4.873E-08
2.36	2.928E-07	5.548E-09	-3.691E-07	-3.338E-08	6.132E-09	7.431E-08
2.49	2.862E-07	9.944E-09	-3.531E-07	-1.964E-08	9.230E-09	9.740E-08
2.63	2.867E-07	1.500E-08	-3.317E-07	-4.661E-09	1.358E-08	1.237E-07
2.76	2.941E-07	2.119E-08	-2.992E-07	1.313E-08	1.993E-08	1.551E-07
2.89	2.862E-07	2.703E-08	-2.281E-07	3.328E-08	2.729E-08	1.802E-07
3.02	2.743E-07	3.306E-08	-1.298E-07	5.531E-08	3.638E-08	2.038E-07
3.15	2.585E-07	3.917E-08	-2.832E-09	7.885E-08	4.734E-08	2.258E-07
3.28	2.408E-07	4.547E-08	1.476E-07	1.036E-07	6.024E-08	2.476E-07
3.41	2.114E-07	4.981E-08	3.146E-07	1.242E-07	7.225E-08	2.577E-07
3.55	1.883E-07	5.576E-08	5.099E-07	1.488E-07	8.809E-08	2.758E-07
3.68	1.694E-07	6.399E-08	7.525E-07	1.795E-07	1.093E-07	3.044E-07
3.81	1.414E-07	6.992E-08	9.905E-07	2.035E-07	1.279E-07	3.217E-07
3.94	1.121E-07	7.566E-08	1.237E-06	2.258E-07	1.469E-07	3.384E-07
4.07	8.180E-08	8.113E-08	1.484E-06	2.459E-07	1.654E-07	3.541E-07
4.20	5.100E-08	8.625E-08	1.722E-06	2.630E-07	1.825E-07	3.688E-07
4.33	2.007E-08	9.095E-08	1.942E-06	2.767E-07	1.973E-07	3.822E-07
4.46	-1.026E-08	9.163E-08	2.054E-06	2.757E-07	2.010E-07	3.797E-07
4.60	-3.934E-08	9.515E-08	2.200E-06	2.806E-07	2.079E-07	3.901E-07
4.73	-7.027E-08	1.019E-07	2.389E-06	2.918E-07	2.178E-07	4.149E-07
4.86	-9.854E-08	1.044E-07	2.438E-06	2.872E-07	2.137E-07	4.241E-07
4.99	-1.255E-07	1.063E-07	2.425E-06	2.776E-07	2.030E-07	4.323E-07
5.12	-1.508E-07	1.076E-07	2.348E-06	2.631E-07	1.856E-07	4.398E-07
5.25	-1.744E-07	1.083E-07	2.205E-06	2.439E-07	1.612E-07	4.465E-07
5.38	-1.887E-07	1.043E-07	1.924E-06	2.121E-07	1.255E-07	4.358E-07
5.52	-2.075E-07	1.037E-07	1.667E-06	1.856E-07	9.009E-08	4.412E-07
5.65	-2.329E-07	1.065E-07	1.412E-06	1.618E-07	5.169E-08	4.638E-07

HAB (mm)	R_{C2H4}	R_{C2H2}	R_{CH4}	R_{CH3}	R_{H2CO}	R_{CO2}
5.78	-2.483E-07	1.047E-07	1.050E-06	1.283E-07	5.951E-09	4.694E-07
5.91	-2.614E-07	1.023E-07	6.555E-07	9.271E-08	-4.224E-08	4.749E-07
6.04	-2.723E-07	9.929E-08	2.421E-07	5.601E-08	-9.130E-08	4.803E-07
6.17	-2.810E-07	9.573E-08	-1.767E-07	1.897E-08	-1.396E-07	4.853E-07
6.30	-2.874E-07	9.160E-08	-5.874E-07	-1.762E-08	-1.854E-07	4.899E-07
6.43	-2.808E-07	8.371E-08	-9.408E-07	-5.103E-08	-2.188E-07	4.756E-07
6.57	-2.827E-07	7.869E-08	-1.284E-06	-8.325E-08	-2.540E-07	4.791E-07
6.70	-2.936E-07	7.599E-08	-1.648E-06	-1.174E-07	-2.938E-07	5.008E-07
6.83	-2.920E-07	6.984E-08	-1.913E-06	-1.453E-07	-3.166E-07	5.039E-07
6.96	-2.886E-07	6.333E-08	-2.121E-06	-1.697E-07	-3.316E-07	5.065E-07
7.09	-2.838E-07	5.652E-08	-2.270E-06	-1.903E-07	-3.387E-07	5.087E-07
7.22	-2.776E-07	4.949E-08	-2.360E-06	-2.067E-07	-3.380E-07	5.102E-07
7.35	-2.701E-07	4.230E-08	-2.391E-06	-2.188E-07	-3.299E-07	5.108E-07
7.48	-2.518E-07	3.371E-08	-2.280E-06	-2.184E-07	-3.036E-07	4.918E-07
7.62	-2.426E-07	2.663E-08	-2.211E-06	-2.220E-07	-2.840E-07	4.909E-07
7.75	-2.417E-07	2.026E-08	-2.184E-06	-2.306E-07	-2.702E-07	5.084E-07
7.88	-2.308E-07	1.289E-08	-2.040E-06	-2.271E-07	-2.423E-07	5.070E-07
8.01	-2.196E-07	5.586E-09	-1.871E-06	-2.204E-07	-2.124E-07	5.057E-07
8.14	-2.080E-07	-1.619E-09	-1.687E-06	-2.111E-07	-1.818E-07	5.044E-07
8.27	-1.963E-07	-8.674E-09	-1.496E-06	-1.995E-07	-1.515E-07	5.033E-07
8.40	-1.777E-07	-1.497E-08	-1.256E-06	-1.793E-07	-1.180E-07	4.836E-07
8.54	-1.663E-07	-2.138E-08	-1.078E-06	-1.652E-07	-9.216E-08	4.827E-07
8.67	-1.611E-07	-2.864E-08	-9.452E-07	-1.561E-07	-7.150E-08	5.007E-07
8.80	-1.498E-07	-3.481E-08	-7.866E-07	-1.403E-07	-5.040E-08	5.005E-07
8.93	-1.389E-07	-4.066E-08	-6.457E-07	-1.246E-07	-3.257E-08	5.005E-07
9.06	-1.285E-07	-4.614E-08	-5.240E-07	-1.093E-07	-1.803E-08	5.003E-07
9.19	-1.186E-07	-5.121E-08	-4.214E-07	-9.467E-08	-6.625E-09	5.000E-07
9.32	-1.092E-07	-5.584E-08	-3.371E-07	-8.090E-08	1.939E-09	4.991E-07
9.45	-9.662E-08	-5.781E-08	-2.594E-07	-6.563E-08	7.754E-09	4.797E-07
9.59	-8.863E-08	-6.145E-08	-2.084E-07	-5.445E-08	1.169E-08	4.783E-07
9.72	-8.428E-08	-6.721E-08	-1.759E-07	-4.614E-08	1.465E-08	4.959E-07
9.85	-7.698E-08	-7.023E-08	-1.460E-07	-3.700E-08	1.599E-08	4.967E-07
9.98	-7.052E-08	-7.293E-08	-1.246E-07	-2.910E-08	1.647E-08	4.973E-07
10.11	-6.445E-08	-7.522E-08	-1.095E-07	-2.237E-08	1.645E-08	4.983E-07
10.24	-5.877E-08	-7.709E-08	-9.879E-08	-1.673E-08	1.619E-08	4.999E-07
10.37	-5.141E-08	-7.565E-08	-8.773E-08	-1.166E-08	1.528E-08	4.834E-07
10.51	-4.645E-08	-7.661E-08	-8.194E-08	-8.070E-09	1.505E-08	4.855E-07
10.64	-4.328E-08	-8.003E-08	-7.975E-08	-5.418E-09	1.552E-08	5.048E-07
10.77	-3.846E-08	-7.995E-08	-7.450E-08	-3.108E-09	1.554E-08	5.037E-07
10.90	-3.378E-08	-7.930E-08	-6.910E-08	-1.364E-09	1.564E-08	4.994E-07
11.03	-2.924E-08	-7.810E-08	-6.347E-08	-9.145E-11	1.579E-08	4.928E-07
11.16	-2.485E-08	-7.643E-08	-5.764E-08	7.822E-10	1.587E-08	4.801E-07
11.29	-2.067E-08	-7.408E-08	-5.182E-08	1.328E-09	1.588E-08	4.668E-07
11.42	-1.327E-08	-6.903E-08	-4.456E-08	1.508E-09	1.613E-08	4.718E-07
11.56	-1.276E-08	-6.728E-08	-4.010E-08	1.542E-09	1.601E-08	4.532E-07
11.69	-1.000E-08	-6.757E-08	-3.759E-08	1.617E-09	1.674E-08	4.719E-07
11.82	-7.775E-09	-6.565E-08	-3.501E-08	1.496E-09	1.688E-08	4.800E-07
11.95	-5.377E-09	-6.399E-08	-3.338E-08	1.298E-09	1.722E-08	5.010E-07
12.08	-3.523E-09	-6.290E-08	-3.314E-08	1.022E-09	1.788E-08	5.392E-07
12.21	-2.139E-09	-6.239E-08	-3.420E-08	6.886E-10	1.886E-08	5.943E-07
12.34	-1.194E-09	-6.228E-08	-3.608E-08	4.079E-10	2.023E-08	6.680E-07
12.47	-5.872E-10	-6.007E-08	-3.665E-08	1.853E-10	2.078E-08	7.126E-07
12.61	-2.754E-10	-5.890E-08	-3.803E-08	5.655E-11	2.185E-08	7.771E-07
12.74	-1.612E-10	-6.173E-08	-4.065E-08	-5.429E-12	2.344E-08	8.432E-07
12.87	-1.880E-11	-5.143E-08	-3.607E-08	-3.252E-11	2.120E-08	7.902E-07

Table K.3 Experimental net rates of CO, H_2O, H_2, H atom, OH and O_2.

HAB (mm)	R_{CO}	R_{H2O}	R_{H2}	R_H	R_{OH}	R_{O2}
0.13	-7.927E-07	-8.039E-06	2.308E-04	-1.184E-06	-1.080E-07	3.849E-06
0.26	-1.005E-06	-1.017E-05	2.609E-04	-1.497E-06	-1.445E-07	5.281E-06
0.39	-9.925E-07	-1.002E-05	2.389E-04	-1.456E-06	-1.415E-07	5.335E-06
0.53	-1.085E-06	-1.091E-05	2.226E-04	-1.561E-06	-1.557E-07	6.131E-06
0.66	-1.232E-06	-1.234E-05	2.018E-04	-1.714E-06	-1.724E-07	7.208E-06
0.79	-1.363E-06	-1.363E-05	1.668E-04	-1.839E-06	-1.855E-07	8.180E-06
0.92	-1.518E-06	-1.521E-05	1.288E-04	-1.994E-06	-1.993E-07	9.195E-06
1.05	-1.695E-06	-1.712E-05	9.205E-05	-2.190E-06	-2.161E-07	1.026E-05
1.18	-1.885E-06	-1.932E-05	5.664E-05	-2.430E-06	-2.362E-07	1.133E-05
1.31	-2.068E-06	-2.140E-05	2.984E-05	-2.655E-06	-2.557E-07	1.227E-05
1.44	-2.162E-06	-2.297E-05	-1.409E-06	-2.855E-06	-2.701E-07	1.268E-05
1.58	-2.287E-06	-2.401E-05	-8.193E-07	-2.928E-06	-2.786E-07	1.317E-05
1.71	-2.526E-06	-2.863E-05	-6.315E-05	-3.648E-06	-3.332E-07	1.457E-05
1.84	-2.575E-06	-3.056E-05	-8.434E-05	-4.009E-06	-3.595E-07	1.483E-05
1.97	-2.552E-06	-3.203E-05	-1.027E-04	-4.357E-06	-3.831E-07	1.476E-05
2.10	-2.457E-06	-3.303E-05	-1.176E-04	-4.692E-06	-4.048E-07	1.442E-05
2.23	-2.286E-06	-3.349E-05	-1.295E-04	-5.006E-06	-4.232E-07	1.379E-05
2.36	-2.041E-06	-3.339E-05	-1.382E-04	-5.293E-06	-4.378E-07	1.290E-05
2.49	-1.660E-06	-3.150E-05	-1.387E-04	-5.340E-06	-4.315E-07	1.130E-05
2.63	-1.291E-06	-3.031E-05	-1.416E-04	-5.550E-06	-4.371E-07	9.957E-06
2.76	-8.989E-07	-2.973E-05	-1.471E-04	-5.945E-06	-4.552E-07	8.744E-06
2.89	-4.104E-07	-2.754E-05	-1.444E-04	-6.094E-06	-4.520E-07	6.994E-06
3.02	1.181E-07	-2.493E-05	-1.401E-04	-6.211E-06	-4.441E-07	5.103E-06
3.15	6.781E-07	-2.193E-05	-1.341E-04	-6.292E-06	-4.311E-07	3.090E-06
3.28	1.257E-06	-1.877E-05	-1.307E-04	-6.372E-06	-4.149E-07	1.010E-06
3.41	1.784E-06	-1.472E-05	-1.208E-04	-6.178E-06	-3.786E-07	-1.126E-06
3.55	2.365E-06	-1.113E-05	-1.157E-04	-6.192E-06	-3.525E-07	-3.295E-06
3.68	3.060E-06	-7.602E-06	-1.150E-04	-6.416E-06	-3.332E-07	-5.742E-06
3.81	3.658E-06	-3.462E-06	-1.101E-04	-6.374E-06	-2.946E-07	-8.112E-06
3.94	4.242E-06	8.161E-07	-1.057E-04	-6.304E-06	-2.501E-07	-1.051E-05
4.07	4.804E-06	5.177E-06	-1.016E-04	-6.210E-06	-2.000E-07	-1.290E-05
4.20	5.334E-06	9.562E-06	-9.777E-05	-6.093E-06	-1.446E-07	-1.526E-05
4.33	5.825E-06	1.393E-05	-9.407E-05	-5.953E-06	-8.442E-08	-1.756E-05
4.46	6.038E-06	1.755E-05	-8.703E-05	-5.576E-06	-1.914E-08	-1.903E-05
4.60	6.419E-06	2.161E-05	-8.349E-05	-5.396E-06	4.684E-08	-2.107E-05
4.73	7.009E-06	2.658E-05	-8.311E-05	-5.387E-06	1.209E-07	-2.389E-05
4.86	7.299E-06	3.062E-05	-7.980E-05	-5.143E-06	1.963E-07	-2.580E-05
4.99	7.534E-06	3.454E-05	-7.654E-05	-4.870E-06	2.741E-07	-2.759E-05
5.12	7.713E-06	3.833E-05	-7.336E-05	-4.569E-06	3.536E-07	-2.926E-05
5.25	7.837E-06	4.197E-05	-7.029E-05	-4.242E-06	4.337E-07	-3.079E-05
5.38	7.614E-06	4.375E-05	-6.483E-05	-3.742E-06	4.946E-07	-3.100E-05
5.52	7.630E-06	4.694E-05	-6.210E-05	-3.372E-06	5.705E-07	-3.222E-05
5.65	7.893E-06	5.191E-05	-6.183E-05	-3.083E-06	6.694E-07	-3.462E-05
5.78	7.817E-06	5.492E-05	-5.932E-05	-2.635E-06	7.437E-07	-3.565E-05
5.91	7.699E-06	5.776E-05	-5.700E-05	-2.158E-06	8.140E-07	-3.657E-05
6.04	7.541E-06	6.038E-05	-5.480E-05	-1.660E-06	8.794E-07	-3.735E-05
6.17	7.345E-06	6.277E-05	-5.273E-05	-1.142E-06	9.388E-07	-3.799E-05
6.30	7.115E-06	6.489E-05	-5.076E-05	-6.115E-07	9.910E-07	-3.849E-05
6.43	6.598E-06	6.425E-05	-4.707E-05	-6.908E-08	9.969E-07	-3.739E-05
6.57	6.318E-06	6.572E-05	-4.530E-05	4.577E-07	1.031E-06	-3.756E-05
6.70	6.246E-06	6.950E-05	-4.525E-05	1.030E-06	1.098E-06	-3.906E-05
6.83	5.913E-06	7.048E-05	-4.355E-05	1.590E-06	1.116E-06	-3.898E-05
6.96	5.568E-06	7.120E-05	-4.194E-05	2.150E-06	1.126E-06	-3.878E-05

Appendix K Species Net Rates

HAB (mm)	R_{CO}	R_{H2O}	R_{H2}	R_{H}	R_{OH}	R_{O2}
7.09	5.215E-06	7.164E-05	-4.042E-05	2.702E-06	1.127E-06	-3.847E-05
7.22	4.857E-06	7.180E-05	-3.897E-05	3.243E-06	1.119E-06	-3.804E-05
7.35	4.498E-06	7.168E-05	-3.759E-05	3.764E-06	1.104E-06	-3.751E-05
7.48	3.989E-06	6.864E-05	-3.493E-05	4.105E-06	1.041E-06	-3.549E-05
7.62	3.650E-06	6.799E-05	-3.369E-05	4.558E-06	1.012E-06	-3.476E-05
7.75	3.448E-06	6.970E-05	-3.377E-05	5.179E-06	1.014E-06	-3.526E-05
7.88	3.117E-06	6.861E-05	-3.262E-05	5.599E-06	9.720E-07	-3.436E-05
8.01	2.801E-06	6.734E-05	-3.154E-05	5.993E-06	9.253E-07	-3.340E-05
8.14	2.500E-06	6.590E-05	-3.053E-05	6.357E-06	8.746E-07	-3.239E-05
8.27	2.216E-06	6.432E-05	-2.958E-05	6.688E-06	8.206E-07	-3.133E-05
8.40	1.877E-06	6.027E-05	-2.760E-05	6.726E-06	7.359E-07	-2.910E-05
8.54	1.636E-06	5.849E-05	-2.674E-05	6.979E-06	6.798E-07	-2.801E-05
8.67	1.467E-06	5.879E-05	-2.688E-05	7.478E-06	6.467E-07	-2.792E-05
8.80	1.254E-06	5.680E-05	-2.601E-05	7.681E-06	5.874E-07	-2.674E-05
8.93	1.060E-06	5.477E-05	-2.513E-05	7.855E-06	5.289E-07	-2.557E-05
9.06	8.853E-07	5.271E-05	-2.426E-05	7.998E-06	4.718E-07	-2.440E-05
9.19	7.288E-07	5.063E-05	-2.338E-05	8.110E-06	4.168E-07	-2.323E-05
9.32	5.898E-07	4.854E-05	-2.249E-05	8.191E-06	3.642E-07	-2.208E-05
9.45	4.497E-07	4.472E-05	-2.080E-05	7.934E-06	3.024E-07	-2.017E-05
9.59	3.457E-07	4.270E-05	-1.993E-05	7.954E-06	2.567E-07	-1.908E-05
9.72	2.644E-07	4.226E-05	-1.980E-05	8.253E-06	2.215E-07	-1.872E-05
9.85	1.828E-07	4.019E-05	-1.888E-05	8.218E-06	1.782E-07	-1.763E-05
9.98	1.133E-07	3.825E-05	-1.807E-05	8.174E-06	1.390E-07	-1.662E-05
10.11	5.439E-08	3.630E-05	-1.728E-05	8.101E-06	1.020E-07	-1.563E-05
10.24	5.043E-09	3.436E-05	-1.650E-05	8.000E-06	6.726E-08	-1.466E-05
10.37	-3.433E-08	3.122E-05	-1.518E-05	7.579E-06	3.332E-08	-1.319E-05
10.51	-6.629E-08	2.933E-05	-1.448E-05	7.421E-06	3.934E-09	-1.228E-05
10.64	-9.560E-08	2.847E-05	-1.429E-05	7.506E-06	-2.365E-08	-1.181E-05
10.77	-1.168E-07	2.643E-05	-1.354E-05	7.266E-06	-4.865E-08	-1.087E-05
10.90	-1.332E-07	2.438E-05	-1.279E-05	6.994E-06	-7.002E-08	-9.940E-06
11.03	-1.452E-07	2.234E-05	-1.203E-05	6.690E-06	-8.836E-08	-9.027E-06
11.16	-1.537E-07	2.037E-05	-1.120E-05	6.395E-06	-1.012E-07	-8.154E-06
11.29	-1.580E-07	1.841E-05	-1.040E-05	6.048E-06	-1.121E-07	-7.307E-06
11.42	-1.528E-07	1.491E-05	-8.810E-06	5.261E-06	-1.428E-07	-5.794E-06
11.56	-1.513E-07	1.448E-05	-8.600E-06	5.131E-06	-1.348E-07	-5.642E-06
11.69	-1.547E-07	1.357E-05	-8.272E-06	4.982E-06	-1.509E-07	-5.236E-06
11.82	-1.503E-07	1.251E-05	-7.874E-06	4.668E-06	-1.611E-07	-4.806E-06
11.95	-1.450E-07	1.148E-05	-7.395E-06	4.336E-06	-1.779E-07	-4.371E-06
12.08	-1.378E-07	1.069E-05	-7.086E-06	3.992E-06	-2.014E-07	-4.037E-06
12.21	-1.287E-07	1.005E-05	-7.075E-06	3.628E-06	-2.318E-07	-3.786E-06
12.34	-1.184E-07	9.474E-06	-7.240E-06	3.185E-06	-2.713E-07	-3.570E-06
12.47	-1.044E-07	8.666E-06	-7.205E-06	2.670E-06	-2.977E-07	-3.277E-06
12.61	-9.217E-08	7.942E-06	-7.644E-06	2.108E-06	-3.341E-07	-3.043E-06
12.74	-9.226E-08	8.132E-06	-8.147E-06	2.036E-06	-3.652E-07	-3.127E-06
12.87	-6.680E-08	6.121E-06	-7.656E-06	1.084E-06	-3.525E-07	-2.420E-06

Appendix L. Fragmentation Magnitude Analyses.

It was found desirable from time to time to examine the question of which species in the flame might be the source of fragment molecules that were measured at a particular mass number. To perform this type of analysis, the signals of the daughter and all possible parents would ideally all be taken at the same height above the burner, on the same day and over a range of electron energies from below the appearance potential to a few eV above it. Also, where the parent species could be introduced into the burner or effusive source, cold gas fragmentation calibration experiments would be performed. Unfortunately, the analyses were attempted after experiments were completed, at less than perfect conditions in most cases. Signal corrections and estimations such as the following were then required:

- use of a third, reference species that was measured on both days, to get the parent and daughter species on the same basis,
- energy corrections, such as those described in Chapter 3, and
- interpolation or use of a data curve to approximate the signal at a different height than that measured.

Two other factors had to be considered: the type of fragmentation (skeletal or H atom elimination) and the energy level with respect to the appearance potential. Measurements of CH_3 appearance from CH_4 revealed that for some H eliminations a much higher amount of fragment would appear at a particular energy above the appearance potential than for skeletal fragmentations. In the other case measured, C_6H_5 from C_6H_6, comparatively little fragment showed up in the first several eV above the appearance potential. Although there was no way of determining which type of behavior a postulated H elimination might exhibit, for those types of fragmentations it was necessary to allow for the possibility of a high fragment signal close to the appearance potential. In general, of course, within the first several eV of the appearance potential (i.e., before all of the molecules were fragmented) more daughter species would be expected at higher electron energies than at lower ones.

In the analyses that follow, electron energies for the species being compared were either at or were corrected to be the same. When comparing measurements made on different days, the electron energies of the reference species measurements were also at (or were corrected to be)

the same value for both measurements. However, it was not necessary for the electron energy of the species being compared to be the same as the energy of the reference species.

The following nomenclature was used in this appendix:

"AP" — appearance potential of the species being considered from the species listed,

"EI" — electron impact ionization method (a preferred value for appearance potentials, because it corresponds to the ionization method used in the experiment),

"I_i" — mass spectrometer signal for species i,

"IEff" — ionization efficiency curve to measure experimental ionization potential or appearance potential,

"IP" — ionization potential,

"RICS" — relative ionization cross-section calibration (see Chapter 3).

Mass 39

Measured intercept is at least 11.9 eV, though interpretations as high as 14.1 eV are possible.

Table L.1 Possible parent species for mass 39, with literature appearance potentials.

Species	AP (eV)
c-C_3H_4 (mass 40)	10.25-11.5 (10.9-11.15 EI)
CH_2=C=CH_2 (mass 40)	11.5-12.02 (12.02 EI)
$CH_3C{\equiv}CH$ (mass 40)	11.8-12.06 (range=EI too)
CH_2=CHCH=CH_2 (mass 54)	11.35-11.71 (11.71 EI)
$CH_3CH_2C{\equiv}CH$ (mass 54)	10.8-11.7 (EI)
$CH_3C{\equiv}CCH_3$ (mass 54)	11.4 (EI)
CH_3CH=C=CH_2 (mass 54)	10.86,11.0
$CH_3COC{\equiv}CH$ (mass 68)	11.55
C_4H_4O (furan) (mass 68)	12.1
C_6H_6 (benzene, mass 78)	13.79-16.9 (14.7-16.1 EI)
four C_6H_6's (mass 78) - not benzene	11.99-14.57 (EI)

Mass 54 as possible parent of mass 39:

Measurements of 6/13/93; at 4.58 mm, derive $I_{39}/I_{44} = 1.5x10^{-2}$ or $4.6x10^{-2}$, depending on which experimental AP one chooses.

Measurements of 7/2/93; interpolated to 4.58 mm, derive I_{54}/I_{44} = 2.7e-2. The low AP measurement of mass 39 is about 60% that of mass 54.

On 6/24/93, appearance of mass 39 from benzene was measured. At AP+4, the fraction I_{39}/I_{78} was about 5%. The signal of mass 39 a much higher fraction of the mass 54 signal, so mass 54 is probably not the (sole) parent of mass 39.

Mass 68 as possible parent of mass 39:

Measurements of 6/13/93; at 4.58 mm, derive $I_{39}/I_{78} = 1.4x10^{-2}$ or $4.1x10^{-2}$, depending on which experimental AP one chooses. Conversion from a CO_2 basis to a C_6H_6 basis via the RICS equation was necessary.

Measurements of 7/8/93; interpolated to 4.58 mm, derive $I_{68}/I_{78} = 9.3x10^{-3}$ to $1.2x10^{-2}$, depending on possible parent. The low AP measurement of mass 39 is *greater* than that of mass 54. Therefore, mass 68 is not the (sole) parent of mass 39.

Results:

1. None of the masses at 54 and 68 are in high enough concentrations to adequately explain the low appearance of mass 39. It could be both masses contribute some.

2. There may be other, unknown species contributing.

3. The high appearance of mass 39 is probably not attributable to a significant extent to the mass 54 and 68 species. Given its magnitude and energy of appearance, it is probably from benzene.

4. Because there is no mass 40 signal measured (enormous interference from argon), its contribution cannot be evaluation.

Mass 41

Measured IP/AP = 12.33.

Table L.2 Possible parent species for mass 41, with literature appearance potentials.

Species	AP (eV)
C_3H_6 (mass 42)	11.4-12.11 (range incl. EI)
c-C_3H_6 (mass 42)	10.74-12.06 (range incl. EI)
1-C_4H_8 (mass 56)	11.28-11.8 (EI)
iso-C_4H_8 (")	11.45-11.8 (EI)
cis-2-C_4H_8 (")	11.33-11.6 (EI)
c-$C_3H_5CH_3$ (")	10.9-11.0?
$(CH_2)_3O$ (mass 58)	11.8 (EI)
3,4-epoxy-1-butene (m70)	11.1
c-C_5H_8=CH_2	10.2, 12.03, 14.05 (EI)
C_6H_{10} (mass 82)	">10.9", 13.1
c-C_6H_{10} (mass 82)	12.12

Species	AP (eV)
c-$C_5H_7CH_3$ (mass 82)	12.28, 12.45
Bicyclo C6H10's (m82)	10.64, 11.65

Mass 42 as possible parent of mass 41:

Masses 41 and 42 were measured at the same time and can be compared directly. Using the more believable of the two IEff lines for mass 41, I_{41} = 990 and I_{42} = 1944, at AP+3.3. That is, mass 41 is 34% of mass 42. *But,* the measured AP is 12.33eV, while the dropoff in the mass 42 signal occurs at 15.6eV. This is 3.27 eV difference.

Compare first with mass 39 from benzene, measured on 6/24/93, where mass 39 appears right where benzene starts to drop off. But this is a skeletal fragmentation, so compare also with methyl from methane (an H elimination like mass 42/41), where for example the mass 16 curve takes a downturn at 17.6eV but the CH_3 curve starts to appears at 14.4. The difference is 3.2eV, as compared with 3.3eV for masses 42/41. Also, at 3.3eV above the AP, the amount of CH_3 is about 36%. So, if the C_3 species is analogous to methane, C_3H_6 (linear or cyclic) could be the parent of mass 41.

Mass 56 as possible parent of mass 41:

Measurements of 6/13/93; at 4.58 mm, derive $I_{41}/I_{44} = 4.9x10^{-2}$.

Measurements of 7/2/93; interpolated to 4.58 mm, derive $I_{56}/I_{44} = 2.6x10^{-2}$ to $3.1x10^{-2}$, depending on the possible parent species. Also, the dropoff in mass 56 (which requires a skeletal fragmentation to produce mass 41) occurs at least 2.2 eV, and as much as 4.1 eV, above the measured AP.

Therefore, the mass 41 signal is *greater* than the mass 56 signal, and the latter is not a significant contributor.

Mass 58 as possible parent of mass 41:

Measurements of 6/13/93; at 4.58 mm, derive $I_{41}/I_{44} = 2.9x10^{-2}$.

Measurements of 7/2/93; interpolated to 4.58 mm, derive $I_{58}/I_{44} = 7.2x10^{-3}$, depending on the possible parent species. Also, the dropoff in mass 56 (which requires a skeletal fragmentation to produce mass 41) occurs at least 2.2 eV, and as much as 4.1 eV, above the measured AP.

Therefore, the mass 41 signal is *greater* than the mass 58 signal, and the latter is not a significant contributor.

Mass 70 as possible parent of mass 41:

Measurements of 6/13/93; at 4.58 mm, derive $I_{41}/I_{78} = 2.1x10^{-2}$ and $2.8x10^{-2}$, depending on the intercept of benzene used for comparison. Conversion from a CO_2 basis to a C_6H_6 basis via the RICS equation was necessary.

Measurements of 7/8/93; interpolated to 4.58 mm, derive $I_{70}/I_{78} = 2.0x10^{-3}$ and $2.8x10^{-3}$, depending on the intercept of benzene used for comparison.

Therefore, the mass 41 signal is *greater* than the mass 70 signal, and the latter is not a significant contributor.

Mass 82 as possible parent of mass 41:

Measurements of 6/13/93; at 4.58 mm, derive $I_{41}/I_{78} = 2.1x10^{-2}$ and $2.8x10^{-2}$, depending on the intercept of benzene used for comparison. Conversion from a CO_2 basis to a C_6H_6 basis via the RICS equation was necessary.

Measurements of 6/30/93; at 4.58 mm, derive $I_{82}/I_{78} = 3.6x10^{-3}$.

Therefore, the mass 41 signal is *greater* than the mass 82 signal, and the latter is not a significant contributor.

Results:

1. None of the masses at 56, 58, 70 and 82 are alone in high enough concentrations to adequately explain the low appearance of mass 41. If these masses make up much of the mass 41 signal, it's likely that more than one mass contributes. The most likely candidate in the group is 56, though the location of its dropoff is significantly different from the AP.

3. A mass 42 contribution is consistent with the behavior seen for the other H elimination studied, CH_4/CH_3. The AP measured is consistent with *both* C_3H_6 and c-C_3H_6.

4. There may be other, unknown, species contributing.

Mass 42

Measured IP/AP = 10.07, 10.11 for the two IEff measurements respectively.

Table L.3 Possible parent species for mass 42, with literature appearance potentials.

Species	AP (eV)
CH_3CHO (mass 44)	10.7 (EI)
C_3H_4=O (mass 56)	9.9
CH_3COCH_3 (mass 58)	10.2-10.7
n-C_4H_{10} (mass 58)	10.77-11.1 (10.77 EI)

Species	AP (eV)
iso-C_4H_{10} (")	10.88 (EI)
C_4H_6O (cyclobutanone) (mass 70)	9.85
C_5H_{12}'s (mass 72)	10.74-10.89
C_6H_{14}'s (mass 86)	10.60-10.86

Mass 44 (low electron energy signal) as possible parent of mass 42:

Measurements of 6/13/93; at 2.5 mm, derive $I_{42}/I_{44total} = 1.4x10^{-1}$.

Measurements of 5/3/93; at 2.5 mm, derive $I_{44low}/I_{44total} = 4.2x10^{-2}$.

Therefore, the mass 42 signal is *greater* than the mass 44 signal, and the latter is not a significant contributor.

Mass 56 as possible parent of mass 42:

Measurements of 6/13/93; at 2.5 mm, derive $I_{42}/I_{44} = 1.4x10^{-1}$.

Measurements of 7/2/93; interpolated to 2.5 mm, derive $I_{56}/I_{44} = 6.8x10^{-2}$.

Therefore, the mass 42 signal is *greater* than the mass 56 signal, and the latter is not a significant contributor.

Mass 58 as possible parent of mass 42:

Measurements of 6/13/93; at 2.5 mm, derive $I_{42}/I_{44} = 1.4x10^{-1}$.

Measurements of 7/2/93; interpolated to 2.5 mm, derive $I_{58}/I_{44} = 2.2x10^{-2}$.

Therefore, the mass 42 signal is *greater* than the mass 58 signal, and the latter is not a significant contributor.

Mass 70 as possible parent of mass 42:

Measurements of 6/13/93; at 2.5 mm, derive $I_{42}/I_{78} = 2.4x10^{-2}$. Conversion from a CO_2 basis to a C_6H_6 basis via the RICS equation was necessary.

Measurements of 7/8/93; interpolated to 2.5 mm, derive $I_{70}/I_{78} = 1.9x10^{-3}$ or $2.6x10^{-3}$, depending on the intercept of benzene used for comparison.

Therefore, the mass 42 signal is *greater* than the mass 70 signal, and the latter is not a significant contributor.

Mass 72 as possible parent of mass 42:

Measurements of 6/13/93; at 2.5 mm, derive $I_{42}/I_{78} = 2.4x10^{-2}$. Conversion from a CO_2 basis to a C_6H_6 basis via the RICS equation was necessary.

Measurements of 7/8/93; interpolated to 2.5 mm, derive $I_{72}/I_{78} = 3.5x10^{-4}$ (difference for the two benzene intercepts was very small).

Therefore, the mass 42 signal is *greater* than the mass 72 signal, and the latter is not a significant contributor.

Mass 86 as possible parent of mass 42:

Measurements of 6/13/93; at 2.5 mm, derive $I_{42}/I_{78} = 2.4x10^{-2}$. Conversion from a CO_2 basis to a C_6H_6 basis via the RICS equation was necessary.

Measurements of 6/30/93; at 2.5 mm, derive $I_{86}/I_{78} = 1.9x10^{-4}$.

Therefore, the mass 42 signal is *greater* than the mass 86 signal, and the latter is not a significant contributor.

Results:

1. There is no possible parent species which is in high enough concentration to expect that a significant portion of the mass 42 signal is from a fragmentation process.

2. The highest possible contributions to the mass 42 signal would come from CH_3CHO, c-C_3H_4=O, CH_3COCH_3, and n-C_4H_{10}. (c-C_3H_4=O comes the closest, with mass 42 being about 67% of the mass 42 and mass 56 signal combined. At only about AP_{meas}+2eV, this is much more fragmentation than would be expected.)

Mass 52

IEff measurements show the intercept to be 14.0-14.7 eV.

Table L.4 Possible parent species for mass 52, with literature appearance potentials.

Species	AP (eV)
$CH_3C{\equiv}CCH_3$ (mass 54)	14
CH_2=CHCH=CH_2 (mass 54)	13.84
Benzene (mass 78)	13.94-15.55 (EI)
C_6H_8's (mass 80)	12.82-13.91
CH_3CH=CHCH=$CHCH_3$ (mass 82)	15.41

Mass 54 as possible parent of mass 52:

Measurements of 5/9/93 and 6/3/93; at 2.9 mm, derive $I_{52}/I_{78} = 1x10^{-1}$ and $3.5x10^{-1}$.

Measurements of 7/2/93; at 2.9 mm, derive $I_{54}/I_{78} = 6.3x10^{-2}$. Conversion from a CO_2 basis to a C_6H_6 basis via the RICS equation was necessary.

Therefore, the mass 52 signal is *greater* than the mass 54 signal, and the latter is not a significant contributor.

Benzene as possible parent of mass 52:

From measurements of the two species on 5/19/93 at 2.9 mm, at the same electron energy (AP+2.5), $I_{52}/I_{78} = 7x10^{-2}$. This is just what would be expected for benzene as the parent species.

Mass 80 as possible parent of mass 52:

Measurements of 5/9/93 and 6/3/93; at 2.9 mm, derive $I_{52}/I_{78} = 1x10^{-1}$ and $3.5x10^{-1}$.

Measurements of 6/30/93; interpolated to 2.9 mm, derive $I_{80}/I_{78} = 1.1x10^{-2}$.

Therefore, the mass 52 signal is *greater* than the mass 80 signal, and the latter is not a significant contributor.

Mass 82 as possible parent of mass 52:

Measurements of 5/9/93 and 6/3/93; at 2.9 mm, derive $I_{52}/I_{78} = 1x10^{-1}$ and $3.5x10^{-1}$.

Measurements of 6/30/93; interpolated to 2.9 mm, derive $I_{82}/I_{78} = 6.0x10^{-3}$.

Therefore, the mass 52 signal is *greater* than the mass 82 signal, and the latter is not a significant contributor.

Results:

1. None of the masses at 54, 80 and 82 are alone in high enough concentrations to adequately explain the appearance of mass 52. If these masses make up much of the mass 41 signal, it's likely that more than one mass would be contributing. There are no good candidates in the above group, though the best of the lot is mass 54.

2. A mass 78 contribution is consistent with the appearance of mass 52. On 6/24/93, appearance of mass 52 from benzene was measured directly. The measured AP was around 16 eV with the bottom of the tail at about 14.6 eV. At AP+2, the fraction I_{52}/I_{78} was about 5%. It looks like most or all of the mass 52 signal is from benzene fragmentation.

Mass 55

Since no ionization efficiency curve was done, there is no experimental intercept. The question being investigated for this mass was whether the large increase in signal in going from 10.3 eV to 12.6 eV might have been from fragmentation. The appearance potentials for C_4H_7 from C_5H_{10} (mass 70) are about 10.3-11.5 eV. The AP from C_4H_8 (mass 56) ranges from 11.2-12.0 eV. The signal from C_4H_8 fragmentation could show up much earlier and stronger than that from mass 70, because it is an H elimination. Also, there is twice as much mass 56 as mass 70. As for H/C/O species, the AP from C_4H_6O is 10.4-10.8eV.

Rough fragment analysis shows that at 12.6 eV (AP+1.0 to AP+1.9 eV), excess mass 55 comprises about 26-32% of the combined signals of excess mass 55 plus mass 56. Since this is an H elimination fragmentation, high levels of fragment are feasible. However, this level of fragmentation is only seen around 2.5-3.5 eV above the appearance potential, in the methane H elimination to CH_3. Some of the increase in signal could therefore be due to other sources, for example from mass 70.

Because of the probable contribution from fragmentation at the higher energy, the lower electron energy measurement was chosen for the mole fraction data.

Mass 56

The measured IP/AP's are 9.8, 10.13, 9.7, and 10.27 eV respectively (average 10.0 eV).

Table L.5 Possible parent species for mass 56, with literature appearance potentials.

Species	AP (eV)
C_5H_{12} (mass 72)	11.0 (EI), 10.4-10.9
C_6H_{12} (mass 84)	11.08-11.45
C_6H_{14}'s (mass 86)	10.2-11
$C_6H_{12}O$'s (mass 100)	9.86-11.1

Mass 100 does not have a significant signal in the flame, leaving the other three species for fragmentation analysis.

Mass 72 as possible parent of mass 56:

Measurements of 5/19/93; at the maximum signal (2.9 mm), derive $I_{56}/I_{78} = 2.2x10^{-2}$. From the data curve, the maximum is about 40% greater than the signal at 1.0 mm. At that height, I_{56}/I_{78} would then be $1.6x10^{-2}$.

Measurements of 7/8/93; at the maximum signal (1.0 mm), derive $I_{72}/I_{78} = 1.3x10^{-3}$.

Therefore, the mass 56 signal is *greater* than the mass 72 signal, and the latter is not a significant contributor.

Mass 84 as possible parent of mass 56:

Measurements of 5/19/93; at 2.9 mm, derive $I_{56}/I_{78} = 2.2x10^{-2}$.

Measurements of 6/30/93; intepolated to 2.9 mm, derive $I_{84}/I_{78} = 1.3x10^{-3}$.

Therefore, the mass 56 signal is *greater* than the mass 84 signal, and the latter is not a significant contributor.

Mass 86 as possible parent of mass 56:

Measurements of 5/19/93; at 2.9 mm, derive $I_{56}/I_{78} = 2.2x10^{-2}$.

Measurements of 6/30/93; intepolated to 2.9 mm, derive $I_{86}/I_{78} \lesssim 1.3x10^{-3}$.

Therefore, the mass 56 signal is *greater* than the mass 86 signal, and the latter is not a significant contributor.

Result:

Mass 56 is purely or nearly purely derived from an ionization process alone, and not fragmentation in the ionizer.

Mass 57

Since no ionization efficiency curve was done, there is no experimental intercept. The question being investigated for this mass was whether the large increase in signal in going from 10.3 eV to 12.6 eV might have been from fragmentation.

Table L.6 Possible parent species for mass 57, with literature appearance potentials.

Species	AP (eV)
i-C_4H_{10} (mass 58)	10.7
n-C_4H_{10} (mass 58)	11.1 (EI)
C_3H_6O (mass 58)	11.5-13.1 (EI)
C_5H_{12}'s (mass 72)	10.35-11.3
C_4H_8O (mass 72)	10.45 (EI)
C_6H_{14}'s (mass 86)	10.5-11.1
$C_5H_{10}O$ (mass 86)	10.6 (EI)

Mass 58 as possible parent of mass 57:

Mass 58 signals are less than the mass 57 signal at the data electron energy, so that is not a likely source of the mass 57 signal.

Mass 72 as possible parent of mass 57:

From the 7/2/93 data measurements, at 1.0 mm, $I_{57}/I_{56} = 0.75$, where I_{57} is the signal from the high electron energy measurement. The mass 57 signal was taken at an energy 0.6 eV higher than mass 56. An estimated correction to the same energy reduces the ratio to 0.57. Therefore, from the fragmentation analysis of mass 56, estimate that $I_{57}/I_{78} \approx 0.57 \times 1.6x10^{-2} = 9x10^{-3}$.

Measurements of 7/8/93; at the maximum signal (1.0 mm), derive $I_{72}/I_{78} = 1.3x10^{-3}$.

Therefore, the mass 56 signal is *greater* than the mass 72 signal, and the latter is not a significant contributor.

Mass 86 as possible parent of mass 57:

From the 7/2/93 data measurements, at 2.9 mm, $I_{57}/I_{56} = 0.53$, where I_{57} is the signal from the high electron energy measurement. The mass 57 signal was taken at an energy 0.6 eV higher than mass 56. An estimated correction to the same energy reduces the ratio to 0.40. Therefore, from the fragmentation analysis of mass 56, estimate that $I_{57}/I_{78} \approx 0.40 \times 2.2\text{x}10^{-2} = 9\text{x}10^{-3}$.

Measurements of 6/30/93; intepolated to 2.9 mm, derive $I_{86}/I_{78} \lesssim 1.3\text{x}10^{-3}$.

Therefore, the mass 56 signal is *greater* than the mass 86 signal, and the latter is not a significant contributor.

Result:

Mass 57 is purely or nearly purely derived from an ionization process alone, and not fragmentation in the ionizer.

Mass 66

The intercept of mass 66 was measured to be 8.7 eV or 9.5 eV, compared to the two intercepts of benzene.

Table L.7 Possible parent species for mass 66, with literature appearance potentials.

Species	AP (eV)
phenol (mass 94)	11.7-12.45 (EI)
c-C_7H_{10} (mass 94)	10.7
bicyclo C_7H_{10} (mass 94)	10.02,10.45
norbornene (mass 94)	9.58
other bi-, tricyclos (mass 94)	9.22-10.15

Mass 94 as possible parent of mass 66:

Mass 94 data were taken on 11/12/92, relative to benzene. Mass 66 data was taken on 11/19/92, also relative to benzene. The ratio of I_{66}/I_{78} to I_{94}/I_{78} ranges from 0.15 to 0.46, both collected at an energy (about 10.9 eV) approximately 0.8 eV below the listed AP from phenol. Even if the acknowledged variation of electron impact appearance potentials from literature values is considered, the amount of mass 66 relative to mass 94 is far too high for a skeletal fragmentation to conclude that a significant amount of mass 66 is from phenol destruction in the ionizer. It is also too high for the other mass 94 possibilities with lower AP's to be significant either, since they also involve skeletal fractures.

Appendix M. Heats of Formation From Thermochemical Kinetics.

The following table contains calculated heats of formation for species for which ionization potential estimates had to be made. (In these cases, Lias et al. (1988) only gives heats of formation for the negative ions.) All computations were performed with the THERM program of Ritter et al. (1990). In certain cases, small modifications to their bond dissociation energies ("BDE") were made. Also, some values for groups or BDE's had to be estimated. When there was no clearly relevant BDE choice for a radical correction, the several possibilities were checked against analogous situations, it possible[51]. Units are kcal/mol.

Table M.1 Heats of formation by thermochemical kinetics, for ionization potential estimates, using THERM.

Species	ΔH^0_{f300}	Species	ΔH^0_{f300}
$HC{\equiv}COH$	20.43	2-methyl,5-hydro-c-C_4H_3O	3.03
HCCCO	55.10	3-methyl,2-hydro-c-C_4H_3O	3.11
$HC{\equiv}CCH_2O$	61.78	$(CH_3)_2C{=}CHCO$	-5.74
$CH_2{=}CHCHOH$	-1.80	1-c-C_5H_8OH	-17.21
$CH_2CH{=}CHOH$	-1.38	2-c-$C_4H_6O(CH_3)$-2-yl	-11.23
C_2H_5CHOH	-20.30	2-c-$C_4H_6O(CH_3)$-3-yl	-7.90
$C_2H_5OCH_2$	-9.20	2-c-C_5H_9O	-11.80
CH_3CHOCH_3	-8.70	c-$C_3H_5C(OH)CH_3$	2.17
$C(CH_3)_2OH$	-26.10	$CH_3CH{=}CHC(OH)CH_3$	-17.94
1-c-$C_3H_2CH_3$-2-yl	93.88	$CH_3C(OH){=}C(CH_2)CH_3$	-19.03
$CH_2{=}CCH{=}CH_2$	59.60	1,3-c-$C_4H_3(CH_3)_2$	53.38
c-$C_3H_4CH_3$ H at CH_3	51.92	c-$C_3(CH_3)_3$	76.40
c-$C_3H_4CH_3$ H at H	49.77	c-$C_5H_6(CH_3)$ [1-ene,2-CH_3]	56.27
c-C4H5O (2-hydrofuran)	12.23	c-C_6H_9	30.63
2,3,4-trihydrofuran	-0.73	$CH_3C{\equiv}CC(CH_3)_2$	55.18
2,3,5-trihydrofuran	-3.80	c-$C_5H_8CH_3$-1-yl	18.29
$CH_2C(CH_3){=}CHOH$	-9.83	1,1-c-$C_3H_4(CH_3)CH_2CH_2$	41.84
$CH_3CHCH{=}CHOH$	-8.74	1,1-c-$C_3H_4(CH_3)CHCH_3$	39.19
$CH_2CH(CH_3)CHOH$	21.60	1,2-c-$C_4H_5(CH_3)_2$ H at CH_3	38.80
CH_3CHCH_2CHOH	21.15	1,2-c-$C_4H_5(CH_3)_2$ H at H	36.65
$CH_3C(OH)CH_2CH_2$	18.00	c-$C_5H_8CH_3$-2-yl	20.44

[51] For example, in estimating the heat of formation of c-$C_3H_2CH_3$, a calculation of cycloprop-2-en-1-yl was performed. The BDE corrections for cyclopentadienyl and primary allyl might equally well have been chosen. The allyl correction gave closer results to literature data, and was therefore used for the c-$C_3H_2CH_3$ calculation.

Species	ΔH^0_{f300}	Species		ΔH^0_{f300}
$CH_3C(OH)=CHCH_3$	-46.68	$C_2H_5C(CH_3)CH=CH_2$		19.34
c-$C_3H_2(CH=CH_2)$	117.22	c-$C_3H_2(CH_3)_2CH_3$	H at CH_3	38.55
1,1-c-$C_3H_3(CH_3)_2$-2-yl	44.12	c-$C_3H_2(CH_3)_2CH_3$	H at H	36.40
c-$C_3H_5(CH_2CH_2)$	49.64	c-$C_3H_5C(CH_3)_2$		37.67
c-$C_3H_5(CHCH_3)$	46.99	$CH_3CH=CHC(CH_3)_2$		16.40
c-$C_4H_6(CH_3)$ H at CH_3	45.97	$(CH_3)_2CC(CH_3)=CH_2$		15.82
c-$C_4H_6(CH_3)$ H at H	43.82	C(C2H5)2(CH3)		1.80
CH3CH2C=CHCH3	48.92	(CH3)2CHC(CH3)2		0.40
(CH3)2CHC=CH2	49.87			

It was also found necessary to estimate the heat of formation of the o-$C_6H_4O_2$ and p-$C_6H_4O_2$ molecules, for a sensitivity analysis in Chapter 7. The heats of formation according to thermochemical kinetics were -35.41 kcal/mol and -44.25 kcal/mol, respectively. Entropies at 298 K of the species were estimated at 78.91 cal/mol-K and 73.25 cal/mol-K.

Appendix N. Reaction Sets for Models Under Review.

Models are given in the format used by CHEMKIN II (Kee et al., 1991).

N.1 Emdee et al. Model.

The basis for this model was Emdee et al. (1992), as received from Brezinsky (1994). Rate constants for which Zhang and McKinnon (1995) performed falloff calculations were replaced with the Zhang and McKinnon values, but only for the flame code solution; the original rate constants were kept for reaction path analysis. Both are listed below, with the originals preceeded by "!". Reactions from the H_2-O_2 system which were taken from Yetter et al. (1991) were revised to reflected argon as the principal component of the bath gas, rather than N_2.

Table N.1 Emdee et al. reaction mechanism, as revised for testing in this work.

```
ELEMENTS
C H O AR
END
SPECIES
CH3           H             O                   OH
H2            O2            CO                  CH4
HO2           H2O2          CO2                 CH3O
H2O           HCO           CH2O          AR
C6H5CH3       C6H5CH2       C6H5CHO       C6H5CO
C6H5C2H5      HOC6H4CH3
C6H5CH2OH     C6H5          C6H6
BIBENZYL      C6H5O         C5H5
CH2OH         C5H5O         C5H6                C4H5
C4H4          C6H5OH        C4H6                C5H4OH
C2H4          C2H2          C2H3                CH2
C5H4O         HCCO          OC6H4CH3
C6H5C2H3
END
REACTIONS
!
!  For reactions from Yetter et al. (1991) ("YDR") I've put in the numbers
!  applicable to Ar as a bath gas, and the YDR collision efficiencies.
!  Where Zhang/JTM applied QRRK to a reaction, I've replaced the
!  EBG reaction with that "low-pressure-ized" reaction.
!               R. Shandross MIT, 1994.
!
!
!
```

```
!  Emdee et al. (1992) model reaction set:
!
H+O2=O+OH                                                  1.906E+14      0     16440
O+H2=H+OH                                                  5.129E+04   2.67      6290
H2+OH=H2O+H                                                2.138E+08   1.51      3430
OH+OH=O+H2O                                                1.230E+04   2.62     -1878
!H2+M=H+H+M                                                4.571E+19   -1.4    104400
H2+M=H+H+M                                                 5.890E+18   -1.1    104380
 H2/3.333/ H2O/16.0/ CO2/5.067/ CO/2.533/ O2/1.14/
!O+O+M=O2+M                                                6.166E+15   -0.5         0
O+O+M=O2+M                                                 1.910E+13      0     -1790
 H2/3.333/ H2O/16.0/ CO2/5.067/ CO/2.533/ O2/1.14/
O+H+M=OH+M                                                 4.677E+18     -1         0
 H2/3.333/ H2O/16.0/ CO2/5.067/ CO/2.533/ O2/1.14/
!H+OH+M=H2O+M                                              2.239E+22     -2         0
H+OH+M=H2O+M                                               8.320E+21     -2         0
 H2/3.333/ H2O/16.0/ CO2/5.067/ CO/2.533/ O2/1.14/
!H+O2+M=HO2+M                                              6.761E+19  -1.42         0
H+O2+M=HO2+M                                               1.510E+15      0     -1000
 H2/3.333/ H2O/16.0/ CO2/5.067/ CO/2.533/ O2/1.14/
H+HO2=H2+O2                                                6.607E+13      0      2130
H+HO2=OH+OH                                                1.698E+14      0       870
HO2+O=O2+OH                                                1.738E+13      0      -400
HO2+OH=H2O+O2                                              1.445E+16     -1         0
HO2+HO2=H2O2+O2                                            3.020E+12      0      1390
!H2O2+M=OH+OH+M                                            1.202E+17      0     45500
H2O2+M=OH+OH+M                                             8.510E+16      0     45500
 H2/3.333/ H2O/16.0/ CO2/5.067/ CO/2.533/ O2/1.14/
H2O2+H=H2O+OH                                              1.000E+13      0      3590
H2O2+H=HO2+H2                                              4.786E+13      0      7950
H2O2+O=OH+HO2                                              9.550E+06      2      3970
H2O2+OH=H2O+HO2                                            7.079E+12      0      1430
!CO+O+M=CO2+M                                              2.510E+13      0     -4540
CO+O+M=CO2+M                                               2.190E+13      0     -4540
 H2/3.333/ H2O/16.0/ CO2/5.067/ CO/2.533/ O2/1.14/
CO+O2=CO2+O                                                2.512E+12      0     47690
CO+OH=CO2+H                                                1.500E+07    1.3      -765
CO+HO2=CO2+OH                                              6.026E+13      0     22950
HCO+M=H+CO+M                                               1.862E+17     -1     17000
 H2/3.333/ H2O/16.0/ CO2/5.067/ CO/2.533/ O2/1.14/
HCO+O2=CO+HO2                                              4.169E+12      0         0
HCO+H=CO+H2                                                7.244E+13      0         0
HCO+O=CO+OH                                                3.020E+13      0         0
HCO+OH=CO+H2O                                              3.020E+13      0         0
CH2O+OH=HCO+H2O                                            3.430E+09   1.18      -447
CH2O+O=HCO+OH                                              1.810E+13      0      3080
CH2O+H=HCO+H2                                              1.000E+14      0      4928
CH2O+HO2=HCO+H2O2                                          1.990E+12      0     11660
CH4=CH3+H                                                  6.138E+14      0    103800
CH4+H=CH3+H2                                               5.470E+07   1.97     11210
CH4+OH=CH3+H2O                                             5.720E+06   1.96      2639
CH4+O=CH3+OH                                               6.930E+08   1.56      8484
CH4+HO2=CH3+H2O2                                           1.810E+11      0     18580
CH3+HO2=CH3O+OH                                            2.000E+13      0      1076
CH3+OH=CH2OH+H                                             1.090E+11    0.4      -708
```

```
!  Emdee et al. (1992) model reaction set:
!
CH3+O=CH2O+H                                    8.430E+13      0        0
CH3+O2=CH3O+O                                   1.990E+18   -1.57    29230
CH2O+CH3=HCO+CH4                                5.540E+03    2.81     5863
HCO+CH3=CH4+CO                                  1.200E+14      0        0
CH3+HO2=CH4+O2                                  3.610E+12      0        0
CH3O+M=CH2O+H+M                                 9.370E+24    -2.7    30590
CH3O+O2=CH2O+HO2                                6.300E+10      0     2600
CH2OH+O2=CH2O+HO2                               2.410E+14      0     5000
CH2OH+M=CH2O+H+M                                1.670E+24    -2.5    34190
!JTM/Zhang value:
C6H5CH2+H=C6H5CH3                               7.230E+86   -20.6    49930
!C6H5CH2+H=C6H5CH3                              1.800E+14      0        0
!Zhang/JTM have a pathway C6H5+CH3=C6H5CH2+H in
!   addition to the following:
!JTM/Zhang value:
C6H5+CH3=C6H5CH3                                7.180E+86   -21.1    49950
!******Replacing the reverse of this with
!   JTM/Zhang value:
!C6H5CH3=C6H5+CH3                               1.400E+16      0    99800
C6H5CH3+O2=C6H5CH2+HO2                          3.000E+14      0    41400
C6H5CH3+OH=C6H5CH2+H2O                          1.265E+13      0     2583
C6H5CH3+H=C6H5CH2+H2                            1.200E+14      0     8235
C6H5CH3+H=C6H6+CH3                              1.200E+13      0     5148
C6H5CH3+O=OC6H4CH3+H                            1.630E+13      0     3418
CH3+C6H5CH3=CH4+C6H5CH2                         3.160E+11      0     9500
C6H5+C6H5CH3=C6H6+C6H5CH2                       2.103E+12      0     4400
C6H5OH+C6H5CH2=C6H5O+C6H5CH3                    1.050E+11      0     9500
HOC6H4CH3+C6H5CH2=OC6H4CH3+C6H5CH3              1.050E+11      0     9500
C6H5CH2+O=C6H5CHO+H                             2.500E+14      0        0
C6H5CH2+O=C6H5+CH2O                             8.000E+13      0        0
C6H5CH2+HO2=C6H5CHO+H+OH                        2.500E+14      0        0
C6H5CH2+HO2=C6H5+CH2O+OH                        8.000E+13      0        0
C6H5CH2+C6H5CH2=BIBENZYL                        2.510E+11    0.4        0
C6H5C2H5=C6H5CH2+CH3                            2.000E+15      0    72700
!JTM/Zhang value:
C6H5CH2+OH=C6H5CH2OH                            7.230E+86   -20.9    47840
!C6H5CH2+OH=C6H5CH2OH                           6.000E+13      0        0
C6H5CH2OH+O2=C6H5CHO+HO2+H                      2.000E+14      0    41400
C6H5CH2OH+OH=C6H5CHO+H2O+H                      8.433E+12      0     2583
C6H5CH2OH+H=C6H5CHO+H2+H                        8.000E+13      0     8235
C6H5CH2OH+H=C6H6+CH2OH                          1.200E+13      0     5148
C6H5CH2OH+C6H5CH2=C6H5CHO+C6H5CH3+H             2.110E+11      0     9500
C6H5CH2OH+C6H5=C6H5CHO+C6H6+H                   1.400E+12      0     4400
C6H5CHO+O2=C6H5CO+HO2                           1.020E+13      0    38950
C6H5CHO+OH=C6H5CO+H2O                           1.710E+09   1.18     -447
C6H5CHO+H=C6H5CO+H2                             5.000E+13      0     4928
C6H5CHO+H=C6H6+HCO                              1.200E+13      0     5148
C6H5CHO+O=C6H5CO+OH                             9.040E+12      0     3080
C6H5CH2+C6H5CHO=C6H5CH3+C6H5CO                  2.770E+03   2.81     5773
CH3+C6H5CHO=CH4+C6H5CO                          2.770E+03   2.81     5773
C6H5+C6H5CHO=C6H6+C6H5CO                        7.010E+11      0     4400
C6H5C2H5+OH=C6H5C2H3+H2O+H                      8.433E+12      0     2583
C6H5C2H5+H=C6H5C2H3+H2+H                        8.000E+13      0     8235
C6H5C2H5+O2=C6H5C2H3+HO2+H                      2.000E+14      0    41400
```

```
!  Emdee et al. (1992) model reaction set:
!
OC6H4CH3+H=HOC6H4CH3                          2.500E+14      0        0
OC6H4CH3=C6H6+H+CO                            2.510E+11      0    43900
HOC6H4CH3+OH=OC6H4CH3+H2O                     6.000E+12      0        0
HOC6H4CH3+H=OC6H4CH3+H2                       1.150E+14      0    12400
HOC6H4CH3+H=C6H5CH3+OH                        2.210E+13      0     7910
HOC6H4CH3+H=C6H5OH+CH3                        1.200E+13      0     5148
C6H5CO=C6H5+CO                                3.981E+14      0    29400
C6H5+H=C6H6                                   2.200E+14      0        0
C6H6+O2=C6H5+HO2                              6.300E+13      0    60000
C6H6+OH=C6H5+H2O                              2.110E+13      0     4570
!Zhang/JTM also have a pathway C6H5O+H=C5H6+O
!   for the following:
!JTM/Zhang (47)*'d:
C6H5O+H=C6H6+O                                3.020E+54  -11.2    64750
!*****Reverse reaction from JTM
!C6H6+O=C6H5O+H                               2.780E+13      0     4910
C6H6+H=C6H5+H2                                2.500E+14      0    16000
C6H5+O2=C6H5O+O                               2.090E+12      0     7470
!JTM/Zhang value:
C6H5O=CO+C5H5                                 1.240E+07    0.5    27800
!*****Reverse reaction from JTM
!C6H5O=CO+C5H5                                2.510E+11      0    43900
!JTM/Zhang (65)*'d:
C6H5O+H=C6H5OH                                7.240E+47   -9.7    20190
!C6H5O+H=C6H5OH                               2.500E+14      0        0
C6H5OH+OH=C6H5O+H2O                           6.000E+12      0        0
C6H5OH+H=C6H6+OH                              2.210E+13      0     7910
C6H5OH+H=C6H5O+H2                             1.150E+14      0    12400
C6H5OH+O=C6H5O+OH                             2.810E+13      0     7352
C2H3+C6H5OH=C2H4+C6H5O                        6.000E+12      0        0
C4H5+C6H5OH=C4H6+C6H5O                        6.000E+12      0        0
C6H5+C6H5OH=C6H6+C6H5O                        4.910E+12      0     4400
!JTM/Zhang value:
C5H5+H=C5H6                                   7.350E+32   -5.8     7470
!C5H5+H=C5H6                                  1.000E+14      0        0
!Zhang/JTM have a pathway C5H5+O=C5H5O in addition
!  to the following:
C5H5+O=C4H5+CO                                1.000E+14      0        0
C5H5+HO2=C5H5O+OH                             3.000E+13      0        0
C5H5+OH=C5H4OH+H                              3.000E+13      0        0
!Zhang/JTM have a pathway C5H6+CO=C6H5OH in
!  addition to the following:
C5H6+O2=C5H5+HO2                              2.000E+13      0    25000
C5H6+HO2=C5H5+H2O2                            1.990E+12      0    11660
C5H6+OH=C5H5+H2O                              3.430E+09   1.18     -447
C5H6+H=C5H5+H2                                2.190E+08   1.77     3000
C5H6+O=C5H5+OH                                1.810E+13      0     3080
C5H6+C2H3=C5H5+C2H4                           6.000E+12      0        0
C5H6+C4H5=C5H5+C4H6                           6.000E+12      0        0
C5H6+C6H5O=C5H5+C6H5OH                        3.160E+11      0     8000
!JTM/Zhang value:
C5H5O=C4H5+CO                                 3.310E+10   -1.2    30250
!C5H5O=C4H5+CO                                2.510E+11      0    43900
```

```
!  Emdee et al. (1992) model reaction set:
!
!JTM/Zhang value:
C5H4O+H=C5H4OH                                    5.360E+31   -5.4     12420
!*****Replaced by reverse JTM reaction
!C5H4OH=C5H4O+H                                   2.100E+13      0     48000
C5H4O=CO+C2H2+C2H2                                1.000E+15      0     78000
C4H5=C2H3+C2H2                                    3.980E+11    0.7     42260
!Zhang/JTM have pathways C2H3+C2H=C4H4 and
!   H+C4H3=C4H4 in addition to the following:
C4H5+M=C4H4+H+M                                   2.981E+33     -5     44320
C4H5+O2=C4H4+HO2                                  1.205E+11      0         0
C2H3+M=C2H2+H+M                                   2.981E+33     -5     44320
C2H3+O2=C2H2+HO2                                  1.205E+11      0         0
!Zhang/JTM have a pathway HCCO+H=HCCOH in addition
!   to the following:
C2H2+O=HCCO+H                                     5.800E+06   2.09      1562
!Zhang/JTM have a pathway CH2+CH=CH2CO in addition
!    to the following:
C2H2+O=CH2+CO                                     1.400E+06   2.09      1562
CH2+O2=H+OH+CO                                    6.022E+11      0         0
CH2+O2=CO+H2O                                     2.410E+11      0         0
HCCO+O2=OH+CO+CO                                  1.460E+12      0      2500
END
```

N.2 Zhang and McKinnon Model.

The basis for this model was Zhang and McKinnon (1995), as received from Zhang (1994). Pressure effects for reactions for which the original authors had performed QRRK calculations were recomputed for 22 torr and a bath gas characteristic of the $\phi = 1.79$, H_2-O_2-C_6H_6-Ar flame. Details of the bath gas properties are given in Appendix C.

Reactions from the H_2-O_2 system which were taken from Yetter et al. (1991) were revised to reflected argon as the principal component of the bath gas, rather than N_2.

Table N.2 Zhang and McKinnon reaction mechanism, as revised for testing in this work.

```
        ELEMENTS H O C AR END
!
        SPECIES
        AR C12H10 C6H6 C6H5OH C6H5O C6H5 C5H6 C5H5O  C5H4OH  C5H5
        C5H4O C4H6 CH2CHCHCH C4H4  H2CCCCH C4H2  C3H4 H2CCCH C3H2
        C2H4 C2H3 C2H2 CH2CO  C2H HCCO CH4 CH3O CH3 CH2O  CH2 CH
        CO2 CO H2O H2 H2O2 HCO HO2  H OH O2 O C6H5(L) C6H4OH C6H4
        C6H2 C6H  C5H3 C5H2 CH2CHCCH2  HCCHCCH C4H H2C4O
        C3H6 C3H5 C3H4P C2H6 C2H5 HCCOH C2O C2 CH3OH CH2OH HCH C
        C5H5(L) C6H3 C7H7 C7H8 C7H8O C8H6 C8H8 C8H10 C10H7 C10H8
        END
!
```

```
        REACTIONS
!
!  This version of the JTM/Zhang mechanism is identical to their's,
!  except that QRRK reactions are for 22 torr, and a bath gas comprised of
!  average RAS flame proportions of Ar, H2, H2O and O2.  9/7/94.
!
!!  The following reactions (marked with "!!") are the original ZM QRRK rate
!!  constants:
!!
!!     C6H5+C6H5=C12H10              4.61E12              -.05          60.0
!!     HCCHCCH+C6H5=C10H8            7.23E86            -21.12       48800.0
!!     HCCHCCH+C6H5=C10H7+H          5.63E77            -17.62       62310.0
!!     C10H7+H=C10H8                 1.01D40             -6.78        206100.
!!     C6H5+C2H3=C8H8                1.332E84           -19.96       53190.0
!!     C6H5+C2H=C8H6                 5.102E13           -17.31       46220.0
!!     C7H7+H=C7H8                   7.23E86            -20.63       49930.0
!!     C6H5+CH3=C7H8                 7.184E86           -21.11       49950.0
!!     C7H7+OH=C7H8O                 7.23E86            -20.91       47840.0
!!     C6H5+CH3=C7H7+H               1.61E57            -11.7        51750.0
!!     C6H5O+H=C6H6+O                3.02E54            -11.21       64750.0
!!     C3H4+C3H2=C6H6                7.383E13            -.69          920.0
!!     C3H4P+C3H2=C6H6               1.42E14             -.78         1030.0
!!     C5H6+CO=C6H5OH                9.00E09             0.0          34600.0
!!     C6H5O+H=C6H5OH                7.24E47            -9.67         20190.0
!!     C6H5O+H=C5H6+CO               1.06E53            -10.74        41360.0
!!     C5H5+CO=C6H5O                 1.241E07            0.45         27800.0
!!     HCCHCCH+C2H2=C6H5(L)          8.32E13             -1.27         4880.0
!!     C6H4+H=C6H5(L)                3.31E66            -15.45        20490.0
!!     C6H3+H=C6H4                   6.04E32             -5.98         7650.0
!!     C2H2+HCCHCCH=C6H4+H           4.10E10              0.63         13550.0
!!     C5H5+CO=C6H4OH                1.38E11             -0.98         51190.0
!!     C4H2+C2H=C6H3                 2.70E31             -6.0          7450.0
!!     C6H2+H=C6H3                   1.30E22             -2.87         6130.0
!!     C5H5+H=C5H6                   7.35E32             -5.78         7470.0
!!     H2CCCH+C2H2=C5H5(L)           1.064E31            -6.92         4780.0
!!     CH2CHCHCH+CO=C5H5O            3.31E10             -1.17         30250.0
!!     H2CCCH+C2H2=C5H5              5.08E53            -12.53        57210.0
!!     C5H5+O=C5H5O                  15.9400             1.49         31630.0
!!     C5H4O+H=C5H4OH                5.36E31             -5.42         12420.0
!!     H+H2CCCCH=C4H4                3.48E25             -4.14         14150.0
!!     C2H3+C2H=C4H4                 9.22E27             -4.28         5510.0
!!     C2H2+C2H=HCCHCCH              4.17E36             -7.33         8780.0
!!     C2H3+CH3=C3H6                 5.554E31            -5.66         6120.0
!!     C2H+CH3=C3H4P                 5.53E38             -8.21         35420.0
!!     CH2+CO=CH2CO                  6.21E08             0.0           0.0
!!     HCCO+H=HCCOH                  7.42E38             -8.44         6150.0
!!
!!   End original ZM QRRK rate constants.
!
!Zhang and McKinnon (1995) model reaction set:
C6H5+C6H6=C12H10+H                              4.00E+11          0          4000
2C5H5=C10H8+H2                                  4.30E+36       -6.3         45671
C6H5+HCCHCCH=C10H8                              5.76E+94      -23.1         58049
C6H5+HCCHCCH=C10H7+H                            9.48E+77      -17.6         65693
C10H8+OH=C10H7+H2O                              2.10E+13          0          4600
C10H7+H=C10H8                                   1.16E+42       -7.3         23392
C10H8+C2H3=C10H7+C2H4                           5.00E+13          0         16000
```

```
!Zhang and McKinnon (1995) model reaction set:
C10H8+C2H=C10H7+C2H2                          5.00E+13      0      16000
C10H8+H=C10H7+H2                              2.50E+14      0      16000
C8H10+OH=C8H8+H2O+H                           8.34E+12      0       2583
C8H10+H=C8H8+H2+H                             8.00E+13      0       8235
C8H10+O2=C8H8+HO2+H                           2.00E+14      0      41400
C7H7+CH3=C8H10                                1.19E+13      0        221
C8H10=C8H8+H2                                 5.01E+12      0      64000
C6H5+C2H3=C8H8                                1.97E+73    -16.9    45926
C6H5+C4H4=C8H8+C2H                            3.20E+11      0       1900
C6H5+C4H6=C8H8+C2H3                           3.20E+11      0       1900
C4H4+C4H4=C8H8                                1.48E+14      0      38003
CH2CHCHCH+C4H4=C8H8+H                         3.16E+11      0        600
C6H6+C2H=C8H6+H                               1.00E+12      0          0
C6H5+C2H=C8H6                                 3.75E+65    -14.7    40046
C6H5+C4H2=C8H6+C2H                            2.00E+13      0          0
C6H5+C4H4=C8H6+C2H3                           3.20E+11      0       1350
CH2CHCHCH+C4H2=C8H6+H                         3.16E+11      0       1800
C7H7+H=C7H8                                   1.76E+92      -22     56509
C6H5+CH3=C7H8                                 1.04E+20     -2.2      2977
C7H8+O2=C7H7+HO2                              3.00E+14      0      41400
C7H8+OH=C7H7+H2O                              1.26E+13      0       2583
C7H8+H=C7H7+H2                                1.20E+14      0       8235
C7H8+H=C6H6+CH3                               1.20E+13      0       5148
C7H8+CH3=C7H7+CH4                             3.16E+11      0       9500
C7H8+C6H5=C7H7+C6H6                           2.10E+12      0       4400
CH2CHCHCH+C3H4=C7H8+H                         2.00E+11      0       3700
CH2CHCHCH+C3H4P=C7H8+H                        3.16E+11      0       3700
C7H7+OH=C7H8O                                 4.20E+97    -23.7    59320
C7H8O+H=C6H6+CH2OH                            1.20E+13      0       5148
C7H8O+H=C7H8+OH                               2.21E+13      0       7910
C7H8O+H=C6H5OH+CH3                            1.20E+13      0       5148
C6H5O+CH3=C7H8O                               1.00E+12      0          0
C7H7+C6H5OH=C7H8+C6H5O                        1.05E+11      0       9500
C6H5+CH3=C7H7+H                               5.50E+02      3.8     18344
C7H7+HO2=C6H5+CH2O+OH                         8.00E+13      0          0
C4H4+C2H2=C6H6                                4.47E+11      0      30090
C6H5+H=C6H6                                   2.20E+14      0          0
C6H6+H=C6H5+H2                                2.50E+14      0      16000
H+C6H5O=C6H6+O                                7.06E+53      -11    66159
C6H6+OH=C6H5+H2O                              1.45E+13      0       4491
C6H6+O2=C6H5+HO2                              6.30E+13      0      60000
C6H5+CH2O=C6H6+HCO                            1.75E+10      0          0
C3H4+C3H2=C6H6                                1.43E+13     -0.5      627
C3H4P+C3H2=C6H6                               2.33E+13     -0.5      715
C3H4+H2CCCH=C6H6+H                            2.20E+11      0       2000
C6H6+OH=C6H5OH+H                              3.54E+09      1       7906
CO+C5H6=C6H5OH                                1.35E+12     -0.6     36031
C6H5OH+H=C6H5O+H2                             1.15E+14      0      12400
C6H5OH+O=C6H5O+OH                             2.81E+13      0       7352
C6H5OH+OH=C6H5O+H2O                           2.95E+06      2       1312
C6H5OH+OH=C6H4OH+H2O                          6.00E+12      0          0
C6H5OH+HO2=C6H5O+H2O2                         3.00E+13      0      15000
C6H5OH+C2H3=C2H4+C6H5O                        6.00E+12      0          0
C6H5OH+CH2CHCHCH=C4H6+C6H5O                   6.00E+12      0          0
C6H5OH+CH2CHCCH2=C4H6+C6H5O                   6.00E+12      0          0
```

```
!Zhang and McKinnon (1995) model reaction set:
C6H5OH+C6H5=C6H6+C6H5O                    4.91E+12      0       4400
H+C6H5O=C6H5OH                            1.35E+41     -7.7     16271
C6H5O+C5H6=C5H5+C6H5OH                    3.16E+11      0       8000
H+C6H5O=C5H6+CO                           1.06E+42     -7.6     35349
C5H5+CO=C6H5O                             7.57E+05      0.8     27315
C6H5+O2=C6H5O+O                           2.09E+12      0       7470
C6H5+OH=C6H5O+H                           5.00E+13      0          0
C6H5+O2=2CO+C2H2+C2H3                     7.50E+13      0       15002
C6H5=C2H2+HCCHCCH                         4.50E+13      0       72530
C6H5=C6H5(L)                              4.09E+21     -2.4     75346
C6H5(L)+H=C6H4+H2                         2.00E+13      0          0
HCCHCCH+C2H2=C6H5(L)                      1.96E+12     -0.7      3755
C6H4+H=C6H5(L)                            2.16E+63    -14.5     19341
C4H4+C2H2=C6H5+H                          1.00E+09      0       29999
C6H4+H=C6H3+H2                            1.50E+14      0     10205.3
C6H3+H=C6H4                               4.18E+29     -5        6445
C6H4+OH=C6H3+H2O                          7.00E+13      0      3011.4
C6H4+C2H=C6H3+C2H2                        2.00E+13      0          0
HCCHCCH+C2H2=C6H4+H                       4.15E+05      2.1     11129
C5H5+CO=C6H4OH                            7.85E+09     -0.6     50703
C6H3+H=C6H2+H2                            2.00E+13      0          0
C4H2+C2H=C6H3                             2.09E+27     -4.7      5949
C6H2+H=C6H3                               4.56E+19     -2.1      5159
C6H2+M=C6H+H+M                            5.00E+16      0       80065
C6H2+OH=C6H+H2O                           1.10E+13      0      7002.7
C6H2+C2H=C6H+C2H2                         2.00E+13      0          0
C4H2+C2H=C6H2+H                           4.00E+13      0          0
2C3H2=C6H2+H2                             2.00E+13      0       85000
C6H2+C2H=C4H+C4H2                         1.00E+13      0          0
C5H6+HO2=C5H5+H2O2                        1.99E+12      0       11660
C5H6+O2=C5H5+HO2                          2.00E+13      0       25000
C5H6+O2=C5H5O+OH                          1.00E+13      0       20712
C5H6+O=C5H5+OH                            1.81E+13      0        3080
C5H6+C2H3=C5H5+C2H4                       6.00E+12      0          0
C5H6+CH2CHCHCH=C5H5+C4H6                  6.00E+12      0          0
C5H6+CH2CHCCH2=C5H5+C4H6                  6.00E+12      0          0
C3H5+C2H2=C5H6+H                          2.95E+32     -5.8      26733
C3H5+C5H5=C5H6+C3H4                       1.00E+12      0          0
C5H5+H=C5H6                               2.92E+29     -4.7       6148
C5H5=C5H5(L)                              1.11E+47    -10.5      55548
H2CCCH+C2H2=C5H5(L)                       5.62E+32     -7.3       6758
CH2CHCHCH+CO=C5H5O                        6.11E-01      1.9      31067
C5H5+OH=C5H4OH+H                          3.00E+13      0          0
C5H5+O=CH2CHCHCH+CO                       1.00E+14      0          0
C5H5+HO2=C5H5O+OH                         3.00E+13      0          0
H2CCCH+C2H2=C5H5                          7.39E+53    -12.5      57313
C5H5+O=C5H5O                              1.24E+25     -3.7       4763
C5H4O+H=C5H4OH                            5.27E+27     -4.2      10863
C5H4O=CO+C2H2+C2H2                        1.00E+15      0       78000
C4H2+HCH=C5H3+H                           1.30E+13      0          0
C4H2+CH2=C5H3+H                           3.00E+13      0          0
C4H2+CH=C5H2+H                            1.00E+14      0          0
C4H6+H2CCCH=CH2CHCCH2+C3H4                1.00E+13      0       22501
C4H6+O=C2H4+CH2CO                         1.00E+12      0          0
C4H6+O=C3H4+CH2O                          1.00E+12      0          0
```

```
!Zhang and McKinnon (1995) model reaction set:
C4H6+OH=C3H5+CH2O                          1.00E+12      0        0
C4H6+OH=C2H5+CH2CO                         1.00E+12      0        0
C4H6+H=CH2CHCHCH+H2                        3.00E+07      2     6000
CH2CHCCH2+M=C4H4+H+M                       2.00E+15      0    42000
CH2CHCHCH+M=C4H4+H+M                       1.00E+14      0    30000
CH2CHCCH2+O2=C4H4+HO2                      1.20E+11      0        0
CH2CHCHCH+O2=C4H4+HO2                      1.20E+11      0        0
CH2CHCHCH+H=CH2CHCCH2+H                    1.00E+14      0        0
CH2CHCHCH+OH=C4H4+H2O                      2.00E+07      2     1000
CH2CHCHCH+H=C4H4+H2                        3.00E+07      2     1000
CH2CHCHCH+C2H2=C6H6+H                      2.80E+03    2.9     1400
CH2CHCHCH+C2H3=C6H6+H2                     2.80E-07    5.6    -1890
2C2H3=CH2CHCCH2+H                          4.00E+13      0        0
CH2CHCCH2+OH=C4H4+H2O                      2.00E+07      2     1000
CH2CHCCH2+H=C4H4+H2                        3.00E+07      2     1000
HCCHCCH+H+M=C4H4+M                         1.00E+15      0        0
H2CCCCH+H+M=C4H4+M                         1.00E+15      0        0
H2CCCCH+H=C4H4                             1.30E+23   -3.4    13208
C4H4+OH=H2CCCCH+H2O                        7.50E+06      2     5000
C4H4+C2H=H2CCCCH+C2H2                      4.00E+13      0        0
C4H4+C2H=HCCHCCH+C2H2                      4.00E+13      0        0
C4H4+H=H2CCCCH+H2                          3.00E+07      2     5000
C4H4+H=HCCHCCH+H2                          2.00E+07      2    15000
H2CCCH+HCH=C4H4+H                          4.00E+13      0        0
C4H4+C2H3=C2H4+H2CCCCH                     5.00E+11      0    16300
C4H4+C2H3=C2H4+HCCHCCH                     5.00E+11      0    16300
C4H4+C2H=C4H2+C2H3                         1.00E+13      0        0
C2H3+C2H=C4H4                              3.05E+25   -3.5     4551
C2H4+C2H=C4H4+H                            1.21E+13      0        0
HCCHCCH+H=H2CCCCH+H                        1.00E+14      0        0
H2CCCCH+M=C4H2+H+M                         2.00E+15      0    48000
HCCHCCH+M=C4H2+H+M                         1.00E+14      0    30000
H2CCCCH+O=CH2CO+C2H                        2.00E+13      0        0
H2CCCCH+O=H2C4O+H                          2.00E+13      0        0
H2CCCCH+O2=CH2CO+HCCO                      1.00E+12      0        0
H2CCCCH+OH=C4H2+H2O                        3.00E+13      0        0
H2CCCCH+H=C4H2+H2                          5.00E+13      0        0
H2CCCCH+H2=C2H2+C2H3                       5.01E+10      0    20000
H2CCCCH+HCH=C3H4+C2H                       2.00E+13      0        0
C2H2+C2H=HCCHCCH                           4.76E+33   -6.4     7801
H2CCCH+CH=H2CCCCH+H                        7.00E+13      0        0
H2CCCH+CH=HCCHCCH+H                        7.00E+13      0        0
C2H2+C2H2=HCCHCCH+H                        1.46E+15      0    70480
C3H2+HCH=H2CCCCH+H                         3.00E+13      0        0
C4H2+O=C3H2+CO                             1.20E+12      0        0
2C3H2=C4H2+C2H2                            2.00E+13      0    85000
C2H2+C2H=C4H2+H                            3.00E+13      0        0
C4H2+M=C4H+H+M                             3.50E+17      0    80065
C4H2+C2H=C4H+C2H2                          2.00E+13      0        0
C3H6=C3H5+H                                2.50E+15      0    86688
C2H3+CH3=C3H6                              6.30E+28   -4.8     5017
C3H6+HO2=C3H5+H2O2                         9.64E+03    2.6    13910
C3H6+CH3=C3H5+CH4                          2.21E+00    3.5     5675
C3H6+O=C3H5+OH                             6.03E+10    0.7     7633
C3H6+O=C2H5+HCO                            1.21E+11    0.1     8960
```

```
!Zhang and McKinnon (1995) model reaction set:
C3H6+O2=C3H5+HO2                          6.03E+13          0       47593
C3H6+CH2OH=C3H5+CH3OH                     6.03E+01          3       11989
C3H6+CH3O=C3H5+CH3OH                      9.00E+01          3       11987
C3H6+C2H=C3H4P+C2H3                       1.21E+13          0           0
C3H6+CH2=C3H5+CH3                         7.23E+11          0        6192
C3H6+C2H5=C3H5+C2H6                       2.23E+00        3.5        6637
C3H6+C2H3=C3H5+C2H4                       2.21E+00        3.5        4682
C3H5+HCO=C3H6+CO                          6.03E+13          0           0
C3H5+CH2OH=C3H6+CH2O                      1.81E+13          0           0
C3H5+CH3O=C3H6+CH2O                       3.01E+13          0           0
C3H5+C2H3=C3H6+C2H2                       4.82E+12          0           0
C3H5+C2H5=C3H6+C2H4                       2.59E+12          0        -131
2C3H5=C3H4+C3H6                           8.43E+10          0        -262
C3H4+H=C3H5                               1.20E+11        0.7        3007
C3H5+H=C3H4+H2                            1.81E+13          0           0
C3H5+OH=C3H4+H2O                          6.03E+12          0           0
CH3+C2H2=C3H5                             2.43E+46      -10.9       19974
C3H5+CH2=C4H6+H                           3.01E+13          0           0
C2H+C3H5=C2H2+C3H4                        1.50E-01          0           0
C2H+C3H5=C2H3+H2CCCH                      2.00E+01          0           0
C3H5+C2H3=C3H4+C2H4                       2.41E+12          0           0
C3H5+C2H5=C3H4+C2H6                       9.64E+11          0        -131
C2H3+CH2OH=C3H5+OH                        1.21E+13          0           0
C2H4+HCH+M=C3H5+H+M                       3.19E+12          0      5285.4
C3H4=C3H4P                                1.90E+29         -5       67303
C3H4+C3H2=3C2H2                           1.70E+13          0       15000
C3H4P+C3H2=3C2H2                          1.70E+13          0       15000
C3H4P+OH=H2CCCH+H2O                       2.00E+07          2        1000
C3H4+O=CO+C2H4                            1.50E+13          0        2103
C3H4+OH=HCO+C2H4                          1.00E+12          0           0
C3H4+M=H2CCCH+H+M                         1.00E+17          0       70000
C3H4P+M=H2CCCH+H+M                        1.00E+17          0       70000
C3H4+CH3=H2CCCH+CH4                       2.00E+12          0        7700
C3H4P+CH3=H2CCCH+CH4                      2.00E+12          0        7700
C3H4+H=C2H2+CH3                           2.00E+13          0        2400
C2H+CH3=C3H4P                             4.16E+33        -6.6       33537
HCH+C2H2+M=C3H4+M                         1.20E+13          0        6600
C2H2+CH2+M=C3H4P+M                        2.23E+14          0           0
C2H3+HCH=C3H4+H                           3.00E+13          0           0
C2H2+CH2+M=C3H4+M                         2.23E+14          0           0
C3H4P+H=CH3+C2H2                          1.00E+14          0        4000
C3H4P+C2H=C2H2+H2CCCH                     1.00E+13          0           0
C3H4+C2H=C2H2+H2CCCH                      1.00E+13          0           0
H2CCCH+O=C3H2+OH                          3.20E+12          0           0
CH3+C2H=H2CCCH+H                          2.41E+13          0           0
C2H+CH2OH=H2CCCH+OH                       1.21E+13          0           0
C2H+C2H5=CH3+H2CCCH                       1.81E+13          0           0
C2H2+HCH=H2CCCH+H                         1.20E+13          0        6600
C2H2+HCCO=H2CCCH+CO                       1.10E+11          0        3000
H2CCCH+O2=CH2CO+HCO                       3.00E+10          0        2868
H2CCCH+H=C3H2+H2                          2.00E+13          0           0
C3H2+O=C2H+HCO                            6.80E+13          0           0
C3H2+OH=C2H2+HCO                          5.00E+13          0           0
H2C4O+H=C2H2+HCCO                         5.00E+13          0        3000
H2C4O+OH=CH2CO+HCCO                       1.00E+07          2        2000
```

```
!Zhang and McKinnon (1995) model reaction set:
C2H6+CH3=C2H5+CH4                                5.50E-01        4        8300
C2H6+H=C2H5+H2                                   5.40E+02      3.5        5210
C2H6+O=C2H5+OH                                   3.00E+07        2        5115
C2H6+OH=C2H5+H2O                                 8.70E+09        1        1810
C2H6+O2=C2H5+HO2                                 1.00E+13        0       51000
C2H6+HO2=C2H5+H2O2                               3.00E+11        0       11500
HCO+C2H5=C2H6+CO                                 1.21E+14        0           0
C2H4+C2H5=C2H3+C2H6                              6.32E+02      3.1       18010
2CH3+M=C2H6+M                                    3.18E+41       -7        2762
  H2/2/ CO/2/ CO2/3/ H2O/5/
CH2+C2H6=CH3+C2H5                                1.20E+14        0           0
C2H5+O=C2H4+OH                                   5.00E+13        0           0
C2H5+O=CH2O+CH3                                  1.61E+13        0           0
HO2+C2H5=C2H4+H2O2                               3.01E+11        0           0
HCH+CH3=C2H5                                     2.53E+20     -3.5        2030
CH3+C2H5=C2H4+CH4                                1.95E+13     -0.5           0
CH3+CH2=C2H5                                     1.11E+19     -3.2        1780
CH2OH+CH3=C2H5+OH                                1.37E+14     -0.4        6589
C2H+C2H5=C2H2+C2H4                               1.81E+12        0           0
C2H5+H=C2H4+H2                                   1.81E+12        0           0
C2H5+H=CH3+CH3                                   1.00E+14        0           0
C2H5+O2=C2H4+HO2                                 8.43E+11        0        3875
C2H4+H+M=C2H5+M                                  6.37E+27     -2.8         -54
2C2H4=C2H5+C2H3                                  4.82E+14        0       71539
C2H5+OH=C2H4+H2O                                 2.41E+13        0           0
C2H5+HO2=CH3+CH2O+OH                             2.40E+13        0           0
C2H4+M=C2H2+H2+M                                 2.60E+17        0       79297
  H2/2.5/ H2O/16/ CO/1.9/ CO2/3.8/ CH4/16/
C2H4+M=C2H3+H+M                                  1.40E+16        0       82360
C2H4+O=CH2O+CH2                                  2.51E+13        0        5000
C2H4+H=C2H3+H2                                   1.33E+06      2.5       12241
2HCH=C2H4                                        1.11E+20     -3.4        2070
HCH+CH3=C2H4+H                                   4.20E+13        0           0
CH3O+C2H3=CH2O+C2H4                              2.41E+13        0           0
CH2CO+CH2=C2H4+CO                                1.60E+14        0           0
C2H3+H2O2=C2H4+HO2                               1.21E+10        0        -596
C2H3+CH2O=C2H4+HCO                               5.43E+03      2.8        5862
C2H3+CH2OH=C2H4+CH2O                             3.01E+13        0           0
CH3+CH2=C2H4+H                                   4.94E+13     -0.1          94
CH+CH4=C2H4+H                                    6.00E+13        0           0
C2H4+O=CH3+HCO                                   1.60E+09      1.2         746
C2H4+OH=C2H3+H2O                                 2.02E+13        0        5955
C2H4+OH=CH3+CH2O                                 2.00E+12        0         960
C2H4+O2=C2H3+HO2                                 4.22E+13        0       57594
C2H4+CH3=C2H3+CH4                                4.16E+12        0    11127.2
C2H4+O=OH+C2H3                                   1.51E+07      1.9        3736
C2H4+C2H2=2C2H3                                  2.41E+13        0       68360
C2H3+HCO=C2H4+CO                                 9.04E+13        0           0
C2H2+H2=C2H3+H                                   4.02E+15     -0.6       65800
C2H3+O=CH2CO+H                                   3.00E+13        0           0
C2H3+O=C2H2+OH                                   3.00E+13        0           0
C2H3+O=CO+CH3                                    3.00E+13        0           0
CH+HCH=C2H3                                      3.09E+14       -2         620
CH+CH3=C2H3+H                                    3.00E+13        0           0
CH2+CH2=C2H3+H                                   2.00E+13        0           0
```

```
!Zhang and McKinnon (1995) model reaction set:
2HCH=C2H3+H                                          7.12E+21     -3.9       2460
CH2OH+C2H2=C2H3+CH2O                                 7.30E+11        0       9004
C2H3+O=HCO+CH2                                       3.00E+13        0          0
C2H3+O2=CH2O+HCO                                     4.00E+12        0       -250
C2H3+O2=C2H2+HO2                                     7.51E+14       -1       2376
C2H3+OH=C2H2+H2O                                     2.00E+13        0          0
C2H3+C2H=2C2H2                                       3.00E+13        0          0
C2H3+CH=HCH+C2H2                                     5.00E+13        0          0
C2H3+CH3=C2H2+CH4                                    3.92E+11        0          0
C2H3+CH2=CH3+C2H2                                    1.81E+13        0          0
C2H2+M=C2H+H+M                                       4.20E+16        0     107000
C2H2+O2=C2H+HO2                                      1.20E+13        0      74475
C2H2+H=CH+CH2                                        1.02E+16        0     125076
C2H+H2=C2H2+H                                        4.09E+05      2.4        864
C2H3+M=C2H2+H+M                                      3.00E+15        0      32006
  H2/2.5/ H2O/16/ CO/1.9/ CO2/3.8/ CH4/16/ CH3OH/5/
C2H2+OH=C2H+H2O                                      3.37E+07        2      14000
C2H2+OH=HCCOH+H                                      5.04E+05      2.3      13500
C2H2+OH=CH2CO+H                                      2.18E-04      4.5      -1000
C2H2+OH=CH3+CO                                       4.83E-04        4      -2000
CH3OH+C2H=CH3O+C2H2                                  1.21E+12        0          0
CH3OH+C2H=CH2OH+C2H2                                 6.03E+12        0          0
C2H+CH4=C2H2+CH3                                     1.81E+12        0        497
HCCO+CH=C2H2+CO                                      5.00E+13        0          0
HCCO+HCCO=C2H2+2CO                                   1.00E+13        0          0
HO2+C2H2=CH2CO+OH                                    6.03E+09        0       7949
HCO+C2H=C2H2+CO                                      6.03E+13        0          0
C+CH3=C2H2+H                                         5.00E+13        0          0
CH2+C2H2=HCH+C2H2                                    4.00E+13        0          0
CH2+CH2=C2H2+H2                                      4.00E+13        0          0
CH3O+C2H=CH2O+C2H2                                   2.41E+13        0          0
2HCH=C2H2+2H                                         4.97E+12      0.2       -150
2HCH=C2H2+H2                                         4.02E+14     -0.5        480
CH+HCH=C2H2+H                                        2.50E+12     -3.7       4190
C2H+CH2OH=C2H2+CH2O                                  3.61E+13        0          0
C2H+C2H=C2H2+C2                                      1.81E+12        0          0
C2H+CH2=CH+C2H2                                      1.81E+13        0          0
C2H2+O=C2H+OH                                        3.16E+15     -0.6      15000
C2H2+O=HCH+CO                                        1.40E+06      2.1       1562
C2H2+O=HCCO+H                                        5.80E+06      2.1       1562
CH2CO+M=HCH+CO+M                                     3.60E+15        0      59235
  H2/2.5/ H2O/16/ CO/1.9/ CO2/3.8/ CH4/16/ CH3OH/5/
CH2CO+O=CH2O+CO                                      2.00E+13        0          0
CH2CO+O=HCO+HCO                                      2.00E+13        0       2293
CH2CO+O=CH2+CO2                                      1.75E+12        0       1350
CH2CO+H=HCCO+H2                                      5.00E+13        0       8000
CH2CO+O=HCCO+OH                                      1.00E+13        0       8000
CH2O+CH=CH2CO+H                                      9.46E+13        0       -515
CH2+CO=CH2CO                                         6.13E+08        0          0
CH2CO+OH=HCCO+H2O                                    7.50E+12        0       2000
CH2CO+OH=CH2O+HCO                                    2.80E+13        0          0
CH2CO+OH=CH3O+CO                                     2.80E+13        0          0
HCCOH+H=CH2CO+H                                      1.00E+13        0          0
HCCO+H=CH2+CO                                        1.00E+14        0          0
HCCO+O=2CO+H                                         1.00E+14        0          0
```

!Zhang and McKinnon (1995) model reaction set:			
HCCO+H=HCCOH	7.54E+38	-8.3	6449
HCCO+OH=C2O+H2O	3.00E+13	0	0
HCCO+CH2=CH2O+C2H	1.00E+13	0	2000
HCCO+O2=2CO+OH	1.46E+12	0	2500
HO2+C2H=HCCO+OH	1.81E+13	0	0
C2H+O2=HCCO+O	5.00E+13	0	1500
C2H+OH=HCCO+H	2.00E+13	0	0
C2H+M=C2+H+M	4.68E+16	0	124000
C2H+O=CO+CH	5.00E+13	0	0
C2H+O2=HCO+CO	2.41E+12	0	0
C2H+O2=H+CO+CO	3.52E+13	0	0
C2H+O2=CO2+CH	3.52E+13	0	0
C2H+OH=CH2+CO	1.81E+13	0	0
C2H+OH=C2+H2O	4.00E+07	2	8000
C+HCH=C2H+H	5.00E+13	0	0
CH+HCH=C2H+2H	5.49E+22	-2.4	11520
C2+H2=C2H+H	4.00E+05	2.4	1000
C2O+H=CH+CO	5.00E+13	0	0
C2O+O=CO+CO	5.00E+13	0	0
C2O+OH=CO+CO+H	2.00E+13	0	0
C2O+O2=2CO+O	2.00E+13	0	0
C2+OH=C2O+H	5.00E+13	0	0
C2+O2=2CO	5.00E+13	0	0
CH4+O2=CH3+HO2	7.94E+13	0	56000
CH4+H=CH3+H2	5.47E+07	2	11210
CH4+OH=CH3+H2O	5.72E+06	2	2639
CH4+O=CH3+OH	6.93E+08	1.6	8484
CH4+HO2=CH3+H2O2	1.81E+11	0	18580
CH3OH+M=CH3+OH+M	8.86E+46	-7.9	102641
CH3OH+M=CH2OH+H+M	7.20E+46	-7.9	107705
CH3OH+CH3=CH2OH+CH4	3.19E+01	3.2	7172
CH3OH+CH3=CH3O+CH4	1.45E+01	3.1	6935
CH3OH+HO2=H2O2+CH2OH	9.80E+13	0	19400
CH3OH+O=OH+CH2OH	3.80E+05	2.5	3080
CH3OH+O=OH+CH3O	1.00E+13	0	4684
CH3OH+O2=CH2OH+HO2	2.05E+13	0	44717
CH3OH+OH=H2O+CH2OH	1.50E+13	0	5960
CH3OH+OH=H2O+CH3O	1.50E+13	0	5960
CH3OH+CH2OH=CH3OH+CH3O	7.83E+09	0	12062
CH3OH+H=CH2OH+H2	3.20E+13	0	6095
CH3OH+H=CH3O+H2	8.06E+12	0	6095
CH3O+M=CH2O+H+M	9.37E+24	-2.7	30590
CH3O+H=CH2O+H2	2.00E+13	0	0
CH3O+OH=CH2O+H2O	1.00E+13	0	0
CH3O+O=CH2O+OH	1.00E+13	0	0
CH3O+O2=CH2O+HO2	6.30E+10	0	2600
CH3O+HO2=CH2O+H2O2	3.01E+11	0	0
CH3O+CO=CH3+CO2	1.75E+13	0	11797
CH2OH+M=CH2O+H+M	1.67E+24	-2.5	34190
CH2OH+O=CH2O+OH	1.00E+13	0	0
CH2OH+O2=CH2O+HO2	2.41E+14	0	5000
CH2OH+OH=CH2O+H2O	1.00E+13	0	0
CH2OH+H=CH2O+H2	2.00E+13	0	0
CH2OH+HO2=CH2O+H2O2	1.20E+13	0	0
CH2OH+HCO=CH3OH+CO	1.20E+14	0	0

!Zhang and McKinnon (1995) model reaction set:			
CH2OH+CH2O=CH3OH+HCO	5.54E+03	2.8	5682
2CH2OH=CH3OH+CH2O	1.20E+13	0	0
CH2OH+HCO=2CH2O	1.81E+14	0	0
CH3+M=CH+H2+M	6.90E+14	0	82500
CH3+H+M=CH4+M	8.00E+26	-3	0
H2/2/ CO/2/ CO2/3/ H2O/5/			
CH3+HO2=CH3O+OH	2.00E+13	0	1076
CH3+O=CH2O+H	6.03E+13	0	0
CH3+O=CH3O	1.78E+14	-2.1	603
CH3+O2=CH3O+O	7.26E+11	0.4	27363
CH3+O2=CH2OH+O	1.29E+13	0	26900
CH3+OH=CH3OH	1.24E+43	-9.5	10471
CH3+OH=CH3O+H	8.93E+11	0	13073
CH3+OH=CH2O+H2	3.98E+10	0	8765
CH3+HO2=CH2OH+OH	2.00E+13	0	0
CH3+HCO=CH4+CO	1.20E+14	0	0
CH3+CH2OH=CH4+CH2O	2.41E+12	0	0
CH3+CH3O=CH4+CH2O	2.41E+13	0	0
CH3+CH2O=CH4+HCO	5.54E+03	2.8	5863
HCH+H+M=CH3+M	2.40E+31	-4.4	0
HCH+H=CH+H2	1.00E+18	-1.6	0
HCH+O=CO+2H	5.00E+13	0	0
HCH+O=CO+H2	3.00E+13	0	0
HCH+O2=CO2+2H	1.60E+12	0	1000
HCH+O2=CH2O+O	5.00E+13	0	9000
HCH+O2=CO2+H2	6.90E+11	0	500
HCH+O2=CO+H2O	1.90E+10	0	-1000
HCH+O2=CO+OH+H	8.60E+10	0	-500
HCH+O2=HCO+OH	4.30E+10	0	-500
HCH+OH=CH+H2O	1.13E+07	2	3000
HCH+OH=CH2O+H	2.50E+13	0	0
HCH+CO2=CH2O+CO	1.10E+11	0	1000
CH2+M=HCH+M	1.00E+13	0	0
H/0.0/ H2O/0.0/ C2H2/0.0/			
CH2+CH4=2CH3	4.00E+13	0	0
CH2+H2=CH3+H	7.00E+13	0	0
CH2+H2O=HCH+H2O	3.00E+13	0	0
CH2+H=HCH+H	2.00E+14	0	0
CH2+O=H+H+CO	3.00E+13	0	0
CH2+O=H2+CO	1.51E+13	0	0
CH2+O2=CO2+2H	1.59E+12	0	1000
CH2+O2=O+CH2O	2.00E+13	0	9000
CH2+O2=H2+CO2	6.90E+11	0	500
CH2+O2=H+CO+OH	1.30E+13	0	1505.7
CH2+OH=CH+H2O	4.50E+13	0	3000
CH2+OH=CH2O+H	3.01E+13	0	0
CH2+H=CH+H2	3.01E+13	0	0
CH2+CO2=CH2O+CO	3.00E+12	0	0
CH2+HO2=CH2O+OH	3.01E+13	0	0
CH2+H2O2=CH3O+OH	3.01E+13	0	0
CH2+HCO=CO+CH3	1.81E+13	0	0
CH2+CH2O=HCO+CH3	1.20E+12	0	0
CH2+O=CH+OH	3.00E+14	0	11923
CH2O+OH=HCO+H2O	3.43E+09	1.2	-447
CH2O+H=HCO+H2	2.19E+08	1.8	3000

```
!Zhang and McKinnon (1995) model reaction set:
CH2O+M=HCO+H+M                                3.31E+16        0       81000
CH2O+O=HCO+OH                                 1.80E+13        0        3080
CH2O+O2=HO2+HCO                               1.23E+06        3       52000
CH2O+HO2=HCO+H2O2                             4.40E+06        2       12000
CH+O=C+OH                                     1.52E+13        0        4732
CH+O=CO+H                                     5.70E+13        0           0
CH+O2=CO+OH                                   3.30E+13        0           0
CH+O2=HCO+O                                   3.30E+13        0           0
CH+OH=HCO+H                                   3.00E+13        0           0
CH+OH=C+H2O                                   4.00E+07        2        3000
CH+CO2=HCO+CO                                 3.40E+12        0         690
CH+H=C+H2                                     1.50E+14        0           0
CH+H2O=CH2O+H                                 1.17E+15     -0.8           0
CH+H2O=CH2OH                                  5.71E+12        0        -755
C+O2=CO+O                                     2.00E+13        0           0
C+OH=CO+H                                     5.00E+13        0           0
HCO+O=CO2+H                                   3.00E+13        0           0
HCO+O2=CO2+OH                                 3.31E+12     -0.4           0
HCO+HO2=CO2+OH+H                              3.00E+13        0           0
HCO+CH3O=CH3OH+CO                             9.04E+13        0           0
2HCO=CH2O+CO                                  4.50E+13        0           0
HCO+O2=CO+HO2                                 3.30E+13     -0.4           0
HCO+OH=CO+H2O                                 3.02E+13        0           0
HCO+M=H+CO+M                                  2.50E+14        0       16802
HCO+H=CO+H2                                   2.00E+14        0           0
HCO+O=CO+OH                                   3.00E+13        0           0
CO+O+M=CO2+M                                  2.51E+13        0       -4540
CO+OH=CO2+H                                   3.09E+11        0         735
CO+O2=CO2+O                                   2.51E+12        0       47690
CO+HO2=CO2+OH                                 6.03E+13        0       22950
H2O2+M=OH+OH+M                                1.20E+17        0       45500
H2O2+H=HO2+H2                                 4.79E+13        0        7950
H2O2+H=OH+H2O                                 1.00E+13        0        3590
H2O2+O=OH+HO2                                 9.55E+06        2        3970
H2O2+O=O2+H2O                                 9.55E+06        2        3970
HO2+H=H2O+O                                   3.00E+13        0        1070
HO2+H=H2+O2                                   6.61E+13        0        2130
HO2+H=OH+OH                                   1.40E+14        0        1073
HO2+OH=H2O+O2                                 7.50E+12        0           0
HO2+HO2=H2O2+O2                               2.00E+12        0           0
H2+OH=H2O+H                                   2.14E+08      1.5        3430
H2+O2=OH+OH                                   1.70E+13        0       47780
H+O2=OH+O                                     1.91E+14        0       16440
H+O2+M=HO2+M                                  3.61E+17     -0.7           0
  H2O/18.6/ CO2/4.2/ H2/2.9/ CO/2.1/
2H+M=H2+M                                     1.00E+18       -1           0
2H+H2=2H2                                     9.20E+16     -0.6           0
2H+H2O=H2+H2O                                 6.00E+19     -1.3           0
2H+CO2=H2+CO2                                 5.49E+20       -2           0
H+OH+M=H2O+M                                  2.24E+22       -2           0
H+O+M=OH+M                                    6.02E+16     -0.6           0
  H2O/5/
OH+H2O2=H2O+HO2                               7.08E+12        0        1430
OH+OH=O+H2O                                   1.23E+04      2.6       -1878
O+HO2=OH+O2                                   1.74E+13        0        -400
```

```
!Zhang and McKinnon (1995) model reaction set:
O+H2=OH+H                                          5.13E+04      2.7       6290
O+O+M=O2+M                                         6.17E+15     -0.5          0
O+OH+M=HO2+M                                       1.00E+17        0          0
```

N.3 Lindstedt and Skevis Model.

As received from Lindstedt (1995). This version was modified for CHEMKIN/PREMIX usage, from the original Lindstedt and Skevis (1994) model. In the revised version, six minor reactions were removed, two were rewritten in the reverse direction, and one reaction was added. The following excerpt from Lindstedt (1995) spells out the changes made and their rationale:

...we also had some significant problems with the numerical stability of CHEMKIN. The[y] have now been solved at the expense of removing six reactions which were found to cause problems below 1000 K. These were,

	Reaction	Source
1.	CH3 + M = CH2(S) + H + M	Markus et al.
2.	C3H4(P) + O2 = C2HO + CH2(T) + OH	Dagaut et al.
3.	C4H2 + C4H2 = C8H2 + H + H	Kiefer et al.
4.	C2H2 + C4H2 = C6H2 + H + H	Kiefer et al.
5.	C2H2 + C6H2 = C8H2 + H + H	Kiefer et al.
6.	C5H6 + O2 = C5H5 + HO2	Emdee et al.

The removal of these reactions regrettably affects the agreement for poly-acetylenic species adversely. We also noted three further problems of which two were of any consequence. The first was a misfit of the thermo for C6H7(L) though this did not play a major role. The second was excess HO2 formation through the following sequence,

7.	C2H5 + O2 = C2H4 + HO2	
8.	C2H5 + M = C2H4 + H + M	Baulch et al.

This problem was removed by writing reaction 8 in the reverse bi-molecular form with a frequency factor of 1E09. The final problem was adressed by writing an isomerisation reaction also in the reverse direction with in this case a frequency factor of 1E10. The new reaction reads

9.	C6H5(B) = C6H5	Our Estimate

The revised reaction mechanism is given in Table N.3. Close inspection reveals several reactions which have been changed other than those noted above. Original versions of changed reactions which involve the species C_5H_6, C_6H_5, C_6H_6, C_6H_5O and C_6H_5OH are indicated in the listijng below. Note that activation energies are listed in J/mol, rather than cal/mol.

Table N.3 Lindstedt and Skevis reaction mechanism, as revised by the original authors.

```
ELEMENTS
H O C AR
END
SPECIES
H       OH      O       HO2     H2      H2O
H2O2    O2      CO      CO2     AR      CH
CHO     CH2T    CH2S    CH2O    CH3
CH3O    CH2OH           CH4     C2H     C2HO    C2H2
C2H2O   CHCOH   C2H3    C2H4    C2H5    C2H6
C3H     C3H2            C3H3    C3H4A   C3H4P   C3H4B
C3H2O   C3H5A           C3H5S   C3H5T   C3H6    C3H7N
C3H7I   C3H8            C4H
C4H2    C4H3N   C4H3I   C4H4    C4H5S   C4H5T   C4H5I
C4H6S   C4H6T   C4H6B   C4H6O   C6H2    C6H3    C6H4L
C6H4C   C6H5    C6H5O   C6H5OH          C6H7L   C6H6A
C6H6B   C6H6D   C6H6S   C6H6M           C6H6F   C6H5A
C6H5B   C5H6    C5H5    C5H5O           C5H4O   C5H4OH
C5H6L   C5H5L   C5H4L   C5H3L           C8H2    CH3OH
C5H2    C2O     C4H2O   C6H7            C6H6
END
REAC      JOULES/MOLE
!!Original versions of changed reactions which involve the
!!   species C5H4O, C5H6, C6H5, C6H6, C6H5O and C6H5OH:
!!C6H5=C6H5B                    4.00E+13                    0              303400
!!C6H6F=C6H6                    7.58E+13                    0              276000
!!Note the change of mechanism to C6H6+O=C6H5O+H for the following reaction
!!   in the revised model:
!!C6H6+O=C6H5OH                 2.40E+13                    0               20500
!!C5H5+O=C4H5T+CO               5.00E+14                    0                   0
!!C5H6+OH=C5H5+H2O              3.43E+09                 1.18                1870
!!The following reaction doesn't appear in the revised model:
!!C5H6+O2=C5H5+HO2              2.00E+13                    0              104600
!!Note change of mechanism to C5H4O=CO+2C2H2 for the following reaction
!!   in the revised model:
!!C5H4O=CO+C4H4                 1.00E+15                    0              326570
!
!Lindstedt and Skevis(1994) model reaction set:    (Ea in J/mol, not cal/mol)
H+O2=OH+O                                          2.00E+14          0        70300
O+H2=OH+H                                          5.12E+04        2.7        26300
OH+H2=H2O+H                                        1.00E+08        1.6        13800
OH+OH=H2O+O                                        1.50E+09        1.1          420
O2+H+M=HO2+M                                       2.00E+18       -0.8            0
  AR/0.4/  O2/0.35/  CO/0.7/  CO2/1.5/ H2O/6.5/
HO2+H=OH+OH                                        1.68E+14          0         3660
HO2+H=H2+O2                                        4.27E+13          0         5900
HO2+OH=H2O+O2                                      2.89E+13          0        -2080
HO2+H=H2O+O                                        3.00E+13          0         7200
HO2+O=OH+O2                                        3.19E+13          0            0
HO2+HO2=H2O2+O2                                    1.86E+12          0         6440
H2O2+H=H2O+OH                                      1.00E+13          0        15000
H2O2+H=HO2+H2                                      1.70E+12          0        15700
H2O2+O=HO2+OH                                      6.60E+11          0        16600
```

```
!Lindstedt and Skevis(1994) model reaction set:    (Ea in J/mol, not cal/mol)
H2O2+OH=H2O+HO2                                  7.83E+12          0          5570
H2O2+M=OH+OH+M                                   1.20E+17          0        190000
  H2/1.87/  AR/1/  O2/1/
H+H+M=H2+M                                       6.53E+17         -1             0
  H2/0/  CO2/0/  H2O/0/
H+H+H2=H2+H2                                     9.20E+16       -0.6             0
H+H+H2O=H2+H2O                                   6.00E+19       -1.3             0
H+H+CO2=H2+CO2                                   5.49E+20         -2             0
H+OH+M=H2O+M                                     2.20E+22         -2             0
  H2/1.87/  AR/1/  O2/1/
O+O+M=O2+M                                       1.00E+17         -1             0
  H2/1.87/  AR/1/  O2/1/
CO+OH=CO2+H                                      4.39E+06        1.5         -3100
CO+HO2=CO2+OH                                    1.50E+14          0         98930
CO+O+M=CO2+M                                     5.30E+13          0        -19008
  H2/1.87/  AR/1/  O2/1/
CO+O2=CO2+O                                      2.50E+12          0        200000
CH+O2=CHO+O                                      3.30E+13          0             0
CH+CO2=CHO+CO                                    3.40E+12          0          2900
CH+O=CO+H                                        4.00E+13          0             0
CH+OH=CHO+H                                      3.00E+13          0             0
CH+H2O=CH2O+H                                    1.17E+15       -0.8             0
CH+CH2O=C2H2O+H                                  9.46E+13          0         -2160
CH+CH2T=C2H2+H                                   4.00E+13          0             0
CH+CH3=C2H3+H                                    3.00E+13          0             0
CH+CH4=C2H4+H                                    6.00E+13          0             0
CH+C2H2=C3H+H2                                   1.00E+14          0         42000
CH+C2H2=C3H2+H                                   1.00E+14          0         42000
CHO+H=CO+H2                                      9.00E+13          0             0
CHO+O=CO+OH                                      3.00E+13          0             0
CHO+O=CO2+H                                      3.00E+13          0             0
CHO+OH=CO+H2O                                    1.00E+14          0             0
CHO+O2=CO+HO2                                    3.00E+11          0             0
CHO+M=CO+H+M                                     1.86E+17         -1         71100
  H2/1.87/  AR/1/  O2/1/
CH2S+H2=CH3+H                                    7.23E+13          0             0
CH2S+H=CH+H2                                     7.00E+13          0             0
CH2S+O=CO+H+H                                    1.50E+13          0             0
CH2S+O=CO+H2                                     1.50E+13          0             0
CH2S+OH=CH2O+H                                   3.00E+13          0             0
CH2S+O2=CO+OH+H                                  3.00E+13          0             0
CH2S+CO2=CH2O+CO                                 3.00E+12          0             0
CH2S+CH3=C2H4+H                                  1.80E+13          0             0
CH2S+CH4=CH3+CH3                                 4.27E+13          0             0
CH2S+C2H2=C3H3+H                                 0.00E+00          0             0
CH2S+C2H2=C3H4B                                  8.00E+13          0             0
CH2S+C2H2O=C2H4+CO                               1.26E+14          0             0
CH2S+C2H4=C3H6                                   6.60E+13          0             0
CH2S+C2H6=C2H5+CH3                               1.14E+14          0             0
CH2S+M=CH2T+M                                    1.00E+13          0             0
  AR/0.4/  CO/0.4/  CO2/0.4/  H2O/4/ CH4/0.7/  C2H2/5/  C2H4/1.4/  C2H6/2.2/
CH2T+H2=CH3+H                                    3.00E+09          0             0
CH2T+H=CH+H2                                     1.10E+14          0             0
CH2T+O=CO+H+H                                    7.22E+13          0             0
```

!Lindstedt and Skevis(1994) model reaction set:	(E_a in J/mol, not cal/mol)		
CH2T+O=CO+H2	3.61E+13	0	0
CH2T+OH=CH+H2O	1.13E+07	2	12560
CH2T+OH=CH2O+H	2.50E+13	0	0
CH2T+O2=CO+H+OH	6.58E+12	0	6240
CH2T+O2=CO2+H+H	6.58E+12	0	6240
CH2T+O2=CH2O+O	6.58E+12	0	6240
CH2T+O2=CO2+H2	2.63E+12	0	6240
CH2T+O2=CO+H2O	2.63E+12	0	6240
CH2T+CO2=CH2O+CO	1.10E+11	0	4187
CH2T+CH2T=C2H2+H+H	1.20E+14	0	3320
CH2T+CH3=C2H4+H	4.00E+13	0	0
CH2T+C2HO=C2H3+CO	3.00E+13	0	0
CH2T+C2H2=C3H4B	1.20E+13	0	27700
CH2T+C2H4=C3H6	1.80E+10	0	0
CH2O+H=CHO+H2	2.29E+08	1.8	12550
CH2O+O=CHO+OH	4.15E+11	0.6	11560
CH2O+OH=CHO+H2O	3.40E+09	1.2	-1870
CH2O+O2=CHO+HO2	6.00E+13	0	170000
CH2O+HO2=CHO+H2O2	2.00E+12	0	48970
CH2O+CH3=CHO+CH4	4.09E+12	0	37000
CH2O+M=CHO+H+M	1.26E+16	0	326000
CH3+CH3=C2H5+H	9.00E+13	0	56540
CH3+CH3(+M)=C2H6(+M) LOW/1.27E+41 -7.00 1.156E+04/ TROE/0.63 23.0 1180.0/ C2H6/5/	3.60E+16	0	0
CH3+O=CH2O+H	8.43E+13	0	0
CH3+OH=CH2OH+H	1.50E+13	0	0
CH3+OH=CH2S+H2O	4.00E+06	0.2	10470
CH3+OH=CH2O+H2	8.00E+12	0	0
CH3+OH=CH3O+H	0.00E+00	0	0
CH3+O2=CH3O+O	1.32E+14	0	131360
CH3+O2=CH2O+OH	3.30E+11	0	37400
CH3+HO2=CH3O+OH	1.80E+13	0	0
CH3+CHO=CH4+CO	1.20E+14	0	0
CH3+M=CH+H2+M	6.90E+14	0	345031
CH3OH+M=CH3+OH+M	1.90E+19	0	384000
CH2OH+H=CH3OH	1.00E+10	0	0
CH2S+H2O=CH3OH	1.00E+10	0	0
CH3OH+H=CH2OH+H2	4.00E+13	0	25500
CH3OH+H=CH3O+H2	4.00E+12	0	25500
CH3OH+H=CH3+H2O	5.01E+12	0	22170
CH3OH+O=CH2OH+OH	3.88E+05	2.5	12900
CH3OH+O=CH3O+OH	1.00E+13	0	19590
CH3OH+OH=CH2OH+H2O	3.00E+04	2.7	-3700
CH3OH+OH=CH3O+H2O	5.30E+03	2.7	-3700
CH3OH+CH3=CH2OH+CH4	3.19E+01	3.2	30000
CH3OH+CH3O=CH2OH+CH3OH	3.01E+11	0	17040
CH3O+H=CH2O+H2	2.00E+13	0	0
CH3O+O=CH2O+OH	6.00E+12	0	0
CH3O+OH=CH2O+H2O	1.80E+13	0	0
CH3O+O2=CH2O+HO2	6.60E+10	0	10880
CH2O+H=CH3O	1.00E+10	0	0
CH2OH+H=CH2O+H2	3.00E+13	0	0

!Lindstedt and Skevis(1994) model reaction set:	(E_a in J/mol, not cal/mol)		
CH2OH+O=CH2O+OH	4.22E+13	0	0
CH2OH+OH=CH2O+H2O	2.40E+13	0	0
CH2OH+O2=CH2O+HO2	1.00E+14	0	21000
CH2OH+M=CH2O+H+M	1.22E+28	-4	133420
CH3+H(+M)=CH4(+M)	2.00E+17	0	0
LOW/0.62E+25 -1.80 0.00E+00/			
TROE/0.37 3315.0 61.0/			
C2H6/5/			
CH4+H=CH3+H2	3.86E+06	2.1	32426
CH4+O=CH3+OH	9.03E+08	1.6	35500
CH4+OH=CH3+H2O	1.56E+07	1.8	11600
CH4+HO2=CH3+H2O2	9.03E+12	0	103090
CH4+O2=CH3+HO2	3.97E+13	0	238000
C2H+H2=C2H2+H	5.67E+10	0.9	8400
C2H+O=CO+CH	1.00E+13	0	0
C2H+OH=C2HO+H	2.00E+13	0	0
C2H+O2=CO+CO+H	3.52E+13	0	0
C2H+CH3=C3H3+H	2.41E+13	0	0
C2HO+H=CH2S+CO	1.50E+14	0	0
C2HO+O=CO+CO+H	9.64E+13	0	0
C2HO+OH=C2O+H2O	3.00E+13	0	0
C2HO+O2=CO+CO+OH	1.00E+13	0	0
C2HO+O2=CO2+CO+H	1.00E+13	0	0
C2HO+CH=C2H2+CO	5.00E+13	0	0
C2HO+C2HO=C2H2+CO+CO	1.00E+13	0	0
C2HO+C2H2=C3H3+CO	1.00E+11	0	12600
C2HO+M=CH+CO+M	6.00E+15	0	246000
C2O+H=CH+CO	5.00E+13	0	0
C2O+O=CO+CO	5.00E+13	0	0
C2O+OH=CO+CO+H	2.00E+13	0	0
C2O+O2=CO+CO+O	2.00E+13	0	0
C2H2+O=CH2T+CO	2.70E+12	0	13300
C2H2+O=C2HO+H	1.53E+13	0	13300
C2H2+OH=C2H+H2O	3.37E+07	2	58615.2
C2H2+OH=CHCOH+H	5.04E+05	2.3	56521.8
C2H2+OH=C2H2O+H	1.10E+13	0	30000
C2H2+OH=CH3+CO	1.21E+12	0	1900
C2H2+O2=C2H+HO2	1.20E+13	0	311700
C2H2+O2=C2HO+OH	2.00E+08	1.5	126000
C2H2+M=C2H+H+M	4.20E+16	0	448000
CHCOH+H=C2H2O+H	1.00E+13	0	0
C2H2O+M=CH2T+CO+M	3.60E+15	0	248000
C2H2O+H=CH3+CO	1.10E+07	0.2	-8640
C2H2O+O=CO2+CH2T	1.75E+12	0	5700
C2H2O+O=C2HO+OH	1.00E+13	0	33500
C2H2O+OH=CH2OH+CO	7.50E+12	0	8370
C2H2O+CH3=C2H5+CO	9.00E+12	0	0
C2H3(+M)=C2H2+H(+M)	2.00E+17	0	166300
LOW/4.160E+41 -7.50 190.4E+03/			
C2H3+H=C2H2+H2	9.64E+13	0	0
C2H3+O=C2H2O+H	3.00E+13	0	0
C2H3+OH=C2H2+H2O	2.00E+13	0	0
C2H3+O2=CHO+CH2O	3.50E+12	0	0
C2H3+CH=C2H2+CH2T	5.00E+13	0	0

!Lindstedt and Skevis(1994) model reaction set:			(E_a in J/mol, not cal/mol)
C2H3+C2H=C2H2+C2H2	3.00E+13	0	0
C2H4+H=C2H3+H2	1.33E+06	2.5	51210
C2H4+O=CH3+CHO	1.32E+08	1.5	1788
C2H4+OH=C2H3+H2O	1.57E+04	2.8	17460
C2H4+M=C2H3+H+M	2.60E+17	0	410700
C2H5+O2=C2H4+HO2	1.02E+10	0	-9140
C2H5+O=CH3+CH2O	6.60E+13	0	0
C2H4+H=C2H5	1.00E+09	0	0
C2H6(+M)=C2H5+H(+M)	8.85E+23	-1.2	427700
LOW/4.900E+42 -0.643E+01 448.4E+03/			
TROE/0.015 -16182 3371/			
C2H6/5/			
C2H6+H=C2H5+H2	1.45E+09	1.5	31000
C2H6+O=C2H5+OH	1.00E+09	1.5	24300
C2H6+OH=C2H5+H2O	7.23E+06	2	3616
C3H+O=C2H+CO	6.80E+13	0	0
C3H+OH=C2H2+CO	6.80E+13	0	0
C3H+O2=C2HO+CO	2.00E+12	0	0
C3H2+O=C2H+CO+H	6.80E+13	0	0
C3H2+OH=C2H2+CO+H	5.00E+13	0	0
C3H2+O2=C2H2+CO2	2.00E+12	0	0
C3H2+M=C3H+H+M	1.00E+15	0	424800
C3H3+H=C3H2+H2	1.00E+12	0	6276
C3H3+O=C3H2O+H	1.40E+14	0	0
C3H3+OH=C3H2O+H2	2.00E+12	0	0
C3H3+O2=C2H2O+CHO	3.00E+10	0	12000
C3H3+M=C3H2+H+M	2.00E+48	-8.5	410222
C3H2O=C2H2+CO	8.51E+14	0	297000
C3H2O+O=CHO+C2HO	1.00E+13	0	0
C3H2O+OH=CHO+C2H2O	1.00E+13	0	0
C2H2+CH3=C3H4A+H	3.10E+12	0	71121
C2H2+CH3=C3H4P+H	6.19E+12	0	71121
C2H2+CH3=C3H5A	1.09E+48	-10.9	119545
C2H2+CH3=C3H5S	2.43E+46	-10.9	83627
C3H4A+H=C3H5T	8.50E+12	0	8370
C3H4A+H=C3H5A	4.00E+12	0	11300
C3H4A+H=C3H3+H2	1.00E+12	0	6276
C3H4A+O=C2H3+CHO	1.10E-02	4.6	-17800
C3H4A+OH=C2H2O+CH3	3.12E+12	0	-1660
C3H4A+OH=C3H3+H2O	1.00E+12	0	6276
C3H4A+O2=C3H3+HO2	4.00E+13	0	257500
C3H4A+CH3=C3H3+CH4	2.00E+12	0	32200
C3H4A+C2H=C3H3+C2H2	1.00E+13	0	0
C3H4A+C3H4A=C3H5A+C3H3	5.00E+14	0	270880
C3H4A+C3H5A=C3H3+C3H6	2.00E+12	0	32240
C3H4A+M=C3H3+H+M	2.00E+18	0	334717
C3H4B=C3H4A	1.51E+14	0	211000
C3H4B=C3H4P	7.08E+13	0	182960
C3H4P+H=C3H5T	6.50E+12	0	8373
C3H4P+H=C3H5S	5.80E+12	0	12980
C3H4P+H=C3H3+H2	1.00E+12	0	6276
C3H4P+O=C2H2O+CH2T	6.40E+12	0	8410
C3H4P+O=C2H3+CHO	3.20E+12	0	8410
C3H4P+O=C2HO+CH3	6.30E+12	0	8410

!Lindstedt and Skevis(1994) model reaction set:			(E_a in J/mol, not cal/mol)
C3H4P+OH=C2H4+CHO	5.00E-04	4.5	-4190
C3H4P+OH=C3H3+H2O	1.00E+12	0	6276
C3H4P+O2=C3H3+HO2	5.00E+12	0	213000
C3H4P+CH3=C3H3+CH4	2.00E+12	0	32200
C3H4P+C2H=C3H3+C2H2	1.00E+13	0	0
C3H4P+C3H5A=C3H3+C3H6	2.00E+12	0	32240
C3H4P+M=C3H3+H+M	4.70E+18	0	334170
C3H5A+H=C3H4A+H2	3.33E+12	0	0
C3H5A+O=C2H4+H+CO	1.81E+14	0	0
C3H5A+O2=CH2O+CH2O+CH	6.30E+11	0	72050
C3H5A+CH3=C3H4A+CH4	3.00E+12	-0.3	-549
C3H5A+C2H3=C2H4+C3H4A	2.41E+12	0	0
C3H5A+C2H5=C2H6+C3H4A	9.60E+11	0	-549
C3H5A+C3H5A=C3H4A+C3H6	8.43E+10	0	-1097
C3H5S+H=C3H4A+H2	3.33E+12	0	0
C3H5S+O=C2H2O+CH3	1.81E+14	0	0
C3H5S+O2=CH3+CH2O+CO	4.34E+11	0	0
C3H5S+CH3=C3H4A+CH4	1.00E+11	0	0
C3H5S+C2H3=C2H4+C3H4A	1.00E+11	0	0
C3H5S+C2H5=C2H6+C3H4A	1.00E+11	0	0
C3H5T+H=C3H4A+H2	3.33E+12	0	0
C3H5T+O=C2HO+CH3+H	1.81E+14	0	0
C3H5T+O2=CH3+CH2O+CO	4.34E+11	0	0
C3H5T+CH3=C3H4A+CH4	1.00E+11	0	0
C3H5T+C2H3=C2H4+C3H4A	1.00E+11	0	0
C3H5T+C2H5=C2H6+C3H4A	1.00E+11	0	0
C3H6=C2H3+CH3	1.10E+21	-1.2	408840
C3H6=C3H5A+H	4.57E+14	0	372200
C3H6=C3H5S+H	7.59E+14	0	424120
C3H6=C3H5T+H	1.45E+15	0	410560
C3H6+H=C3H5A+H2	1.73E+05	2.5	10425
C3H6+H=C3H5S+H2	4.10E+05	2.5	40980
C3H6+H=C3H5T+H2	8.04E+05	2.5	51390
C3H6+O=C2H5+CHO	5.22E+07	1.6	-2629
C3H6+O=C2H4+CH2O	3.48E+07	1.6	-2629
C3H6+O=CH3+CH3+CO	6.96E+07	1.6	-2629
C3H6+OH=C3H5A+H2O	3.12E+06	2	-1247
C3H6+OH=C3H5S+H2O	1.11E+06	2	6069
C3H6+OH=C3H5T+H2O	2.14E+06	2	11622
C3H6+O2=C3H5A+HO2	1.95E+12	0	163280
C3H6+O2=C3H5S+HO2	2.00E+13	0	199290
C3H6+O2=C3H5T+HO2	2.00E+13	0	184220
C3H6+CH3=C3H5A+CH4	2.22E+00	3.5	23740
C3H6+CH3=C3H5S+CH4	8.42E-01	3.5	48770
C3H6+CH3=C3H5T+CH4	1.35E+00	3.5	53760
C3H6+C2H5=C3H5A+C2H6	2.22E+00	3.5	27770
C3H7N+H=C3H8	2.00E+13	0	0
C3H7N+O2=C3H6+HO2	1.00E+12	0	20910
C3H7N=C2H4+CH3	3.00E+14	0	139000
C3H6+H=C3H7N	7.23E+12	0	12140
C3H7I+H=C3H8	2.00E+13	0	0
C3H7I+O2=C3H6+HO2	1.00E+12	0	12500
C3H7I=C2H4+CH3	2.00E+10	0	123500
C3H7I=C3H6+H	6.00E+13	0	154390
C3H8(+M)=C2H5+CH3(+M)	1.10E+20	0	353000

!Lindstedt and Skevis(1994) model reaction set:			(E_a in J/mol, not cal/mol)
LOW/7.828E+18 0.0 271.87E+03/			
TROE/0.24 38.0 1946.0/			
C3H8+H=C3H7N+H2	1.30E+14	0	40600
C3H8+H=C3H7I+H2	1.00E+13	0	34900
C3H8+O=C3H7N+OH	3.00E+13	0	24100
C3H8+O=C3H7I+OH	2.60E+13	0	18700
C3H8+OH=C3H7N+H2O	5.75E+08	1.4	3558
C3H8+OH=C3H7I+H2O	4.79E+08	1.4	3558
C3H8+CH3=C3H7N+CH4	9.03E-01	3.7	29900
C3H8+CH3=C3H7I+CH4	1.51E+00	3.5	22900
C2H2+C2H2=C4H3N+H	1.00E+12	0	276140
C2H2+C2H2=C4H3I+H	2.00E+12	0	268000
C2H2+C2H2=C4H2+H2	1.51E+13	0	178770
C3H2+CH2T=C4H3I+H	3.00E+13	0	0
C3H3+CH=C4H3N+H	7.00E+13	0	0
C3H3+CH=C4H3I+H	7.00E+13	0	0
C3H3+CH2T=C4H4+H	4.00E+13	0	0
C2H+C2H2=C4H2+H	1.20E+14	0	0
C2H+C4H2=C6H2+H	1.20E+14	0	0
C2H+C6H2=C8H2+H	1.20E+14	0	0
C2H+C2H=C4H+H	1.00E+14	0	0
C4H+H2=C4H2+H	4.07E+05	2.4	840
C4H+C2H2=C6H2+H	1.20E+14	0	0
C4H+C4H2=C8H2+H	1.20E+14	0	0
C4H2=C4H+H	7.80E+14	0	502400
C4H2+C4H2=C8H2+H2	1.50E+13	0	178770
C2H2+C4H2=C6H2+H2	1.50E+13	0	178770
C2H2+C6H2=C8H2+H2	1.50E+13	0	178770
C4H2+O=C3H2+CO	9.00E+11	0	0
C4H2+OH=C4H2O+H	6.69E+12	0	-1716
C4H2O+OH=C2H2+CO+CO+H	1.00E+15	0	0
C4H3N(+M)=C4H2+H(+M)	1.00E+17	0	150720
LOW/1.00E+14 0.0 125.52E+03/			
C4H3N+H=C4H2+H2	8.10E+13	0	0
C4H3N+OH=C4H2+H2O	3.00E+13	0	0
C4H3I=C4H3N	1.50E+13	0	283450
C4H3I(+M)=C4H2+H(+M)	1.00E+17	0	230270
LOW/2.00E+15 0.0 200.83E+03/			
C4H3I+H=C4H2+H2	8.10E+13	0	0
C4H3I+O=C2H2O+C2H	2.00E+13	0	0
C4H3I+OH=C4H2+H2O	3.00E+13	0	0
C4H3I+O2=C2H2O+C2HO	1.00E+13	0	0
C4H4=C4H3I+H	8.63E+09	0	247000
C4H4+H=C4H3N+H2	2.00E+07	2	25170
C4H4+O=C3H4A+CO	3.00E+12	0	0
C4H4+OH=C4H3N+H2O	1.00E+07	2	12600
C4H4+C2H=C4H3I+C2H2	3.98E+13	0	0
C4H5S(+M)=C4H4+H(+M)	1.00E+17	0	209200
LOW/2.00E+15 0.0 175.73E+03/			
C4H5S+H=C4H4+H2	1.00E+14	0	0
C4H5S+OH=C4H4+H2O	2.00E+07	2	4180
C4H5S=C4H5T	1.50E+13	0	283450
C4H5T(+M)=C4H4+H(+M)	1.00E+17	0	154900
LOW/1.00E+14 0.0 125.52E+03/			

!Lindstedt and Skevis(1994) model reaction set:			(E_a in J/mol, not cal/mol)
C4H5T=C2H2+C2H3	2.00E+12	0	192464
C4H5T+H=C4H4+H2	1.00E+14	0	0
C4H5T+OH=C4H4+H2O	2.00E+07	2	4180
C4H5I=C4H5T	1.50E+13	0	283450
C4H5I(+M)=C4H4+H(+M)	1.00E+17	0	209340
LOW/2.00E+15 0.0 175.73E+03/			
C4H5I+H=C4H4+H2	1.00E+14	1	0
C4H5I+OH=C4H4+H2O	2.00E+07	2	4180
C4H6S=C3H3+CH3	1.00E+12	0	248900
C4H6S=C4H5I+H	4.20E+15	0	387100
C4H6S+H=C2H3+C2H4	4.00E+11	0	0
C4H6S+H=C4H5S+H2	1.00E+14	0	60710
C4H6S+OH=C4H5S+H2O	1.62E+13	0	0
C4H6S+CH3=C4H5S+CH4	7.00E+13	0	0
C2H3+C2H3=C4H6T	2.00E+13	0	0
C4H6T=C4H5I+H	4.20E+15	0	414216
C4H6T+H=C4H5T+H2	6.30E+10	0.7	25100
C4H6T+H=C2H3+C2H4	5.00E+11	0	0
C4H6T+O=C4H6O	6.30E+08	1.5	3592
C4H6T+OH=C4H5T+H2O	2.00E+07	2	20930
C4H6T+O2=C4H5T+HO2	4.00E+13	0	242000
C4H6T+C2H3=C4H5T+C2H4	6.31E+13	0	60700
C4H6T+CH3=C4H5T+CH4	7.00E+13	0	12500
C4H6T+C3H3=C4H5T+C3H4A	1.00E+13	0	75312
CH2S+C3H4P=C4H6B	1.80E+14	0	0
C4H6B=C4H6T	3.00E+13	0	177000
C4H6B=C4H6S	3.00E+13	0	183000
C4H6O=C3H6+CO	3.16E+13	0	249790
C3H3+C3H2=C6H4L+H	1.00E+13	0	0
C3H3+C3H3=C6H6A	1.00E+13	0	0
C3H3+C3H3=C6H6B	1.00E+13	0	0
C3H3+C3H3=C6H6S	1.00E+13	0	0
C3H3+C3H4A=C6H7L	3.00E+11	0	12560
C4H3N+C2H2=C6H5B	4.12E+06	1.6	10467
C4H4+C2H3=C6H7L	1.90E+12	0	10500
C4H5T+C2H2=C6H7L	1.73E+06	1.8	9378
C6H3+H=C6H2+H2	1.00E+14	0	0
C6H3+O=C6H2+OH	2.00E+13	0	0
C6H3+OH=C6H2+H2O	2.00E+13	0	0
C6H4L+H=C6H3+H2	1.00E+14	0	0
C6H4L+O=C6H3+OH	2.00E+13	0	0
C6H4L+OH=C6H3+H2O	2.00E+13	0	0
C6H4C=C6H4L	1.00E+12	0	138072
C6H5B=C6H4L+H	2.50E+58	-13.8	208000
C6H5B+H=C6H4L+H2	1.00E+14	0	0
C6H5B+O=C6H4L+OH	2.00E+13	0	0
C6H5B+OH=C6H4L+H2O	2.00E+13	0	0
C6H5B=C6H5A	1.00E+10	0	0
C6H5A=C6H4L+H	6.00E+11	0	188000
C6H5A+H=C6H4L+H2	1.00E+14	0	0
C6H5A+O=C6H4L+OH	2.00E+13	0	0
C6H5A+OH=C6H4L+H2O	2.00E+13	0	0
C6H5B=C6H5	1.00E+10	0	0
C6H5=C6H4C+H	3.00E+13	0	372376
C6H5+H=C6H4C+H2	1.50E+14	0	0

!Lindstedt and Skevis(1994) model reaction set:			(E_a in J/mol, not cal/mol)
C6H5+O=C6H4C+OH	2.00E+13	0	0
C6H5+OH=C6H4C+H2O	2.00E+13	0	0
C6H5+HO2=C6H5O+OH	5.00E+13	0	4186
C6H5+O2=C6H5O+O	2.09E+12	0	31250
C6H6A=C6H6S	5.40E+11	0	149660
C6H6S=C6H6M	5.00E+11	0	92000
C6H6S=C6H6F	5.00E+11	0	132400
C6H6M=C6H6F	4.26E+13	0	206000
C6H6B=C6H6F	5.00E+11	0	144000
C6H6B=C6H6D	1.00E+12	0	224000
C6H6F=C6H6D	1.00E+13	0	342000
C6H6D=C6H6	5.00E+11	0	200000
C6H6F=C6H6	7.58E+13	0	309000
C6H6A=C6H5A+H	1.40E+15	0	326600
C6H6B=C6H5A+H	7.00E+14	0	326600
C6H6A+H=C6H5A+H2	1.00E+14	0	0
C6H6A+O=C6H5A+OH	2.00E+13	0	0
C6H6A+OH=C6H5A+H2O	2.00E+13	0	0
C6H6B+H=C6H5A+H2	1.00E+14	0	0
C6H6B+O=C6H5A+OH	2.00E+13	0	0
C6H6B+OH=C6H5A+H2O	2.00E+13	0	0
C6H6D+H=C6H5B+H2	1.00E+14	0	46000
C6H6D+O=C6H5B+OH	2.00E+13	0	0
C6H6D+OH=C6H5B+H2O	2.00E+13	0	12600
C6H5+H=C6H6	2.20E+14	0	0
C6H6+H=C6H5+H2	2.50E+14	0	66940
C6H6+O=C6H5O+H	2.40E+13	0	19530
C6H6+O=C6H5+OH	2.00E+13	0	61520
C6H6+OH=C6H5+H2O	1.63E+08	1.4	6100
C6H6+OH=C6H5OH+H	1.32E+13	0	44315
C6H6+O2=C6H5+HO2	6.30E+13	0	251040
C6H6+CH3=C6H5+CH4	4.36E-04	5	51497
C6H5O+H=C6H5OH	2.50E+14	0	0
C6H5OH+C5H5=C6H5O+C5H6	2.67E+14	0	105620
C6H5OH+H=C6H5O+H2	1.15E+14	0	51920
C6H5OH+O=C6H5O+OH	2.81E+13	0	30780
C6H5OH+OH=C6H5O+H2O	6.00E+12	0	0
C6H5O=C5H5+CO	4.50E+11	0	183680
C6H6+H=C6H7	4.00E+13	0	18042
C6H7=C6H7L	3.00E+14	0	209200
C3H5A+C2H2=C5H6+H	4.00E+14	0	104145
C5H5+H=C5H6	1.00E+14	0	0
C5H5+O=C4H5T+CO	1.00E+14	0	0
C5H5+O=C5H5O	1.00E+13	0	0
C5H5+OH=C5H4OH+H	3.00E+13	0	0
C5H5+HO2=C5H5O+OH	3.00E+13	0	0
C5H6+H=C5H5+H2	2.19E+08	1.8	12550
C5H6+O=C5H5+OH	1.81E+13	0	12870
C5H6+OH=C5H5+H2O	3.43E+09	1.2	-1870
C5H6+HO2=C5H5+H2O2	2.00E+12	0	48780
C5H6+O2=C5H5O+OH	1.00E+13	0	86659
C5H5O=C4H5T+CO	2.51E+11	0	183680
C5H4OH=C5H4O+H	2.10E+13	0	200830
C5H4O=CO+C2H2+C2H2	1.00E+15	0	326570
C5H6=C5H6L	1.00E+14	0	235000

!Lindstedt and Skevis(1994) model reaction set:	(E_a in J/mol, not cal/mol)		
C5H5=C5H5L	1.00E+14	0	334000
C3H3+C2H2=C5H5L	1.00E+09	0	0
C5H5L+H=C5H6L	1.00E+13	0	0
C5H6L+H=C5H5L+H2	1.00E+12	0	0
C5H6L+O=C3H2O+C2H3+H	2.00E+13	0	126000
C5H6L+OH=C5H5L+H2O	1.00E+13	0	0
C5H5L+H=C5H4L+H2	1.00E+13	0	0
C5H5L+O=C4H5I+CO	1.00E+14	0	0
C5H5L+OH=C5H4L+H2O	1.00E+13	0	0
C5H5L+O2=C2H3+C2HO+CHO	1.00E+12	0	155000
C5H4L+H=C5H3L+H2	1.00E+13	0	0
C5H4L+OH=C5H3L+H2O	1.00E+13	0	0
C5H3L+H=C5H4L	1.00E+13	0	0
C5H3L+H=C5H2+H2	1.00E+13	0	0
C5H3L+O=C4H3I+CO	1.00E+14	0	0
C5H3L+OH=C5H2+H2O	1.00E+13	0	0
C5H2+OH=C4H2+CHO	1.00E+12	0	0
C4H2+CH2S=C5H3L+H	3.00E+13	0	0
C4H2+CH2T=C5H3L+H	1.30E+13	0	18100
C4H2+CH=C5H2+H	1.00E+14	0	0
C4H6T+C3H3=C4H5T+C3H4P	1.00E+13	0	75312
C4H6S+C3H3=C4H5S+C3H4A	1.00E+13	0	0
C4H6S+C3H3=C4H5S+C3H4P	1.00E+13	0	0
C4H6T+H=C3H4A+CH3	1.20E+12	0	8786
C4H6S+H=C3H4A+CH3	6.00E+12	0	8786

END

Appendix O. Flame Code Thermochemistry and Transport Parameters.

Parameters are given in the format used by CHEMKIN II (Kee et al., 1991) and TRANFIT (Kee et al., 1986). As noted in Chapter 7, the Zhang and McKinnon (1995) thermochemical data (based on the CHEMKIN Thermodynamic Database, Kee et al., 1994) with some modifications, was used for reaction path analyses. Those modifications, plus other thermochemical and transport parameters not documented elsewhere, are given in Section O.4.

O.1 Emdee et al. Model.

As received from Brezinsky (1994).

O.1.1 Thermochemistry Parameters

```
THERMO
   300.000  1000.000  5000.000
AR                120186AR  1               G  0300.00   5000.00  1000.00      1
 2.50000000E+00 0.00000000E+00 0.00000000E+00 0.00000000E+00 0.00000000E+00    2
-7.45375000E+02 4.36600065E+00 2.50000000E+00 0.00000000E+00 0.00000000E+00    3
 0.00000000E+00 0.00000000E+00-7.45375000E+02 4.36600065E+00                   4
C2H2              121386C   2H   2          G  0300.00   5000.00  1000.00      1
 4.43677044E+00 5.37603907E-03-1.91281674E-06 3.28637895E-10-2.15670953E-14    2
 2.56676641E+04-2.80033827E+00 2.01356220E+00 1.51904458E-02-1.61631888E-05    3
 9.07899178E-09-1.91274600E-12 2.61244434E+04 8.80537796E+00                   4
C2H4              121286C   2H   4          G  0300.00   5000.00  1000.00      1
 3.52841878E+00 1.14851845E-02-4.41838529E-06 7.84460053E-10-5.26684849E-14    2
 4.42828857E+03 2.23038912E+00-8.61487985E-01 2.79616285E-02-3.38867721E-05    3
 2.78515220E-08-9.73787891E-12 5.57304590E+03 2.42114868E+01                   4
C4H4              121686C   4H   4          G  0300.00   5000.00  1000.00      1
 8.89214897E+00 1.09088495E-02-3.59495971E-06 5.19341903E-10-2.68089214E-14    2
 3.32843477E+04-2.17269440E+01 2.14033699E+00 2.46050470E-02-3.63916570E-06    3
-1.53040141E-08 8.89646083E-12 3.53740000E+04 1.42824774E+01                   4
C5H6               20387C   5H   6          G  0300.00   5000.00  1000.00      1
 9.68981457E+00 1.83826201E-02-6.26488418E-06 9.39337719E-10-5.08770814E-14    2
 1.10212422E+04-3.12290802E+01-3.19673920E+00 4.08136100E-02 6.81650533E-07    3
-3.13745900E-08 1.57722307E-11 1.52906758E+04 3.86993866E+01                   4
C6H6               20387C   6H   6          G  0300.00   5000.00  1000.00      1
 1.29107399E+01 1.72329657E-02-5.02421062E-06 5.89349680E-10-1.94752119E-14    2
 3.66451172E+03-5.00269928E+01-3.13801193E+00 4.72310297E-02-2.96220787E-06    3
-3.26281899E-08 1.71869186E-11 8.89003125E+03 3.65757294E+01                   4
CH2               120186C   1H   2          G  0250.00   4000.00  1000.00      1
 3.63640785E+00 1.93305663E-03-1.68701632E-07-1.00989939E-10 1.80825576E-14    2
 4.53413398E+04 2.15656066E+00 3.76223707E+00 1.15981908E-03 2.48958543E-07    3
 8.80083562E-10-7.33243544E-13 4.53679063E+04 1.71257758E+00                   4
CH2O              121286C   1H   2O   1     G  0300.00   5000.00  1000.00      1
 2.99560618E+00 6.68132119E-03-2.62895469E-06 4.73715289E-10-3.21251747E-14    2
```

```
!  Emdee et al. thermochemical data.
!
-1.53203691E+04 6.91257238E+00 1.65273118E+00 1.26314387E-02-1.88816848E-05    3
 2.05003143E-08-8.41323712E-12-1.48654043E+04 1.37848196E+01                   4
CH2OH             120186H   3C   1O   1     G  0250.00   4000.00  1000.00     1
 6.32752037E+00 3.60827078E-03-3.20154726E-07-1.93874999E-10 3.50970473E-14    2
-4.47450928E+03-8.32936573E+00 2.86262846E+00 1.00152725E-02-5.28543581E-07    3
-5.13853982E-09 2.24604103E-12-3.34967871E+03 1.03979378E+01                   4
CH3               121286C   1H   3          G  0300.00   5000.00  1000.00     1
 2.84405160E+00 6.13797410E-03-2.23034522E-06 3.78516080E-10-2.45215903E-14    2
 1.64378086E+04 5.45269728E+00 2.43044281E+00 1.11240987E-02-1.68022034E-05    3
 1.62182872E-08-5.86495262E-12 1.64237813E+04 6.78979397E+00                   4
CH3O              121686C   1H   3O   1     G  0300.00   3000.00  1000.00     1
 3.77079964E+00 7.87149742E-03-2.65638391E-06 3.94443145E-10-2.11261638E-14    2
 1.27832520E+02 2.92957497E+00 2.10620403E+00 7.21659511E-03 5.33847197E-06    3
-7.37763628E-09 2.07561052E-12 9.78601074E+02 1.31521769E+01                   4
CH4               121286C   1H   4          G  0300.00   5000.00  1000.00     1
 1.68347883E+00 1.02372356E-02-3.87512864E-06 6.78558487E-10-4.50342312E-14    2
-1.00807871E+04 9.62339497E+00 7.78741479E-01 1.74766835E-02-2.78340904E-05    3
 3.04970804E-08-1.22393068E-11-9.82522852E+03 1.37221947E+01                   4
CO                121286C   1O   1          G  0300.00   5000.00  1000.00     1
 3.02507806E+00 1.44268852E-03-5.63082779E-07 1.01858133E-10-6.91095156E-15    2
-1.42683496E+04 6.10821772E+00 3.26245165E+00 1.51194085E-03-3.88175522E-06    3
 5.58194424E-09-2.47495123E-12-1.43105391E+04 4.84889698E+00                   4
CO2               121286C   1O   2          G  0300.00   5000.00  1000.00     1
 4.45362282E+00 3.14016873E-03-1.27841054E-06 2.39399667E-10-1.66903319E-14    2
-4.89669609E+04-9.55395877E-01 2.27572465E+00 9.92207229E-03-1.04091132E-05    3
 6.86668678E-09-2.11728009E-12-4.83731406E+04 1.01884880E+01                   4
H                 120186H   1            G  0300.00   5000.00  1000.00     1
 2.50000000E+00 0.00000000E+00 0.00000000E+00 0.00000000E+00 0.00000000E+00    2
 2.54716270E+04-4.60117638E-01 2.50000000E+00 0.00000000E+00 0.00000000E+00    3
 0.00000000E+00 0.00000000E+00 2.54716270E+04-4.60117608E-01                   4
H2                121286H   2            G  0300.00   5000.00  1000.00     1
 2.99142337E+00 7.00064411E-04-5.63382869E-08-9.23157818E-12 1.58275179E-15    2
-8.35033997E+02-1.35511017E+00 3.29812431E+00 8.24944174E-04-8.14301529E-07    3
-9.47543433E-11 4.13487224E-13-1.01252087E+03-3.29409409E+00                   4
H2O                20387H   2O   1          G  0300.00   5000.00  1000.00     1
 2.67214561E+00 3.05629289E-03-8.73026011E-07 1.20099639E-10-6.39161787E-15    2
-2.98992090E+04 6.86281681E+00 3.38684249E+00 3.47498246E-03-6.35469633E-06    3
 6.96858127E-09-2.50658847E-12-3.02081133E+04 2.59023285E+00                   4
H2O2              120186H   2O   2          G  0300.00   5000.00  1000.00     1
 4.57316685E+00 4.33613639E-03-1.47468882E-06 2.34890357E-10-1.43165356E-14    2
-1.80069609E+04 5.01136959E-01 3.38875365E+00 6.56922581E-03-1.48501258E-07    3
-4.62580552E-09 2.47151475E-12-1.76631465E+04 6.78536320E+00                   4
HCCO               32387H   1C   2O   1     G  0300.00   4000.00  1000.00     1
 6.75807285E+00 2.00040033E-03-2.02760731E-07-1.04113183E-10 1.96516472E-14    2
 1.90151328E+04-9.07126236E+00 5.04796505E+00 4.45347792E-03 2.26828277E-07    3
-1.48209456E-09 2.25074150E-13 1.96589180E+04 4.81843948E-01                   4
HO2                20387H   1O   2          G  0300.00   5000.00  1000.00     1
 4.07219124E+00 2.13129632E-03-5.30814532E-07 6.11226902E-11-2.84116471E-15    2
 9.36629296E+01 3.47602940E+00 2.97996306E+00 4.99669695E-03-3.79099697E-06    3
 2.35419240E-09-8.08902424E-13 4.29135834E+02 9.22272396E+00                   4
O                 120186O   1            G  0300.00   5000.00  1000.00     1
 2.54205966E+00-2.75506191E-05-3.10280335E-09 4.55106742E-12-4.36805150E-16    2
 2.92308027E+04 4.92030811E+00 2.94642878E+00-1.63816649E-03 2.42103170E-06    3
-1.60284319E-09 3.89069636E-13 2.91476445E+04 2.96399498E+00                   4
O2                121386O   2            G  0300.00   5000.00  1000.00     1
```

```
!  Emdee et al. thermochemical data.
!
 3.69757819E+00 6.13519689E-04-1.25884199E-07 1.77528148E-11-1.13643531E-15    2
-1.23393018E+03 3.18916559E+00 3.21293640E+00 1.12748635E-03-5.75615047E-07    3
 1.31287723E-09-8.76855392E-13-1.00524902E+03 6.03473759E+00                   4
OH                121286O   1H   1          G  0300.00   5000.00  1000.00     1
 2.88273048E+00 1.01397431E-03-2.27687707E-07 2.17468370E-11-5.12630534E-16    2
 3.88688794E+03 5.59571219E+00 3.63726592E+00 1.85091049E-04-1.67616463E-06    3
 2.38720266E-09-8.43144185E-13 3.60678174E+03 1.35886049E+00                   4
C4H6              PW-APIC   4H   6          G   300.000  5000.000              1
+4.55600000E+00+2.57600004E-02-1.21199997E-05+2.18799999E-09+0.00000000E+00    2
+1.06500000E+04-1.23400000E-01-2.52900000E+00+5.42100008E-02-5.37399986E-05    3
+2.85200003E-08-6.08799998E-12+1.20200000E+04+3.39200000E+01                   4
C6H5              L12/84C   6H   5    0    0G   300.000  5000.000 1000.000    1
 0.11431418E+02 0.17019045E-01-0.58387241E-05 0.88094687E-09-0.48050417E-13    2
 0.33942348E+05-0.38574219E+02-0.23405075E+01 0.42760305E-01-0.25518166E-05    3
-0.30668716E-07 0.16245519E-10 0.38376734E+05 0.35617355E+02                   4
C6H5O             L12/84C   6H   5O   1    0G   300.000  5000.000 1000.000    1
 0.13833984E+02 0.17618403E-01-0.60696257E-05 0.91988173E-09-0.50449181E-13    2
-0.69212549E+03-0.50392990E+02-0.18219433E+01 0.48122510E-01-0.46792302E-05    3
-0.34018594E-07 0.18649637E-10 0.42429180E+04 0.33526199E+02                   4
C6H5OH            L12/84C   6H   6O   1    0G   300.000  5000.000 1000.000    1
 0.14930705E+02 0.18346462E-01-0.61796381E-05 0.91533114E-09-0.48830826E-13    2
-0.18379656E+05-0.55983917E+02-0.16495714E+01 0.52105546E-01-0.69632842E-05    3
-0.36011539E-07 0.20483074E-10-0.13292336E+05 0.32357330E+02                   4
C2H3      BENSON 88      C   2H   3    0    0G   300.000  5000.000 1384.000    01
 4.98632615E+00 6.74210478E-03-2.31088203E-06 3.59124380E-10-2.08449928E-14    2
 3.12665642E+04-2.59023245E+00 2.46978485E+00 1.15950612E-02-6.06325764E-06    3
 1.85458682E-09-2.87093484E-13 3.23161752E+04 1.14112313E+01                   4
C4H5      BENSON 88      C   4H   5    0    0G   300.000  5000.000 1400.000    11
 1.09319148E+01 1.12577926E-02-3.82466213E-06 5.90906138E-10-3.41605706E-14    2
 3.55451038E+04-3.26454973E+01 6.94982037E-01 4.01246346E-02-3.60998164E-05    3
 1.71826737E-08-3.27377307E-12 3.86582614E+04 2.06646321E+01                   4
C5H4O       5/ 2/90      C   5H   4O   1    0G   300.000  5000.000 1389.000    01
 1.33020143E+01 1.29090773E-02-4.55425968E-06 7.22010615E-10-4.25087252E-14    2
-4.58547917E+03-5.02244575E+01-2.95685650E+00 5.07722289E-02-3.78981734E-05    3
 1.39325529E-08-2.03155485E-12 1.02174969E+03 3.70541785E+01                   4
C5H5      BOZZELLI       C   5H   5    0    0G   300.000  5000.000 1400.000    01
 1.34351894E+01 1.26452160E-02-4.42858813E-06 6.98682634E-10-4.09970231E-14    2
 2.06536455E+04-5.32987048E+01-6.29416088E+00 6.57550731E-02-6.00914914E-05    3
 2.73875793E-08-4.92425888E-12 2.67607327E+04 5.00994833E+01                   4
C5H4OH    THERM          C   5H   5O   1    0G   300.000  5000.000 1406.000    11
 1.49801651E+01 1.29977504E-02-4.44659387E-06 6.90532769E-10-4.00736033E-14    2
-6.21452008E+02-5.56115890E+01-4.12577307E+00 6.80489898E-02-6.60482345E-05    3
 3.19378134E-08-6.02014894E-12 4.94419361E+03 4.32564735E+01                   4
C6H5CH3           T 9/81C   7H   8    0    0G   300.000  5000.000              1
 0.13957725E+02 0.24616607E-01-0.83795358E-05 0.12537165E-08-0.67675520E-13    2
-0.10295066E+04-0.52245728E+02-0.25368824E+01 0.52898869E-01 0.14038515E-05    3
-0.40762323E-07 0.20377519E-10 0.44778477E+04 0.37415115E+02                   4
C6H5C2H5                  C   8H  10    0    0G   300.000  5000.000 1397.000    21
 2.02816724E+01 2.59464082E-02-8.92667064E-06 1.39161163E-09-8.09786280E-14    2
-6.88695837E+03-8.65892579E+01-5.93600077E+00 8.94618416E-02-6.81230510E-05    3
 2.66103734E-08-4.21398102E-12 1.94317497E+03 5.33309542E+01                   4
C6H5CH2OH  3/ 8/90       C   7H   8O   1    0G   300.000  5000.000 1396.000    21
 1.81575155E+01 2.26620146E-02-7.79454113E-06 1.21491074E-09-7.06883434E-14    2
-2.13319736E+04-7.19512787E+01-3.72475901E+00 7.42375044E-02-5.41481788E-05    3
 2.01178934E-08-3.02199053E-12-1.38224993E+04 4.53342817E+01                   4
```

```
!  Emdee et al. thermochemical data.
!
BIBENZYL                C  14H  14    0    0G   300.000  5000.000 1392.000    21
 3.48131330E+01 3.78396057E-02-1.27934440E-05 1.97366490E-09-1.14091685E-13    2
-3.11362732E+02-1.63384186E+02-1.05318902E+01 1.48504587E-01-1.15713218E-04    3
 4.52836955E-08-7.06388895E-12 1.47378885E+04 7.80962493E+01                   4
HOC6H4CH3 AVG CRESOL    C   7H   8O   1    0G   300.000  5000.000 1400.000    21
 1.97311724E+01 2.12245074E-02-7.27602659E-06 1.13158989E-09-6.57395287E-14    2
-2.50451776E+04-8.18783394E+01-4.17663565E+00 8.29479164E-02-6.92618926E-05    3
 2.97047387E-08-5.12027914E-12-1.73715284E+04 4.43681107E+01                   4
OC6H4CH3  AVG CRESOL    C   7H   7O   1    0G   300.000  5000.000 1398.000    11
 2.00333477E+01 1.83142467E-02-6.17265091E-06 9.50353551E-10-5.48634044E-14    2
-7.76864165E+03-8.60606102E+01-3.82920147E+00 7.73376217E-02-6.15929083E-05    3
 2.43728641E-08-3.80779615E-12 2.89377185E+01 4.06647799E+01                   4
C5H5O       5/16/90 THERMC   5H   5O   1    0G   300.000  5000.000 1392.000    01
 1.48322894E+01 1.40483376E-02-4.92302051E-06 7.77041219E-10-4.56103939E-14    2
 1.45523665E+04-5.73228191E+01-2.83112840E+00 5.67277287E-02-4.44757303E-05    3
 1.74924447E-08-2.76004847E-12 2.04992154E+04 3.69634411E+01                   4
C6H5C2H3  TRC TABLES    C   8H   8    0    0G   300.000  5000.000 1400.000    11
 1.94675525E+01 2.19916239E-02-7.56672249E-06 1.17967158E-09-6.86483959E-14    2
 8.16106600E+03-8.19394370E+01-5.75443698E+00 8.70398896E-02-7.28533682E-05    3
 3.12720079E-08-5.39379278E-12 1.62673706E+04 5.12775455E+01                   4
C6H5CHO     5/16/90 THERMC   7H   6O   1    0G   300.000  5000.000 1386.000    11
 1.74024893E+01 1.89508317E-02-6.58694307E-06 1.03413046E-09-6.04793155E-14    2
-1.31418522E+04-6.83371315E+01-2.37082285E+00 6.28843128E-02-4.26460754E-05    3
 1.39416083E-08-1.74474949E-12-6.11656186E+03 3.85478773E+01                   4
C6H5CO      THERM        C   7H   5O   1    0G   300.000  5000.000 1392.000    11
 1.75116258E+01 1.62650511E-02-5.65051892E-06 8.86922680E-10-5.18657990E-14    2
 4.67641545E+03-6.70531966E+01-1.56729686E+00 5.99817511E-02-4.29153585E-05    3
 1.48666854E-08-1.98938453E-12 1.12873830E+04 3.55490009E+01                   4
C6H5CH2    TROE,JPC,1990 C   7H   7    0    0G   300.000  5000.000 1392.000    11
 1.77752663E+01 1.88366755E-02-6.58968982E-06 1.03873424E-09-6.09096279E-14    2
 1.65061292E+04-7.37168331E+01-3.82523574E+00 7.22854694E-02-5.81397283E-05    3
 2.40211852E-08-4.03015544E-12 2.37153019E+04 4.12436407E+01                   4
END
```

O.1.2 Transport Parameters

```
AR                0    136.500     3.330     0.000     0.000     0.000
C2H2              1    209.000     4.100     0.000     0.000     2.500
C2H3              2    209.000     4.100     0.000     0.000     1.000 ! *
C2H4              2    280.800     3.971     0.000     0.000     1.500
C6H5              2    412.300     5.349     0.000     0.000     1.000 ! JAM
C6H5O             2    450.000     5.500     0.000     0.000     1.000 ! JAM
C6H6              2    412.300     5.349     0.000     0.000     1.000 ! SVE
CH2               1    144.000     3.800     0.000     0.000     0.000
CH2O              2    498.000     3.590     0.000     0.000     2.000
CH2OH             2    417.000     3.690     1.700     0.000     2.000
CH3               1    144.000     3.800     0.000     0.000     0.000
CH3O              2    417.000     3.690     1.700     0.000     2.000
CH4               2    141.400     3.746     0.000     2.600    13.000
CO                1     98.100     3.650     0.000     1.950     1.800
CO2               1    244.000     3.763     0.000     2.650     2.100
H                 0    145.000     2.050     0.000     0.000     0.000
H2                1     38.000     2.920     0.000     0.790   280.000
H2O               2    572.400     2.605     1.844     0.000     4.000
H2O2              2    107.400     3.458     0.000     0.000     3.800
```

```
HCCO            2   150.000     2.500     0.000     0.000     1.000 ! *
HCO             2   498.000     3.590     0.000     0.000     0.000
HO2             2   107.400     3.458     0.000     0.000     1.000 ! *
O               0    80.000     2.750     0.000     0.000     0.000
O2              1   107.400     3.458     0.000     1.600     3.800
OH              1    80.000     2.750     0.000     0.000     0.000
C6H5CH3         2   465         5.196     0.4       0.0       1.0
C6H5CHO         2   593         5.47      2.8       0.0       1.0
C6H5C2H5        2   485         5.425     0.4       0.0       1.0
HOC6H4CH3       2   567         5.60      1.6       0.0       1.0
C6H5CH2OH       2   572         5.82      1.7       0.0       1.0
BIBENZYL        2   620         7.24      0.0       0.0       1.0
C5H6            2   389         5.10      0.0       0.0       1.0
C6H5OH          2   548         5.09      1.6       0.0       1.0
C4H6            2   329         5.07      0.0       0.0       1.0
C6H5C2H3        2   501         6.03      0.1       0.0       1.0
C6H6            2   432         4.860     0.0       0.0       1.0
C6H5CH2         2   465         5.2       0.4       0.0       1.0
C6H5CO          2   593         5.5       2.8       0.0       1.0
C6H5            2   432         4.9       0.0       0.0       1.0
C6H5O           2   548         5.1       1.6       0.0       1.0
C5H5            2   389         5.1       0.0       0.0       1.0
C5H5O           2   494         5.2       1.6       0.0       1.0
C4H5            2   329         5.1       0.0       0.0       1.0
C5H4OH          2   494         5.2       1.6       0.0       1.0
C5H4O           2   484         5.1       1.6       0.0       1.0
OC6H4CH3        2   567         5.6       1.6       0.0       1.0
C4H4            1   357.000     5.180     0.000     0.000     1.000
```

O.2 Zhang and McKinnon Model.

As received from Zhang (1994).

O.2.1 Thermochemistry Parameters

```
THERMO
   300.000  1000.000  5000.000
AR                120186AR  1               G  0300.00   5000.00  1000.00      1
 0.02500000E+02 0.00000000E+00 0.00000000E+00 0.00000000E+00 0.00000000E+00    2
-0.07453750E+04 0.04366000E+02 0.02500000E+02 0.00000000E+00 0.00000000E+00    3
 0.00000000E+00 0.00000000E+00-0.07453750E+04 0.04366000E+02                   4
C                 121086C   1               G  0300.00   5000.00  1000.00      1
 0.02602087E+02-0.01787081E-02 0.09087041E-06-0.11499333E-10 0.03310844E-14    2
 0.08542154E+06 0.04195177E+02 0.02498584E+02 0.08085776E-03-0.02697697E-05    3
 0.03040729E-08-0.11066518E-12 0.08545878E+06 0.04753459E+02                   4
CH4               121286C   1H   4          G  0300.00   5000.00  1000.00      1
 0.01683478E+02 0.10237236E-01-0.03875128E-04 0.06785585E-08-0.04503423E-12    2
-0.10080787E+05 0.09623395E+02 0.07787415E+01 0.01747668E+00-0.02783409E-03    3
 0.03049708E-06-0.12239307E-10-0.09825229E+05 0.13722195E+02                   4
C2                121286C   2               G  0300.00   5000.00  1000.00      1
 0.04135978E+02 0.06531618E-03 0.01837099E-05-0.05295085E-09 0.04712137E-13    2
 0.09967272E+06 0.07472923E+01 0.06996045E+02-0.07400601E-01 0.03234703E-04    3
 0.04802535E-07-0.03295917E-10 0.09897487E+06-0.13862268E+02                   4
```

```
!  Zhang and McKinnon thermochemical data.
!
C2H                 20387C   2H   1          G  0300.00   5000.00  1000.00      1
 0.04427688E+02 0.02216268E-01-0.06048952E-05 0.09882517E-09-0.07351179E-13    2
 0.06590415E+06-0.11994418E+01 0.03050667E+02 0.06051674E-01-0.04956634E-04    3
 0.02804159E-07-0.08193332E-11 0.06630011E+06 0.05954361E+02                   4
C2H2                121386C   2H   2          G  0300.00   5000.00  1000.00      1
 0.04436770E+02 0.05376039E-01-0.01912816E-04 0.03286379E-08-0.02156709E-12    2
 0.02566766E+06-0.02800338E+02 0.02013562E+02 0.15190446E-01-0.16163189E-04    3
 0.09078992E-07-0.01912746E-10 0.02612444E+06 0.08805378E+02                   4
C2H3                12787C   2H   3          G  0300.00   5000.00  1000.00      1
 0.05933468E+02 0.04017745E-01-0.03966739E-05-0.14412666E-09 0.02378643E-12    2
 0.03185434E+06-0.08530313E+02 0.02459276E+02 0.07371476E-01 0.02109872E-04    3
-0.13216421E-08-0.11847838E-11 0.03335225E+06 0.11556202E+02                   4
C2H4                121286C   2H   4          G  0300.00   5000.00  1000.00      1
 0.03528418E+02 0.11485185E-01-0.04418385E-04 0.07844600E-08-0.05266848E-12    2
 0.04428288E+05 0.02230389E+02-0.08614880E+01 0.02796162E+00-0.03388677E-03    3
 0.02785152E-06-0.09737879E-10 0.05573046E+05 0.02421148E+03                   4
C2H5                12387C   2H   5          G  0300.00   5000.00  1000.00      1
 0.07190480E+02 0.06484077E-01-0.06428064E-05-0.02347879E-08 0.03880877E-12    2
 0.10674549E+05-0.14780892E+02 0.02690701E+02 0.08719133E-01 0.04419838E-04    3
 0.09338703E-08-0.03927773E-10 0.12870404E+05 0.12138195E+02                   4
C2H6                121686C   2H   6          G  0300.00   4000.00  1000.00      1
 0.04825938E+02 0.13840429E-01-0.04557258E-04 0.06724967E-08-0.03598161E-12    2
-0.12717793E+05-0.05239506E+02 0.14625388E+01 0.15494667E-01 0.05780507E-04    3
-0.12578319E-07 0.04586267E-10-0.11239176E+05 0.14432295E+02                   4
C2O                 121286C   2O   1          G  0300.00   5000.00  1000.00      1
 0.04849809E+02 0.02947585E-01-0.10907286E-05 0.01792562E-08-0.11157585E-13    2
 0.03282055E+06-0.06453225E+01 0.03368850E+02 0.08241803E-01-0.08765145E-04    3
 0.05569262E-07-0.15400086E-11 0.03317081E+06 0.06713314E+02                   4
C3H2                121686C   3H   2          G  0300.00   5000.00  1000.00      1
 0.06530853E+02 0.05870316E-01-0.01720776E-04 0.02127498E-08-0.08291910E-13    2
 0.05115213E+06-0.11227278E+02 0.02691077E+02 0.14803664E-01-0.03250551E-04    3
-0.08644363E-07 0.05284877E-10 0.05219072E+06 0.08757391E+02                   4
C3H5                U12/77C   3H   5          G  0300.00   5000.00  1000.00      1
 0.79091978E+01 0.12115255E-01-0.41175863E-05 0.61566796E-09-0.33235733E-13    2
 0.12354156E+05-0.19672333E+02-0.54100400E+00 0.27284101E-01-0.96365329E-06    3
-0.19129462E-07 0.98394175E-11 0.15130395E+05 0.26067337E+02                   4
C3H6                120186C   3H   6          G  0300.00   5000.00  1000.00      1
 0.06732257E+02 0.14908336E-01-0.04949899E-04 0.07212022E-08-0.03766204E-12    2
-0.09235703E+04-0.13313348E+02 0.14933071E+01 0.02092517E+00 0.04486794E-04    3
-0.16689121E-07 0.07158146E-10 0.10748264E+04 0.16145340E+02                   4
C4H                 121686C   4H   1          G  0300.00   5000.00  1000.00      1
 0.06242882E+02 0.06193682E-01-0.02085931E-04 0.03082203E-08-0.16364826E-13    2
 0.07568019E+06-0.07210806E+02 0.05023247E+02 0.07092375E-01-0.06073762E-07    3
-0.02275752E-07 0.08086994E-11 0.07623812E+06-0.06942594E+00                   4
C4H2                121686C   4H   2          G  0300.00   5000.00  1000.00      1
 0.09031407E+02 0.06047252E-01-0.01948788E-04 0.02754863E-08-0.13856080E-13    2
 0.05294735E+06-0.02385067E+03 0.04005191E+02 0.01981000E+00-0.09865877E-04    3
-0.06635158E-07 0.06077413E-10 0.05424065E+06 0.01845736E+02                   4
C4H4                      C   4H   4          G   300.00   5000.00  1404.000     1
 1.00207062E+01 9.67390881E-03-3.23076021E-06 4.93586227E-10-2.83175163E-14    2
 3.26359855E+04-2.84768495E+01 1.01074067E+00 3.33151781E-02-2.73656162E-05    3
 1.17824083E-08-2.04860686E-12 3.54881795E+04 1.89625510E+01                   4
C4H6                120186C   4H   6          G  0300.00   5000.00  1000.00      1
 0.08046583E+02 0.16485251E-01-0.05522227E-04 0.08123593E-08-0.04295078E-12    2
 0.13701305E+05-0.01800457E+03 0.03197108E+02 0.02025591E+00 0.06510192E-04    3
```

```
!  Zhang and McKinnon thermochemical data.
!
-0.16584423E-07 0.06400282E-10 0.15715203E+05 0.09895660E+02                    4
C5H2                20587C   5H   2          G  0300.00   5000.00  1000.00     1
 0.11329175E+02 0.07424056E-01-0.02628188E-04 0.04082541E-08-0.02301332E-12    2
 0.07878706E+06-0.03617117E+03 0.03062321E+02 0.02709998E+00-0.10091697E-04    3
-0.12727451E-07 0.09167219E-10 0.08114969E+06 0.07071078E+02                    4
C5H3                20387C   5H   3          G  0300.00   5000.00  1000.00     1
 0.10787622E+02 0.09539619E-01-0.03206744E-04 0.04733323E-08-0.02512135E-12    2
 0.06392904E+06-0.03005444E+03 0.04328720E+02 0.02352480E+00-0.05856723E-04    3
-0.12154494E-07 0.07726478E-10 0.06588531E+06 0.04173258E+02                    4
C5H4O                    C   5H   4O   1     G   300.00   5000.00  1387.000    1
 1.32914560E+01 1.29138911E-02-4.55514943E-06 7.22080955E-10-4.25104153E-14    2
-4.57568023E+03-5.01428656E+01-2.97337632E+00 5.10458345E-02-3.85513684E-05    3
 1.44491809E-08-2.16384604E-12 1.01932661E+03 3.70964885E+01                    4
C5H5                     C   5H   5          G   300.00   5000.00  1401.000    1
 1.35679630E+01 1.24463855E-02-4.34198158E-06 6.83368587E-10-4.00352578E-14    2
 2.06107056E+04-5.40332736E+01-5.81161873E+00 6.34164614E-02-5.62131189E-05    3
 2.47724300E-08-4.31219658E-12 2.66964534E+04 4.79019561E+01                    4
C5H5O                    C   5H   5O   1     G   300.00   5000.00  1391.000    1
 1.48359646E+01 1.40333516E-02-4.91531955E-06 7.75582831E-10-4.55153340E-14    2
 1.45580753E+04-5.73214147E+01-2.82370598E+00 5.68195777E-02-4.47287341E-05    3
 1.76910566E-08-2.80968491E-12 2.04947862E+04 3.69083876E+01                    4
C5H4OH                   C   5H   5O   1     G   300.00   5000.00  1411.000    1
 1.53245379E+01 1.23087049E-02-4.04243988E-06 6.11260166E-10-3.48376790E-14    2
-7.00902608E+02-5.74376976E+01-4.21524798E+00 6.79625301E-02-6.49157951E-05    3
 3.06252731E-08-5.61255626E-12 4.96710972E+03 4.37575334E+01                    4
C5H6                20387C   5H   6          G  0300.00   5000.00  1000.00     1
 0.09689815E+02 0.01838262E+00-0.06264884E-04 0.09393377E-08-0.05087708E-12    2
 0.11021242E+05-0.03122908E+03-0.03196739E+02 0.04081361E+00 0.06816505E-05    3
-0.03137459E-06 0.15772230E-10 0.15290676E+05 0.03869938E+03                    4
C6H                121686C   6H   1          G  0300.00   5000.00  1000.00     1
 0.11587352E+02 0.07295362E-01-0.02466008E-04 0.03407045E-08-0.14981855E-13    2
 0.10314481E+06-0.03172578E+03 0.04769848E+02 0.02457279E+00-0.07561252E-04    3
-0.14806908E-07 0.09768053E-10 0.10485231E+06 0.03241530E+02                    4
C6H2               121686C   6H   2          G  0300.00   5000.00  1000.00     1
 0.12756519E+02 0.08034381E-01-0.02618215E-04 0.03725060E-08-0.01878850E-12    2
 0.08075469E+06-0.04041262E+03 0.05751085E+02 0.02636719E+00-0.11667596E-04    3
-0.10714498E-07 0.08790297E-10 0.08262012E+06-0.04335532E+02                    4
C6H3                20387C   6H   3          G  0300.00   5000.00  1000.00     1
 0.12761181E+02 0.10385573E-01-0.03479192E-04 0.05109733E-08-0.02690965E-12    2
 0.07477706E+06-0.03891745E+03 0.05007089E+02 0.02692851E+00-0.05919865E-04    3
-0.15272335E-07 0.09408310E-10 0.07713200E+06 0.02225621E+02                    4
C6H5                82489C   6H   5          G  0300.00   4000.00  1000.00     1
 0.15775887E+02 0.09651109E-01-0.09429416E-05-0.05469111E-08 0.10265216E-12    2
 0.03302698E+06-0.06176280E+03 0.11435567E+00 0.03627324E+00 0.11582856E-05    3
-0.02196964E-06 0.08463556E-10 0.03836054E+06 0.02380117E+03                    4
C6H5(L)             82489C   6H   5          G  0300.00   4000.00  1000.00     1
 0.01721540E+03 0.08621068E-01-0.08221340E-05-0.04752164E-08 0.08844086E-12    2
 0.06385819E+06-0.06139128E+03 0.04854268E+02 0.03031659E+00 0.01742892E-05    3
-0.01811010E-06 0.07392511E-10 0.06798733E+06 0.05854934E+02                    4
C6H5O               82489C   6H   5O   1     G  0300.00   4000.00  1000.00     1
 0.01822638E+03 0.10039851E-01-0.09915668E-05-0.05672804E-08 0.10683716E-12    2
-0.02620846E+05-0.07361390E+03 0.11074965E+01 0.03956945E+00 0.08497295E-05    3
-0.02436311E-06 0.09650659E-10 0.03159672E+05 0.01973496E+03                    4
C6H5OH              82489C   6H   6O   1     G  0300.00   4000.00  1000.00     1
 0.01821632E+03 0.11424269E-01-0.10966843E-05-0.06427442E-08 0.11988930E-12    2
```

```
!  Zhang and McKinnon thermochemical data.
!
-0.02053664E+06-0.07304233E+03 0.13914556E+01 0.03931957E+00 0.01777096E-04    3
-0.02277673E-06 0.08309659E-10-0.14721809E+05 0.01917813E+03                   4
C6H6               20387C   6H   6          G  0300.00   5000.00  1000.00     1
 0.12910740E+02 0.01723296E+00-0.05024210E-04 0.05893497E-08-0.01947521E-12    2
 0.03664511E+05-0.05002699E+03-0.03138012E+02 0.04723103E+00-0.02962207E-04    3
-0.03262819E-06 0.01718691E-09 0.08890031E+05 0.03657573E+03                   4
C7H7               WARTZC   7H   7          G  0300.00   4000.00  1000.00     1
 0.14765557E+02 0.21834318E-01-0.74497539E-05 0.11167121E-08-0.60388706E-13    2
 0.16991187E+05-0.56287125E+02-0.20902777E+01 0.53650826E-01-0.37096879E-05    3
-0.38106585E-07 0.20462368E-10 0.22393387E+05 0.34406097E+02                   4
C7H8               WARTZC   7H   8          G  0300.00   4000.00  1000.00     1
 0.13957725E+02 0.24616607E-01-0.83795358E-05 0.12537165E-08-0.67675520E-13    2
-0.10295066E+04-0.52245728E+02-0.25368824E+01 0.52898869E-01 0.14038515E-05    3
-0.40762323E-07 0.20377519E-10 0.44778477E+04 0.37415115E+02                   4
C8H10                10C   8H  10          G  0300.00   5000.00  1000.00     1
 0.15268401E+02 0.34433573E-01-0.13685810E-04 0.21177802E-08-0.11564062E-12    2
-0.61602461E+04-0.59529587E+02-0.16422014E+01 0.58058664E-01 0.55675910E-05    3
-0.45693085E-07 0.21727536E-10 0.10412372E+03 0.34509140E+02                   4
C10H8            Gardib8C  10H   8          G  0300.00   5000.00  1000.00     1
 0.19726501E+02 0.28167639E-01-0.96896429E-05 0.14654855E-08-0.80134955E-13    2
 0.85581797E+04-0.86023239E+02-0.46547480E+01 0.74611127E-01-0.53069607E-05    3
-0.54125859E-07 0.29066527E-10 0.16325324E+05 0.45005463E+02                   4
CH                 121286C   1H   1          G  0300.00   5000.00  1000.00     1
 0.02196223E+02 0.02340381E-01-0.07058201E-05 0.09007582E-09-0.03855040E-13    2
 0.07086723E+06 0.09178373E+02 0.03200202E+02 0.02072875E-01-0.05134431E-04    3
 0.05733890E-07-0.01955533E-10 0.07045259E+06 0.03331587E+02                   4
CH2CO              121686C   2H   2O   1     G  0300.00   5000.00  1000.00     1
 0.06038817E+02 0.05804840E-01-0.01920953E-04 0.02794484E-08-0.14588676E-13    2
-0.08583402E+05-0.07657581E+02 0.02974970E+02 0.12118712E-01-0.02345045E-04    3
-0.06466685E-07 0.03905649E-10-0.07632636E+05 0.08673553E+02                   4
CH2O               121286C   1H   2O   1     G  0300.00   5000.00  1000.00     1
 0.02995606E+02 0.06681321E-01-0.02628954E-04 0.04737153E-08-0.03212517E-12    2
-0.15320369E+05 0.06912572E+02 0.16527311E+01 0.12631439E-01-0.01888168E-03    3
 0.02050031E-06-0.08413237E-10-0.14865404E+05 0.13784820E+02                   4
CH2OH              120186H   3C   1O   1     G  0250.00   4000.00  1000.00     1
 0.06327520E+02 0.03608270E-01-0.03201547E-05-0.01938750E-08 0.03509704E-12    2
-0.04474509E+05-0.08329365E+02 0.02862628E+02 0.10015273E-01-0.05285435E-05    3
-0.05138539E-07 0.02246041E-10-0.03349678E+05 0.10397938E+02                   4
CH3                121286C   1H   3          G  0300.00   5000.00  1000.00     1
 0.02844051E+02 0.06137974E-01-0.02230345E-04 0.03785161E-08-0.02452159E-12    2
 0.16437809E+05 0.05452697E+02 0.02430442E+02 0.11124099E-01-0.01680220E-03    3
 0.16218288E-07-0.05864952E-10 0.16423781E+05 0.06789794E+02                   4
CH3O               121686C   1H   3O   1     G  0300.00   3000.00  1000.00     1
 0.03770799E+02 0.07871497E-01-0.02656384E-04 0.03944431E-08-0.02112616E-12    2
 0.12783252E+03 0.02929575E+02 0.02106204E+02 0.07216595E-01 0.05338472E-04    3
-0.07377636E-07 0.02075610E-10 0.09786011E+04 0.13152177E+02                   4
CH3OH              121686C   1H   4O   1     G  0300.00   5000.00  1000.00     1
 0.04029061E+02 0.09376593E-01-0.03050254E-04 0.04358793E-08-0.02224723E-12    2
-0.02615791E+06 0.02378195E+02 0.02660115E+02 0.07341508E-01 0.07170050E-04    3
-0.08793194E-07 0.02390570E-10-0.02535348E+06 0.11232631E+02                   4
CO                 121286C   1O   1          G  0300.00   5000.00  1000.00     1
 0.03025078E+02 0.14426885E-02-0.05630827E-05 0.10185813E-09-0.06910951E-13    2
-0.14268350E+05 0.06108217E+02 0.03262451E+02 0.15119409E-02-0.03881755E-04    3
 0.05581944E-07-0.02474951E-10-0.14310539E+05 0.04848897E+02                   4
CO2                121286C   1O   2          G  0300.00   5000.00  1000.00     1
```

```
!  Zhang and McKinnon thermochemical data.
!
 0.04453623E+02 0.03140168E-01-0.12784105E-05 0.02393996E-08-0.16690333E-13    2
-0.04896696E+06-0.09553959E+01 0.02275724E+02 0.09922072E-01-0.10409113E-04    3
 0.06866686E-07-0.02117280E-10-0.04837314E+06 0.10188488E+02                   4
H                 120186H   1               G  0300.00   5000.00  1000.00     1
 0.02500000E+02 0.00000000E+00 0.00000000E+00 0.00000000E+00 0.00000000E+00    2
 0.02547162E+06-0.04601176E+01 0.02500000E+02 0.00000000E+00 0.00000000E+00    3
 0.00000000E+00 0.00000000E+00 0.02547162E+06-0.04601176E+01                   4
H2                121286H   2               G  0300.00   5000.00  1000.00     1
 0.02991423E+02 0.07000644E-02-0.05633828E-06-0.09231578E-10 0.15827519E-14    2
-0.08350340E+04-0.13551101E+01 0.03298124E+02 0.08249441E-02-0.08143015E-05    3
-0.09475434E-09 0.04134872E-11-0.10125209E+04-0.03294094E+02                   4
H2C4O             120189H   2C   4O   1     G  0300.00   4000.00  1000.00     1
 0.10268878E+02 0.04896164E-01-0.04885080E-05-0.02708566E-08 0.05107013E-12    2
 0.02346902E+06-0.02815985E+03 0.04810971E+02 0.13139988E-01 0.09865073E-05    3
-0.06120720E-07 0.16400028E-11 0.02545803E+06 0.02113424E+02                   4
H2CCCCH            82489C   4H   3          G  0300.00   4000.00  1000.00     1
 0.11314095E+02 0.05014414E-01-0.05350444E-05-0.02825309E-08 0.05403279E-12    2
 0.05181211E+06-0.03062434E+03 0.06545799E+02 0.12424768E-01 0.05603226E-05    3
-0.05631141E-07 0.16652183E-11 0.05352502E+06-0.04264082E+02                   4
H2CCCH             82489C   3H   3          G  0300.00   4000.00  1000.00     1
 0.08831047E+02 0.04357194E-01-0.04109066E-05-0.02368723E-08 0.04376520E-12    2
 0.03847419E+06-0.02177919E+03 0.04754199E+02 0.11080277E-01 0.02793323E-05    3
-0.05479212E-07 0.01949629E-10 0.03988883E+06 0.05854549E+01                   4
H2O                20387H   2O   1          G  0300.00   5000.00  1000.00     1
 0.02672145E+02 0.03056293E-01-0.08730260E-05 0.12009964E-09-0.06391618E-13    2
-0.02989921E+06 0.06862817E+02 0.03386842E+02 0.03474982E-01-0.06354696E-04    3
 0.06968581E-07-0.02506588E-10-0.03020811E+06 0.02590232E+02                   4
H2O2               120186H   2O   2          G  0300.00   5000.00  1000.00     1
 0.04573167E+02 0.04336136E-01-0.14746888E-05 0.02348903E-08-0.14316536E-13    2
-0.01800696E+06 0.05011369E+01 0.03388753E+02 0.06569226E-01-0.14850125E-06    3
-0.04625805E-07 0.02471514E-10-0.01766314E+06 0.06785363E+02                   4
HCCHCCH            82489C   4H   3          G  0300.00   4000.00  1000.00     1
 0.10752738E+02 0.05381153E-01-0.05549637E-05-0.03052266E-08 0.05761740E-12    2
 0.06121419E+06-0.02973025E+03 0.04153881E+02 0.01726287E+00-0.02389374E-05    3
-0.10187000E-07 0.04340504E-10 0.06338070E+06 0.06036506E+02                   4
HCCO               32387H   1C   2O   1     G  0300.00   4000.00  1000.00     1
 0.06758073E+02 0.02000400E-01-0.02027607E-05-0.10411318E-09 0.01965164E-12    2
 0.01901513E+06-0.09071262E+02 0.05047965E+02 0.04453478E-01 0.02268282E-05    3
-0.14820945E-08 0.02250741E-11 0.01965891E+06 0.04818439E+01                   4
HCCOH              32387H   2C   2O   1     G  0300.00   4000.00  1000.00     1
 0.07328324E+02 0.03336416E-01-0.03024705E-05-0.01781106E-08 0.03245168E-12    2
 0.07598258E+05-0.14012140E+02 0.03899465E+02 0.09701075E-01-0.03119309E-05    3
-0.05537732E-07 0.02465732E-10 0.08701190E+05 0.04491874E+02                   4
HCO                121286H   1C   1O   1     G  0300.00   5000.00  1000.00     1
 0.03557271E+02 0.03345572E-01-0.13350060E-05 0.02470572E-08-0.01713850E-12    2
 0.03916324E+05 0.05552299E+02 0.02898329E+02 0.06199146E-01-0.09623084E-04    3
 0.10898249E-07-0.04574885E-10 0.04159922E+05 0.08983614E+02                   4
HO2                20387H   1O   2          G  0300.00   5000.00  1000.00     1
 0.04072191E+02 0.02131296E-01-0.05308145E-05 0.06112269E-09-0.02841164E-13    2
-0.15797270E+03 0.03476029E+02 0.02979963E+02 0.04996697E-01-0.03790997E-04    3
 0.02354192E-07-0.08089024E-11 0.01762273E+04 0.09222724E+02                   4
O                 120186O   1               G  0300.00   5000.00  1000.00     1
 0.02542059E+02-0.02755061E-03-0.03102803E-07 0.04551067E-10-0.04368051E-14    2
 0.02923080E+06 0.04920308E+02 0.02946428E+02-0.16381665E-02 0.02421031E-04    3
-0.16028431E-08 0.03890696E-11 0.02914764E+06 0.02963995E+02                   4
```

```
!  Zhang and McKinnon thermochemical data.
!
O2                121386O   2               G  0300.00   5000.00  1000.00      1
 0.03697578E+02 0.06135197E-02-0.12588420E-06 0.01775281E-09-0.11364354E-14    2
-0.12339301E+04 0.03189165E+02 0.03212936E+02 0.11274864E-02-0.05756150E-05    3
 0.13138773E-08-0.08768554E-11-0.10052490E+04 0.06034737E+02                  4
OH                121286O   1H   1           G  0300.00   5000.00  1000.00      1
 0.02882730E+02 0.10139743E-02-0.02276877E-05 0.02174683E-09-0.05126305E-14    2
 0.03886888E+05 0.05595712E+02 0.03637266E+02 0.01850910E-02-0.16761646E-05    3
 0.02387202E-07-0.08431442E-11 0.03606781E+05 0.13588605E+01                  4
C12H10            T01/83C  12H  10          G   300.00   5000.00  1398.000     1
 2.76343526E+01 2.86963585E-02-8.99420034E-06 1.28842095E-09-7.00070141E-14    2
 1.17738049E+04-1.19958174E+02 2.42974541E+01 3.43776994E-02-1.21992197E-05    3
 1.90723902E-09-7.84868672E-14 1.32240822E+04-1.01155748E+02                  4
C3H4               40687C   3H   4          G   300.00   5000.00  1385.000     1
 7.98479832E+00 9.00742888E-03-3.03812525E-06 4.67662711E-10-2.69836951E-14    2
 2.02727111E+04-2.24484016E+01 7.96068546E-01 2.61442059E-02-1.90422255E-05    3
 7.44999425E-09-1.22184246E-12 2.27607548E+04 1.60819810E+01                  4
C3H4P              40687C   3H   4          G   300.00   5000.00  1385.000     1
 7.98479832E+00 9.00742888E-03-3.03812525E-06 4.67662711E-10-2.69836951E-14    2
 1.93164957E+04-2.24484016E+01 7.96068546E-01 2.61442059E-02-1.90422255E-05    3
 7.44999425E-09-1.22184246E-12 2.18045394E+04 1.60819810E+01                  4
CH2CHCCH2               C   4H   5          G   300.00   5000.00  1413.000     1
 1.11854536E+01 1.06049024E-02-3.42268950E-06 5.10812979E-10-2.88272523E-14    2
 3.24441710E+04-3.39237401E+01 1.05514961E+00 3.77996411E-02-3.15008221E-05    3
 1.36464976E-08-2.36025391E-12 3.55501864E+04 1.91307649E+01                  4
CH2CHCHCH               C   4H   5          G   300.00   5000.00  1413.000     1
 1.11854536E+01 1.06049024E-02-3.42268950E-06 5.10812979E-10-2.88272523E-14    2
 3.86847347E+04-3.39237401E+01 1.05514961E+00 3.77996411E-02-3.15008221E-05    3
 1.36464976E-08-2.36025391E-12 4.17907501E+04 1.91307649E+01                  4
C6H4OH            MOPAC C   6H   5O   1     G   300.00   5000.00  1404.000     1
 1.45068436E+01 1.59404980E-02-5.37246333E-06 8.26250158E-10-4.76347968E-14    2
 9.52783213E+03-5.58395061E+01-3.09604127E+00 6.10439698E-02-4.99110690E-05    3
 2.08646723E-08-3.49237193E-12 1.51688735E+04 3.71626206E+01                  4
C5H5(L)           MOPAC C   5H   5          G   300.00   5000.00  1401.000     1
 1.15143692E+01 1.32586113E-02-4.41495859E-06 6.73083711E-10-3.85558960E-14    2
 3.70799582E+04-3.53820788E+01 1.14470900E+00 3.95517480E-02-3.04137636E-05    3
 1.25168727E-08-2.11652249E-12 4.04708347E+04 1.95690968E+01                  4
C8H8              EBG   C   8H   8          G   300.00   5000.00  1397.000     1
 1.97218275E+01 2.13671373E-02-7.18301846E-06 1.10346973E-09-6.35885595E-14    2
 8.09327433E+03-8.32435075E+01-5.59026555E+00 8.59858562E-02-7.07697538E-05    3
 2.96387500E-08-4.96343461E-12 1.62297563E+04 5.05773921E+01                  4
C8H10             EBG   C   8H  10          G   300.00   5000.00  1390.000     1
 2.14713086E+01 2.49558342E-02-8.42478694E-06 1.29835947E-09-7.49993230E-14    2
-7.46898472E+03-9.36428065E+01-6.24730659E+00 8.99995431E-02-6.56895331E-05    3
 2.37336850E-08-3.37085410E-12 1.97071484E+03 5.48599202E+01                  4
C7H7              EBG   C   7H   7          G   300.00   5000.00  1390.000     1
 1.79096766E+01 1.83682476E-02-6.26657678E-06 9.72300701E-10-5.64192872E-14    2
 1.65219791E+04-7.43297801E+01-3.83376615E+00 7.20782523E-02-5.73515788E-05    3
 2.31788229E-08-3.76671810E-12 2.37165997E+04 4.13057853E+01                  4
C7H8              EBG   C   7H   8          G   300.00   5000.00  1393.000     1
 1.70319326E+01 2.08285471E-02-6.90952198E-06 1.04955780E-09-5.99307668E-14    2
-7.80653050E+02-6.60852736E+01 1.34198333E+01 2.70927672E-02-1.15073246E-05    3
 3.04497250E-09-4.81138453E-13 8.79493570E+02-4.56030693E+01                  4
C7H8O             EBG   C   7H   8O   1     G   300.00   5000.00  1386.000     1
 1.91919825E+01 2.19714408E-02-7.42997382E-06 1.14635969E-09-6.62717108E-14    2
-2.18095070E+04-7.82183334E+01-4.10842859E+00 7.49994656E-02-5.21053820E-05    3
```

```
!  Zhang and McKinnon thermochemical data.
!
 1.75996769E-08-2.28346014E-12-1.37101009E+04 4.71979266E+01                   4
C6H4               MOPAC C   6H   4          G   300.00   5000.00  1405.000     1
 1.23312011E+01 1.27232213E-02-4.26224174E-06 6.52339627E-10-3.74660297E-14    2
 5.27630546E+04-4.05641744E+01 3.90077286E-01 4.58355028E-02-4.02468421E-05    3
 1.85500296E-08-3.42138397E-12 5.63954748E+04 2.17272556E+01                   4
C8H6               MOPAC C   8H   6          G   300.00   5000.00  1405.000     1
 1.66351836E+01 1.92798599E-02-6.53286309E-06 1.00805333E-09-5.82414666E-14    2
 2.90016559E+04-6.75140560E+01-4.49996942E+00 7.48975828E-02-6.33659826E-05    3
 2.75708834E-08-4.80311439E-12 3.56617392E+04 4.36862915E+01                   4
C10H7              mopac C  10H   7          G   300.00   5000.00  1431.000     1
 1.77174588E+01 2.67239869E-02-8.72730540E-06 1.31405429E-09-7.46517931E-14    2
 3.78635946E+04-7.55942936E+01-4.97706841E+00 7.81519562E-02-5.09523896E-05    3
 1.59157709E-08-1.79646453E-12 4.56870324E+04 4.64894159E+01                   4
HCH                120186C   1H   2          G  0250.00   4000.00  1000.00     1
 0.03636407E+02 0.01933056E-01-0.01687016E-05-0.10098994E-09 0.01808255E-12    2
 0.04534134E+06 0.02156560E+02 0.03762237E+02 0.11598191E-02 0.02489585E-05    3
 0.08800836E-08-0.07332435E-11 0.04536790E+06 0.01712577E+02                   4
CH2                 31287C   1H   2          G  0300.00   4000.00  1000.00     1
 0.03552888E+02 0.02066788E-01-0.01914116E-05-0.11046733E-09 0.02021349E-12    2
 0.04984975E+06 0.01686570E+02 0.03971265E+02-0.01699088E-02 0.10253689E-05    3
 0.02492550E-07-0.01981266E-10 0.04989367E+06 0.05753207E+00                   4
```

O.2.2 Transport Parameters

```
AR                0    136.500     3.330     0.000     0.000     0.000
C                 0     71.400     3.298     0.000     0.000     0.000 ! *
C2                1     97.530     3.621     0.000     1.760     4.000
C2O               1    232.400     3.828     0.000     0.000     1.000 ! *
C2H               1    209.000     4.100     0.000     0.000     2.500
C2H2              1    209.000     4.100     0.000     0.000     2.500
C2H3              2    209.000     4.100     0.000     0.000     1.000 ! *
C2H4              2    280.800     3.971     0.000     0.000     1.500
C2H5              2    252.300     4.302     0.000     0.000     1.500
C2H6              2    252.300     4.302     0.000     0.000     1.500
C3H2              2    209.000     4.100     0.000     0.000     1.000 ! *
C3H4              1    252.000     4.760     0.000     0.000     1.000
C3H4P             1    252.000     4.760     0.000     0.000     1.000 ! JAM
C3H5              2    266.800     4.982     0.000     0.000     1.000 ! cp
C3H6              2    266.800     4.982     0.000     0.000     1.000
C4H4              2    357.000     5.180     0.000     0.000     1.000    !
C4H6              2    357.000     5.180     0.000     0.000     1.000
C4H               1    357.000     5.180     0.000     0.000     1.000
C4H2              1    357.000     5.180     0.000     0.000     1.000
C4H6              2    357.000     5.176     0.000     0.000     1.000    !
C5H2              1    357.000     5.180     0.000     0.000     1.000
C5H3              1    357.000     5.180     0.000     0.000     1.000
C5H5              1    357.000     5.180     0.000     0.000     1.000    !
C5H5(L)           1    357.000     5.180     0.000     0.000     1.000    !
C5H6              1    357.000     5.180     0.000     0.000     1.000    !
C6H               1    357.000     5.180     0.000     0.000     1.000
C6H2              1    357.000     5.180     0.000     0.000     1.000
C6H3              1    357.000     5.180     0.000     0.000     1.000 ! CP
C6H5              2    412.300     5.349     0.000     0.000     1.000 ! JAM
C6H4              2    412.300     5.349     0.000     0.000     1.000 ! JAM
```

```
!  Zhang and McKinnon transport data.
!
C6H5(L)              2   412.300      5.349      0.000      0.000      1.000 ! JAM
C5H4O                2   450.000      5.500      0.000      0.000      1.000 !     !
C5H5O                2   450.000      5.500      0.000      0.000      1.000 !     !
C6H5O                2   450.000      5.500      0.000      0.000      1.000 ! JAM
C6H4OH               2   450.000      5.500      0.000      0.000      1.000!CP=c6h5o
C5H4OH               2   450.000      5.500      0.000      0.000      1.000 !     !
C6H5OH               2   450.000      5.500      0.000      0.000      1.000 !     !
C6H6                 2   412.300      5.349      0.000      0.000      1.000 ! SVE
C7H7                 2   450.000      5.549      0.000      0.000      1.000 ! cp
C7H8                 2   450.000      5.549      0.000      0.000      1.000 ! cp
C7H8O                2   450.000      5.754      0.000      0.000      1.000 !ro=1.8
C8H6                 2   450.000      5.646      0.000      0.000      1.000 ! cp
C8H8                 2   450.000      5.683      0.000      0.000      1.000 ! cp !
C8H10                2   450.000      5.719      0.000      0.000      1.000 ! cp
C10H7                2   450.000      6.090      0.000      0.000      1.000 ! cp !
C10H8                2   450.000      6.090      0.000      0.000      1.000 ! cp !
C12H10               2   450.000      6.477      0.000      0.000      1.000 !ro=1.8!
CH                   1    80.000      2.750      0.000      0.000      0.000
CH2                  1   144.000      3.800      0.000      0.000      0.000
HCH                  1   144.000      3.800      0.000      0.000      0.000
CH2CHCCH2            2   357.000      5.180      0.000      0.000      1.000 ! JAM
CH2CHCHCH            2   357.000      5.180      0.000      0.000      1.000 ! JAM
CH2CO                2   436.000      3.970      0.000      0.000      2.000
CH2O                 2   498.000      3.590      0.000      0.000      2.000
CH2OH                2   417.000      3.690      1.700      0.000      2.000
CH3                  1   144.000      3.800      0.000      0.000      0.000
CH3O                 2   417.000      3.690      1.700      0.000      2.000
CH3OH                2   481.800      3.626      0.000      0.000      1.000 ! SVE
CH4                  2   141.400      3.746      0.000      2.600     13.000
CO                   1    98.100      3.650      0.000      1.950      1.800
CO2                  1   244.000      3.763      0.000      2.650      2.100
H                    0   145.000      2.050      0.000      0.000      0.000
H2C4O                2   357.000      5.180      0.000      0.000      1.000 ! JAM
H2                   1    38.000      2.920      0.000      0.790    280.000
H2CCCCH              2   357.000      5.180      0.000      0.000      1.000 ! JAM
H2CCCH               2   252.000      4.760      0.000      0.000      1.000 ! JAM
H2O                  2   572.400      2.605      1.844      0.000      4.000
H2O2                 2   107.400      3.458      0.000      0.000      3.800
HCCHCCH              2   357.000      5.180      0.000      0.000      1.000 ! JAM
HCCO                 2   150.000      2.500      0.000      0.000      1.000 ! *
HCCOH                2   436.000      3.970      0.000      0.000      2.000
HCO                  2   498.000      3.590      0.000      0.000      0.000
HO2                  2   107.400      3.458      0.000      0.000      1.000 ! *
O                    0    80.000      2.750      0.000      0.000      0.000
O2                   1   107.400      3.458      0.000      1.600      3.800
OH                   1    80.000      2.750      0.000      0.000      0.000
```

O.3 Lindstedt and Skevis Model.

As received from Lindstedt (1995).

O.3.1 Thermochemistry Parameters

```
THERMO ALL
300.00 5000.00 1000.00
C6H6                 20387C   6H   6          G  0300.00   5000.00  1000.00      1
 0.12910740E+02 0.17232966E-01-0.50242106E-05 0.58934968E-09-0.19475212E-13    2
 0.36645117E+04-0.50026993E+02-0.31380119E+01 0.47231030E-01-0.29622079E-05    3
-0.32628190E-07 0.17186919E-10 0.88900312E+04 0.36575729E+02                   4
H                    120186H   1               G  0300.00   5000.00  1000.00      1
 0.25000000E+01 0.00000000E+00 0.00000000E+00 0.00000000E+00 0.00000000E+00    2
 0.25471627E+05-0.46011763E+00 0.25000000E+01 0.00000000E+00 0.00000000E+00    3
 0.00000000E+00 0.00000000E+00 0.25471627E+05-0.46011762E+00                   4
OH                   121286O   1H   1          G  0300.00   5000.00  1000.00      1
 0.28827305E+01 0.10139743E-02-0.22768771E-06 0.21746837E-10-0.51263053E-15    2
 0.38868879E+04 0.55957122E+01 0.36372659E+01 0.18509105E-03-0.16761646E-05    3
 0.23872027E-08-0.84314418E-12 0.36067817E+04 0.13588605E+01                   4
O                    120186O   1               G  0300.00   5000.00  1000.00      1
 0.25420597E+01-0.27550619E-04-0.31028033E-08 0.45510674E-11-0.43680515E-15    2
 0.29230803E+05 0.49203081E+01 0.29464288E+01-0.16381665E-02 0.24210317E-05    3
-0.16028432E-08 0.38906963E-12 0.29147644E+05 0.29639949E+01                   4
HO2                  20387H   1O   2          G  0300.00   5000.00  1000.00      1
 0.41722659E+01 0.18812098E-02-0.34629297E-06 0.19468516E-10 0.17609153E-15    2
 0.61818851E+02 0.29577974E+01 0.43017880E+01-0.47490201E-02 0.21157953E-04    3
-0.24275961E-07 0.92920670E-11 0.29480876E+03 0.37167010E+01                   4
H2                   121286H   2               G  0300.00   5000.00  1000.00      1
 0.29914234E+01 0.70006441E-03-0.56338287E-07-0.92315782E-11 0.15827518E-14    2
-0.83503399E+03-0.13551102E+01 0.32981243E+01 0.82494417E-03-0.81430153E-06    3
-0.94754343E-10 0.41348722E-12-0.10125209E+04-0.32940941E+01                   4
H2O                  20387H   2O   1          G  0300.00   5000.00  1000.00      1
 0.26721456E+01 0.30562929E-02-0.87302601E-06 0.12009964E-09-0.63916179E-14    2
-0.29899209E+05 0.68628168E+01 0.33868425E+01 0.34749825E-02-0.63546963E-05    3
 0.69685813E-08-0.25065884E-11-0.30208113E+05 0.25902328E+01                   4
H2O2                 120186H   2O   2          G  0300.00   5000.00  1000.00      1
 0.45731667E+01 0.43361363E-02-0.14746888E-05 0.23489037E-09-0.14316536E-13    2
-0.18006961E+05 0.50113696E+00 0.33887536E+01 0.65692260E-02-0.14850126E-06    3
-0.46258055E-08 0.24715147E-11-0.17663147E+05 0.67853631E+01                   4
O2                   121386O   2               G  0300.00   5000.00  1000.00      1
 0.36975782E+01 0.61351969E-03-0.12588419E-06 0.17752815E-10-0.11364353E-14    2
-0.12339302E+04 0.31891656E+01 0.32129364E+01 0.11274863E-02-0.57561505E-06    3
 0.13138772E-08-0.87685539E-12-0.10052490E+04 0.60347376E+01                   4
CO                   121286C   1O   1          G  0300.00   5000.00  1000.00      1
 0.30250781E+01 0.14426885E-02-0.56308278E-06 0.10185813E-09-0.69109515E-14    2
-0.14268349E+05 0.61082177E+01 0.32624516E+01 0.15119408E-02-0.38817552E-05    3
 0.55819442E-08-0.24749512E-11-0.14310539E+05 0.48488969E+01                   4
CO2                  121286C   1O   2          G  0300.00   5000.00  1000.00      1
 0.44536228E+01 0.31401687E-02-0.12784105E-05 0.23939967E-09-0.16690332E-13    2
-0.48966961E+05-0.95539588E+00 0.22757246E+01 0.99220723E-02-0.10409113E-04    3
 0.68666868E-08-0.21172801E-11-0.48373141E+05 0.10188488E+02                   4
AR                      AR  1               G  0300.00   5000.00  1000.00      1
 0.02926640E+02 0.01487977E-01-0.05684761E-05 0.01009704E-08-0.06753351E-13    2
-0.09227977E+04 0.05980528E+02 0.03298677E+02 0.01408240E-01-0.03963222E-04    3
 0.05641515E-07-0.02444855E-10-0.01020900E+05 0.03950372E+02                   4
CH                   121286C   1H   1          G  0300.00   5000.00  1000.00      1
 0.25209062E+01 0.17653726E-02-0.46147581E-06 0.59288567E-10-0.33473209E-14    2
 0.71134082E+05 0.74053223E+01 0.34898166E+01 0.32383554E-03-0.16889906E-05    3
 0.31621733E-08-0.14060907E-11 0.70799939E+05 0.20840111E+01                   4
```

```
!  Lindstedt and Skevis thermochemical data.
!
CHO                     C   1H   1O   1     G  0300.00   5000.00  1000.00      1
 0.35572712E+01 0.33455728E-02-0.13350060E-05 0.24705726E-09-0.17138509E-13    2
 0.39163245E+04 0.55522995E+01 0.28983297E+01 0.61991466E-02-0.96230842E-05    3
 0.10898249E-07-0.45748852E-11 0.41599219E+04 0.89836139E+01                  4
CH2S                 31287C   1H   2          G  0300.00   5000.00  1000.00      1
 0.35528886E+01 0.20667882E-02-0.19141160E-06-0.11046734E-09 0.20213496E-13    2
 0.49849754E+05 0.16865700E+01 0.39712651E+01-0.16990887E-03 0.10253688E-05    3
 0.24925508E-08-0.19812663E-11 0.49893676E+05 0.57532072E-01                  4
CH2T                120186C   1H   2          G  0300.00   5000.00  1000.00      1
 0.36364078E+01 0.19330566E-02-0.16870163E-06-0.10098994E-09 0.18082558E-13    2
 0.45341339E+05 0.21565606E+01 0.37622371E+01 0.11598191E-02 0.24895854E-06    3
 0.88008356E-09-0.73324354E-12 0.45367906E+05 0.17125776E+01                  4
CH2O                121286C   1H   2O   1     G  0300.00   5000.00  1000.00      1
 0.31694807E+01 0.61932742E-02-0.22505981E-05 0.36598245E-09-0.22015410E-13    2
-0.14478425E+05 0.60423533E+01 0.47937036E+01-0.99081518E-02 0.37321459E-04    3
-0.37927902E-07 0.13177015E-10-0.14308955E+05 0.60288702E+00-0.13059098E+05    4
CH3                 121286C   1H   3          G  0300.00   5000.00  1000.00      1
 0.28440516E+01 0.61379741E-02-0.22303452E-05 0.37851608E-09-0.24521590E-13    2
 0.16437808E+05 0.54526973E+01 0.24304428E+01 0.11124099E-01-0.16802203E-04    3
 0.16218287E-07-0.58649526E-11 0.16423781E+05 0.67897939E+01                  4
CH3O                121686C   1H   3O   1     G  0300.00   5000.00  1000.00      1
 0.37707996E+01 0.78714974E-02-0.26563839E-05 0.39444314E-09-0.21126164E-13    2
 0.12783252E+03 0.29295749E+01 0.21062040E+01 0.72165951E-02 0.53384719E-05    3
-0.73776363E-08 0.20756105E-11 0.97860107E+03 0.13152177E+02                  4
CH2OH               120186H   3C   1O   1     G  0300.00   5000.00  1000.00      1
 0.46776733E+01 0.65608772E-02-0.22636864E-05 0.35530469E-09-0.20842959E-13    2
-0.28928048E+04 0.48041879E+00 0.38644027E+01 0.55913161E-02 0.59514635E-05    3
-0.10477176E-07 0.43793199E-11-0.25050493E+04 0.54710652E+01                  4
CH4                 121286C   1H   4          G  0300.00   5000.00  1000.00      1
 0.16834788E+01 0.10237235E-01-0.38751286E-05 0.67855849E-09-0.45034231E-13    2
-0.10080787E+05 0.96233949E+01 0.77874148E+00 0.17476683E-01-0.27834090E-04    3
 0.30497080E-07-0.12239307E-10-0.98252285E+04 0.13722195E+02                  4
C2H                  81193C   2H   1          G  0300.00   5000.00  1000.00      1
 0.40553334E+01 0.35212890E-02-0.12531130E-05 0.19513214E-09-0.11276587E-13    2
 0.66668674E+05 0.12209775E+01 0.23114439E+01 0.97218264E-02-0.10166438E-04    3
 0.58435851E-08-0.13028789E-11 0.67150882E+05 0.99824423E+01                  4
C2HO                    C   2H   1O   1     G  0300.00   5000.00  1000.00      1
 0.42603635E+01 0.48274243E-02-0.16661974E-05 0.26140685E-09-0.15325901E-13    2
 0.17880484E+05 0.39788463E+01 0.27659287E+01 0.14174259E-01-0.23260615E-04    3
 0.21573491E-07-0.75853929E-11 0.18085633E+05 0.10540898E+02                  4
C2H2                    C   2H   2          G  0300.00   5000.00  1000.00      1
 0.44367704E+01 0.53760391E-02-0.19128167E-05 0.32863789E-09-0.21567095E-13    2
 0.25667664E+05-0.28003383E+01 0.20135622E+01 0.15190446E-01-0.16163189E-04    3
 0.90789918E-08-0.19127460E-11 0.26124443E+05 0.88053779E+01                  4
C2H2O                   C   2H   2O   1     G  0300.00   5000.00  1000.00      1
 0.60388174E+01 0.58048405E-02-0.19209538E-05 0.27944846E-09-0.14588675E-13    2
-0.85834023E+04-0.76575813E+01 0.29749708E+01 0.12118712E-01-0.23450457E-05    3
-0.64666850E-08 0.39056492E-11-0.76326367E+04 0.86735525E+01                  4
CHCOH                   C   2H   2O   1     G  0300.00   5000.00  1000.00      1
 0.63660255E+01 0.55038729E-02-0.18851901E-05 0.29446414E-09-0.17218598E-13    2
 0.89184965E+04-0.82504705E+01 0.19654173E+01 0.25585205E-01-0.38773334E-04    3
 0.31566335E-07-0.10081670E-10 0.97694090E+04 0.12602749E+02                  4
C2H3                 12787C   2H   3          G  0300.00   5000.00  1000.00      1
 0.59334679E+01 0.40177456E-02-0.39667395E-06-0.14412665E-09 0.23786435E-13    2
 0.33854346E+05-0.85303125E+01 0.24592764E+01 0.73714764E-02 0.21098729E-05    3
```

```
!  Lindstedt and Skevis thermochemical data.
!
-0.13216421E-08-0.11847838E-11 0.35352250E+05 0.11556202E+02                   4
C2H4               121286C   2H   4          G  0300.00   5000.00  1000.00     1
 0.35284188E+01 0.11485184E-01-0.44183853E-05 0.78446005E-09-0.52668485E-13    2
 0.44282886E+04 0.22303891E+01-0.86148798E+00 0.27961628E-01-0.33886772E-04    3
 0.27851522E-07-0.97378789E-11 0.55730459E+04 0.24211487E+02                   4
C2H5               12387C   2H   5          G  0300.00   5000.00  1000.00     1
 0.42878814E+01 0.12433893E-01-0.44139119E-05 0.70654102E-09-0.42035136E-13    2
 0.12056455E+05 0.84602583E+00 0.43058580E+01-0.41833638E-02 0.49707270E-04    3
-0.59905874E-07 0.23048478E-10 0.12841714E+05 0.47100236E+01                   4
C2H6               121686C   2H   6          G  0300.00   5000.00  1000.00     1
 0.48259382E+01 0.13840429E-01-0.45572588E-05 0.67249672E-09-0.35981614E-13    2
-0.12717793E+05-0.52395067E+01 0.14625387E+01 0.15494667E-01 0.57805073E-05    3
-0.12578319E-07 0.45862671E-11-0.11239176E+05 0.14432295E+02                   4
C3H                    C   3H   1          G  0300.00   5000.00  1000.00     1
 0.34671283E+01 0.62969122E-02-0.22708676E-05 0.36749291E-09-0.22034692E-13    2
 0.80801495E+05 0.53527629E+01 0.24726647E+01 0.85316627E-02-0.63505996E-05    3
 0.56681332E-08-0.24832298E-11 0.81205573E+05 0.10875808E+02                   4
C3H2               102193H   2C   3          G  0300.00   5000.00  1000.00     1
 0.62476406E+01 0.56755154E-02-0.19541329E-05 0.31686787E-09-0.19722528E-13    2
 0.54930960E+05-0.96791278E+01 0.36613541E+01 0.89364130E-02 0.35404269E-05    3
-0.11072967E-07 0.52009416E-11 0.55858605E+05 0.46695742E+01                   4
C3H3                   C   3H   3          G  0300.00   5000.00  1000.00     1
 0.66416953E+01 0.80859651E-02-0.28479238E-05 0.45353447E-09-0.26828535E-13    2
 0.38979395E+05-0.10400071E+02 0.18283782E+01 0.23784171E-01-0.21923663E-04    3
 0.10007755E-07-0.13902579E-11 0.40186308E+05 0.13844912E+02                   4
C3H4A                  C   3H   4          G  0300.00   5000.00  1000.00     1
 0.63168722E+01 0.11133728E-01-0.39629378E-05 0.63564238E-09-0.37875540E-13    2
 0.20117495E+05-0.10995766E+02 0.26130445E+01 0.12122575E-01 0.18539880E-04    3
-0.34525149E-07 0.15335079E-10 0.21541567E+05 0.10226139E+02                   4
C3H4P                  C   3H   4          G  0300.00   5000.00  1000.00     1
 0.60252400E+01 0.11336542E-01-0.40223391E-05 0.64376063E-09-0.38299635E-13    2
 0.19620942E+05-0.86043785E+01 0.26803869E+01 0.15799651E-01 0.25070596E-05    3
-0.13657623E-07 0.66154285E-11 0.20802374E+05 0.98769351E+01                   4
C3H4B                  C   3H   4          G  0300.00   5000.00  1000.00     1
 0.66999931E+01 0.10357372E-01-0.34551167E-05 0.50652949E-09-0.26682276E-13    2
 0.30199051E+05-0.13378770E+02-0.24621047E-01 0.23197215E-01-0.18474357E-05    3
-0.15927593E-07 0.86846155E-11 0.32334137E+05 0.22729762E+02                   4
C3H5A                  C   3H   5          G  0300.00   5000.00  1000.00     1
 0.09651539E+02 0.08075596E-01-0.07965424E-05-0.04650696E-08 0.08603281E-12    2
 0.15300955E+05-0.02837848E+03 0.02276486E+02 0.01985564E+00 0.11238421E-05    3
-0.10145757E-07 0.03441342E-10 0.01789496E+06 0.12214139E+02                   4
C3H5S                  C   3H   5          G  0300.00   5000.00  1000.00     1
 0.09209764E+02 0.07871412E-01-0.07724522E-05-0.04497357E-08 0.08377272E-12    2
 0.02853967E+06-0.02383444E+03 0.03161863E+02 0.15180997E-01 0.02722659E-04    3
-0.05177112E-07 0.05435286E-12 0.03095547E+06 0.10468980E+02                   4
C3H5T                  C   3H   5          G  0300.00   5000.00  1000.00     1
 0.09101018E+02 0.07964167E-01-0.07884945E-05-0.04562036E-08 0.08529212E-12    2
 0.02670680E+06-0.02301634E+03 0.03385811E+02 0.14045337E-01 0.03204127E-04    3
-0.03824120E-07-0.09053742E-11 0.02909066E+06 0.09755734E+02                   4
C3H6               120186C   3H   6          G  0300.00   5000.00  1000.00     1
 0.67213974E 01 0.14931757E-01-0.49652353E-05 0.72510753E-09-0.38001476E-13    2
-0.92453149E 03-0.12155617E 02 0.14575157E 01 0.21142263E-01 0.40468012E-05    3
-0.16319003E-07 0.70475153E-11 0.10740208E 04 0.17399460E 02                   4
C3H7N                  C   3H   7          G  0300.00   5000.00  1000.00     1
 0.77026987E 01 0.16044203E-01-0.52833220E-05 0.76298590E-09-0.39392284E-13    2
```

```
!  Lindstedt and Skevis thermochemical data.
!
 0.82984336E 04-0.15480180E 02 0.10515518E 01 0.25991980E-01 0.23800540E-05    3
-0.19609569E-07 0.93732470E-11 0.10631863E 05 0.21122559E 02                   4
C3H7I                   C   3H   7          G  0300.00   5000.00  1000.00     1
 0.65294638E 01 0.17193288E-01-0.57153220E-05 0.83408080E-09-0.43663532E-13    2
 0.77179102E 04-0.91399021E 01 0.14461584E 01 0.20988975E-01 0.77172672E-05    3
-0.18481391E-07 0.71269024E-11 0.98206094E 04 0.20108200E 02                   4
C3H8               120186C   3H   8          G  0300.00   5000.00  1000.00     1
 0.75252171E+01 0.18890340E-01-0.62839244E-05 0.91793728E-09-0.48124099E-13    2
-0.16464547E+05-0.17843903E+02 0.89692080E+00 0.26689861E-01 0.54314251E-05    3
-0.21260007E-07 0.92433301E-11-0.13954918E+05 0.19355331E+02                   4
C4H                121686C   4H   1          G  0300.00   5000.00  1000.00     1
 0.62428318E+01 0.61936825E-02-0.20859315E-05 0.30822034E-09-0.16364825E-13    2
 0.94300187E+05-0.72108059E+01 0.50232468E+01 0.70923753E-02-0.60737619E-08    3
-0.22757522E-08 0.80869941E-12 0.94858125E+05-0.69425940E-01                   4
C4H2               121686C   4H   2          G  0300.00   5000.00  1000.00     1
 0.86670035E+01 0.67166371E-02-0.23544995E-05 0.37383079E-09-0.22118914E-13    2
 0.52878439E+05-0.21114205E+02-0.39518508E+00 0.51955813E-01-0.91786616E-04    3
 0.80523929E-07-0.26917088E-10 0.54473214E+05 0.20969101E+02                   4
C4H3N                   C   4H   3          G  0300.00   4000.00  1000.00     1
 0.10752738E+02 0.05381153E-01-0.05549637E-05-0.03052266E-08 0.05761740E-12    2
 0.06121419E+06-0.02973025E+03 0.04153881E+02 0.01726287E+00-0.02389374E-05    3
-0.10187000E-07 0.04340504E-10 0.06338070E+06 0.06036506E+02                   4
C4H3I                   C   4H   3          G  0300.00   5000.00  1000.00     1
 0.84874201E+01 0.86908937E-02-0.28544437E-05 0.41200798E-09-0.21301093E-13    2
 0.54044069E+05-0.19018509E+02 0.35539713E+01 0.19461986E-01-0.48102484E-05    3
-0.97301225E-08 0.62390535E-11 0.55527377E+05 0.70829868E+01                   4
C4H4                    C   4H   4          G  0300.00   5000.00  1000.00     1
 0.88921490E+01 0.10908850E-01-0.35949597E-05 0.51934190E-09-0.26808921E-13    2
 0.29966522E+05-0.21726944E+02 0.21403370E+01 0.24605047E-01-0.36391657E-05    3
-0.15304014E-07 0.88964608E-11 0.32056170E+05 0.14282477E+02                   4
C4H5S                   C   4H   5          G  0300.00   5000.00  1000.00     1
 0.40734210E 01 0.24907370E-01-0.13229540E-04 0.34159060E-08-0.34874460E-12    2
 0.33975420E 05 0.43252930E 01-0.19509230E 01 0.53281440E-01-0.65306770E-04    3
 0.46994220E-07-0.14204880E-10 0.35048460E 05 0.32542460E 02                   4
C4H5T                   C   4H   5          G  0300.00   5000.00  1000.00     1
 0.72559180E 01 0.17141310E-01-0.74350450E-05 0.16410520E-08-0.15360780E-12    2
 0.38227410E 05-0.12422830E 02-0.20329280E 01 0.53630530E-01-0.63382690E-04    3
 0.40641440E-07-0.10398020E-10 0.40219650E 05 0.32787830E 02                   4
C4H5I                   C   4H   5          G  0300.00   5000.00  1000.00     1
 0.72559180E 01 0.17141310E-01-0.74350450E-05 0.16410520E-08-0.15360780E-12    2
 0.36339860E 05-0.13420580E 02 0.10251400E 02-0.25627670E-01 0.10715090E-03    3
-0.11090190E-06 0.37550050E-10 0.37128550E 05-0.20574530E 02                   4
C4H6S                   C   4H   6          G  0300.00   5000.00  1000.00     1
 0.17815570E 02-0.42575020E-02 0.10511850E-04-0.44738440E-08 0.58481380E-12    2
 0.12673420E 05-0.69826620E 02 0.10234670E 01 0.34959190E-01-0.22009050E-04    3
 0.69422720E-08-0.78791870E-12 0.18117990E 05 0.19750660E 02                   4
C4H6T                   C   4H   6          G  0300.00   5000.00  1000.00     1
 0.71309430E 01 0.20640080E-01-0.93239060E-05 0.21473070E-08-0.20613610E-12    2
 0.96126540E 04-0.14172220E 02-0.25309000E 01 0.53879690E-01-0.51739330E-04    3
 0.25107200E-07-0.43247260E-11 0.11876910E 05 0.33913880E 02                   4
C4H6B                   C   4H   6          G  0300.00   5000.00  1000.00     1
 0.77061882E+01 0.15477240E-01-0.22161657E-05-0.17662189E-08 0.57283106E-12    2
 0.25267377E+05-0.15592457E+02-0.19918253E+02 0.17644100E+00-0.35904226E-03    3
 0.33266232E-06-0.11036895E-09 0.29933167E+05 0.10893895E+03                   4
C4H6O                   C   4H   6O   1     G  0300.00   5000.00  1000.00     1
```

```
!  Lindstedt and Skevis thermochemical data.
!
 0.49302578E+01 0.30160125E-01-0.16567141E-04 0.44492734E-08-0.46829386E-12    2
-0.15047124E+05 0.38153801E+01 0.23550308E+00 0.48366807E-01-0.44811732E-04    3
 0.24686299E-07-0.59726694E-11-0.13999238E+05 0.26791668E+02                   4
C6H2               121686C   6H   2          G  0300.00   5000.00  1000.00     1
 0.12532801E+02 0.87766321E-02-0.31329616E-05 0.50371820E-09-0.30071921E-13    2
 0.79784338E+05-0.38858580E+02-0.54109216E+00 0.74532628E-01-0.13578252E-03    3
 0.12226630E-06-0.41825207E-10 0.82115132E+05 0.21882710E+02                   4
C8H2               121686C   8H   2          G  0300.00   5000.00  1000.00     1
 0.17007524E+02 0.93656848E-02-0.30485718E-05 0.47653534E-09-0.29169032E-13    2
 0.10628021E+06-0.59224564E+02 0.12470437E+01 0.78392526E-01-0.12416148E-03    3
 0.98381697E-07-0.30063943E-10 0.10942891E+06 0.16048227E+02                   4
C3H2O                  C   3H   2O   1     G  0300.00   5000.00  1000.00     1
 0.57542202E+01 0.16024155E-01-0.89997933E-05 0.23647714E-08-0.23824583E-12    2
 0.10893523E+05-0.17259618E+01 0.18049291E+01 0.25715641E-01-0.15713782E-04    3
 0.22703604E-08 0.81809272E-12 0.12047403E+05 0.18987669E+02                   4
CH3OH              121686C   1H   4O   1     G  0300.00   5000.00  1000.00     1
 0.36012593E+01 0.10243223E-01-0.35999217E-05 0.57251951E-09-0.33912719E-13    2
-0.25997155E+05 0.47056025E+01 0.57153948E+01-0.15230920E-01 0.65244182E-04    3
-0.71080873E-07 0.26135383E-10-0.25642765E+05-0.15040970E+01                   4
C6H3                20387C   6H   3          G  0300.00   5000.00  1000.00     1
 0.12761181E+02 0.10385573E-01-0.34791929E-05 0.51097326E-09-0.26909651E-13    2
 0.74777062E+05-0.38917450E+02 0.50070896E+01 0.26928518E-01-0.59198655E-05    3
-0.15272335E-07 0.94083101E-11 0.77132000E+05 0.22256212E+01                   4
C6H4L                  C   6H   4          G  0300.00   5000.00  1000.00     1
 0.17183117E+02 0.66487658E-02-0.12416263E-05 0.14697448E-09-0.91398013E-14    2
 0.55076954E+05-0.64435183E+02 0.19323139E+01 0.39032183E-01-0.69227109E-05    3
-0.27093357E-07 0.15730252E-10 0.59691948E+05 0.16516023E+02                   4
C6H5                82489C   6H   5          G  0300.00   5000.00  1000.00     1
 0.11433509E+02 0.17014805E-01-0.58358992E-05 0.88020347E-09-0.47983644E-13    2
 0.34941625E+05-0.38578339E+02-0.22878075E+01 0.42416330E-01-0.17666744E-05    3
-0.31422520E-07 0.16505464E-10 0.39370789E+05 0.35398270E+02                   4
C6H5O                  C   6H   5O   1     G  0300.00   5000.00  1000.00     1
 0.13833984E 02 0.17618403E-01-0.60696257E-05 0.91988173E-09-0.50449181E-13    2
-0.69212549E 03-0.50392990E 02-0.18219433E 01 0.48122510E-01-0.46792302E-05    3
-0.34018594E-07 0.18649637E-10 0.42429180E 04 0.33526199E 02                   4
C6H5OH                 C   6H   6O   1     G  0300.00   5000.00  1000.00     1
 0.14943568E+02 0.18317845E-01-0.61606479E-05 0.91048524E-09-0.48410806E-13    2
-0.18386828E+05-0.56096741E+02-0.16677656E+01 0.52091170E-01-0.67895007E-05    3
-0.36257116E-07 0.20586241E-10-0.13287539E+05 0.32421951E+02                   4
C5H6                20387C   5H   6          G  0300.00   5000.00  1000.00     1
 0.96898146E+01 0.18382620E-01-0.62648842E-05 0.93933772E-09-0.50877081E-13    2
 0.11021242E+05-0.31229080E+02-0.31967392E+01 0.40813610E-01 0.68165053E-06    3
-0.31374590E-07 0.15772231E-10 0.15290676E+05 0.38699387E+02                   4
C5H5               101993H   5C   5          G  0300.00   5000.00  1000.00     1
 0.10844072E+02 0.15392831E-01-0.55630422E-05 0.90189440E-09-0.54156619E-13    2
 0.26950886E+05-0.35254983E+02-0.95902849E+00 0.31396777E-01 0.26724050E-04    3
-0.68942183E-07 0.33301983E-10 0.30779441E+05 0.29072780E+02                   4
C5H5O                  H   5C   5O   1     G  0300.00   5000.00  1000.00     1
 0.73219724E+01 0.26217271E-01-0.10394357E-04 0.69805534E-09 0.30307525E-12    2
 0.86725078E+04-0.13395977E+02-0.91274900E+01 0.89092843E-01-0.98929631E-04    3
 0.55164946E-07-0.12054646E-10 0.12050769E+05 0.66558670E+02                   4
C5H4O                  H   4C   5O   1     G  0300.00   5000.00  1000.00     1
 0.16174722E+01 0.37716053E-01-0.23935409E-04 0.72674178E-08-0.84449082E-12    2
-0.32129492E+03 0.13399043E+02-0.33123374E+01 0.54107033E-01-0.48252157E-04    3
 0.26132914E-07-0.68544311E-11 0.10042001E+04 0.38434387E+02                   4
```

```
!  Lindstedt and Skevis thermochemical data.
!
C5H4OH                    H   5C   5O   1      G  0300.00   5000.00  1000.00      1
 0.82749834E+01 0.25455624E-01-0.11891672E-04 0.20921516E-08-0.16007544E-13    2
 0.65311050E+04-0.18165775E+02-0.75077271E+01 0.86810358E-01-0.99664867E-04    3
 0.56890869E-07-0.12613540E-10 0.97140107E+04 0.58272274E+02                   4
C5H5L                     H   5C   5          G  0300.00   5000.00  1000.00      1
 0.94095519E+01 0.13173708E-01-0.40061435E-05 0.59642775E-09-0.35402340E-13    2
 0.41667887E+05-0.22571166E+02 0.22059680E+01 0.39193876E-01-0.40875017E-04    3
 0.25229634E-07-0.65871791E-11 0.43303065E+05 0.13030572E+02                   4
C5H6L                     H   6C   5          G  0300.00   5000.00  1000.00      1
 0.18941353E+02 0.85102411E-02-0.14014643E-05 0.00000000E+00 0.00000000E+00    2
 0.21152123E+05-0.76903470E+02-0.56457147E+00 0.48115796E-01-0.23131123E-04    3
 0.00000000E+00 0.00000000E+00 0.27947513E+05 0.28939042E+02                   4
C5H4L                     H   4C   5          G  0300.00   5000.00  1000.00      1
 0.91465524E+01 0.12847056E-01-0.32463853E-05 0.39700433E-09-0.19573305E-13    2
 0.47414730E+05-0.20999841E+02 0.17646776E+01 0.45425568E-01-0.58400827E-04    3
 0.43937642E-07-0.13555336E-10 0.48714156E+05 0.13861447E+02                   4
C5H3L                     H   3C   5          G  0300.00   5000.00  1000.00      1
 0.10296658E+02 0.10470124E-01-0.37746103E-05 0.61077326E-09-0.36621089E-13    2
 0.63403545E+05-0.27338507E+02 0.15946538E+01 0.43378369E-01-0.56253789E-04    3
 0.41304029E-07-0.12456939E-10 0.65455235E+05 0.15644812E+02                   4
C5H2                20587C   5H   2          G  0300.00   5000.00  1000.00      1
 0.11329175E+02 0.74240565E-02-0.26281887E-05 0.40825410E-09-0.23013326E-13    2
 0.78787062E+05-0.36184340E+02 0.30623217E+01 0.27099982E-01-0.10091697E-04    3
-0.12727451E-07 0.91672191E-11 0.81149687E+05 0.70842413E+01                   4
C6H4C              111293H   4C   6          G  0300.00   5000.00  1000.00      1
 0.10582770E+02 0.15914908E-01-0.58202018E-05 0.95108725E-09-0.57425956E-13    2
 0.52834650E+05-0.32571269E+02 0.28042240E+00 0.26170563E-01 0.29996638E-04    3
-0.63979566E-07 0.29103081E-10 0.56470786E+05 0.24784179E+02                   4
C6H6A                     H   6C   6          G  0300.00   5000.00  1000.00      1
 0.13411768E+02 0.14720221E-01-0.50817705E-05 0.79886354E-09-0.46950844E-13    2
 0.46417676E+05-0.41652032E+02 0.77929707E+00 0.54372126E-01-0.47873814E-04    3
 0.16187164E-07 0.33735744E-12 0.49564288E+05 0.22128592E+02                   4
C6H6B                     H   6C   6          G  0300.00   5000.00  1000.00      1
 0.13411768E+02 0.14720221E-01-0.50817705E-05 0.79886354E-09-0.46950844E-13    2
 0.46417676E+05-0.41652032E+02 0.77929707E+00 0.54372126E-01-0.47873814E-04    3
 0.16187164E-07 0.33735744E-12 0.49564288E+05 0.22128592E+02                   4
C6H6D                     H   6C   6          G  0300.00   5000.00  1000.00      1
 0.13411768E+02 0.14720221E-01-0.50817705E-05 0.79886354E-09-0.46950844E-13    2
 0.34835236E+05-0.41652032E+02 0.77929707E+00 0.54372126E-01-0.47873814E-04    3
 0.16187164E-07 0.33735744E-12 0.37981848E+05 0.22128592E+02                   4
C6H5A                     H   5C   6          G  0300.00   5000.00  1000.00      1
 0.13411768E+02 0.14720221E-01-0.50817705E-05 0.79886354E-09-0.46950844E-13    2
 0.59803716E+05-0.42552032E+02 0.77929707E+00 0.54372126E-01-0.47873814E-04    3
 0.16187164E-07 0.33735744E-12 0.62950312E+05 0.21228592E+02                   4
C6H5B                     H   5C   6          G  0300.00   5000.00  1000.00      1
 0.13411768E+02 0.14720221E-01-0.50817705E-05 0.79886354E-09-0.46950844E-13    2
 0.65450312E+05-0.42552032E+02 0.77929707E+00 0.54372126E-01-0.47873814E-04    3
 0.16187164E-07 0.33735744E-12 0.67996908E+05 0.21228592E+02                   4
C6H7               82489C   6H   7          G  0300.00   5000.00  1000.00      1
 0.12801758E+02 0.21924749E-01-0.79713001E-05 0.12972935E-08-0.78100416E-13    2
 0.17889539E+05-0.45804341E+02-0.10303140E+00 0.34393354E-01 0.39788466E-04    3
-0.85116612E-07 0.39012224E-10 0.22425515E+05 0.26022350E+02                   4
C6H7L                     H   7C   6          G  0300.00   5000.00  1000.00      1
 0.01755221E+03 0.01227080E+00-0.01185742E-04-0.06959661E-08 0.01301326E-11    2
 0.01624581E+06-0.07166589E+03 0.04639166E+01 0.03975928E+00 0.02529095E-04    3
```

```
!  Lindstedt and Skevis thermochemical data.
!
-0.02223792E-06 0.07557053E-10 0.02225169E+06 0.02235387E+03                   4
C6H6S                   H   6C   6          G  0300.00   5000.00  1000.00      1
 0.13411768E+02 0.14720221E-01-0.50817705E-05 0.79886354E-09-0.46950844E-13    2
 0.43134058E+05-0.41652032E+02 0.77929707E+00 0.54372126E-01-0.47873814E-04    3
 0.16187164E-07 0.33735744E-12 0.46280670E+05 0.22128592E+02                   4
C6H6F                   H   6C   6          G  0300.00   5000.00  1000.00      1
 0.13411768E+02 0.14720221E-01-0.50817705E-05 0.79886354E-09-0.46950844E-13    2
 0.20846783E+05-0.46451032E+02 0.77929707E+00 0.54372126E-01-0.47873814E-04    3
 0.16187164E-07 0.33735744E-12 0.23993395E+05 0.17329458E+02                   4
C6H6M                   H   6C   6          G  0300.00   5000.00  1000.00      1
 0.13411768E+02 0.14720221E-01-0.50817705E-05 0.79886354E-09-0.46950844E-13    2
 0.34835236E+05-0.46451032E+02 0.77929707E+00 0.54372126E-01-0.47873814E-04    3
 0.16187164E-07 0.33735744E-12 0.37981848E+05 0.17329458E+02                   4
C2O                     C   2O   1          G  0300.00   5000.00  1000.00      1
 0.51512722E+01 0.23726722E-02-0.76135971E-06 0.11706415E-09-0.70257804E-14    2
 0.33241888E+05-0.22183135E+01 0.28648610E+01 0.11990216E-01-0.18362448E-04    3
 0.15769739E-07-0.53897452E-11 0.33749932E+05 0.88867772E+01                   4
C4H2O                   H   2C   4O   1     G  0300.00   5000.00  1000.00      1
 0.10268878E+02 0.04896164E-01-0.04885080E-05-0.02708566E-08 0.05107013E-12    2
 0.02346902E+06-0.02815985E+03 0.04810971E+02 0.13139988E-01 0.09865073E-05    3
-0.06120720E-07 0.16400028E-11 0.02545803E+06 0.02113424E+02                   4
END
```

O.3.2 Transport Parameters

```
AR                  1    97.530     3.621     0.000     1.760     4.000
C6H6                2   412.300     5.349     0.000     0.000     1.000 ! SVE
H                   0    37.000     2.708     0.000     0.000  1000.000
OH                  1    80.000     2.750     0.000     0.000    10.000
O                   0    80.000     2.750     0.000     0.000  1000.000
HO2                 2   107.400     3.458     0.000     0.000     3.000 ! *
H2                  1    59.700     2.827     0.000     0.790   280.000
H2O                 2   572.400     2.605     1.844     0.000     4.000
H2O2                2   107.400     3.458     0.000     0.000     3.800
O2                  1   107.400     3.458     0.000     1.600     3.800
CO                  1    98.100     3.650     0.000     1.950     1.800
CO2                 1   244.000     3.763     0.000     2.650     2.100
CH                  1    80.000     2.750     0.000     0.000     2.000
CHO                 2   498.000     3.590     0.000     0.000     2.000
CH2T                1   144.000     3.800     0.000     0.000    13.000
CH2S                1   144.000     3.800     0.000     0.000    13.000
CH2O                2   498.000     3.590     0.000     0.000     2.000
CH3                 1   144.000     3.800     0.000     0.000    13.000
CH3O                2   498.000     3.590     1.700     0.000     2.000
CH2OH               2   498.000     3.590     1.700     0.000     2.000
CH4                 2   141.400     3.746     0.000     2.600    13.000
C2H                 1   209.000     4.100     0.000     0.000     2.500
C2HO                1   150.000     2.500     0.000     0.000     2.000
C2H2                1   209.000     4.100     0.000     0.000     2.500
C2H2O               2   436.000     3.970     0.000     0.000     2.000 ! *
CHCOH               2   436.000     3.970     0.000     0.000     2.000 ! *
C2H3                2   209.000     4.100     0.000     0.000     2.000 ! *
C2H4                2   280.800     3.971     0.000     0.000     2.000
C2H5                2   252.300     4.302     0.000     0.000     2.000
```

```
!  Lindstedt and Skevis transport data.
!
C2H6              2   252.300     4.302     0.000     0.000     2.000
C3H               2   209.000     4.100     0.000     0.000     1.000
C3H2              2   209.000     4.100     0.000     0.000     1.000 ! *
C3H3              1   252.000     4.760     0.000     0.000     1.000
C3H4A             1   252.000     4.760     0.000     0.000     1.000
C3H4P             1   252.000     4.760     0.000     0.000     1.000
C3H4B             2   252.000     4.760     0.000     0.000     1.000
C3H5A             2   252.000     4.760     0.000     0.000     1.000
C3H5S             2   252.000     4.760     0.000     0.000     1.000
C3H5T             2   252.000     4.760     0.000     0.000     1.000
C3H6              2   266.800     4.982     0.000     0.000     1.000
C3H7N             2   266.800     4.982     0.000     0.000     1.000
C3H7I             2   266.800     4.982     0.000     0.000     1.000
C3H8              2   266.800     4.982     0.000     0.000     1.000
C4H               1   357.000     5.180     0.000     0.000     1.000
C4H2              1   357.000     5.180     0.000     0.000     1.000
C4H3N             1   357.000     5.180     0.000     0.000     1.000
C4H3I             1   357.000     5.180     0.000     0.000     1.000
C4H4              1   357.000     5.180     0.000     0.000     1.000
C4H5S             2   357.000     5.180     0.000     0.000     1.000
C4H5T             2   357.000     5.180     0.000     0.000     1.000
C4H5I             2   330.000     5.280     0.000     0.000     1.000
C4H6S             2   330.000     5.280     0.000     0.000     1.000
C4H6T             2   330.000     5.280     0.000     0.000     1.000
C4H6B             2   330.000     5.280     0.000     0.000     1.000
C4H6O             2   374.400     5.494     0.000     0.000     1.000
C6H2              1   297.100     6.182     0.000     0.000     1.000
C8H2              1    50.000     6.000     0.000     0.000     1.000
C3H2O             2   209.000     4.100     0.000     0.000     1.000
CH3OH             2   481.800     3.626     0.000     0.000     1.000 ! SVE
C6H3              1   297.100     6.182     0.000     0.000     1.000
C6H4L             2   412.300     5.349     0.000     0.000     1.000 ! JAM
C6H5              2   412.300     5.349     0.000     0.000     1.000 ! JAM
C6H5O             2   412.300     5.349     0.000     0.000     1.000 ! JAM
C6H5OH            2   412.300     5.349     0.000     0.000     1.000 ! JAM
C5H6              1   391.410     5.209     0.000     0.000     1.000
C5H5              1   426.960     5.029     0.000     0.000     1.000
C5H5O             2   278.490     6.234     0.000     0.000     1.000
C5H4O             2   278.490     6.234     0.000     0.000     1.000
C5H4OH            2   278.490     6.234     0.000     0.000     1.000
C5H6L             1   391.410     5.209     0.000     0.000     1.000
C5H5L             1   426.960     5.029     0.000     0.000     1.000
C5H3L             1   426.960     5.029     0.000     0.000     1.000
C5H4L             1   426.960     5.029     0.000     0.000     1.000
C5H2              1   426.960     5.029     0.000     0.000     1.000
C6H4C             2   412.300     5.349     0.000     0.000     1.000 ! JAM
C6H6A             2   412.300     5.349     0.000     0.000     1.000 ! JAM
C6H6B             2   412.300     5.349     0.000     0.000     1.000 ! JAM
C6H6D             2   412.300     5.349     0.000     0.000     1.000 ! JAM
C6H5A             2   412.300     5.349     0.000     0.000     1.000 ! JAM
C6H5B             2   412.300     5.349     0.000     0.000     1.000 ! JAM
C6H7              2   412.300     5.349     0.000     0.000     1.000 ! JAM
C6H7L             2   412.300     5.349     0.000     0.000     1.000 ! JAM
C6H6S             2   412.300     5.349     0.000     0.000     1.000 ! JAM
C6H6F             2   412.300     5.349     0.000     0.000     1.000 ! JAM
```

```
!  Lindstedt and Skevis transport data.
!
C6H6M              2   412.300      5.349      0.000      0.000      1.000 ! JAM
C2O                1   150.000      2.500      0.000      0.000      2.000
C4H2O              2   374.400      5.494      0.000      0.000      1.000
```

O.4 Parameters Introduced in This Work.

Thermochemical parameters were needed for the flame code simulation of a rich benzene flame, and for net rate analyses when equilibrium constants were required. Also, the thermochemistry for C_6H_5, C_6H_5O and C_6H_5OH in the Sandia set were replaced with parameters from Burcat et al. (1985) for certain calculations, in a database referred to in this work as "modified Sandia thermochemistry." (Note that other heat of formation estimations were performed in this work, for various purposes other than those just described. Those calculations are recorded in Appendix M, where all of the thermochemical kinetics computations are described.)

O.4.1 Thermochemistry Parameters

1. *Parameters for flame code simulation with revised model.* KEY: "THERM" refers to parameters estimated by thermochemical kinetics, using the program THERM by Ritter et al. (1990); "TSANG" refers to Tsang (1986); "MOPAC" refers to an estimation by semi-emirical quantum mechanics, using the program by Stewart (1990).

```
C6H813 RAS12/14/94 THERMC   6H   8          G   300.000  5000.000 1396.000    01
 1.53625259E+01 2.08675112E-02-7.19203048E-06 1.12251633E-09-6.53733380E-14    2
 4.62118283E+03-6.26703913E+01-5.81337476E+00 7.22248431E-02-5.52161741E-05    3
 2.16975324E-08-3.46304555E-12 1.17578006E+04 5.03398935E+01                   4
C6H814 RAS12/14/94 THERMC   6H   8          G   300.000  5000.000 1394.000    01
 1.50866863E+01 2.11483961E-02-7.29888357E-06 1.14020521E-09-6.64432988E-14    2
 5.02632710E+03-6.19776093E+01-5.34206341E+00 6.96903834E-02-5.16349220E-05    3
 1.96729152E-08-3.05521699E-12 1.20241900E+04 4.74226109E+01                   4
C6H7   RAS01/19/95 TSANGC   6H   7    0    0G   300.000  2500.000 1000.000    01
 2.51495534E+00 4.32714617E-02-2.43043200E-05 6.66824985E-09-7.24113668E-13    2
 2.21043349E+04 8.73039795E+00-4.95929904E+00 6.11287329E-02-3.00150127E-05    3
-6.44910254E-09 7.71986166E-12 2.41440610E+04 4.76202502E+01                   4
C6H6OH     3/23/95 MOPACC   6H   7O   1    0G   300.000  5000.000 1400.000    1
 6.15925825E+00 4.18663376E-02-2.33225432E-05 6.37246733E-09-6.90755957E-13    2
 1.03419779E+03-7.21077924E+00-4.94895390E+00 7.56352277E-02-5.58570274E-05    3
 1.37758982E-08 1.77955931E-12 3.75787222E+03 4.89349949E+01                   4
```

2. *Other parameters for net rate analyses.* KEY: "RITTER90" refers to Ritter et al. (1990); "DAVICO95" refers to Burcat et al. (1985) thermochemistry but with ΔH_f^0(phenyl) from Davico et al. (1995); "YULIN" refers to Yu and Lin (1994), with the heat of formation (35.5

kcal/mol) calculated from a fit of the data with an RRKM calculation.

```
1-C4H3      5/19/95 THERMC   4H   3    0    0G   300.000  5000.000 1401.000     1
 1.08882913E+01 6.50355968E-03-2.16694795E-06 3.30972065E-10-1.89983375E-14    2
 5.95536284E+04-3.17037965E+01 6.89941647E-01 3.55996328E-02-3.43006650E-05    3
 1.64111389E-08-3.05900603E-12 6.25353925E+04 2.11435401E+01                   4
C6H5             DAVICO95C   6H   5    0    0G   300.000  2500.000 1000.000     1
 3.50879535E+00 3.48298254E-02-1.97252461E-05 5.45378513E-09-5.96252202E-13    2
 3.79263965E+04 3.95529312E+00-3.94856270E+00 5.42601903E-02-3.11063934E-05    3
-9.59225530E-10 5.22478085E-12 3.99013339E+04 4.24115182E+01                   4
C6H5(L)     5/ 9/95 THERMC   6H   5    0    0G   300.000  5000.000 1387.000     1
 1.64468639E+01 1.18841552E-02-4.18655991E-06 6.62936178E-10-3.89945068E-14    2
 6.34442025E+04-5.99575959E+01 1.02825316E+00 5.49828289E-02-5.24456488E-05    3
 2.57123032E-08-4.99962199E-12 6.82130798E+04 2.05465046E+01                   4
C5H4CH3          RITTER90C   7H   7    0    0G   300.000  2500.000 1000.000     1
 2.59436709E+00 4.27785291E-02-2.21900864E-05 5.54844418E-09-5.81887598E-13    2
 2.13423954E+04 1.05145396E+01-2.35803844E+00 5.53222792E-02-2.97720288E-05    3
 2.47879544E-09 2.47624729E-12 2.27060253E+04 3.62304487E+01                   4
C6H6O              THERMC   6H   6    0    1G   300.000  2500.000 1000.000     1
 5.86900676E+00 3.97206423E-02-2.26418935E-05 6.28969901E-09-6.89992066E-13    2
 2.74839697E+04-6.17719846E+00-5.43451842E+00 7.50387373E-02-5.91947994E-05    3
 1.79175892E-08 2.19777790E-13 3.02238228E+04 5.07597393E+01                   4
C6H5OO             YULINC   6H   5    0    2G   300.000  2500.000 1500.000     1
 1.81577904E+01 1.56948561E-02-5.44691513E-06 8.54249718E-10-4.99219126E-14
 9.26550172E+03-7.47248801E+01-4.49111204E+00 7.56652813E-02-6.70887553E-05
 2.98226442E-08-5.25122304E-12 1.63582080E+04 4.42982349E+01
```

3. *Parameters for "modified Sandia thermochemistry."* One change was made to the Burcat et al. values: the heat of formation of phenoxy radical was set to 9.3 kcal/mol. (See Chapter 7 for further information on this change.)

```
C6H5        3/24/95NASA85C   6H   5         G   300.000  5000.000 1000.000     1
 3.50879535E+00 3.48298254E-02-1.97252461E-05 5.45378513E-09-5.96252202E-13    2
 3.66055026E+04 3.95529312E+00-3.94856270E+00 5.42601903E-02-3.11063934E-05    3
-9.59225530E-10 5.22478085E-12 3.85804400E+04 4.24115182E+01                   4
C6H5O       3/24/95NASA85C   6H   5O   1    0G   300.000  5000.000 1000.000     1
 5.46396853E+00 3.64718323E-02-2.08036360E-05 5.78476879E-09-6.35266571E-13    2
 1.02112013E+03-5.47541329E+00-4.33407781E+00 6.61551088E-02-4.97266437E-05    3
 1.31146597E-08 1.07163299E-12 3.44467814E+03 4.41152985E+01                   4
C6H5OH      3/24/95NASA85C   6H   6O   1    0G   300.000  5000.000 1000.000     1
 6.92687855E+00 3.62810564E-02-2.00924422E-05 5.47100509E-09-5.91899353E-13    2
-1.57311164E+04-1.29922819E+01-4.96342676E+00 7.59185430E-02-6.65786995E-05    3
 2.64847633E-08-2.86718827E-12-1.29625171E+04 4.63129156E+01                   4
```

O.4.2 Transport Parameters

New transport data were only needed for testing the proposed model in the flame code simulation of a rich benzene flame. Three species were introduced, two isomers of cyclohexadiene and the adduct of the $OH+C_6H_6$ reaction. Transport parameters for the three new species were estimated from other molecules of their size and type.

C6H813	2	412.300	5.549	0.000	0.000	1.000 ! slightly larger than benzene
C6H814	2	412.300	5.549	0.000	0.000	1.000 ! slightly larger than benzene
C6H6OH	2	450.000	5.500	0.000	0.000	1.000 ! same as phenol

Appendix P. Analytical Testing Results for Purity of Benzene Feedstock.

The following information was taken from Herbert V. Schuster, Inc.'s Laboratory Report No. 20590A, dated 7/26/95. The laboratory is located at 5 Hayward St., Quincy, MA 02171-2493.

Sample Identification: Lab Sample Number: M6424, Benzene (Liquid), No Code. Sample received in a 2.5 mL graduated glass vial with a black opaque screw-on plastic cap.

Gas Chromatography Conditions:

Model:	Perkin Elmer Sigma 2000
Column:	5% Carbowax 20M, 60/80 Carbopack BAW Glass, ¼ inch x 8 feet
Column Temperature:	80°C
Injector/Detector Temperature:	130°C
Helium Flow Rate:	30 mL per minute
Hydrogen Flow Rate:	20 psi
Air Flow Rate:	12 psi

Results:

Cyclohexane:	5.8 ppm
Cyclohexene:	None Detected
Cyclohexadiene:	None Detected

Appendix Q. Isotopic Contribution Factors.

As mentioned in Chapter 3, when a peak being measured was one or two amu higher than another species having a significant signal, a correction for the isotopic contribution from the lighter species was required. For example, mass 80 required a correction for the signal of C_6H_5D and $^{13}CC_5H_6$, where D is deuterium (^2H). From the natural isotopic abundance table of CRC (1985):

P_C = probability of $^{12}C = 0.9890$

P_H = probability of $^1H = 0.99985$

P_O = probability of $^{16}O = 0.99762$

P_{O17} = probability of $^{17}O = 0.00038$

P_{O18} = probability of $^{18}O = 0.002$

Note that the probability of finding ^{13}C is $(1\text{-}P_C)$ and the probability of finding ^2H is $(1\text{-}P_H)$.

The probability that a species with x carbons and y hydrogens will have a molecular weight n = (12x+y) amu is

$$P_{n=12x+y} = P_C^x P_H^y. \tag{Q-1}$$

As this is the nominal molecular weight, $P_{n=12x+y}$ will be referred to simply as "P_n." Regarding the probability that a species would have a molecular weight of $n+1$, two terms are needed. The first term covers the contribution of a single ^{13}C with no other heavy isotopes, and the second accounts for one ^2H and no other heavy isotopes:

$$P_{n+1} = x \cdot \left[(1-P_C)P_C^{x-1}P_H^y\right] + y \cdot \left[P_C^x(1-P_H)P_H^{y-1}\right] \tag{Q-2}$$

The factor in front of each term in brackets accounts for the fact that one is not only interested in the probability that a *particular* carbon or hydrogen is heavy and the other atoms normal, but that *any* carbon or hydrogen is heavy and the other atoms normal. The formula for P_{n+2} is

$$P_{n+2} = \binom{x}{2}(1-P_C)^2P_C^{x-2}P_H^y + \binom{y}{2}P_C^x(1-P_H)^2P_H^{y-2} + xy(1-P_C)P_C^{2x-1}(1-P_H)P_H^{2y-1} \tag{Q-3}$$

where $\binom{i}{2} = \frac{i!}{(i-2)!2!} = \frac{i(i-1)}{2}$. The first term is for the case of two ^{13}C atoms, the middle term for two ^2H atoms, and the last for one ^{13}C and one ^2H.

The formulae for molecules containing *z* oxygen atoms are derived in a similar manner, but one also must account for second oxygen isomer, ^{18}O, when calculating P_{n+2}.

$$P_n = P_C^x P_H^y P_O^z \tag{Q-4}$$

$$P_{n+1} = x(1-P_C)P_C^{x-1}P_H^y P_O^z + yP_C^x(1-P_H)P_H^{y-1}P_O^z + zP_C^x P_H^y P_{O17} P_O^{z-1} \tag{Q-5}$$

$$\begin{aligned} P_{n+2} = \binom{x}{2}(1-P_C)^2 P_C^{x-2}P_H^y P_O^z + \binom{y}{2}P_C^x(1-P_H)^2 P_H^{y-2}P_O^z + \binom{z}{2}P_C^x P_H^y P_{O17}^2 P_O^{z-2} + zP_C^x P_H^y P_{O18} P_O^{z-1} \\ +xy(1-P_C)P_C^{2x-1}(1-P_H)P_H^{2y-1}P_O^{2z} + xz(1-P_C)P_C^{2x-1}P_H^{2y}P_{O17}P_O^{2z-1} \\ +yzP_C^{2x}(1-P_H)P_H^{2y-1}P_{O17}P_O^{2z-1} \end{aligned} \tag{Q-6}$$

In practical application of these factors, if the total signal of a species which nominally should weigh *n* amu is I_n, then the measured signal is $I_{meas} = I_n P_n$. Typically, one wishes to multiply the measured signal at peak *n* by a correction factor to get the contribution of the species to *n+1*. Since the contribution to *n+1* is $I_n P_{n+1}$, the correction factor is

$$f_{isotopic} = \frac{I_n P_{n+1}}{I_{meas}} = \frac{I_n P_{n+1}}{I_n P_n} = \frac{P_{n+1}}{P_n}. \tag{Q-7}$$

It would seem that one also needs to multiply the measured signal at *n* by $1/P_n$ to get the true amount of signal attributable to the species of that nominal molecular weight. In practice, however, this is not done:

1. In the case of major stable species, the signal ratio $\frac{I_n}{I_{Ar}}$ and the sensitivity $S_{n,Ar}$ both have the same ratio of correction factors, $\frac{P_{Ar}}{P_n}$. The factors cancel out, since the signal ratio is in the numerator and the sensitivity is in the denominator. The mass discrimination factor is the ratio of two signal ratios, each with the same correction factor, so no adjustment is needed for $\alpha_{n,Ar}$.

2. For species calibrated by the relative ionization cross-section method, the species and its reference are usually of similar molecular weights. Therefore the ratio of correction factors is generally close to unity. Even in the case of a large difference in molecular weights, the adjustment is not large compared to the overall factor of two error inherent in the calibration method. For example, if phenol were measured with respect to CO (which is not the case — C_6H_6 is the reference species), the ratio of correction factors would only be 1.06.

The isotopic contribution factors used in this work are listed in Tables Q.1 and Q.2.

Table Q.1 Isotopic contribution correction factors for species containing only hydrogen and/or carbon.

Species	n (MW)	P_n	P_{n+1}/P_n	P_{n+2}/P_n	Remainder
H	1	9.999E-01	1.500E-04	----------	1.100E-19
H_2	2	9.997E-01	3.001E-04	2.251E-08	2.600E-17
CH	13	9.889E-01	1.127E-02	1.650E-06	1.800E-08
CH_2	14	9.887E-01	1.142E-02	3.322E-06	3.800E-08
CH_3	15	9.886E-01	1.157E-02	5.016E-06	5.700E-08
CH_4	16	9.884E-01	1.172E-02	6.732E-06	7.800E-08
C_2H	25	9.780E-01	2.240E-02	1.270E-04	9.000E-08
C_2H_2	26	9.778E-01	2.255E-02	1.303E-04	1.800E-07
C_2H_3	27	9.777E-01	2.270E-02	1.336E-04	2.700E-07
C_2H_4	28	9.775E-01	2.285E-02	1.369E-04	3.700E-07
C_2H_5	29	9.774E-01	2.300E-02	1.402E-04	4.600E-07
C_2H_6	30	9.772E-01	2.315E-02	1.436E-04	5.600E-07
C_3H	37	9.672E-01	3.352E-02	3.760E-04	1.500E-06
C_3H_2	38	9.671E-01	3.367E-02	3.808E-04	1.800E-06
C_3H_3	39	9.669E-01	3.382E-02	3.857E-04	2.000E-06
C_3H_4	40	9.668E-01	3.397E-02	3.906E-04	2.200E-06
C_3H_5	41	9.666E-01	3.412E-02	3.955E-04	2.400E-06
C_3H_6	42	9.665E-01	3.427E-02	4.005E-04	2.600E-06
C_3H_7	43	9.664E-01	3.442E-02	4.055E-04	2.900E-06
C_3H_8	44	9.662E-01	3.457E-02	4.104E-04	3.100E-06
C_4H	49	9.566E-01	4.464E-02	7.486E-04	5.700E-06
C_4H_2	50	9.564E-01	4.479E-02	7.550E-04	6.100E-06
C_4H_3	51	9.563E-01	4.494E-02	7.615E-04	6.400E-06
C_4H_4	52	9.562E-01	4.509E-02	7.679E-04	6.800E-06
C_4H_5	53	9.560E-01	4.524E-02	7.744E-04	7.200E-06
C_4H_6	54	9.559E-01	4.539E-02	7.809E-04	7.600E-06
C_4H_7	55	9.557E-01	4.554E-02	7.874E-04	8.000E-06
C_4H_8	56	9.556E-01	4.569E-02	7.939E-04	8.400E-06
C_4H_9	57	9.554E-01	4.584E-02	8.004E-04	8.800E-06
C_4H_{10}	58	9.553E-01	4.599E-02	8.070E-04	9.200E-06
C_5H	61	9.461E-01	5.576E-02	1.245E-03	1.400E-05
C_5H_2	62	9.459E-01	5.591E-02	1.253E-03	1.400E-05
C_5H_3	63	9.458E-01	5.606E-02	1.261E-03	1.500E-05
C_5H_4	64	9.456E-01	5.621E-02	1.269E-03	1.600E-05
C_5H_5	65	9.455E-01	5.636E-02	1.277E-03	1.600E-05
C_5H_6	66	9.454E-01	5.651E-02	1.285E-03	1.700E-05
C_5H_7	67	9.452E-01	5.666E-02	1.293E-03	1.700E-05
C_5H_8	68	9.451E-01	5.681E-02	1.301E-03	1.800E-05
C_5H_9	69	9.449E-01	5.696E-02	1.309E-03	1.900E-05
C_5H_{10}	70	9.448E-01	5.711E-02	1.317E-03	1.900E-05
C_5H_{11}	71	9.446E-01	5.726E-02	1.325E-03	2.000E-05
C_5H_{12}	72	9.445E-01	5.741E-02	1.333E-03	2.100E-05
C_6H	73	9.357E-01	6.688E-02	1.865E-03	2.700E-05
C_6H_2	74	9.355E-01	6.703E-02	1.874E-03	2.800E-05
C_6H_3	75	9.354E-01	6.718E-02	1.884E-03	2.900E-05
C_6H_4	76	9.352E-01	6.733E-02	1.893E-03	2.900E-05
C_6H_5	77	9.351E-01	6.748E-02	1.903E-03	3.000E-05

Species	n (MW)	P_n	P_{n+1}/P_n	P_{n+2}/P_n	Remainder
C_6H_6	78	9.350E-01	6.763E-02	1.912E-03	3.100E-05
C_6H_7	79	9.348E-01	6.778E-02	1.922E-03	3.200E-05
C_6H_8	80	9.347E-01	6.793E-02	1.931E-03	3.300E-05
C_6H_9	81	9.345E-01	6.808E-02	1.941E-03	3.400E-05
C_6H_{10}	82	9.344E-01	6.823E-02	1.950E-03	3.500E-05
C_6H_{11}	83	9.343E-01	6.838E-02	1.960E-03	3.600E-05
C_6H_{12}	84	9.341E-01	6.853E-02	1.969E-03	3.700E-05
C_6H_{13}	85	9.340E-01	6.868E-02	1.979E-03	3.700E-05
C_6H_{14}	86	9.338E-01	6.883E-02	1.989E-03	3.800E-05
C_7H	85	9.254E-01	7.801E-02	2.609E-03	4.600E-05
C_7H_2	86	9.252E-01	7.816E-02	2.620E-03	4.700E-05
C_7H_3	87	9.251E-01	7.831E-02	2.630E-03	4.900E-05
C_7H_4	88	9.249E-01	7.846E-02	2.641E-03	5.000E-05
C_7H_5	89	9.248E-01	7.861E-02	2.652E-03	5.100E-05
C_7H_6	90	9.247E-01	7.876E-02	2.663E-03	5.200E-05
C_7H_7	91	9.245E-01	7.891E-02	2.674E-03	5.300E-05
C_7H_8	92	9.244E-01	7.906E-02	2.685E-03	5.500E-05
C_7H_9	93	9.243E-01	7.921E-02	2.696E-03	5.600E-05
C_7H_{10}	94	9.241E-01	7.936E-02	2.707E-03	5.700E-05
C_7H_{11}	95	9.240E-01	7.951E-02	2.718E-03	5.800E-05
C_7H_{12}	96	9.238E-01	7.966E-02	2.729E-03	5.900E-05
C_7H_{13}	97	9.237E-01	7.981E-02	2.740E-03	6.100E-05
C_7H_{14}	98	9.236E-01	7.996E-02	2.751E-03	6.200E-05
C_7H_{15}	99	9.234E-01	8.011E-02	2.762E-03	6.300E-05
C_7H_{16}	100	9.233E-01	8.026E-02	2.773E-03	6.400E-05

Table Q.2 Isotopic contribution correction factors for species containing oxygen.

Species	n (MW)	P_n	P_{n+1}/P_n	P_{n+2}/P_n	Remainder
O	16	9.976E-01	3.809E-04	2.005E-03	4.900E-17
OH	17	9.975E-01	5.309E-04	2.005E-03	3.000E-07
H_2O	18	9.973E-01	6.810E-04	2.005E-03	6.000E-07
O_2	32	9.953E-01	7.618E-04	4.010E-03	5.500E-06
HO_2	33	9.951E-01	9.118E-04	4.010E-03	6.100E-06
H_2O_2	34	9.950E-01	1.062E-03	4.010E-03	6.700E-06
CO	28	9.867E-01	1.150E-02	2.009E-03	2.200E-05
CHO	29	9.865E-01	1.165E-02	2.011E-03	2.200E-05
CH_2O	30	9.864E-01	1.180E-02	2.012E-03	2.300E-05
CH_3O	31	9.862E-01	1.195E-02	2.014E-03	2.300E-05
CH_4O	32	9.861E-01	1.210E-02	2.016E-03	2.300E-05
C_2HO	41	9.757E-01	2.278E-02	2.140E-03	4.400E-05
C_2H_2O	42	9.755E-01	2.293E-02	2.143E-03	4.500E-05
C_2H_3O	43	9.754E-01	2.308E-02	2.147E-03	4.500E-05
C_2H_4O	44	9.752E-01	2.323E-02	2.150E-03	4.600E-05
CO_2	44	9.843E-01	1.188E-02	4.018E-03	5.000E-05
C_3H_2O	54	9.648E-01	3.405E-02	2.398E-03	6.800E-05
C_3H_3O	55	9.646E-01	3.420E-02	2.403E-03	6.900E-05
C_4H_2O	66	9.542E-01	4.517E-02	2.776E-03	9.400E-05
C_4H_3O	67	9.540E-01	4.532E-02	2.783E-03	9.500E-05

Species	n (MW)	P_n	P_{n+1}/P_n	P_{n+2}/P_n	Remainder
C_4H_5O	69	9.537E-01	4.562E-02	2.796E-03	9.600E-05
C_4H_6O	70	9.536E-01	4.577E-02	2.802E-03	9.700E-05
C_5H_5O	81	9.432E-01	5.674E-02	3.302E-03	1.300E-04
C_5H_6O	82	9.431E-01	5.689E-02	3.310E-03	1.300E-04
C_6H_2O	90	9.333E-01	6.742E-02	3.903E-03	1.600E-04
C_6H_5O	93	9.329E-01	6.787E-02	3.931E-03	1.600E-04
C_6H_6O	94	9.327E-01	6.802E-02	3.941E-03	1.600E-04
C_6H_7O	95	9.326E-01	6.817E-02	3.950E-03	1.600E-04
C_7H_8O	108	9.222E-01	7.944E-02	4.717E-03	2.100E-04
$C_6H_5O_2$	109	9.306E-01	6.825E-02	5.960E-03	3.000E-04
$C_6H_6O_2$	110	9.305E-01	6.840E-02	5.970E-03	3.000E-04
$C_4H_4O_4$	116	9.471E-01	4.661E-02	8.853E-03	3.900E-04
$C_6H_5O_3$	125	9.284E-01	6.863E-02	7.989E-03	4.400E-04
$C_6H_6O_4$	142	9.261E-01	6.916E-02	1.003E-02	5.900E-04

References

Ackermann, L., Hippler, H., Pagsberg, P., Reihs, C. and Troe, J., *J. Phys. Chem.*, **94**, 5427 (1990).

Alfassi, Z.B., Benson, S.W., and Golden, D.M., *J. Am. Chem. Soc.*, **95**, 4784 (1973).

Amano, A., Horie, O. and Hanh, N.H., *Int. J. Chem. Kinet.*, **8**, 321 (1976).

Anderson, R.L., *Temperature: Its Measurement and Control in Science and Industry*, **4**, 927 (1972).

Asaba, T. and Fujii, N., *13th Symposium (Int.) on Combustion*, The Combustion Institute (1971), p. 155.

Astholtz, D.C., Troe, J. and Wieters, W., *J. Phys. Chem.*, **70**, 5107 (1979).

Avramenko, L.I., Kolesnikova, R.V. and Savinova, G.I., *Izv. Akad. Nauk SSSR, Ser. Khim.*, **1**, 24 (1965).

Back, M.H., *J. Phys. Chem.*, **93**, 6880 (1989).

Bajaj, P.N., Rensselaer Polytechnic Institute, personal communication from Fontijn, A. to Howard, J.B. (1994).

Baldwin, R.R. and Mayor, L., *Trans. Farad. Soc.*, **56**, 93 (1960).

Baldwin, R.R., Fuller, M.E., Hillman, J.S., Jackson, D. and Walker, R.W., *J. Chem. Soc. Farad. Trans. I*, **70**, 635 (1974).

Baldwin, R.R., Scott, M. and Walker, R.W., *21st Symposium (Int.) on Combustion*, The Combustion Institute (1986), p. 991.

Bargmann, R.E., "Matrices and Determinants," in CRC Standard Mathematical Tables, 21st Edition, CRC Press: Boca Raton (1973), pp. 117-139.

Bauer, S.H. and Aten, C.F., *J. Chem. Phys.*, **39**, 1253 (1963).

Baulch, D.L., Drysdale, D.D., Horne, D.G. and Lloyd, A.C., Evaluated Kinetic Data for High Temperature Reactions, Vol. 1: Homogeneous Gas Phase Reactions of the H_2-O_2 System, Butterworths: London (1972).

Baulch, D.L., Cobos, C.J., Cox, R.A., Esser, C., Frank, P., Just, Th., Kerr, J.A., Pilling, M.J., Troe, J., Walker, R.W. and Warnatz, J., *J. Phys. Chem. Ref. Data*, **21**, 411 (1992).

Bedford, R.E., *High Temperatures - High Pressures*, **4**, 241 (1972).

Benson, S. W., Thermochemical Kinetics, John Wiley & Sons: New York (1976).

Benson, S.W. and Shaw, R., *Tran. Faraday Soc.*, **63**, 985 (1967a).

Benson, S.W. and Shaw, R., *J. Am. Chem. Soc.*, **89**, 5351 (1967b).

Beran, J.A. and Kevan, L., *J. Phys. Chem.*, **73**, 3866 (1969).

Berry, R.J., *Temperature: Its Measurement and Control in Science and Industry*, **4**, 937 (1972).

Bettens, B. and Cyprès, R., Proceedings of the Round Table Conference, Heerlen, Feb. 18, 1971.

Beyer, T. and Swinehardt, D.F., *Comm. ACM*, **16**, 379 (1973).

Biordi, J.C., Lazzara, C.P., and Papp, J.F., *Combust. Flame*, **21**, 371 (1974).

Bittker, D.A., Detailed Mechanism of Benzene Oxidation, *NASA Tech. Memo. 100202*, (1987).

Bittker, D.A., *Combust. Sci. Tech.*, **79**, 49 (1991).

Bittner, J.B., A Molecular Beam Mass Spectrometric Study of Fuel-Rich and Sooting Benzene-Oxygen Flames, Sc.D. Thesis, Department of Chemical Engineering, Massachussetts Institute of Technology (1981).

Bittner, J.D. and Howard, J.B., *18th Symposium (Int.) on Combustion*, The Combustion Institute (1981), p. 1105.

Bley, U., Dransfeld, P., Himme, B., Koch, M., Temps, F., and Wagner, H.Gg., *22nd Symposium (Int.) on Combustion*, The Combustion Institute (1989), p. 997.

Bonanno, R.A., Kim, P., Lee, J.-H. and Timmons, R.B., *J. Chem. Phys.*, **57**, 1377 (1972).

Bonhoeffer, K.F. and Harteck, P., *Z. physik. Chem. A*, **139**, 64 (1928).

Boocock, G. and Cvetanović, R.J., *Can. J. Chem.*, **39**, 2436 (1961).

Braun-Unkhoff, M., Frank, P. and Just, Th., *22nd Symp. (Int.) Combust.*, The Combustion Institute (1989), p. 1053.

Brezinsky, K., *Prog. Energy Combust. Sci.*, **12**, 1 (1986).

Brezinsky, K., Princeton University, personal communication (1994).

Brooks, C.T., Peacock, S.J. and Reuben, B.G., *J. Chem. Soc. Faraday Trans. 1*, **75**, 652 (1979).

References

Bruinsma, O.S.L., Geertsma, R.S., Bank, P. and Moulijn, J.A., *Fuel*, **67**, 327 (1988)

Burcat, A., Zeleznik, F.J., and McBride, B.J., Ideal Gas Thermodynamic Properties for the Phenyl, Phenoxy and o-Biphenyl Radicals, *NASA Technical Memorandum 83800* (1985).

Caddell, J. P., Temperature Measurements in Low-Pressure Stoichiometric and Fuel-Rich Flames of Toluene and Butadiene, B.S. Thesis, Department of Chemical Engineering, Massachussetts Institute of Technology (1984).

Cherian, M.A., Rhodes, P., Simpson, R.J. and Dixon-Lewis, G., *18th Symp. (Int.) Combust.*, The Combustion Institute (1981), p. 385.

Chevalier, C. and Warnatz, J., *Am. Chem. Soc., Div. Fuel Chem. Preprints,* **36**, 1486 (1991).

Colket, III, M.B., *Am. Chem. Soc., Div. Fuel Chem. Preprints,* **31**, 98 (1986a).

Colket, III, M.B., *21st Symp. (Int.) Combust.*, The Combustion Institute (1986b), p. 851.

Cole, J.A., A Molecular-Beam Mass-Spectrometric Study of Stoichiometric and Fuel-Rich 1,3-Butadiene Flames, M.S. Thesis, Department of Chemical Engineering, Massachusetts Institute of Technology (1982).

Cole, J.A., Bittner, J.D., Longwell, J.P. and Howard, J.B., The Chemistry of Combustion Processes, *ACS Symposium Series, No. 249*, Sloane, T.M., ed. (1984a).

Cole, J.A., Bittner, J.D., Longwell, J.P. and Howard, J.B., *Combustion and Flame*, **56**, 51 (1984b).

Collins, J.H., Winters, R.E. and Engerholm, G.G., *J. Chem. Phys.*, **49**, 2469 (1968).

Colussi, A.J., Singleton, D.L., Irwin, R.S., and Cvetanović, R.J., *J. Phys. Chem.*, **79**, 1900 (1975).

Colussi, A.J., Zabel, F. and Benson, S.W., *Int. J. Chem. Kinet.*, **9**, 161 (1977).

CRC, Handbook of Chemistry and Physics, 66th Edition, Weast, R.C., ed., CRC Press: Boca Raton (1985).

Cvetanović, R.J. and Singleton, D.L., *Rev. Chem. Intermed.*, **5**, 183 (1984).

Cyprès, R. and Bettens, B., *Tetrahedron*, **30**, 1253 (1974).

Davico, G.E., Bierbaum, V.M., DePuy, C.H., Ellison, G.B. and Squires, R.R., *J. Am. Chem. Soc.*, **117**, 2590 (1995).

Davis, D.D., Bollinger, W. and Fischer, S., *J. Phys. Chem.*, **79**, 293 (1975).

Day, M.J., Dixon-Lewis, G. and Thompson, K., *Proc. Roy. Soc. Lond. A*, **330**, 199 (1972).

Dayton, D.C., Faust, C.M., Anderson, W.R., and Sausa, R.C., *Combust. Flame*, **99**, 323 (1994).

Dean, A.M., *J. Phys. Chem.*, **89**, 4600 (1985).

Dean, A.M., *J. Phys. Chem.*, **94**, 1432 (1990).

Dean, A.M., Bozzelli, J.W. and Ritter, E.R., *Comb. Sci. Tech.*, **80**, 63 (1991).

Deutsch, H. and Schmidt, M., *Contrib. Plasma Phys.*, **25**, 475 (1985).

Deutsch, H., Margreiter, D. and Mark, T.D., *Int. J. Mass Spectrom. Ion Proc.*, **93**, 259 (1989).

Dewar, M.J.S., Gardiner, Jr., W.C., Frenklach, M. and Oref, I., *J. Am. Chem. Soc.*, **109**, 4456 (1987).

Dibeler, V.H., Reese, R.M. and Mohler, F.L., *J. Chem. Phys.*, **26**, 304 (1957).

Di Lauro, C., Neto, N., and Califano, S., *J. Molec. Struct.*, **3**, 219 (1969).

Dixon-Lewis, G., *Proc. Roy. Soc. Lond. A*, **298**, 495 (1967).

Dixon-Lewis, G., *Proc. Roy. Soc. A*, **307**, 111 (1968).

Dixon-Lewis, G., *Phil. Trans. R. Soc. London*, **292**, 45 (1979).

Dixon-Lewis, G., *Archivum Combustionis*, **4**, 279 (1984).

Djuric, N.Lj., Cadez, I.M. and Kurepa, M.V., *Int. J. Mass Spectrom. Ion Proc.*, **83**, R7 (1988).

Dougherty, E.P., Hwang, J.T. and Rabitz, H., *J. Chem. Phys.*, **71**, 1794 (1979).

Dougherty, E.P. and Rabitz, H., *J. Chem. Phys.*, **72**, 6571 (1980).

Doyle, G.J., Lloyd, A.C., Darnall, K.R., Winer, A.M. and Pitts, Jr., A.M., *Envir. Sci. Tech*, **9**, 237 (1975).

Duncan, F.J. and Trotman-Dickenson, A.F., *J. Chem. Soc.*, 4672 (1962)

Ellis, R.J. and Frey, H.M., *J. Chem. Soc. A [Inorg. Phys. Theor.]*, 553 (1966).

Emanuel, G., *Int. J. Chem. Kinet.*, **4**, 591 (1972).

References

Emdee, J.L., Brezinsky, K. and Glassman, I., *J. Phys. Chem.*, **96**, 2151 (1992).

Fahr, A. and Stein, S.E., *22nd Symp. (Int.) Combust.*, The Combustion Institute (1989), p. 1023.

Fairbanks, D. and Wilke, C.R., *Ind. and Eng. Chem.*, **42**, 471 (1950).

Faist, S.M., Analysis of Stable Species in a Benzene-Oxygen-Argon Laminar Premixed Flame by Chemical and Spectroscopic Techniques: Applications to Soot Formation and Combustion Chamber Deposits, M.S. Thesis, Department of Chemical Engineering, Massachussetts Institute of Technology (1979).

Fenimore, C.P. and Jones, G.W., *10th Symp. (Int.) Combust.*, The Combustion Institute (1965), p. 489.

Fenimore, C.P. and Jones, G.W., *J. Phys. Chem.*, **71**, 593 (1967).

Field, F.H. and Franklin, J.L., Electron Impact Phenomena, Academic Press: New York (1970).

Fitch, W.L. and Sauter, A.D., *Anal. Chem.*, **55**, 832 (1983).

Fite, W.L. and Brackmann, R.T., *Phys. Rev.*, **113**, 815 (1959).

Fite, W.L., Expansion of Gases From Molecular Beam Sources, Research Note #1, Extranuclear Laboratories, Inc.: Pittsburgh (1971).

Fite, W.L., Siegel, M.W., Brackmann, R.T., McKeown, M., Kurzweg, L., Waruszewski, W., Schaeffer, R.A., and Corridon, J., manual from The Seventh Annual Fall School in Practical Quadrupole Mass Spectrometry, Extranuclear Laboratories, Inc., Pittsburgh, PA (1980).

Fontijn, A. and Mahmud, K., Abstracts for the Combustion Research Contractors Meeting, Sandia National Laboratories Combustion Research Facility and U.S. Department of Energy Office of Basic Energy Sciences, (1989), p. 93.

Forst, W., Theory of Unimolecular Reactions, Academic Press: New York (1973), p. 184.

Fox, R.E. and Hickam, W.M., *J. Chem. Phys.*, **22**, 2059 (1954).

Fox, R.E., Hickam, W.M., Grove, D.J. and Kjeldaas, Jr., T., *Rev. Sci. Instrum.*, **26**, 1101 (1955).

Frank, P., Herzler, J., Just, Th. and Wahl, C., *25th Symp. (Int.) Combust.*, The Combustion Institute, in press.

Frenklach, M., Clary, D.W., Gardiner, Jr., W.C., and Stein, S.E., *20th Symp. (Int.) Combust.*, The Combustion Institute (1985), p. 887.

Frenklach, M. and Wang, H., *23rd Symp. (Int.) Combust.*, The Combustion Institute (1990), p. 1559.

Frenklach, M. and Wang, H., *Phys. Rev. B*, **43**, 1520 (1991).

Fristrom, R.M. and Westenberg, A.A., Flame Structure, McGraw-Hill: New York (1965), p. 250.

Fritz, B., Handwerk, V., Preidel, M. and Zellner, R., *Ber. Bunsenges. Phys. Chem.*, **89**, 343 (1985).

Frost, D.C. and McDowell, C.A., *Proc. Roy. Soc. London A*, **241**, 194 (1957).

Fujii, N. and Asaba, T., *14th Symp. (Int.) Combust.*, The Combustion Institute (1973), p. 433.

Furukawa, K., James, D.G.L. and Papic, M.M., *Int. J. Chem. Kinet.*, **6**, 337 (1974).

Gardiner, Jr., W.C. and Troe, J., "Rate Coefficients of Thermal Dissociation, Isomerization, and Recombination Reactions," Chapter 4 of Combustion Chemistry, ed. by Gardiner, Jr., W.C., Springer-Verlag: New York (1984), p. 173.

Gaynor, B.J., Gilbert, R.G., King, K.D. and Harman P.J., *Aust. J. Chem.*, **34**, 449 (1981).

Giddings, J.C. and Hirschfelder, J.O., *6th Symp. (Int.) on Combustion*, The Combustion Institute (1957), p. 199.

Gilbert, R.G., *QCPE*, **3**, 64 (1983).

Gilbert, R.G., Luther, K.,and Troe, J., *Ber. Bunsenges. Phys. Chem.*, **87**, 169 (1983).

Gonzalez Ureña, A., Hoffman, S.M.A., Smith, D.J. and Grice, R., *J. Chem. Soc., Farad. Trans. 2*, **82**, 1537 (1986).

Grovenstein, E. and Mosher, A.J., *J. Amer. Chem. Soc.*, **92**, 3810 (1970).

Halstead, C.J. and Jenkins, D.R., *Trans. Farad. Soc.*, **65**, 3013 (1969).

Harrison, A.G., Jones, E.G., Gupta, S.K. and Nagy, G.P., *Can. J. Chem.*, **44**, 1967 (1966).

Hausmann, M., Hebgen, P. and Homann, K.-H., *24th Symp. (Int.) Combust.*, The Combustion Institute (1992), 793.

He, Y.Z., Mallard, W.G. and Tsang, W., *J. Phys. Chem.*, **92**, 2196 (1988).

Herron, J.T. and Schiff, H.I., *Can. J. Chem.*, **36**, 1159 (1958).

Hoyermann, K., Preuss, A.W. and Wagner H.Gg., *Ber. Bunsenges. Phys. Chem.*, **79**, 156 (1975).

References

Hsu, D.S.Y., Lin, C.Y. and Lin, M.C., *20th Symp. (Int.) Combust.*, The Combustion Institute (1984), p. 623.

Hsu, W.L., *J. Appl. Phys.*, **72**, 3102 (1992).

Jackson, M.G. and Laurendeau, N.M., *Energy & Fuels*, **1**, 405 (1987).

James, D.G.L. and Suart, R.D., *Trans. Faraday Soc.*, **64**, 2752 (1968).

Jones, R.H., Olander, D.R., Siekhaus, W.J. and Schwarz, J.A., *J. Vac. Sci. Technol.*, **9**, 1429 (1972).

Kaskan, W.E., *Combust. Flame*, **2**, 286, (1958).

Kazakov, A., Wang, H. and Frenklach, M., *Combust. Flame*, **100**, 111 (1995).

Kee, R.J., Dixon-Lewis, G., Warnatz, J., Coltrin, M.E. and Miller, J.A., A FORTRAN Computer Code Package for the Evaluation of Gas-Phase Multicomponent Transport Properties, *Sandia Report SAND86-8246* (1986).

Kee, R.J., Grcar, J.F., Smooke, M.D. and Miller, J.A., A FORTRAN Program for Modeling Steady Laminar One-Dimensional Premixed Flames, *Sandia Report SAND85-8240* (1985).

Kee, R.J., Rupley, R.J, and Miller, J.A. , CHEMKIN II: A FORTRAN Chemical Kinetics Package for the Analysis of Gas-Phase Chemical Kinetics, *Sandia Report SAND89-8009* (1991).

Kee, R.J., Rupley, F.M. and Miller, J.A., The Chemkin Thermodynamic Data Base, *Sandia Report SAND87-8215B* (1994).

Kent, J. H., *Combust. Flame*, **14**, 279 (1970).

Kern, R.D., Wu, C.H., Skinner, G.B., Rao, V.S., Kiefer, J.H., Towers, J.A. and Mizerka, L.J., *20th Symp. (Int.) Combust.*, The Combustion Institute (1985), p. 789.

Keselica, D. S., Yttria and Yttria-Beryllia Coatings for Ultra-fine Butt-welded Thermocouple Wires, Final UROP Project Report, Department of Chemical Engineering, Massachusetts Institute of Technology (1982).

Kiefer, J.H., Mizerka, L.J., Patel, M.R., and Wei, H.-C., *J. Phys. Chem.*, **89**, 2013 (1985).

Kieffer, L.J. and Dunn, G.H., *Rev. Mod. Phys.* **38**, 1 (1966).

Kim, P., Lee, J.H., Bonanno, R.J. and Timmons, R.B., *J. Phys. Chem.*, **59**, 4593 (1973).

Kingery, W. D., Introduction to Ceramics, Wiley, New York (1960), p. 393.

References

Knispel, R., Koch, R., Siese, M. and Zetzsch, C., *Ber. Bunsenges. Phys. Chem.*, **94**, 1375 (1990).

Ko, T., Adusei, G.Y. and Fontijn, A., *J. Phys. Chem.*, **95**, 8745 (1991).

Koda, S., Endo, Y., Tsuchiya, S., and Hirota, E., *J. Phys. Chem.*, **95**, 1241 (1991).

Kramers, H., *Physics*, **12**, 61 (1946).

Lam, F.W., Longwell, J.P. and Howard, J.B., *23rd Symp. (Int.) Combust.*, The Combustion Institute (1990), 1477.

Lampe, F.W., Franklin, J.L. and Field, F.H., *J. Am. Chem. Soc.*, **79**, 6129 (1957).

Larson, C.W. and Rabinovitch, B.S., *J. Chem. Phys.*, **51**, 2293 (1969).

Laurendeau, N.M. and Goldsmith, J.E.M., *Combust. Sci. and Tech.*, **63**, 139 (1989).

Lazzara, C.P., Biordi, J.C. and Papp, J.F., *Combust. Flame*, **21**, 371 (1973).

Lebiedzik, J., Advanced Research Instruments Corporation, personal communication (1992).

Leidreiter, H.I. and Wagner, H.Gg., *Z. Phys. Chem. Neue Folge*, **165**, 1 (1989).

Levin, R.D. and Lias, S.G., Ionization Potential and Appearance Potential Measurements, 1971-1981, *NSRDS-NBS 71*, U.S. Govt. Printing Office: Washington, D.C. (1982).

Levin, E. M., Robbins, C. R., and McMurdie, H. F., in Phase Diagrams for Ceramists, ed. by M. K. Reser, The American Ceramic Society, Westville (1964), vol. I, p. 100.

Levine, R.D. and Bernstein, R.B., Molecular Reaction Dynamics, Oxford University Press: New York (1974), Section 4.4.

Lias, S.G., Bartmess, J.E., Liebman, J.F., Holmes, J.L., Levin, R.D. and Mallard, W.G., *J. Phys. Chem. Ref. Data*, **17**, Suppl. 1 (1988).

Lin, C.-Y. and Lin M.C., *Fall Techical Meeting, Eastern States: The Combustion Institute*, Clearwater, FL, December 3-5, 1984, 86-1.

Lin, C.-Y. and Lin M.C., *Fall Techical Meeting, Eastern States: The Combustion Institute*, Gaithersburg, MD, November 2-5, 1987, 7-1.

Lindemann, F.A., *Trans. Faraday Soc.*, **17**, 598 (1922).

Lindstedt, R.P., Imperial College, personal communications (1994).

Lindstedt, R.P., Imperial College, personal communications (1995).

Lindstedt, R.P. and Skevis, G., *Combustion and Flame*, **99**, 551 (1994); *Am. Chem. Soc., Div. Fuel Chem. Preprints,* **39**, 147 (1994).

Lorenz, K. and Zellner, R., *Ber. Bunsenges. Phys. Chem.*, **87**, 629 (1983).

Louw, R., Dijks, J.H.M., and Mulder, P., *Recl. Trav. Chim. Pays-Bas*, **103**, 271 (1984).

Louw, R. and Lucas, H.J., *Recueil*, **92**, 55 (1973).

Lovell, A.B., Brezinsky, K. and Glassman, I., *Int. J. Chem. Kinet.*, **21**, 547 (1989).

Lovell, A.B., Brezinsky, K. and Glassman, I., *22nd Symposium (Int.) on Combustion*, The Combustion Institute (1989), p. 1063.

Madronich, S. and Felder, W., *J. Phys. Chem.*, **89**, 3556 (1985).

Majer, J.R. and Patrick, C.R., *Trans. Farad. Soc.*, **58**, 17 (1962).

Mallard, W.G., Westley, F., Herron, J.T., Hampson, R.F., and Frizzell, D.H., NIST Chemical Kinetics Database - Ver. 5.0, (1993).

Mani, I. and Sauer, Jr., M.C., *Adv. Chem. Ser.*, **82**, 142 (1968).

Manion, J.A. and Louw, R., *J. Phys. Chem.*, **93**, 3563 (1989).

Marcoux, P.J. and Setser, D.W., *J. Phys. Chem.*, **82**, 97 (1978).

Marcus, R.A., *J. Chem. Phys.*, **20**, 359 (1952).

Marcus, R.A., *J. Chem. Phys.*, **43**, 2658 (1965).

Marcus, R.A., *J. Chem. Phys.*, **52**, 1018 (1970).

Margreiter, D., Deutsch, H., Schmidt, M. and Mark, T.D., *Int. J. Mass Spectrom. Ion Proc.*, **100**, 157 (1990).

Mark, T.D. and Egger, F., *Int. J. Mass Spectrom. Ion Proc.*, **20**, 89 (1976).

McKinnon, J.T., Chemical and Physical Mechanisms of Soot Formation, Ph.D. Thesis, Department of Chemical Engineering, Massachussetts Institute of Technology (1989).

McLain, A.G., Jachimowski, C.J. and Wilson, C.H., Chemical Kinetic Modeling of Benzene and Toluene Oxidation Behind Shock Waves, *NASA Technical Papter 1472*, (1979).

Melton, C.E. and Hamill, W.H., *J. Chem. Phys.*, **41**, 3464 (1964).

Metal and Ceramics Information Center, Battelle, Engineering Property Data on Selected Ceramics. Volume III, Single Oxides, Battelle Columbus Laboratories, Columbus (1981), p. 5.4.2-20.

Miller, J.A., Mitchell, R.E., Smooke, M.D. and Kee, R.J., *19th Symp. (Int.) Combust.*, The Combustion Institute (1982), p. 181.

Miller, J.A., Smooke, M.D., Green, R.M. and Kee, R.J., *Combust. Sci. Tech.*, **34**, 149 (1983).

Morrison, R.T. and Boyd, R.N., Organic Chemistry, Allyn and Bacon: Boston (1973), p. 596.

Mulder, P., Gas Phase Thermal Oxidation of Benzene Derivatives, Ph.D thesis, Center for Chemistry and the Environment, Gorlaeus Laboratory, University of Leiden, Netherlands (1987).

Neoh, K.G., Soot Burnout in Flames, Sc.D. Thesis, Department of Chemical Engineering, Massachussetts Institute of Technology (1980).

Nicovich, J.M., Gump, C.A. and Ravishankara, A.R., *J. Phys. Chem.*, **86**, 1684 (1982).

Nicovich, J.M. and Ravishankara, A.R., *J. Phys. Chem.*, **88**, 2534 (1984).

Norrish, R.G.W. and Taylor, G.W., *Proc. Roy. Soc. Lond. A*, **234**, 160 (1956).

Oikawa, S., Tsuda, M., Okamura, Y. and Urabe, T., *J. Am. Chem. Soc.*, **106**, 6751 (1984).

Olson, D.B. and Calcote, H.F., *18th Symp. (Int.) Combust.*, The Combustion Institute (1981), p. 453.

Orchard, S.W. and Thrush, B.A., *Proc. R. Soc. London A*, **337**, 257 (1974).

Oref, I. and Tardy, D.C., *Chem. Rev.*, **90** 1407 (1990).

Padly, P.J. and Sugden, T.M., *7th Symp. (Int.) on Combustion*, The Combustion Institute (1958), p. 235.

Peeters, J., Lambert, J.F., Hertoghe, P. and Van Tiggelen, A., *13th Symp. (Int.) Combust.*, The Combustion Institute (1971), p. 321.

Peeters, J. and Vinckier, C., *15th Symp. (Int.) Combust.*, The Combustion Institute (1975), p. 969.

Perry, R.A., Atkinson, R. and Pitts, J.N., *J. Phys. Chem.*, **81**, 296 (1977).

Preidel, M. and Zellner, R., *Ber. Bunsenges. Phys. Chem.*, **93**, 1417 (1989).

Pryor, W.A., Lin, T.H., Stanley, J.P. and Henderson, R.W., *J. Am. Chem. Soc.*, **95**, 6993 (1973).

Puri, R., Santoro, R.J. and Smyth, K.C., *Combust. Flame*, **97**, 125 (1994).

Quack, M. and Troe, J., "Unimolecular Reactions and Energy Transfer of Highly Excited Molecules," Chapter 5 of Gas Kinetics and Energy Transfer, Volume 2, The Chemical Society, Burlington House: London (1977), p. 175.

Rao, V.S. and Skinner, G.B., *J. Phys. Chem.*, **92**, 2442 (1988).

Rapp, D. and Englander-Golden, P., *J. Chem. Phys.*, **43**, 1471 (1965).

Ritter, E.R. and Bozzelli, J.W., THERM: Thermodynamic Property Estimation of Gas Phase Radicals and Molecules, *12th Int. CODATA Conf.*, July 15-19, 1990.

Ritter, E.R., Bozzelli, J.W. and Dean, A.M., *J. Phys. Chem.*, **94**, 2493 (1990).

Robaugh, D. and Tsang, W., *J. Phys. Chem.*, **90**, 4159 (1986).

Robinson, P.J. and Holbrook, K.A., Unimolecular Reactions, John Wiley & Sons: London (1972).

Rosenstock, H.M., Draxl, K., Steiner, B.W. and Herron, J.T., *J. Phys. Chem. Ref. Data*, **6**, Suppl. 1, (1977).

Rotzoll, G., *Int. J. Chem. Kinet.*, **17**, 637 (1985).

Rupley, R.J., Sandia National Laboratories, personal communications (1994).

Russell, G.A. and Bridger, R.F., *J. Amer. Chem. Soc.*, **85**, 3765 (1963).

Santoro, R.J. and Glassman, I., *Combust. Sci. Tech.*, **19**, 161 (1979).

Sauer, Jr., M.C. and Ward, B., *J. Phys. Chem.*, **71**, 3971 (1967).

Sauer, Jr., M.C. and Mani, I., *J. Phys. Chem.*, **74**, 59 (1970).

Savitsky, A. and Golay, M.J.E., *Anal. Chem.*, **36**, 1627 (1964).

Schiff, H.I. and Steacie, E.W.R., *Can. J. Chem.*, **29**, 1 (1951).

Schmidt, H., *Annal. Phys.*, **29**, 971 (1909).

Seery, D.J. and Zabielski, M.F., *18th Symp. (Int.) Combust.*, The Combustion Institute (1981), p. 397.

Seery, D.J., United Technologies Research Center, personal communication (1994).

Shandross, R.A. and Howard, J.B., *QCPE Bulletin*, **7**, 73 (1987).

Shandross, R.A. and Howard, J.B., unpublished revisions to RRKM program, (1988-1995).

Shandross, R.A., Longwell, J.P. and Howard, J.B., *Combust. Flame*, **85**, 282 (1991).

Shimanouchi, *Natl. Stand. Ref. Data Ser., Natl. Bur. Stand.*, **39** (1972).

Sibener, S.J., Buss, R.J., Casavecchia, P., Hirooka, T. and Lee, Y.T., *J. Phys. Chem.*, **72**, 4341 (1980).

Singh, H.J. and Kern, R.D., *Combust. Flame*, **54**, 49 (1983).

Sloane, T.M., *J. Chem. Phys.*, **67**, 2267 (1977).

Sloane, T.M., *Chem. Phys. Letters*, **54**, 269 (1978).

Smith, O.I., Wang, S.N., Tseregounis, S. and Westbrook, C.K., *Combust. Sci. Technol.*, **30**, 241 (1983).

Smith, R.D. and Johnson, A.L., *Combust. Flame*, **51**, 1 (1983).

Sol, V.M., Louw, R. and Mulder, P., Organic Free Radicals, ed. by Fischer, H. and Heimgartner, H., Springer-Verlag: Berlin (1988), p. 135.

Spielmann, R. and Cramers, C.A., *Chromatographia*, **5**, 295 (1972).

Steinier, J., Termonia, Y. and Deltour, J., *Anal. Chem.*, **44**, 1906 (1972).

Stewart, J.J.P., MOPAC, version 6.0, distributed by Quantum Chemistry Program Exchange, Indiana University Chemistry Department (1990).

Stidham, H.D., *Spectrochim. Acta*, **21**, 23 (1965).

Tabares, F.L. and Gonzalez Ureña, A., *J. Phys. Chem.*, **87**, 4933 (1983).

Tardy, D.C. and Malins, R.J., *J. Phys. Chem.*, **83**, 93 (1979).

Tardy, D.C. and Rabinovitch, B.S., *Chem. Rev.*, **77**, 369 (1977).

Tatang, M.A., Direct Incorporation of Uncertainty in Chemical and Environmental Engineering Systems, Ph.D. Thesis, Department of Chemical Engineering, Massachussetts Institute of Technology (1995).

Troe, J., *J. Chem. Phys.*, **11**, 4745 (1977a).

Troe, J., *J. Chem. Phys.*, **11**, 4758 (1977b).

Troe, J., *J. Phys. Chem.*, **83**, 114 (1979).

Troe, J., *Ber. Bunsenges. Phys. Chem.*, **87**, 161 (1983).

Tsang, W., *J. Phys. Chem.*, **90**, 1152 (1986).

Tsang, W., personal communication (1995).

Tsang, W. and Hampson, R.F, *J. Phys. Chem. Ref. Data*, **15**, 1087 (1986).

Tully, F.P., Ravishankara, A.R., Thompson, R.L., Nicovich, J.M., Shah, R.C., Kreutter, N.M. and Wine, P.H., *J. Phys. Chem.*, **85**, 2262 (1981).

Turecek, F., Brabec, L., Hanus, V., Zima, V. and Pytela, O., *Int. J. Mass Spectrom. Ion Proc.*, **97**, 117 (1990).

Vandooren, J. and Bian, J., *23rd Symp. (Int.) Combust.*, The Combustion Institute (1990), p. 341.

Vandooren, J. and Peeters, J., and Van Tiggelen, P.J., *15th Symp. (Int.) Combust.*, The Combustion Institute (1975), p. 745.

Vaughn, C.B., Formation of Soot and Polycyclic Aromatic Hydrocarbons in a Jet-Stirred Reactor, Ph.D. Thesis, Department of Chemical Engineering, Massachussetts Institute of Technology (1988).

Venkat, C., High Temperature Oxidation of Aromatic Hydrocarbons, M.S. Thesis, Department of Chemical Engineering, Princeton University (1981).

Venkat, C., Brezinsky, K. and Glassman, I., *19th Symp. (Int.) Combust.*, The Combustion Institute (1982), p. 143.

Waage, E.V. and Rabinovitch, B.S., *Chem. Rev.*, **70**, 377 (1970).

Wallington, T.J., Neuman, D.M. and Kurlyo, M.J., *Int. J. Chem. Kinet.*, **19**, 725 (1987).

Warnatz, J., *Ber. Bunsenges. Phys. Chem.*, **83**, 950 (1979).

Warnatz, J., *Comb. Sci. Techn.*, **34**, 201 (1983).

Warnatz, J., "Rate Coefficients in the C/H/O System," Chapter 5 of Combustion Chemistry, ed. by Gardiner, Jr., W.C., Springer-Verlag: New York (1984), p. 197.

Weider, G.M. and Marcus, R.A., *J. Chem. Phys.*, **37**, 1835 (1962).

Wersborg, B., Physical Mechanisms of Carbon Formation in Flames, Sc.D. Thesis, Department of Chemical Engineering, Massachussetts Institute of Technology (1972).

References

Westbrook, C.K., *Combust. Sci. Tech.*, **29**, 67 (1982).

Westbrook, C.K. and Dryer, F.L., *Prog. Energy Comb. Sci.*, **10**, 1 (1984).

Westmoreland, P.R., Experimental and Theoretical Analysis of Oxidation and Growth Chemistry in a Fuel-Rich Acetylene Flame, Ph.D. Thesis, Department of Chemical Engineering, Massachussetts Institute of Technology (1986).

Westmoreland, P.R., Dean, A.M., Howard, J.B., and Longwell, J.P., *J. Phys. Chem.*, **93**, 8171 (1989).

Westmoreland, P.R., Program UQRRK in Quantum-RRK programs for the Personal Computer, unpublished programs, (1992a).

Westmoreland, P.R., *Combust. Sci. Tech.*, **82**, 151 (1992b).

Westmoreland, P.R., personal communication (1995).

Winters, R.E., Collins, J.H. and Courchene, W.L., *J. Chem. Phys.*, **45**, 1931 (1966).

Witte, F., Urbanik, E. and Zetsch, C., *J. Phys. Chem.*, **90**, 3251 (1986).

Yetter, R.A., Dryer, F.L. and Rabitz, H., *Combust. Sci. Tech.*, **79**, 97 (1991).

Yu, T. and Lin, M.C., *J. Amer. Chem. Soc.*, **116**, 9571 (1994).

Yu, T., Lin, M.C., and Melius, C.F., *Int. J. Chem. Kinet.*, **26**, 1095 (1994).

Zachariah, M.R. and Smith, O.I., *Combust. Flame*, **69**, 125 (1987).

Zhang, H.-Y., Colorado School of Mines, personal communication (1994).

Zhang, H.-Y., and McKinnon, J.T., *Combust. Sci. Tech.*, in press (1995).

Zysk, E.D., *Temperature: Its Measurement and Control in Science and Industry*, **3**, 135 (1963).

Biographical Note

Mr. Shandross is a native of Chicago, Illinois, born to Abe and Rose Shandross on October 3, 1957. Upon entering the worldly sphere, he found himself "the baby of the family," after Marianne, Susan and Gary. He has remained in that position to this day, in spite of vocal protestations to the contrary.

Mr. Shandross' first six years after age one were spent in River Edge, New Jersey, living next door to Cletus Boyer, down the block from Mickey Mantle, and not too far from Bill Parcells. Several miles away was a kid named Randi Donnis, whom he did not to his knowledge meet. At age seven, he dragged the family back to Chicago, where they spent many years in Rogers Park. There he attended Daniel Boone Elementary School and Steven Tyng Mather High School. He broke free in 1975.

With a passel of grants and the National Merit and Illinois State scholarships, Mr. Shandross attended Northwestern University in Evanston, Illinois. Having always been interested in learning to protect himself, he began the study of martial arts; first Kempo (for nine months), followed by T'ai Chi Ch'uan, which occupies his spare time to this day. Also while in Evanston, he spent many hours living and learning with the (mostly) gentle crew of a rebellious Pi Kappa Alpha house, known as Pike — one of two coed Pike houses in the nation. Ominously enough, the other was at MIT. Mr. Shandross graduated from NU in 1979 with a BS in Environmental Engineering, and also ominously, with a concentration in Chemical Engineering.

Fresh with ambition, Mr. Shandross joined the Waste Management Division of the Region V office of the U.S. Environmental Protection Agency. His area of specialization was hazardous waste management, and in his six years at U.S. EPA, he served many roles in that program. He was appointed State Implementation Officer for Indiana, and in that capacity was the primary technical focal point for the Federal program in that State. Mr. Shandross was fortunate to be involved in site investigations, enforcement, permit review and writing, regulatory and programmatic development. He was also effectively a consultant to the State, the regulated community, and other departments within the Federal government.

In 1985, Mr. Shandross resigned from the EPA so that he could pursue a Master's degree at MIT. Shortly after his arrival, he was hornswaggled by his curriculum advisor, one Prof. John

P. Longwell, into entering the Ph.D. program. So little did he know about what was in store for him that he was excited about the prospect. What he was to find out was that the project he undertook was in fact *two* Ph.D. theses. The first thesis, an unwritten tome, was an empirical unfolding of enlightened intrametaphysical knowledge, the summation of which is — in the LaBroglie spirit of one-paragraph theses — the following:

> In an experiment consisting of a large room full of ten-year old equipment, every instrument and portion of the apparatus will eventually break down over the course of an investigation, in a sequential manner such that a complete experiment will not be achievable without replacement of at least two-thirds of said equipment.

That work having been completed, Mr. Shandross performed the entirety of the data collection, reduction, analysis and writing found in this document in the span of four years.

During the spiritual awakening of the data collection phase, Mr. Shandross met and ultimately married the previously-unknown Randi Donnis. The joyous event occurred on May 29, 1994. They intend to whoop it up for a month in celebration of the completion of this work, so you'd best be advised to call back in mid-October.

THESIS PROCESSING SLIP

FIXED FIELD: ill _____ name _____

index _____ biblio _____

▶ COPIES: (Archives) Aero Dewey Eng Hum

Lindgren Music Rotch (Science)

TITLE VARIES ▶☐ _____

NAME VARIES: ▶☐ _____

IMPRINT (COPYRIGHT) _____

▶ COLLATION 555p

▶ ADD DEGREE: _____ ▶ DEPT.: _____

SUPERVISORS: _____

NOTES:

cat'r: date:

page: F54

▶ DEPT: Chem. Eng

▶ YEAR: 1996 ▶ DEGREE: Ph.D.

▶ NAME SHANDROSS, Richard Allen